PROCEEDINGS OF THE NINETY-SEVENTH ANNUAL CONGRESS OF THE SOUTH AFRICAN SUGAR TECHNOLOGISTS' ASSOCIATION

held at the International Convention Centre, Durban,12-14 August 2025

PROCEEDINGS OF THE NINETY-SEVENTH ANNUAL CONGRESS OF THE SOUTH AFRICAN SUGAR TECHNOLOGISTS' ASSOCIATION

held at the International Convention Centre, Durban,12-14 August 2025

ISSN 1028-3781

Published by:

South African Sugar Technologists' Association

C/o South African Sugarcane Research Institute
Private Bag X02, Mount Edgecombe, KwaZulu-Natal, 4300, RSA
Tel: 27(0) 31 508-7543 Fax: 27(0) 31 508-7420
E-mail: sasta.secretariat@sugar.org.za
Website: www.sasta.co.za

First Edition: August 2025
ISSN 1028-3781

Copyright Reserved
© 2025

No part of this publication may be reproduced, stored in a retrieval system, or transmitted in any form or by any means, electronic, mechanical photocopying, recording or otherwise without the written permission of the copyright owner.

The South African Sugar Technologists' Association was founded in 1926. It is an organisation of technical workers and others directly interested in the technical aspect of the South African sugar industry. It operates under the aegis of the South African Sugar Association, but is governed under its own constitution by a Council elected by its members.

DISCLAIMER

This publication is provided on an 'as is' basis without warranties of any kind, either expressed or implied, including, but not limited to, warranties of title or implied warranties of merchantability of fitness for a particular purpose. The information contained in this publication is for general information purposes only. It does not constitute professional, technical, financial or other advice to the user of this publication and must not be relied upon as such by any person whatsoever. The use of this publication is at the user's own risk.

The authors/creators of the information contained in this publication have tried to ensure that the information contained herein is correct, but errors or inaccuracies may exist or the information may be incomplete, unreliable or no longer up to date. Therefore, no warranties of any nature whatsoever are given, and any liability to any person in respect of anything and in respect of the consequences of anything done or omitted to be done, wholly or partly in reliance upon the whole or any part hereof, are disclaimed, including and without limitation any contractual, dialectal, direct, consequential or financial damages or losses.

On no account will the organisers and/or any of the contributors or any person or entity involved in creating, producing or distributing the information and/or software available in this publication, be liable for any such damages arising out of the use of or inability to use this publication.

Although the greatest care has been taken in the compilation of the entire contents, the editors and publishers do not accept responsibility for errors or omissions.

CONTENTS

Editorial Panel, Referees and Reviewers		v
Exhibitors and sponsors		vi
Plenary Session		
A Review of South African Sugarcane Production in the 2024/25 Season: Climate, Production and Economics	***Sithole P**, Nicholson RJ and Wilkinson DG*	1
Biosecurity: An Overview of the 2023/2024 Season (Short Communication)	***Basdew IH**, McFarlane SA and Wilkinson DG*	15
100th Annual Review of the Milling Season - Southern Africa (2022/2023)	***Mbuyazi M, Ndinisa VN, Davis SB and Bhyrodeyal L***	28
Current Topics in Sugarcane-Based Material Research in South Africa	*Ayingeneye J, Govender K, Mphahlele J, Ndlovu N**, Stark A***	29
Assessing the Financial Viability of Sustainable Aviation Fuels (SAF) Production from Sugarcane in South Africa: An Ex-Ante Analysis	***Mvelase L,** Ferrer S*	46
An Analysis of the Financial Viability and Environmental Impact of Food Products, Biochemicals, Biofuels, and Biomaterials as Potential Diversification Strategies for the Sugar Industry	*Louw J, Louw JP, **Brobbey MS**, Foxon KM and Gorgens JF*	54
Sustainable Acrylic Acid and Propylene Glycol Production in a Sugarcane Biorefinery: A Techno-Economic and Environmental Analysis	***Brobbey M,** Louw J, Gorgens J*	63
Characterising Past Climate Change in The South African Sugar Industry: Preliminary Findings for Temperature and Rainfall, 1980-2024	***Sithole P** and Clark D*	74
Agriculture Session 1: Small Scale Growers		
Investigating the Impact of Skills Development Training on Farmer's Performance and Livelihoods: A Case of Small-Scale Sugarcane Growers in the Umfolozi Mill Area KZN	***Qwabe S***	81
Guidelines for the Field Establishment of NovaCane® Plants	***Tweddle PB,** McFarlane SA and Snyman SJ*	84
The Role of the South African Sugarcane Research Institute's Insect Rearing Programme in Pest Control	***Nzama S,** Gillespie D and Malinga L*	85
Standing the Test of Time: Sugarcane Biotechnology Research Collaboration Between the Institute for Plant Biotechnology, Stellenbosch University, and the South African Sugarcane Research Institute	*Van der Vyver C **and Snyman SJ***	89
Identification and Validation of Molecular Markers for Resistance to *Eldana Saccharina* Walker (Lepidoptera: Pyralidae)	***Jacob R**, Singh S and Joshi S*	90

Agriculture Session 2: Biology		
The Isolation and Characterisation of Lactic Acid Bacteria (LAB) Involved in Cane Deterioration	***Tererai R,*** *Rambwawasvika and Mutatu W*	91
An Investigation of the Population Dynamics of Yellow Sugarcane Aphid with Particular Emphasis on Movement Patterns Between Plants	***Basdew I*** *and Xaba B*	92
Analysing The Expression of Insecticidal Proteins in Genetically Modified Sugarcane	***Makhetha T,*** *Joshi S, Albertse E and Ghai M*	93
From Many to One: A Pipeline for Selecting a Dual Trait Commercial Genetically Modified Sugarcane Event	***Meyer G,*** *Albertse E, Jacob R, Khanyi H and Snyman SJ*	100
Control of Yellow Sugarcane Aphids using Entomopathogenic Fungi	***Nguvu G*** *and Mndzawe D*	101
Agriculture Session 3: Digital and Precision Agriculture		
Automated Field Boundary Detection, Delineation, and Extraction Using Sentinel-2 Satellite Imagery	***Poona, N***	102
Modelling Leaf Nitrogen by Using Multi-Temporal *In Situ* Infrared Spectroscopy	***Makhaye A****, Tyilekile S and Poona N*	107
Optimizing Field Monitoring Through NDVI-Based Anomaly Detection Using Drone Imagery: A Pilot Study at Dwangwa Estate	***Msowoya M***	113
Introducing Digital Data Collection for Biosecurity Surveys at the South African Sugarcane Research Institute (SASRI)	***Thompson I,*** *Stranack RA, McFarlane SA, Basdew IH, Merile S and Velem T*	118
Creating A Multi-User Digital Data Collection System for Ratoon Stunt (RSD)	***Radebe S****, McFarlane S, Stranack R, Thompson I, Maduray R, Torlage J and Edmonds J*	126
Agriculture Session 4: Nutrition		
Mapping the Soil pH Variability in Sugarcane Fields of the Zimbabwe Sugar Industry From 2018-2024	***Marungudze A,*** *Mampangesi S, Rambwawasvika H, Washington Mutatu W*	127
Trends and Challenges in Sulphur Management for South African Sugarcane Industry	***Elephant D****, Zulu S, Mdlambuzi T*	128
Volatilisation Losses from Surface-Applied Nitrogenous Fertilizers in the Sugarcane-Growing Soils of Zimbabwe: Laboratory Scale Study	***Maidza T****, Rambwawasvika H, Chibarabada T, Mutatu W*	140
The Integration of Soybean into Sugarcane Farming Systems: Enhancing Soil Fertility and Weed Control	***Phiri J***	150
Agriculture Session 5: Agronomy and Management		
A Data-Driven Approach to Support the On-Farm Management of Sugarcane Varieties in The KwaZulu-Natal Midlands Region	***Hoffman N,*** *Clark D, Kadwa M, Paraskevopoulos A, van Heerden R, Wilkinson D and Botha P*	151
Effects of Harvest Season and Soil Type on Sugarcane Ratoon Yield Decline	***Dlamini N and Zhou M***	157

Rising Groundwater Levels in Sugarcane Fields and their Impact on Agricultural Water Management	***Mabaya G,*** *Nkala P and Gumindoga W*	164
Factory Session 1: Boilers		
The Hidden Costs of Over-Designing Boiler Back-end Equipment	***Mienie B*** *and* ***Dauvellier R***	176
Controlling Boiler Swell and Shrink	***Wannenburg E***	188
Boiler Equipment: Typical Anomalies and Their Efficiency Consequences	***Wilke C,*** *Marais F and Rawlins B*	199
CFD Study on Bagasse Spreader Airflow and Deflector Plate Configurations: Impacts on Fuel Distribution and Boiler Performance	***Rawlins B****, Marais F and De Villers E*	214
Shaft Mounted Planetary Mill Drive for Economic Expansion and Mill Performance Improvement	***Patil M,*** *Carroll B and Kristensen P*	229
The Retrofitting of Boiler-Induced Draft Fan Rotors to Increase Efficiency and The Associated Energy Savings	***Frost M***	243
Factory Session 2: Energy		
Energy Savings Utilising Dimple Tube Technology	***Bezuidenhoudt D,*** *Stevens M, Yeo W and Gokool M*	252
Why Grid Codes Matter for Embedded Generators – Comparing Utility vs Factory Perspectives	***Ahlschlager R,*** *Seebran P and Gent R*	266
Killing-the-Joule: Enhancing Energy Efficiency Through Strategic and Practical Initiatives at Hulett Refinery	***Reddy J,*** *Rambukus Z and Maharaj N*	277
Factory Session 3: Processing		
The Benefits of Installing Mud Belt Filters in The Simunye Sugar Mill in the 2024/25 Crushing Season	***Dlamini M****, Kugara R and Kunene T*	291
A Review of Sucrose Solubility in Impure Cane Sugar Solutions Used in Raw Sugar Factory Pan Stations	***Rahiman S,*** *Mbuthuma Y, Love D and Davis S*	306
The Use of Supersaturation for Crystallisation Control	***Muir BM*** *and Rózsa, J*	327
The Analysis of Lime on Melt by Double Alkalinity Titration	***Naicker A,*** *Ngcobo S, Naidoo YL, Walthew D and Myeza N*	350
Factory Session 4: Processing (2)		
A Review of the Physical Properties of A-Massecuite That Affect Batch Centrifugal Performance	***Munsamy S***	351
Optimisation of the Back end of Standalone Refinery	***Dlamini EM,*** *Maharaj N and Rambakus Z*	361
Design and Optimisation of a Batch Reactor for The Digestion Stage in The Production of Potassium Sulphate from Stillage at a Pilot Scale	*Mutatu W, Nyemba T,* ***Marungudze A*** *and Rambwawasvika H*	372

Factory Session 5: Measurement /Labs		
The SMRI Factory Laboratory Certification Scheme: Ensuring Credible and Reliable Laboratory Results	***Ngema M,*** *Naidoo YL, Mbuyazi M and Pillay V*	373
The SMRI Factory Improvement Initiative	***Mbuyazi M*** *and* ***Ndinisa V***	374
Comparison of Near Infra-Red Spectroscopy (NIRS) and The Conventional Direct Analysis of Cane (DAC) in The Determination of Cane Quality Parameters	*Siyakisa F, Rambwawasvika H, Mutatu W and* ***Tererai R***	406
GENERAL SASTA INFORMATION		
SASTA Officers 1926 – 2025		407
SASTA Awards 1926 – 2025		409

Editorial Panel 2025

Dr Shailesh Joshi ((Editor-in-Chief)
Mrs Sharon McFarlane (Editor: Agriculture)
Mr Gavin Smith (Factory Programme)
Mr Steve Davis (Editor: Factory)
Dr Sharon Rees (Technical Editor)

Referees and Reviewers 2025

Ewald Albertse
Dr Carolyn Baker
Iona Basdew
Kim Booysen
Celo Chili
Steve Davis
Dr Dimpho Elephant
Jan Erasmus
Katherine Foxon
Matthew Furniss
Thomas Gibbs
Andrew Gielink
Dr Natalie Hoffman
Dr Matthew Jones
Dr Shailesh Joshi
Dr Ashiel Jumman
Dr Muhammad Kadwa
Dr Malcolm Keeping
Dr Tsion Kidane
Warren Lawlor
Dr Goden Mabaya
Shaun Madho
Samkelo Matsebula
Alan Mead
Dave Meadows
Fred Mncube
Dr Sandile Mthimkhulu
Stanley Munsamy
Rishen Naidoo
Seelan Naidoo
Nkosinathi Vincent Ndinisa
Sanet Nel
Thobile Nxumalo
Bheki Nzama
Steve Peacock
Navin Ramjuan
Althaf Rassol
Peter Rein
Dr Ruth Rhodes
Paul Schorn
Alex Searle
Nadeem Shrubrati
Dr Abraham Singels
Ish Singh
Leon Smith
Dr Sandy Snyman
Prof Annegret Stark
Nico Stolz
Dr Rowan Stranack
Brian Tait
Dr Louis Titshall
Prof Solomon Tsfamichael
Dr Rianto van Antwerpen
Dr Riekert van Heerden
William Yeo

Sponsors and Exhibitors

Agrihawk

AISCO Africa / Western Irrigation

Alignment with Laser

Alliance Consulting Engineers

Anhui VSD Special Chain

Anton Paar South Africa

Babcock Africa

Babcock Ntuthuko Engineering (Pty) Ltd

Bell Equipment

BMA / Sucrotech

BMG

Bonfiglioli

Bosch Projects

Brenley Engineering Sales

Bruker South Africa

Buckman

CMG Pumps

C.R.I. Pumps S.A.

Everllence South Africa

Fortek - Kolhapur Auto Works

Fortek – S B Reshellers

Hagglunds Drives SA

Hanna Instruments (Pty) Ltd

Haver & Boecker oHG - BEHN + BATES

Ilembe Foundry

John Thompson

Kirton Mechanical Equipment

Lakeside Equipment

Lasec®

Mecosa

Metrohm South Africa

Netafim SA

Pfeifer & Langen GmbH

PPI Pumps

Process Valve Corporation

Process Vacuum / PPI Pumps

Rheinmetall Resonant South Africa

Rheochem

Rossi Southern Africa

Rotex / GNV Enterprises (Pty) Ltd

Rotortek

SEW - EURODRIVE

SGM / SU Group

Shrijee Process Engineering Works

Sonkor Engineering Pty Ltd

South African Sugar Association (SASA)

South African Sugar Technologists' Association (SASTA)

Sugarequip

The Rotex Group

Three Star Engineering Works Pvt Limited

Timken South Africa (Pty) Ltd

Turbine Generator Services

TWIMS

United Scientific SA

Voitechnik

Weg Africa

REVIEW PAPER

A REVIEW OF SOUTH AFRICAN SUGARCANE PRODUCTION IN THE 2024/25 SEASON: CLIMATE, PRODUCTION AND ECONOMICS

Sithole P[1], Maluleke IM[2], Nicholson RJ[2] and Wilkinson DG[1]

[1]South African Sugarcane Research Institute, Private Bag X02, Mount Edgecombe, 4300, South Africa
[2]South African Cane Growers' Association, 170 Flanders Drive, Mount Edgecombe, 4300, South Africa

Phillemon.Sithole@sugar.org.za; Ikageng.Maluleke@canegrowers.co.za; Richard.Nicholson@sacanegrowers.co.za; David.Wilkinson@sugar.org.za

Abstract

The objective of this paper is to characterise sugarcane production in South Africa for the 2024/25 milling season, from an agricultural perspective. The review helps to provide an insight into the successes and shortcomings of the industry's recent production strategies and to flag areas that may require intervention, to improve productivity.

The season was characterised by erratic summer rainfall, followed by a prolonged dry spell in the winter of 2024. This was not entirely unexpected, due to the prevailing El Niño state of the El Niño-Southern Oscillation. Cane yield and production decreased across all the rainfed mill supply areas, when compared to recent seasons, due to the poor rainfall distribution. The estimated industry average cane yield (66.3 t/ha) was the lowest since the drought-affected 2016/17 season. The industry average estimated recoverable crystal, which is a measure of cane quality, was slightly better than that of the previous season and the five-season mean because of better natural ripening under the drier conditions. However, the prolonged dry conditions caused the cane quality to decline, as the season progressed. The forced premature harvest of frost-damaged cane in parts of the Midlands and Zululand regions also contributed to the poor cane quality.

Grower revenue per ton of cane improved slightly, relative to the previous season, due to the marginal gain in the Recoverable Value (RV) price. However, grower profitability, in both the rainfed and irrigated areas, was negatively affected by the low cane yields and higher operating costs.

The forced carry-over cane crisis that affected growers in the coastal and Midlands mill supply areas in recent seasons is now over. This, coupled with the favourable RV price, motivated growers to resume crop establishment. Concerted efforts are required to ensure an adequate supply of good seedcane and, ultimately, to improve cane supplies in the forthcoming seasons.

Keywords: sugarcane, production, yield, quality, climate, El Niño, profitability

Introduction

The South African (SA) sugar industry produced 16.47 million tons (Mt) of cane in the 2024/25 season from an estimated 244 311 ha harvested. This was a significant decrease from the 17.91 and 17.94 Mt of cane produced in the 2022/23 and 2023/24 seasons, respectively (Figure 1), despite a slight increase in the estimated area harvested. Consequently, sugar production declined to 1.87 Mt in 2024/25, compared to the corresponding figures of 1.93 and 2.01 Mt for the previous two seasons (Sithole *et al.,* 2024). The average estimated cane yield for the industry was 66.3 t/ha, compared to 76.4 t/ha for 2022/23 and 73.5 t/ha for 2023/24. Large declines in production and yield were observed in all the rainfed mill supply areas (MSAs), while there was a general slight increase for the irrigated areas, when compared to the previous season.

The forced carry-over cane crisis that growers in the coastal and Midlands MSAs have been grappling with for the previous five seasons (Sithole *et al.,* 2023) is now over. Poor growing conditions during the 2024/25 season resulted in most mills closing earlier than scheduled, due to cane shortages, and therefore, there was no forced carry-over cane in the 2024/25 season. This motivated growers to refocus their activities and to prioritise the re-establishment of fallow and abandoned fields, which resulted in the slight increase in the estimated area under cane (AUC) in 2024, compared to 2023 (Figure 1). This trend is expected to continue into the 2025/26 season as the industry aims to improve cane supply in those regions.

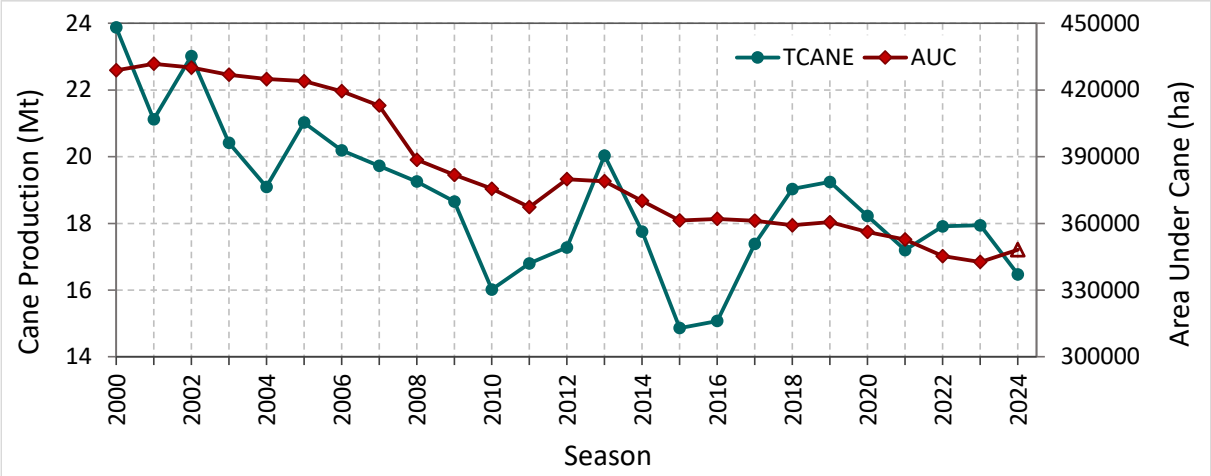


Figure 1. Industry cane production (TCANE, Mt) and area under cane (AUC, ha) per season, from 2000/01 (2000) to 2024/25 (2024). The triangle for the 2024 AUC represents an estimated value

The objective of this paper is to characterise cane production in South Africa for the 2024/25 season, from an agricultural perspective. Production indicators of cane yield and quality were related to major production factors, such as the climate, irrigation capacity and economic conditions. This review aims to provide an insight into the industry's successes and challenges in the recent production strategies which, in turn, will help to identify opportunities for improved production efficiency in the future.

Methodology

General

A similar approach to those in the previous reviews was followed (van den Berg *et al.*, 2008; Singels *et al.*, 2014; Sithole *et al.*, 2022). Production and climate data were analysed mostly at MSA level, and they were then upscaled to the regional and/or industry level. The Canesim Crop Forecasting System (CCFS) (Bezuidenhout & Singels, 2007), at a spatial scale of the Homogenous Climate Zones (HCZ) (Bezuidenhout & Gers, 2002), was used to evaluate the climatic potential.

Figure 2 shows the agroclimatic regions and the location of the 12 sugar mills of the South African sugar industry. The 2024/25 growing and milling season will henceforth be referred to as the 2024 season, and the previous seasons, e.g. 2022/23 and 2023/24, as the 2022 and 2023 seasons, respectively.

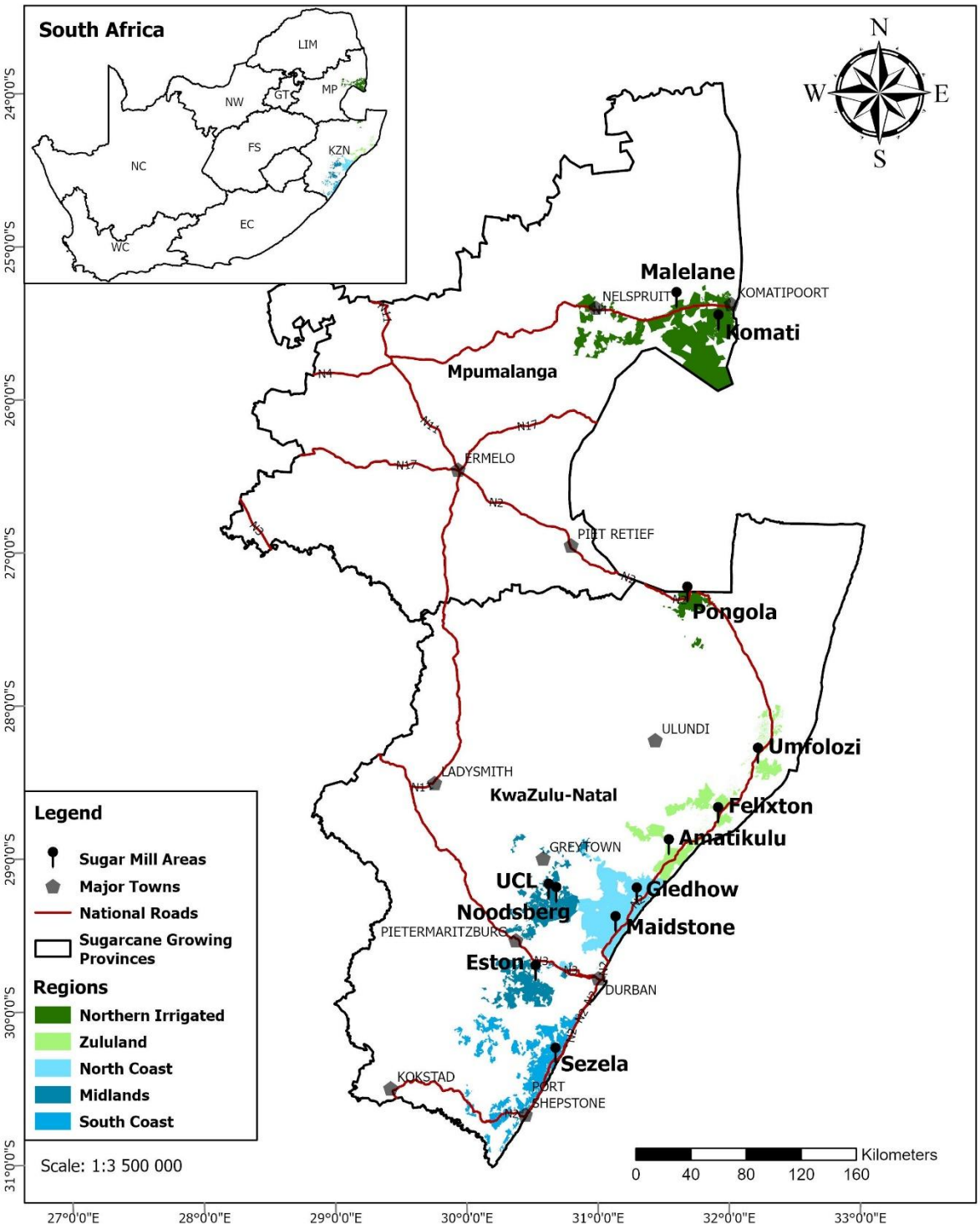


Figure 2. A map of the South African sugar industry showing the sugar mills and the main agro-climatic regions (Source: South African Sugarcane Research Institute, Geographic Information Systems Office)

Climate and irrigation water supply

Climate records from various weather stations and aggregated to MSA level, were obtained from the SASRI weather data portal, https://sasri.sasa.org.za/weatherweb. The twelve-month totals (or means) leading up to each month of the 2024 milling season (e.g. 1 April 2023 to 31 March 2024, 1 May 2023 to 30 April 2024, and so on), were compared to the corresponding long-term mean (LTM) values. The seasonal averages were then compared to the corresponding figures for other past seasons, e.g. 2022 and 2023. The monthly rainfall distribution and reference soil water content (SWC) trends throughout the season were also analysed. The SWC is a measure of the plant-available soil water calculated for rainfed conditions for a soil with a total available water (TAW) of 100 mm and with a full canopy cane crop growing on it.

Weekly irrigation water allocations were obtained from the respective Water Boards for each water source in the irrigated areas, and they were analysed in the same way as in previous reviews (Singels *et al.*, 2014; Sithole *et al.*, 2022).

Production

Cane production (cane delivered to the mills) and cane quality data were obtained from the South African Sugar Association (SASA) Cane Testing Service database. Similar approaches as those used in previous reviews (Jones *et al*., 2021) were followed to establish the area harvested. The average cane yield for each MSA, was calculated as the total tons of cane produced, divided by the total area harvested for the season.

MSA average simulated yields from the CCFS were used to assess the climatic yield potential, as determined by the climatic conditions and irrigation water availability. Unexpected changes in the usual harvest age, the effects of profuse flowering, as well as crop damage from extreme weather events, such as flooding, lodging, hail or frost, were not accounted for in the simulations.

Economics

To assess the performance and sustainability of the SA sugarcane industry, several economic indicators affecting sugarcane growers were examined. These indicators provide an insight into the growers' financial viability, productivity and responsiveness to market and policy changes. The key metrics include gross income, production costs, profitability margins, income per ton of RV, as well as cost components such as planting, harvesting and transport. Together, these indicators offer a comprehensive view of the economic dynamics that shape both large-scale and small-scale sugarcane farming operations.

The economic analysis was drawn from a combination of survey data, official government reports, as well as inflation-based projections to estimate the production economics for the 2024 season, compared to the actual and estimated data of the past seasons (2022 and 2023), respectively. This approach was to ensure consistency and relevance, by incorporating actual cost data, where available, and applying recognised indices and inflation rates to estimate the missing data, as was the case in recent review papers (Sithole *et al.,* 2022; Sithole *et al.*, 2023).

Income and production cost data for large- and small-scale (producing less than approximately 1 800 TCANE per season) farms from all the 12 MSAs for the 2022 season were obtained from a survey conducted by the SA Cane Growers' Association (SACGA, 2024a; 2024b). Data for the 2023 season were estimated by using indices from the Crops and Markets Reports released by the Department of Agriculture, Land Reform and Rural Development (2024). The projections for the 2024 season were based on the average Consumer Price Index (CPI) for the year 2024 (Statistics South Africa, 2024). Estimates for the 2023 season are based on the actual changes in prices and costs, while projections for the 2024 season were based on the average inflationary increase. The average cost and income statistics reported in this study were determined by weighting the MSA values by the deliveries of large-scale growers (LSGs) in each MSA. The small-scale grower (SSG) data for 2023 were updated through a 2023/24

cost survey, with 2024 estimates based on CPI and regional input cost changes from the SA Canegrowers' staff.

Results and Discussion

Climate

On average, the industry received near-normal rainfall for the 2024 season, with some MSAs getting slightly below and others slightly above the LTM rainfall (Figure 3). The 2024 rainfall was, however, below that of the previous two seasons (2022 and 2023) in all the MSAs.

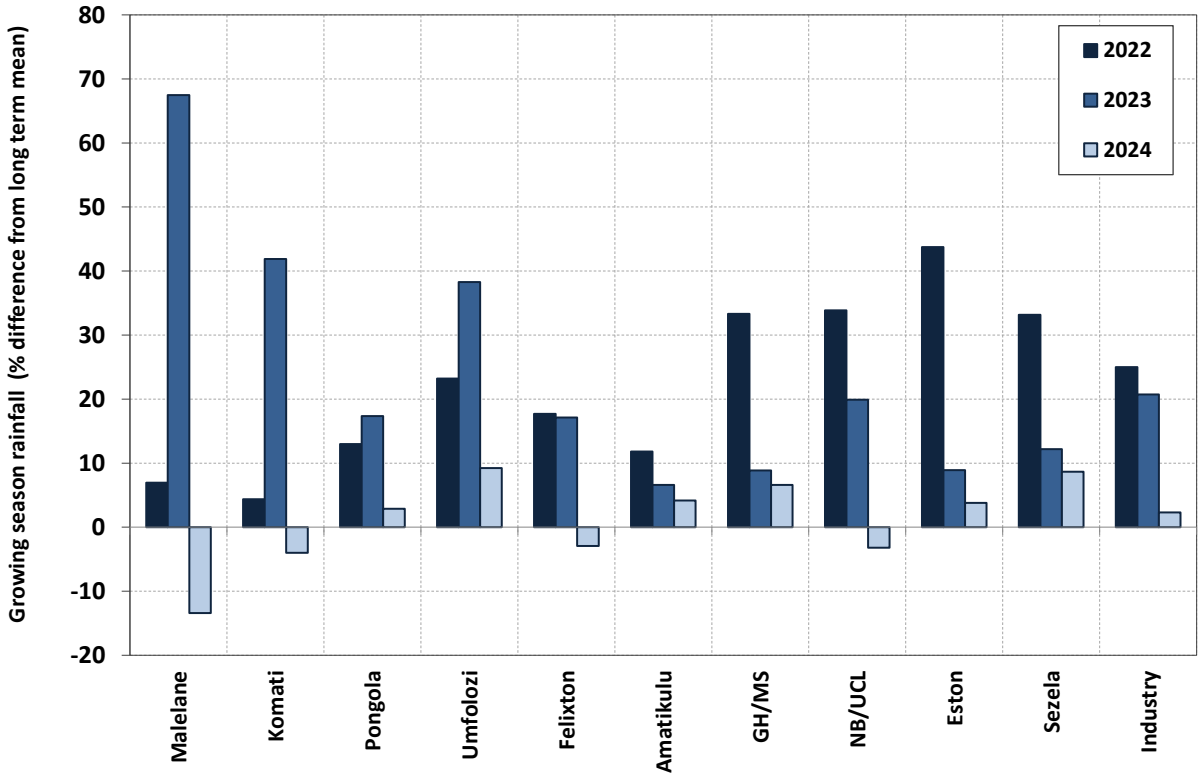


Figure 3. The 12-month total rainfall for the 2024 season expressed as a percentage difference from the long-term mean for the mill supply areas and the industry average for the 2024 season, compared to the 2022 and 2023 seasons. GH/MS are the combined figures for Gledhow and Maidstone, while NB/UCL are the figures for Noodsberg and UCL

The general expectation leading up to the 2023/24 summer season was that it would be a hot and dry summer, due to the prevailing strong El Niño conditions of the El Niño-Southern Oscillation (ENSO). When compared to recent El Niño-affected seasons (2010 and 2016), the rainfall during the 2024 season was much better, with an industry average of 102% of the LTM, compared to 87% for 2010 and 70% for 2016.

The rainfall distribution in most of the rainfed areas from the onset of the 2023/24 summer rainfall season was typically characterised by heavy downpours (October and December, 2023; January 2024), followed by extended periods of little rainfall (Figure 4). This resulted in severe soil water depletion in some areas and subsequent crop water stress, especially during most of winter in 2024 (Figure 5). In the irrigated areas, the average summer rainfall was below the LTM, but good rainfall in December 2023 and the heavy rainfall in March 2024, which was associated with tropical storm *Filipo,* ensured that irrigation water sources were well replenished. No severe irrigation water restrictions were experienced during the 2024 season, unlike 2016, when severe restrictions were applied, due to diminished water supplies from all the major water sources, following similar El Niño conditions during the 2015/16 summer.

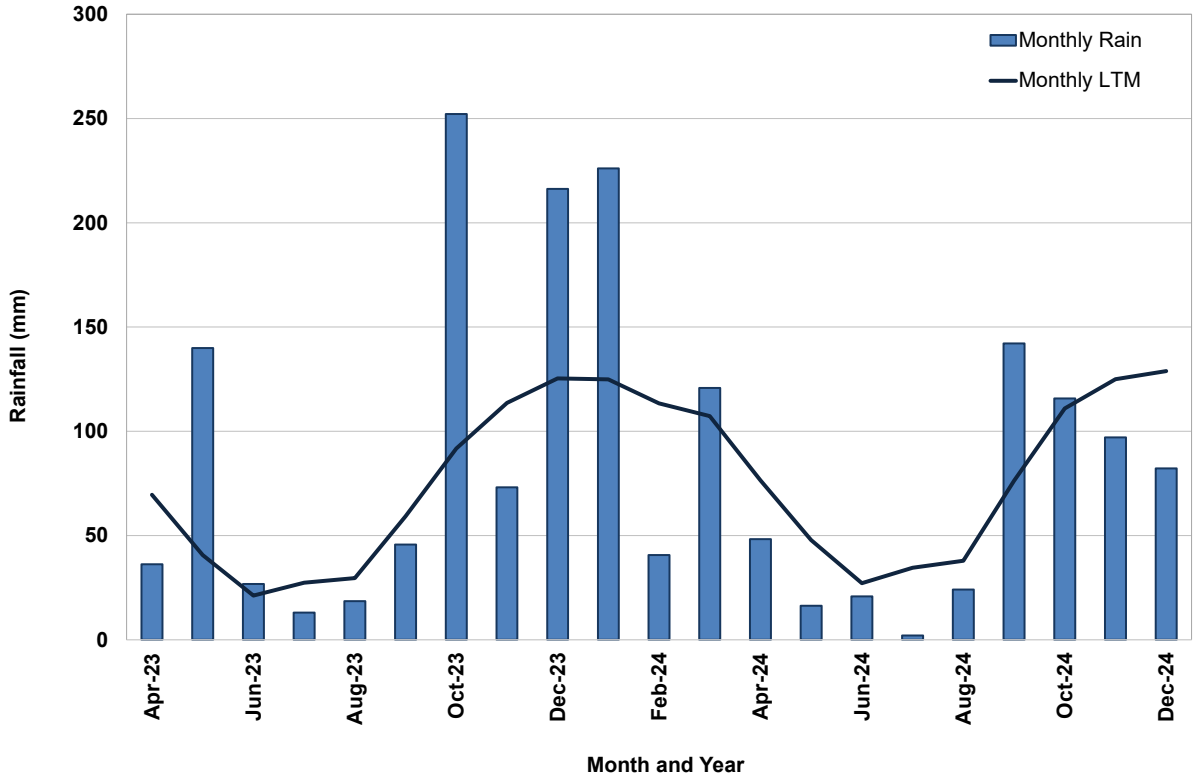


Figure 4. The average monthly rainfall, weighted by the area under cane, for the rainfed North Coast region of KwaZulu-Natal from April 2023 to December 2024, compared to the long-term mean (LTM)

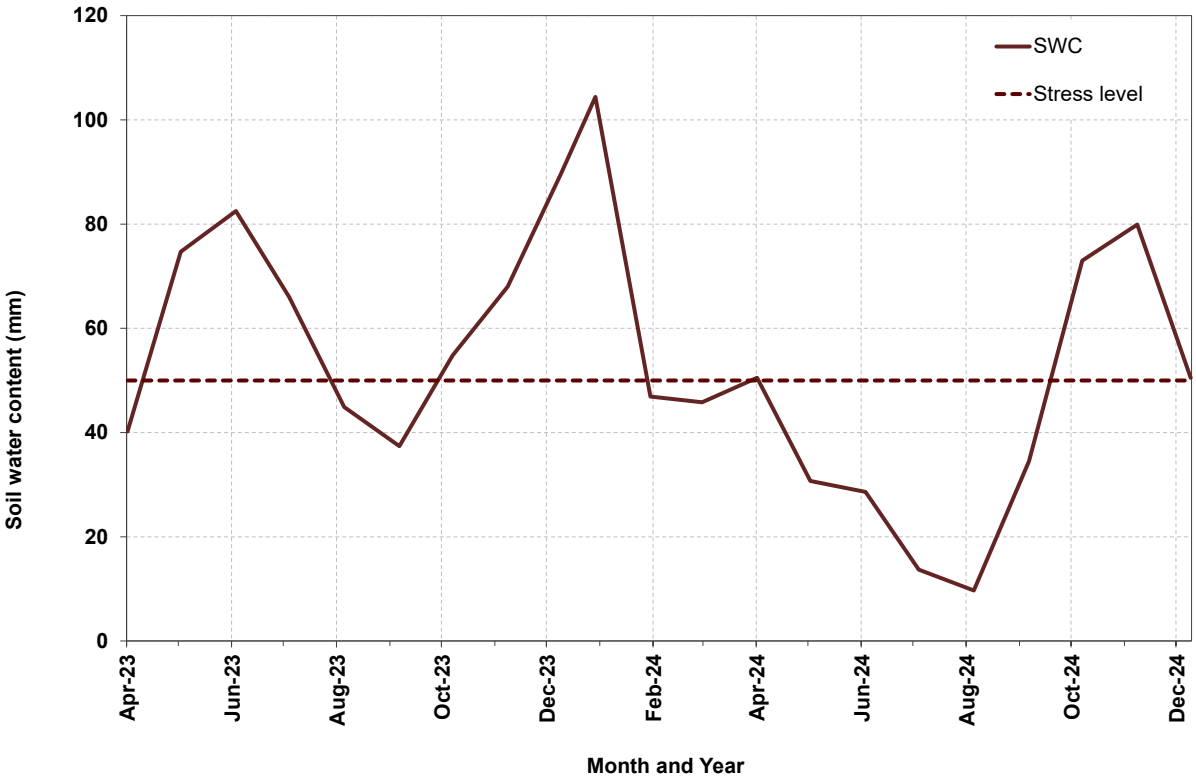


Figure 5. Monthly reference available soil water content (SWC) for the Maidstone mill supply area for April 2023 to December 2024. The broken line (---) represents the 50% depletion level, below which crop water stress is assumed to commence

Daily minimum temperatures during the 2024 winter were generally mild, but a cold snap with sub-zero temperatures in early July in parts of the Midlands (Figure 6), Zululand and Mpumalanga resulted in black frost and subsequent crop damage. The estimated total cane area affected exceeded 3 500 ha for the Midlands region alone (Wilkinson, D. pers. comm., 2025).

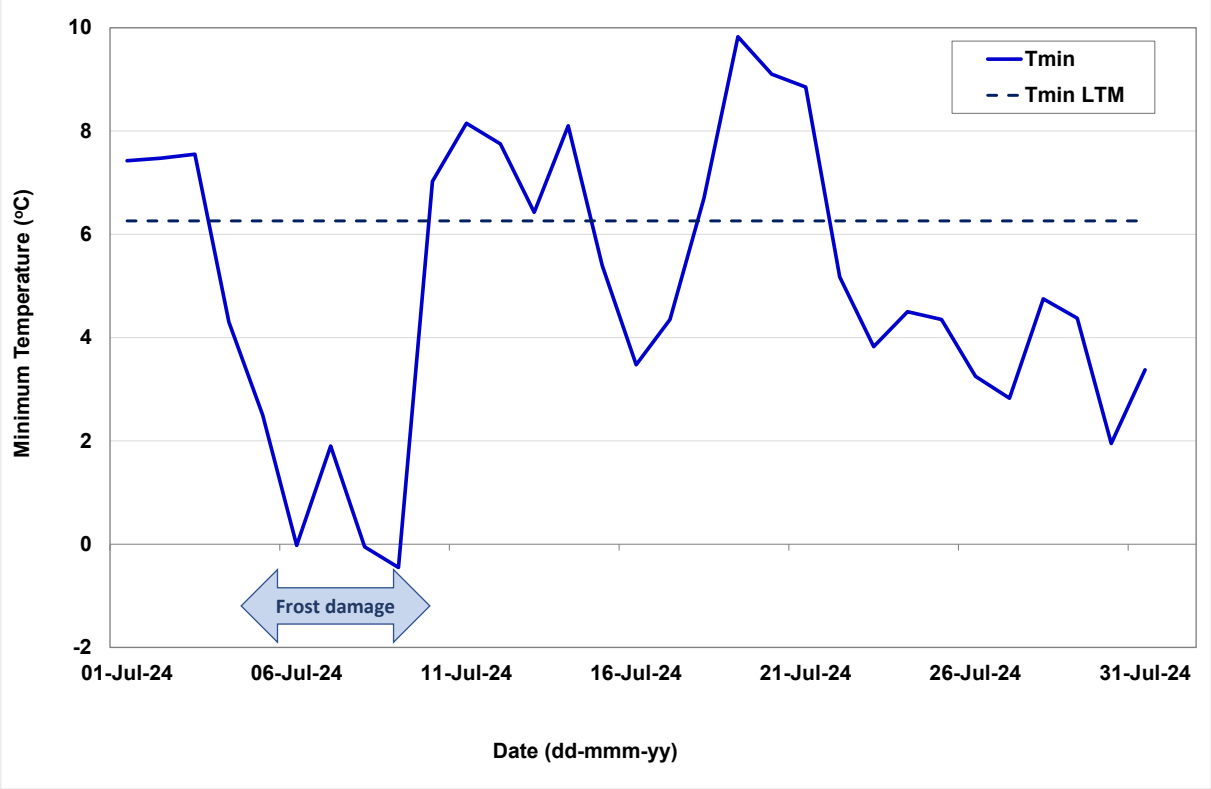


Figure 6. Average daily minimum temperature (Tmin) for the Midlands North region for July 2024, compared to the corresponding monthly long-term mean (Tmin LTM)

The dry summer months, especially in the irrigated north region, recorded higher-than-normal incidents of extreme high temperatures (with daily maxima exceeding 40°C), which may have had a negative effect on cane growth, especially where irrigation was not optimal.

Production and yields

The industry total cane production (16.5 Mt) and the average estimated yield (66 t/ha) for 2024 were the lowest since 2016, when the industry experienced a severe drought (Singels *et al.*, 2017). Sugar production was also lower than most recent seasons, but surprisingly, higher than that for the 2021 season, when more cane (17.2 Mt) was crushed. This suggests improved milling (sugar extraction) efficiency, in addition to the slightly improved cane quality (see the section on cane quality).

At MSA level, average estimated yields for 2024 were lower than the previous two seasons (2022 and 2023) for all the rainfed mill supply areas (Figure 7). In the northern irrigated areas, the average estimated yields for 2024 were mostly lower than the previous two seasons and the five-season mean, but slightly higher than those for 2023, for the Komati and Malelane MSAs.

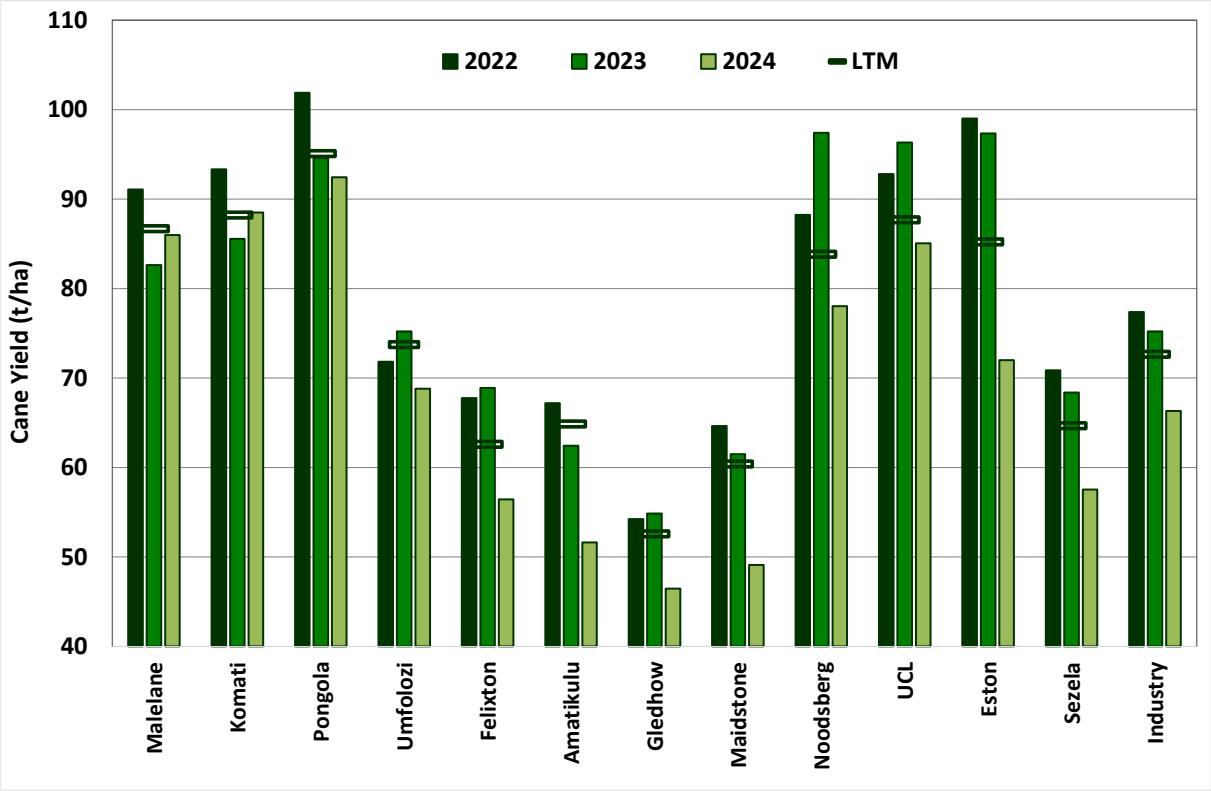


Figure 7. Estimated average cane yield for the mill supply areas and for the industry for the 2024 season, compared to the 2022, 2023 and five-season mean (LTM) yields

The decline in rainfed production and yield from 2022 and 2023 was mainly due to the difference in climatic conditions, notably the lower rainfall (Figure 3). This was reflected by Canesim simulations, which indicated that the climatic yield potential for 2024 was below that of the 2023 season (Figure 8) for all the rainfed MSAs.

Yield improvements from 2023 were anticipated in the irrigated areas, following the suspension of rolling blackouts in March 2024. This was the case for the Malelane and Komati MSAs, but there was a slight 2.3% yield decline for Pongola. No consistent pattern existed between simulated and actual yields among all of the three irrigated MSAs. These discrepancies between the actual and simulated yield trends were due to the difficulties associated with accurately accounting for the impacts of the severe rolling black-outs during 2023 (Sithole *et al*., 2024) in the simulated yields. The yield losses associated with the yellow sugarcane aphid (*Sipha flava*) infestations and the reduced age of the harvest in the late season crop (due to low cane supplies) were also not accounted for in the simulated yields.

Other factors affecting the cane yields in 2024 included frost damage, particularly in the Midlands region, which forced the early harvesting of the affected fields. Overall, the low yields across the industry resulted in cane being harvested at a progressively younger age, as the season progressed, and eventually most mills closed earlier than scheduled, due to the diminished cane supplies.

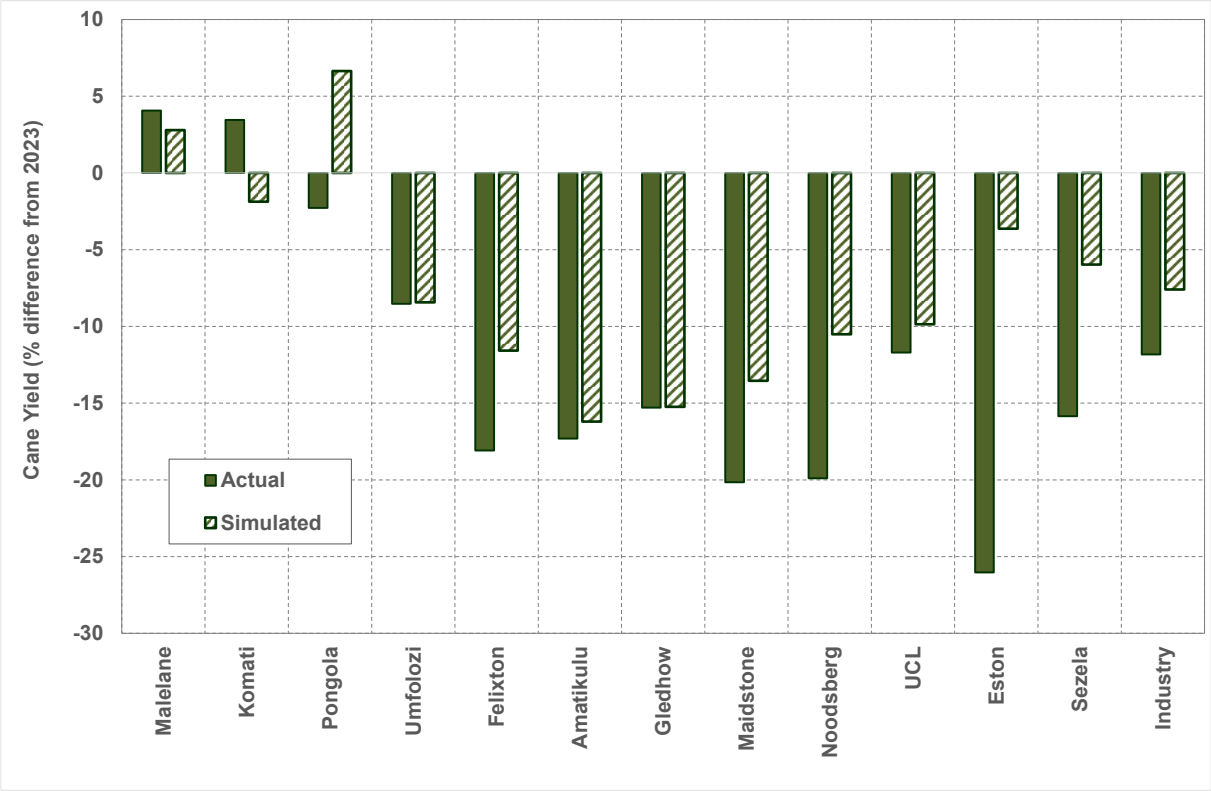


Figure 8. Average estimated and simulated yields for 2024 expressed as a percentage difference from the 2023 season yields

Cane quality

Cane quality was slightly better in 2024 than in 2023 for most MSAs, and for the industry as a whole (Figure 9). The reduced forced-carryover cane in the Midlands meant that less poor quality, over-aged cane was delivered at the start of the season. The general dry conditions between the 2024 autumn and spring initially helped to improve cane quality through natural cane ripening. However, as the dry spell continued beyond winter, cane quality in the rainfed areas began to deteriorate due to severe water stress and in association with increased Eldana damage and sour rot. The frost damage in July 2024 also had a negative impact on cane quality, due to cane deterioration and the forced harvesting of young, frosted cane. Towards the end of the season, low cane supplies in most MSAs forced premature harvesting in many fields, which negatively impacted cane yield and quality. Despite the overall improved cane quality, compared to the previous two seasons, the industry average cane quality remained low (ERC% = 11.16) compared to the period 2017-2019 (with an ERC% range of 11.48-11.52), when forced carry-over cane was not a major contributing factor to cane quality.

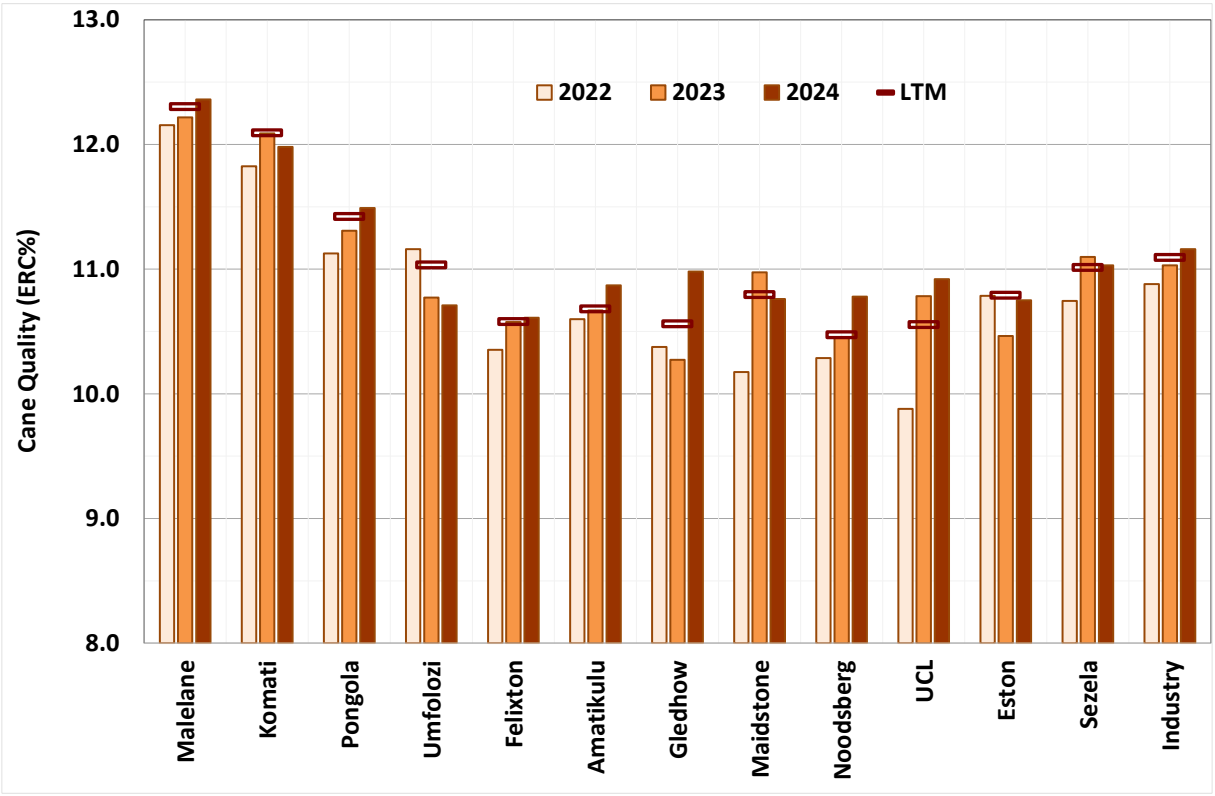


Figure 9. Overall estimated recoverable crystal content of cane (ERC%), a measure of cane quality, at mill supply area and industry levels for the 2024 season, compared to the 2022 and 2023 seasons and the five-season mean (LTM)

Economics and grower profitability

The SA sugar industry experienced mixed economic conditions between the 2023 and 2024 seasons, with signs of both resilience and pressure in key performance areas, as shown in Table 1.

Table 1. Key economic indicators for the South African sugar industry during the 2023 and 2024 seasons (Source: SACGA, 2024 and SACGA, 2025)

Season	2023	2024	Percentage change (%)
**Sugar: RV Ratio	93.43	93.65	0.2
Gross Sugar production (t)	2 005 208	1 885 789	-6.0
Local market demand (t)	1 510 902	1 443 291	-4.5
*Sugar imports (t)	359 955	375 542	4.3
*Sugar exports (t)	496 866	431 464	-13.2
#11 World Price (weighted average: USc/lb.)	24.58	20.45	-16.8
R/US$ exchange Rate (weighted average)	19.26	18.58	-3.5
**RV price (R/t)	7429.76	7 665.63	3.2

*2023 figures revised **RV = Recoverable Value

The sugar to Recoverable Value (RV) ratio, which indicates the efficiency of sugar extraction from cane, increased slightly from 93.43% to 93.65%. This marginal increase reflects a slight improvement in cane quality, or more favourable processing conditions. A notable contraction was observed in the gross sugar production, which declined by 6% and was largely attributed to the below-average growing conditions, as reported earlier. The Health Promotion Levy

(HPL) remained unchanged, but the local sugar demand decreased by 4.5% in 2024, compared to 2023, which explains the corresponding increase in sugar imports. The 4.3% increase in sugar imports for 2024, compared to the 2023 season, was due to insufficient import tariff protection.

Sugar exports also declined significantly, i.e. by 13.2% from the previous season, mostly due to the smaller crop size. The international #11 world sugar price dropped sharply by 16.8%, from 24.58 US cents/lb to 20.45 US cents/lb. This substantial decline, coupled with a 3.5% appreciation of the Rand against the US dollar (from R19.26 to R18.58), placed further downward pressure on the export income. Despite the broader industry contraction, the RV price per ton increased by 3.2%, from R7 429.76 to R7 665.63, mainly due to lower export exposure, lower industry costs and the first business rescue default repayments from both Tongaat Hulett Sugar and Gledhow Sugar Company.

Large-scale grower profitability

Figure 10 indicates that there was a moderate improvement in the LSG's gross income per ton of cane for the 2024 season, which was largely driven by a 3.2% rise in the RV price. In the rainfed areas, the rising costs continued to erode grower profitability, with a 32.0% drop in their Net Farm Income, while in the irrigated areas, grower profitability remained largely stable, with only a 4.3% drop in their Net Farm Income, when compared to 2023. Growers in rainfed areas, especially in the Midlands, still struggled with the after-effects of forced carry-over cane from the previous seasons, which had a negative impact on their farm income in 2024. It is important to acknowledge that the cost per hectare typically escalates annually, irrespective of the yield performance. However, a yield decline reduces the total cane output, as was the case in the 2024 season. This elevated the cost per ton, thereby exerting downward pressure on the Net Farm Income per ton. Consequently, while an improved RV price may result in a higher income, the combined effect of the increasing input costs and reduced yields compromised the overall farm efficiency and financial sustainability.

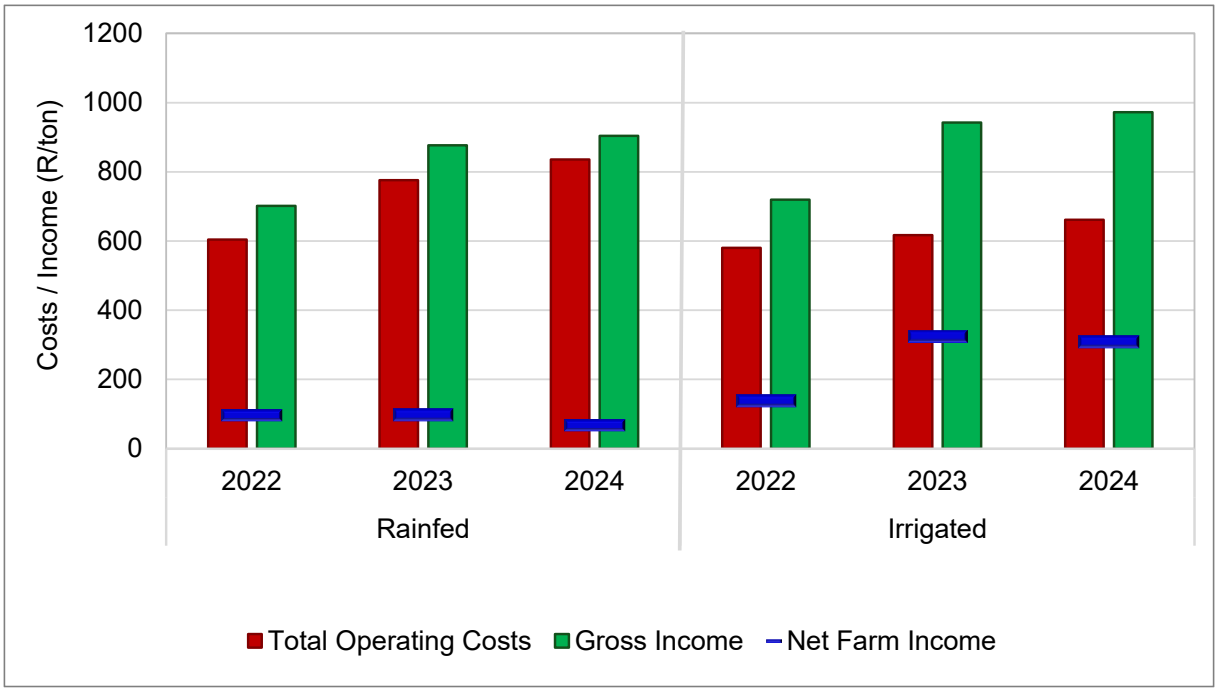


Figure 10. Total operating costs and net farm income (defined as the difference between gross income and total operational cost and excluding managerial costs, interest, rent and leases, depreciation, and tax) per ton of cane harvested for a typical rainfed and irrigated large-scale grower during the 2022, 2023 and 2024 seasons (Source: SACGA, 2024a)

Small-scale grower profitability

SSGs typically operate on a smaller scale than LSGs, with an average Area Under Cane of approximately 2 hectares. The survey results for 2023, compared with estimated results for 2024, show a 7.0% increase in the gross and cane (per ton) income for SSGs in both rainfed and irrigated regions. On the other hand, the operating costs for rainfed and irrigated growers increased by 7.8% and 10.9%, respectively (Table 2). The profitability for SSGs under rainfed conditions showed an improvement of 4.2%, compared to 2023, while the corresponding figure for irrigated conditions was a 1.5% increase. However, when the income was assessed, excluding the industry support, there was a decline in their profit margins.

Table 2. Gross and other income, operating costs, and net farm income per ton of cane harvested for a typical rainfed and irrigated small-scale grower for the 2023 and 2024 seasons (Source: SACGA, 2024c)

SSG Crop Budget (per ton)	**Rainfed**			**Irrigated**		
Year	***2023**	**2024**	**Year on Year % change**	***2023**	**2024**	**Year on Year % change**
Gross Income	**R901.30**	**R964.39**	**7.0**	**R1 036.78**	**R1 109.35**	**7.0**
Cane Income	R707.98	R757.54	7.0	R843.46	R902.51	7.0
*VAT Flat Rate	R64.34	R68.84	7.0	R64.34	R68.84	7.0
**SPF	R41.11	R43.99	7.0	R41.11	R43.99	7.0
Transformation Intervention Income	R87.87	R94.02	7.0	R87.87	R94.02	7.0
Total Operating Costs	**R651.45**	**R702.02**	7.8	**R606.24**	**R672.25**	**10.9**
Profit/Loss	**R249.85**	**R260.37**	4.2	**R430.54**	**R437.11**	**1.5**
Profit/Loss – no industry support	**R56.53**	**R53.52**	**-5.3**	**R237.22**	**R230.26**	**-2.9**

*VAT – Value added tax.
**SPF – Supplementary Payment Fund (given to SSGs)
*** Updated figures from survey results

Table 2 highlights the vital role of industry support provided through various mechanisms, including the Supplementary Payment Fund (SPF), the VAT Flat Rate (an industry-administered SARS VAT rebate for SSGs), and the Transformation Intervention Funds. Through these funds, SSGs can maintain a stable source of income, despite the challenges that they face in their socio-economic environment.

Conclusions

Cane production in 2024/25 was the lowest since the drought-affected 2016/17 season. This production decline was mainly due to the less-favourable growing conditions, especially for the rainfed areas where erratic rainfall, associated with the prevailing El Niño conditions, resulted in widespread yield losses.

The dry conditions during 2024 initially resulted in an enhanced cane quality from natural ripening. However, cane quality deteriorated as the season progressed, and with the

intensifying water-stress conditions. Severe frost damage in the Midlands and a shortage of cane supply towards the end of the season further exacerbated the poor cane quality situation.

Growers received a slightly improved revenue per ton of cane, when compared to 2023/24, due to the marginal (3.2%) increase in the RV price, while small-scale growers continued to benefit from various industry support interventions. However, the decline in the cane supply increased the production costs per ton of cane, thereby reducing the net farm income. As a result, the overall profitability in 2024 was lower than in 2023.

The decline in cane supply, as well as the consequent elimination of the carry-over cane crisis of recent seasons in the rainfed areas, motivated growers to resume normal replanting operations in abandoned and fallow fields. This resulted in a slight increase in the area under cane, a trend which is expected to continue in the 2025/26 season. Concerted efforts are needed to produce adequate quality seed-cane, in order to alleviate the seed-cane shortages that are reported in many regions. This should help to improve the cane supplies from 2026/27 onwards, assuming that there are good growing conditions.

Acknowledgements

The authors thank the SASRI extension specialists for their overall input. We also acknowledge the services of the SASRI Agromet team, SASA's Cane Testing Services, Industry Affairs, as well as the SA Canegrowers' Association, for capturing and making available the various data that were used for this review.

References

Bezuidenhout CN and Gers C (2002). Homogeneous climate zones for the South African sugar industry: Preliminary boundaries. *Proc S Afr Sug Technol Ass* 76: 601-605.

Bezuidenhout CN and Singels A (2007). Operational forecasting of South African sugarcane production: Part 2 - System evaluation. *Agric Syst* 92(1–3): 39-51. Available at: https://doi.org/10.1016/j.agsy.2006.03.002

Department of Agriculture, Land Reform and Rural Development (2024). Crops and Markets: 2nd Quarter 2024, Volume 105, No. 1000, Department of Statistics and Economic Analysis. Available at: www.dalrrd.gov.za

Jones MR, McFarlane SA, Nicholson RJ, Basdew I, Sithole P and Stranack RA (2021). A review of South African sugarcane production in the 2020/21 season. *Proc S Afr Sug Technol Ass* 93: 1-23.

SACGA (2024). Restricted Distribution – RV Price – Final Price 2023-24. Internal publication of the South African Cane Growers' Association. Mount Edgecombe, South Africa.

SACGA (2024a). Annual Large-scale Grower Cost Survey 2022/23. Internal publication of the South African Cane Growers' Association. Mount Edgecombe, South Africa.

SACGA (2024b) Small-scale Grower Survey. Internal publication of the South African Cane Growers' Association. Mount Edgecombe, South Africa.

SACGA (2024c). Small-scale Growers VAT Rebate Report. Internal publication of the South African Cane Growers' Association, ref: G.078.2022 RJN/rjn. Mount Edgecombe, South Africa.

SACGA (2025). Restricted Distribution – RV Price – Final Price 2024-25. Internal publication of the South African Cane Growers' Association. Mount Edgecombe, South Africa.

Singels A, Leslie G, McFarlane S, Schoeman J and Gabriel A (2014). South African sugarcane production in 2013/14: A record-breaking season. *Proc S Afr Sug Technol Ass* 87: 1-22.

Singels A, McFarlane S, Nicholson R, Way M and Sithole P (2017). Review of South African sugarcane production in the 2016/2017 season: Light at the end of the tunnel? *Proc S Afr Sug Technol Ass* 90: 1-19.

Sithole P, Jones MR, Nicholson RJ and van Antwerpen R (2022). A review of South African sugarcane production in the 2021/22 season: climate, production and economics. *Proc S Afr Sug Technol Ass* 94: 1-20.

Sithole P, Nicholson RJ and Stranack RA (2023). A review of South African sugarcane production in the 2022/2023 season: climate, production and economics. *Proc S Afr Sug Technol Ass* 95: 1-16.

Sithole P, Nicholson RJ, van Heerden PDR and Stranack RA (2024). A review of South African sugarcane production in the 2023/2024 season: climate, production and economics. *Proc S Afr Sug Technol Ass* 96: 1-17.

Statistics South Africa (2023) CPI History: Table B CPI Headline, Statistical Release, P0141, Statistics South Africa. Available at: http://www.statssa.gov.za/publications/P0141/CPIHistory.pdf?

Statistics South Africa (2024) CPI History: Table B CPI Headline, Statistical Release, P0141, Statistics South Africa. Available online: CPIHistory.pdf (statssa.gov.za)

van den Berg M, Singels A, Armitage RM, Way MJ and McFarlane SA (2008). South African sugarcane production in the 2007-2008 milling season: An unfulfilled promise? *Proc S Afr. Sug Technol Ass* 81: 51-67.

FULL PAPER

BIOSECURITY: AN OVERVIEW OF THE 2023/2024 SEASON

Basdew IH, McFarlane SA and Wilkinson DG

SA Sugarcane Research Institute, 170 Flanders Drive, Mount Edgecombe, 4300

Iona.Basdew@sugar.org.za; Sharon.McFarlane@sugar.org.za;
David.Wilkinson@sugar.org.za

Abstract

This biosecurity review characterises the South African sugarcane industry from a pest and disease perspective for the 2023/2024 milling season, compared with the previous seasons. Eldana infestation levels across all regions for 2023/2024 were not significantly different from the 2022/2023 season. However, the mean percent stalk length red was generally higher across most regions, with the industry mean exceeding that of the previous two seasons. The incidence and severity of the yellow sugarcane aphid has remained a problem, with the Pongola, Midlands South, Zululand, North Coast, Umfolozi and uMzimkhulu regions reporting a higher-than-usual incidence over the past summer. The 2023 longhorn beetle surveys revealed that four fields in Entumeni and three fields in Melmoth all tested positive for larvae. These fields have been eradicated and are currently fallow. White grub surveys showed an increase in the grub numbers from 2023 to 2024, with *Schizonycha* spp. being most abundant. While the overall smut situation in the industry was similar to the 5-year mean, higher levels were recorded in commercial fields in the Zululand and Midlands regions. Ratoon Stunt (RSD) was diagnosed in 6% of the commercial fields and in 2% of the intended seed-cane sources that were tested, which exceeded the 5- and 10-year means for both categories. The mosaic levels remained extremely low in the industry. Symptoms of one or more of the three rusts infecting sugarcane in South Africa were reported in approximately 3% of the area that was inspected during routine pest and disease surveys. The factors that are likely to have influenced the occurrence of the major pests and diseases in the industry will be highlighted, along with the management strategies that have been adopted to address these issues.

Keywords: sugarcane, pests, diseases, biosecurity, monitoring, management

Introduction

The South African sugarcane industry covers approximately 350 000 hectares, from southern KwaZulu-Natal to the Mpumalanga Lowveld (Sithole *et al*. 2023), and it encompasses a wide range of environmental conditions that favour the development of different pests and diseases. The industry is subdivided into Control Areas, as defined by the Local Pest, Disease and Variety Control Committees of the South African Sugar Association (SASA) (Stranack, 2021). The Sugar Act (Act 9 of 1978) and the Sugar Industry Agreement (2000), which make provision for the establishment of these Committees, provide a means of protecting the industry against the effects of pests and diseases, through the routine monitoring of prospective seed-cane sources and commercial fields.

The last three seasons have placed the South African sugarcane industry under a great degree of pressure, mainly from the perspective of carry-over issues and climate-driven pest and disease outbreaks (Sithole *et al*., 2023). This paper will present the trends derived from the pest and disease surveys that were conducted during the 2023-2024 season.

Methodology

Pest Data

Eldana saccharina

The SASRI Biosecurity Inspectorate conducted industry-wide *Eldana saccharina* (Eldana) surveys during the 2023/2024 season (starting 01 June 2023 and ending 31 May 2024). Eldana infestations are quantified as the number of larvae and pupae per 100 stalks (e/100) and these were averaged for different Pest and Disease (P&D) areas over the 12-month period. The percent stalk length red (%SLR) due to Eldana infestation was also determined over the 12-month period. The seasonal average infestation levels plus %SLR for the different P&D areas and for the industry, were compared to those of the previous two seasons, plus the mean over the last five and ten seasons.

Other pests

Surveys for thrips, white grub and longhorn beetles were also conducted. The presence and severity of *Sipha flava* (Yellow Sugarcane Aphid, YSA) was continually monitored during the season.

Surveys for *Chilo sacchariphagus* remain ongoing. SASRI, in collaboration with Cropwatch Africa, monitors a total of thirty-six pheromone traps that have been placed in strategic positions in KwaZulu-Natal, Mpumalanga and the Limpopo Province. Surveillance reports are sent to SASRI monthly. Twenty-seven traps have been placed around the cane fields, seven at the border posts, and two around the natural vegetation in the Kruger National Park.

Disease Data

Smut and mosaic

Smut (*Sporisorium scitamineum*) and mosaic (sugarcane mosaic virus) surveys are conducted by the SASRI Biosecurity Inspectorate annually, usually when the cane is three to six months old. This is done by inspecting a specified number of 50 m lengths of cane row in each field. The number of row sections inspected is dependent on the field size and it is assumed that there are 100 stools in each 50 m row length, i.e., two stools per metre. The number of off-types is also recorded. Disease prevalence is expressed as the proportion, or percent, of the fields inspected that were infected (Nutter *et al*., 1991). The disease incidence is expressed as the percent stools examined that were infected.

The selection of the fields for inspection varies between LPD&VCC areas. In some areas fields are randomly selected for the survey, while in others, fields planted to varieties known to be susceptible to smut or mosaic may also be targeted. Generally, the Biosecurity Inspectorate aims to visit each farm at least once a year, but this depends largely on the number of teams operating in the area and the size of the area to be covered. Therefore, it is not possible to make comparisons between LPD&VCC areas, but the trends over the years within these areas can be analysed.

A total of 8 690 commercial fields, covering an area of approximately 41 500 ha, were inspected for smut, mosaic and off-types in the 2023-24 season. This represented approximately 12% of the area under cane. In addition, a total of 1 450 seed-cane fields representing over 2 200 ha were inspected, with these fields requiring one or two repeat surveys to comply with approved and certified seed-cane standards, respectively.

Ratoon stunt (RSD)

Since ratoon stunt (RSD, *Leifsonia xyli* subsp. *xyli*) does not have any obvious external symptoms, and the diagnosis is based on the serological analysis of expressed xylem sap from stalk samples (McFarlane *et al*., 1999). Routine surveys of commercial and seed-cane fields are conducted annually by the Biosecurity Inspectorate, in order to identify RSD-infected fields. The Biosecurity Inspectorate collects 20 stalks from obviously-stunted stools from commercial fields of 5 ha (or less), and additional samples are collected from larger fields. Forty stalks are collected from seed-cane fields of 1 ha or less.

A total of 7 322 commercial and seed-cane samples were processed in the RSD diagnostic laboratory at Mount Edgecombe during the period under review. These samples represented 4 591 commercial fields that covered approximately 22 000 ha, and 890 seed-cane nurseries.

Other diseases

Observational information for other diseases, such as rust, was also recorded.

Results and Discussion

Pests

Eldana

During the 2023/0024 season, approximately 89 308 ha under cane were surveyed for Eldana infestation. Eldana infestation levels (e/100) for the 2023/2024 season, across all regions, were not significantly different from those of the previous season (Figure 1). The 2023/2024 industry mean (e/100 = 1.33) was slightly above the 5-year mean (e/100 = 1.28), but this did not show any statistically-significant difference. The 2023/2024 industry mean was significantly lower than the 10-year mean (e/100 = 2.05). Pongola, Umfolozi, Felixton, Entumeni, North Coast and Sezela showed lower e/100 than the previous season; however, these differences were not statistically different from the year before. Although the Mpumalanga, Amatikulu, uMzimkhulu, Midlands North and Midlands South regions all showed a higher e/100 than the 2022/2023 season, these comparisons were again not statistically-different from each other. The %SLR was generally higher across most regions (Figure 2). Pongola, Felixton, Entumeni, Amatikulu, North Coast, uMzimkhulu, Midlands North and Midlands South showed a higher %SLR during 2023/2024 than during 2022/2023. The industry mean for 2023/2024 (%SLR = 0.63) was insignificantly lower than the 2022/2023 (%SLR = 0.64), but higher than the 2021/2022 (%SLR = 0.55) mean (these variances were not statistically different), but it was below the 10-year mean (%SLR = 0.83).

A concerning feature of the 2023/2024 season is that some regions of the industry experienced more severe Eldana infestations than previous years, with the surveys having reported e/100 ranging from 29-40. Other areas have reported an increase in the prevalence of the pest, but not in e/100, which might raise the possibility of more severe Eldana infestations in the 2024/2025 season. Both the spread and the severity of infestations could possibly be attributable to the high quantity of carry-over cane over the past three seasons, which has resulted in the excessive ageing of the crop in-field. This, coupled with a milder winter, was a likely contributing factor that has encouraged the persistence of Eldana in those carry-over fields. The carry-over issues experienced over the past three seasons could also have exacerbated the %SLR, as studies have shown that the damage assessed the previous October can increase between 2-4 times, if that field is carried over into April/May the following year (https://sasri.org.za/farming-manuals/#150-194-pests). The scouting and implementation of robust control measures need to remain a priority going forward, especially on ageing cane.

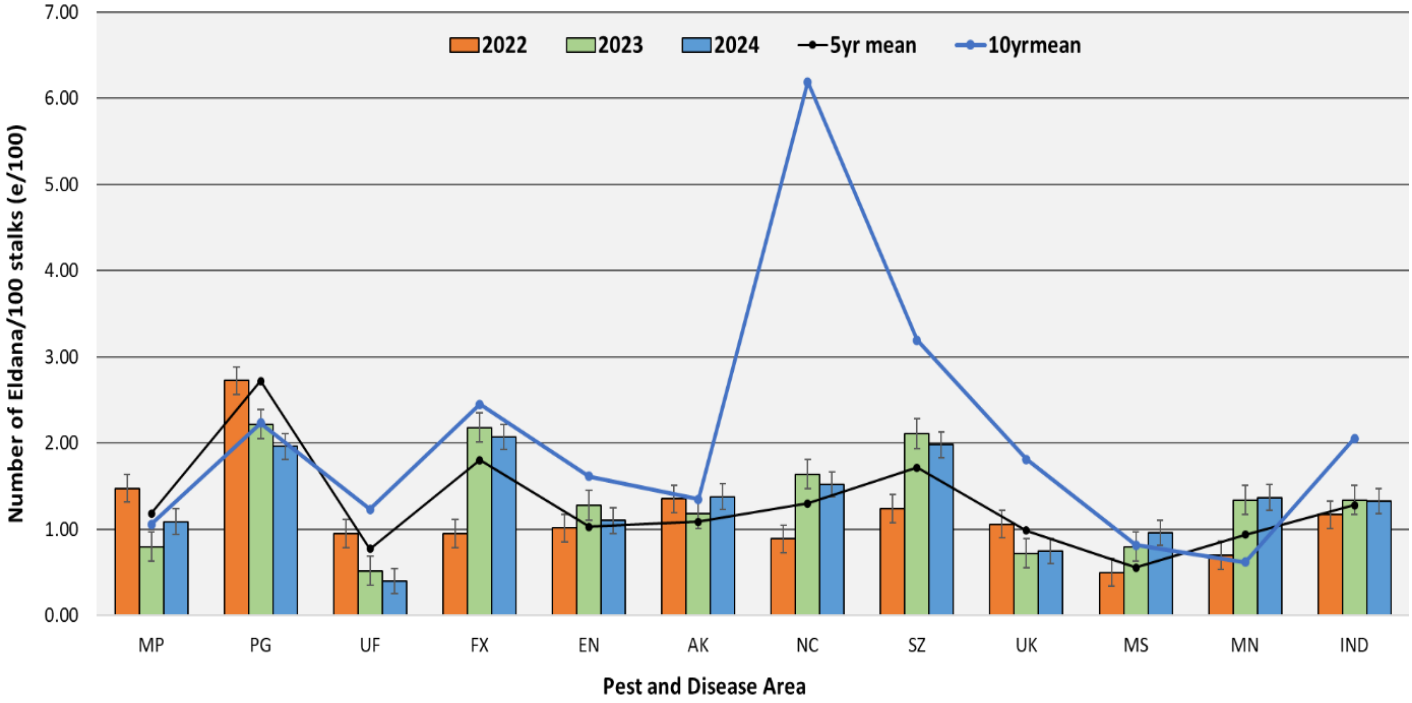


Figure 1. Eldana infestation for different pest and disease areas and for the industry as a whole for the 2023/2024 season, compared to the previous two seasons, and to the long-term mean over the past five seasons and 10 seasons. MP = Mpumalanga, PG = Pongola, UF = Umfolozi, FX = Felixton, EN = Entumeni, AK = Amatikulu, NC = North Coast; SZ = Sezela; UK = uMzimkhulu; MS = Midlands South; MN = Midlands North; IND = industry

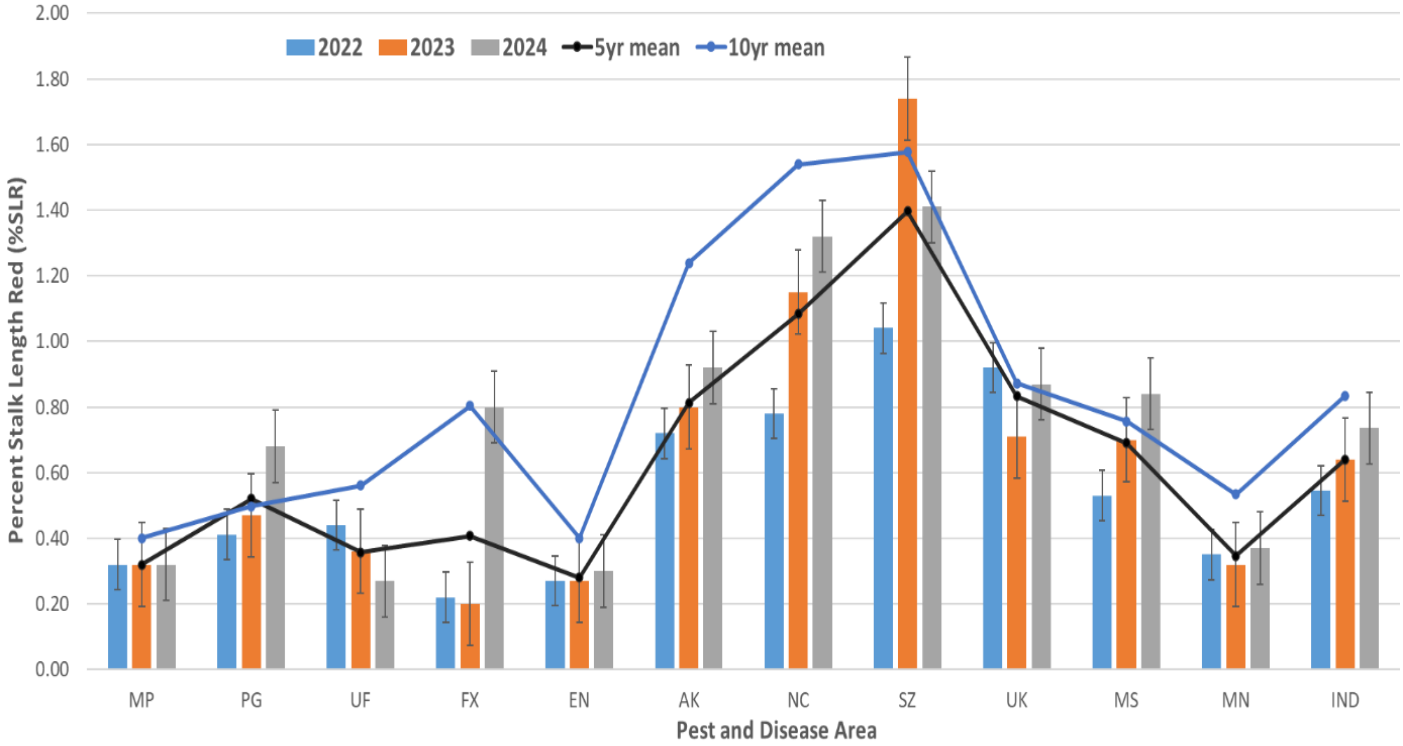


Figure 2. Percent stalk length red (%SLR) due to Eldana infestation for different pest and disease areas and for the industry as a whole for the 2023/2024 season, compared to the previous two seasons, and to the long-term mean over the past five seasons and 10 seasons. MP = Mpumalanga, PG = Pongola, UF = Umfolozi, FX = Felixton, EN = Entumeni, AK = Amatikulu, NC = North Coast; SZ = Sezela; UK = uMzimkhulu; MS = Midlands South; MN = Midlands North; IND = industry.

Yellow sugarcane aphid

The incidence of the yellow sugarcane aphid and the severity of infestation remains an ongoing problem throughout the South African sugar industry. This pest also occurs in eSwatini, Mozambique, Zimbabwe and Zambia. A notable observation from the Midlands North region over the 2023/2024 summer saw the most significant outbreak of YSA in the last ten years. However, there was a relative abundance of predatory insects where the infestations were prevalent. Most growers in the area opted not to apply insecticides to manage the infestations, and within three weeks the cane had begun to recover well. Other regions that reported a higher-than-normal incidence of infestation this past summer included Pongola, Midlands South, Zululand (North, Central, South), North Coast, Umfolozi and uMzimkhulu. It is likely that the hot, dry weather experienced during the summer of 2023/2024 could have exacerbated the level of infestation experienced across the industry. SASRI continues to engage with growers and to undertake research to promote the long-term practical in-field management of the pest. This information is disseminated to growers as it becomes available, in the form of newsletters, ad-hoc publications or grower events.

Longhorn beetle

Survey data of the Longhorn Beetle (LHB), *Cacosceles newmanii*, from the 2023/2024 season yielded results that have raised some concern. During the surveys that are conducted every

two months (or ad-hoc), four fields tested positive for LHB grubs in August 2023 in the Entumeni area. All four fields have been eradicated and are currently lying fallow. In November/December 2023, a further two fields tested positive for grubs in Melmoth. One field has been eradicated, and the second field is in the process of eradication. A further field tested positive in Melmoth in April/May 2024. These fields have been harvested and eradicated. These results show that LHB is not just found within the Entumeni region. It therefore remains paramount to continue with the surveys, in order to adequately inform the industry on the way forward and to map their movement from the point of first discovery in Entumeni in 2015.

White grub

White grub surveys showed an increase in the grub numbers from the 2022/2023 season (with 249 grubs captured) to 2023/2024 season (with 282 grubs captured). The *Schizonycha* spp. were most abundant, with minimal captures of *Hypopholis* spp. (7 grubs) and *Pegylis* spp. (3 grubs and 1 adult). The age and variety of the cane appeared to have no effect on the number of grubs that were captured during each survey. However, the captures were higher in number where the cane was grown in proximity to either maize or timber plantations (mainly wattle), as these crops also serve as a food source for many beetle species. No insecticides are currently registered for use against the white grub on cane in South Africa. Therefore, where infestations have been severe, growers were advised to rotovate those fields and to expose the grubs to sunlight (grubs are photosensitive) and natural predators, such as birds and small rodents.

Chilo sacchariphagus

Chilo sacchariphagus, the Chilo stem borer, remains a potential threat to the South African sugarcane industry and its monitoring remains ongoing, in collaboration with Cropwatch Africa. No suspect specimens were received for identification over the past 12 months, and communication channels remain open between SASRI and Cropwatch Africa. Furthermore, a revised Bio-incursion Plan has been developed for the management of a potential *C. sacchariphagus* incursion into South Africa.

Thrips (Fulmekiola serrata)

The long-term sampling programme that is in place for thrips has confirmed consistent seasonal trends of a general peak in activity from November to January, with a drop in the population numbers from March until October/November. The populations appeared to be consistent with the seasonal changes, with no notable deviations to report. Thrips remain a serious pest throughout the cane industry. However, with the arsenal of registered insecticides that are at the disposal of the grower, its management has been undertaken in a relatively efficient manner.

Other pests

With regard to other matters, the Lowveld region reported a severe leafhopper infestation in the Kaalrug area during the 2023/24 season. This highly-sporadic infestation was followed by the development of sooty mould on the affected cane. The infestation could not be chemically managed, as there are no insecticide registrations for leafhoppers on South African cane. The infestation did not persist, and the cane was able to recover. The uMzimkhulu region reported a spike in trash caterpillar infestation after the 2023 harvest. This infestation was also sporadic, it did not persist, and the cane was able to recover.

Diseases

Smut

For the period under review, 19% of the commercial fields inspected in the industry (Figure 3a), which covered 21% of the inspected area, were infected with smut. This was similar to the 5- and 10-year means. Smut was identified in 0.15% of the stools that were inspected, which is lower than the previous season and the 5- and 10-year means (Figure 3b).

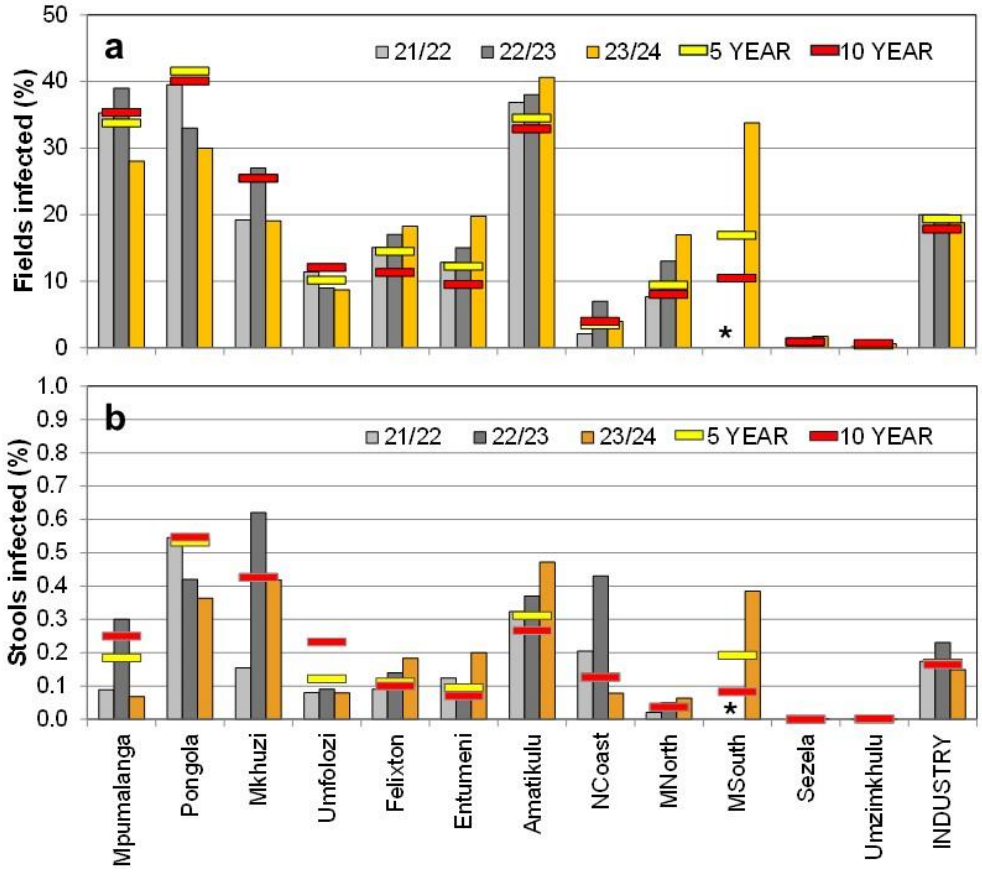


Figure 3. Smut (a) prevalence and (b) incidence in the South African sugarcane industry, June 2023 to May 2024 (commercial fields only), compared with the previous two seasons; * indicates small sample size

Both the smut incidence and prevalence have decreased in Pongola in recent years, and they are currently well below the 5- and 10-year means after the adoption of an integrated management strategy stipulated by the Pongola LPD&VCC, which was supported by the majority of growers. In addition, reduced crop stress as a result of improvements in some irrigation systems and an adequate water supply (Sithole *et al*., 2023) are likely to have had an impact on the smut levels in the area. The incidence of smut is known to increase with moisture stress and drier, warmer winters (James, 1972; Rutherford *et al.* 2003). However, while good progress has been made, smut remains prevalent in Pongola, with 30% of the approximately 5 200 ha inspected being infected to some degree, and the incidence of smut remains high in some fields, particularly in N41 (Figure 4). As part of the integrated management strategy for Pongola, no further planting of this variety is permitted, and any fields above the permissible limit are flagged for eradication.

Smut levels exceeded the 5- and 10- year means in Felixton, Entumeni and Amatikulu (Figures 3a and b). Several varieties grown in the region have shown some susceptibility, with smut being particularly common and severe in the popular varieties of N54 and N59 (Figure 4). Similarly, smut was highest in these varieties, along with NCo376, in the North Coast area, although its incidence and prevalence were lower than in previous seasons. Poorly-distributed rainfall, which resulted in extended periods of dry weather in recent years, along with mild winters (Sithole *et al*., 2023), would have contributed to increases in some areas.

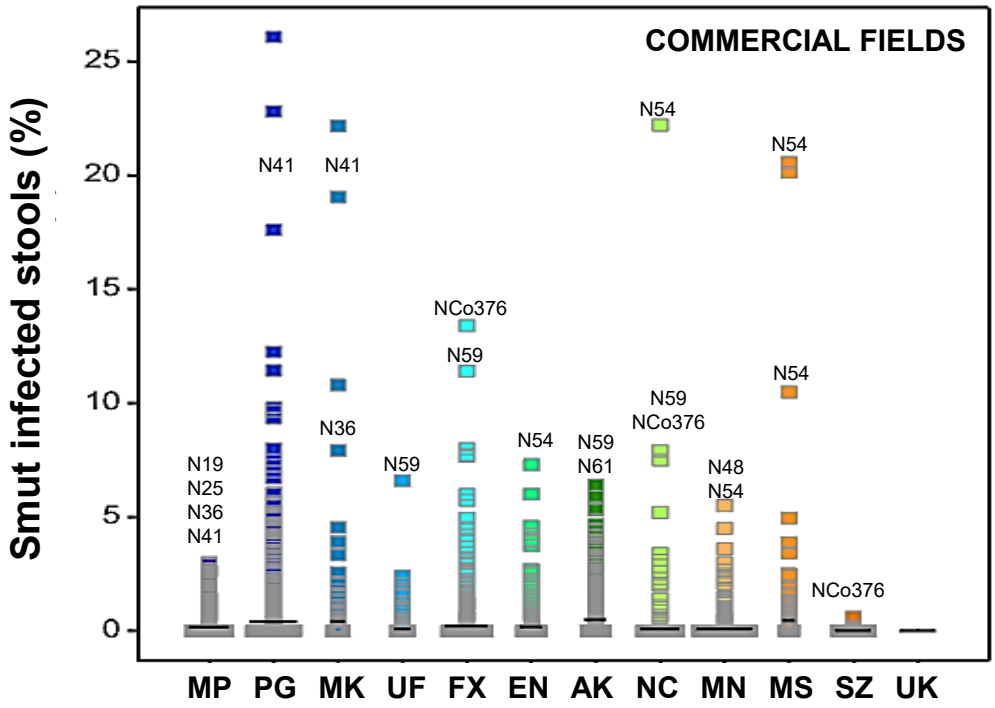


Figure 4. Percent smut-infected stools by Pest and Disease Control Area. Each square indicates smut incidence in an inspected field, different colours are used to differentiate the Pest and Disease Control Areas. Fields with the highest incidence are annotated with the variety name(s). Pest and disease area abbreviations: MP = Mpumalanga; PG = Pongola; MK = Mkhuze / Makhathini, UF = Umfolozi; FX = Felixton; EN = Entumeni; AK = Amatikulu; NC = North Coast; MN = Midlands North; MS = Midlands South; SZ = Sezela; UK = uMzimkhulu.

High levels of smut in N54 contributed to an increase in the incidence and prevalence recorded in the Midlands region (Figures 3a, 3b and 4). Smut incidence exceeded 10% stools infected in three fields of N54 on an irrigated farm in the Midlands South area. These fields are due to be replanted. A focus on eldana and seed-cane inspections has resulted in a limited number of commercial fields being inspected for diseases in recent years in Midlands South. The current estimate of the disease status is based on inspections in 216 fields covering an area of 666 ha (approximately 2% of the area under cane). Smut tends to be less problematic in the Sezela and uMzimkhulu areas.

Mosaic

Mosaic levels remained low in the industry, with the disease being observed in 1% of the fields that were inspected (Figure 5).

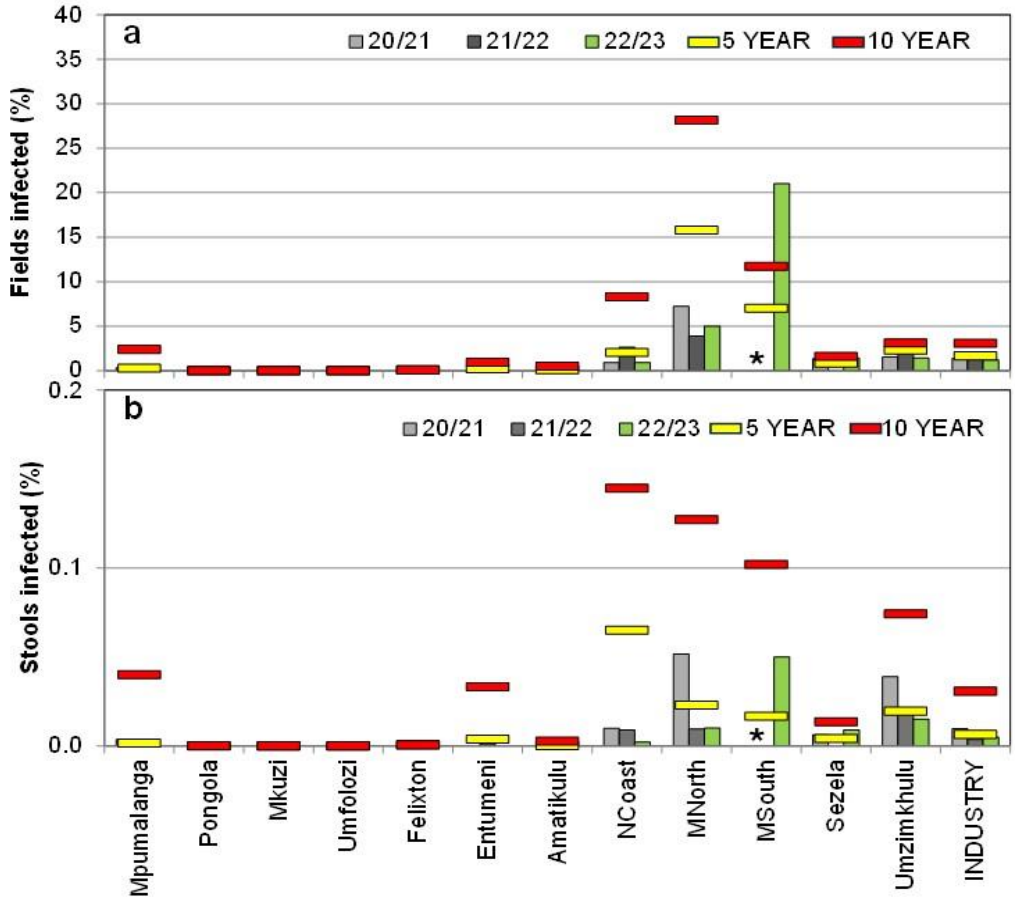


Figure 5. Mosaic (a) prevalence and (b) incidence in the South African sugarcane industry, June 2023 to May 2024 (commercial fields only), compared with the previous two seasons; *indicates small sample size

Mosaic is more common in the southern and midlands areas, but was detected in Pongola in February 2024. This was the first report of the disease in this area since 1997, when it was found in N19. To date, mosaic has been identified on three farms (six fields of N57 and two fields of N36), with the infected fields covering an area of approximately 24 ha. Five of these fields (12 ha) have been eradicated and the remainder have been rogued and will be eradicated after harvest. The current permissible limit for mosaic in Pongola is zero. Varietal resistance has been key in managing mosaic in the industry. The varieties that were most commonly infected were N12, NCo376 and N57 (Figure 6). Notably, no mosaic was detected in the 55 N12 Zapyr fields that were inspected, all but one of which were seed-cane fields covering approximately 56 ha.

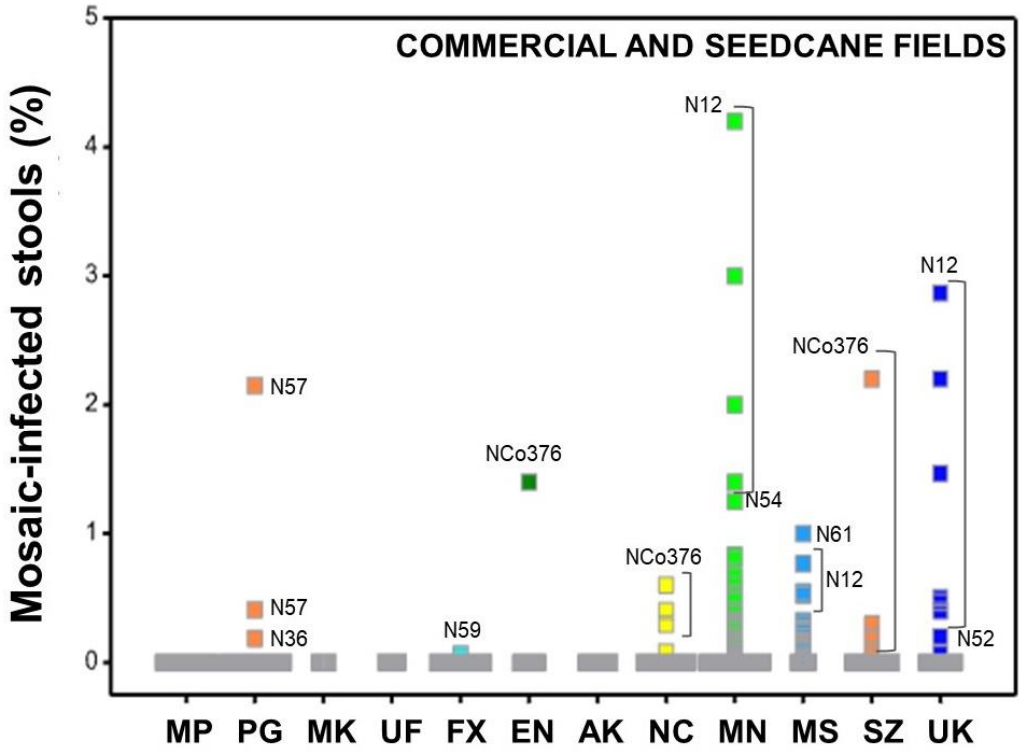


Figure 6. Percent mosaic-infected stools by Pest and Disease Control Area in commercial and seed-cane fields. Each square indicates mosaic incidence in an inspected field, different colours are used to differentiate the Pest and Disease Control Areas. Fields with the highest incidence are annotated with the variety name(s). Pest and disease area abbreviations: MP = Mpumalanga; PG = Pongola; MK = Mkhuze / Makhathini, UF = Umfolozi; FX = Felixton; EN = Entumeni; AK = Amatikulu; NC = North Coast; MN = Midlands North; MS = Midlands South; SZ = Sezela; UK = uMzimkhulu.

Ratoon stunt (RSD)

Ratoon stunt (RSD) was diagnosed in 6% of the commercial fields tested (Figure 7), which represented approximately 2 130 ha of the 22 000 ha that were sampled. This was higher than the previous season and the 5- and 10-year means. The disease was diagnosed in more than 15% of the commercial fields tested in Pongola and Umfolozi. The RSD incidence in seed-cane was higher than in the previous two seasons, with 1.9% of the fields testing positive in 2023-24. This increase was influenced by a number of samples collected from commercial fields, which were intended for use as seed-cane from one farm in Umfolozi, testing positive for RSD. In addition, five of the 93 seed-cane fields tested in Umzimkhulu were found to be infected. With the continued drive to meet the seed-cane 2028 target of establishing certified and approved nurseries to meet the seed-cane needs of each LPD&VCC Area, the undesirable practice of using commercial fields for seed-cane purposes is expected to decrease over time.

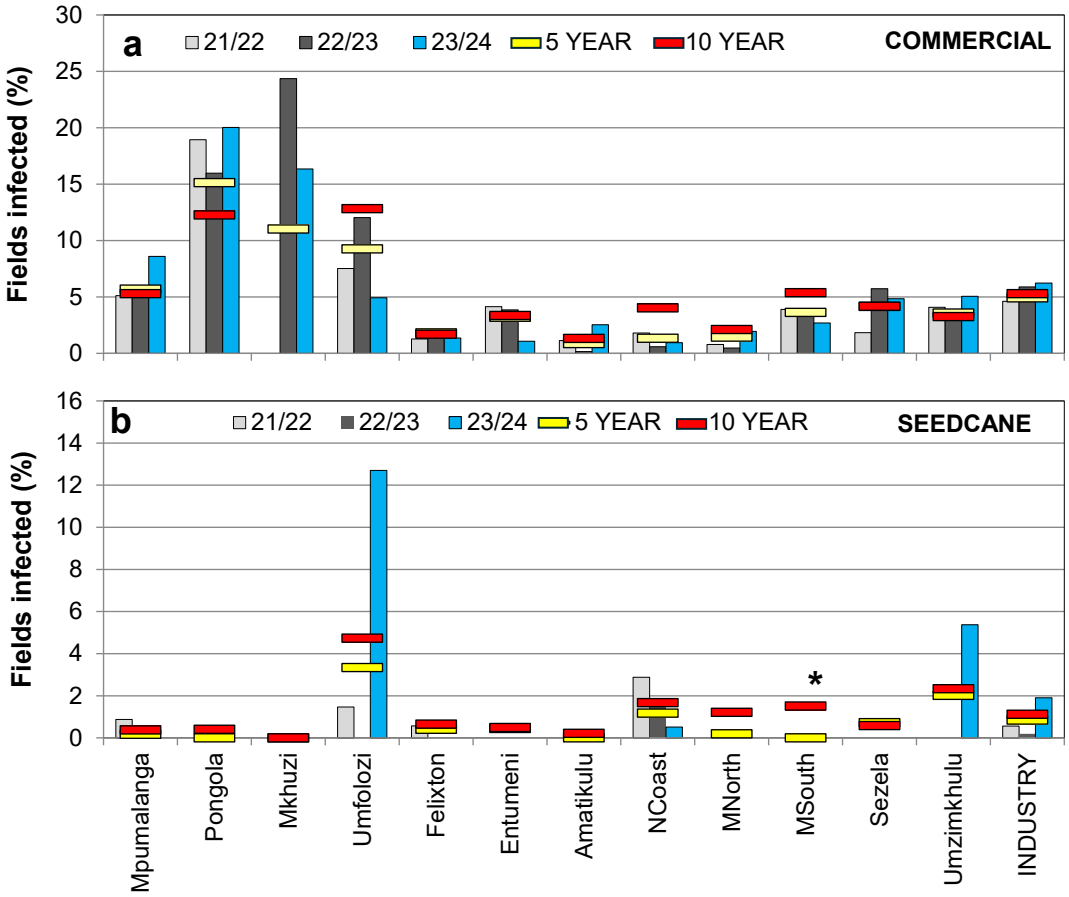


Figure 7. Ratoon stunt (RSD) incidence in (a) commercial and (b) intended seed-cane sources in the South African sugarcane industry, June 2023 to May 2024, compared with the previous two seasons; * indicates small sample size

Rust

Observational disease data are now being recorded when fields are being inspected for smut, mosaic and eldana, by using the ArcGIS Survey123 application that was developed at SASRI for the Biosecurity Inspectorate (Thompson *et al*., 2025). Based on these data, 3% of the approximately 62 400 ha of sugarcane inspected showed varying degrees of rust infection. This is most likely an underestimate. Distinguishing some of the foliar symptoms in the field and rating the extent and severity of the symptoms can be challenging, and therefore, ongoing training is required. The accuracy of the data should also improve, as the Inspectorate becomes more familiar and confident with the technology.

Most varieties have shown some susceptibility to orange rust, with moderate-to-severe symptoms being observed on several varieties from January through May each season (Table 1).

Table 1. Orange rust observations in the South African sugar industry

Rainfed varieties			
Not common		Common and sometime severe	
N48	N61	N12	N62
N54	N72	N12 Zapyr	N63
N55	N74	N39	N66
N59		N41	N75
		N52	N76
		N58	
Irrigated varieties			
Not common		Common and sometime severe	
N19	N40	N19	N57
N36	N53	N23	N60
		N41	N70
		N49	

Yield losses of 10 to 26% have recently been reported in orange rust-infected fields in Reunion (Dijoux *et al*., 2023), and 19% in moderate-to-severely infected N60 in South Africa (Kistan & McFarlane, 2024). Sporadic outbreaks of brown and tawny rust were reported in spring and early summer. Although not widely used, fungicides were generally applied by drone.

Biosecurity training

Pest and Disease training for Biosecurity personnel was conducted across all regions. The training was comprised of in-field pest and disease identification, Eldana and disease surveys, proper in-field sanitation of knives when collecting stalk samples, the identification of predatory insects, white grub surveys and navigation through the Survey123 App. This training is essential for ensuring the accuracy and reliability of the survey data that are submitted for analysis and used to inform decisions regarding pest and disease issues in the growers' fields. During these training events, the supervisors and inspectors are also reminded that their vigilance is key when conducting surveys to detect new pest and disease threats in the industry.

Conclusion

The issues encountered this season with Eldana and YSA infestations, are likely to persist into the forthcoming season, particularly due to the carry-over problems experienced in most regions. The YSA research portfolio is frequently enriched with new facets, in order to gain optimal value from the results. It is envisaged that these data that consider the soil, plant and environmental factors will be translated into field applicable methodologies, in order to better manage the infestations in the long-term.

With the continued drive to establish commercial fields with approved seed-cane, a decrease in the incidence of systemic diseases, such as smut and RSD, is expected over time. However, the extended warm, dry winters, as well as the extreme summer temperatures experienced in recent years, may fuel outbreaks of smut and contribute to greater yield reductions when the crops are infected with RSD and smut. The prevalence and severity of rust is also strongly influenced by climatic conditions. Research on supplementing and adapting integrated strategies is ongoing for the improved and more sustainable management of the most important diseases in the industry.

Acknowledgements

The authors would like to thank SASRI Extension Specialists, Biosecurity Inspectorate, Secretaries and the RSD Diagnostic Service for their invaluable support over the course of the survey period.

References

Basdew IH, McFarlane SA and Stranack RA (2023). Biosecurity: an overview of the 2021/2022 season. *Proc S Afr Sug Technol Ass* 95: 17-21.

Dijoux J, Dumont T, Paysan M, Legrand C, Hervouet C, Barau L, Rott P and Hoarau JY (2023). Effects of orange rust on sugarcane yield traits in a multi-environment breeding program. *Euphytica* 219(4): 49.

James GL. 1972. Smut incidence in variety trials. *Proc S Afr Sug Technol Ass* 46: 211–215.

Kistan CJ and McFarlane SA (2024). Orange rust: Preliminary research findings. *Proc S Afr Sug Technol Ass* 96: 133.

McFarlane SA, Bailey RA and Subramoney DS (1999). The introduction of a serological method for large-scale diagnosis of RSD in the South African sugar industry. *Proc S Afr Sug Technol Ass* 73: 123-127.

Nutter, FW Jr (2001). Disease assessment terms and concepts. In: *Encyclopedia of Plant Pathology*, OC Maloy and TD Murray, eds. John Wiley and Sons, Inc., New York, NY. Pages 312-323.

Rutherford RS, McFarlane SA, van Antwerpen T and McFarlane K. 2003. The use of varieties to minimise losses from sugarcane diseases in South Africa. *Proc S Afr Sug Technol Ass* 77: 180-188.

SASRI (2023). Controlling Eldana in the South African cane industry. https://sasri.org.za/wpfd_file/controlling-eldana-in-the-south-african-sugar-industry/

Singels A, Leslie G, McFarlane S, Schoeman J and Gabriel A (2014). South African sugarcane production in 2013/14: A record-breaking season. *Proc S Afr Sug Technol Ass* 87: 1-22.

Sithole P, Nicholson RJ and Stranack RA (2023). A review of South African sugarcane production in the 2022/23 season: Climate, production and economics. *Proc S Afr Sug Technol Ass* 95: 1-16.

Stranack RA (2021). Review of the regularisation and centralisation of the biosecurity function in the South African sugar industry: 2015-2019. *Proc S Afr Sug Technol Ass* 93: 25-38.

Thompson IB, Stranack RA, McFarlane SA, Basdew IH, Merile, S and Velem T (2025). Introducing digital data collection for biosecurity surveys at the South African Sugarcane Research Institute (SASRI). *Proc S Afr Sug Technol* Ass (in press).

100TH ANNUAL REVIEW OF THE MILLING SEASON IN SOUTHERN AFRICA (2024/2025)

Mbuyazi M, Ndinisa NV, Davis SB, and Bhyrodeyal, L

Sugar Milling Research Institute NPC, c/o University of KwaZulu-Natal, Durban, 4041, South Africa
mmbuyazi@smri.org, nndinisa@smri.org,*sdavis@smri.org,*
lbhyrodeyal@smri.org

Abstract

The performance, throughput, and other relevant aspects of the sugar industry in Southern Africa for the 2024/25 milling season are presented and discussed. The data from sugar mills in South Africa (SA), Eswatini, Malawi, Mozambique, Tanzania, Zambia, and Zimbabwe are included. The milling season review is considered in terms of the tonnes of cane that were harvested, the cane quality, as well as the time efficiencies, recoveries and losses. The performance is compared to the results of the previous seasons. The 2024/25 season was another good season for the SA milling operations whilst performance in the other countries was mixed, with some countries showing a decline in performance. The industry performance continued to improve in SA, although it was a short season characterised by a significant dry spell. Most sugar mills closed earlier than their planned mill closure dates, due to lack of cane supply to sustain operations. The recorded overall factory performance parameters show an improving trajectory and have been assisted by good crop management, a reduction in the amount of carryover cane and improved processing efficiencies.

Keywords: sugarcane, sugar factories, cane quality, crop size, performance, recovery

Note: The South African Sugar Millers' Association NPC (SASMA) has taken a decision not to distribute the performance data of the individual factories in southern Africa; therefore, a full paper is not available in the proceedings. However, the Sugar Milling Research Institute NPC (SMRI) will present an annual review of the Southern African milling season at the SASTA Congress, using industry trends, rather than mill-specific data.

FULL PAPER

CURRENT PROGRESS IN SUGARCANE-BASED MATERIAL RESEARCH

Ayingeneye J[1], Govender K[1], Mphahlele IJ[1], Ndlovu N[1], Stark A[1]

[1]SMRI/DSTI/NRF SARChI Chair Sugarcane Biorefining in South Africa, Discipline of Chemical Engineering, University of KwaZulu-Natal, Durban, South Africa

starka@ukzn.ac.za

Abstract

The beneficiation of industrial residues is a major aspect of the *South African Sugarcane Value Chain Master Plan to 2030*, aiming to diversify and stabilise this industry economically, which is of national importance. In the policy space, the country has recently also made much progress in terms of the Extended Producer Responsibility Regulations, which seek to translate the current linear, take-make-dispose economy into a Circular Economy. In this context, one of the key issues is to find outlets for recycled materials, such as plastics. The coal mining industry has to deal with a legacy of unused coal fines, which is a cause for environmental concern. On the other hand, as a developing country, South Africa possesses vast potential for economic growth, in particular in the energy, consumer product and construction sectors.

Industrial symbiosis is a concept that seeks to build networks across industries that do not traditionally transact. The aim of this contribution is to showcase the current research, development and innovation at the SMRI/DSTI/NRF SARChI Chair in Sugarcane Biorefining in South Africa, by focusing on the production of materials. After a brief literature review of the current local sugarcane-derived material research, the Chair's recent activities on the manufacture and properties of three materials are presented, namely, bagasse-based particleboards, and coal briquettes from coal fines, which both use an organosolv lignin derived from sugarcane, as well as composites from recycled polypropylene and bagasse. Technical aspects of the production of these materials, characterisation results and application areas are discussed in order to highlight the opportunities for sector-overarching collaboration.

***Keywords*:** sugarcane bagasse, material development, material characterisation, material application, biorefinery, industrial symbiosis

Introduction

In 2020, the South African plastics industry contributed ZAR 68 billion (20%) to the manufacturing gross domestic product (TIPS, 2024), with the key players being Sasol and Safripol. Since 2012, South Africa (SA) is a net importer of both primary plastics and plastic goods, which indicates a growing domestic demand (Plastics SA, 2020). In 2023, SA had a consumption of over 362 kt per annum of polypropylene (PP; 23% of all plastics consumed), of which only 82 kt were recycled (23%) (Plastics SA, 2024). Important policy documents published in the recent past have highlighted that, while the government sees the plastics industry as instrumental for the economic development of the country, as evidenced by the draft *Plastics Industry Master Plan for Growth* (Plastics SA, 2020), it is cognisant of the environmental and social effects of plastic pollution, and therefore it introduced the *Extended Producer Responsibility (EPR) Regulations* in 2021 (NEMWA, 2020). The EPR regulations place the responsibility of recovering and recycling packaging materials on those who produce

them, and they stipulate certain percentage recycling rates that have to be met, for example, for polyolefins, such as PP, the recycling target is 50% in Year 5. It is therefore clear that the local plastics industry should be interested in establishing markets that can increase the demand for recycled polypropylene (r-PP). In principle, PP can be recycled into new PP products; however, PP from household packaging is difficult to separate and it is therefore returned at a lower quality. One market for lower-grade r-PP is in the production of composites, i.e. materials that are comprised of plastics and biomass fibres. The application areas of such PP-based composites include automotive parts and building materials (Gozdecki *et al.*, 2014; Anggono *et al.*, 2018; Várdai *et al.*, 2019; Sezgin *et al.*, 2021; Piekarczuk *et al.*, 2025).

Coal remains a major contributor to SA's electricity generation (85%) (Cowling, 2024). It has been estimated that for every ton of coal produced, 0.24 t of coal fines and other discards are generated, which amounted to a total of 2 billion tons by 2017 (Lloyd, 2019) and which are often poorly managed in defunct dumps (National Inventory: Discard & Duff Coal; 2001). Coal mining discards are detrimental as they contribute to air pollution, acid rain and leached metal ions (Olawale *et al.*, 2020), and they increase the risk of spontaneous incineration, as well as fibrosis in humans (Wang *et al.*, 2022). To curb these effects, some coal fines can be reclaimed and are presently used in brick production (e.g. by Hercules Bricks). In 2016, CoalTech announced the launch of a 120 kt per annum pellet plant that is based on coal waste (Anon, 2016), but it still needs to be commercialised. In general, research is scarce on briquettes and similar materials that use coal fines, although some researchers have reported that bio-based binders can give suitable briquettes for both residential and industrial use (Balrai *et al.*, 2021; Papin *et al.*, 2015; Manyuchi *et al.*, 2018; Waanders *et al*., 2020; Marx *et al.*, 2023).

The *Master Plan for the Commercial Forestry Sector in South Africa: 2020-2025* (DTIC, 2020) indicates that the lack of new afforestation is a major constraint, as it limits the sustainable growth of this industry. On the other hand, there is demand for locally-produced fibreboard in the southern African markets, and PG Bison (2024) has recently commissioned a new 780 m^3/d manufacturing facility in Mkhondo.

The sugar industry is an important contributor to the SA economy, producing 18 Mt of cane and 2 Mt of sugar in the 2023/24 season (Sithole *et al.*, 2024). In order to curb the pressures in this industry, which over the past two decades has led to a decline in sugar production (-25%), in the number of sugarcane farmers (-60%) and in industry-related jobs (-45%) (SASA, 2020), the industry has developed its *Sugarcane Value Chain Master Plan to 2030* (SASA, 2020), which includes the diversification of the product portfolio. Through biorefining, energy products, chemicals and materials would be produced to supplement the sugar-derived income. In this regard, sugarcane bagasse (SCB) is of particular interest, because even with the installed low-pressure boilers that provide process energy to the sugar mills, excess bagasse is available, which can be diverted to biorefining (Guest *et al.*, 2019).

At one of the SA sugar mills, namely the Sezela mill of Illovo Sugar Africa, a furfural-producing biorefinery plant is already in operation, in which SCB is treated with steam at high pressures and temperatures (steam explosion) to hydrolyse hemicellulose, which is followed by its conversion into furfural. A solid residue is the by-product, which is mainly composed of cellulose and lignin, which will hereafter be referred to as steam-exploded sugarcane bagasse (SCB_{StEx}). At present, it is used as boiler feed to produce energy. Its physical form (fine powder), as well as its reported composition (52-55% cellulose, 2-7% hemicellulose and 29-40% lignin (Ramos *et al.*, 2015; Moghaddam *et al.*, 2017; do Espirito Santo *et al.*, 2019)) make it an attractive feedstock for other biorefinery operations, once the cellulose and lignin are efficiently separated and further processed.

Lignin is the second-most abundant natural polymer in the biosphere, and the most abundant resource of bio-aromatics (Ragauskas *et al.*, 2014; Fernández-Rodríguez *et al.*, 2017). Chemically, lignin is an aromatic polymer that results from the non-structured connection of three phenylpropanoid types (*p*-hydroxyphenyl, guaiacyl and syringyl) and it contains various

chemical functional groups (Gosselink *et al.*, 2010). Historically, lignin has been obtained in a derivatised form as a waste product from the wood-pulping industry (Mastrolitti *et al.*, 2021; Becker & Wittmann, 2019), but more recently, organosolv processes (Gomes *et al.*, 2020; Mastrolitti *et al.*, 2021) have been developed in which the native structure of the polymer is retained. Organosolv lignins have a relatively low molecular weight (1000-6000 g/mol) and are sulphur- and ash-free (<1%). Furthermore, organosolv lignins possess favourable properties for material production, including a high hydrophobicity, which renders them insoluble in aqueous solutions, but soluble in some organic solvents (Tribot *et al.*, 2019; Kazzaz & Fatehi, 2020; Mastrolitti *et al.*, 2021). Not surprisingly, organosolv lignins have recently been investigated as additives, binders, plasticisers and fillers in resins, adhesives, flame retardants, elastomers, polymer composites etc. (Gordobil *et al.*, 2016; Kazzaz & Fatehi, 2020; Mastrolitti *et al.*, 2021).

This brief analysis of key sectors of the SA economy has led to the hypothesis that opportunities for joint ventures exist, where value addition can be harnessed by cross-cutting industrial symbiosis, which guides the materials focus area of this Research Chair (Figure 1). To the best of our knowledge, the production of organosolv lignin from SCB has not been explored, and we present results on the production of lignin, as well as its application in the production of briquettes from coal fines and of particleboards from SCB. The former will support the remediation of the local coal discard dumps, while producing a higher value energy product. The latter can support the forestry sector by supplementing the feedstock basis with SCB, and decreasing the environmental effects of urea-formaldehyde resins, by substituting it with a bio-based lignin binder. Furthermore, SCB-based composites made from recycled plastic can contribute to the success of the EPR, while providing materials for the automotive and building industries.

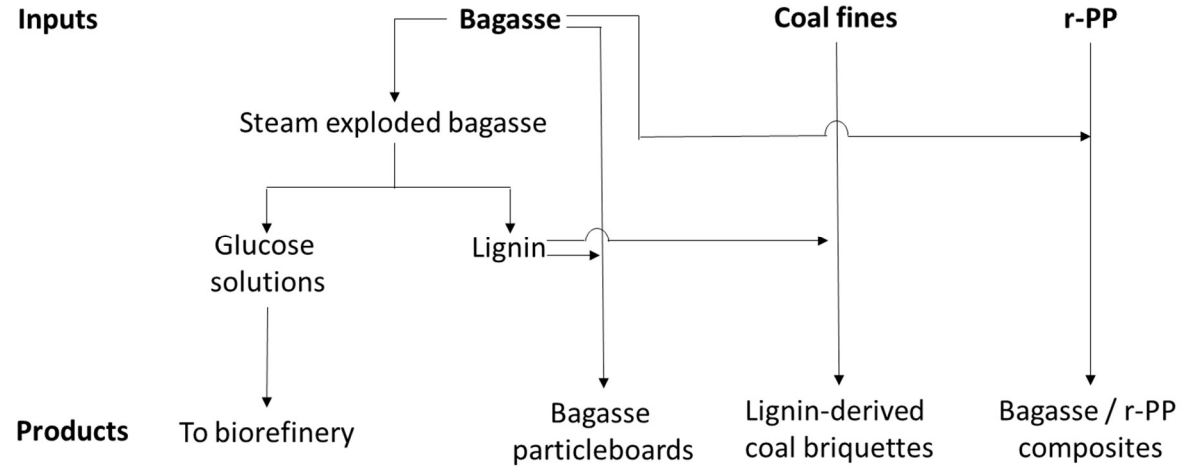


Figure 1. Overview of the materials currently investigated at this Research Chair

Methodology

Materials and chemicals

Untreated sugarcane bagasse (SCB_{unt}) for bagasse-polypropylene composites, as well as particleboards, were supplied by the Sugar Milling Research Institute NPC (SMRI), Durban. The residue from the furfural plant, SCB_{StEx}, was provided by Illovo Sugar Africa at Sezela. BisonBord® and urea-formaldehyde resin were purchased from PG Bison (PGB) and Resinkem, respectively. Recycled polypropylene (r-PP) waste with a particle size of 200 µm was acquired from the Council for Scientific and Industrial Research (CSIR), Pretoria. For the enzymatic hydrolysis, Cellic CTec2 (Novozymes A/S, Denmark), as well as a glucose testing

kit (Megazyme, Ireland), were used. Coal acquired from the Uitkomst Colliery, Utrecht, was used to model coal fines. Hide Glue (HG) and talc were purchased from African Glue Industries and Merck, respectively.

Organosolv lignin extraction

Organosolv lignin was obtained by Soxhlet extraction; samples of 10 g SCB_{StEx} were extracted with 200 cm^3 of various solvents, including tetrahydrofuran (THF), ethyl acetate, chloroform, butanone and ethanol, using a biomass-to-solvent ratio of 1:20 (w/v). After extraction, the dissolved lignin was separated by filtration, and the resulting delignified solid residue ($SCB_{StEx-Del}$) was washed twice (2 x 50 cm^3) with the same solvent, rinsed with deionised water at 70°C and dried at 50°C overnight. The respective solid residues were subjected to enzymatic hydrolysis, as described below. The lignin filtrate was concentrated by using a rotary evaporator to yield solid lignin. The lignin yields are expressed as a percentage, relative to the theoretically-available lignin in SCB_{StEx}. Extractions were carried out in duplicate, with a standard deviation between runs of <0.7% yield. Lignin that was produced by using THF was used as a binder in the production of tablets from coal fines and of particleboards from SCB.

Enzymatic hydrolysis

Enzymatic hydrolysis of the delignified solid residues ($SCB_{StEx-Del}$) obtained from extraction with the different organic solvents was performed. During the enzymatic digestibility tests, the sample was submerged in 0.05 M sodium citrate buffer (pH 4.8) with solid loading of 10% (w/v) in a working volume of 10 cm^3. The loading of the cellulase enzyme Cellic CTec2 was 10 filter paper unit (FPU)/g of dry weight of the sample. Enzymatic hydrolysis was performed at 50°C, with an agitation of 120 rpm for 72 h. Glucose yields were determined by using the Megazyme glucose kit, and are expressed as glucose yield relative to the theoretical glucose yield after the quantitative hydrolysis of all the cellulose available in SCB_{StEx}.

Compositional analyses

The compositional analysis of SCB_{StEx} was conducted prior to lignin extraction, by following NREL standard protocols (Sluiter *et al.*, 2012). SCB_{StEx} was found to comprise of 51 ± 0.3% cellulose, 6 ± 0.0% hemicellulose, 31 ± 0.1% lignin, 5.7 ± 0.1% extractives and 6.0 ± 0.1% ash. The compositions of SCB, as well as bagasse pretreated with either citric or sulphuric acid for particleboard production, were determined by following the procedures of Undersander *et al.* (1993). The values presented are the averages between triplicate runs, with standard deviations below 1%.

SCB preparation for particleboard production

SCB was dried at 85°C until its moisture content was below 10%, and it was then shredded by using a Fritsch Pulverisette (Model 11). A homogeneous particle size fraction between 1 and 2 mm was obtained by sieving, using laboratory sieve trays. Samples of 350 g SCB were pretreated at 110°C for 30 min, using either 5 m/v% citric or 1.5 m/v% sulphuric acid (CA and SA), respectively, according to Vaz *et al.* (2021). After the subsequent cooling, filtration and washing, the biomasses were dried at 60°C until the moisture content was between 15 and 20 wt.%.

Fibre analysis of SCB, and acid-pretreated SCB

Scanning Electron Microscopy (SEM) imaging was performed at the Microscopy and Microanalysis Unit of the University of KwaZulu-Natal, after sputtering with gold in a Quorum Q150R ES gold coater, using a Zeiss Ultra Plus Field Emission Gun Scanning Electron Microscope with an acceleration voltage of 5 kV.

Particleboard production

In addition to using the acid-pretreated SCB directly, particleboard feedstocks were prepared from these by adding THF-extracted SCB lignin. For this purpose, the required amount of lignin (2.5, 7.5 and 12.5 wt.% relative to the untreated SCB) was re-dissolved in THF and sprayed on the pretreated SCB, prior to drying. For comparison, urea-formaldehyde resin (UF) at 7.5% was added to SA-retreated SCB, prior to drying. The pretreated SCB and pretreated SCB-adhesive mixtures were compressed at 60°C at 2.2 MPa for 6 h to a thickness of between 6.1 and 8.5 mm (a standard deviation of thickness between two boards with same pretreatment/composition: <0.04 mm), using a mould (150 x 300 mm) and a Mobi-Jack 20-Ton Shop Press (Ram type, MOB 5002). After compression, the particleboards were removed from the mould, cooled at room temperature for 1 hour before being weighed and stored in airtight bags, prior to material testing. The samples were named according to the amount of the auxiliary THF-derived lignin added. CA and SA stand for citric acid- and sulphuric acid-pretreated SCB, respectively, L for lignin, followed by the percentage amount of lignin added.

Particleboard testing and characterisation

The manufactured particleboards were tested according to the South African National (SANS) or European (EN) Standards: Thickness swelling (TS) and water absorption (WA): SANS 6012:2004; Modulus of Elasticity (MoE) and Modulus of Rupture (MoR): SANS 6015:2004; Density: EN312:2010. The density, water absorption and thickness swelling measurements were performed in duplicate, with standard deviations of <0.05 g/cm^3, 1.3% and 2.7%, respectively. Due to the limited access to instrumentation time, MoE and MoR were only measured once per board, at the material testing facility One Eighty Degrees, in Cape Town.

SCB preparation for composite material production

SCB fines were washed with water and dried overnight at 60°C. Dried SCB was then immersed in a solution of sodium hydroxide (6 wt.%; biomass-to-liquid ratio 1:5; 25°C) and stirred continuously for 6 h. SCB was filtered off and washed with deionised water until the filtrate was pH neutral. The pretreated SCB was oven-dried at 80°C for 24 h, then stored in an airtight container.

Composite material production

Pretreated SCB fines were mixed with recycled PP at different concentrations (5, 10, 15 and 20 wt.%) using a Process 11 co-rotating twin-screw extruder, L/D = 40, Thermo Scientific, USA, and extruded at 180°C, with a screw speed of 23 rpm at 112 bar. The composite blends, which were in granular form (nurdles), were processed to yield dog bone-shaped specimens by using an injection moulding machine (e-mac 50) at 180°C and 450 bar after being dried overnight at 105°C.

Composite characterisation and testing

The degradation and thermal stability of the composites were investigated by using thermogravimetric analysis (Thermal Universal V 4.5 A). The samples were heated in the range of 30-550°C at a heating rate of 10°C/min under a nitrogen atmosphere (20 cm^3/min). Using an Instron 5966 tester, the tensile properties were assessed by using a load cell of 10 kN and a crosshead speed of 55 mm/min, in accordance with the American Society for Testing and Materials (ASTM) standard D638. Four specimens of each composition were tested, and the average and standard deviation were recorded. A CEAST Pendulum Resil Impactor II with a notch radius of 0.25 mm and a depth of 2 mm was used to determine the impact properties. Specimens were notched at one side. The pendulum hammer had a 15 J impact energy. Tests were conducted according to ISO179. Four specimens each were analysed, and the standard

deviation recorded. The SEM morphology of the fracture surface of composites was investigated by sputter-coating samples with gold, using Quorum Q150RS, and they were investigated by using a Phenom Pharos desktop scanning electron microscope at 15 kV.

Coal fines preparation

Lump coal was crushed by using a hammer mill at 1240 rpm, and then sieved to yield artificial coal fines with an average particle size distribution of 49, 48 and 3% in the >1.18 mm, 0.25-1.18 mm, and <0.25 mm ranges, respectively.

Coal-binder mixture preparation and tablet production

Hide Glue (HG) or Organosolv Lignin (OL) were dissolved in either water or tetrahydrofuran, respectively, at a ratio of 1:3 (wt/v), and coal fines added to make up the binder composition, as specified in Table 1. Where indicated, 2% talc was added for lubrication. The resulting mixtures were subjected to mixing and solvent removal by using a rotary evaporator at 100 mbar, 60-75°C and 3 rpm. From the dried mixtures, tablets were obtained by using an Erweka Apparatebau AR400 Tablet press machine that was set at a 5.5 mm punch height. The nomenclature of the various resulting fuel tablets is as follows: binder type/s (OL, HG or OL+HG) – coal (C) – lubricant talc (T), and the values in the ensuing bracket indicate the percentage composition, i.e. binder/s:coal:talc.

Table 1. Composition of prepared coal fines tablets

Fuel code	**Composition (%)**		
	Binder/s	**Coal**	**Lubricant (talc)**
OL – C – T (30:70:0)	30.0	70.0	0.0
HG – C – T (30:70:0)	30.0	70.0	0.0
(OL+HG) – C – T ((13+13): 75:0)	12.5 + 12.5	75.0	0.0
OL – C – T (29:69:2)	29.4	68.6	2.0
HG – C – T (29:69:2)	29.4	68.6	2.0

Coal tablet testing and characterisation

A hand-held Monsanto type hardness tester with a 0 to 20 N capacity was used to measure hardness. The friability was analysed by means of an Erweka Tap single-drum friability tester that was set at 3 minutes per cycle test. The standard deviations for hardness and friability were <0.4 N (average of 5 tablets) and 6.2% (average of 10 tablets) per batch, respectively. The Calorific Values (CV) of the coal and binders were determined by using a CAL3K-F Oxygen Bomb Calorimeter, according to the ASTM standard D5865-2. Analyses were conducted in duplicate and the standard deviations were below 0.2 MJ/kg. Thermogravimetric analysis was conducted using a thermogravimetric analyser (TGA) according to ASTM 7582-15: in an inert atmosphere, the samples were heated from 30 to 107°C at 16°C/min, and held for 60 min (release of moisture), followed by heating at 30°C/min to 950°C, and held for 7 min. (release of volatile matter). The samples were cooled to 600°C, and the gas was switched to an oxidative atmosphere (air). At a rate of 3°C/min, the samples were heated to 750°C and held for 10 min (oxidation of carbonaceous material). The remaining residue is termed ash.

The flow-rates of air and nitrogen gases were set at 16 cm^3/min, and samples of 20 mg each were analysed.

Results and Discussions

Lignin extraction and cellulose hydrolysis

The extracted lignin and the produced glucose yields, calculated as a percentage of the lignin and cellulose fractions of dry SCB_{StEx} used in the process, as well as the overall biomass usage (efficiency), are presented in Figure 2.

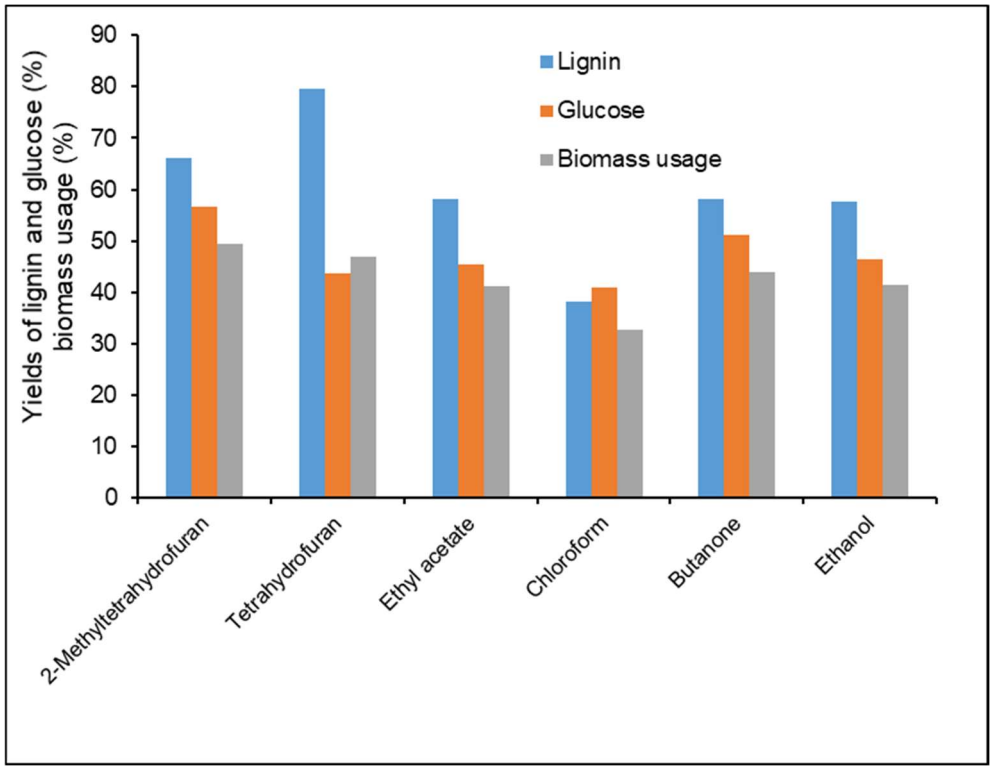


Figure 2. Yields of lignin obtained by extraction from SCB_{StEx} with various solvents, yields of glucose obtained by enzymatic hydrolysis from $SCB_{StEx\text{-}Del}$, as well as overall biomass usage in the combined process, all relative to SCB_{StEx}.

Extraction with THF gave the highest yields of lignin, which amounted to 80% of the lignin in SCB_{StEx}, followed by 2-methyltetrahydrofuran. The latter solvent is particularly interesting, as it can be produced from furfural by hydrogenation.

The lignin fractions were fully characterised (data not shown), by using UV-Vis, FTIR and NMR spectroscopies, as well as size-exclusion chromatography, and indicated a solvent dependence of the resulting chemical lignin structure. THF-extracted lignin was found to possess weight-average and number-average molecular weights of 7912 and 3830 g/mol, respectively, with a polydispersity index of 2.1.

Extraction with either 2-methyltetrahydrofuran or butanone, followed by hydrolysis, gave the highest glucose yields (57 and 51%, respectively). Hence, the solvent choice is one parameter by which a biorefinery can control the degree to which lignin extraction and glucose production occurs. Interestingly, the residual lignin in $SCB_{StEx\text{-}Del}$ did not affect the hydrolysis with enzymes, contrary to literature reports (Ghose & Bisaria, 1979; Silva *et al.*, 2018; Xu *et al.*,

2023). Final decision-making on the solvent choice will depend on the product prices and application areas of both lignin and glucose. Biomass usage should also be considered, because the residue of the enzymatic hydrolysis could either be used as fuel to generate process energies, or otherwise, it has to be disposed of. The maximum biomass usage was 49%, when 2-methyltetrahydrofuran was used as an extracting solvent.

Since the material production described in this paper focuses on the use of lignin in material production, THF was selected as the extractant, to ensure high yields.

Lignin applications

1. Sugarcane bagasse-based particleboards

Table 2 shows the compositional analysis of untreated SCB, as well as CA- and SA-pretreated SCB.

Table 2. Compositional analysis of untreated SCB, as well as Citric Acid (CA)- and Sulphuric Acid (SA)-pretreated SCB

	Extractives (%)	**Cellulose (%)**	**Hemicellulose (%)**	**Lignin (%)**	**Ash (%)**
Not pretreated	2.3	46.3	32.4	15.9	3.1
CA-pretreated	0.3	46.4	28.7	21.5	3.2
SA-pretreated	0.4	56.9	6.7	32.7	3.2

The pretreatment of SCB, using the CA protocol, led to a weight loss of 37%, due to solubilisation. The solubilisation was relatively unselective, with fractional losses of 91, 37, 44, 15 and 34% for extractives, cellulose, hemicellulose, lignin and ash, respectively.

On the other hand, when treated with the SA protocol, a total biomass loss of 45% was found, with fractional losses of 91, 32, 89, 0 and 42%, respectively. In other words, hemicellulose is more preferentially removed with SA than with CA, while preserving a high lignin content. It can be deduced from the literature that a low hemicellulose content is beneficial for the production of particleboards with suitable physical and mechanical properties (Vaz *et al.,* 2021). In addition, due to the binding properties of lignin, it can be hypothesised that a protocol should be chosen that preserves the lignin content of the biomass. Following this reasoning, SA-pretreated SCB should lead to better particleboards than when the pretreatment is done with citric acid.

The SEM images (data not shown) of non-pretreated SCB show that the fibre bundles are anchored and that the fibres are compact and intact. CA-pretreated SCB fibres display a rugged fibre structure and the partial dismemberment of smaller fibrils. The cross-sectional image indicates a partial collapse of the cellulose bundles. On the other hand, SA-pretreated SCB fibres have a comparatively lower degree of fibril dismemberment and collapse of fibre bundles, when compared to CA-pretreated SCB. This aligns with the compositional results.

Particleboards were produced, as described in the Methodology section, with and without the addition of THF-extracted SCB lignin. Table 3 gives an overview of the densities, water absorption and thickness swelling after 24 h contact with water, Moduli of Elasticity and Rupture.

Table 3. Overview of the particleboards' total lignin content, and resulting properties (density, water absorption, thickness swelling, Modulus of Elasticity (MoE) and Modulus of Rupture (MoR))

Sample[1]	Total lignin[2] (%)	Density (g cm^{-3})	Water absorption (%)	Thickness swelling (%)	MoE (MPa)[3]	MoR (MPa)[3]
CA	22	0.74	59	43	1700	3.0
CAL 2.5	24	0.83	57	39	650	2.0
CAL 7.5	28	0.83	55	35	1600	2.5
CAL 12.5	32	0.94	40	25	3150	4.5
SA	33	0.78	28	23	5350	5.0
SAL 2.5	35	1.08	18	17	6800	3.0
SAL 7.5	39	1.02	15	12	9800	5.5
SAL 12.5	42	1.27	3	4	15150	10.5
SAUF 7.5	30	0.98	4	4	7650	5.0
PGB	n/a	0.53	5	3	9750	14

[1] CA, SA: citric or sulphuric acid-pretreated SCB; L: lignin added; 2.5, 7.5, 12.5: percentage of lignin added relative to the untreated SCB; SAUF: sulphuric acid-pretreated SCB bonded with 7.5% urea-formaldehyde; BisonBord® purchased from PG Bison. [2] lignin content of the pretreated SCB plus added THF-derived SCB lignin (where applicable). [3] MoE and MoR data is rounded to the nearest 50 MPa and 0.5 MPa, respectively, according to SANS 6015: 2004

Table 3 shows that all particleboards had densities that comply with medium-density particleboards (0.5-1.0 g/cm; ASTM D1554-10), except for SAL 12.5, which was somewhat denser. The density of the CA-pretreated SCB boards is slightly lower than that of SA-pretreated SCB boards.

It was found that the densities, MoE and MoR of particleboards increase with the increasing lignin content, irrespective of the pretreatment method. Similarly, both the water absorption and thickness swelling decrease systematically with the increasing lignin content. Due to the higher lignin content in the SA-pretreated SCB, the resulting particleboards possess better properties than the respective CA-pretreated particleboards. Clearly, the hydrophobic character of lignin is essential for providing particleboards that can resist degradation, when in contact with water.

For comparison, a Urea-Formaldehyde (UF) particleboard was produced from SA-pretreated SCB, in order to compare the performance of lignin to a conventional binder. The comparison between SAL 7.5 and SAUF 7.5 shows that, while densities and MoRs were similar, the SAUF board featured a lower water absorption and thickness swelling, but also a lower MoE. It is noteworthy that SAL 12.5 gave similar properties as SAUF 7.5 (water absorption, thickness swelling), but surpassed it with regards to MoE and MoR. This emphasises the rigidity and eco-friendliness of lignin-based particleboards, despite the reported low reactivity and weak bond strength of unmodified lignin, compared to UF resin (Zhao *et al.*, 2024; Zhao *et al.*, 2025).

Furthermore, a commercial BisonBord® was purchased. This board had a much lower density than any of the SCB-based boards. SAL 12.5 surpassed the commercial board in all aspects, except for a somewhat lower MoR value.

The best SCB-particleboard of this study (SAL 12.5) was compared to international industry standards. According to EN310: 2010 (medium-density boards), for boards with a nominal thickness of between 6 to 13 mm, the maximum percentage of the thickness swelling within 24 h of exposure to water is below 10-19%, depending on board class. Both, the commercial PGB board and SAL12.5 comply with this requirement. The minimum Modulus of Rupture is between 11 and 22 MPa. The PGB board would fulfil the requirements of a P2 or P3 board in this regard, while SAL 12.5 would only be rated as P2 board. The further addition of lignin would likely increase the values of MoR even further. The minimum requirement for the Modulus of Elasticity in bending is between 1800 and 3350 MPa. Both the PGB and the SAL 12.5 board fulfil the requirements of boards with P1 to P7 specifications. In summary, SAL12.5 complies in all the categories with a P2-type board (boards for interior fitments, including furniture, for dry conditions), while PGB would also fulfil those of P3 (non-load-bearing boards for use in humid conditions). That being said, it should be noted that not all aspects of EN312 were tested, and future research will expand to surface soundness and cycling tests (for applications in humid conditions).

2. *Sugarcane bagasse-based polypropylene composites*

For composite extrusions, it is important to ensure that none of the components of the composite are thermally degraded during the process. A thermogravimetric analysis study was therefore conducted, and Figure 3 shows the results of r-PP, NaOH-pretreated SCB, as well as the composites that were prepared.

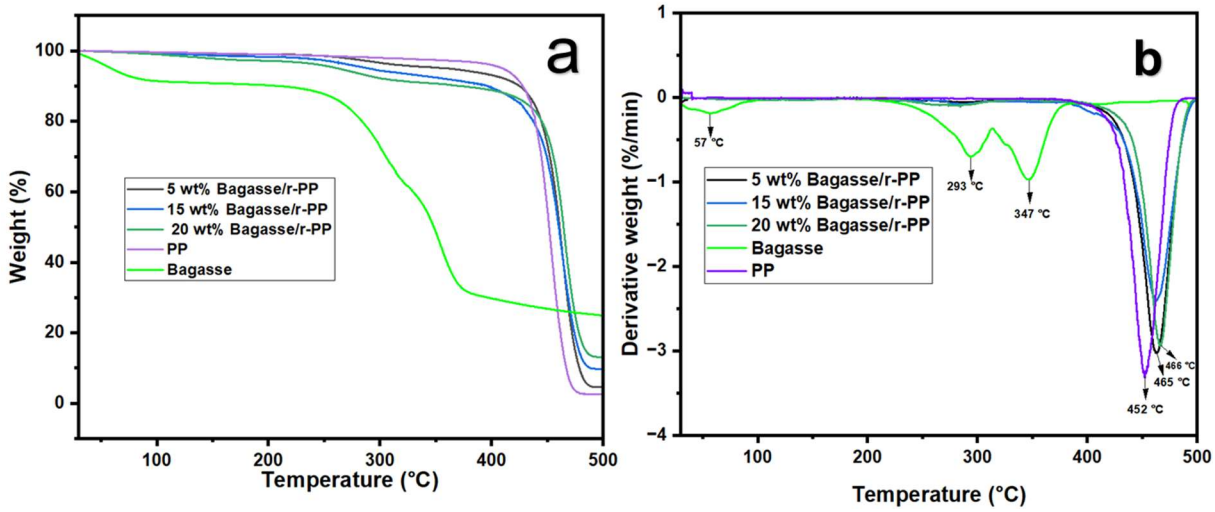


Figure 3. Thermogravimetric analysis (a) and derivative weight (b) of the recycled PP, bagasse, and bagasse/recycled PP composites

For SCB, an initial weight loss starting at 30°C (moisture evaporation) was observed, followed by a two-step loss starting at 225°C (breakdown of glycosidic bonds of cellulose and hemicellulose (Luz *et al*; 2008)). Inflection points occur at 293 and 347°C, with 26% of a char residue.

r-PP remained thermally stable up to 420°C, with an inflection point at 452°C, which is attributed to the degradation of saturated carbon-carbon bonds. Little residue remained (3%). All the composites of SCB and r-PP remained stable upon heating. A minor weight loss was detected (<7%) at temperatures up to 330°C, which could be due to the exposed SCB fibres at the surface of the composites. Major decomposition was experienced at temperatures above 380°C, with inflection points around 465°C. The residues of the composite degradation correlate with the composition, and are somewhat higher than the theoretical mass-weighted composite contributions of r-PP and SCB to the residue. From this study, it was concluded that

the SCB/r-PP composites can be processed without decomposition at temperatures below 200°C.

The amount of stress that a material can bear before breaking, as well as its stiffness, are determined by its tensile strength and tensile modulus, respectively. The tensile strength decreased continuously from 29 MPa (r-PP only) to 23 MPa upon addition of up to 20 wt.% SCB, while the tensile modulus increased from 650 to 800 MPa (data not shown). The impact strength, which is an indication of the stress a material can withstand when exposed to a sudden shock, decreased from 36 kJ/m (r-PP only) to 8 kJ/m (20 wt.% SCB).

Irrespective of the detrimental effects of the addition of SCB pretreated by NaOH on the mechanical properties, it should be noted that these composites still meet the requirements for materials in certain applications, such as lightweight, non-load-bearing structures (Devadiga *et al.*, 2020). These findings are supported by relevant studies that suggest the potential use of sugarcane SCB composite production.

The composites' morphology at the impact fracture surface was evaluated by using SEM, as shown in Figure 4. The pretreated SCB showed ordered strands of fibre, while the r-PP exhibited a smooth and irregularly-fractured surface. Increasing the amount of SCB in the composite leads to a roughening of the fracture surface, as well as the visual voids that are caused by fibre pull-out from the matrix. These voids show that SCB and r-PP show poor adhesion, which decreases their mechanical strength (Smariha *et al.*, 2013; Arrakhiz *et al.*, 2013).

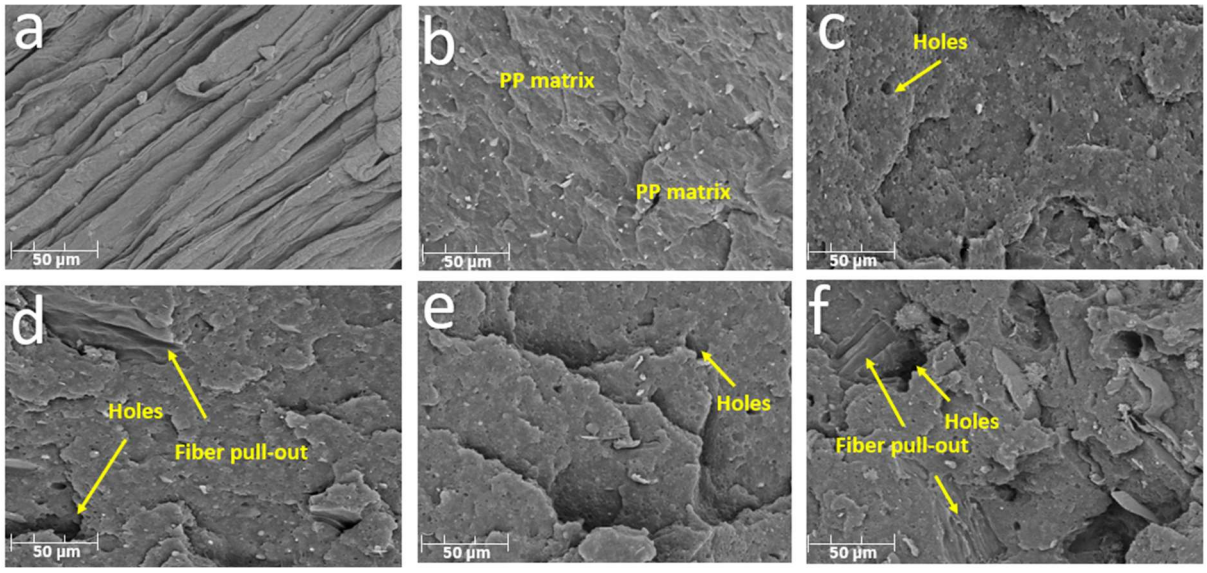


Figure 4. SEM micrographs of (a) pretreated SCB, (b) r-PP, and bagasse / r-PP composites with (c) 5, (d) 10, (e) 15, and (f) 20 wt.% bagasse content at the impact fracture surface

3. Sugarcane bagasse-based lignin as a binder for coal fines briquette production

Preliminary compression investigations were conducted on a pharmaceutical tabletting machine to obtain information on the general trends regarding hardness and friability, when various bio-based binders were used to produce tablets from coal fines. This allowed for relatively small batch sizes, and hence, chemical consumption, when compared to briquette production. Tablets with a diameter of 13 mm and a weight ranging from 330 mg to 485 mg were prepared, as shown in Table 4. Several binders, including Kraft lignin, lignosulfonate, bone glue, molasses, pine gum rosin, SCB_{StEx} and others, were assessed. in In a systematic

study, the binder concentrations were altered between 5 and 30%, and in certain cases, 2% of a lubricant, i.e. hydrated magnesium silicate (talc) was added to improve tablet ejection. However, in this paper, we only present the results with Organosolv Lignin (OL), which was extracted from SCB_{StEx} by using THF, as outlined in the Methodology section, and we compare to similar tablets made from commercial Hide Glue (HG).

In the pharmaceutical industry, hardness testing determines the breaking force and can be interpreted as the tensile strength, while friability describes the tendency to disintegrate, when handled. Both are therefore measures of the structural integrity of tablets, to ensure that they can withstand physical stress during handling, packaging and transportation. For comparison, for pharmaceutical tablets, the acceptable hardness values for oral tablets lie between 40-100 N (Amidon *et al.*, 2017), while friabilities of between 0.5 and 1% weight loss are considered acceptable.

Table 4 shows that tablets with a higher hardness and lower friability were obtained with hide glue, both in the presence and absence of talc (Entries 2 and 5), while OL led to tablets with a lower structural integrity. The combination of OL and hide glue as additives resulted in no improvement, when compared to experiments where only OL was used as a binder.

Table 4: Physical properties of prepared tablets

Entry	Mixture	Weight (mg) [1]	STD (mg) [2]	Hardness (N)	Friability (%)	CV (MJ/kg) [3]
1	OL – C – T (30:70:0)	454	3.9	0.7	99.2	28.5
2	HG – C – T (30:70:0)	330	3.3	8.0	1.7	25.4
3	(OL+HG) – C – T ((12.5+12.5):75:0)	486	5.7	0.8	100.0	27.2
4	OL – C – T (29:69:2)	453	4.7	0.6	99.7	28.1
5	HG – C – T (29:69:2)	473	0.3	5.8	1.5	25.0

[1] average of 10 tablets; [2] STD: standard deviation; [3] calculated from the calorific values of the pure constituents of the mixtures.

The calorific values of the tablets (Table 4) were determined from their constituent materials: coal fines (28.5 MJ/kg), organosolv lignin (28.4 MJ/kg) and hide glue (18.2 MJ/kg). It is worth noting that organosolv lignin has a very similar calorific value to coal, which highlights its potential to substitute coal in energy-related applications. Not surprisingly, the organosolv-derived tablets feature higher calorific values than those derived from hide glue.

Important information can be obtained about the suitability of a mixture as fuel by using thermogravimetric analysis. Volatile matter, which is the weight loss experienced from the dry material in the absence of auxiliary oxygen during the experiment, is related to the ease of fuel ignition. An ideal fuel should also combust completely, leaving little ash (inorganic material) behind. ASTM 7582-15 details the TGA temperature programme, as described in the Methodology section. Table 5 summarises the findings of the coal fines tablet analyses.

Table 5 shows that coal fines and hide glue both had a relatively high ash content of 12 and 15%, respectively, while organosolv lignin had an ash content of below 0.5%. This led to high ash contents of all coal tablets made using hide glue, while the use of organosolv lignin resulted in lower ash contents. On the other hand, due to the fact that both OL and HG have similar volatile matter contents, this property is similar in all binder-coal mixtures prepared.

Table 5. Volatile matter, fixed carbon (carbonaceous matter) and ash content of coal fines tablets (dry basis)

Analyte	Volatile matter (%)	Fixed carbon (%)	Ash (%)
Coal fines	27	61	12
OL	65	35	0 (0.4)
HG	71	14	15
OL – C – T (30:70:0)	38	53	9
HG – C – T (30:70:0)	40	47	13
(OL+HG) – C – T ((12.5+12.5):75:0)	37	52	11
OL – C – T (29:69:2)	37	52	9
HG – C – T (29:69:2)	39	46	13

Conclusions

In conclusion, the residue from the furfural process, steam-exploded bagasse, is an ideal feedstock for the production of organosolv lignin, and high lignin and glucose yields can be obtained. The THF-derived lignin was successfully applied as a promising binder for all-bagasse particleboards, which is of interest, not only because residual bagasse could be diverted to a growing market, but also because the use of carcinogenic formaldehyde resin is avoided. Future research will focus on process optimisation, and assess other acids in terms of their ability to selectively remove hemicellulose in the pretreatment, while retaining the lignin content of SCB. Organic acids are of particular interest in that regard, for reducing the sulphur content in the effluent.

SCB can also be used together with r-PP to prepare composite materials for light-weight applications, and work is currently underway to investigate the effects of alternative pretreatment protocols, as well as surface modifications, to enhance the interactions between the SCB and r-PP.

It is concluded that using organosolv lignin as a binder, results in the coal fines tablets having a similarly-high calorific value as coal, with a somewhat higher volatile matter and lower ash content. However, at the present stage, the structural integrity of the tablets is limited. Current studies are investigating the stability of disk-shaped briquettes that are produced from these, and similar, mixtures. The study has also shown that other bio-based binders, such as hide glue, could lead to suitable fuel blends. Other sugarcane-derived by-products of the industry, in particular molasses, will be included in future studies.

Acknowledgments

This work is based on the research supported, in part, by the National Research Foundation of South Africa (Grant Number: 115465, SMRI/DSTI/NRF South African Research Chair (SARChI) Sugarcane Biorefining in South Africa). The authors acknowledge C Kruger (Illovo Sugar Africa, Sezela), the Sugar Milling Research Institute, the Council for Scientific and Industrial Research (CSIR) and the Technology Innovation Agency (TIA) for the provision of sugarcane bagasse residue from the furfural plant, for the provision of sugarcane bagasse, for student co-supervision (J.I.M., N.N.), for access to the research infrastructure, and for their financial support. For co-supervision, the authors thank D Lokhat (K.G.; Chemical Engineering, University of KwaZulu-Natal (UKZN), V Chunilall (N.N. and J.I.M., CSIR Durban) and V Ojijo (J.I.M., CSIR Pretoria), as well as Y Sewsunker (UKZN, now at the University of the Western Cape) for producing the enzymatic hydrolysis data, and T Govender

(Pharmaceutical Sciences, UKZN) for providing access to their tabletting machine and tablet characterisation equipment.

References

Amidon GE, Secreast PH and Mudie D (2017). Particle, powder and compact characterization. In: *Developing Solid Oral Dosage Forms*, 2nd ed., Elsevier, p. 271-293.

Anggono J, Sugondo S, Alim R, Purwaningsih H, Sugondo S, Alim R, Purwaningsih H and Wibawa A (2018). Performance and evaluation of low-cost sugarcane bagasse - polypropylene bio-composites as candidate material for Automotive Parcel Tray. *Materials Science Forum* 923: 40-46.

Anon (2016). Coal fines to pellets moving ahead in South Africa. International Mining. https://im-mining.com/2016/02/18/coal-fines-to-pellets-moving-ahead-in-south-africa/ [Accessed 28.04.2025].

Arrakhiz FZ, Malha M, Bouhfid R, Benmoussa K and Qaiss A (2013). Tensile, flexural and torsional properties of chemically treated alfa, coir and bagasse reinforced polypropylene. *Composites Part B: Engineering* 47: 35-41.

Balraj A, Krishnan J, Selvarajan K and Sukumar K (2021). Potential use of biomass and coal-fine waste for making briquette for sustainable energy and environment. *Environmental Science and Pollution Research* 28: 63516-63522.

Becker J and Wittmann C (2019). A field of dreams: Lignin valorisation into chemicals, materials, fuels and health-care products. *Biotechnology Advances* 37: 107360.

Cowling N (2024). Power production breakdown in South Africa 2022, by source. https://www.statista.com/statistics/1237610/south-africa-distribution-of-electricity-production-by-source/ [Accessed 28.04.2025].

Devadiga DG, Bhat KS and Mahesha GT (2020). Sugarcane bagasse fibre reinforced composites: Recent advances and applications. *Cogent Engineering* DOI: 10.1080/23311916.2020.1823159.

DTIC (Department Trade, Industry and Competition) (2020). Master Plan for the Commercial Forestry Sector in South Africa 2020-2025. https://www.dffe.gov.za/sites/default/files/docs/strategy.framework/forestry/sectormasterplan2020.2025.pdf [Accessed 08.01.2025].

do Espirito Santo MC, Cardoso EB, Guimaraes FEG, DeAzevedo ER, da Cunha GP, Novotny EH, Pellegrini VdOH, Chandel AK, Silveira MHL and Polikarpov I (2019). Multi-faceted characterization of sugarcane bagasse under different steam explosion severity conditions leading to distinct enzymatic hydrolysis yields. *Industrial Crops and Products* 139: 111542.

Fernández-Rodríguez J, Erdocia X, Sánchez C, Alriols MG and Labidi J (2017). Lignin depolymerization for phenolic monomers production by sustainable processes. *Journal of Energy Chemistry* 26: 622-631.

Ghose T and Bisaria V (1979). Studies on the mechanism of enzymatic hydrolysis of cellulosic substances. *Biotechnology and Bioengineering* 21: 131-146.

Gomes MG, Gurgel LVA, Baffi MA and Pasquini D (2020). Pretreatment of sugarcane bagasse using citric acid and its use in enzymatic hydrolysis. *Renewable Energy* 157: 332-341.

Gordobil O, Egüés I and Labidi J (2016). Modification of eucalyptus and spruce organosolv lignins with fatty acids to use as filler in PLA. *Reactive and Functional Polymers* 104: 45-52.

Gosselink RJ, van Dam JE, de Jong E, Scott EL, Sanders JP, Li J and Gellerstedt G (2010). Fractionation, analysis and PCA modeling of properties of four technical lignins for prediction of their application potential in binders. *Holzforschung* 64: 193-200.

Gozdecki C, Wilczynski A, Kociszewski M and Zajchowski S (2014). Properties of wood–plastic composites made of milled particleboard and polypropylene. *European Journal of Wood and Wood Products* 73: 87-95.

Guest K, Stark A and Starkzak M (2019). Development and verification of an Aspen Plus® model of a sugarcane biorefinery. *Proceedings of the South African Sugar Technologists' Association* 92: 254-273.

Hercules Bricks, https://herculesbricks.co.za/manufacturing.html, [Accessed 28.04.2025].

Kazzaz AE and Fatehi P (2020). Technical lignin and its potential modification routes: A mini-review. *Industrial Crops and Products* 154: 112732.

Lloyd T (2019). The myth of 'clean coal' https://cer.org.za/wp-content/uploads/2019/01/The-Myth-of-Clean-Coal-Technical-Report-January-2019.pdf [Accessed 28.04.2025].

Luz SM, Del Tio J, Rocha GJM, Gonçalves AR and Del'Arco Jr AP (2008). Cellulose and cellulignin from sugarcane bagasse reinforced polypropylene composites: Effect of acetylation on mechanical and thermal properties. *Composites Part A: Applied Science and Manufacturing* 39: 1362-1369.

Manyuchi MM, Mbohwa C and Muzenda E (2018). Value addition of coal fines and sawdust to briquettes using molasses as a binder. *South African Journal of Chemical Engineering* 26: 70-73.

Marx S, Laubser ANE, Bunt JR, Venter RJ, Uwanoma RC and Strydom CA (2023). Evaluation of sugar cane bagasse hydrothermal liquefaction products for co-gasification with coal as green coal pellet production. *Bioresource Technology Reports* 22:101503.

Mastrolitti S, Borsella E, Giuliano A, Petrone M, de Bari I, Gosselink R, van Erven G, Annevelink E, Traintafyllidis K and Stichnothe H (2021). Sustainable lignin valorisation: Technical lignin, processes and market development *IEA Bioenergy Task 42 & LignoCOST*.

Moghaddam L, Rencoret J, Maliger VR, Rackemann DW, Harrison MD, Gutiérrez A, del Río JC and Doherty WO (2017). Structural characteristics of bagasse furfural residue and its lignin component. An NMR, Py-GC/MS, and FTIR study. *ACS Sustainable Chemistry & Engineering* 5: 4846-4855.

National inventory discard and duff coal – 2001. https://www.dmre.gov.za/Portals/0/Energy_Website/Coal/coal_discard_report.pdf [Accessed 28.04.2025].

NEMWA (National Environmental Management: Waste Act) (2020). Draft Amendments to the regulations and notices regarding extended producer responsibility. https://www.dffe.gov.za/sites/default/files/legislations/nemwa_extendedproducerresponsibilty202regulationsnotices_g44295gon239.pdf [Accessed 08.01.2025].

Olawale JT, Edeki OG and Cowan AK (2020). Bacterial degradation of coal discard and geologically weathered coal. *International Journal of Coal Science & Technology* 7: 405-416.

PG Bison (2024). PG Bison unveils new Supawood Medium-Density Fibreboard (MDF) line in Mkhondo. https://pgbison.co.za/new-supawood-medium-density-fibreboard/ [Accessed 17.04.2025].

Papin AV, Ignatova AY, Nevedrov AV and Cherkasova TG (2015). Fuel briquetting using finely disperse waste of coal mining and processing. *Journal of Mining Science* 51: 895-900.

Piekarczuk A, Szewczak E, Kozikowska E and Gobebiowski L (2025). 3D Scanning of wood–plastic composite decking after cyclic thermal action. *Materials* 18: 97, DOI:10.3390/ma18010097.

Plastics SA (2020). Plastics, People and Planet: An Annual Review. https://www.plasticsinfo.co.za/wp-content/uploads/2020/08/Master-Plan-for-Growth-Draft-Jun-30_2020.pdf [Accessed 08.01.2025].

Plastics SA (2024). Annual review 2023-2024. https://www.plasticsinfo.co.za/wp-content/uploads/2024/11/20241021_PSA-Annual-Review_20232024_low-res.pdf, [Accessed 28.04.2025].

Ragauskas AJ, Beckham GT, Biddy MJ, Chandra R, Chen F, Davis MF, Davison BH, Dixon RA, Gilna P and Keller M (2014). Lignin valorisation: improving lignin processing in the biorefinery. *Science* 344: 1246843.

Ramos LP, da Silva L, Ballem AC, Pitarelo AP, Chiarello LM and Silveira MHL (2015). Enzymatic hydrolysis of steam-exploded sugarcane bagasse using high total solids and low enzyme loadings. *Bioresource Technology* 175: 195-202.

Samariha A, Bastani A, Nemati M, Kiaei M, Nostrati H and Farsi M (2013). Investigation of the mechanical properties of bagasse flour/polypropylene composites. *Mechanics of Composite Materials* 49: 447-4564.

SASA (South African Sugar Association) (2020). South African Sugarcane Value Chain Master Plan to 2030. https://sasa.org.za/wp-content/uploads/2024/05/SA-Sugar-Master-Plan-1.pdf [Accessed 08.01.2025].

Sezgin H, Kucukali-Ozturk M, Berkalp OB and Yalcin-Enis I (2021). Design of composite insulation panels containing 100% recycled cotton fibres and polyethylene/polypropylene packaging wastes. *Journal of Cleaner Production* 304: 127132.

Silva TAL, Zamora HDZ, Varão LHR, Prado NS, Baffi MA and Pasquini D (2018). Effect of steam explosion pretreatment catalysed by organic acid and alkali on chemical and structural properties and enzymatic hydrolysis of sugarcane bagasse. *Waste and Biomass Valorisation* 9: 2191-2201.

Sithole P, Nickolson RJ, van Heerden PDR and Stranack RA (2024). A review of South African sugarcane production in the 2023/24 season: Climate, production and economics. *Proceedings of the South African Sugar Technologists' Association* 96: 1-17.

Sluiter A, Hames B, Ruiz R, Scarlata C, Sluiter J, Templeton D and Crocker D (2012). Determination of structural carbohydrates and lignin in biomass. NREL *Laboratory Analytical Procedure TP-510-42618*.

TIPS (Trade and Industrial Policy Strategies) (2024). Industry Study Plastics. https://www.tips.org.za/manufacturing-data/manufacturing-sectors/item/4747-industry-study-plastics [Accessed 08.01.2025].

Tribot A, Amer G, Alio MA, de Baynast H, Delattre C, Pons A, Mathias JD, Callois JM, Vial C and Michaud P (2019). Wood-lignin: Supply, extraction processes and use as bio-based material. *European Polymer Journal* 112: 228-240.

Undersander D, Mertens DR and Thiex N (1993). Forage analyses procedures. *National Forage Testing Association*. https://www.foragetesting.org/lab-procedures [last accessed 27.04.2025].

Várdai R, Lummerstorfer T, Pretschuh C, Jarabek M, Gahleitner M, Pukanszky B and Renner K (2019). Impact modification of PP/wood composites: A new approach using hybrid fibres. *eXPRESS Polymer Letters* 13: 223-234.

Vaz FL, da Rocha Lins J, Alencar BRA, de Abreu IBS, Vidal EE, Ribeiro E, Sampaio EVdSB, Menezes RSC and Dutra ED (2021). Chemical pretreatment of sugarcane bagasse with liquid fraction recycling. *Renewable Energy* 174: 666-673.

Waanders FB, Marx S and Bunt JR (2020). Production of a carbonaceous feedstock material from a waste carbon source. US 10,711,214, to North-West University.

Wang W, Mu M, Zou Y, Li B, Cao H, Hu D and Tao X (2022). Inflammation and fibrosis in the coal dust-exposed lung described by confocal Raman spectroscopy. *Peer J*: e13632.

Xu X, Wang K, Zhou Y, Lai C, Zhang D, Xia C and Pugazhendhi A (2023). Comparison of organosolv pretreatment of masson pine with different solvents in promoting delignification and enzymatic hydrolysis efficiency. *Fuel* 338: 127361.

Zhao D, Li Z, Zhang Y and Fu P (2025). The role of lignin in adhesives for lignin-based formaldehyde-based resins: a review. *Biomass Conversion and Biorefinery* DOI: 10.1007/s13399-024-06397-1.

Zhao L, Li W, Cheng Y, Zhao J, Tian D, Huang M and Shen F (2024). Preparation and evaluation of lignin-phenol-formaldehyde resin as wood adhesive using unmodified lignin. *Industrial Crops and Products* 211: 118168.

SHORT COMMUNICATION

ASSESSING THE FINANCIAL VIABILITY OF SUSTAINABLE AVIATION FUELS (SAF) PRODUCTION FROM SUGARCANE IN SOUTH AFRICA: AN EX-ANTE ANALYSIS

L Mvelase and SRD Ferrer

Discipline of Agricultural Economics, School of Agriculture, Earth and Environmental Sciences, University of KwaZulu-Natal, P/Bag X01, Scottsville, Pietermaritzburg, 3209, South Africa.

mvelaselm@yahoo.com

Abstract

This paper assesses the economic feasibility of Sustainable Aviation Fuel (SAF) production from sugarcane A-Molasses in South Africa, through an Alcohol to Jet fuel (AtJ) production pathway. Two possible scenarios were considered, namely, the existing (Brownfield) and the non-existing (Greenfield) project scenarios. Capital budgeting techniques and a Cost Benefit Analysis (CBA) were used to assess the economic feasibility of SAF production. The results showed that the production of SAF is not financially viable without government support for both the Brownfield and Greenfield project. The results showed that the production is viable at a price of at least R60.20/litre for the Brownfield project and a price of at least R69.85/litre for the Greenfield project. Therefore, it is slightly financially feasible to produce SAF in the Brownfield project scenario, than it is in the Greenfield project scenario. The study findings therefore give rise to a recommendation that there should be no investment in SAF until there is sufficient government subsidy for production to be viable.

Keywords: Sustainable aviation fuels, economic feasibility, sugarcane

Introduction

The increasing global interest in electric battery-powered motor vehicles has reduced the certainty of the long-term demand for biofuels as an alternative to crude fuels for motor vehicles. According to the International Energy Agency (IEA, 2024), between 2020 and 2022, the share of electric motor vehicle sales more than doubled, as it increased from 4% in 2020 to 14% in 2022. The sales of battery electric motor vehicles are anticipated to continue increasing, and the rollout of electric motor vehicles is anticipated to replace 5 million barrels of crude oil per day by 2030 (IEA, 2024).

The regulations by the Carbon Offsetting and Reduction Scheme for International Aviation (CORSIA), which require nations to use SAF instead of conventional jet fuels to minimise the Green House Gas (GHG) emissions of the aviation sector, present a promising medium-term demand for the South African biofuel industry (ICAO, 2024). The bio-based (including sugarcane-based) jet fuels can be considered as SAF, since they meet the key sustainability requirements, i.e. they do not compete with food crops or water use, and they reduce the GHG emissions throughout their life-cycle relative to conventional jet fuels.

The aim of this study was to make a relevant contribution to knowledge by assessing the minimum selling price in South Africa that will make sugarcane-based SAF producers break-even, and to assess the financial feasibility of sugarcane-based SAF production. The study is based on two scenarios, namely, the Brownfield project and Greenfield project scenarios. The Greenfield project scenario involves the construction of the new bioethanol-to-SAF processing plants, whereas the Brownfield project scenario involves the repurposing of the existing fuel refineries to blend ethanol, which is transported from the existing sugar mills, into jet fuels.

Material and Methods

Research method

The capital budgeting methods of CBA were used to assess the financial feasibility of SAF. The capital budgeting methods are divided into two categories, the real Discounted Cash Flow (DCF) methods and the non-DCF cash flow analysis methods (Mollah *et al*.,2021). In this study, the real DCF methods were considered because they account for the time value of money concepts through discounting. These methods include the Net Present Value (NPV)(Equation 1), the Internal Rate of Return (IRR) (Equation 2) and the Benefit Cost Ratio (BCR) (Equation 3) methods.

$$NPV=\sum_{i=1}^{n}\frac{C_t}{(1+r)^n}-C_t,0 \quad \ldots(1)$$

$$0=\sum_{i=1}^{n}\frac{C_t}{(1+IRR)^n}-C_t,0 \quad \ldots(2)$$

$$BCR=\frac{\Sigma B_i/(1+r)^n}{\Sigma C_i/(1+r)^n} \quad \ldots(3)$$

Where n is the lifetime of an investment, C_t is the net cashflow in time t, r is the real interest rate and C_t,0 is the initial investment cost of the project.

Data sources and procedures

Since no SAF production is currently taking place in Africa, this study relied on data obtained from local and international literature sources. The summarised parameters used for assessing the financial feasibility of SAF production in South Africa are outlined in Table 1. The exchange rates obtained from the South African Reserve Bank Quarterly Bulletin (SARB, 2024) were used to convert international currencies into South African Rands. Furthermore, nominal figures were converted into real figures by using the inflation rate statistics obtained from the SARB (2024). The costs and the selling prices are presented per ton of SAF. The data on the plant size capacity of 300 million litres of SAF is the countrywide expected capacity when A-molasses are converted into SAF (Bole-Rented *et al*., 2022).

Th secondary data that were used to supplement these analyses were obtained from the SA Canegrowers' Association. These data include information on the Recoverable Value price (RV) of sugarcane that was used as a proxy for the cost of the SAF feedstock over the project's lifetime.

In the baseline scenario, the average world price for jet fuels, which is estimated to range between 0.6 USD to 1 USD (Bonnefoy & Schaufele, 2022), was used as a baseline price for SAF. This price is necessary to determine whether SAF will be competitive with the conventional jet fuels. The second scenario involved using the current world price of SAF, which was estimated to be 0,92 USD by Seymour *et al*. (2024), to determine whether or not the current world price of SAF makes the production financially viable in South Africa which, in turn, forms the basis for determining the minimum selling price required to make SAFs viable. Thereafter, a sensitivity analysis was used to determine the break-even price for SAF production, which is interpreted as the Minimum Selling Price (MSP) for SAF.

Table 1. Summarised parameters for conducting the discounted cash flow analysis

Process Parameter	Units/quantities	Sources of information
SAF production capacity	300 000 000 litres	Bole-Rentel *et al*. (2022)
Jet fuel price	R14.79/litre	
SAF price	R22.37/litre	Seymore *et al*. (2024)
Feedstock Cost-intermediate processing: A-Molasses	R4 914/ton	SACGA (2024)
Real Discount rate	10%	Mullins *et al*. (2014)
Project lifetime	26 Years	Tierney & Bird, (2020)
Total Feedstock Processing Cost	R23 479	Pavlenko *et al*. (2019)
Processing Cost-Intermediate Processing	R10 197/ton	
Processing cost-final product SAF processing	R8 367/ton	
Cost of finishing step to produce SAF		
Construction/Capital Cost		Pavlenko *et al*. (2019)
Production facilities and Buildings	R1 699/ton	
Transport equipment	R831/ton	
Information, computer and telecommunication equipment	R302/ton	
Machinery and other equipment	R227/ton	
Processing equipment	R227/ton	
Infrastructure	R113/ton	
Security and environment installation	R76/ton	
Storage of liquid products	R38/ton	
Other Units and plant Capex	R264/ton	
Variable Cost	R2 645/ton	Pavlenko *et al*. (2019)
Fixed Cost	R3 705/ton	Pavlenko *et al*. (2019)

Source: Authors' own computations

Results and Discussion

CBA results

The economic feasibility results of the Brownfield and Greenfield project scenarios are outlined in Table 2. In the Greenfield project scenario (Table 2), when the price of SAF is assumed to be equivalent to the current world price of jet fuels (R14.79/litre), i.e. using the current price of jet fuel as a baseline price, the production of SAF was found to not be profitable. The resulting NPV at this price was estimated at -R152 331 million, the IRR was 0% and the BCR was estimated to be 0.24. At the current world price of SAF (R22.37/litre), its production was also found to not be financially feasible i.e. the NPV was estimated to be -R131 346, the IRR was estimated to be 0% and the BCR was estimated to be 0.32. The sensitivity analysis shows that a MSP of at least R69.85/l is sufficient for SAF producers to break-even.

Like the Greenfield project, the Brownfield project scenario production of SAF was also not sustainable at the current world price of jet fuels (R14.79/litre), i.e. the NPV, IRR and BCR

were estimated to be -R126 686 million, 0% and 0.24, respectively. Its production was also found to not be financially feasible at the current world selling price of SAF (R22.37), i.e. the negative NPV (-R105 721), the 0% IRR and the BCR of less than 1 (0.37). The MSP required to make producers break-even is R60.59/litre.

Table 2. The economic feasibility results of SAF under the Greenfield project scenario

	Greenfield scenario			
Evaluation Criteria	R14.79/litre	R22.37/litre	R69.85/litre	R75/litre
Net Present Value (NPV), 2024 Prices (R Millions)	-R152 311	-R131 346	R0	R14 221
Internal Rate of Return	0%	0%	10%	19.0%
Benefit Cost Ratio	0.21	0.32	1.00	1.07
		Brownfield scenario		
Net Present Value (NPV), 2024 prices (R Millions)	-R126 686	-R105 721	R0	R25.62
Internal Rate of Return	0%	0%	10%	36.4%
Benefit Cost Ratio	0.24	0.37	1	1.15

Source: Authors' own computations

Sensitivity analysis results

The results of the sensitivity analysis for the Greenfield scenario are outlined in Figure 1 (a and b). For the sake of simplicity, the sensitivity analysis involved assessing the sensitivity of NPV to changes in the price of SAF and the real discount rate. Under a real discount rate of 10%, changes in the SAF selling prices for the Greenfield project scenario revealed that the production of SAF is not financially viable at a selling price that is less than R69.9/litre.

Reducing the real discount rate to 8% does improve the feasibility of SAF under the Greenfield scenario, but not by much. At this discount rate, the MSP decreased from 69.9 to 69.1 (i.e. a 1.2% decrease).

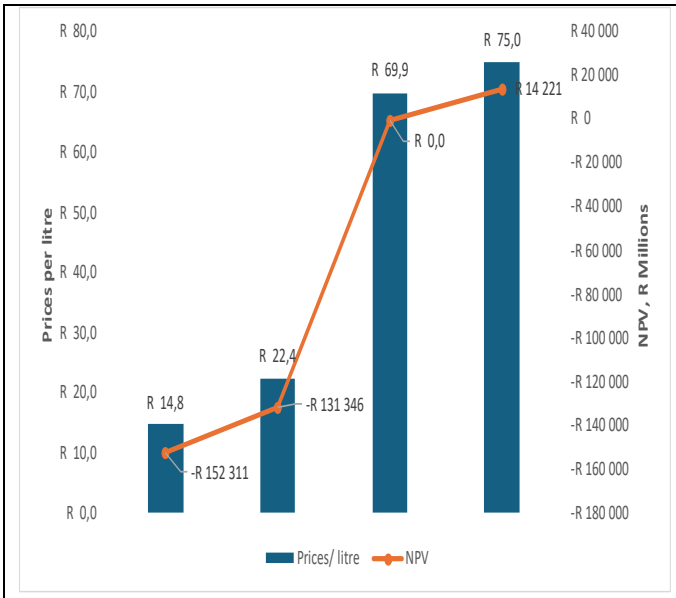


Figure 1a. NPV Sensitivity at 10% real discount rate

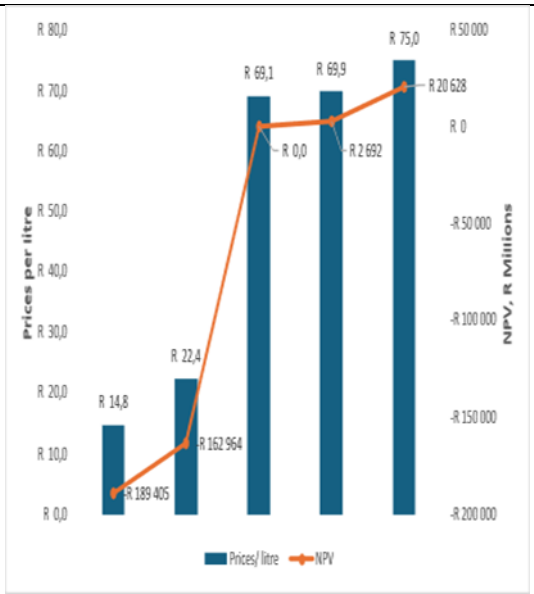


Figure 1b. NPV sensitivity at 8% real discount rate.

Figure 1. The sensitivity of NPV to changes in the price of SAF under the Greenfield project at 10% and 8% discount rate

The results of the sensitivity analysis for the Brownfield scenario are outlined in Figure 2 (a and b). Under the Brownfield project scenario, the MSP that is required to make SAF production financially viable is R60.6/litre. For all prices above R60.6/litre, the production is even more favourable, and for prices below R60.6/litre, the production is not feasible. Like the Greenfield project scenario, decreasing the real discount rate under the Brownfield project scenario does improve the viability of SAF production, but only slightly, as shown in Figure 6.4. The MSP required for SAF producers to break-even drops from R60.6/litre to R60.2/litre (0.67% drop in MSP).

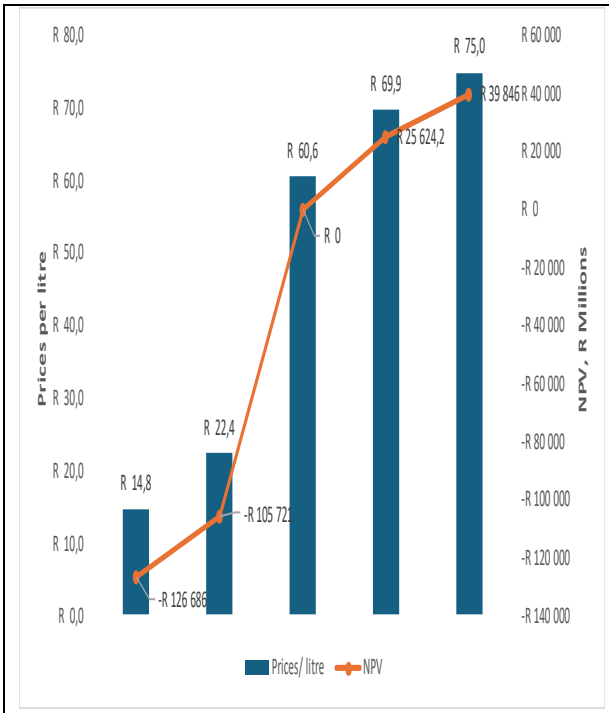


Figure 2a. NPV Sensitivity at 10% real discount rate

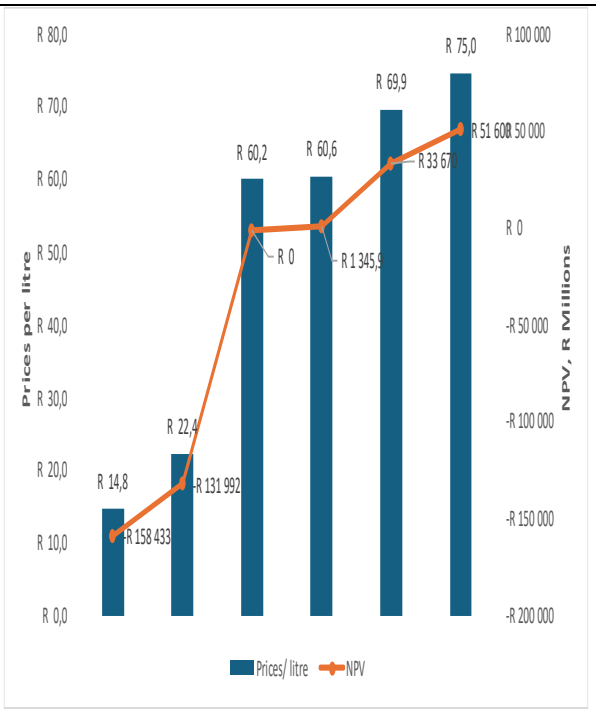


Figure 2b. NPV sensitivity at 8% real discount rate

Figure 2. The sensitivity of NPV to changes in the price of SAF under the Brownfield project at a real discount rate of 10% and 8%

Discussion

The price of SAF is not currently competitive with the price of jet fuels. At the selling price equivalent to the current world price of jet fuels, SAF production incurs a financial loss under both the Greenfield and the Brownfield project scenarios. Some studies (e.g. Broun *et al.*, 2024; Watson *et al.*,2024) also found that SAF production was expensive, relative to conventional jet fuels. This factor must be addressed, in order to make SAF financially-attractive to investors. The losses in the Brownfield project scenario are, however, 16.82% less than those of the Greenfield project scenario, primarily because the Greenfield scenario assumes the high capital expenditure that is associated with the construction of the refineries of bioethanol to jet fuel, whereas the Brownfield project involves repurposing the already-existing infrastructure at a significantly lower capital cost. The break-even price for SAF production under the Greenfield scenario was higher than that of the Brownfield project (R69.85/litre vs R60.21/litre); therefore, with the Brownfield project, the prices at which prospective SAF producers will start realising a profit are much less than the prices for the Greenfield project. This will make the existing oil refineries scenario attractive again..

The sensitivity analysis results revealed that changing the real discount rates has an insignificant impact on the economic feasibility of SAF. It changes in SAF selling prices that could significantly affect the viability of SAF. Interventions that are designed to stimulate the production of SAF should, therefore, aim to address the negative impact that the selling price has on the attractiveness of SAF to consumers, i.e. the jet fuel manufacturers. A subsidy, or price support, from the government is one of the interventions that could decrease the MSP of SAF by minimising SAF production costs.

Conclusions and Recommendations

The production of SAF in South Africa at the current world price of jet fuels is currently not financially-feasible for both the Greenfield and the Brownfield project scenarios without substantial subsidisation. The Brownfield project is, however, more promising than the Greenfield project scenario. The NPV, at the current world price of SAF, was 16.85% higher than that for the Greenfield project scenario. In the Brownfield project scenario, the MSP that is required to make SAF producers break-even was 15.28% lower than the MSP required in the Greenfield project scenario. The study therefore recommends financial support from government and private investors, since the production of SAF is financially unfeasible in the absence of financial support.

References

Bole-Rentel T, Chireshe F and Reeler J (2022). Fuel for the future: A blueprint for the production of sustainable aviation fuel in South Africa. South Africa, Cape Town, South Africa: World Wide Fund for Nature.

Bonnefoy PA and Schaufele R (2022). Placing Costs Associated with LTAG Integrated Scenarios in Context. https://www.icao.int/environmental-protection/Documents/EnvironmentalReports/2022/ENVReport2022_Art100.pdf (Accessed 10 May 2024).

Braun M, Grimme W and Oesingmann K (2024). Pathway to net zero: Reviewing sustainable aviation fuels, environmental impacts and pricing. *Journal of Air Transport Management* 117: 1-13.https://doi.org/10.1016/j.jairtraman.2024.102580

ICAO (2024). Carbon Offsetting and Reduction Scheme for International Aviation (CORSIA). Montreal, Canada: International Civil Aviation Organization.

IEA (2024). Global EV Outlook 2024. Paris, France: International Energy Agency https://www.iea.org/reports/global-ev-outlook-2024

Mollah AS, Rouf A and Rana SM (2021). A study on capital budgeting practices of some selected companies in Bangladesh. *PSU Research Review* 7(2): 137-151. http://dx.doi.org/10.1108/PRR-10-2020-0035.

Mullins D, Botha JP, Mosaka DD, Jurgens FX and Majoro TJ (2014). A manual for cost benefit analysis in South Africa, with specific reference to water resource development. Water Research Commission Report No TT 598/14, Pretoria, Republic of South Africa.

Ndokwana A and Fore S (2018). Economic assessment of bioethanol production from maize in South Africa. *Journal of Engineering, Design and Technology* 16(6): 973-994. https://doi.org/10.1108/JEDT-05-2017-0052.

Pavlenko N, Searle S and Christensen A (2019). The cost of supporting alternative jet fuels in the European Union. The International Council for Clean Transportation (ICCT) working paper 2019-05. Washington, D.C.

SARB (2024). Quarterly Bulletin, June 2024. Pretoria, South Africa: South African Reserve Bank.

Seymour K, Held M, Stolz B, Georges G and Boulouchos K (2024). Future costs of power-to-liquid sustainable aviation fuels produced from hybrid solar PV-wind plants in Europe. *Sustainable Energy and Fuels* 8: 811-825. DOI: 10.1039/d3se00978e.

Tierney S and Bird L (2020). Setting the record straight about renewable energy. World Resources Institute (WRI), Washington DC. https://www.wri.org/insights/setting-record-straight-about-renewable-energy (Accessed 15 June 2024).

Watson MJ, Machado PG, da Silva AV, Saltar Y, Ribeiro CO, Nascimento CAO and Dowling AW (2024). Sustainable aviation fuel technologies, costs, emissions, policies and markets: A critical review. *Journal of Cleaner Production* 449: 141472. https://doi.org/10.1016/j.jclepro.2024.141472

SHORT COMMUNICATION

AN ANALYSIS OF THE FINANCIAL VIABILITY AND ENVIRONMENTAL IMPACT OF FOOD PRODUCTS, BIOCHEMICALS, BIOFUELS AND BIOMATERIALS AS POTENTIAL DIVERSIFICATION STRATEGIES FOR THE SUGAR INDUSTRY

Louw, J[1], Louw, JP[1], Brobbey MS[1], Foxon, KM[2] and Görgens JF[1]

[1]Department of Chemical Engineering, Stellenbosch University, Stellenbosch, South Africa
[2]Sugar Milling Research Institute NPC, c/o University of KwaZulu-Natal, Durban, South Africa

jeannelouw@sun.ac.za, jplouw@sun.ac.za, 24661724@sun.ac.za, kfoxon@smri.org, jgorgens@sun.ac.za

Abstract

The Sugar Value Chain Master Plan 2030 was implemented with the goal of transforming the local sugar industry to achieve sustainability for its stakeholders, the bioeconomy, and society at large. A key component of the future sustainability of the local sugar industry is finding economically-viable diversification options. This has been the focus of previous and current projects conducted by the Sugar Milling Research Institute (SMRI) and the NRF Research Chair in Sugarcane Biorefineries at Stellenbosch University. The economic performance of over forty (40) possible products that can be made from A-molasses, such as biochemicals, biofuels, biopolymers and food-type products, was compared by using standardised methods for process simulations, techno-economic assessment, and life-cycle analysis. The Aspen Plus® process simulation tool was used to generate mass and energy balance data for each production process. The mass and energy balance data were used to conduct an economic analysis for each potential diversification product. The Minimum Selling Price (MSP) for a reasonable return on investment in relation to the product's current market price was used to assess its economic viability. The cradle-to-gate system boundary approach was used to estimate the greenhouse gas (GHG) emissions associated with 20 of these products. The estimated MSPs range from nearly 0% to 400% of the market price, depending on the product, with more than 15 products having MSPs lower than 150% of the market price. The estimated GHG emissions ranged between 0.8 and 8.0 CO2eq/kg, with about 40% of the products having GHG emissions lower than 1.0 CO2eq/kg. Identifying economically-viable and environmentally-sustainable products for the diversification of the South African sugar industry should be possible by comparing their economic feasibility and reduction in GHG emissions, compared to fossil-based products. These identified products should be prioritised for further feasibility studies, with the purpose of creating investment opportunities for the South African sugar industry.

Keywords: *Sugarcane biorefinery, product diversification, techno-economic analysis, sustainability*

Introduction

In order to achieve future economic sustainability, sugar mills around the world are responding to the stagnation in traditional markets by diversifying their product portfolios and collaborating on the co-production of value-added bioproducts (food ingredients, biofuels, bioenergy and industrial chemicals) by means of the concept of biorefineries (Rosales-Calderon and Arantes,

2019). Such biorefineries may use by-products and waste streams as feedstocks, including sugarcane bagasse, brown-leaf harvest leftovers, molasses, and occasionally, clarified juice. The diversification of sugarcane processing to produce products with a higher value than the equivalent world market prices for raw sugar has the potential to improve the financial viability of the industry and to make progress towards environmental and social sustainability. The prioritisation and benchmarking of appropriate, economically-feasible bioproducts for diversification is required, in order to direct the available feedstock to potential bioproducts of the highest economic feasibility (Louw *et al.*, 2023).

The economic and environmental performance of a wide number of potential bioproducts that can be produced as feedstock from A-molasses have been considered over the past 3-4 years in various post-graduate projects, as part of the on-going work within the NRF research chair in Sugarcane Biorefineries at the Stellenbosch University under Prof Johann Görgens, most of which having been published in peer-reviewed journals (Amanful et al., 2024; Brobbey et al., 2023; Brobbey et al., 2024; Brobbey et al., 2024; Cronjé et al., 2023; Dogbe et al., 2020; Gouws et al., 2024; Gouws et al., 2024; Klaver et al., 2024; Janus Louw et al., 2024; Janus Louw et al., 2023; Petersen et al., 2024; Phasha et al., 2025; Ratshoshi et al., 2021, 2024; Rode et al., 2024; Sikazwe et al., 2024; Van Heerden et al., 2023; van Heerden et al., 2024). This paper provides a comparison of the economic performance of 40 possible diversification products, as well as the environmental performance of 20 of these products.

Methodology/Approach

Products considered

The bio-products that were considered included big-volume products, such as 1,2-propanediol (1,2-PDO), 1,3-butadiene (1,3-BD), 1,4-butanediol (1,4-BDO), acrylonitrile, acrylic acid, adipic acid, citric acid, ethyl acetate, glycerol, lactic acid, monoethylene glycol (MEG), monosodium glutamate (MSG), polyethylene (PE), polyethylene furanoate (PEF), polyethylene terephthalate (PET), propylene, sorbitol, terephthalic acid and p-xylene. It also included sets of related small-volume items that could be produced as a suite, which include allulose, collagen, erythritol, isomaltulose, short-chain fructo-oligosachharides (scFOS), thaumatin and tryptophan. Lastly, it included small volume items that are already on the market, but which have a lot of room for growth in market sizes, such as 1,3-propanediol (1,3-PDO), 2,3-butanediol (2,3-BDO), 2,5-furandicarboxylic acid (2,5-FDCA), 5-hydroxymethylfurfural (5-HMF), 3-hydroxypropionic acid (3-HP), butyric acid, ethyl lactate, glucaric acid, isosorbide, itaconic acid, levulinic acid, muconic acid, polybutylene adipate terephthalate (PBAT), polybutylene succinate (PBS), succinic acid, polyhydroxyalkanoates (PHA) and polylactic acid (PLA).

Economic modelling

The overall economic benchmarking methodology is shown in Figure *1*.

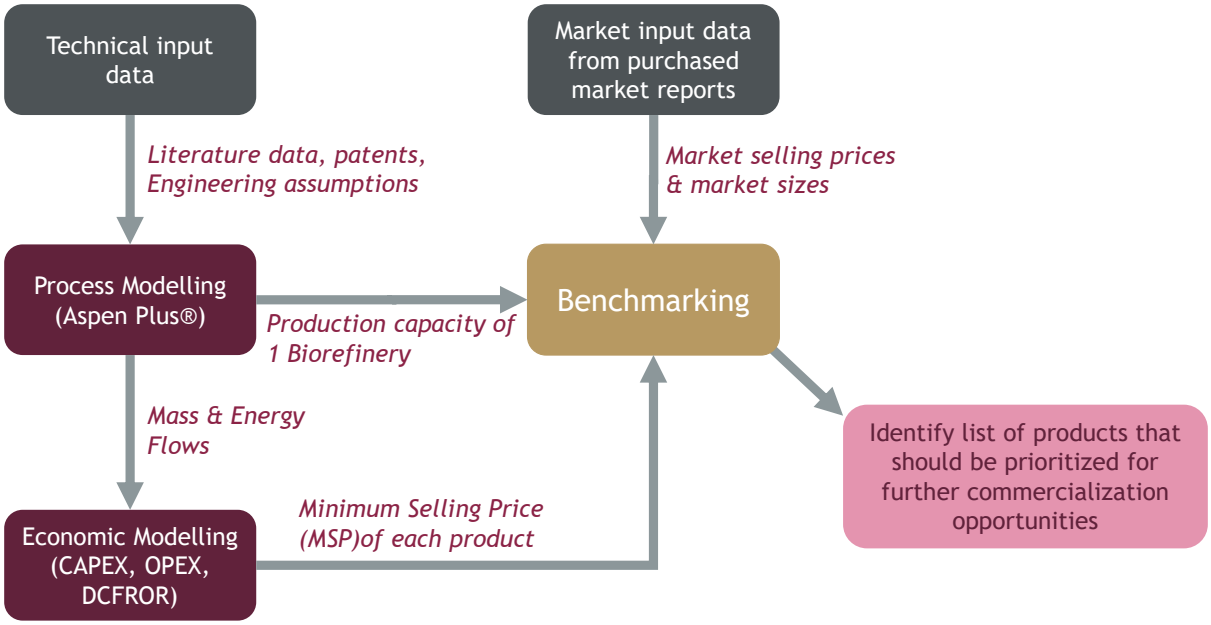


Figure 1. Overall economic benchmarking methodology

A process model for the production process of each product that was considered was built in Aspen Plus®. The biorefinery (bioproduct production process) was designed to be annexed to a typical existing sugar mill with a cane-crushing capacity of 300 t/h. A-molasses diverted from the sugar mill was considered as feedstock to the biorefinery. The biorefinery was designed to be energy-self-sufficient, employing bagasse and harvesting residues (in cases where the amount of bagasse is not sufficient to meet the energy demand of the biorefinery and sugar mill) as energy sources, to produce steam and electricity for both the sugar mill and the biorefinery. The production process for each bioproduct was based on technical information from publicly-available literature sources. Each biorefinery scenario was created by using comparable technical input assumptions, such as the feedstock type, flow rate and annual operating time (Table *1*). All of the A-molasses from 1 sugar mill was diverted to the biorefinery as feedstock, making the biorefinery scale A-molasses restricted.

Table 1. Technical and economic input data

Parameter	**Value**
Annual production time	5 000 hours
Feedstock	A-molasses
A-molasses flow rate	25.4 tonnes/h
Base year of analysis	2023
Discount rate	20% (real)
Project lifetime	25 years
Depreciation method	Straight line over 5 years
Plant location	South Africa

The mass and energy flow data that were obtained from the Aspen Plus® process simulations were used to determine the operating and capital costs for each scenario. A Discounted Cash Flow (DCF) analysis was consequently performed for each biorefinery scenario, utilising the same economic input assumptions, such as the base year of study, the anticipated discount rate, the location of the facility, the project lifetime, etc (see Table *1*). From the DCF analysis, the Minimum Selling Price (MSP) of each bioproduct was determined.

The MSP for each bioproduct was compared to the market prices (fossil-based and bio-based, if applicable) which were derived from acquired market reports(Global Market Insights, 2021; Grand View Research, 2021b, 2021d, 2021f, 2021e, 2021g, 2021c, 2021a; Industrial Plastics Market, 2020). In addition, the expected market share that the production from a single biorefinery would occupy was calculated by comparing the annual production rate for each bioproduct to the size of the product's present market. Based on these findings, the bioproducts were ranked by using a combination of each product's market share and the percentage difference between its MSP and market price.

Environmental Assessment

The greenhouse gas (GHG) emissions for each biorefinery scenario were quantified in terms of CO2-equivalent emissions per kilogram of the product produced. The system boundary was defined as cradle-to-gate, where the cradle includes sugarcane cultivation and the gate refers to the biorefinery gate (as shown in Figure 2). Using the CML-IA baseline technique (Version 3.08, EU25), which was created by the Centre of Environmental Sciences (CML) at Leiden University, in partnership with Technische Universität Berlin, a midpoint Life-Cycle Impact Assessment (LCIA) approach was used. The Roundtable on Sustainable Biomaterials (RSB) GHG calculator tool, or pertinent literature, were used to derive the Emission Factors (EFs) for raw materials that were not listed in the SimaPro Eco-invent database. CO_2eq emissions from sugarcane cultivation and milling were allocated between the sugar, A-molasses, and bagasse on an economic basis, upstream of the biorefinery. All emissions from the bioconversion stage were fully allocated to the biorefinery products.

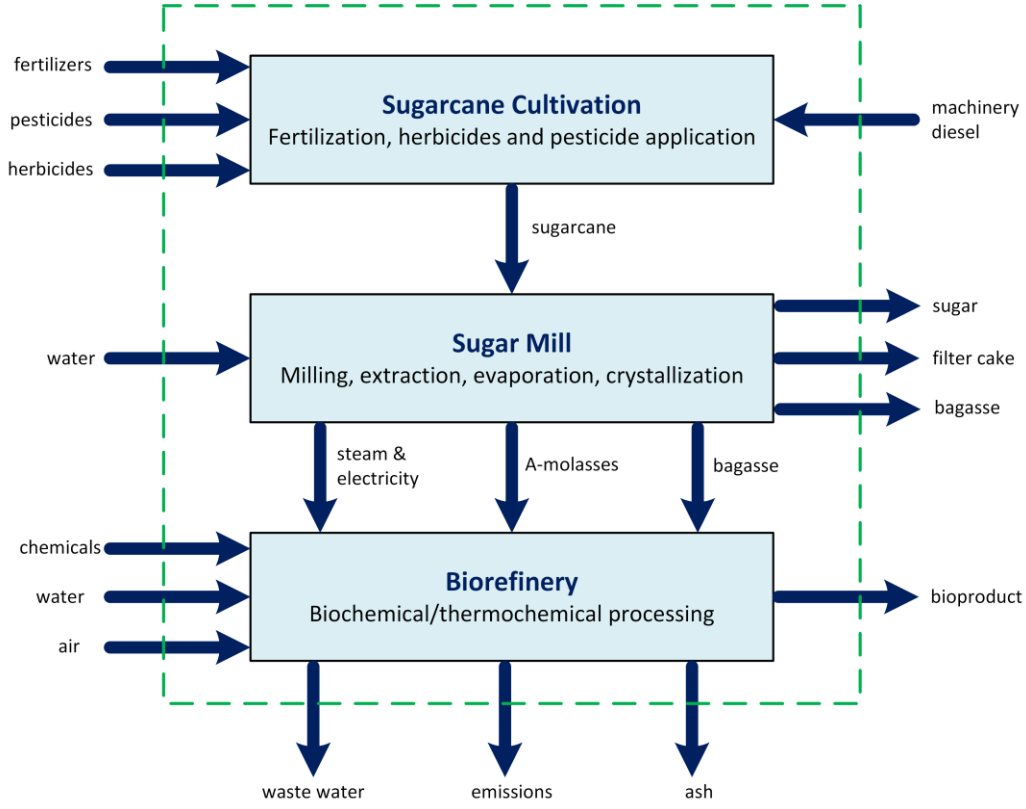
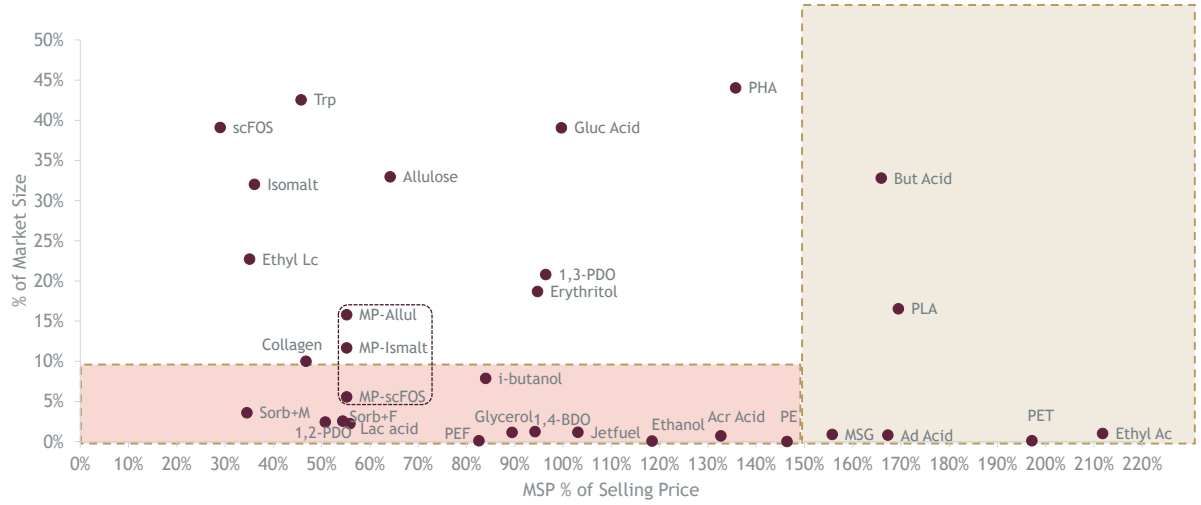


Figure 2. System boundary for GHG emissions calculations

Results and Discussion

Economic Performance Comparison

The MSPs, as a percentage of the market price of each product, are plotted against the production rate as a percentage of the market size that one biorefinery will occupy, if all the A-molasses from one sugar mill is used as feedstock to the biorefinery (see Figure *3*). Products that are not shown on the graph are outside the 50% market size production rate and 220% MSP range and include citric acid, propylene, terephthalic acid, acrylonitrile, 1,3-butadiene, PBS and isosorbide. Products that are considered as possible viable options with MSPs between 0 and 150% of the current selling price, and production rates less than 10% of the market size, include lactic acid, ethanol, 1,4-BDO, isobutanol, sorbitol, aviation fuel, 1,2-PDO, glycerol and acrylic acid. The multi-product sweetener scenario could be viable on a smaller production scale. Products that are currently non-viable (i.e. with MSPs higher than 150% of the market price) include butyric acid, PLA, erythritol, adipic acid, PET and ethyl acetate. If the global market size of ethyl lactate, allulose, isumaltulose, scFOS, tryptophan, glucaric acid, PHA, 1,3-PDO, collagen, isosorbide, PBS and succinic acid increase, these products might be economically-viable diversification options.



Trp: Tryptophan	But Acid: Butyric Acid	Ethyl Lc: Ethyl lactate	MP: Multi-product sweetners	Sorb+M: Sorbitol + Mannitol
Ethyl Ac: Ethyl Acetate	Lac acid: Lactic Acid	Acr Acid: Acrylic Acid	Ad Acid: Adipic Acid	Sorb+F: Sorbitol + fructose

Figure 3. Screening results summary based on economic results and market information

Environmental Performance Comparison

Figure *4* shows the total and non-biogenic GHG emissions for each scenario. The best performing scenarios (non-biogenic CO_{2eq} emissions < 1 kg per kg) include ScFOS, lactic acid, ethanol, ethyl acetate, 1,3 PDO, glycerol, 1,4-BDO, 2,3-BDO and ethyl lactate. These products were mostly produced by biological processes, like fermentation or enzymatic conversion, which often require fewer and less significant chemical inputs. The comparison of the non-biogenic GHG emissions and the total emissions demonstrate how important it is for integrated biorefineries to use biomass as an energy source, in order to achieve low greenhouse gas emissions for bio-based products. At the sugarcane cultivation and milling stage, non-biogenic CO_2eq emissions primarily arise from the use of diesel-powered agricultural machinery, the transport of cane to the mill (by road and rail), the production and transport of agrochemicals

(fertilisers, herbicides and pesticides), as well as the electricity used for irrigation. These typically represent the largest share of the total emissions that are associated with the bioproducts. At the bioconversion stage, the sources of non-biogenic CO_2eq vary by product, but are generally linked to the production of fermentation nutrients, chemical solvents, catalysts and other raw materials. Minor contributions may also result from the small methane releases in vent streams from the wastewater treatment. In the energy generation stage, non-biogenic CO_2eq emissions are typically present as carbon monoxide and methane in boiler stack gases.

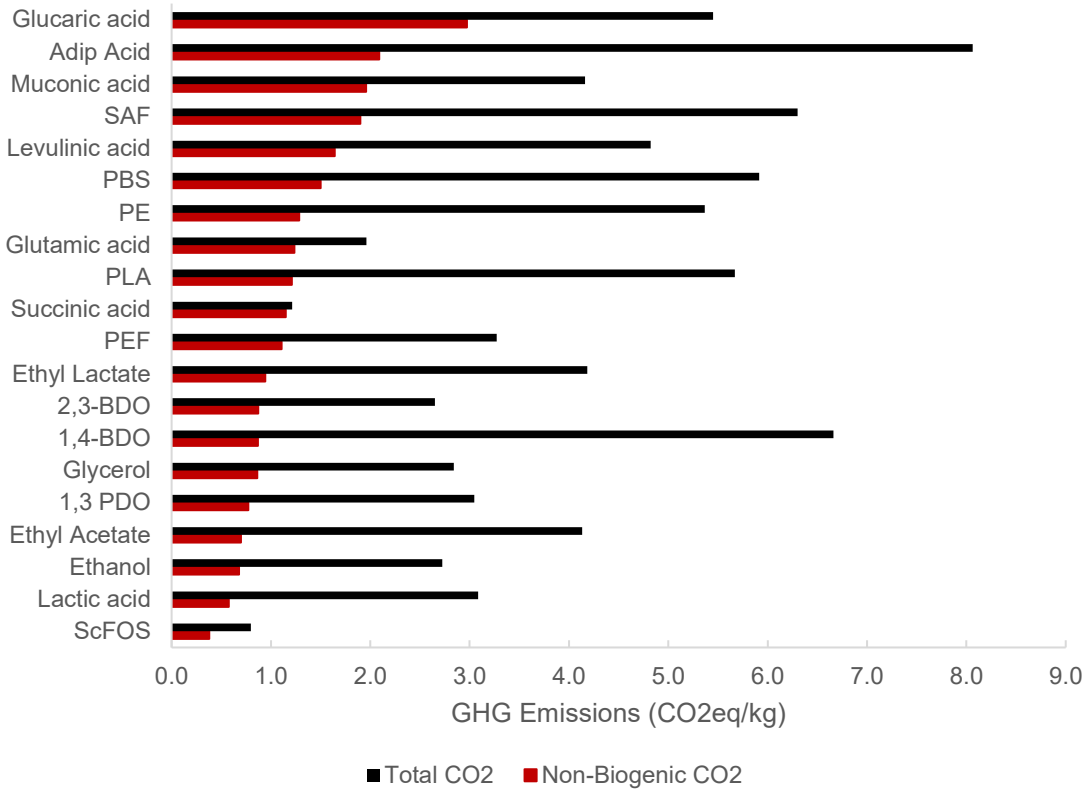


Figure 4. Total and non-biogenic GHG emissions for each scenario

Conclusion

The study demonstrates how a systematic economic benchmarking strategy may be used to select possible diversification products for the South African sugar industry. Short-listed products could be considered for more in-depth and time-consuming feasibility studies and commercial process design. It can also show which markets are most likely to require price premiums for a certain bio-based product to be profitable, and which processes still require technology breakthroughs to increase their economic viability. It also highlights the importance of obtaining accurate market information (the market sizes and selling prices). This work is still on-going within the NRF research chair in Sugarcane Biorefineries at Stellenbosch University. The next step will be to complete the GHG emissions calculations for all of the 40 products considered in the economic analysis and to rank these products through a multi-criteria analysis, in order to determine which products will be the most sustainable (economical and environmental) diversification opportunities.

Acknowledgments

This study was financially supported by the Chemical Engineering Department of Stellenbosch University, as well as the National Research Foundation (NRF), Grant Number 114614. The authors also acknowledge Aspen Technology Inc. for providing the Aspen Plus® academic license that was used for the process simulations in the study. We also acknowledge SimaPro for the LCA software academic licence.

References

Amanful, B. *et al.* (2024) 'Stochastic techno-economic analysis for the co-production of alternative sweeteners in sugarcane biorefineries', *Food and Bioproducts Processing*, 143, pp. 9–20. Available at: https://doi.org/10.1016/j.fbp.2023.10.006.

Brobbey, M.S. *et al.* (2024) 'Effect of production scale on the techno-economic viability and environmental life cycle analysis of lactic acid production in a sugarcane biorefinery', *Food and Bioproducts Processing*, 148, pp. 269–284. Available at: https://doi.org/10.1016/J.FBP.2024.09.020.

Brobbey, M.S., Louw, J. and Görgens, J.F. (2023) 'Biobased acrylic acid production in a sugarcane biorefinery: A techno-economic assessment using lactic acid, 3-hydroxypropionic acid and glycerol as intermediates', *Chemical Engineering Research and Design*, 193, pp. 367–382. Available at: https://doi.org/https://doi.org/10.1016/j.cherd.2023.03.034.

Brobbey, M.S., Louw, J. and Görgens, J.F. (2024) 'Biobased propylene glycol production in a sugarcane biorefinery through lactic acid, glycerol, or sorbitol: A techno-economic and environmental evaluation of intermediates and downstream processing methods', *Biochemical Engineering Journal*, 205. Available at: https://doi.org/10.1016/j.bej.2024.109292.

Cronjé, Y. *et al.* (2023) 'A critical review of multiple alternative pathways for the production of a high-value bioproduct from sugarcane mill byproducts: the case of adipic acid', *Biofuel Research Journal*. Green Wave Publishing of Canada, pp. 1933–1947. Available at: https://doi.org/10.18331/BRJ2023.10.3.5.

Dogbe, E.S., Mandegari, M. and Görgens, J.F. (2020) 'Revitalizing the sugarcane industry by adding value to A-molasses in biorefineries', *Biofuels, Bioproducts and Biorefining*, 14(5), pp. 1089–1104. Available at: https://doi.org/10.1002/bbb.2122.

Global Market Insigths (2021) *Global Short-chain Fructooligosaccharides Market*.

Gouws, M.R., Dogbe, E.S., *et al.* (2024) 'Comparative techno-economics of 1,3-butadiene production from sugarcane feedstocks via ethanol or 2,3-butanediol as intermediates', *Industrial Crops and Products*, 208, p. 117872. Available at: https://doi.org/10.1016/J.INDCROP.2023.117872.

Gouws, M.R., Bosman, C.E., *et al.* (2024) 'Comparative techno-economics of 2,3-butanediol, polyhydroxybutyrate and citric acid production in a biorefinery using 1G and 1G2G sugarcane-based feedstocks', *Chemical Engineering Science*, 286. Available at: https://doi.org/10.1016/j.ces.2023.119649.

Grand View Research (2021a) *Adipic Acid Market*.

Grand View Research (2021b) *Bio-based Platform Chemicals Market*.

Grand View Research (2021c) *Global Ethyl Acetate Market*.

Grand View Research (2021d) *Global Glycerol Market*.

Grand View Research (2021e) *Glutamic Acid Market*.

Grand View Research (2021f) *Lactic Acid Market*.

Grand View Research (2021g) *Polylactic Acid Market*.

vanHeerden, C. *et al.* (2024) 'Techno-economics and environmental assessment of sorbitol and itaconic acid production from sugarcane-based feedstock', *Chemical Engineering Science*, 299, p. 120431. Available at: https://doi.org/10.1016/J.CES.2024.120431.

VanHeerden, C., Farzad, S. and Görgens, J.F. (2023) 'Techno-Economic and Environmental Assessments of 1,3-Propanediol and Xylooligosaccharide Production Annexed to a Typical Sugar Mill', *ACS Sustainable Chemistry and Engineering*, 11(46), pp. 16453–16468. Available at: https://doi.org/10.1021/acssuschemeng.3c03338.

Grand View Research (2020) *Industrial Plastics Market*.

Klaver, M. *et al.* (2024) 'Economic validation and comparison of microbial tryptophan, erythritol and collagen production in an integrated sugarcane biorefinery', *Biochemical Engineering Journal*, 212, p. 109505. Available at: https://doi.org/10.1016/J.BEJ.2024.109505.

Louw, J. *et al.* (2023) 'Prioritisation of biomass-derived products for biorefineries based on economic feasibility: A review on the comparability of techno-economic assessment results', *Renewable and Sustainable Energy Reviews*, 188. Available at: https://doi.org/10.1016/j.rser.2023.113840.

Louw, J., Farzad, S. and Görgens, J.F. (2023) 'Polyethylene furanoate: technoeconomic analysis of biobased production', *Biofuels, Bioproducts and Biorefining*, 17(1), pp. 135–152. Available at: https://doi.org/10.1002/bbb.2430.

Louw, J., Farzad, S. and Görgens, J.F. (2024) 'Production of biobased polyethylene terephthalate and its precursors for diversification in the global sugarcane industry', *Biochemical Engineering Journal*, 210, p. 109404. Available at: https://doi.org/10.1016/J.BEJ.2024.109404.

Petersen, A.M., Louw, J. and Görgens, J.F. (2024) 'Economic and Environmental Comparison of the Monosodium Glutamate (MSG) Production Processes from A-Molasses in an Integrated Sugarcane Biorefinery', *International Journal of Chemical Engineering*, 2024(1), p. 2077515. Available at: https://doi.org/10.1155/2024/2077515.

Phasha, M.J., Petersen, A.M. and Görgens, J.F. (2025) 'Process flowsheet development for bio-ethyl acetate production from sugar mill feedstocks: A techno-economic approach', *Chemical Engineering Research and Design*, 217, pp. 252–266. Available at: https://doi.org/10.1016/J.CHERD.2025.03.026.

Ratshoshi, B.K., Farzad, S. and Görgens, J.F. (2021) 'Techno-economic assessment of polylactic acid and polybutylene succinate production in an integrated sugarcane biorefinery', *Biofuels, Bioproducts and Biorefining*, 15(6), pp. 1871–1887. Available at: https://doi.org/10.1002/BBB.2287.

Ratshoshi, B.K., Farzad, S. and Görgens, J.F. (2024) 'A techno-economic study of Polybutylene adipate terephthalate (PBAT) production from molasses in an integrated

sugarcane biorefinery', *Food and Bioproducts Processing*, 145, pp. 11–20. Available at: https://doi.org/10.1016/j.fbp.2024.01.011.

Rode, L. *et al.* (2024) 'Biobased propylene and acrylonitrile production in a sugarcane biorefinery: Identification of preferred production routes via techno-economic and environmental assessments', *Biomass and Bioenergy*, 190, p. 107399. Available at: https://doi.org/10.1016/J.BIOMBIOE.2024.107399.

Rosales-Calderon, O. and Arantes, V. (2019) 'A review on commercial-scale high-value products that can be produced alongside cellulosic ethanol', *Biotechnology for Biofuels*, 12(1). Available at: https://doi.org/10.1186/S13068-019-1529-1.

Sikazwe, M.K., Louw, J. and Görgens, J.F. (2024) 'Microbe and bioprocess performances for sustainable production of biobased 2,3-butanediol in a sugarcane biorefinery; a technoeconomic and environmental analysis', *Clean Technologies and Environmental Policy*, 26, pp. 4505–4519. Available at: https://doi.org/10.1007/s10098-024-02843-w.

SHORT COMMUNICATION

SUSTAINABLE ACRYLIC ACID OR PROPYLENE GLYCOL PRODUCTION IN A SUGARCANE BIOREFINERY: A TECHNO-ECONOMIC AND ENVIRONMENTAL ANALYSIS

Brobbey MS[1], Louw J[1] and Gorgens J[1]

[1]Department of Chemical Engineering, Stellenbosch University, South Africa

brobbey@sun.ac.za, jeannelouw@sun.ac.za, jgorgens@sun.ac.za

Abstract

The potential to produce sustainable Acrylic Acid (AA) or Propylene Glycol (PG) in biorefineries annexed to existing sugar mills in South Africa was evaluated based on the conversion of the available feedstocks into Lactic Acid (LA) as the platform chemical. Both A-molasses only (1G) and a combination of A-molasses with lignocelluloses (bagasse and harvesting residues, 1G2G) as feedstocks were investigated, which resulted in four biorefinery process scenarios, i.e. 1G AA, 1G2G AA, 1G PG and 1G2G PG. These scenarios were simulated in Aspen Plus® to provide technical inputs for an economic feasibility assessment, by using a discounted cash flow analysis, while the environmental performance was evaluated by using a Life Cycle Assessment (LCA) in SimaPro®.

Propylene glycol production had a higher energy demand, but a greater product yield, than AA. Subsequently, the Minimum Selling Prices (MSPs) were 1,991 US$.t^{-1} for PG and 2,059 US$.t^{-1} for AA, with Internal Rates of Return (IRRs) around 16%. Adding 2G feedstocks (1G2G scenarios) resulted in a 4% and 17% increase in MSPs of AA and PG, respectively, which translated into green price premiums of 11% for PG and 29% for AA, compared to fossil-based market prices. For the environmental assessment, the Global Warming Potentials (GWPs) of 0.95 $kg_{CO2\ eq}$/ kg_{PG} for 1G PG and 0.70 $kg_{CO2\ eq}$/ kg_{PG} for 1G2G PG production were most notable, and lower than the 1.09$_{kg\ CO2\ eq}$/ kg_{AA} for 1G AA and 0.92 $kg_{CO2\ eq}$/ kg_{AA} for 1G2G AA. The GWPs were lower than the fossil-based products that they would potentially replace. The integration of lignocellulosic residues with A-molasses in 1G2G substantially lowered the environmental impacts per kg of the product and, combined with its competitive economic performance, it positioned them as the viable pathways for sustainable chemical production in South Africa.

Keywords: A-molasses, biorefinery, techno-economic analysis, acrylic acid, propylene glycol, lactic acid

Introduction

In recent years, there has been an increased sense of urgency to transition away from fossil resources, which has given rise to significant interest in the development of integrated biorefineries that are capable of converting biomass into value-added products, such as biofuels, biochemicals and biomaterials (Mandegari *et al.*, 2017; Ntimbani *et al.*, 2021). Sugarcane is among the most extensively studied biomass resources due to its high efficiency in converting solar energy and its ability to generate both sugar-rich and lignocellulosic residues that are suitable for biorefinery processes (Rosales-Calderon & Arantes, 2019).

However, the global sugar industry faces considerable economic challenges due to the declining demand and volatile international prices, which have prompted the pursuit of more diversified product portfolios to enhance the sustainability and profitability of the industry (Farzad *et al*., 2017).

Integrating biorefineries into existing sugar mill facilities offers a pathway for revitalising the sugar industry, particularly in countries like South Africa, where sugarcane is a major agricultural commodity (Dogbe *et al*., 2020). By modifying the traditional three-stage crystallisation process to yield A-molasses, a sucrose-rich by-product, sugar mills can feed a 1G biorefinery, while second-generation (2G) lignocellulosic resources, such as bagasse and harvesting residues, can also be considered for further valorisation. This co-utilisation model maximises the biomass value, reduces the dependence on volatile sugar markets and enables the production of high-value chemicals (Dogbe *et al*., 2020).

Acrylic Acid (AA) and Propylene Glycol (PG) are two value-added chemicals that can be considered for manufacture in sugarcane biorefineries owing to their extensive industrial applications. The global demand of AA was estimated to be 5 750 kilo tons in 2014 and it is projected to reach a market value of US$ 20 billion by 2031 (Grand View Research, 2016). PG has a notable global market size, with a projected market value of 4.7 billion US$ by 2024, at a Cumulative Annual Growth Rate (CAGR) of 4.4% (Gonzalez-Garay *et al.*, 2017). AA is widely used in the manufacture of adhesives, paints and textiles, while PG is used in the pharmaceutical, food and polymer industries, due to its favourable physicochemical properties and low toxicity. Currently, both AA and PG are produced primarily from fossil-based feedstocks through energy-intensive processes and high emissions, about 4.0 $kg_{CO2\ eq}$/ kg_{PG} for PG and as high as 7.7 $kg_{CO2\ eq}$/ kg_{AA} for AA (Brobbey *et al*., 2023, 2024; Buitelaar *et al*., 2020; Gonzalez-Garay *et al*., 2017; Louw *et al*., 2023).

This study compares the economic performance and environmental impacts associated with producing AA or PG in an annexed sugarcane biorefinery, where sugar-containing feedstocks are first fermented into lactic acid, prior to further chemical conversion into AA or PG. By integrating A-molasses and lignocellulosic residues in the production of LA-derived AA and PG, the study aims to determine whether biomass diversification enhances the competitiveness and sustainability of the South African sugarcane industry. Ultimately, the work provides strategic insights into the preferred chemical products that would offer the most attractive investments in biorefineries in a circular, fossil-independent bioeconomy.

Methodology/Approach

This study evaluates four biorefinery configurations annexed to a typical existing sugar mill in South Africa. The mill has a cane-crushing capacity of 300 $t \cdot h^{-1}$ and produces 38.4 $t \cdot h^{-1}$ of raw sugar and 11.6 $t \cdot h^{-1}$ of C-molasses (Dogbe *et al.*, 2018). In these configurations, A-molasses (25.4 $t \cdot h^{-1}$) was diverted as feedstock to the biorefinery, which reduced the sugar production and eliminated C-molasses as co-product. The A-molasses stream considered in the simulation has a composition of 54 wt.% sucrose, 22 wt.% water, 12 wt.% fructose and 12 wt.% glucose (Dogbe *et al.*, 2018). In addition, the mill provides surplus utilities, including 15.0 $t \cdot h^{-1}$ of high-pressure steam, 15.5 $t \cdot h^{-1}$ of low-pressure steam and 1.86 MW of electricity, to the biorefinery, which is made available due to the reduced sugar flowrate by not extracting the sugar from A-molasses. Lignocellulosic residues (65 $t \cdot h^{-1}$ dry matter) in the form of bagasse (45 $t \cdot h^{-1}$ with a moisture content of 50.8%) and field residues (20 $t \cdot h^{-1}$ dry matter with

a moisture content of 14.9%) were also available. A left-over amount of 21.6 $t \cdot h^{-1}$ DM bagasse remains after meeting the energy needs of the mill, with the field residues being unused (Dogbe *et al*., 2018; Farzad *et al*., 2017). A green-cane-harvesting strategy is assumed to preserve the soil fertility by leaving the tops (green leaves) in the field and only making the brown-leaf component of sugarcane harvesting residues available (Farzad *et al*., 2017). The sugar mill and the biorefinery are energy self-sufficient, with no external fuel used to provide energy. Four scenarios were developed based on two types of feedstocks: A-molasses only (1G) and a combination of A-molasses with lignocellulosic residues (bagasse and harvesting residues; 1G2G) namely, 1G acrylic acid (AA) (Figure 1a), 1G2G AA (Figure 1b), 1G propylene glycol (PG) (Figure 1c) and 1G2G PG (Figure 1d), which are based on Lactic Acid (LA) as an intermediate.

Process simulations were developed by using Aspen Plus® v14. The feedstock compositions, conversion yields and operating conditions were based on literature data and previous studies (Brobbey *et al*., 2023, 2024; Humbird *et al*., 2011). Where necessary, missing component data were supplemented by using user-defined components and external sources.

Process description

1G LA production (Figure 1) involved hydrolysing the A-molasses to glucose and fructose with a 98% yield (Cronjé *et al*., 2023), followed by fermentation, using *Lactobacillus delbrueckii Uc-3*, with a LA yield of 0.95 $g.g^{-1}$ (Dumbrepatil *et al.,* 2008). Biomass was removed by centrifugation and residual sugars were eliminated via membrane filtration. In the 1G2G scenarios, lignocellulose was pretreated by using steam explosion followed by enzymatic hydrolysis with an overall yield of 60.4 g combined sugar/100 g DM sugarcane lignocellulose (Nieder-Heitmann *et al*., 2020), which resulted in a 2G sugar stream. Separate fermenters (Figures 1b, d) were used for the 1G and 2G sugar streams to optimise the yields, as a suitable strain that can efficiently co-ferment both the molasses and lignocellulose-derived sugars, to produce LA with high titres that are acceptable for industrial application, but which are not yet available (Ratshoshi *et al*., 2021). The combined LA broth was then centrifuged prior to further processing. A bypass ratio was used to allocate a portion of the available lignocelluloses to process energy generation, while only the remaining portion was processed for pretreatment-hydrolysis-fermentation, to ensure the sugar mill and biorefinery are energy self-sufficient.

For AA production (Figures 1a, b), the crude LA stream was diluted to 80 wt.% water and dehydrated in a fixed-bed reactor at 375°C and 26 bar, using phosphate-based catalysts, with yield of 0.85 $g \cdot g^{-1}$ (Godlewski *et al*., 2018; Lingoes & Collias, 2018). The reactor output underwent multistage separation, including solvent extraction with ethyl acetate and distillation, to achieve >99 wt.% AA purity. The waste solvent was recovered and the remaining wastewater treated onsite. PG production (Figures 1c, d) involved concentrating LA to 50 wt.%, then hydrogenating it at 200°C and 7.2 bar over a Cu/SiO_2 catalyst with a yield of 0.882 $g \cdot g^{-1}$ (Cortright *et al*., 2002). Hydrogen was recycled to maintain a molar ratio of 146:1. The product stream was purified by using two-stage distillation to recover PG at >99 wt.% purity.

An onsite Wastewater Treatment (WWT, Figure 1) system, which featured anaerobic digestion for biogas recovery, aerobic digestion and a reverse osmosis unit for water recycling, was included in all scenarios. Biogas was used for electricity generation or hydrogen production, depending on the scenario. Sludge was either combusted or processed for additional energy recovery.

Economic and environmental assessment

An economic analysis used mass and energy data from the Aspen Plus® simulations to estimate the equipment size and cost. The capital and operating costs were derived from literature and scaled to the plant year of 2021, using Chemical Engineering Plant Construction Index (CEPCI) values (Davis *et al*., 2016; Dutta *et al*., 2016). A summary of the main parameters used in the economics is given in Table 1. A discounted cash flow method was applied to calculate the Minimum Selling Prices (MSPs), the Internal Rate of Return (IRR), as well as the required green price premiums, compared to the market prices for fossil-based products (Expert Market Research, 2023).

The goal of the LCA was to evaluate and compare the environmental impacts of producing AA and PG from LA that is derived from A-molasses only, or from a combination of A-molasses and lignocelluloses. The functional unit was defined as the production of a 1 kg of product. A cradle-to-biorefinery-gate system boundary was used, including sugarcane cultivation, milling, Wastewater Treatment (WWT), Combined Heat and Power (CHP) generation, and AA or PG production. An economic allocation was used to allocate the environmental burdens for sugar, A-molasses, bagasse and filter cake, with the inventory data for cane cultivation sourced from Farzad *et al.* (2017). Mass and energy data for the biorefinery and WWT were derived from Aspen Plus® simulations. The LCA was conducted using SimaPro® (V9.4.0.2) with the CML-IA baseline v3.08 method with few impact categories considered in this study, namely, abiotic depletion, the Global Warming Potential (GWP_{100a}) and Ozone Depletion Layer (ODP). The off-gas from the hydrogen production section in PG production and the flue gas after energy generation for both scenarios was treated as emissions to air and accounted for in the analysis. Similarly, the solid residues and sludge from the wastewater treatment section were modelled as municipal sludge waste and also accounted for in the analysis.

Table 1. Main economic analysis parameters

Parameter	Value	References
Annual operating hours	5000 h	
Project life	25 years	
Discount rate	20%	
Equity	100%	
Income tax rate	28%	
Depreciation	Straight line over 5 years	
Salvage value	0	
Cash flow calculation basis (IRR method)	2 years	
Start-up time	2 years	
First year capacity (% design)	50%	
Second year capacity (% design)	75%	
Cost year	2021	
CEPCI (2021)	776.3	Towering Skills (ToweringSkills, 2023)
A-molasses cost US$.t^{-1}	199.6[2]	Dogbe *et al. (Dogbe et al*., 2019)
Bagasse cost US$.t^{-1}	29.96[2]	Dogbe *et al.* (Dogbe *et al*., 2019)
Ethyl acetate US$.t^{-1}	1,450	Okoro *et al.* (Okoro *et al*., 2022)
Triethylamine US$.t^{-1}	1,500	Ratshoshi *et al.* (Ratshoshi *et al*., 2021)
$Mg(OH)_2$ cost US$.t^{-1}	300	Mandegari *et al.* (2017)
Hydrogen US$.t^{-1}	4,780[3]	Statista (2021)
Phosphate catalyst US$.t^{-1}	5,180[1]	
Cu/SiO_2 catalyst US$.t^{-1}	9,280[1]	

[1] Estimated using composition from experiment and materials library from CatCost (catcost.chemcatbio.org/)
[2] Costs are recalculated for the new plant year of 2021 from a study by Dogbe *et al.* (*et al*2019).
[3]Green hydrogen cost estimated as an average of price obtained from www.statista.com

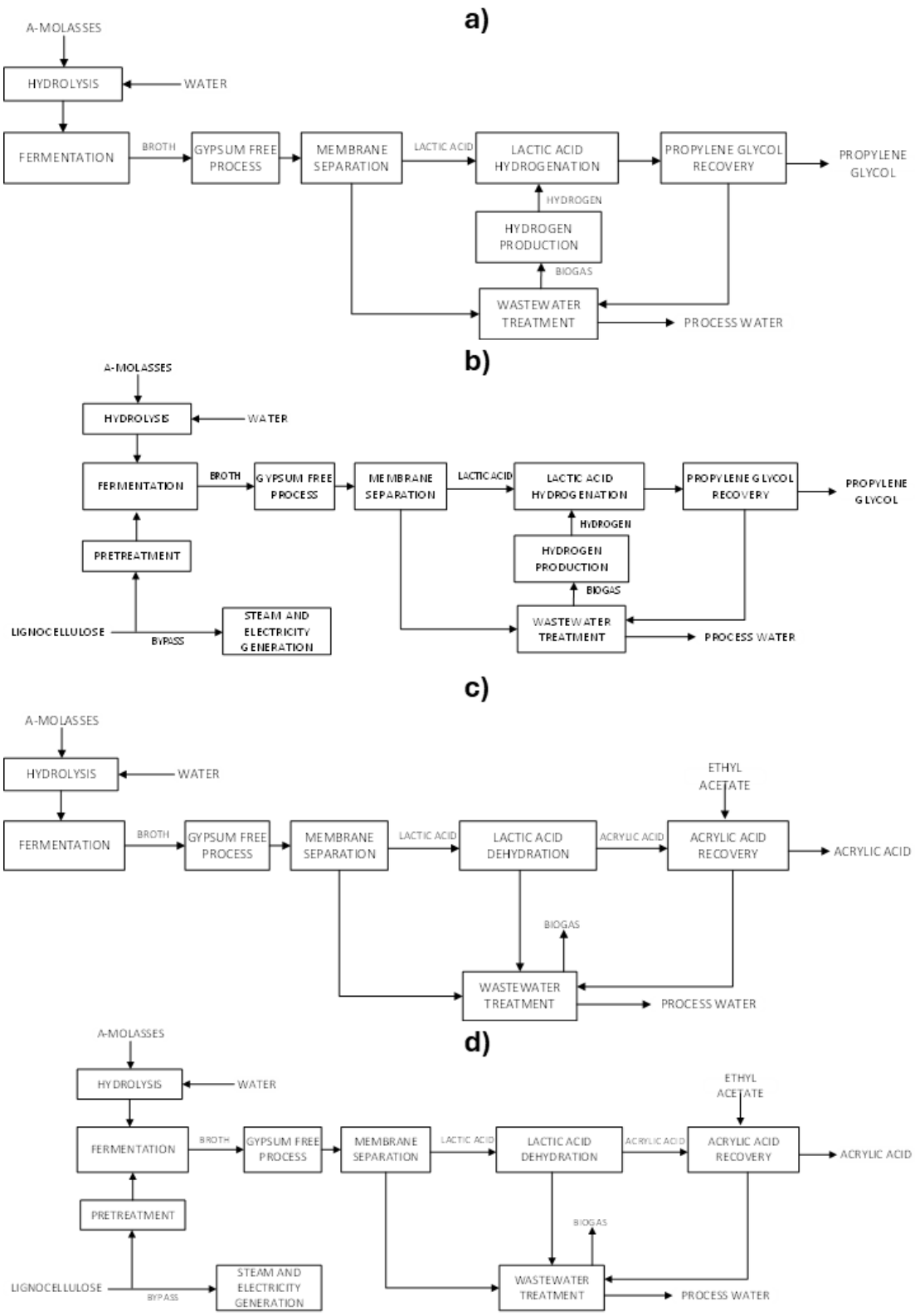


Figure 1. Process flow diagram for (a) 1G AA, (b) 1G2G AA (c) 1G PG and (d) 1G2G PG

Results and Discussion

Mass and energy balance

The mass and energy results (Table 2) showed that PG scenarios (1G PG and 1G2G PG) produced between ~13-20% more of the final product for the 1G and 1G2G systems, compared to the AA scenarios. Despite identical Lactic Acid (LA) yields from the A-molasses, the higher final yield of PG on LA (0.88 g/g) for PG, compared to 0.85 g/g for AA, allowed for the increased annual PG production. While 1G PG achieved the highest yield (0.49 g/g of feedstock), incorporating the lignocellulosic feedstock (2G) reduced the overall yields, due to its lower sugar yield (0.60 g/g dry matter of lignocellulose).

Table 2. Summary results for the four biorefinery scenarios

Parameter	1G AA	1G2G AA	1G PG	1G2G PG
A-molasses feed [a], $t.h^{-1}$	25.4	25.4	25.4	25.4
Total bagasse available [a], $t.h^{-1}$	43.9	43.9	43.9	43.9
Bagasse used as feed		40.4	-	27.9
Bagasse used for energy	27.8	3.5	43.9	16.1
Brown leaves rate [a], $t.h^{-1}$	23.5	23.5	23.5	23.5
Brown leaves used as feed	-	-	-	-
Brown leaves used for energy	-	23.5	12.6	23.5
Product rate, $t.h^{-1}$	10.4	13.7	12.6	15.6
Overall yield, $g_{product}/g_{feed}$	0.41	0.21	0.49	0.29
Heating Demand, MW	33.1	63.1	17.8	55.4
Cooling Demand, MW	42.6	50.7	88.2	24.7
Electricity Demand, MW	3.2	6.2	15.5	13.6
CAPEX, Million US$	137	359	134	361
OPEX, $US\$.y^{-1}$	54	70	55	73
MSP, $US\$.t^{-1}$	2,058	2,404	1,991	2,065
IRR, % at market price	16	12	17	16
Green Premium	11	29	10	11
Abiotic depletion, $MJ/kg_{product}$	16.23	13.55	11.13	9.51
GWP100a, kg CO_2 eq./$kg_{product}$	1.09	0.92	0.95	0.70
ODP, g CFC-11 eq./$kg_{product}$	1.98×10^{-4}	1.73×10^{-4}	1.68×10^{-4}	1.38×10^{-4}

[a] Flowrate given in wet basis

A closer look at the energy demands showed that PG production demanded more utilities, particularly for cooling and electricity. The 1G PG scenario had a cooling demand that was 121% higher than that of 1G AA, due to hydrogen compression and recycling requirements. However, 1G2G PG benefited from heat integration by lowering the cooling and electricity demand by 50% and 30%, respectively (data not shown). In contrast, AA production was more heat-intensive, due to the distillation requirement to break the azeotrope, with 12GG AA exhibiting the highest heat demand (see Table 2).

Economic assessment

The CAPEX for the scenarios ranged from US$ 134-361 million, with higher costs observed for the 1G2G configurations, due to additional pretreatment requirements. Notably, AA purification was >100% more expensive than PG, due to the complex solvent extraction and distillation purification configuration. Hydrogen production represented 7-9% of the equipment cost for PG production.

The operating costs (OPEX) were primarily driven by feedstock, accounting for 35-47%, with the use of lignocellulose increasing the costs in 1G2G systems. The chemicals and nutrients used in fermentation also constituted a significant share (20-35%). AA scenarios incurred additional solvent costs (ethyl acetate), while PG required hydrogen procurement (~2% of OPEX). The fixed operating costs were generally higher for 1G2G setups, due to the added labour and maintenance demands.

The Minimum Selling Price (MSP) was lowest for 1G PG (1,991 US$.$t^{-1}$), followed by 1G AA (2,058 US$.$t^{-1}$). 1G configurations demonstrated a higher profitability with IRRs of 16-17%, requiring green price premiums of 10 and 11% for PG and AA, respectively. The 1G2G process configurations had IRRs of 12 and 16% for AA and PG, respectively, demonstrating the financial competitiveness of these configurations (see Table 1). For PG production scenarios, the green price premium for 1G2G AA was 18% higher than its 1G counterpart. The range of green price premiums (12 to 17%) were similar to those reported for other industrial green chemicals, which indicated that both AA and PG from the LA platform were economically viable. However, for the 1G2G scenarios, the production of PG performed better than AA production.

Environmental performances

The environmental impact analysis (Table 1) indicated that the 1G or 1G2G scenarios for AA and PG had similar burdens across the categories investigated per kg of product. A-molasses contributed significantly (>20%) to the categories, largely due to the fossil fuel emissions during sugarcane processing. This resulted mainly from the harvesting stage, where fertilizers and the transport of the harvested cane results in the emissions, which is further accounted for by using the economic allocation (Farzad *et al*., 2017; Nieder-Heitmann *et al.*, 2019). Incorporating 2G feedstock reduced the burdens by 12-17% because of the higher product throughput. 1G2G scenarios demonstrated environmental advantages, showing reduced Global Warming Potentials (GWPs) of 0.92 kg $_{CO_2eq.}$/kg $_{product}$ and 0.70 kg $_{CO_2\ eq.}$/kg $_{product}$ for AA and PG, respectively, compared to 1.09 and 0.95 kg $_{CO_2\ eq.}$/kg $_{product}$ for the 1G counterparts. AA scenario had higher emissions (45%, Table 1) for abiotic depletion, due to the use of the ethyl acetate solvent. The GWP of PG production scenarios were lower due to the absence of solvents in the downstream processing, and hydrogen production from the internal biogas in the PG scenarios further reduced the environmental burdens, compared to externally-sourced hydrogen. PG production was subsequently more environmentally preferred, compared to AA, although they are not significantly different. On a product basis, the GWP for PG obtained in the study range from 0.70-0.95 kg$_{CO2\ eq}$/ kg $_{PG}$, which is significantly lower than the emissions of about 4.0 kg$_{CO2\ eq}$/ kg$_{PG}$ reported for fossil-based PG (Nachtergaele *et al*., 2019). For AA production, a range of 0.90-1.09 kg $_{CO2\ eq}$/ kg$_{AA}$ was obtained, which was lower than the reported values of 4.07−7.65 kg $_{CO2\ eq}$/ kg$_{AA}$ for fossil-based AA. The GWPs were lower than the fossil-based products that they would potentially replace.

Conclusion

This study assessed the techno-economic and environmental performance of producing Acrylic Acid (AA) and Propylene Glycol (PG) from Lactic Acid (LA) in A-molasses only (1G) or combined A-molasses and lignocelluloses (1G2G) sugarcane biorefineries. The 1G processes were found to be more economically attractive, with Minimum Selling Prices (MSPs) of 2 059 US$.t^{-1} and 1 991 US$.t^{-1} for AA and PG, respectively, and IRRs of about 16%. The 1G2G configurations had slightly higher MSPs, which translated to reduced IRRs, with AA production being less competitive. However, the integration of lignocellulosic residues in 1G2G scenarios substantially improved the environmental performance, particularly in terms of their Global Warming Potential (GWP), which made these routes more sustainable overall. Despite the slightly-reduced economic competitiveness, the 1G2G configurations present a promising pathway when environmental sustainability is also considered. The 1G2G scenarios offer a viable balance of economic and environmental performance and can be recommended as sustainable option for bio-based chemical production in South Africa.

Acknowledgments

This study was financially supported by the National Research Foundation of South Africa (Grant 114614). The authors also acknowledge Aspen Technology Inc. for providing the Aspen Plus® academic license that was used for the process simulations in the study.

References

Brobbey, M. S., Louw, J., & Görgens, J. F. (2023). Biobased acrylic acid production in a sugarcane biorefinery: A techno-economic assessment using lactic acid, 3-hydroxypropionic acid and glycerol as intermediates. Chemical Engineering Research and Design, 193, 367–382. https://doi.org/10.1016/j.cherd.2023.03.034

Brobbey, M. S., Louw, J., & Görgens, J. F. (2024). Biobased propylene glycol production in a sugarcane biorefinery through lactic acid, glycerol, or sorbitol: A techno-economic and environmental evaluation of intermediates and downstream processing methods. Biochemical Engineering Journal, 205(March), 109292. https://doi.org/10.1016/j.bej.2024.109292

Buitelaar, M. M., Van Daatselaar, E., Van Teijlingen, D. G., Stokvis, H. I., Wendt, J. D., De Sousa Ribeiro, R. J., Brooks, A. M. M., Kamphuis, E. C., Lopez Montoya, S., Van Putten, J. C., Van Der Ham, A. G. J., Van Den Berg, H., & Lange, J. P. (2020). Process Designs for Converting Propylene Glycol to Acrylic Acid via Lactic Acid and Allyl Alcohol. Ind. Eng. Chem. Res., 59(3), 1183–1192. https://doi.org/10.1021/acs.iecr.9b04334

Cortright, R. D., Sanchez-Castillo, M., & Dumesic, J. A. (2002). Conversion of biomass to 1,2-propanediol by selective catalytic hydrogenation of lactic acid over silica-supported copper. Appl. Catal. B, 39(4), 353–359. https://doi.org/10.1016/S0926-3373(02)00121-2

Cronjé, Y., Farzad, S., Mandegari, M., & Görgens, J. F. (2023). A critical review of multiple alternative pathways for the production of a high-value bioproduct from sugarcane mill byproducts: the case of adipic acid. Biofuel Research Journal, 10(3), 1933–1947. https://doi.org/10.18331/BRJ2023.10.3.5

Davis, R., Markham, J., Kinchin, C., Grundl, N., Tan, E., & Humbird, D. (2016). Process Design and Economics for the Production of Algal Biomass: Algal Biomass Production in Open

Pond Systems and Processing Through Dewatering for Downstream Conversion. In National Renewable Energy Laboratory (Issue February). www.nrel.gov/publications

Dogbe, E. S., Mandegari, M. A., & Görgens, J. F. (2018). Exergetic diagnosis and performance analysis of a typical sugar mill based on Aspen Plus® simulation of the process. Energy, 145, 614–625. https://doi.org/10.1016/j.energy.2017.12.134

Dogbe, E. S., Mandegari, M., & Görgens, J. F. (2019). Assessment of the thermodynamic performance improvement of a typical sugar mill through the integration of waste-heat recovery technologies. Appl. Therm. Eng., 158(May), 113768. https://doi.org/10.1016/j.applthermaleng.2019.113768

Dogbe, E. S., Mandegari, M., & Görgens, J. F. (2020). Revitalizing the sugarcane industry by adding value to A-molasses in biorefineries. Biofuels Bioprod. Bioref., 14(5), 1089–1104. https://doi.org/10.1002/bbb.2122

Dumbrepatil, A., Adsul, M., Chaudhari, S., Khire, J., & Gokhale, D. (2008). Utilization of molasses sugar for lactic acid production by Lactobacillus delbrueckii subsp. delbrueckii mutant Uc-3 in batch fermentation. Applied and Environmental Microbiology, 74(1), 333–335. https://doi.org/10.1128/AEM.01595-07

Dutta, A., Schaidle, J. A., Humbird, D., Baddour, F. G., & Sahir, A. (2016). Conceptual Process Design and Techno-Economic Assessment of Ex Situ Catalytic Fast Pyrolysis of Biomass: A Fixed Bed Reactor Implementation Scenario for Future Feasibility. Topics in Catalysis, 59(1), 2–18. https://doi.org/10.1007/s11244-015-0500-z

Farzad, S., Mandegari, M. A., Guo, M., Haigh, K. F., Shah, N., & Görgens, J. F. (2017). Multi-product biorefineries from lignocelluloses: A pathway to revitalisation of the sugar industry? Biotechnology for Biofuels, 10(1), 1–24. https://doi.org/10.1186/s13068-017-0761-9

Godlewski, J. E., Lingoes, J. V., Velasquez, J. E., & Collias, D. I. (2018). Purification of bio-based acrylic acid to crude and glacial acrylic acid (U.S. Patent Application No. US 2018/0127348 A1). The Procter & Gamble Company. https://patents.google.com/patent/US20180127348A1/en

Gonzalez-Garay, A., Gonzalez-Miquel, M., & Guillen-Gosalbez, G. (2017). High-Value Propylene Glycol from Low-Value Biodiesel Glycerol: A Techno-Economic and Environmental Assessment under Uncertainty. ACS Sustainable Chemistry and Engineering, 5(7), 5723–5732. https://doi.org/10.1021/acssuschemeng.7b00286

Grand View Research. (2016). Acrylic Acid Market Size. Grand View Research, Inc. https://www.grandviewresearch.com/industry-analysis/acrylic-acid-market

Humbird, D., Davis, R., Tao, L., Kinchin, C., Hsu, D., Aden, A., Schoen, P., Lukas, J., Olthof, B., Worley, M., Sexton, D., & Dudgeon, D. (2011). Process design and economics for conversion of lignocellulosic biomass to ethanol. NREL Technical Report NREL/TP-5100-51400, 303(May 2011), 275–3000. https://doi.org/10.4324/9780429290602-8

Lingoes, J. V., & Collias, D. I. (2018). Catalytic conversion of lactic acid to acrylic acid (US 9 , 926 , 256 B2). United States Patent.

Louw, J., Dogbe, E. S., Yang, B., & Görgens, J. F. (2023). Prioritisation of biomass-derived products for biorefineries based on economic feasibility: A review on the comparability of techno-economic assessment results. Renewable and Sustainable Energy Reviews, 188(September). https://doi.org/10.1016/j.rser.2023.113840

Mandegari, M. A., Farzad, S., & Görgens, J. F. (2017). Recent trends on techno-economic assessment (TEA) of sugarcane biorefineries. Biofuel Res. J., 4(3), 704–712. https://doi.org/10.18331/BRJ2017.4.3.7

Mandegari, M. A., Farzad, S., van Rensburg, E., & Görgens, J. F. (2017). Multi‐criteria analysis of a biorefinery for co‐production of lactic acid and ethanol from sugarcane lignocellulose. Biofuels Bioprod. Bioref., 11(6), 971–990. https://doi.org/10.1002/bbb.1801

Nachtergaele, P., De Meester, S., & Dewulf, J. (2019). Environmental sustainability assessment of renewables-based propylene glycol at full industrial scale production. J. Chem. Technol. Biotechnol., 94(6), 1808–1815. https://doi.org/10.1002/jctb.5951

Nieder-Heitmann, M., Haigh, K. F., & Görgens, J. F. (2019). Life cycle assessment and multi-criteria analysis of sugarcane biorefinery scenarios: Finding a sustainable solution for the South African sugar industry. J. Clean. Prod., 239, 118039. https://doi.org/10.1016/j.jclepro.2019.118039

Nieder-Heitmann, M., Haigh, K., Louw, J., Görgens, J. F., Nieder‐Heitmann, M., Haigh, K., Louw, J., & Görgens, J. F. (2020). Economic evaluation and comparison of succinic acid and electricity co-production from sugarcane bagasse and trash lignocelluloses in a biorefinery, using different pretreatment methods: dilute acid (H2SO4), alkaline (NaOH), organosolv, ammonia fibre expa. Biofuels, Bioproducts and Biorefining, 14(1), 55–77. https://doi.org/10.1002/bbb.2020

Ntimbani, R. N., Farzad, S., & Görgens, J. F. (2021). Techno-economic assessment of one-stage furfural and cellulosic ethanol co-production from sugarcane bagasse and harvest residues feedstock mixture. Industrial Crops and Products, 162(February), 113272. https://doi.org/10.1016/j.indcrop.2021.113272

Okoro, O. V., Nie, L., Alimoradi, H., & Shavandi, A. (2022). Waste Apple Pomace Conversion to Acrylic Acid: Economic and Potential Environmental Impact Assessments. Fermentation, 8(1), 21. https://doi.org/10.3390/fermentation8010021

Ratshoshi, B. K., Farzad, S., & Görgens, J. F. (2021). Techno-economic assessment of polylactic acid and polybutylene succinate production in an integrated sugarcane biorefinery. Biofuels, Bioproducts and Biorefining, 15(6), 1871–1887. https://doi.org/10.1002/bbb.2287

Rosales-Calderon, O., & Arantes, V. (2019). A review on commercial-scale high-value products that can be produced alongside cellulosic ethanol. Biotechnol. Biofuels, 12(1), 240. https://doi.org/10.1186/s13068-019-1529-1

Statista. (2021). Global Green Hydrogen Projects' Selling Prices 2021 | Statista. https://www.statista.com/statistics/1260117/projected-selling-prices-of-large-scale-hydrogen-green-projects/

ToweringSkills. (2023). Financial Analysis, Cost Indices. https://www.toweringskills.com/financial-analysis/cost-indices/#chemical-engineering-plant-cost-index-cepci

SHORT COMMUNICATION

CHARACTERISING PAST CLIMATE CHANGE IN THE SOUTH AFRICAN SUGAR INDUSTRY: PRELIMINARY FINDINGS FOR TEMPERATURE AND RAINFALL, 1980-2024

Sithole P and Clark D

South African Sugarcane Research Institute, Private Bag X02, Mount Edgecombe,

4300, South Africa

phillemon.sithole@sugar.org.za; david.clark@sugar.org.za

Abstract

Climate change, past and future, manifests as long-term changes in the annual or seasonal rainfall and air temperature values, as well as changes in their variability, for rainfall in particular. These changes pose a significant threat to agricultural systems, sugar production included. Projected future climate change and variability patterns for the South African sugar industry have been reported but, to date, little attempt has been made to characterise and quantify the real changes, in order to confirm or refute the perceived changes. This paper aims to characterise the changes in the rainfall and temperature across all the major sugarcane-producing regions of South Africa. The long-term (1980-2024) daily air temperature and rainfall records from the representative weather stations in each region were analysed by using the Climpact climate analysis tool to generate several climate change indicators. The preliminary findings showed a clear increase in the daily maximum and average temperatures for all the regions, but there was no clear trend for the minimum temperature. The rainfall analyses produced no clear trend for the annual rainfall amounts or extreme events for most of the regions, due to the high levels of inter-annual variability. Only the Midlands region showed a significant increasing trend in the annual total rainfall. The next steps in the study will be to expand the analysis to include additional study sites and to assess the impact of the increased maximum temperature and rainfall variability on sugarcane production in each region.

***Keywords*:** Climate, temperature, rainfall, climate change, climate variability, sugarcane

Introduction

Sugarcane is grown in the eastern parts of South Africa, which receive relatively high rainfall. However, the inter-annual variability in weather (rainfall, air temperature, relative humidity and wind), as well as the cyclical variations due to the El Niño and La Niña phases of the El Niño-Southern Oscillation (ENSO), are a significant source of risk for sugarcane production, especially in the rainfed production areas, but also due to their impact on the available water resources in irrigated areas. In addition, there are risks associated with climate change, namely, the long-term changes in the annual or seasonal rainfall and temperature values and their variability.

The Intergovernmental Panel on Climate Change (IPCC) has reported rising global average temperatures, with the past few decades experiencing an accelerated warming trend (IPCC, 2023). The IPCC also reports that there is stronger evidence over the past 10 years of observed changes in climate extremes, including heatwaves, heavy rainfall events, droughts and tropical cyclones (IPCC, 2023). Climate extremes will not only have a direct impact on sugarcane production, but they will also have an impact on the Gross Domestic Product (GDP), employment in the sugar industry and foreign exchange earnings. Climate change could also result in a spatial shift in the optimal sugarcane production areas.

The projected future climate change and its impact on agricultural production, both globally and in South Africa, have been receiving increasing research attention in recent years. However, little work has been done to characterise and quantify the past climate change in the sugarcane-producing regions of South Africa, in order to confirm or to refute the perceived changes. Singels *et al.* (2005) reported a 0.75°C temperature increase and an increase in rainfall variability between 1954 and 2004 at Mt Edgecombe. Jones *et al*. (2015) reported a decreasing rainfall trend in Zululand for the period 1980-2010. Strydom and Savage (2018) found that the microclimate had changed in the KwaZulu-Natal Midlands, with an increase in the annual average air temperature being greater than the African and global observations, an increase in the relative humidity and, in some areas, a significant decrease in the rainfall. In a study in the uMngeni Catchment of KwaZulu-Natal, Strydom *et al*. (2020) noted the increased daytime temperatures and changes in the atmospheric water vapour pressure at some locations, but no significant changes in the annual rainfall totals, despite the high levels of inter-annual variability.

The valuable weather database collected and curated by SASRI over several decades provides an opportunity to investigate the past climate change. The purpose of this short communication is to report some preliminary findings of a study that aims to characterise the changes in rainfall and temperature, using historic climate data, across all the major sugarcane-producing regions of South Africa.

Methodology

Daily maximum and minimum air temperature and rainfall data for six sites across the South African sugar belt were obtained from the SASRI weather database (https://sasri.sasa.org.za/weatherweb) for the period 1980 to 2024. Daily mean temperature was calculated as the average of the daily maximum and minimum temperature. The six sites, all with suitable long and complete datasets, were carefully selected to ensure the representation of all the major agroclimatic regions of the sugar industry. The selected sites and the regions represented were:

- Komati - Mpumalanga Lowveld, irrigated;
- Pongola – Northern Zululand, irrigated;
- Umfolozi – Zululand, partially-irrigated;
- Mount Edgecombe - North Coast, rainfed;
- Noodsberg - Midlands, rainfed; and
- Sezela – South Coast, rainfed.

Climpact (https://climpact-sci.org/) is an R-based software package that was developed for the World Meteorological Organisation (WMO) for the calculation of various climate indices associated with temperature and rainfall extremes for climate monitoring assessments (Zhang *et al*., 2011). Climpact was used to generate selected climate indices (see Table 1) for each of the six sites. These indices were deemed suitable for the study due to their relevance in agricultural applications in general and, in particular, the sugarcane-producing areas of South Africa. The data quality control functions of Climpact were used to ensure and enhance the integrity and temporal consistency of the data. The overall trend of the time series was determined in Climpact, using the Sen's slope. The P-value associated with the Sen's slope was calculated by using the Mann-Kendal test to determine whether the observed trend was significant at a confidence level of 0.05.

Results and Discussion

A total of 12 climatic indices, based on the annualised values relating to the air temperature and rainfall extremes, were used to assess climate change in the sugar industry. The findings are presented in Table 1.

Table 1. Selected Climpact air temperature- and rainfall-related indices for the six study sites. The values indicate the slope (rate of change in units/decade (based on annual records), and the units are as specified). Bold and italicised values indicate significant (P<0.05) rates of change

Short name	**Long name**	**Definition**	**Units** (per decade)	**Rate of Change (units per decade)**					
				KOM	**PON**	**UMF**	**MTE**	**NDS**	**SEZ**
CDD	Consecutive Dry Days	Maximum number of consecutive dry days (when PR<1.0 mm)	days	1.30	***4.44***	-1.10	1.40	-0.66	***3.40***
FD	Frost Days	Number of days when TN<0°C	days	0.00	0.00	0.00	0.00	0.00	0.00
GDD	Growing Degree Days	Annual sum of TM - n (where n is a user-defined base temperature and TM > n). Here n=10°C.	°C	***91.70***	***72.60***	***66.50***	***88.30***	***88.00***	6.30
PRTOT	Annual total wet-day PR	Sum of daily PR≥1.0 mm	mm	19.20	4.50	1.30	22.00	***46.70***	54.00
R10mm	Number of heavy rain days	Number of days when PR ≥ 10 mm	days	0.66	0.00	0.00	0.64	***1.67***	0.00
R20mm	Number of very heavy rain days	Number of days when PR ≥ 20 mm	days	0.56	0.39	0.00	0.70	0.65	0.31
TMm	Mean TM	Mean daily mean temperature	°C	***0.24***	***0.20***	***0.17***	***0.24***	***0.24***	0.02
TNm	Mean TN	Mean daily minimum temperature	°C	0.14	0.04	-0.07	0.00	***0.21***	-0.20
TNn	Min TN	Coldest daily TN	°C	0.08	0.07	-0.24	-0.17	0.07	-0.09
TXm	Mean TX	Mean daily maximum temperature	°C	***0.40***	***0.40***	***0.46***	***0.50***	***0.30***	***0.22***
TXx	Max TX	Warmest daily TX	°C	***0.71***	***0.48***	***0.95***	***0.60***	***0.66***	***0.88***
TXge38	TX of at least 38°C	Number of days when TX ≥ 38°C	days	***3.30***	***0.60***	***1.20***	0.00	0.00	0.00

TX = maximum air temperature, TN = minimum air temperature, TM = mean air temperature, PR = precipitation (rainfall). KOM = Komatipoort, PON = Pongola, UMF = Umfolozi, MTE = Mount Edgecombe, NDS = Noodsberg, SEZ = Sezela

Maximum Temperature

The results showed a statistically significant increasing trend for all the indices relating to maximum temperature at all the study sites (Table 1). The annual absolute daily maximum temperature (TXx) showed an increasing rate range of 0.48 to 0.95°C per decade, with Umfolozi recording the highest increase. The increase in the annual mean daily maximum temperature (TXm) ranged between 0.22°C per decade (Sezela) and 0.46°C per decade (Umfolozi). There was also an increasing trend in the number of days with extreme maximum temperatures (at least 38°C, TXge38) with the potential of inducing heat stress in sugarcane in the irrigated areas. The number of days with extreme maximum temperatures increased at a rate of 1.2 days per decade for Umfolozi and 3.3 days per decade for Komatipoort, where up to 35 days per annum with extreme temperatures have occurred (2016). The years with the peak numbers of days with extreme maximum temperatures (Figure 1) coincide mostly with the El Niño phenomenon, due to the associated hot and dry conditions.

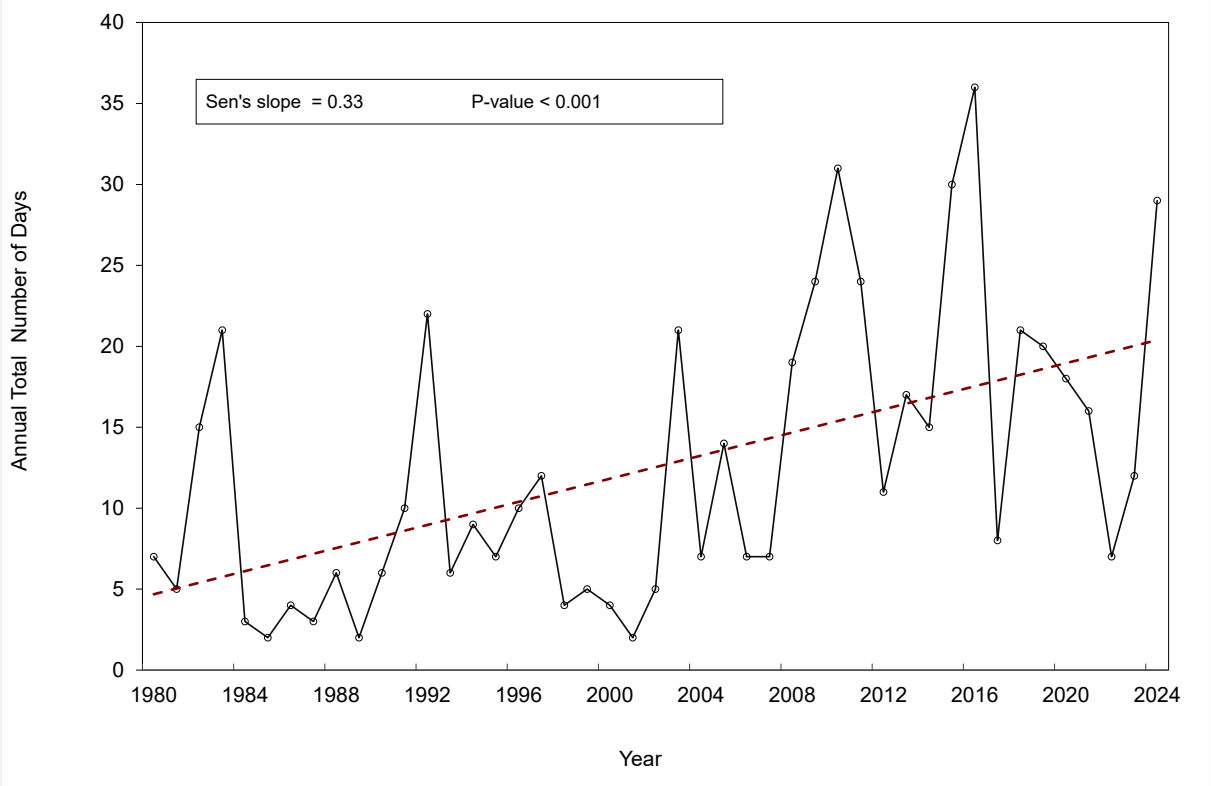


Figure 1. Annual total number of days when maximum temperature was more than 38°C at Komatipoort between 1980 and 2024. The dashed line is the Sen's slope, which represents the overall annual rate of change (increase) over that period.

The increasing trend of maximum temperatures resulted in an increase in the daily mean temperatures (TMm) across all the sites, with the highest rate of increase of 0.24°C per decade was observed at Noodsberg, Komatipoort and Mount Edgecombe. Consequently, the growing degree days (base 10°C) (GDD) showed a significant increasing trend for all the sites, ranging from 63- to 92-degree-days per decade. This has potentially wide implications for sugarcane production, both positive and negative. Higher temperatures promote a faster growth rate, which potentially increases radiation interception and results in better yields (Jones *et al.,* 2015). However, they could also result in increased water stress and related risks during periods of inadequate soil water availability, in both rainfed and irrigated areas. Cane quality could also be affected negatively, due to increased vegetative growth under warmer conditions when soil water is not limiting (Singels *et al.,* 2005). Higher temperatures may potentially result

in shorter harvesting cycles, e.g. in the Midlands, but they could also pose increased pest and disease pressure.

These results confirm and add to the evidence of a climate that is becoming more extreme and at similar magnitudes to the values reported by others (Nayamuth, 2005; IPCC 2023; Strydom *et al*. 2020) with respect to average and maximum temperatures. Singels *et al* (2023) projected temperature increases of about 2°C, with little spatial variation across the South African sugar industry, for the 2046-2065 time-period (relative to the 1971-1990 baseline period), with uncertainty around the rainfall projections.

Minimum Temperature

There was no definite trend for the minimum temperature (TNm and TNn), including the related indices, like frost days (FD), across all the sites. The average (TNm) and absolute (TNn) annual minimum temperatures decreased slightly at three sites (Umfolozi, Mount Edgecombe and Sezela) and increased at the other three sites. However, all these trends were not significant, except for Noodsberg, where the data suggested a significant increase in the mean daily minimum temperature at a rate of 0.21°C per decade. Less severe minimum temperatures would be expected to have a positive effect on germination, seedling development, ratoonability and yield (Sanghera, 2020). The increasing trend of the minimum temperature for Mount Edgecombe, reported by Singels *et al*. (2005), could not be confirmed in this study. The minimum temperature data across all six sites showed high levels of inter-annual variability, but with no significant trend.

Rainfall

No significant trend was observed for the annual total rainfall (PRTOT) for all sites, except for Noodsberg. Other rainfall-related indices, like the days with extreme rainfall, also showed no significant changes at most sites (Table 1). An analysis of the rainfall data by month and season did not indicate any noticeable shift in the rainfall seasonality either. The only exception was Noodsberg, where the annual total rainfall showed a significant increasing rate of nearly 47 mm per decade (Figure 2), coupled with an increasing trend for the number of rainfall events, recording at least 10 mm (R10 mm). On the other hand, four of the sites showed an increasing number of days without rainfall, with Pongola and Sezela having a significantly-increasing rate of consecutive dry days per year (CDD) at 4.4 and 3.4 days per decade, respectively.

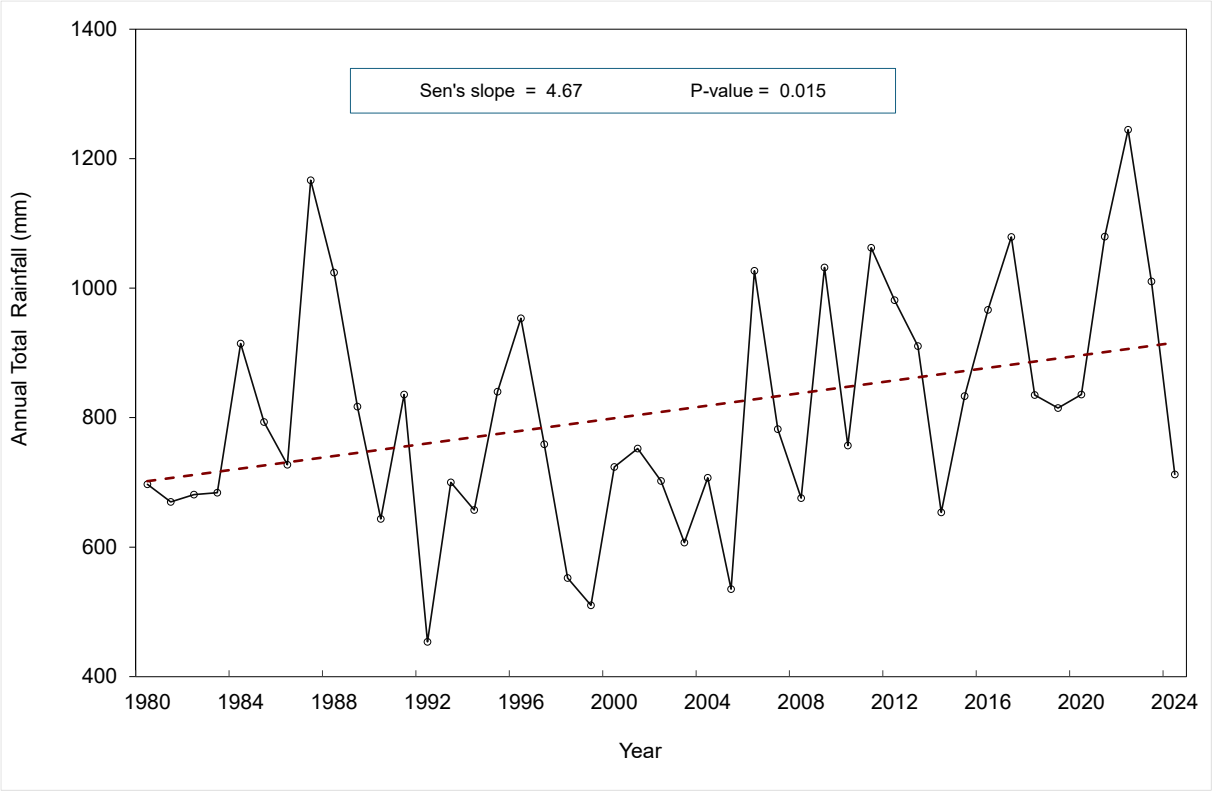


Figure 2. Annual total rainfall for Noodsberg between 1980 and 2024, for daily rainfall events of at least 1.0 mm (PRTOT). The dashed line is the Sen's slope, which represents the overall annual rate of change (increase) over that period.

Overall, the rainfall data also showed a high inter-annual variability, which is often linked to the ENSO phenomena (high during La Niña conditions and low under El Niño conditions), and which is in line with the previous findings by Singels *et al*. (2005) and Strydom *et al.* (2020). Jones *et al*. (2015) reported small changes in the projected annual rainfall at the three sites investigated and commented that there were considerable variations in the rainfall trends between different projections.

The increasing number of consecutive dry days for Pongola and Sezela indicate an increased risk of lower yields related to water availability, especially in rainfed crops. An analysis of the trends in the sub-daily rainfall intensity would be useful for informing the design and implementation of erosion and runoff control structures.

Conclusions

Across all the study sites, an increase in the daily maximum and average temperature and all the related extreme heat indices was the clearest and most significant trend established in this study. The associated increase in the growing degree days may have implications for sugarcane maturity, while also posing pest and disease threats, e.g. in the Midlands. There was no evidence of trends in cold weather extremes across all the study sites. The study results suggest that rainfall is becoming more variable, with more large events and more consecutive dry days, in general, but there was no noticeable trend in the annual total rainfall, except for the Midlands, where increasing annual totals were observed at Noodsberg. The northern irrigated areas, while getting warmer, are not really getting wetter, which raises concern over the irrigation water demand and availability in future, due to the elevated crop water use. In the rainfed and cooler areas, higher temperatures may promote more vigorous growth, but they will also increase the risk and severity of water stress during periods of drought. This study will

be extended to more sites across the industry, in order to help assess the related impacts on sugarcane production and quality.

Future Work

Work is underway to increase the number of study sites, in order to ensure that all parts of the industry are adequately represented and, where possible, to corroborate the regional trends. Thereafter, climate-driven parameters, such as the potential and simulated evapotranspiration from sugarcane production, thermal discomfort and fire danger indices, will also be analysed. Finally, the impact of climate change on sugarcane production in South Africa over the same period will be analysed to evaluate the trends in production.

References

IPCC (2023). Summary for Policymakers. In: *Climate Change 2023: Synthesis Report*. Contribution of Working Groups I, II and III to the Sixth Assessment Report of the Intergovernmental Panel on Climate Change. IPCC, Geneva, Switzerland.

Jones MR and Singels A (2015). Analysing yield trends in the South African sugar industry. *Agric Syst* 141: 24-35.

Jones MR, Singels A and Ruane AC (2015). Simulated impacts of climate change on the water use and yield of irrigated sugarcane in South Africa. *Agric Sys* 139: 260-270. Online: https://doi.org/10.1016/j.agsy.2015.07.007

Nayamuth AR (2005). Climate change: Impact, adaptation and implications for a sustainable sugar industry. *Proc Int Soc Sug Cane Technol* 25(2): 69-77.

Sanghera G (2020). Sugarcane disorders associated with temperature extremes and mitigation strategies. *East African Scholars J Agri Life Sci* 3(4): 101-114.

Singels A, van den Berg M and van Antwerpen R (2005). Climate change and yield decline: an analysis of the actual and simulated yield data from the BT1 field experiment. *Proc S Afr Sug Technol Ass* 79: 491-494.

Singels A, Jones MR and Lumsden J (2023). Potential for sugarcane production under current and future climates in South Africa: Sugar and ethanol yields, and crop water use. *Sug Tech* 25(2), 473-481. Online: https://doi.org/10.1007/s12355-022-01227-y

Strydom S, Jewitt GPW, Savage MJ and Clulow AD (2020). Long-term trends and variability in the microclimates of the uMngeni Catchment, KwaZulu-Natal, South Africa, and the potential impacts on water resources. *Theor Appl Climatol* 140:1171-1184.

Strydom S and Savage MJ (2018). Observed variability and trends in the microclimate of the Midlands of KwaZulu-Natal and its influence on fire danger. *Int J Clim* 38: 751-760.

Zhang X, Alexander L, Hegerl GC, Jones P, Tank AK, Peterson TC, Trewin B and Zwiers FW (2011). Indices for monitoring changes in extremes based on daily temperature and precipitation data. *Wiley Interdiscip Rev Clim Chang* 2: 851–70 Online: http://dx.doi.org/10.1002/wcc.147.

SHORT COMMUNICATION

INVESTIGATING THE IMPACT OF SKILLS DEVELOPMENT TRAINING ON FARMERS' PERFORMANCE AND LIVELIHOODS: A CASE STUDY OF SMALL-SCALE SUGARCANE GROWERS IN THE UMFOLOZI MILL AREA, KZN

Qwabe S

[1]*Umfolozi Sugar Mill,Cnr Mill Road & Club Lane, Mtubatuba,3935*

sqwabe@usm.co.za

Abstract

Small-scale sugarcane growers encounter a variety of obstacles that impact their livelihoods and performance. This study aimed to investigate the impact of farmer development training on the farmer's performance and livelihood. It was conducted in the Umfolozi Mill Area, and it employed a quantitative research approach by using a questionnaire.

A total of 30 small-scale sugarcane farmers who had received training and who supplied sugarcane to Umfolozi Sugar Mill, participated as the respondents in this study. They agreed that the training was useful and had made them better farmers. The impact of training on farmers can be summarised as follows: an increase in their job satisfaction level, an increase in farm productivity, an increase in income, cost- and time-savings, an increased knowledge, as well as increased networking.

There is a strong interest among growers for ongoing training, in order to further enhance their sugarcane production businesses. This eagerness underscores the value that they place on continuous learning and development. The study highlights the need to involve more youth and emerging farmers in future training initiatives, to ensure the long-term sustainability and growth of the small-scale grower sector in the Umfolozi Mill area.

Keywords: Small-scale growers, training, Umfolozi Mill area, sugarcane, livelihood, performance

Introduction

The problem that was investigated in this study is the low educational attainment among small-scale growers, unskilled labour, as well as the low adoption rate of best management practices, which are the contributing factors that lead to yield losses in sugarcane production. On-farm training skills courses have been conducted by the sugar industry training providers (Shukela Training Centre) through the Grower Development Account (SASA, 2013). The training programmes are aimed at developing farmers on how to become productive; however, to the best of my knowledge, the information concerning the impact of skills development training on the farmers' performance and their livelihoods has not been examined comprehensively.

This study aims to investigate the potential impact of skills development training on the farmers' performance and livelihoods in the Umfolozi Mill area of KwaZulu-Natal. In addition, the research seeks to evaluate the attitudes of small-scale growers towards skills development training, to identify the skills gap and training needs of small-scale growers for future agricultural advancement, to determine the extent of productivity improvement after training, and to justify the financial investment in the training and development programmes.

The results gathered from this study will assist in structuring future training programmes, in order to enhance the knowledge and skills of sugarcane growers. It will also allow extension officers and other South African sugar industry stakeholders to redesign their activities for transferring knowledge about sugarcane, in order to improve productivity.

Materials and Methods

A questionnaire was designed. Only 30 respondents were selected from a population of 50 small-scale sugarcane growers who had received training. The decision to select only 30 participants was influenced by the limitations imposed during the COVID-19 pandemic. The list of small-scale growers in the area was sourced from the Umfolozi Sugar Mill training and development database. Growers were then categorised into sub-zones and local associations.

The data were collected by using structured questions in the form of questionnaires, which ensured their uniformity. To provide clarification and accommodate varying levels of education, some farmers struggled to understand the questions, when reading them independently; therefore, face-to-face interviews were utilised to administer the questionnaires. Participants were asked the same set of questions, and in the same order, to ensure consistency. The researcher scheduled the appointments in advance, in order to confirm the respondents' availability, and the interviews were conducted at locations that were convenient for them. The data were analysed by coding the responses in Microsoft Excel.

Results and Discussion

A significant number of the small-scale growers who were interviewed were aged 61 and above (38.7%), with 32.3% being between 41-50 years. Youth participation was minimal, comprising only 3.2%, which indicated the limited engagement of young individuals in sugarcane production. The skills and knowledge that they have acquired have enabled growers to perform their farming operations more effectively, which has led to an improvement in their performance levels. Growers reported an increased motivation, which has translated into enhanced work efficiency. Compared to the period before their training, the growers have exhibited a notable improvement in their farming operations. The reported outcomes included increased productivity, improved cane quality, an increased income and enhanced sustainability. This information is based on their personal stories, cane payment statements and the cane quality analysis results.

The most frequently mentioned training needs were related to budgeting and record-keeping, the RV payment system and chemical ripening. Sugarcane Husbandry emerged as the most attended training course. Growers described this course as comprehensive and impactful, particularly because it covered the full production cycle, from planting to harvest. The respondents believed that such training not only equipped them with a technical knowledge, but it also instilled greater motivation and confidence in their operations.

Conclusion

The findings of this study are specific to the Umfolozi Mill area on the northern coast of KZN and may not be representative of all sugarcane-growing regions. However, the concerns and insights shared by growers, particularly relating to the ageing demographics, the low youth involvement, and the gaps in production knowledge, may not be isolated to this region. While this study did not seek to compare different regions, the challenges that were raised could reflect a broader pattern in the small-scale grower sector, which merits further investigation. Future research should consider conducting similar studies across sugarcane-growing regions to identify their commonalities and variations in both the challenges and the impact of training. This would support the development of regionally responsive training programmes and could contribute toward establishing a baseline for assessing training effectiveness on a wider scale.

Acknowledgments

The author acknowledges the participation of small-scale growers and the support of the Umfolozi Sugar Mill Cane Supply Manager, S Mahlinza.

References

South African Sugar Association [SASA] (2013). The South African sugar industry directory 2013/2014, SASA, Durban, South Africa.

POSTER SUMMARY

GUIDELINES FOR THE FIELD ESTABLISHMENT OF NOVACANE® PLANTS

Tweddle PB[1,2], McFarlane SA[1] and Snyman SJ[1,3]

[1]South African Sugarcane Research Institute, P/Bag X02, Mount Edgecombe, 4300, South Africa
[2]Bioresources Engineering, School of Engineering, University of KwaZulu-Natal, Rabie Saunders Building, Agriculture Campus, 62 Carbis Road, Scottsville, Pietermaritzburg, 3201
[3]University of KwaZulu-Natal, School of Life Sciences, Westville Campus, P/Bag X54001, Durban, 4000, South Africa

peter.tweddle@sugar.org.za

Abstract

NovaCane® technology provides a rapid method for the bulking up of disease-free, true-to-type sugarcane plantlets. Some varieties are particularly affected by the tissue culture process, which is commonly manifested as thinner stalk diameters. NovaCane® plantlets are more fragile than vegetatively-propagated setts (transplants) and require appropriate care when transitioning from a moderately-protected nursery environment to the field.

This poster contains:

- shared experiences from SASRI Extension Specialists covering NovaCane® plantlet establishment for irrigated and rainfed growing scenarios;
- important observations from a SASRI field trial for the N78 NovaCane® variety; and
- considerations and best practices for the field establishment of NovaCane® plantlets.

The trial findings include:

- NovaCane® plantlets that were hardened-off in black plastic trays with inserts had an ±10% lower plantlet mortality, compared with those in white polystyrene trays;
- N78 NovaCane® showed prolific tillering and radial growth from the base of the plantlets;
- individual elongated thin stalks were observed in N78 NovaCane® plantlets prior to the development of the whole plant stalk;
- deeper planting with ridging treatments improved the stalk diameter taper profiles, when compared with shallow furrow plantings; and
- the stalk diameters of the N78 NovaCane® ratoon crop increased from 81% to 86% in the 2023 and 2024 crop cycle, respectively, relative to the non-tissue culture N78 ratoon crops.

Best practices for the field establishment of NovaCane® plantlets considers the seasonal timing and climatic conditions when establishing the crop, the requirements for the field and soil preparation, plantlet care to minimise the transition from a nursery to a field environment, as well as early crop establishment and the husbandry requirements.

Keywords: NovaCane®, tissue culture, best practice, acclimation, crop establishment

POSTER SUMMARY

THE ROLE OF THE SOUTH AFRICAN SUGARCANE RESEARCH INSTITUTE'S INSECT-REARING PROGRAMME IN PEST CONTROL

Nzama SN[1], Gillespie DY[2] and Malinga LN[1,3]

[1]*South African Sugarcane Research Institute, P/Bag X02, Mount Edgecombe, 4300, South Africa*
[2]*28 Niagara Drive, Waterfall, 3610, South Africa*
[3]*School of Life Sciences, University of KwaZulu-Natal, Pietermaritzburg, South Africa*

sindisiwe.nzama@sugar.org.za, gillespiedenise13@gmail.com, lawrence.malinga@sugar.org.za

Abstract

Successful insect-rearing is fundamental to entomological research and pest control practices. Artificial diets have proven to be critical in advancing insect mass production for various research purposes (Cohen, 2001). For over 100 years, artificial diets have been used for rearing insects, with the first diet being developed for the rearing of the blue bottle fly, *Calliphora vomitoria* (Diptera: Calliphoridae) (Bogdanow, 1908; Piper, 2017). The effectiveness of artificial diets was recognised in the 1950s when the predatory ladybug, *Coccinella septempunctata*, was successfully reared on a diet composed of prey dry powder (Liu *et al.*, 2022). The screw-worm *Cochliomyia hominivorax* (Diptera: Calliphoridae) was also successfully reared on an artificial diet, and it was completely eradicated by using the sterile male release technique in the south-eastern United States (Lindquist *et al*., 1992). Since then, numerous diets have been described for phytophagous insects, particularly the economic pest species of the Noctuid and Pyralid families (Singh, 1977).

The South African Sugarcane Research Institute's (SASRI's) insect-rearing programme was initiated in 1981 to focus on the mass rearing of the stalk borer, *Eldana saccharina* Walker (Lepidoptera: Pyralidae). Eldana is a notable pest in the sugarcane industry which, if not controlled, could result in a total loss of over R1 billion per season (Rutherford, 2015). Small, prefabricated laboratories at SASRI were used to rear Eldana and its biological control agents, such as *Xanthopimpla stemmator* (Hymenoptera: Ichneumonidae) and *Sturmiopsis parasitica* (Diptera: Tachinidae). Over time, it was recommended that the control measures for Eldana should be based on the Integrated Pest Management (IPM) approach, which included host-plant resistance, push-pull technology, biological control and the Sterile Insect Technique (SIT) (Chinheya *et al*., 2009; Cockburn, 2013). As a result, the rearing programme advanced into large-scale rearing in 1988 when a custom-designed, environmentally-controlled, multi-room Insect-Rearing Unit (IRU) was commissioned. The focus of the IRU shifted to incorporate IPM programmes, particularly the proof-of-concept evaluation of the Sterile Insect Technique (SIT).

An artificial diet for rearing Eldana has been developed and refined over the years, and it is now virtually contamination-free, yielding high-quality insects. The complete rearing of Eldana on an artificial diet was first achieved in the 1940s (Dick, 1945). This diet consisted of cooked maize meal inoculated with the common food spoilage mould, *Mucor hiemalis*, the presence of which allowed for the better development of the larvae (Dick, 1945). Further diet development by Atkinson (1978), Graham and Conlong (1988), Rutherford and van Staden (1991), Gillespie (1993), Walton and Conlong (2016) and Woods *et al*. (2020) all produced improved Eldana diets. These diets continuously increased the quality and production of the insects required for IPM programmes, whilst reducing the production costs. The current diet used in the IRU is based on a 'rabbit pellet diet' that was originally developed for the European

corn borer *Ostrinia nubilalis* Hubner (Lepidoptera: Crambidae) (Beck *et al*., 1949). This diet has been refined and optimized by Ngomane *et al*. (2022) for effective mass rearing of Eldana.

Another invasive pest, the longhorn beetle *Cacosceles newmannii* (Coleoptera: Cerambycidae), is currently being reared in the IRU. No artificial diet has been successfully developed for this pest because of its extended life-cycle of two years.

Other end-users of the IRU include specialists who are conducting research in the SASRI's Crop Protection Programme, Biotechnology Department and academic institutions. In addition, the IRU provides specialist training to local and international rearing institutions, as requested. The most notable milestones achieved since the unit's inception almost 40 years ago are as follows: (i) an efficient rearing facility with climate control, (ii) the implementation of Standard Operational Procedures with workflow patterns, (iii) health and safety and microbial contamination control measures, and (iv) the mass production of Eldana to provide material for research programmes.

***Keywords**:* Insect rearing, pest control, IPM, contamination

References:

Atkinson, PR (1978). Mass rearing and artificial infestation methods for *Eldana saccharina* Walker (Lepidoptera: Pyralidae). Proceedings of the South African Sugar Technologists' Association 52: 143 -145

Beck, SD, Lilly, JH and Stauffer, JF (1949). Nutrition of the European corn borer, *Pyrausta nubialis* (HBN.) Development of a satisfactory purified diet for larval growth. Annals of the Entomological Society of America 42: 483- 496.

Bogdanow, EA (1908). About the dependence of the growth of larvae of bacteria and enzymes and about variability and inheritance in the flesh flies. Archives of Anatomy and Physiology 6: 173-200.

Chinheya, CC, Mutambara-Mabveni, ARS and Chinwada, P (2009). Assessment of damage due to *Eldana saccharina* Walker (Lepidoptera: Ppyralidae) in sugarcane. Proceedings of the South African Sugar Technologists' Association 82: 446-456.

Cockburn, JJ (2013). Implementation of the push-pull strategy for *Eldana saccharina* control on sugarcane in KwaZulu-Natal, South Africa. Unpublished MSc Thesis. North-West University, South Africa.

Cohen, AC (2001). Formalizing Insect Rearing and Artificial Diet Technology. American Entomologist 47: 198-206.

Dick, J (1945). Some data on the biology of the sugarcane borer (*Eldana saccharina*, Wlk.). Proceedings of the South African Sugar Technologists' Association 23: 75 – 79.

Gillespie, DY (1993). Development of mass-rearing methods for the sugarcane borer *Eldana saccharina* Walker (Lepidoptera: Pyralidae) II: Diet gelling agents. Proceedings of the South African Sugar Technologists' Association 67: 127- 130.

Graham, DY and Conlong, DE (1988). Improved laboratory rearing of *Eldana saccharina* (Lepidoptera: Pyralidae) and its indigenous parasitoid *Goniozus natalensis* (Hymenoptera: Bethylidae). Proceedings of the South African Sugar Technologists' Association 62:116-119.

Lindquist, DA, Abusowa, M and Hall, MJR (1992). The New World screwworm fly in Libya: a review of its introduction and eradication. Medical and Veterinary Entomology 6: 2–8.

Liu, C, Liu, H, Wu, X, Xiao, K, He, H, Huang, Q and Pu, D (2022). Effects of artificial diet on the biological characteristics of the ladybeetle *Coccinella septempunctata*. Entomological research 52(4): 223-231.

Ngomane, NC Pieterse, E Woods, MJ and Conlong, DE (2022). Formulation of Artificial Diets for Mass-Rearing *Eldana saccharina* Walker (Lepidoptera: Pyralidae) Using the Carcass Milling Technique. Insects 13: 316 - 335.

Piper, MD (2017). Using artificial diets to understand the nutritional physiology of *Drosophila melanogaster*. Current Opinion in Insect Science 23:104 -111.

Rutherford R.S. and Van Staden J. (1991). Development of defined synthetic diets for the culturing of *Eldana saccharina* Walker (Lepidoptera: Pyralidae). Proceedings of the South African Sugar Technologists' Association 65: 80 – 86.

Rutherford, RS (2015). IPM for Eldana Control: An Integrated Pest Management (IPM) Approach for the Control of the Stalk Borer *Eldana saccharina* Walker (Lepidoptera: Pyralidae). South African Sugarcane Research Institute, South Africa.

Singh, P (1977). Artificial diets for insects, mites and spiders. Plenum Press, New York

Walton, AJ and Conlong, DE (2016). General biology of *Eldana saccharina* Walker (Lepidoptera: Pyralidae): A target for the sterile insect technique. Florida Entomologist 99 (1): 30 - 35.

Woods, M.J., Conlong, D.E., Ngomane, N., Gillespie, D., Hoffman, L.C. and; Pieterse, E. (2020). The development of an improved artificial diet for the mass-rearing of *Eldana saccharina* Walker (Lepidoptera: Pyralidae). J. Sci. Food. Agric., 100: 4678–4687.

POSTER SUMMARY

STANDING THE TEST OF TIME: SUGARCANE BIOTECHNOLOGY RESEARCH COLLABORATION BETWEEN THE INSTITUTE FOR PLANT BIOTECHNOLOGY, STELLENBOSCH UNIVERSITY, AND THE SOUTH AFRICAN SUGARCANE RESEARCH INSTITUTE

Van der Vyver C[1] and Snyman SJ[2]

[1]Institute for Plant Biotechnology, Stellenbosch University, Stellenbosch, South Africa
[2]South African Sugarcane Research Institute (SASRI), 170 Flanders Drive, Mount Edgecombe, South Africa

Abstract

Biotechnology-related interventions have supported sugarcane research in South Africa since the early 1990's. The longstanding research collaboration between the Institute for Plant Biotechnology (IPB) at the Stellenbosch University and the South African Sugarcane Research Institute (SASRI) has contributed to the advances in this modern field of biotechnology, which are aimed at variety improvement and sustainable sugarcane cultivation. Working together, these two institutes have developed a toolbox of expertise in *in vitro* culture and genetic modification (GM) technology, mutation breeding and, more recently, genome editing. In the process, 73 postgraduate students (including 21 BSc Honours students) have been trained, 39 international peer-reviewed papers have been published, and four patent applications have been submitted. The transgenic sugarcane plants generated at the two institutes were developed as part of the fundamental sucrose metabolism research and for higher sucrose yields and enhanced drought tolerance. As a result of almost three decades of research collaboration between the IPB and SASRI, a vast knowledge of, and skill-sets in, sugarcane biotechniques and functional genomics have been established. Ongoing collaborative research will be invaluable in customising the approaches for future sugarcane improvement, to ensure its sustainable cultivation in local agroclimatic regions.

Keywords: Sucrose metabolism, drought tolerance, genetic modification, sugarcane improvement, capacity building

POSTER SUMMARY

THE IDENTIFICATION AND VALIDATION OF MOLECULAR MARKERS FOR RESISTANCE TO *ELDANA SACCHARINA* WALKER (LEPIDOPTERA: PYRALIDAE)

Jacob RM[1], Singh S and Joshi SV[1,2]

[1]*SA Sugarcane Research Institute, Mount Edgecombe, South Africa*

[2]*School of Life Sciences, College of Agriculture, Engineering and Science, University of KwaZulu-Natal, Durban, South Africa*

robyn.jacob@sugar.org.za, selina.singh@sugar.org.za, shailesh.joshi@sugar.org.za

Abstract

The identification of gene markers for pest resistance in crops, for use in marker-assisted selection, is a powerful tool that accelerates breeding programmes; it enables the development of robust, pest-resistant varieties, while reducing the reliance on chemical pesticides. An RNA-seq study was conducted, using resistant cultivar N33 and susceptible cultivar N11 to identify gene/s that exist naturally within the sugarcane genome for defence responses to *Eldana saccharina*. A gene of unknown function was identified by its wound-induced expression in the resistant sugarcane cultivar only. Further investigations showed that the gene is part of a Presence-Absence Variation (PAV) region, an extreme form of structural variation in which a segment of DNA is present in some individuals but absent in others. A rapid and robust genotyping assay was developed to easily detect the PAV region from a sugarcane leaf sample. The assay is cost-effective, when compared with early genotyping methods, and it allows the high throughput genotyping of many samples. The outcome from genotyping studies revealed that the PAV region was present in 66% of commercial sugarcane N cultivars, whilst its presence ranged from 42% to 58% in unreleased genotypes across different breeding programmes that cater for the sugar industry. A significant positive correlation was observed between the PAV region and Eldana resistance in genotypes from the coastal long-cycle breeding programme. These genotypes were selected under high pest pressure. Information on a gene's heritability is crucial in marker-assisted breeding, because it indicates how reliably the gene's trait will be transferred to the progeny, which ensures consistent improvement across generations. Although sugarcane has a complex polyploid genome, the heritability analysis has indicated that the PAV is inherited in a simple Mendelian pattern. This makes it a promising candidate as a molecular marker for Eldana resistance screening in the early stages of the breeding programme. This is the first report of a PAV region in sugarcane that is associated with increased Eldana resistance.

Keywords: Marker-assisted breeding, presence-absence variation, Eldana, sugarcane resistance

POSTER SUMMARY

THE ISOLATION AND CHARACTERISATION OF LACTIC ACID BACTERIA (LAB) INVOLVED IN CANE DETERIORATION

Tererai MR[1], Rambwawasvika H[2] and Mutatu W[2]

[1]Department *of Biotechnology and Biochemistry, University of Zimbabwe*
[2]*Zimbabwe Sugar Association Experiment Station, Private Bag 7006, Chiredzi*

mrtererai@gmail.com, hrambwawasvika@zsaes.org.zw, wmutatu@zsaes.org.zw

Abstract

The burn-/harvest-to-crush gap, or the time between harvesting and processing, makes the already-significant post-harvest sucrose loss of sugarcane even worse. The microbes that proliferate during this time period convert sucrose into less desirable compounds, such as organic acids and exopolysaccharides. While we know about the economics of this deterioration, we still do not fully understand the microbial organisms that are involved. This study aimed to isolate and characterise the bacteria associated with cane degeneration, by focusing on lactic acid bacteria. The juice from burnt sugarcane was extracted and serially diluted in a peptone broth to enrich the microbial community. The lactic acid bacteria were isolated by using De Man, Rogosa and Sharpe (MRS) agar. After methylene blue staining, the microscopic examination of the morphology showed coccoid cells in a chain formation. The cell wall properties were determined by Gram staining, and the isolates were Gram-positive. Two bromocresol green and phenol red pH indicator assays were used to biochemically validate the production of lactic acid. The juice samples were inoculated to model and assess the cane deterioration, and key parameters, such as the pH, Brix%, Pol%, sucrose, reducing sugars and microbial counts, were monitored over a set period of time. The results showed that there is lactic acid bacteria involvement in cane degradation. When grown on the MRS agar, a slimy, mucilaginous growth was consistently produced and the degree of growth was positively correlated with the initial juice concentration, which indicated dextran production. The microscopic results and Gram staining matched the morphology of L. mesenteroides. Biochemical tests confirmed the production of lactic acid. The quantitative analysis of cane juice showed a decline in the Brix%, Pol% and sucrose levels, which was directly caused by microbial activity. The reducing sugars remained low, which suggests that, perhaps with the help of dextransucrase, the glucose and fructose were quickly converted into dextrans and organic acids. The pH was relatively stable within the range that is conducive to microbial growth. Notably, a significant increase in microbial colony counts was observed, which shows the rapid growth potential of lactic acid bacteria in the sugarcane juice matrix. In summary, this study shows that lactic acid bacteria cause sugarcane deterioration, due to their rapid growth and the conversion of sucrose into lactic acid and dextran. The creation of mitigation strategies requires a more in-depth understanding of these microbial dynamics. The identification of specific deterioration mechanisms, the creation of focused prevention strategies, as well as the use of genomic techniques to describe lactic acid bacteria strains, should be the top priority of future research.

Keywords: Burn-to-crush delays, microbial degradation, lactic acid bacteria

POSTER SUMMARY

AN INVESTIGATION INTO THE POPULATION DYNAMICS OF THE YELLOW SUGARCANE APHID, WITH PARTICULAR EMPHASIS ON ITS MOVEMENT PATTERNS BETWEEN PLANTS

Basdew IH and Xaba B

SA Sugarcane Research Institute, 170 Flanders Drive, Mount Edgecombe, 4300

Iona.Basdew@sugar.org.za; Busisiwe.Xaba@sugar.org.za

Abstract

The Yellow Sugarcane Aphid (YSA), a confounding pest of sugarcane, has plagued the industry since it first arrived in South Africa in 2013. Damage is characterised by yellow-brown leaf lesions at the insect feeding-points, which translate to a reduced photosynthetic capacity and, eventually, to a reduction in the crop yield. The spatio-temporal dynamics of the YSA has not been well-understood or documented within the entomological arena. Field observations describe their infestation as often moving from a low to a high state, or vice versa, within a relatively short space of time, with no apparent agronomic or climatic change/correlation. Whilst many of these observations have been anecdotal, a similar trend appears to exist wherever the YSA is a problem on sugarcane. This study sought to enrich the knowledge-base that is currently available on the biology and behaviour of YSA, by intensively monitoring colonies for their movement between plants, changes in their feeding behaviour and the development of alates, under greenhouse conditions over time. After two years of study, the key findings can confirm that YSA move from plant-to-plant via the plant canopy and that they move between plants via a marching action on the ground. The movement of YSA between plants was most prolific in the late afternoon into the evening, which implies a level of photosensitivity. Temperature fluctuations did not affect their movement between plants. However, their movement did correlate with plant stress, where the greater the damage that was incurred on the leaves by the growing colonies, the greater the migration of 24- to 38-day-old aphids from infested plants to uninfested healthy plants. Less than 5% of each population during each round of the study produced winged alates. The YSA behaviour appeared to have been influenced by both biotic (mites, scale, hover fly) and abiotic (chemical residue) factors, as evidenced by a reduction in their movement and reproductive vigour upon exposure to these stimuli. Adult aphids also showed their ability to move from damaged plants towards uninfested, healthy plants at a maximum of 4 m at a time. A further observation was an abundance of ants, specifically the *Lepisiota* spp., in the immediate vicinity of YSA colonies. The ant/YSA interaction has been consistently observed on commercial cane in the field, not only on the *Lepisiota* spp, but also on the *Linepthema* spp, *Tetramorium* spp. *and Lasius* spp. It is currently not clear whether a synergistic relationship exists between the two species, or if it might be a case of 'mistaken identity', where the ants expect the YSA to produce honeydew (a food-source for ants), which the YSA does not do. This presents an avenue for further research where the ant/YSA interactions could be intensively monitored over time, under controlled conditions. By understanding the movement patterns and ecological interactions of the YSAs, future research and pest control practices can be better tailored to mitigate their impact on sugarcane crops. A typical example could be to time the application of insecticides to the late afternoon, in order to catch the YSA as they begin moving between plants.

Keywords: Yellow sugarcane aphid, pest behaviour, pest management, population dynamics

SHORT COMMUNICATION

ANALYSING THE EXPRESSION OF INSECTICIDAL PROTEINS IN GENETICALLY MODIFIED SUGARCANE

Makhetha T[1,2], Joshi S[1,2], Albertse E[1] and Ghai M[2]

[1]South African Sugarcane Research Institute, 170 Flanders Drive, Mount Edgecombe, South Africa
[2]University of KwaZulu-Natal, Westville, Durban, South Africa

tumo.makhetha@sugar.org.za, shailesh.joshi@sugar.org.za, ewald.albertse@sugar.org.za, ghai@ukzn.ac.za

Abstract

The introduction of insecticidal transgenes into sugarcane is targeted at introducing resistance to the highly destructive and endemic *Eldana saccharina* Walker L., which has a great impact on sugarcane production. The selection of events with low transgene copies and high expression levels is crucial for the successful and effective commercial application of genetically modified (GM) sugarcane for the management of the insect pest. The aim of this study was to determine the relationship between transgene integration and expression levels in GM sugarcane events. Ten GM events were obtained from SASRI and analysed for transgene copy numbers and mRNA expression, using chamber-based digital PCR (cdPCR). Leaf protein levels were measured by using enzyme-linked immunosorbent assay (ELISA) kits. An analysis by cdPCR revealed random variable transgene copies amongst the events, ranging from 1 to 18 (*Cry1Ab*) and 3 to 19 (*Cry2Ab*). The quantification of transgenic transcripts showed a similar variation with mRNA concentrations of *Cry1Ab*, which ranged from 26.2 to 1129.0 copies/µl, while those of *Cry2Ab* were found to range from 28.4 to 502.9 copies/µl. An analysis of the protein concentration also detected variable levels among the events. The concentration of Cry1Ab protein was found to range from 3.3 to 266.0 ng/g fresh weight, while Cry2Ab was found to range from 5.8 to 52 ng/g fresh weight. A statistical analysis revealed the absence of a significant relationship between the transgene copy number and both the gene expression and protein concentration. However, a relationship between the mRNA quantity and protein concentration was detected. The current study is one of the early applications of cdPCR for the transgene copy number and expression analysis in GM sugarcane, and it provides an insight into the incorporation of this technology in expression analysis for the profiling of transgenic lines.

***Keywords*:** Gene copy, gene expression, protein concentration, cdPCR, ELISA

Introduction

Transgenesis, which involves the introduction of foreign DNA within the genome of sugarcane, has the potential to revolutionise the sugar industry by producing plants with various agronomically-beneficial traits (Iqbal *et al*., 2021). The development of genetically modified (GM) sugarcane varieties containing insecticidal transgenes at SASRI has made significant progress towards regulatory approval (Meyer *et al*., 2022). The intention of these transgenes is to provide susceptible varieties with a resistance to the highly destructive African sugarcane borer, *Eldana saccharina*, which severely affects both the cane yield and sugar quality (Goebel & Way, 2003; Meyer *et al*., 2022).

The commercial release of these GM varieties will greatly complement the Integrated Pest Management (IPM) strategies for effectively managing sugarcane borer in highly infested production regions (Kos *et al*., 2009). However, the success of these GM varieties depends largely on achieving high expression levels of the insecticidal proteins, to ensure effective larval mortality and to delay the development of pest resistance to the proteins (Gryspeirt & Gregoire, 2012). As SASRI develops numerous GM events, it is essential to screen for high expressing lines and for further evaluation in pot and field trials, with the goal of identifying elite lines that are suitable for commercial release.

Methodology

In this study, we conducted a GM profiling analysis by using copy number estimation, transcript abundance measurements and protein quantification techniques to identify events for further investigation. Genomic DNA (gDNA) and RNA were extracted from ten TN71 events containing *Cry1Ab* and *Cry2Ab* transgenes; in order to estimate the transgene, copy number relative to a sample of known copies. Reverse transcription was performed to convert the isolated RNA into complementary DNA (cDNA) for a transcript abundance analysis. Both the transgene copy number and transcript levels were quantified by using the QIAcuity Digital PCR System (Qiagen, Hilden, Germany) with specific primer assays. The copy numbers were determined relative to a reference sample containing the known copy numbers of the target transgenes. The transcript abundance was normalised by using two endogenous reference genes to calculate the relative expression levels. Total protein was extracted from the leaves of the GM events and the concentration of Cry1Ab and Cry2Ab proteins was measured by using quantitative ELISA kits (Envirologix, Portland, USA).

Results and Discussion

A copy number analysis is crucial for understanding the integration of transgenes in GM plants, as it plays a significant role in determining the expression of the introduced traits (Li *et al*., 2017). Furthermore, having a knowledge of transgene copy numbers is a regulatory requirement for biosafety assessments and compliance (Liang *et al*., 2022). By using cdPCR, copy number estimation revealed that the transgenes integrated in the TN71 events were variable. The absolute mRNA concentration and corresponding copy numbers of both transgenes in the TN71 events are summarised in Table 1. The *Cry1Ab* copy numbers ranged from 1 to 13, while those of *Cry2Ab* ranged from 3 to 19. This variability can be attributed to the use of particle bombardment, a transformation method that does not allow precise control over the number of inserted copies and results in the random integration within the genome (Ismagul *et al*., 2018; Wang *et al*., 2022). In addition, it was expected that the two *Cry* transgenes would have a different copy number, as they were introduced on different genetic constructs. Variations were also observed in the transgene expression levels and protein concentrations amongst the evaluated events. The absolute quantification of the mRNA showed that *Cry1Ab* transcripts ranged from 26.2 to 1129.0, while those of *Cry2Ab* ranged from 28.4 to 502.9 (Table 1). The relative transgene expression analysis (Figure 1A) indicated that event TN71-243 exhibited the highest relative expression of both transgenes [*Cry1Ab* (39-fold); *Cry2Ab* (14-fold)] relative to the lowest expressing events.

The protein concentration, which was measured by ELISA, showed that amongst the TN71 events, the Cry1Ab protein levels ranged from a 3.2 to 266.0 ng/g fresh leaf weight, while the Cry2Ab ranged from 5.0 to 52.0 ng/g (Table 1). Among the evaluated lines, TN71-472 exhibited the highest protein concentrations for both transgenes. The observed variations in transgene expression and protein concentration could largely be attributed to genomic factors, such as the positional effects and their interaction with nearby genes (Eszterhas *et al*., 2002).Overall, the copy number, gene expression and protein quantification analyses demonstrated that both the *Cry1Ab* and *Cry2Ab* transgenes were successfully integrated and expressed in the TN71

events, which resulted in the production of adequate insecticidal proteins for effective resistance against sugarcane borer (Jacob *et al*., 2023)

in plants occurs at various levels. Therefore, comparing transgene transcript levels and protein concentration can provide valuable insights into the rate of protein translation and the extent of post-transcriptional regulation (Baginsky *et al*., 2010). We analysed data from the transgene copy number, gene expression and protein concentration studies by using Pearson correlation statistics to assess the relationship between these traits in TN71 events (Figure 1B). The results indicated a low-to-moderate correlation between the transgene copy number and the transcript levels. Specifically, the correlation coefficient between the *Cry1Ab* copy numbers and *Cry1Ab* transcripts was found to be 0.33 ($p<0.05$), while it was 0.44 ($p<.0001$) for *Cry2Ab.* Similarly, a low-to-moderate and positive correlation was observed between the transgene copy number, transgene expression and protein concentration. These findings were consistent with those of previous studies, which reported the lack of a strong, positive correlation between the transgene copy number, gene expression and protein concentrations in sugarcane (Gao *et al*., 2016; Gao *et al*., 2018). Few studies have explored the correlation between transgene expression and protein concentration in sugarcane. In the present study, a moderate positive correlation was observed between the transcript levels and the protein concentrations for both Cry1Ab and Cry2Ab, with coefficient correlations of 0.49 ($p<0.05$) and 0.62 ($p<0.05$), respectively. These values suggest that the mRNA expression levels in GM sugarcane can serve as a reliable indicator of subsequent transgenic protein accumulation. Moreover, our findings align with those of Smitha *et al*. (2021), who suggested that integrating mRNA and protein quantification methods is the most accurate approach for determining transgene expression profiles in plants.

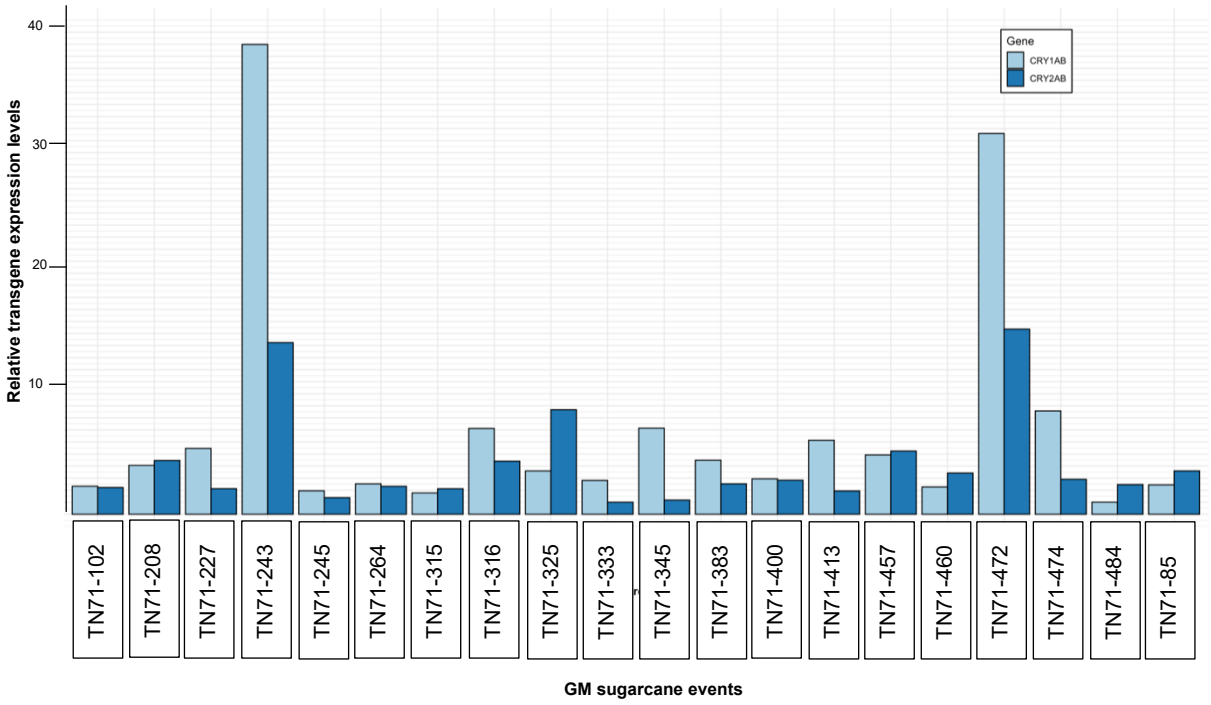
Unlike qPCR, which reports gene expression as fold changes, cdPCR quantifies target transcript concentrations without requiring a standard curve (Lancikova & Hricoka, 2020). By partitioning samples into thousands of individual PCR reactions, cdPCR offers an enhanced sensitivity, which makes it especially useful for detecting low transcript concentrations in events with minimal expression levels (Basu, 2017; Maheshwari *et al*., 2017). The routine integration of gene expression and protein analysis into the molecular characterisation workflow at SASRI will enhance the efficient and reliable selection of elite events for their advancement to field trials. Over the years, qPCR has become a gold standard for gene expression analysis (van Guilder *et al*., 2018). In this study, we successfully developed a transgene expression assay that is based on cdPCR, which is a next-generation PCR technology that utilises sample partitioning. Unlike qPCR, which reports gene expression as fold changes, cdPCR quantifies the target transcript without requiring a standard curve (Lancikova & Hricoka, 2020). By partitioning samples into thousands of individual PCR reactions, cdPCR offers enhanced sensitivity, which makes it especially useful for detecting low transcript concentrations in events with minimal expression levels (Basu, 2017; Maheshwari *et al*., 2017).

Table 1. Concentration and copy numbers of *Cry1Ab* and *Cry2Ab* transgenes in TN71 sugarcane events determined by absolute quantification, using cdPCR

GM event	*Cry1Ab* (copies/µl)	*Cry2Ab* (copies/µl)	*Cry1Ab* Copy number	*Cry2Ab* Copy number	*Cry1Ab* transcripts (copies/µl)	*Cry2Ab* transcripts (copies/µl)	*Cry1Ab* protein (ng/g FW)	*Cry2Ab* protein (ng/g FW)
TN71-85	150.3	274.8	3	7	141.5	254.4	49.1	8.8
TN71-102	42.75	183.9	1	6	69.6	81.1	15.1	9.8
TN71-208	226.2	229.7	4	9	59.9	28.4	51.6	16.1
TN71-227	759.2	236.9	8	8	1129.0	502.9	12.8	5.0
TN71-243	353.6	307.0	8	10	218.4	188.7	6.76	5.8
TN71-245	424.3	361.0	8	10	132.2	147.9	3.2	6.9
TN71-264	597.9	193.4	13	9	71.6	104.6	48.4	17.8
TN71-315	127.6	79.9	2	3	375.0	282.5	76.7	7.3
TN71-316	827.8	457.8	13	15	265.3	780.5	21.2	11.5
TN71-325[a]	47.23	394.6	1	16	167.4	72.8	36.0	27.7
TN71-333	343.0	109.8	7	3	272.1	54.7	21.7	11.1
TN71-345[b]	146.1	98.13	2	3	310.0	212.7	76.8	9.5
TN71-383	551.1	286.4	11	10	235.5	275.8	40.8	11.5
TN71-400	272.8	323.5	6	13	292.0	112.2	38.1	17.7
TN71-413	371.6	241.8	7	5	229.7	298.1	76.7	11.9
TN71-460	111.8	495.4	2	15	869.7	515.4	3.31	29.2
TN71-457	552.0	252.9	10	9	450.6	185.7	31.3	12.1
TN71-472	557.0	354.3	10	6	26.2	78.5	266.0	52.0
TN71-474	432.0	292.9	11	14	141.5	254.4	68.4	21.3
TN71-484	221.0	497.5	4	19	69.6	81.1	3.9	10.2

[a]*Cry1Ab* reference sample, [b]*Cry2Ab* reference sample, FW – Fresh Weight leaf tissue

A



B

Cry2Ab variables	*Cry1Ab* variables: Copy number	*Cry1Ab* variables: Transcript abundance	*Cry1Ab* variables: Protein content
Copy number	1.00	0.33 0.0024	0.18 0.1116
Transcript abundance	0.44 <0.0001	1.00	0.49 <0.0001
Protein content	0.30 0.0062	0.62 <0.0001	1.00

Figure 1. Analysis of transgene copy number, gene expression and protein concentration in TN71 events. (A) Relative transgene expression in, and (B) Pearson correlation analysis of, *Cry1Ab* and *Cry2Ab* variables in TN71 events

Concluding Remarks

The current genetic modification programme at SASRI focuses on developing high foreign transgene-expressing sugarcane varieties, in order to confer effective resistance against the highly destructive sugarcane borer, *E. saccharina*. In this study, we demonstrated the application of cdPCR and ELISA for the assessment of transgene integration, gene expression and protein accumulation in independent GM events that were developed at SASRI. The high levels of transcript abundance and insecticidal protein detected in TN71 events suggest a strong potential for effective resistance to *E. saccharina* in subsequent screening trials.

References

Baginsky S, Henning L, Zimmermann P and Gruissem W (2010). Gene expression analysis, proteomics and network discovery. *Plant Physiol* 152: 402-410.

Basu AS (2017). Digital Assays Part 1: partition statistics and digital PCR. *SLAS Technol.* 22: 369-386.

Eszterhas SK, Bouhassira EE, Martin DIK and Feiring S (2002). Transcriptional interference by independently regulated genes occurs in any relative arrangement and is influenced by chromosomal integration position. *Mol Cell Biol* 22: 469-479.

Gao S, Yang YY, Guo J, Su Y, Wu Q, Wang C and Que Y (2018). Particle bombardment of the *Cry2A* gene cassette induces stem borer resistance in sugarcane. *Int J Mol Sci* 19: 1692.

Gao S, Yang YY, Wang C, Guo J, Zhou D, Wu Q, Su Y, Xu L and Que Y (2016). Transgenic sugarcane with a *Cry1Ac* gene exhibited better phenotypic traits and enhanced resistance against sugarcane borer. *PLoS One* 11: 153929.

Goebel FR and Way MJ (2003). Investigation of the impact of Eldana saccharina (Lepidoptera: Pyralidae) on the sugarcane yield in field trials in Zululand. *Proc S Afr Sug Technol Assoc* 77: 256-265.

Gryspeirt A and Gregoire JC (2012). Effectiveness of the high dose/refuge strategy for managing pest resistance to *Bacillus thuringiensis* (Bt) plants expressing one or two toxins. *Toxins* 4: 810-835.

Iqbal A, Khan RS, Khan MA, Gul K, Jalil F, Shah DA, Rahman H and Ahmed T (2020). Genetic engineering approaches for enhanced insect resistance in sugarcane. *Mol Biotechnol* 63: 557-568.

Jacob RM, Ligege RW, Meyer GM and Snyman SJ (2023). Screening transgenic sugarcane plants for resistance to eldana larvae. *Proc S Afr Sug Technol Assoc* 95: 186.

Kos M, van Loon JJA, Dicke M and Vet LEM (2009). Transgenic plants as vital components of integrated pest management. *Trends Biotechnol* 27: 621-627.

Lancikova V and Hricova A (2020). Digital absolute gene expression analysis of essential starch-related genes in a radiation developed *Amaranthus cruentus* L. variety in comparison with real-time PCR. *Plants* 9: 966.

Liang J, Yang X, Jiao Y, Wang D, Zhao Q, Sun Y, Li Y and Wu K (2022). The evolution of China's regulation of agricultural biotechnology. *aBiotech* 3: 237-249.

Li R, Quan S, Yan X, Biswas S, Zhang D and Shi J (2017). Molecular characterization of genetically modified crops: challenges and strategies. *Biotechnol Adv* 35: 302-309.

Maheshwari Y, Selvaraj V, Hajeri S and Yokomi R (2017). Application of droplet digital PCR for the quantitative detection of *Spiroplasma citri* in comparison with real-time PCR. *PLoS One* 12: 184751.

Meyer GM, Khanyi H, Albertse E, Jacob R and Snyman SJ (2022). Behind the scenes: generation and analysis of genetically modified insect resistant sugarcane. *Proc S Afr Sug Technol Assoc* 94: 69.

Smitha PK, Bathula C, Kumar AM, Chandrashekara KN, Dhar SK and Das M (2021). Correlation of Cry1Ac mRNA and protein abundance in transgenic *Gossypium hirsutum* plants. *3Biotech* 22: 289.

Van Guilder HD, Vrana KE and Freeman WM (2018). Twenty-five years of quantitative PCR for expression analysis. *Biotechniques* 44: 619-626.

POSTER SUMMARY

FROM MANY TO ONE: A PIPELINE FOR SELECTING A DUAL-TRAIT COMMERCIAL GENETICALLY MODIFIED SUGARCANE EVENT

Meyer GM[1], Albertse E[1], Jacob RM[1], Khanyi H[1] and Snyman SJ[1,2]

[1]South African Sugarcane Research Institute, Private Bag X02, Mount Edgecombe, Durban, 4300, South Africa

[2]School of Life Sciences, University of KwaZulu-Natal, Private Bag X54001, Durban, South Africa

gwethlyn.meyer@sugar.org.za, ewald.albertse@sugar.org.za, robyn.jacob@sugar.org.za, hlobisile.khanyi@sugar.org.za, sandy.snyman@sugar.org.za

Abstract

Integrated Pest Management (IPM) mitigates *Eldana saccharina* losses in South African sugarcane. Incorporating *Bacillus thuringiensis* (Bt) *Cry* genes into sugarcane using genetic modification (GM) enhances IPM, reduces the crop's environmental impact and improves its economic value. At SASRI, insect resistance is being combined with tolerance to the herbicide imazapyr, which is conferred by the mutated acetolactate synthase (*mALS*) sugarcane gene.

To meet the South African regulations, insecticidal GM events must contain low- or single-copy genes that express at high levels while maintaining their substantive equivalence to the unmodified wild type. We have developed a screening pipeline to characterise and select events in the laboratory, streamlining numbers that advance to contained facility testing.

Those plants containing the *mALS* gene, detected using polymerase chain reaction (PCR), are tested for CRY protein expression using commercially available lateral flow devices. Positive plants are screened for a low *Cry* gene copy number using digital PCR before being tested in an *in vitro* plantlet bioassay (IVPB). Events resistant to feeding by eldana larvae in the IVPB advance to an *in vitro* re-rooting assay on imazapyr-containing medium. Plants are considered imazapyr tolerant if their roots regrow to >10mm within two weeks.

A case study demonstrates the stringency of this pipeline: over an 18-month period 1,283 GM events were produced from 300 bombardments. Each screening step eliminated between 30 and 56% of the events entering that stage, except for the IVPB step, where 82% were retained. Only seven percent of generated events successfully passed through the laboratory pipeline and proceeded to assessment in SASRI's contained facilities.

Keywords: Bt sugarcane, genetic modification, insect-resistance, Eldana bioassays, integrated pest management, imazapyr tolerance

POSTER SUMMARY

CONTROL OF YELLOW SUGARCANE APHIDS USING ENTOMOPATHOGENIC FUNGI

Nguvu GM[1] and Mndzawe DM[1]

[1]Estate Agriculture Department, Kilombero Sugar Company, P. O. Box 50 Kidatu, Morogoro, Tanzania

gnguvu@illovo.co.tz

Abstract

This study aimed at assessing the efficacy of entomopathogenic fungi in controlling the infestation of yellow sugarcane aphids. Experimental trial was established at Kilombero Estate Agriculture, field 520A having variety NCo376, known to be prone to YSA. Experimental plots dimensions were 18 rows spaced at 1.8m and 300m length. Experimental design was Randomized Complete Block Design with five treatments; *Beauveria bassiana* at 0.5 and 1.0 kg/ha, *Lecanicillium lecanii* at 0.5 and 1.0 kg/ha, tested against a negative control where nothing was applied. Treatments were applied using DJI-Agras T30 drone at 120 l/ha spray mix cruising 3 m above the crop every week for 4 consecutive weeks between 28th September and 26th October 2024. Scouting for YSA and beneficial organisms was done before each spray and one week after the last spray. Data collected were analysed using Minitab™ Statistical Software. Results showed that there was no statistical significance between the treatments (p-value 0.135), while the coefficients for the weeks indicated significant decreases in the percent infestation over time at 0.05 significance level. Multiple Regression Model suggested that both treatments and weeks have significant effects on percent infestation, with weeks having a stronger linear effect and both variables having quadratic effects that modify the overall relationship. Entomopathogenic fungi holds a significance promise for managing insect-pest in sugarcane. However, the timing of application plays a big role in increasing efficiency, therefore, application just at the economic threshold level should be advocated, and high humidities should also be considered for continuous fungal growth.

Keywords: Yellow Sugarcane Aphid, biological control, entomopathogenic fungi, Integrated Pest Management, sugarcane, pest

SHORT COMMUNICATION

AUTOMATED FIELD BOUNDARY DETECTION, DELINEATION AND EXTRACTION, USING SENTINEL-2 SATELLITE IMAGERY

Poona NK

South African Sugarcane Research Institute (SASRI), Mount Edgecombe, 4302, South Africa

Nitesh.Poona@sugar.org.za

Abstract

Accurate and up-to-date field boundary data are crucial for implementing precision agriculture, for the monitoring and evaluation of land cover change, and for resource planning. Field boundaries are foundational for mapping and monitoring the area under cane, developing biomass/yield models, optimising irrigation, fertilizer and chemical inputs, as well as improving the planting and harvesting efficiency. The advent of free-to-use Sentinel-2 (S-2) remotely-sensed satellite data and related geospatial tools provides the means for developing a workflow for producing accurate and up-to-date crop field boundary data, for the entire area under cane. S-2, with 13 spectral bands, a 10-60 m spatial resolution, a 290 km swath, a 2- to 5-day temporal resolution, and an archive since 2015, provides an opportune data source for delineating crop panel/field boundaries. This study employed S-2 imagery, existing boundary data for the Nkomazi region in Mpumalanga Province and Midlands North (MN) region in the KwaZulu-Natal Province, as well as proprietary boundary detection algorithms, for automated field boundary detection, delineation and extraction. The two proprietary algorithms employed in this study were Algorithm 1 (Al-1), which is based on semantic segmentation and deep learning, and Algorithm 2 (Al-2), which is based on super-resolution image reconstruction using a deep learning-based technique. A first model (A1), employing Al-1 and 10 m S-2 imagery in Nkomazi, yielded an F-score of 0.73. An F-score of 0.82 was achieved after fine-tuning the model – Model A2. Two subsequent models employed Al-2 and 10 m S-2 imagery in Nkomazi (Model B) and MN (Model C). Model B yielded an F-score of 0.9857, whereas Model C yielded an F-score of 0.9889. The results demonstrate the potential operational value of the models, particularly Models B and C that were developed by using Al-2.

Keywords: Sugarcane, field boundary, Sentinel-2 (S-2), super-resolution, automated workflow, precision agriculture

Introduction

The traditional approach to extracting crop field boundaries is manual digitisation from high resolution aerial photographs and/or very high-resolution drone imagery. However, manually digitising expansive agricultural areas, such as the area under cane in South Africa, is impractical. Consequently, researchers are investigating protocols for automatically identifying, delineating and extracting crop field boundaries from remotely-sensed imagery. Several studies have applied semantic segmentation, coupled with deep learning, for boundary detection and extraction. For example, Waldner and Diakogiannis (2020) employed 10 m resolution S-2 imagery with ResUNet, a deep Convolutional Neural Network (CNN), to extract field boundaries in South Africa's Maize Quadrangle. The study achieved overall accuracies of above 91%, with F-scores above 0.89. Lu *et al*. (2023) successfully employed the AttMobile-DeeplabV3+ network, based on a CNN, to extract farm boundaries from drone imagery in Beijing, China. The authors reported a producer's accuracy of 96.62%. Anaraki *et al.* (2025) trained a U-Net model by using Google Earth satellite images and drone imagery for extracting agricultural field boundaries in Iran and Ethiopia. The F-scores ranged from 0.70

to 0.82. Chen *et al*. (2025) proposed BS-GAN, a semi-supervised segmentation network that is based on Generative Adversarial networks (GANs). The authors evaluated their Boundary Segmentation network (BS-GAN) for extracting boundaries of various land types, including agricultural land, from high-resolution aerial images of Vaihingen and Gaofen satellite imagery of Potsdam. The F-scores ranged from 0.88 to 0.93.

Super-resolution image reconstruction of the 10 m S-2 bands, using deep learning-based techniques, can produce a higher-quality S-2 image with a spatial resolution of up to 1 m. For example, Kramer *et al*. (2024) enhanced the three 10 m S-2 RGB bands to 5 m by using 20 cm aerial orthophotos and a CNN and GAN. Similarly, Wang *et al*. (2024) enhanced the three 10 m S-2 bands to 4 m by using 4 m Gaofen-2 satellite imagery and a cascaded GAN. Sharifi and Safari (2025) employed transformer-based deep learning models to enhance the three 60 m S-2 bands and six 20 m S-2 red edge and SWIR bands to 10 m. The Sentinel-2 Deep Resolution 3 (S2DR3) model by Digifarm (https://digifarm.io/) increases the spatial resolution of all 12 S-2 bands to 1 m (Chanev *et al*., 2025). This study investigates the feasibility of utilising free-to-use S-2 satellite data to develop a workflow for identifying, delineating and extracting crop field boundaries via two methodologies, namely, by employing semantic segmentation with deep learning and employing super-resolution with feature detection, using deep learning.

Materials and Methods

Image and field boundary data

Free-to-use S-2 multispectral satellite imagery captured in 2023 and 2024 were employed in this study for identifying, delineating and extracting crop field boundaries. The reference field boundary data for Nkomazi were acquired from the Malelane and Komatipoort Mill Group Boards. The Midlands North reference dataset was acquired from the Noodsberg Cane-growers Association. The reference datasets comprised field boundaries of all the sugarcane fields in their respective regions.

Image analysis

Image processing was undertaken in two phases. In Phase 1, the 10 m S-2 images and the Nkomazi reference dataset were analysed by using AI-1, based on semantic segmentation and deep learning. Following training and testing of the original model (A1), a fine-tuning process was undertaken, whereby varying label weights, augmentation and learning rates were iteratively applied. In Phase 2, super-resolution 1 m S-2 images were derived using the Super Resolution Model that is a key component of AI-2 (Figure 1). AI-2 was applied to the Nkomazi (Model B) and Midlands North (Model C) reference dataset.

For all models, the model accuracy was assessed using the F-score: $F = \frac{2xUAxPA}{UA+PA}$, where UA is the user's accuracy ($UA = \frac{TP}{TP+FN}$) and PA is the producer's accuracy ($PA = \frac{TP}{TP+FP}$), where TP = true positive, FP = false positive, and FN = false negative.

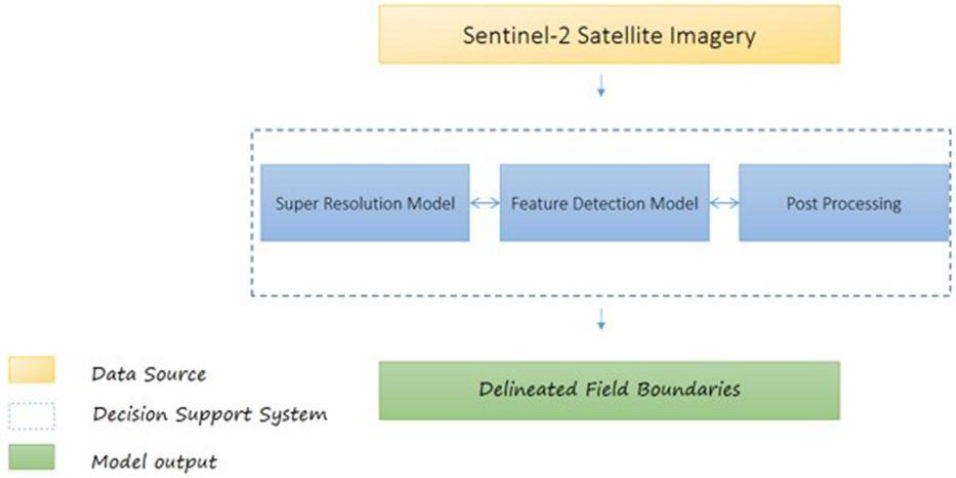


Figure 1. Conceptual framework of the proprietary algorithm AI-2 employed in this study.

Results and Discussion

The results for Model A1 (the original model) and Model A2 (the fine-tuned model) based on the Nkomazi reference dataset and AI-1, is shown in Figure 2. Model A1 produced an F-score of 0.73, whereas Model A2 produced an F-score of 0.82. The fine-tuned Model (A2) has excluded the centre-pivot irrigation field in the lower left of the image, despite the model yielding a higher F-score of 0.82. Fine-tuning a model often results in a compromise, whereby the accuracy in some parts of the output will increase whereas the accuracy in other parts will decrease, despite the increase in overall accuracy. Overall, the original Model (A1) and the fine-tuned model (A2) ignored fields that were not included in the Nkomazi reference dataset. This situation illustrates a key limitation of AI-1 – the requirement for a complete ground truth dataset. The reference dataset for Nkomazi contained only the boundaries of the sugarcane fields. There were no boundary data for non-sugarcane fields (such as other crops and timber), waterbodies and non-agricultural areas. Consequently, the models underperformed in terms of overall accuracy.

Comparing the results of Model A1 (F-score = 0.73) and A2 (F-score = 0.82) with the results of Model B (F-score = 0.9857), it is evident that AI-2 outperformed AI-1 for Nkomazi. The output of Model B (Figure 2) illustrates that AI-2 captured all the fields, including those fields that were not included in the reference dataset. Similar results can be seen in the output of Model C (Figure 2; F-score = 0.9889), where AI-2 has captured all fields, including sub-fields (panels). The outputs of AI-2 will require post-processing to clean up the unnecessary/unrequired sub-field boundaries.

Comparing the results of this study to the results of Waldner and Diakogiannis (2020), who employed 10 m S-2 with semantic segmentation and a deep CNN for field boundary extraction, achieving an F-score of 0.89, it is evident that AI-2, based on super-resolution image reconstruction of the 10 m S-2 bands, using deep learning-based techniques, produced superior results, with an F-score of 0.9857 and 0.9889. Comparative results, with F-scores ranging from 0.88 to 0.93, were achieved by Chen *et al*. (2025), who employed BS-GAN with high resolution aerial images and Gaofen satellite imagery. This study demonstrates the value of image downscaling, specifically the downscaling of S-2 imagery for field boundary detection, delineation and extraction. In addition, the results show that costly aerial imagery may not be required in cases where S-2 free-to-use imagery is downscaled to 1 m.

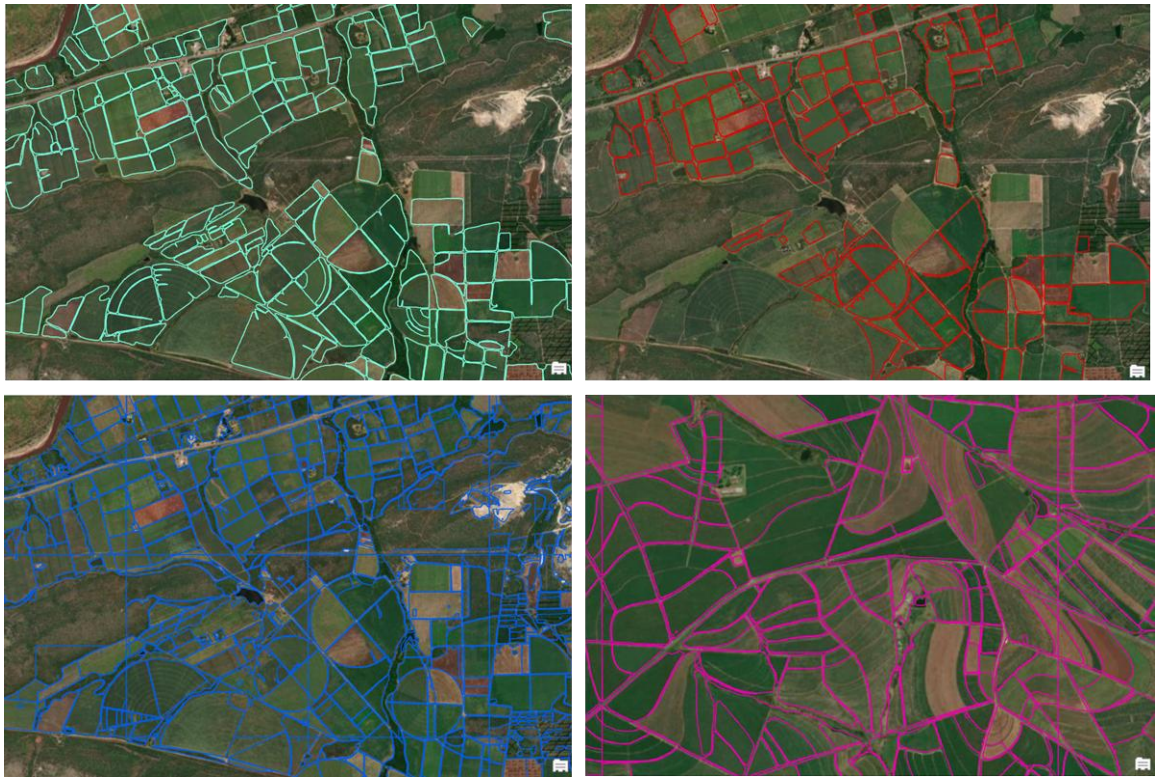


Figure 2. The output of Model A1 (top left), Model A2 (top right), Model B (bottom left), and Model C (bottom right)

Conclusion

The results obtained in this study illustrate the operational potential of using S-2 remotely-sensed satellite imagery for developing a protocol for automated field boundary detection, delineation and extraction. A further calibration/validation of the models is envisaged for other growing regions. The ultimate goal is to develop a protocol for the area under cane, thereby ensuring up-to-date accurate field boundaries.

Acknowledgements

The South African Sugarcane Research Institute is thanked for funding the research, and the two commercial entities are appreciated for their scientific contributions to the success of the study.

References

Anaraki NR, Tahmasbi M and Kheradpisheh SR (2025). Detecting cadastral boundary from satellite images using U-Net model. https://doi.org/10.48550/arXiv.2502.11044.

Chanev M, Kamenova I, Dimitrov P and Filchev L (2025). Evaluation of Sentinel-2 deep resolution 3.0 data for winter crop identification and organic barley yield prediction. *Remote Sensing* 17(6). https://doi.org.10.3390/rs17060957.

Chen Y, Yang Z, Zhang L and Cai W (2025). A semi-supervised boundary segmentation network for remote-sensing images. *Scientific Reports* 15. https://doi.org.10.1038/s41598-025-85125-9.

Chen Z, Coa A, Deng H, Mi X and Yang J (2024). Accurate contour preservation for semantic segmentation by mitigating the impact of pseudo-boundaries. *International Journal of Applied Earth Observation and Geoinformation* 126(103615): 1-10. https://doi.org.10.1016/j.jag.2023.103615.

Kramer P, Steinhardt A and Pedretscher B (2024). Enhancing Sentinel-2 image resolution: evaluating advanced techniques based on convolutional and generative neural networks. https://doi.org/10.48550/arXiv.2410.00516.

Lu H, Wang H, Ma Z, Ren Y, Fu W, Shan Y, Hu S, Zhang G and Meng Z (2023). Farmland boundary extraction based on the AttMobile-DeeplabV3+ network and least squares fitting of straight lines. *Frontiers in Plant Science* 14: 1-15. https://doi.org.10.3389/fpls.2023.1228590.

Sharifi A and Safari MM (2025). Enhancing the spatial resolution of Sentinel-2 images through super-resolution using transformer-based deep-learning models. IEEE *Journal of Selected Topics in Applied Earth Observations and Remote Sensing* 18: 4805-4820. https://doi.org.10.1109/JSTARS.2025.3526260.

Waldner F and Diakogiannis FI (2020). Deep learning on edge: extracting field boundaries from satellite images with a convolutional neural network. *Remote Sensing of Environment* 245. https://doi.org.10.1016/j.rse.2020.111741.

Wang X, Ao Z, Li R, Fu Y, Xue Y and Ge YI (2024). Super-resolution image reconstruction method between Sentinel-2 and Gaofen-2 based on cascaded generative adversarial networks. *Applied Sciences* 14(12). https://doi.org.10.3390/app14125013.

SHORT COMMUNICATION

MODELLING LEAF NITROGEN BY USING MULTI-TEMPORAL *IN SITU* INFRARED SPECTROSCOPY

Makhaye A, Tyilekile S and Poona NK

Plant Environment Resource Centre, South Africa Sugarcane Research Institute, P/Bag X02, Mount Edgecombe, 4300, South Africa

Anelisa.Makhaye@sugar.org.za, Sikelela.Tyilekile@sugar.org.za, Nitesh.Poona@sugar.org.za

Abstract

Sugarcane is a high nutrient-use crop, where balanced nutrition is essential for ensuring optimal sugarcane productivity, quality and yield. Nutrient uptake was assessed by using leaf sampling and an analysis was undertaken at predefined periods to permit diagnostic interpretation. A leaf analysis guides growers regarding the potential nutrient uptake issues in their fields. Visible and Near-Infrared Spectroscopy (VNIRS) has shown promise for estimating the leaf nutrient concentration, most notably nitrogen (N), in standing crops. VNIRS can permit the rapid and near-real-time assessment of a crop's nutritional status, to permit better N management and to improve its nutrient-use efficiency. A multi-temporal assessment of the leaf N could provide an insight into the plant's N uptake and the optimal management of N in the fertilizer input. The goal of this study was to develop a methodology to estimate the leaf nitrogen (N) by using *in situ* hyperspectral data (350-2500 nm) and Machine Learning (ML) techniques. The study was conducted across five trials at Pongola (A + B), Komatipoort, and Mount Edgecombe (A) for the ripener trials, and Mount Edgecombe (B) for the long-term residue and fertilizer management trial, using a FieldSpec 4 Hi-Res spectroradiometer. Spectral data were collected monthly, over six months, from 40 randomly-selected plots, and the leaf samples were sent for laboratory analysis. The third fully expanded leaf from ten plants per plot were scanned. The Random Forest (RF) algorithm was used to develop regression models. The results showed that the N concentrations were highly variable, with respect to leaf age and location, with the R2 values ranging from 0.41 to 0.82. The combined dataset of Pongola and Komati (an irrigated region) yielded the best overall prediction of (R2 = 0.82), which illustrated the potential for modelling the leaf N during the growing season by using VNIRS.

Keywords: Sugarcane, leaf nitrogen, spectral measurements, leaf nutrient, Random Forest (RF), regression models

Introduction

Nitrogen (N) is a key element in the growth, development and yield of a crop and it is often a limiting nutrient in agricultural production. The nitrogen status of crops is assessed by means of a laboratory analysis of soil or plant tissue samples, which informs fertiliser recommendations that are aimed at maximising the yield and nutrient-use efficiency (Abdel-Rahman, 2008). The emergence of remote-sensing technologies, especially Visible and Near-

Infrared Spectroscopy (VNIRS), has enabled the non-destructive *in situ* and near-real time estimation of leaf nutrient concentrations in standing crops.

Poona *et al*. (2023) investigated the use of *in situ* spectroscopy data and machine learning to predict the leaf N content in sugarcane. Spectral data were collected once-off from 4- to 5-month-old sugarcane in Pongola, Komatipoort and Mount Edgecombe. The results were promising, and they demonstrated the potential of using VNIRS and machine learning as a tool to manage N fertiliser application. The utility of VNIRS for estimating the leaf N has also been explored in several studies by using multi-temporal data.

Reyes-Trujillo *et al*. (2021) estimated the canopy N of sugarcane using *in situ* spectroscopy in plant cane and first ratoon cane over a six-month period. Partial Least Squares Regression (PLSR) was employed for developing the models. The results indicated that the best nitrogen estimation was during the early growth stages of the first ratoon (R^2 = 0.98; RMSE = 1.16 g kg^{-1}). The authors noted that canopy reflectance was sensitive to the nitrogen rates in the Near Infrared (NIR) and Red-Edge (RE) region. Silva *et al*. (2024) explored the potential of VNIRS in sugarcane for quantifying the leaf N for different growing regions and vegetative stages. On five occasions, spectral data were collected between 140-260 Days After Cutting (DAC). Spectral models were developed by using PLSR. Using data from all-time points, the model achieved a moderate predictive performance (R^2 = 0.53; RMSE = 2.15 g kg^{-1}). Similarly, Fiorio *et al*. (2024) employed spectral data across different vegetative growth stages. On eight occasions, spectral data were collected between 67-313 DAC. Spectral models were developed by using PLSR. Using data from the all-time points, the model achieved a high predictive performance (R^2 of 0.72; RMSE of 1.41 g kg^{-1}). In addition, the most important features (wavelengths) that were determined by using the Variable Importance in Projection, were located in the visible, RE and Shortwave Infrared (SWIR) regions.

These studies highlight the utility of multi-temporal VNIRS as a rapid and non-destructive approach to leaf N management. The objectives of this study were to evaluate the VNIR (400 nm-1 200 nm) and shortwave infrared (SWIR; 1 200 nm-2 400 nm) wavelengths to model the leaf N in sugarcane leaves and to determine the wavelength ranges that are applicable for predicting the leaf N in sugarcane.

Materials and Methods

Spectral data collection

Leaf spectral measurements were taken in five trials on twelve-month crops in Pongola (A + B), Komatipoort and Mount Edgecombe (A) for ripener trials and, Mount Edgecombe (B) for the long-term residue and fertilizer management trial, using the ASD FieldSpec 4 Hi-Res spectroradiometer (Malvern Panalytical (Pty) Ltd) with a spectral range of 350-2500 nm. Within each ripener trial, 40 plots were randomly selected and scanned monthly, over a 6-month period, starting at a crop age of 4-5 months. For the long-term residue and fertilizer management trial, all 32 plots were selected and scanned monthly over a six-month period, starting at a crop age of 4-5 months. The spectral measurements were collected from ten random leaves per plot, using the third fully-expanded leaf.

Leaf sampling

Leaf sampling coincided with the spectral measurements, i.e. at the crop ages ranging from 4-10 months. For each sampled plot, 30 to 40 leaf samples were collected; the midribs were removed and discarded before being sent to the laboratory for a leaf nutrient analysis. Spectral data and leaf sampling were undertaken within the same week.

Spectral data analysis and model development

The ten spectral measurements from each plot were aggregated to a single leaf spectrum per plot and the spectral data were exported to the software ViewSpec Pro (Malvern Panalytical (Pty) Ltd, 2014) and converted into reflectance values (Re *et al*., 2024). The Random Forest (RF) algorithm (Poona *et al*., 2023) was employed for building regression models, using default hyperparameter values. Modelling was conducted by using the Random Forest Regressor implementation in Python (v7.2.2). The RF of feature importance was calculated by using the Gini impurity coefficient.

Results and Discussion

The study focused on the combined results across the trial sites, as presented in Table 1. These represent the best-performing Random Forest regression models that were developed in the study.

Model performance

The results in Table 1 represent the best-performing RF models for the combined sites in the rainfed (Mount Edgecombe) and irrigated (Pongola and Komatipoort) regions. The R^2 ranged from 0.41 to 0.82, with the Root Mean Squared Error (RMSE) ranging from 1.01 g kg^{-1} to 2.63 g kg^{-1}. These results compare favourably with the results of Fiorio *et al*. (2024) and Silva *et al*. (2024) who achieved R^2 values of 0.72 and 0.53, with RMSE values of 1.41 g kg^{-1} and 2.15 g kg^{-1} respectively. While the RF model demonstrated promising results, it is acknowledged that the model relied solely on hyperspectral data, without integrating the environmental and agronomic variables, such as the rainfall, soil water content, fertiliser timing in application and soil properties, all of which influence the nutrient uptake.

Table 1. Random Forest regression of predicted R^2 values, crop age and the trial sites.

Trial Location	**4-5 month**		**5-6 month**		**6-7 month**		**7-8 month**		**8-9 month**		**9-10 month**	
	R^2	RMSE g kg^{-1}	R^2	RMSE g kg^{-1}	R^2	RMSE g kg^{-1}	R^2	RMSE g kg^{-1}	R^2	RMSE g kg^{-1}	R^2	RMSE g kg^{-1}
Mount Edgecombe (A + B)	0,61	1,62	Null	Null	0,57	2,12	0,66	1,29	0,41	1,97	0,43	1,01
Pongola (A + B) & Komatipoort	0,75	2,61	0,68	1,66	0,70	2,05	0,57	2,63	0,82	1,65	0,73	2,63

Environmental effects on the spectral response and the model's performance

In the rainfed region [Mount Edgecombe (A) and Mount Edgecombe (B)], the R^2 values ranged from 0.61 with a RMSE of 1.62 g kg^{-1} at 4 to 5 months, to R^2 of 0.43 with a RMSE of 1.01 g kg^{-1} at 9 to 10 months. Conversely, in the irrigated region (Pongola (A + B) and Komatipoort), the R^2 values ranged from 0.75 with a RMSE of 2.61 g kg^{-1} at 4 to 5 months, to R^2 of 0.57 with a RMSE of 2,63 g kg^{-1} at 7 to 8 months, which showed an expected trend, as compared with the rainfed region. The higher R^2 of 0.82 at 8 to 9 months likely reflects a combination of a clearer spectral expression of the nitrogen status, favourable environmental conditions and stable leaf N levels, rather than an actual high N uptake. While early growth stages are where the N demand peaks, the later stages may offer more distinct remote-sensing signals for N estimation (Yang *et al*., 2024). This could be due to the rainfall, which drove the nutrient mobility in the soil (especially nitrate), which affected the root function. In addition, the Soil Water Content (SWC) could have impacted the nutrient solubility, microbial activity and root uptake.

The influence of environmental factors, particularly the rainfall and soil moisture, may have affected the accuracy of the spectral predictions in this study. Rainfall increases the soil water content, which can enhance the nutrient solubility and microbial activity, thereby influencing the root uptake and the overall physiological status of the plant (Reisig, 2023). These changes can alter key traits, such as the leaf N concentration, chlorophyll content and water status factors, which are directly linked to the spectral reflectance patterns. As a result, differences in the soil moisture across the study sites may have introduced a variability in the spectral signal, potentially obscuring the N-related absorption features and reducing the clarity of the spectral measurements. This environmental variability could partly explain the inconsistencies or reductions in the model's performance, as the spectral data reflect not only the N levels, but also other physiological responses that are influenced by water availability. Since the spectral measurements were collected multi-temporarily, without including data for the site-specific rainfall or soil moisture conditions, it is possible that these factors acted as confounding variables. In addition, the split fertilizer application could have synchronised the nutrient availability with the peak demand and reduced the leaching losses (Yang *et al*., 2024).

Figure 1 presents the laboratory-derived leaf N concentrations across the crop ages for five sites. Notably, the highest N concentration (2.63%) was observed in young cane at 4½-month-old cane in the Komati region. In the Pongola region, both trials (A + B) had a high N peak on 5- and 6-month-old cane. This aligns with the grand growth phase (3-7 months), when the crop experiences a peak nutrient uptake that is driven by the high demand for canopy expansion and biomass accumulation. As the crop progresses into the maturation phase (8-12 months), the nitrogen uptake generally decreases as the vegetative growth slows and the plant shifts its focus toward sucrose accumulation in the stalk (Khan, 2023). However, the model still showed a strong performance during this period, which suggests that interrelated factors, such as nutrient remobilisation, environmental conditions, and fertilizer timing, may influence the nitrogen status, even in the later stages of growth.

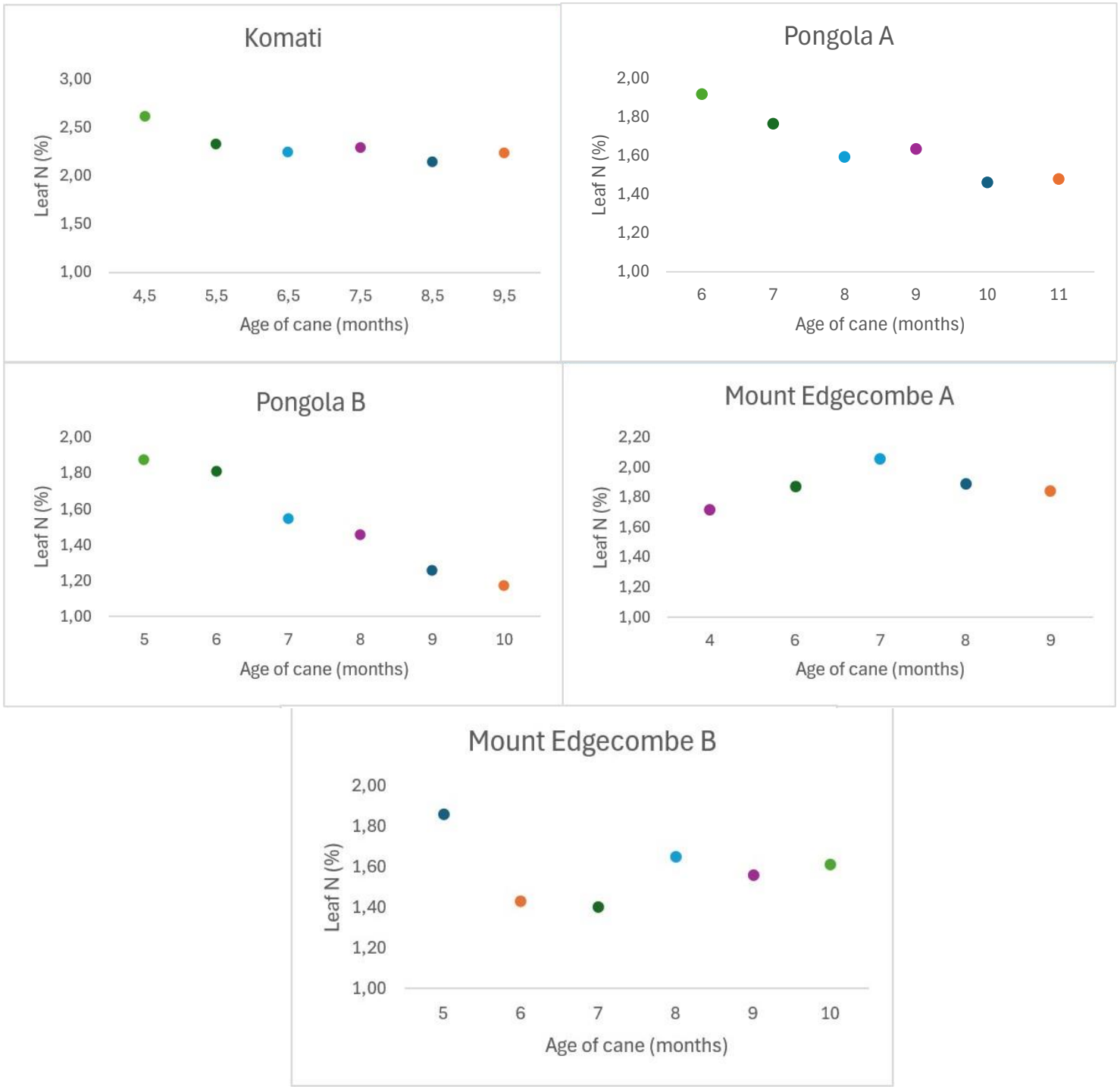


Figure 1. Leaf N across crop ages in months for the five sites.

Feature performance

Overall, the most important features, as ranked by RF using the Gini impurity, were located primarily in the VIS (~400 to 700 nm) and SWIR (~1200 to 2500 nm) regions. Important features were mostly located in the VIS and SWIR for the rainfed models, whereas for the irrigated models, the important features were mostly located in the NIR.

Conclusion

Preliminary work, combining hyperspectral reflectance data with Random Forest modelling, has shown the potential for predicting leaf nitrogen. Future work should focus on expanding the dataset to improve the prediction accuracy. In addition, incorporating the soil moisture and rainfall data may enhance the model's performance. Further investigation is also needed to identify the key spectral features for the development of targeted spectral indices.

Acknowledgements

The author wishes to express their appreciation to the South African Sugarcane Research Institute for supporting this study. We extend our heartfelt gratitude to FAS for analysing the leaf samples. Riekert Van Heerden, Sibusiso Zulu (Ripener Evaluation Trials) and Thandile Mdlambuzi (long-term residue and fertilizer management Trial) for allowing us to utilise the trials, as well as to the Research Support Team at the Komati and Pongola research farms, alongside those at Mount Edgecombe for their assistance in gathering data.

References

Abdel-Rahman EM, Ahmed FB and van den Berg M (2008). Imaging spectroscopy for estimating sugarcane leaf nitrogen concentration. In *Remote Sensing for Agriculture, Ecosystems, and Hydrology* 7104: 263-274.

Fiorio PR, Silva CAAC, Rizzo R, Demattê JAM, dos Santos Luciano AC and da Silva MA (2024). Prediction of leaf nitrogen in sugarcane (Saccharum spp.) by Vis-NIR-SWIR spectroradiometry. *Heliyon* 10(5): 1-13.

Khan ME (2023). Sugarcane crop developmental stages and water requirement: a review. *Pakistan Sugar Journal* 38(2): 11-15.

Poona NK, Radebe T and Titshall LW (2023). Modelling leaf nitrogen using in-situ infrared spectroscopy: a preliminary study. *In Proceedings of the Annual Congress-South African Sugar Technologists Association* 95: 214-217.

Reyes-Trujillo A, Daza-Torres MC, Galindez-Jamioy CA, Rosero-García EE, Muñoz-Arboleda F and Solarte-Rodriguez E (2021). Estimating canopy nitrogen concentration of sugarcane crop using *in situ* spectroscopy. *Heliyon* 7(3): 1-10.

Ré NC, Silva CAAC, Oliveira AKDS, Caron ML, Nilsson MS, Duft DG and Fiorio PR (2024). VIS-NIR-SWIR spectroscopy in sugarcane (Saccharum officinarum L.) cultivation for phytosanitary purposes. *Ciência Rural* 55(3): 1-15.

Reisig, D. (2023). Soil moisture influence on nutrient availability in the soil. *Global Journal of Plant and Soil Sciences* 7(4): 1-2.

Silva CAAC, Rizzo R, da Silva MA, Caron ML and Fiorio PR (2024). Spatio-Temporal Generalization of VIS-NIR-SWIR Spectral Models for Nitrogen Prediction in Sugarcane Leaves. *Remote Sensing* 16(22): 1-18.

Yang L, Zhou Y, Meng B, Zhan J, Xi M, Deng Y, Wu W, Lakshmanan P, Chen X and Zhang F (2024). High sugarcane yield and large reduction in reactive nitrogen loss can be achieved by lowering nitrogen input. *Agriculture, Ecosystems & Environment* 369(109032): 1-24.

POSTER SUMMARY

OPTIMISING FIELD MONITORING THROUGH NDVI-BASED ANOMALY DETECTION USING DRONE IMAGERY: A PILOT STUDY AT DWANGWA ESTATE

Msowoya M

Agriculture Engineering Section, Department of Agriculture, Dwangwa Estate, Illovo Sugar Malawi

mmsowoya@illovo.co.za, mmsowoya150@gmail.com

Abstract

Manual field scouting at Dwangwa Estate is currently the primary method for detecting crop anomalies, but it is time-consuming, labour-intensive and subject to human error. This pilot study introduced drone-based, multispectral imaging and NDVI classification to enhance field monitoring by enabling the early, spatially-precise detection of anomalies, such as gaps, ponding and crop stress in sugarcane fields.

The study was conducted over 70 hectares covered by ratoon and plant cane, using a DJI Phantom 4 Multispectral drone. NDVI maps were generated and classified into four vigour zones (low, medium, high and excellent) using Pix4Dfields and QGIS. Sixty ground-truth points validated the classification accuracy, while the operational usability was assessed through feedback from nine field staff.

The results showed that 43% of the fields exhibited low NDVI values, with 97% of these areas confirmed to have actual problems, including disease, pest damage, ponding and missing stands. Drone-assisted monitoring reduced the full-field scouting time by over 45%. Field staff rated the drone maps 4.5 out of 5 for their decision support value. The integration with Avenza Maps facilitated precise field navigation and targeted interventions.

This study demonstrates that a drone-based NDVI analysis is a feasible, efficient and practical tool for optimising sugarcane field monitoring at an estate level. It enables the earlier detection of stress, better resource allocation and improved decision-making, which makes it a promising approach for modernising the agricultural monitoring practices. The further scaling and integration of this technology into routine operations, regular mapping, as well as the establishment of a centralised database for improved long-term strategic decision-making, are highly recommended.

Keywords
NDVI, drone imagery, field monitoring, precision agriculture, sugarcane, GIS

Introduction

Manual scouting is the current method that is used for field monitoring at Dwangwa Estate. While effective to some extent, it is time-consuming, labour-intensive, and prone to subjectivity and human error. This pilot project introduced NDVI-based drone imagery to optimise field monitoring by enabling the early, spatially-accurate detection of anomalies such as gaps, ponding and crop stress.

The study aimed to assess whether integrating drone technology could improve the speed, accuracy and decision-support value of the field monitoring processes.

Objectives

- to introduce a drone-based NDVI analysis to support field monitoring
- to detect anomalies (gaps, ponding and stress zones) and to classify by NDVI;
- to compare drone-based outputs with field observations for accuracy; and
- to assess its feasibility and usability at estate level.

Materials and Methods

Study site

- Four (4) fields, Dwangwa Estate, Nkhotakota District, Malawi
- Area: 70 ha (ratoon plus plant fields)

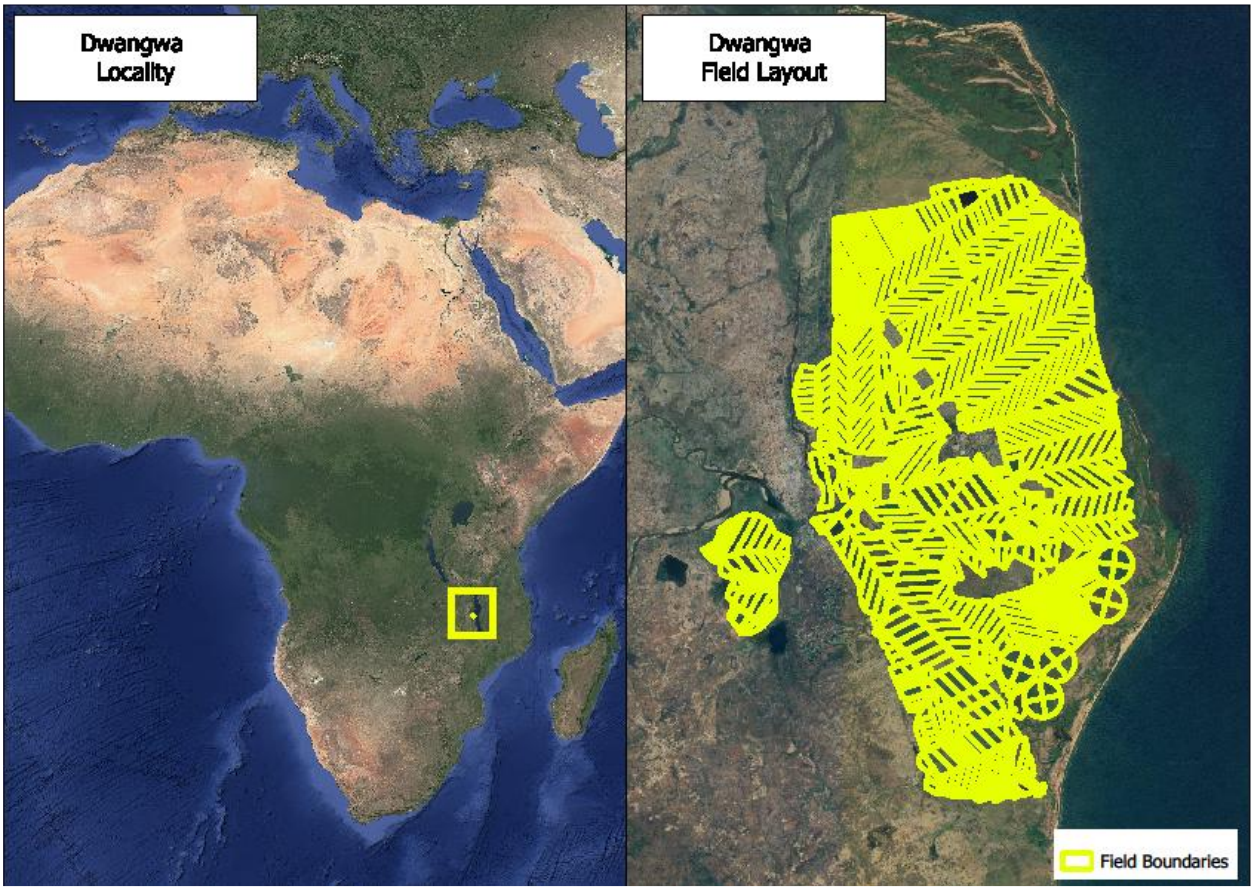


Figure 1. Dwangwa Estate – Field Layout

Drone and sensor

- DJI Phantom 4 Multispectral (P4M)
- 6-band camera (RGB + Red Edge + NIR)
- Ground sampling distance: 5.2 cm/pixel

- Frontlap/Sidelap: 80% / 70%

Processing and classification

- Pix4Dfields: Orthomosaic, radiometric correction, NDVI generation
- QGIS: NDVI classification into four (4) zones:
    - ❖ Low (0.00 - 0.39)
    - ❖ Medium (0.40 - 0.59)
    - ❖ High **(**0.60 - 0.80)
    - ❖ Excellent (0.60 - 1.00)
- Avenza Maps used for offline field inspection navigation
- *Ground truthing and feedback*
- 60 ground-truth points used to validate the classification
- Informal interviews with nine (9) field staff (managers, supervisors and field scouters)
- Operational feedback collected verbally, post-mapping

Results

NDVI map analysis

- 43.0%: Low vigour
- 35.4%: Medium
- 21.6%: High
-

Validation accuracy

- 97% of the areas that showed low NDVI values on the map were confirmed to have actual problems in the field; and
- the anomalies included disease- and pest-affected cane, ponding and missing stands.
-

Operational insights

- managers used maps to prioritise scouting and to intervene faster;
- time required for full - field scouting was reduced by more than 45%; and
- feedback rated drone maps 4.5/5 for decision support.

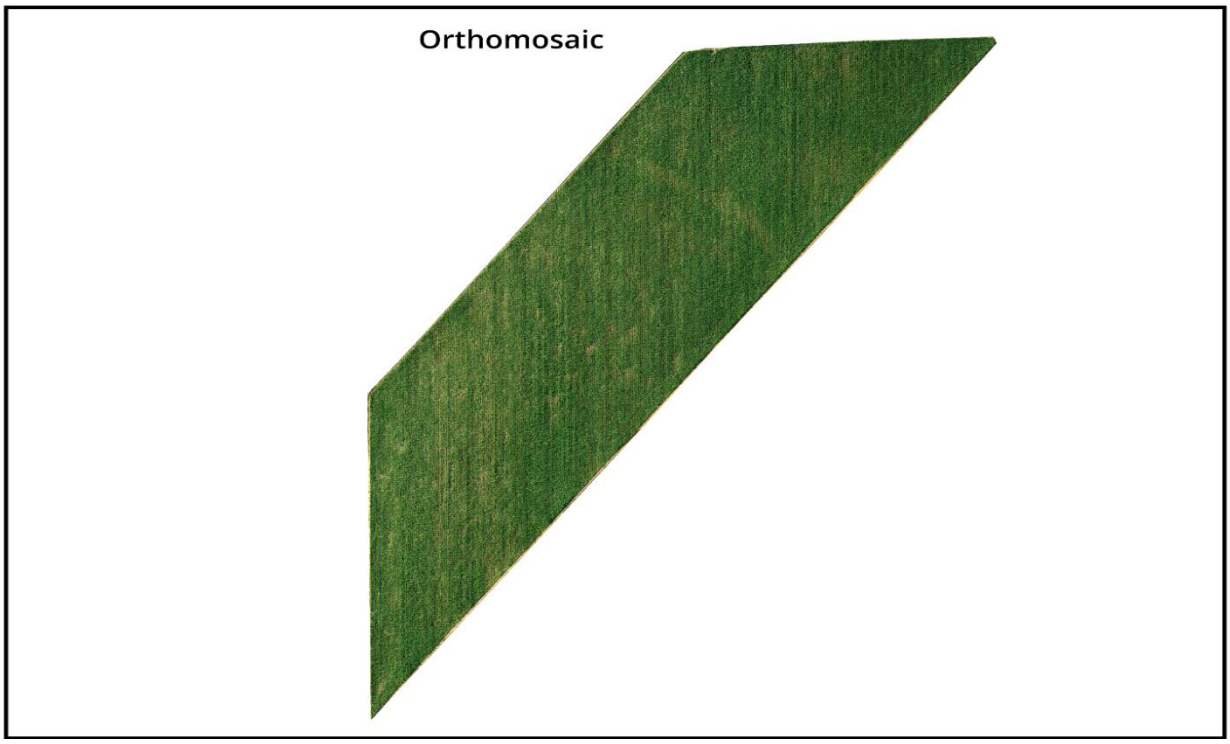


Figure 2. Orthomosaic - Field B

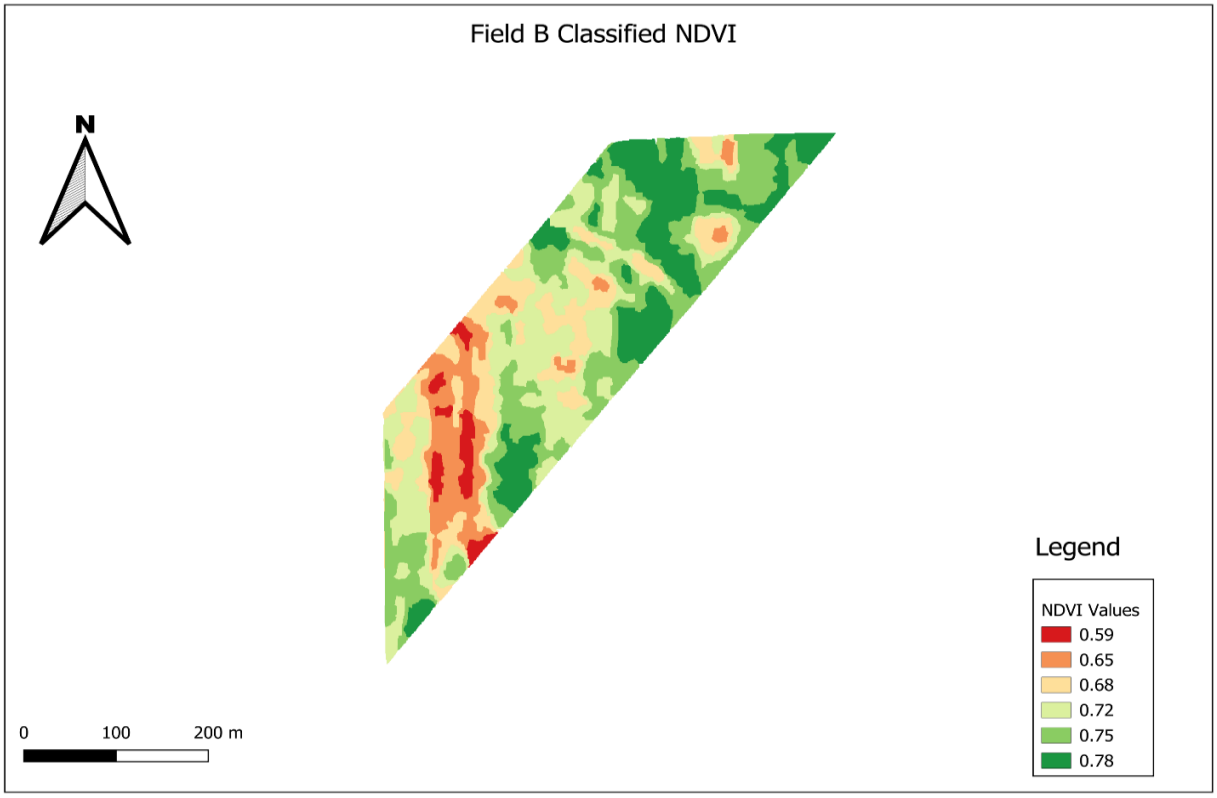


Figure 3. Field B Classified NDVI

Discussion

This pilot study demonstrated that drone-assisted NDVI monitoring significantly improved the anomaly detection efficiency over manual scouting alone. While the DJI P4M is not recommended for scaled commercial use, it served the pilot purpose well. The key benefits included time-saving, the visual clarity of anomalies, as well as more focused in-field checks.
The integration of spatial maps into Avenza made it easier for the field staff to track and locate the affected areas with precision, especially in large fields. The challenges included cloud interference, as well as initial training needs.

Feasibility and Usability

- Usability rating: Strong positive feedback from the field teams and management.
-

Conclusion

This pilot study showed that incorporating a drone-based NDVI analysis into field monitoring workflows can optimise the detection accuracy and reduce the field inspection time. The approach is promising for large estate operations that are aiming to modernise their monitoring practices.

Acknowledgments

The author would like to express her sincere gratitude to Illovo Sugar Malawi, and Illovo Africa as a whole, for their support of this project. Special thanks go to the various departments and teams at the Dwangwa Estate, whose support was instrumental during the project phase.

In particular, I would like to acknowledge the invaluable support and guidance of Mr Zizi Kayira (a Learning and Development Specialist and my MIT Programme Coordinator), Mr Alvine Gwara (Agriculture Engineering Manager and my Line Manager), Mr Thumbiko Nkwawa Zingwe-Banda (of Unitrans Dwangwa, Malawi), and Mr Gavin Taylor (Illovo Africa GIS Lead). Your encouragement, commitment and support greatly contributed to the success of this work.

Above all, I give thanks to my Heavenly Father for making everything possible. May His name be glorified forever and ever.

SHORT COMMUNICATION

INTRODUCING DIGITAL DATA COLLECTION FOR BIOSECURITY SURVEYS AT THE SOUTH AFRICAN SUGARCANE RESEARCH INSTITUTE (SASRI)

Thompson IB, Stranack RA, McFarlane SA, Basdew IH, Merile, S and Velem T

South African Sugarcane Research Institute, Private Bag X02, Mount Edgecombe 4300, South Africa

ingrid.thompson@sugar.org.za, stranackr@gmail.com, Sharon.McFarlane@sugar.org.za, iona.basdew@sugar.org.za , sibongile.merile@sugar.org.za, tulani.velem@sugar.org.za

Abstract

Pests and diseases pose a significant challenge to the South African sugar industry. To address these threats, 24 field inspection teams operate within the 12 Local Pest, Disease and Variety Control Committee (LPD&VCC) control areas across the industry. These teams, collectively known as the Biosecurity Inspectorate, are managed by the South African Sugarcane Research Institute (SASRI). The Inspectorate provides LPD&VCCs and individual growers with vital field data, which enables informed decision-making for the effective monitoring and management of biosecurity threats.

Until recently, a paper-based data collection system was used by the Inspectorate in the field for pest and disease surveys, and the data were manually captured in an electronic format by administrators in each LPD&VCC area. To improve the efficiency of the data capture and processing, electronic data capture systems using ArcGIS Survey123 were configured for mobile devices that can be used in the field. Initially, forms were developed for routine surveys for the stalk borer *Eldana saccharina*, and for disease surveys, where fields are inspected for smut (*Sporisorium scitamineum*), mosaic (sugarcane mosaic virus) and off-type varieties. The electronic data capture system offers many benefits, including increased efficiency and improved accuracy. Inspected fields are geo-referenced, and the captured data are stored in a geodatabase. The system is real-time and allows the visualisation of data using operational dashboards that are linked to the field data. In addition, each form includes a section for capturing valuable observational data for other pests and diseases. Applications for ratoon stunt (RSD, *Leifsonia xyli* subsp. *xyli*), certified and approved seedcane inspections, as well as fallow field inspections, are currently in development, which will ultimately be combined into a seedcane tracking application.

Keywords: ArcGIS Pro, biosecurity, dashboard, GIS, pest and disease, PostgreSQL, Survey 123

Introduction

The South African sugar industry operates across two provinces, KwaZulu-Natal and Mpumalanga, and it plays a pivotal role in the national agricultural economy by means of its contribution to employment, rural development and export earnings (Baiyegunhi, 2024). However, sugarcane production remains vulnerable to an array of pests and diseases that

adversely affect the yield, quality, and long-term sustainability of sugarcane. In this context, biosecurity, defined as a strategic and integrated approach to the analysis and management of risks to agriculture, has become increasingly central to the resilience of the industry (Stranack, 2021).

Biosecurity management within the South African sugarcane industry is structured around a network of Local Pest, Disease and Variety Control Committees (LPD&VCCs), which the Biosecurity Inspectorate supports. The Inspectorate is responsible for conducting routine field inspections, it monitors the prevalence of pests and diseases and delivers timely information to direct local decision-making processes (Stranack, 2021). Historically, these activities depended on paper-based data collection systems, which were time-intensive and susceptible to transcription errors, data loss and inefficiencies in data management and reporting.

The Biosecurity Inspectorate focuses primarily on three key areas: Eldana inspections, disease inspections, as well as surveys for ratoon stunt (RSD; *Leifsonia xyli* subsp*. xyli*). This paper concentrates on the digital transformation of Eldana and disease inspection results. Eldana (*Eldana saccharina*), the indigenous stalk borer, represents the most significant pest threat to the industry, and it is responsible for yield losses that are estimated at approximately US$62 million annually (Zhou, 2022). Disease surveillance efforts centre on the detection of smut (*Sporisorium scitamineum*), mosaic (sugarcane mosaic virus) and the identification of off-type varieties. Smut is most prevalent in the coastal and irrigated regions, while mosaic predominates at higher altitudes (Zhou, 2022). According to McFarlane *et al*. (2018), losses attributable to smut and mosaic were estimated at R15 million per annum.

The digital transformation of biosecurity in the sugar industry, particularly through the integration of Geographic Information Systems (GIS) and mobile data collection technologies, offers significant opportunities to enhance surveillance systems. The adoption of real-time data collection, geo-referencing and automated reporting dashboards facilitates a more proactive and responsive approach to pest and disease management. This paper describes the implementation of a GIS-based electronic data capture system that employs ArcGIS Survey123 for use by the Biosecurity Inspectorate and evaluates the benefits and prospects for future development.

Survey123 for ArcGIS is a form-centric data collection application developed by the Environmental Systems Research Institute (Esri); it is designed to enable the efficient collection, sharing and analysis of survey data, via web and mobile devices, in both online and offline environments. Emphasising simplicity and usability, Survey123 has been widely adopted in sectors including environmental management, public health, agriculture and urban planning (Teucher *et al.*, 2022). A major advantage of Survey123 is its seamless integration within the broader ArcGIS ecosystem. Data captured through Survey123 are stored in feature layers that are hosted on ArcGIS Online or Arcterprise, and they can be connected to external Relational Database Management Systems (RDBMS), such as PostgreSQL. Using the relational data store capabilities of ArcGIS Enterprise, combined with PostGIS extensions or ArcGIS Pro functionalities, organisations can achieve advanced spatial analytics and maintain robust, scalable and enterprise-grade data storage systems (Teucher *et al*., 2022). This architecture ensures long-term data governance, back-up and complex spatial querying.

The visualisation and analysis of Survey123 data are further enhanced by tools, such as ArcGIS Dashboards and ArcGIS Experience Builder. ArcGIS Dashboards provide stakeholders with a real-time, interactive visualisation of the survey data, which enables the efficient monitoring of the key indicators, a spatial analysis of the responses, and dynamic reporting, which does not require extensive GIS expertise (Esri, 2024). Dashboards serve a critical function in operational awareness, situational monitoring and informed decision-making. ArcGIS Experience Builder extends these capabilities by offering a no-code/low-code environment for developing customised web applications that integrate maps, survey data, analytical tools and bespoke user interfaces (Esri, 2024). This flexibility facilitates the creation of end-to-end digital workflows, from field data capture to stakeholder engagement and decision support.

From an academic perspective, Survey123 exemplifies a significant advancement in the fields of Participatory GIS (PGIS), Mobile GIS and Spatial Data Infrastructure (SDI). Its integration of intelligent form logic, enterprise-level database connectivity, real-time visualisation, and spatial analysis capabilities, positions it as a key technology for organisations that aim to develop spatially-enabled, data-driven decision support systems (Esri, 2024).

Background and rationale

The impetus for digitising pest and disease monitoring within the sugar industry arises from the inherent limitations associated with manual data collection methods. Traditional paper-based systems are frequently challenging to standardise, they are prone to physical damage or loss, and they impose administrative burdens related to post-collection digitisation. Furthermore, the absence of spatial referencing in the conventional approaches restricts the capacity to analyse the geographic distribution of biosecurity threats, thereby impeding their timely detection and the response efforts.

In response to these challenges, the South African Sugarcane Research Institute (SASRI) initiated the development of a digital surveillance system, following the centralisation of biosecurity operations within the sugar industry (Stranack, 2021). The objective was to design a user-friendly, mobile-compatible solution that enables biosecurity teams to capture data directly at the inspection site. Through the utilisation of Esri's ArcGIS platform, particularly the Survey123 application, SASRI configured a geospatially-enabled, real-time data collection system to replace the legacy paper-based workflows (Esri, 2022).

Materials and Methods

The development and implementation of a digital data collection system for pest and disease surveillance were conducted by using several key phases:

Requirements gathering and form design

An extensive consultation process was undertaken with the field inspectors, biosecurity supervisors, extension specialists, researchers, and Local Pest, Disease and Variety Control Committee (LPD&VCC) administrators, in order to document their workflows and specific data requirements. Insights from these engagements informed the design of the data collection schema and domain structures within ArcGIS Pro, which ensured a standardised approach across all the LPD&VCC regions.

The data capture schemas for Eldana and disease surveillance were subsequently published within a PostgreSQL relational database. Using ArcGIS Survey123 Connect, the forms were further customised for each LPD&VCC area, to enhance their usability and regional relevance. Regional customisations included the pre-loading of farm names and grower information, ecological zone (ecozone) classifications, biosecurity personnel lists, sugarcane variety lists, crop types and chemical (pesticide) registries.

Eldana inspection forms

The Eldana inspection form was designed to capture critical parameters directly from the field assessments. Biosecurity supervisors record the number of stalks sampled per field (typically 100 stalks), the average stalk height, as well as the cumulative length of the red-coloured damage symptoms observed within the stalks. These measurements are used in a preconfigured equation to calculate the percentage of red tissue per stalk sample, and they serve as a proxy for the extent of Eldana damage. In addition to the physical measurements, the number of Eldana larvae, Eldana pupae and Sesamia larvae found within the sampled stalks are recorded. The larval counts indicate the current infestation levels within a field, and they provide an estimate of the potential for a field to act as a source of infestation to the adjacent fields.

Disease inspection forms

The disease inspection forms are structured to differentiate the required level of detail, based on the type of sugarcane field that is surveyed, i.e. whether it is commercial, certified seedcane or approved seedcane. Field observations involve quantifying smut and mosaic incidence. Preloaded formulae automatically calculate the infection percentages based on the number of infected sugarcane stools. In addition, the forms capture information on the off-type varieties within the surveyed fields. Off-types represent a significant risk to the varietal purity, especially in certified and approved seedcane programmes; in addition, they may be a source of important systemic diseases, such as RSD, smut or mosaic, if they are carried over from a previously-infected field.

General pest and disease observations

Beyond the specific targets of the surveys, inspectors also document any occurrence of general pests and diseases that are encountered during the field visits. These incidental observations are rated for their severity, using a qualitative scale, and they are supported by photographic evidence that is captured through the Survey123 platform.

Geodatabase integration and dashboard visualisation

All field-collected data are synchronised in real time with a PostgreSQL geodatabase that is hosted within the ArcGIS Enterprise environment. This centralised storage enables the secure, structured management of surveillance data across all of the operational regions. To enhance data interpretation and to support decision-making processes, custom operational dashboards are configured by using ArcGIS Dashboards and ArcGIS Experience Builder (Esri, 2022). These interactive dashboards provide real-time visualisations of the key indicators, including inspection coverage, the incidence of pests and diseases, as well as the

identification of emerging biosecurity hotspots, through dynamic maps, charts, spreadsheets and summary tables.

Data security and access management

Robust data governance protocols were implemented to safeguard the integrity, confidentiality, and availability of the surveillance data. Biosecurity supervisors are assigned submission rights, which limits their access to data entry functions only, while biosecurity managers and researchers are granted broader privileges, for data analysis and reporting purposes. Furthermore, regular automated back-ups are scheduled, to ensure data preservation and to mitigate the risk of data loss.

Results

The implementation of the GIS-based electronic data capture system resulted in notable improvements across multiple operational dimensions:

Improved efficiency

The adoption of Survey123 for data collection significantly reduces the time required for field inspections, if the conventional method is completely omitted. Biosecurity supervisors are able to complete and submit digital forms directly from the field, which eliminates the need to return to the office to submit paper-based forms. The submitted inspection data from the field is sent to the database and dashboards in real-time. This streamlined workflow facilitates faster reporting to the growers' LPD&VCCs, thereby accelerating the decision-making processes.

Enhanced data accuracy

The data quality and reliability improved markedly through the use of predefined input options, mandatory fields to ensure data completeness, as well as real-time GPS location tagging. Built-in validation rules within the Survey123 forms reduce human error and minimise ambiguity in data interpretation (Esri, 2022).

Real-time monitoring

The integration of ArcGIS Dashboards enables extension and biosecurity, researchers and managers to monitor the inspection progress and the pest and disease trends in real time. For instance, sudden increases in the incidence of smut, or the detection of new off-type varieties, could be immediately flagged for follow-up action. In addition, the Experience Builder applications linked to the dashboards allowed LPD&VCC administrators to export field data directly into spreadsheets, which eliminated the need to manually transcribe the information from paper forms and to streamline the generation of grower reports.

Spatial intelligence

The collection of geo-referenced data facilitates an advanced spatial analysis, which enables the identification of outbreak clusters and temporal patterns. This spatial intelligence supports targeted interventions, such as the site-specific application of chemical controls or the strategic deployment of resistant sugarcane varieties.

Flexibility and scalability

The modular architecture of the digital system allows for the rapid development and deployment of additional data capture forms. New modules are currently under development. The RSD application includes a number of steps, from stalk sample collection to the uploading of test results. In addition, separate applications cover certified and approved seedcane inspections and fallow field assessments, which will be integrated into a broader seedcane-tracking framework.

Enhanced collaboration and communication

The deployment of digital dashboards significantly improves the communication and co-ordination between biosecurity teams, extension specialists, researchers and management units. It is now possible to share dashboard summaries and alerts almost instantaneously, which facilitates more agile and informed decision-making. Notably, some LPD&VCC meetings have begun to incorporate live dashboard displays to guide their discussions, which indicates a deeper institutional integration of the technology. While the system rollout has already yielded positive outcomes, project implementation is ongoing.

Discussion

The development and implementation of a digital surveillance system represents a logical progression in the centralisation of biosecurity operations within the South African sugar industry (Stranack, 2021). The adoption of digital tools has introduced a paradigm shift in the collection, analysis and application of biosecurity data, with the integration of GIS technologies and mobile data capture transforming surveillance operations. This initiative demonstrates that geospatially enabled, real-time data collection systems can provide timely, spatially accurate and actionable insights to inform pest and disease management strategies.

Introducing new technology into a multi-regional operation presents a combination of challenges and benefits that required careful management. One of the most time-consuming challenges was achieving the standardisation of terminology and data collection formats across all LPD&VCC areas. This was achieved through regular consultation with all the relevant stakeholders. These interactions played a critical role in promoting buy-in, addressing region-specific concerns and fostering a shared understanding of the new requirements. Tailored training sessions and ongoing support were necessary to build confidence and competence in using the new tools effectively in the field.

A critical consideration for the future evolution of the system is its interoperability with existing industry databases and research platforms. Achieving seamless integration will enhance the value of the surveillance data for research initiatives, trend forecasting and the development of evidence-based policies. Although technical challenges remain, particularly regarding network connectivity in remote areas, the offline capabilities of Survey123 partially mitigate this constraint. User feedback has been largely positive, with field personnel reporting an increased confidence in their ability to capture and manage data, as well as a heightened sense of ownership over the quality and integrity of the information collected.
Nonetheless, continuous investment in technical support, device management and user training remains essential. Frequent updates to core domains, such as grower lists, gazetted variety databases and personnel records, necessitate ongoing maintenance and refresher

training, in order to maintain operational consistency. These dynamic elements require careful planning and a flexible design, to ensure that the system remains current and reliable. As part of this process, important decisions had to be made regarding the management of different domain types, whether it is within the central PostgreSQL database for broader integration, or customised directly within ArcGIS Connect for field-specific workflows and deployment efficiency. Furthermore, robust contingency planning is required, including the provision of back-up devices in the event of equipment failure, loss or theft, in order to ensure the continuity of field operations in the event of equipment failure. To mitigate these risks, older but functional mobile devices must be strategically deployed as back-up units across all regions ensures that the field operations can continue with minimal disruption.

In addition, the extensive geospatial dataset generated by this platform presents significant opportunities for longitudinal research on pest and disease dynamics, the impact of climate variability, as well as the effectiveness of management interventions. Aggregated and anonymised datasets could also underpin industry-wide policy development, particularly about varietal deployment and resource prioritisation.

Conclusion

The digitisation of pest and disease surveillance activities within the South African sugar industry has substantially improved the efficiency, accuracy and responsiveness of biosecurity operations. By leveraging ArcGIS Survey123 and the associated geospatial dashboards, stakeholders now benefit from access to real-time, location-specific data that enhance operational decision-making and strategic planning. This initiative not only strengthens biosecurity practices within the sugar industry, but it also offers a model for similar digital transformation efforts in other agricultural sectors. Realising the full potential of the system will require sustained innovation, stakeholder engagement and strategic partnerships, which will ensure its adaptability and relevance in an evolving agricultural landscape.

References

Baiyegunhi LJS (2024). Examining the impact of human capital and innovation on farm productivity in the KwaZulu-Natal North Coast, South Africa. *Agrekon* 63(1-2): 51-64.

Esri (2022). Survey123 for ArcGIS: Modernising field data collection. Environmental Systems Research Institute.

Esri (2024). Survey123 for ArcGIS documentation. Environmental Systems Research Institute.

McFarlane SA, Zhou MM and Rutherford RS (2018). Progress in reducing disease incidence in the South African sugarcane industry. *Proceedings of the South Africa Sugar Technologist Association* 91: 70-73

Stranack RA (2021). Centralisation of biosecurity services in the South African sugar industry. *South African Sugar Journal* 105: 45-49.

Teucher M, Thurkow D, Alb P and Conrad C (2022). Digital *in situ* data collection in earth observation, monitoring and agriculture - Progress towards digital agriculture. *Remote Sensing* 14(1): 2-15.

Zhou M (2022). History and current status of sugarcane breeding, germplasm development and supporting molecular research in South Africa. *Sugar Technologies* 24(1): 86-96.

POSTER SUMMARY

CREATING A MULTI-USER DIGITAL DATA COLLECTION SYSTEM FOR RATOON STUNT

Radebe S, McFarlane SA, Stranack RA, Thompson I, Maduray R, Torlage J and Edmonds J

South African Sugarcane Research Institute, Private Bag X02, Mount Edgecombe 4300, South Africa

sinenhlanhla.radebe@sugar.org.za, sharon.mcfarlane@sugar.org.za, stranackr@gmail.com, ingrid.mthembu@sugar.org.za, renata.maduray@sugar.org.za, joleen.torlage@sugar.org.za, janet.edmonds@sugar.org.za

Abstract

Ratoon Stunt Disease (RSD; *Leifsonia xyli* subsp. *xyli*) causes substantial yield losses in sugarcane and has a significant economic impact on crop production. The disease slows down growth, which results in a reduction in the stalk height and diameter. Due to a lack of obvious visible symptoms, RSD is frequently overlooked, which leads to its accidental spread through infected seedcane, ineffective crop eradication and contaminated equipment during harvesting. In order to identify the infected fields, Xylem sap is extracted from stalk samples that are collected by the SASRI Biosecurity Inspectorate. Field data are collected by using traditional paper-based data collection forms, which are then captured in spreadsheets by administrators in the different regional offices. The spreadsheets and the sap samples are then sent to the SASRI RSD laboratory at Mount Edgecombe for analysis. The results are uploaded to the ORACLE database and distributed to the growers. Although the paper-based system is standardised throughout the industry, it is complex, with multiple users contributing towards the final RSD database. Moreover, the samples taken from fields are not geographically referenced. ArcGIS Survey123 was used to create a multi-user data collection system which consists of mobile devices, smart forms, computers, a web-based RSD data capture system and the visual representation of RSD incidence. Sampled fields are geographically referenced, and the data are submitted to the central ArcGIS Portal, where they can be accessed by the administrators who can annotate the spreadsheet in the portal. The RSD laboratory staff have access to upload the results after the sample analysis. The data are sent to both the ORACLE database and Postgres geodatabase, and they are linked to the RSD Dashboard. This allows Extension Specialists and Biosecurity Inspectorate technical staff to view the sampling events and the related incidence of RSD, thereby providing timeous recommendations to growers on how to manage the disease.

***Keywords**:* Ratoon Stunt Disease, RSD, Survey123, Dashboard, smart forms, biosecurity

POSTER SUMMARY

MAPPING THE SOIL pH VARIABILITY IN SUGARCANE FIELDS OF THE ZIMBABWE SUGAR INDUSTRY FROM 2018-2024

Marungudze A, Mampangesi S, Rambwawasvika H and Mutatu W

Zimbabwe Sugarcane Research Institute, Chiredzi, Zimbabwe

marungudzealan7@gmail.com, sg.mampengesi@gmail.com, hrambwawasvika@zsaes.org.zw, wmutatu@zsaes.org.zw

Abstract

The soil's pH is a critical determinant of nutrient availability, microbial activity and crop performance. For sugarcane production in the Zimbabwe sugar industry, optimal productivity is achieved when the soil pH is maintained between 5.5 and 6.5. In Zimbabwe's Lowveld, where all the sugarcane is irrigated due to the low rainfall, it is essential to understand the soil's pH dynamics for sustainable production. This study investigates the spatial and temporal variability in the soil's pH across the Zimbabwe sugar industry, by using soil analysis data from samples collected between 2018 and 2024.

The soil pH measurements obtained via the $CaCl_2$ potentiometric method, and sourced from the ZSAES soil laboratory, were analysed, cleaned and classified into seven pH categories using Python. QGIS was used to map the spatial pH trends, by using digitised shapefiles of the field sections. The resulting thematic maps, which are colour-coded by their critical pH thresholds, enabled the identification of areas that require site-specific interventions.

The findings revealed a progressive shift toward alkalinity, particularly after 2020. In 2022, over 81% of the fields recorded pH values above 6.5, and 537 fields were classified as strongly alkaline (pH>7.5). Although the acidic conditions (pH<5.5) remained rare, they persisted in isolated blocks. The rise in pH is likely due to over-irrigation and the inherently-sodic nature of some soils, especially in the Hippo Valley. Spatial mapping showed persistent alkalinity in the northern Hippo Valley, while acidic patches were observed in the Triangle Estates.

The study highlights the increasing prevalence of alkaline soils, which poses a risk to the availability of nutrients, as well as to the sugarcane yield. It underscores the importance of precision soil management, particularly-targeted amendments and improved irrigation practices, in order to maintain optimal pH conditions and to ensure the long-term health of the soil.

Keywords: Soil pH, sugarcane, precision agriculture, alkalinity, GIS, sodicity, acidity

FULL PAPER

TRENDS AND CHALLENGES IN SULPHUR MANAGEMENT FOR THE SOUTH AFRICAN SUGAR INDUSTRY

Elephant DE[1], Zulu SL and Mdlambuzi T[1]

[1]South Africa Sugarcane Research Institute, P/Bag X02, Mount Edgecombe, 4300,

South Africa

Dimpho.Elephant@sugar.org.za; Sibusiso.Zulu@sugar.org.za;
Thandile.Mdlambuzi@sugar.org.za

Abstract

Sulphur (S), an essential secondary macronutrient, has been under-researched, despite its importance. In 2018, the Fertiliser Advisory Services (FAS) adopted a resin-based S test, which revealed widespread deficiencies across the South African sugar industry. This study analysed the S trends from 2019 to 2024, using 91 587 topsoil samples, and it assessed the impact of management strategies by using BT1 (no gypsum), chemical ripener, and plant breeding trials (with gypsum), as well as an incubation study on a sandy Catref soil. The results indicated a general decline in the soil S levels over the six-year period, with over 50% of the annual samples showing deficiencies (<15 mg/L). The soil S levels correlated positively with the clay and organic matter content, highlighting that soil with a low clay and organic matter content is being rapidly depleted of S. Similarly, S correlated positively with the soil pH which could be due to the mineralisation of organic matter and improved desorption at a high soil pH, as well as the precipitation of aluminium sulphate at a low pH. The BT1 data showed S levels in unfertilised soils decreasing over the years, and then plateauing at 8 mg/L. This is possibly due to inadequate S replenishment in this trial. Several research trial data showed that levels often returned to the baseline, despite gypsum and ammonium sulphate applications, which is likely due to leaching, or the amount that is applied matching the amount that is removed at harvest. Notably, ameliorants such as granulated CMS and a spent mushroom compost substrate, significantly improved the S levels of the Catref soil. Further research is required to fully understand the S dynamics and to develop optimised management practices, in order to enhance crop sustainability.

Keywords: Saccharum officinarum, organic matter mineralisation, crop nutrition, soil testing, gypsum, anion exchange resin

Introduction

Sulphur (S) is widely recognised as a critical secondary macronutrient after nitrogen (N), phosphorus (P) and potassium (K) (Meyer, 1985), and it is essential for plant metabolic functions, such as protein and enzyme synthesis, chlorophyll formation and nitrogen use efficiency (Havlin *et al*., 2016; Gerson & Hinckley, 2023). In many crops, including sugarcane, the demand for S is comparable to that of P (Havlin *et al*., 2016). However, its importance has often been overlooked in nutrient management programmes, largely due to historical reliance on atmospheric S deposition and incidental inputs from fertilisers.

Sugarcane, a high-biomass and nutrient-demanding crop, relies on an adequate S supply to maintain optimal growth and metabolic function, particularly in amino acid and enzyme synthesis. In South Africa, sugarcane is predominantly grown in regions with sandy soils with a variable rainfall and a low organic matter content. These conditions exacerbate S leaching and have reduced the S retention capacity, which may lead to S deficiencies. Sulphur

deficiency has recently emerged as a widespread global issue in crops, including sugarcane (Ghosh, 2022). This is driven by a combination of environmental and agricultural shifts. A key factor has been the substantial reduction in atmospheric S deposition, due to the improved air quality regulations that are aimed at curbing industrial emissions (McGrath *et al*., 1996; Blake-Kalff *et al*., 2000). In addition, the increased use of S-free fertilisers, such as urea and mono-ammonium phosphate, coupled with intensified cropping practices and greater biomass removal, has increased the crop S demand without receiving the corresponding replenishment (Scherer, 2001; Haneklaus *et al*., 2008).

Sulphur deficiencies in the South African sugar industry were first reported by Meyer (1985) and later by van der Laan and Miles (2010). The persistence of S deficiencies during this period may be attributed to the lack of a routine S analysis in the Fertiliser Advisory Services (FAS). However, in 2018, FAS adopted an anion exchange resin-based S test and a baseline survey revealed widespread deficiencies (Elephant *et al*., 2019). A subsequent survey also revealed the continued prevalence of S deficiencies (Titshall *et al*., 2023), which underscored the need to explore the S dynamics in the South African sugar industry further and to identify the causes of the deficiencies, as well as the management practices that can be used to correct them. This study aims to characterise the S trends over time, using industry-wide diagnostic data, and to evaluate the S dynamics in field trials and in an incubation study. The goal is to generate evidence to inform more effective and sustainable S fertilisation strategies in the South African sugar industry, which are tailored to the local environmental conditions and crop demands.

Materials and Methods

FAS database

Routine topsoil (0-20 cm) fertility analysis data for sugarcane crops were extracted from the FAS database for the period 2019 to 2024. The data were grouped according to the years, the organic matter content, soil texture and soil pH. The analysis of the samples was done using the FAS routine procedures described in Titshall *et al*. (2023). Specific to this paper, S was extracted using the anion exchange resin method (Miles *et al*., 2013), the soil pH was measured in calcium chloride (Miles *et al*., 2014), and the clay and organic matter content were estimated using mid-infrared spectroscopy (Mathadeen *et al*., 2013). The analysis of data was primarily done with the summary statistics using JASP (JASP Version 0.19, 2024) which provided the mean, the Standard Deviation (SD), median, 1st and 3rd quartile (25th and 75th percentile) and the minimum (min) and maximum (max) values.

BT1 trial data

The BT1 trial commenced in 1939 in Mount Edgecombe and is located on the Mayo soil form of the Glenecho family (Soil Classification Working Group, 1991; Mthimkhulu *et al*., 2018). The average clay and organic matter content, and the soil pH for the whole trial are presented in Table 1. BT1 is the oldest long-term sugarcane trial that investigates the effects of residue and fertiliser management on the soil properties and yields. The residue management treatments are: (i) green cane harvested with the retention of a residue blanket (100% cover); (ii) burning prior to harvest, with the tops left scattered on the plots (approximately 67% cover); and (iii) burning prior to harvest, with all the tops raked off the plots. The fertiliser management treatments are unfertilised and fertilised annually with 140 kg N/ha, 28 kg P/ha and 140 kg K/ha. The P source for the first 50 years was single superphosphate, which was switched to mono-ammonium phosphate to the present study period. The experiment was replicated four times in a randomised split-plot design. Topsoil (0-20 cm) samples taken in 2016 to 2024 were used for this paper to assess the trends in S over time. The results were subjected to a two-way Analysis of Variance (ANOVA) using JASP (JASP Version 0.19, 2024). The interaction

between residue management and time was not significant, and thus only fertiliser management is considered.

Table 1. Clay, Organic Matter content (OM), soil pH and average Mean Annual Precipitation (MAP during study periods) for the BT1, breeding and ripener trials and incubation study. Fields G1 and G2 were used for breeding in Glenside, while M1, P1 and Komatipoort were the ripener trials in Mount Edgecombe, Pongola and Komatipoort, respectively. Catref was used for the incubation study

Field	Clay (%)	OM (%)	soil pH_{CaCl2}	MAP (mm)
BT1	54	6.15	4.53	1180
G1	9	0.90	4.21	927
G2	9	1.50	4.16	927
M1	27	1.69	5.21	1107
P1	24	1.35	5.23	702
Komatipoort	43	3.01	7.05	864
Catref	13	2.10	4.51	-

Breeding and ripener trials

Two breeding trial fields located in Glenside (designated G1 and G2) on sandy soil with a low organic matter content were used (Table 1). Both fields were sampled at 0-20 cm and analysed in 2022, revealing S deficiencies. Gypsum was subsequently applied to both fields in 2022. Field G1 received 500 kg/ha, while G2 received 3 t/ha, which corresponded to 93 kg S/ha and 558 kg S/ha, respectively. The fields were sampled again after the 2024 harvest. The 2022 S results are presented as the ‘pre-treatment’, and the 2024 results as the ‘post-harvest’.

Three ripener trials located in Mount Edgecombe (M1), Pongola (P1) and Komatipoort were also used. The soils were loamy at the M1 and P1 sites and clayey at the Komatipoort site (Table 1). In Mount Edgecombe, the soil analysis in 2023 revealed a S deficiency, which was corrected by applying 250 kg/ha of gypsum (equivalent to 46.5 kg S/ha). This trial site was sampled again at 0-20 cm after the harvest in 2024. The 2023 results are presented as the ‘pre-treatment’, and the 2024 results as the ‘post-harvest’. Similarly, the soil analysis in P1 during 2020 revealed low S levels, which were treated with 500 kg/ha of gypsum. This site was sampled again after the harvest in 2021. The 2020 results are presented as the ‘pre-treatment’, and the 2021 results as the ‘post-harvest’. The soil in Komatipoort also showed S deficiencies in 2021. These were initially corrected with an application of 500 kg/ha of gypsum. However, the post-harvest soil analysis in 2022 indicated a persistent deficiency, which was then addressed by applying 550 kg/ha of ammonium sulphate (equivalent to 132 kg S/ha). This trial was sampled again after the harvest in 2023.

Incubation study

The incubation study was conducted in 2015 on a sandy Catref soil with 9% clay, 2.10 organic matter and soil a pH of 4.51 (Table 1). The details of the incubation are presented elsewhere (Elephant *et al*., 2016). In summary, several inorganic and organic ameliorants were applied to the Catref soils at different rates and then incubated for four weeks at 50% water-holding capacity. The soil ameliorants were dolomitic lime, Calmasil, Flyash, Langfos, Quarry dust, liquid molasses (CMS), granulated CMS, Filterpress, Chicken litter, a spent mushroom

compost substrate and Vermicast. The elemental contents and applications are presented in Table 2. Sulphur was extracted by using the anion exchange resin method and the results were subjected to one-way ANOVA, using JASP (JASP Version 0.19, 2024).

Table 2. Description of the soil ameliorants used in the incubation study, their rate of application and their nutrient content (adapted from Elephant *et al*., 2016)

Product	Description	Rate (t/ ha)	Total C (%)	Total N (%)	P (%)	K (%)	Ca (%)	Mg (%)
Lime	Kulu dolomitic lime	**10**			0.02	0.03	28.50	10.10
Calmasil	Calmasil	**10**			0.02	0.03	26.70	6.16
Langfos	Langfos	**1.6**			5.23	0.20	8.48	0.12
Q dust	Quarry dust (dwyka tillite)	**15**			0.15	2.12	3.06	2.08
CL	Chicken litter	**10**	27.03	3.00	0.62	2.08	1.52	3.12
SMS	Spent mushroom compost substrate	**10**	12.68	1.00	0.26	1.28	3.11	1.55
Flyash	Flyash	**50**	nd	0.13	0.09	0.36	0.31	1.58
Filterpress	Filterpress	**50**	6.62	0.32	0.24	0.11	0.50	1.55
Vermicast	Vermicast	**10**	3.94	0.64	0.47	0.38	0.91	0.26
CMS_L	Liquid CMS	**6.0**	nd	0.85	0.11	8.59	-	-
CMS_G	Granular CMS	**1.0**	1.67	11.63	7.03	14.96	0.34	0.33

nd = no data

Results

Trends in sulphur levels from 2019 to 2024, using the FAS database

A total of 91 587 topsoil samples were submitted for sugarcane fertility analysis between 2019 and 2024, with the lowest samples of 13 861 received in 2022 and the highest of 16 952 in 2020 (Table 3). The mean S levels varied annually, with the lowest mean of 19.73 mg/L in 2024 and the highest of 24.21 mg/L in 2019. This trend may indicate a steady decline in the S levels over the years. Despite the mean being above the threshold of 15 mg/L, the median for all years was significantly below this threshold. This suggests that the means were skewed by high maximum values, and that more than 50% of the submitted samples each year were well below the threshold.

A further analysis of the collected data revealed a significant correlation between the mean S levels and other soil properties. Specifically, the mean S levels correlated with the organic matter content (Table 4). This trend held across the 25th, 50th and 75th percentiles, showing higher S levels in soils with a higher organic matter content. Over 75% of the samples with less than 1.0% organic matter were deficient in S. This proportion dropped to over 50% for samples with 1.0-2.0% organic matter, and below 50% for samples with more than 2.0% organic matter content.

Table 3: Summary statistics for resin extractable sulphur (mg/ L) measured in Fertiliser **Advisory Services laboratory from 2019 to 2024. The current threshold for resin extractable sulphur is 15 mg/ L**

Year	2019	2020	2021	2022	2023	2024
No. of Samples	16 024	16 952	14 717	13 861	13 425	16 608
Mean	24.21	20.98	23.98	22.83	22.12	19.73
Std. Deviation	65.70	44.29	72.79	54.60	43.00	44.64
Minimum	3.00	3.00	3.00	3.00	3.00	3.00
25th percentile	5.70	4.90	5.00	5.70	5.50	5.00
50th percentile	11.40	9.70	10.30	10.50	10.60	9.40
75th percentile	25.73	22.00	23.60	22.80	22.10	19.33
Maximum	5049	2548	3136	2940	1787	2574

Table 4: Summary statistics for resin extractable sulphur (mg/ L) associated with various categories of soil organic matter content, soil texture and soil pH. Sand, loam and clay categories were characterised by a <20, 20-32 and >32% clay content, respectively.

Organic matter content	0 – 0.5%	0.5 – 1.0%	1.0 – 1.5%	1.5 – 2.0%	>2.0%
No. of Samples	11 087	16 911	19 196	18 834	25 559
Mean	9.67	13.52	16.74	23.16	36.93
Std. Deviation	40.73	57.42	45.04	45.53	68.12
Minimum	3.00	3.00	3.00	3.00	3.00
25th percentile	3.00	3.56	5.17	7.25	11.49
50th percentile	4.05	5.99	8.56	12.45	21.98
75th percentile	7.84	10.69	15.74	23.28	44.08
Maximum	2921	2802	2737	2574	5049

Soil texture	Sand	Loam	Clay
No. of Samples	35 133	23 908	32 546
Mean	9.66	23.99	34.55
Std. Deviation	37.96	63.90	60.99
Minimum	3.00	3.00	3.00
25th percentile	3.07	7.18	10.93
50th percentile	5.18	12.29	20.27
75th percentile	8.61	23.25	40.21
Maximum	2802	3329	5049

Soil pH	3.0 – 4.0	4.0 – 5.0	5.0 – 6.0	6.0 – 7.0	7.0 – 8.0	8.0 – 9.0
No. of Samples	1917	40 328	15 578	6375	2185	18
Mean	14.86	19.06	15.81	21.53	31.40	366.40
Std. Deviation	26.59	35.95	53.46	107.39	109.55	1171
Minimum	3.00	3.00	3.00	3.00	3.00	11.34
25th percentile	4.32	5.34	4.41	5.53	8.34	27.61
50th percentile	8.61	10.26	7.81	9.82	14.32	65.88
75th percentile	17.71	21.17	14.28	17.28	26.96	151.77
Maximum	919	2574	2737	3329	3136	5049

In addition to organic matter, the mean S levels also correlated with the clay content, with lower levels observed on sandy soils (Table 4). This trend held across the 25th, 50th and 75th percentiles, and the maximum values also showed higher S levels in clayey soils. Over 75% of sandy soils were deficient in S. This proportion dropped to over 50% for loamy soils and fell below 50% for clayey soils.

Finally, a positive correlation was found between the mean S levels and the soil pH, with lower S levels observed in acidic soils (Table 4). This trend was consistent across the 25th, 50th and 75th percentiles, showing progressively higher S levels in soils with an increasing pH. Over 50% of soils with a pH below 7.0 were deficient in S. This proportion decreased to below 25% for soils with a pH above 8.0, although the number of samples in this higher pH range was smaller.

BT1 trial data

The resin-extractable S was consistently higher in the fertilised treatment, compared to the unfertilised treatment, with both treatments exhibiting a steady decline over time (Figure 1). The average annual S removal was 43 t S/ha in the fertilised treatment and 16 t S/ha in the unfertilised treatment (data not shown). In the unfertilised treatment, S levels declined below the critical threshold of 15 mg/L and plateaued at approximately 8 mg/L.

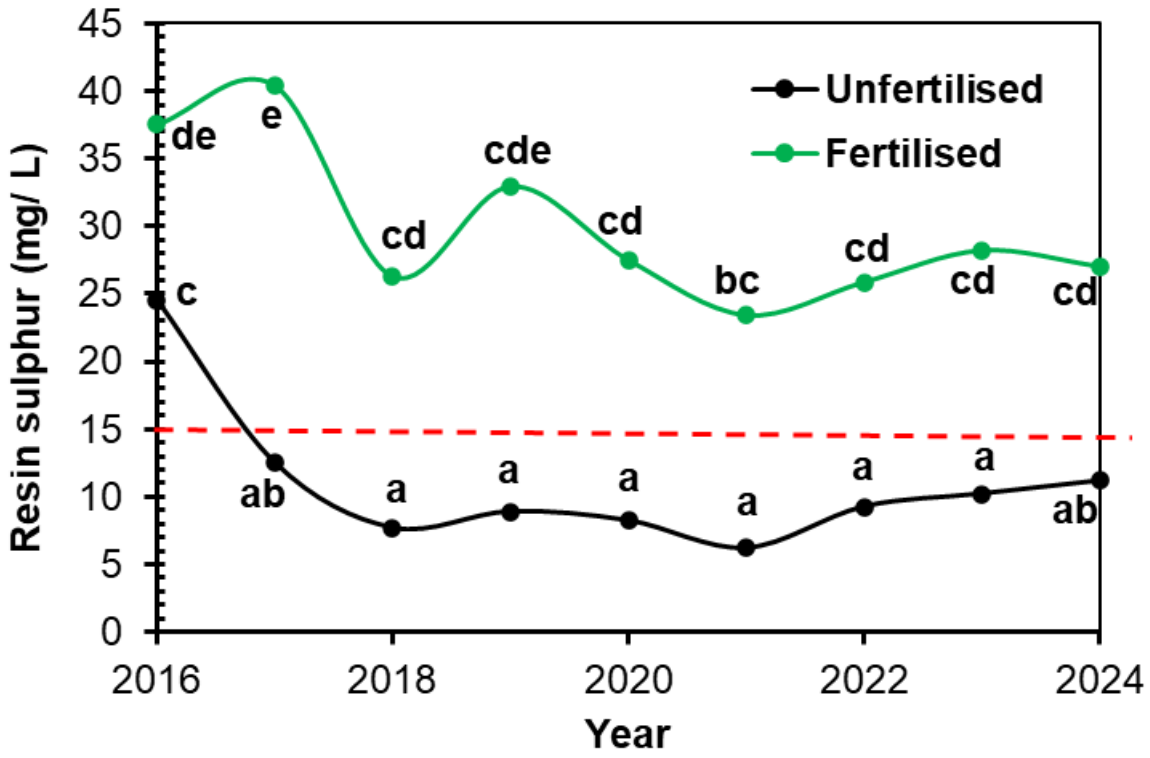


Figure 1. Changes in the resin extractable sulphur over time of unfertilised and fertilised treatments in the BT1 trial. The red-dashed line represents the resin extractable sulphur threshold value of 15 mg/ L. The different lowercase letters indicate significant differences at p<0.05.

Breeding and ripener trials

The post-harvest S levels in soils treated with gypsum (or ammonium sulphate) showed variability. At Glenside (G1 and G2), Mount Edgecombe and Komatipoort, the pre-treatment S levels were below the critical threshold (Figure 2). Following the harvest, the S levels in G1, M1 and Komatipoort returned to their pre-treatment values, while in G2 and P1, they exceeded both the pre-treatment levels and the threshold (Figure 2a, b). The sulphur levels in Komatipoort were consistently below the threshold for 2021-2023.

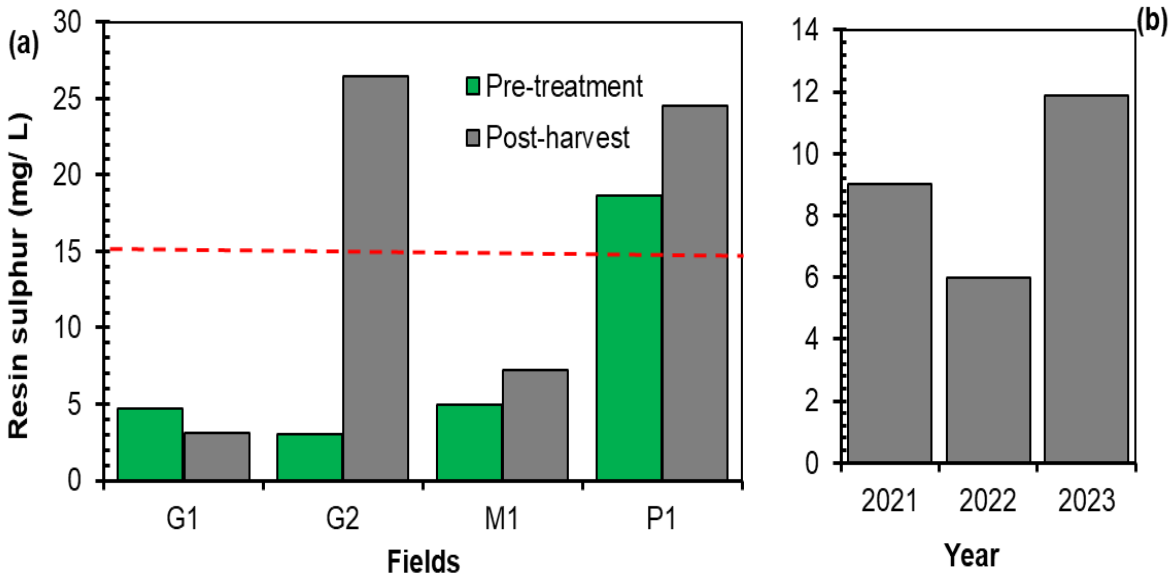


Figure 2. **Resin extractable sulphur levels: (a) before and after gypsum application at Glenside (G1 and G2), Mount Edgecombe (M1) and Pongola (P1); and (b) in Komatipoort across 2021, 2022 and 2023. The red-dashed line represents the resin-extractable sulphur threshold value of 15 mg/L**

Incubation study

The various soil ameliorants that were tested exhibited differing effects on the S levels (Figure 3). Although the application rates of the soil ameliorants varied, the S levels were not measured in the applied materials, and the incubation was conducted with a sandy soil in a closed system; however, the results still provided useful insights into the potential contribution of different ameliorants to increasing soil S levels. Gypsum applied at 5 t/ha and 10 t/ha resulted in S levels of 535 and 916 mg/L, respectively (data not shown). In contrast, the other inorganic ameliorants, including dolomitic lime, Calmasil, fly ash, Langfos and quarry dust, did not significantly increase the S levels (Figure 3). Similarly, organic ameliorants, such as filterpress and vermicast, had no notable effect on the S levels. However, chicken litter, liquid CMS, granulated CMS and a spent mushroom compost substrate increased S levels to 17, 22, 50 and 52 mg/L, respectively.

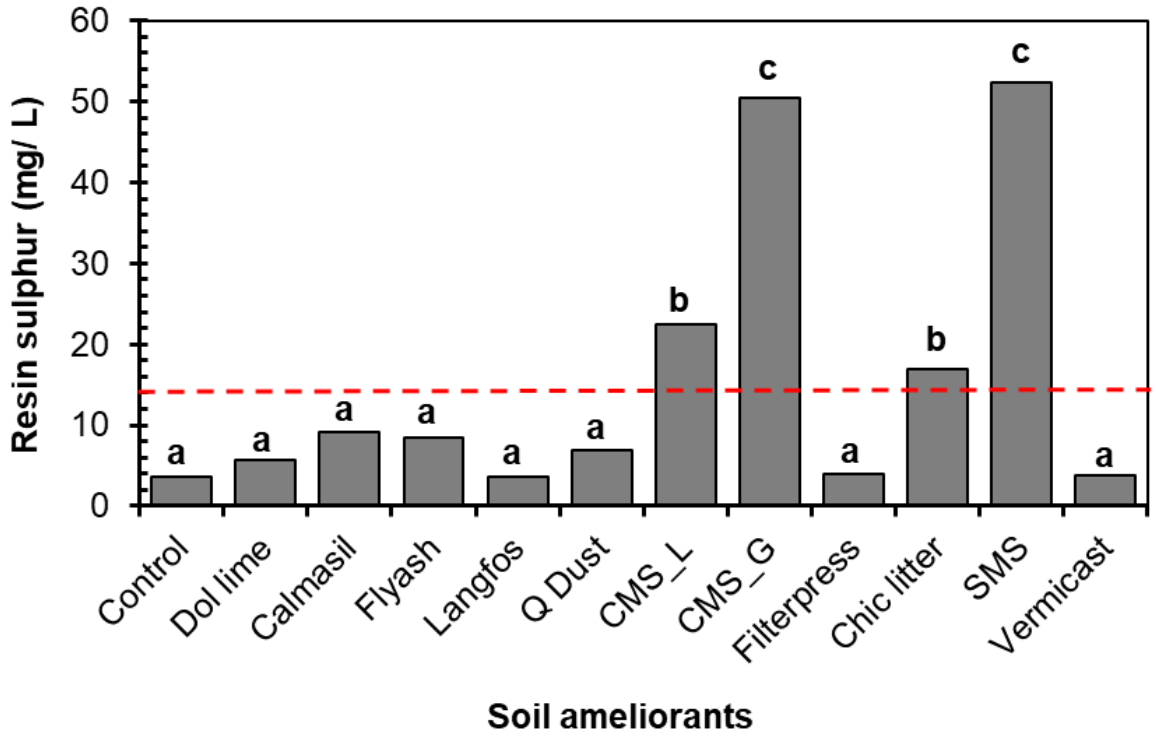


Figure 3. The effects of various inorganic and organic ameliorants on resin extractable sulphur. The different lowercase letters indicate significant differences at $p<0.05$. The red-dashed line represents the resin extractable sulphur threshold value of 15 mg/ L.

Discussion

The widespread S deficiencies observed in the FAS database align with the previous findings by Elephant *et al*. (2019) and Titshall *et al*. (2023). These persistent deficiencies in the South African sugar industry can be attributed to four primary factors: firstly, the lack of S replenishment following its removal during harvest leads to nutrient depletion; secondly, the addition of S through ameliorants may be insufficient if: (a) the applied amount merely equals the harvested amount, (b) it is leached into the subsoil, or (c) it is immobilised through soil reactions. This latter point is influenced by soil properties, such as the clay and organic matter content, and the soil pH, while depletion caused by harvest depends on the crop yields and the quantity of S applied.

Sulphur removal during harvest

The amount of S removed during harvest necessitates replenishment by means of the application of various carriers. When this replenishment does not occur, or the applied amount only matches the removed amount, the deficiencies persist, as evidenced by the FAS data. This is further supported by the declining S levels over time in the BT1 trial for both fertilised and unfertilised treatments. The rate of this decline is directly influenced by the annual removal, which was 43 t S/ha in the fertilised treatment and 16 t S/ha in the unfertilised treatment. Conversely, the higher S levels in the fertilised treatment, compared to the unfertilised treatment in BT1, can be attributed to the legacy effects from a long-term (50 years) single superphosphate application, which contains sulphur. Similarly, the return of post-harvest S levels to pre-treatment levels in the M1 trial occurred because the 47 kg S/ha that was applied was equivalent to the 46 kg S/ha that was removed during harvest.

Relationship between the sulphur levels and soil properties

The positive correlations observed in the FAS data between the S levels and the clay, organic matter and soil pH provide valuable insights for its management. The strong link between S and organic matter is well-established, with early research by Meyer (1985) reporting a correlation coefficient of 0.76, and more recent studies (Titshall *et al*., 2023) confirming the potential for S mineralisation from organic matter. These authors further suggested that organic matter should be taken into account when formulating the S recommendations. While the specific relationship between the S and clay content has not been extensively studied within the South African sugar industry, these results align with the established soil science principles. A higher clay content is known to facilitate the better storage of organic matter (Miles *et al*., 2016), which, as discussed earlier, can contribute to higher S levels. In addition, S is prone to leaching in sandy soils (Riley *et al*., 2002), which leads to lower observed levels. This observation has a practical implication for sugarcane management, which suggests that S application may need to be more frequent on sandy soils, in order to maintain adequate levels for optimal growth. The increased availability of S at a higher pH has been reported previously (Barrow & Hartemink, 2023) and can be ascribed to three main mechanisms. Firstly, a higher pH promotes the better mineralisation of organic matter (Wang & Kuzyakov, 2024), thereby facilitating the release of S from the organic matter (Titshall *et al*., 2023). Secondly, soils with a higher pH generally have a greater proportion of negative surface charges, which reduces the sorption of negatively-charged sulphate ions, thus improving their availability in the soil solution (Barrow & Debnath, 2015). Lastly, under low soil pH conditions, S can react with aluminium ions to form aluminium sulphate precipitates (Mthimkhulu *et al*., 2022), which effectively reduces the concentration of plant-available S.

The contribution of clay and organic matter content to S retention was evident in the BT1, G1, G2 and P1 trials. The higher clay and organic matter content in BT1 may have contributed to S retention and it may have also enabled its slow release over time. Furthermore, the observed plateau in S levels, even as it is continually removed through harvesting, suggests that replenishment is occurring from the soil reserves, such as the adsorbed and organically-bound S. These results may also indicate that the rate of decline is influenced by soil properties, such as clay and organic matter, as well as the quantities of S in the soil reserves. This was corroborated by the contrasting post-harvest S levels in G1 and P1, despite both sites receiving 93 kg S/ ha. The low clay and organic matter in G1 resulted in a return to pre-treatment levels, which is indicative of leaching, in addition its removal by the crop, while the higher clay content in P1 (24%) led to higher post-harvest levels. The substantially low post-harvest S in G2, despite having a high application rate of 558 kg S/ ha and a similar clay content to G1, further suggests significant leaching in soils with a low retention capacity.

However, the results from Komatipoort were confounding. This site received a high S application rate and has soil properties that are generally associated with improved S retention, including a higher clay and organic matter content. Despite these favourable conditions, the post-harvest S levels remained low and below the threshold. In addition, the relatively-high pH at this site would typically promote the mineralisation and release of S from the organic matter. Further research is therefore required to understand the mechanism that is responsible for the unexpectedly low S availability in this particular soil. In addition, the incubation study cautions that pH modification alone is not sufficient to improve the S levels in soils that lack reserves; lime and Calmasil increased the pH, but did not improve the available S in the sandy Catref soil, which is most likely due to a lack of reserves.

Soil ameliorants and sulphur supplies

The effectiveness of different soil amendments in supplying S varied considerably. As expected, gypsum was the most effective for increasing the available S. Notably, certain organic products, particularly granulated CMS and the spent mushroom compost substrate,

significantly improved the S levels and also offer additional benefits, such as improved microbial activity, soil structure and organic matter content. In contrast, inorganic ameliorants like lime, Calmasil and fly ash showed limited efficacy in raising the S levels, especially in soils with low reserves. This underscores the importance of carefully selecting amendments that are based on the specific site conditions and nutrient targets.

Conclusions

The findings from the FAS database, long-term trials and incubation study collectively indicated a widespread challenge in maintaining adequate S levels for sugarcane production. A significant proportion of soils exhibit S deficiencies, which are most likely driven by its continuous removal during harvest and the lack of consistent replenishment. Soil properties, particularly the organic matter, clay content and pH, exert a strong influence on the availability of S through their effects on its retention, release and loss mechanisms. While traditional S sources, like gypsum, are effective, their management needs to consider soil-specific factors, in order to minimise losses, for example, by leaching. Furthermore, certain organic amendments show promise as alternative S sources while offering additional soil health benefits. Ultimately, effective S management in sugarcane requires a site-specific approach that integrates an understanding of its removal rate, the soil characteristics and the appropriate selection and application of S-containing amendments, in order to ensure sustainable yields.

References

Barrow NJ and Debnath A (2015). Effect of phosphate status and pH on sulphate sorption and desorption. *Eur J Soil Sci* 66(2): 286-297.

Barrow NJ and Hartemink AE (2023). The effects of pH on nutrient availability depend on both soils and plants. *Plant Soil* 487(1): 21-37.

Blake-Kalff MMA, Hawkesford MJ, Zhao FJ and McGrath SP (2000). Diagnosing sulfur deficiency in field-grown oilseed rape (Brassica napus L.) and wheat (Triticum aestivum L.). *Plant Soil* 225: 95-107.

Elephant D, Miles N and Dlungele P (2016). Evaluation of the impact of a range of soil ameliorants on soil chemical and biological properties. *Proc S Afr Sug Technol Ass* 89: 170-180.

Elephant DE, Titshall LW and Mthimkhulu S (2019). Sulphur status of soils from southern African sugarcane-producing regions. Proc S Afr Sug Technol Ass 92: 69-72.

Gerson JR and Hinckley ELS (2023). It is time to develop sustainable management of agricultural sulfur. *Earth's Future* 11(11): e2023EF003723

Ghosh GK (2022). Crop productivity and quality vis-a-vis sulphur management strategies in Indian agriculture. In: *Souvenir, National Seminar on "Recent Developments in Nutrient Management Strategies for Sustainable Agriculture: The Indian Context* (p. 57).

Haneklaus S, Bloem E and Schnug E (2008). History of sulfur deficiency in crops. *Sulfur: A Missing Link between Soils, Crops and Nutrition* 50: 45-58.

Havlin JL, Tisdale SL, Nelson WL and Beaton JD (2016). Soil fertility and fertilisers. Pearson Education India.

Mathadeen P, Miles N and Manson AD (2013). Infrared reflectance spectroscopy for the rapid measurement of agronomically-important soil properties. *Proc S Afr Sug Technol Ass* 86: 108-113.

McGrath SP, Zhao FJ and Withers PJA (1996). Development of sulphur deficiency in crops and its treatment. *Proceedings of the Fertiliser Society* 379: 48.

Meyer JH (1985). Sulphur availability in soils of the South African sugar industry. *Proc S Afr Sug Technol Ass* 59: 190-194.

Miles N, Elephant D and Mathadeen P (2013). Prediction of phosphorus availability and fixation in soils of the southern African sugar industry. *Proc S Afr Sug Technol Ass* 86: 145-148.

Miles N, Manson AD, Rhodes R, van Antwerpen R and Weigel A (2014). Extractable silicon in soils of the South African sugar industry and relationships with crop uptake. *Commun Soil Sci Plan Anal* 45(22): 2949-2958.

Miles N, van Antwerpen R and Ramburan S (2016). Soil organic matter under sugarcane: levels, composition and dynamics. *Proc S Afr Sug Technol Ass* 89: 161–169.

Mthimkhulu S, Miles N, van Antwerpen R and Elephant D (2018). Effect of residue and fertiliser management on soil fertility in a long-term sugarcane trial in South Africa. *S Afr J Plant Soil* 35(4): 307-315.

Mthimkhulu SS, Elephant DE, Miles N and Titshall LW (2022). The short-term effects of surface-applied dolomitic lime and gypsum on soil chemical properties and yields of sugarcane ratoon crops in KwaZulu-Natal, South Africa. *S Afr J Plant Soil* 39(2): 102-111.

Riley NG, Zhao FJ, and McGrath SP (2002). Leaching losses of sulphur from different forms of sulphur fertilisers: a field lysimeter study. *Soil Use Manag* 18(2): 120-126.

Scherer HW (2001). Sulphur in crop production. *Eur J Agron* 14(2): 81-111.

Titshall L, Naicker N, and Mdlambuzi T (2023). An overview of the soil fertility status of the South African sugarcane industry from 2017 to 2022. *Proc S Afr Sug Technol Ass* 95: 193-209.

van der Laan M and Miles N (2010). Nutrition of the South African sugar crop: Current status and long-term trends. *Proc S Afr Sugar Technol Ass* 83: 195-204.

Wang C and Kuzyakov Y (2024). Soil organic matter priming: The pH effects. *Glob Change Biol* 30(6): 17349.

SHORT COMMUNICATION

VOLATILISATION LOSSES FROM SURFACE-APPLIED NITROGENOUS FERTILISERS IN THE SUGARCANE-GROWING SOILS OF ZIMBABWE: LABORATORY-SCALE STUDY

Maidza TK[1], Rambwawasvika H[2,3], Chibarabada TP[2] and Mutatu W[2]

[1]Department of Soil Science and Environment, University of Zimbabwe, Mount Pleasant, Box MP167, Harare, Zimbabwe
[2]Zimbabwe Sugar Association Experiment Station, P/Bag 7006, Chiredzi, Zimbabwe
[3]Department of Chemical Engineering, Delft University of Technology, Van der Maasweg 9, 2629 HZ Delft, Netherlands

trishkmaidza@gmail.com, H.Rambwawasvika@tudelft.nl,tpchibarabada@zsaes.org.zw; wmutatu@zsaes.org.zw

Abstract

The volatilisation of nitrogen (N) fertiliser represents a major pathway of nutrient loss in sugarcane cultivation, which potentially leads to reduced crop yields and inefficient fertiliser use. This study quantified the ammonia volatilisation losses from surface-applied nitrogenous fertilizer, under controlled laboratory conditions, using soils from Zimbabwe's sugarcane-growing regions. Four N sources, white urea, carbon-coated urea, urease-inhibited urea and ammonium nitrate were evaluated across soils with a varying pH and texture, under laboratory conditions. The results showed that volatilisation losses were highest in alkaline soils (pH>7.0), with white urea losing up to 85% of its N content over a 14-day period. Among the fertilisers, white urea exhibited the highest volatilisation, followed by carbon-coated urea and ammonium nitrate, while urease-inhibited urea showed the lowest losses. Soils with a higher clay content (greater than 35%) exhibited significantly lower volatilisation than sandy soils. These findings highlight the critical influence of soil properties on nitrogen use efficiency, and they emphasise the need for informed fertiliser selection, in order to enhance productivity and environmental sustainability in sugarcane farming.

Keywords: nitrogen volatilisation, urea, urease inhibitor, ammonium nitrate, sugarcane, soil properties

Introduction

Nitrogen is a vital nutrient in sugarcane production, which directly influences biomass accumulation and the sugar yield (Meyer *et al*., 2007; Boschiero *et al*., 2020). To meet the high nutrient demands of sugarcane, large quantities of nitrogenous fertilisers are routinely applied (Mthimkhulu & Miles, 2017; Titshall *et al*., 2023). In Zimbabwe, the most commonly-used nitrogen sources include urea, Ammonium Nitrate (AN), and Calcium Ammonium Nitrate (CAN), with urea being the preferred choice, due to its high nitrogen content (46%) and cost-effectiveness (Clowes

& Breakwell, 1998; Degaspari *et al*., 2020). However, urea is highly susceptible to ammonia volatilisation, especially when it is surface applied, without incorporation (Oliveira *et al*., 2023).

Nitrogen losses through volatilisation, along with leaching, runoff and denitrification, significantly reduce the fertiliser-use efficiency and they increase the environmental risks (Yang *et al*., 2018). Ammonia volatilisation occurs when urea is hydrolysed to ammonium, which is then lost as gaseous ammonia, particularly under a high pH, warm temperatures and partially wet conditions (Sigurdarson *et al*., 2018).

In order to mitigate against nitrogen losses, fertiliser innovations have been developed, such as coated urea and urease inhibitors. Despite their availability, many farmers remain unaware of their benefits, or they lack guidance on their effective use, particularly in the wake of Zimbabwe's land-reform programme, which introduced a wave of inexperienced farmers.

This study aimed to quantify the volatilisation losses from various nitrogen fertilisers under the different soil conditions found in Zimbabwe's sugarcane-growing regions, under laboratory conditions. By identifying the influence of the soil pH and texture on nitrogen losses, the research provides actionable insights into fertiliser selection and the management for improved nitrogen-use efficiency and sustainable sugarcane production.

Materials and Methods

Experimental site

The experiment was conducted under laboratory conditions at the Zimbabwe Sugar Association Experiment Station (ZSAES), which is located in Chiredzi in the south-eastern Lowveld of Zimbabwe, along the Ngundu-Tanganda road (21°01'57"S; 31°36'58"E; 430 m above sea level). The region is semi-arid, and it receives an average annual rainfall of 550-600 mm, with hot summers (a daily max >30°C), short cool winters and night-time temperatures that range from 6-9°C.

The Zimbabwe Sugar Industry (ZSI) features two dominant soil types, namely, basalt-derived self-churning clays (Vertisols) and siallitic soils derived from gneisses (Clowes & Breakwell, 1998). Vertisols are prevalent in the Hippo Valley, while siallitic soils dominate the Triangle, Mkwasine and ZSAES areas. This study was conducted in the ZSAES Industrial and Agricultural Chemistry Laboratory, using soils that were sampled from the major sugarcane-growing regions.

Sampling and sample preparation

Soil selection was guided by the 2023-2024 ZSAES Agricultural and Industrial Chemistry soil database, which contains historical data on the pH, texture and clay content. Targeted soils were sampled from Triangle, the Hippo Valley, Mkwasine and ZSAES, using a Dutch auger at a depth of 0-30 cm, which corresponds to the primary root zone for sugarcane (Clowes & Breakwell, 1998). A diagonal sampling technique was employed, as described by Chikazaza *et al*. (2022).

The samples were transported in polythene bags and they were air-dried upon arrival at the laboratory. They were crushed with a wooden mallet to break the aggregates and then sieved through a 2 mm mesh (Chikazaza *et al*., 2022).

Soil analysis

All soil samples were analysed for their physico-chemical properties, including their pH, Electrical Conductivity (EC), total nitrogen content, water-holding capacity and texture. The soil pH was determined by using a 1:5 volume-to-volume suspension of soil in a 0.01 M calcium chloride ($CaCl_2$) solution, and the measurements were taken by using a Mettler Toledo Seven Excellence multiparameter meter. The electrical conductivity was measured by using the same instrument on a 1:5 suspension of soil in distilled water. Soil texture was assessed by using the Bouyoucos hydrometer method, as outlined by Beretta *et al*. (2014), which quantifies the proportions of sand, silt and clay. The total soil nitrogen was quantified by using the Kjeldahl digestion method (FAO, 2021), which involves acid digestion, distillation and titration, to determine the concentration of ammoniacal nitrogen.

Experimental set-up and design

The experiment was laid out in a Completely Randomised Design (CRD), following a 2×4 factorial arrangement. Factor A consisted of two soil characteristics, the pH and clay content, while Factor B included four fertiliser treatments: white urea, carbon-coated urea, urease-inhibited urea, ammonium nitrate, as well as a control treatment with no fertiliser. The control was included, in order to verify that the observed nitrogen losses were due to the applied fertilisers, and not to experimental error.

For each treatment, 50 grams of air-dried soil were accurately weighed and placed into individual petri dishes. Fertiliser granules were uniformly applied on the soil surface to deliver a nitrogen rate that was equivalent to 0.46 grams of N per dish. The soil moisture was brought to the field capacity by using distilled water, and the moisture content was kept constant throughout the experimental period.

The treated soils were left to volatilise under controlled laboratory conditions, with the assumption that the nitrogen loss would primarily be influenced by the varying soil pH and texture. Each experimental set, one focusing on the pH and the other on the texture, included 15 treatments, which were each replicated three times, resulting in 45 experimental units per set. Volatilisation was monitored over a period of 14 consecutive days, during which daily observations were made. Nitrogen concentrations were measured both at the beginning of the experiment (to establish the baseline levels) and at the end of the volatilisation period, by using the Kjeldahl method. Nitrogen loss, due to volatilisation, was estimated as the difference between the total nitrogen applied and the residual nitrogen remaining in the soil after the experimental period.

Statistical analysis of data

The data were analysed by using Genstat Release 23.1. A two-way ANOVA was performed to test for significant differences in nitrogen volatilisation among the treatments. The treatment means were separated by using the Least Significant Difference (LSD) at a 5% significance level.

Results and Discussion

Characteristics of the soils used in the study

The soils used in this study varied in their pH and clay content, to represent the typical sugarcane-growing conditions in Zimbabwe. In the pH experiment, the pH values ranged from 4.88 to 8.02, while in the texture experiment, the soils had a clay content that ranged from 9% to 50%.

Effect of pH on ammonia volatilisation

Ammonia volatilisation losses were monitored over 14 days by using five nitrogen fertiliser treatments across soils with low (less than 4.88), medium (4.88 to 6.20) and high (greater than 8.02) pH levels. The results showed a strong positive correlation between the increasing soil pH and nitrogen loss ($F=3193.68$; $p<0.001$), with the highest losses being observed in alkaline soils. White urea exhibited the greatest susceptibility to volatilisation across all pH levels, particularly at a high pH, while urease-inhibited urea showed the lowest losses (Figure 1).

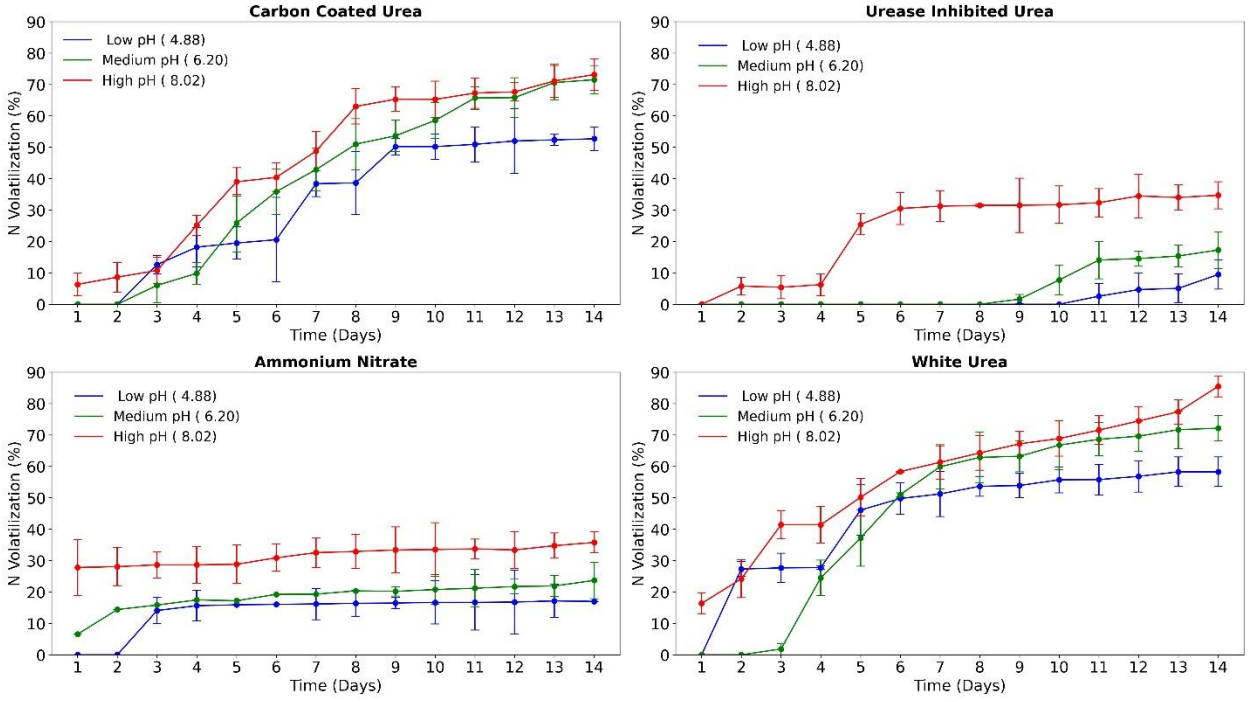


Figure 1. Effect of pH on volatilisation losses from different fertilisers over 14 days

This trend aligns with the chemical equilibrium between the ammonium ions and the ammonia in soil. A higher pH increases the hydroxide ion concentration, shifting the equilibrium toward ammonia, which is volatile and easily lost to the atmosphere (Freney *et al*., 1983; du Preez & Burger, 1988). The higher losses in white urea from this study (up to 80%), compared to the losses of about 50% from the du Preez and Burger (1988) study, may be due to the longer monitoring duration of 14 days vs 3 days, the differences in their measurement methods, and the surface application of fertilisers without soil incorporation, under laboratory conditions.

Effect of the fertiliser type on volatilisation at different pH levels

The fertiliser type significantly influenced the volatilisation losses ($F=19142.42$; $p<0.001$). The cumulative nitrogen losses were as follows (Figure 2): white urea (49.39%), carbon-coated urea (39.58%), ammonium nitrate (21.25%), urease-inhibited urea (10.18%) and the control (0.34%). The losses were highest in the high-pH soils (mean = 31.95%), followed by the medium (21.89%) and low-pH soils (18.61%).

The effectiveness of urease-inhibited urea can be attributed to the presence of Agrotain, which delays urea hydrolysis and reduces the early release of ammonia. In contrast, white urea hydrolyses rapidly, forming ammonium carbonate, which elevates the local pH and promotes volatilisation. Carbon-coated urea showed slightly-reduced losses, which are likely due to the microbial stimulation around the granule that moderates hydrolysis. The control plots showed negligible losses, which confirmed the validity of the experimental set-up.

A significant interaction was observed between the fertiliser type and the soil pH ($F=320.98$; $p<0.001$). The white urea losses increased markedly across the defined soil pH categories: 44.42% for a low pH (<4.88), 46.40% for a medium pH (4.89-6.20) and 57.33% for a high pH (>6.21). In contrast, urease-inhibited urea losses were minimal at a low (1.51%) and medium pH (5.17%), and they increased only moderately under a high pH (23.85%). The daily volatilisation followed a sigmoidal trend, namely, slow at first, accelerating mid-period and plateauing towards Day 14. The white urea lost up to 85% of its N under a high pH by Day 14, while the urease-inhibited urea showed delayed and limited losses (Figure 2).

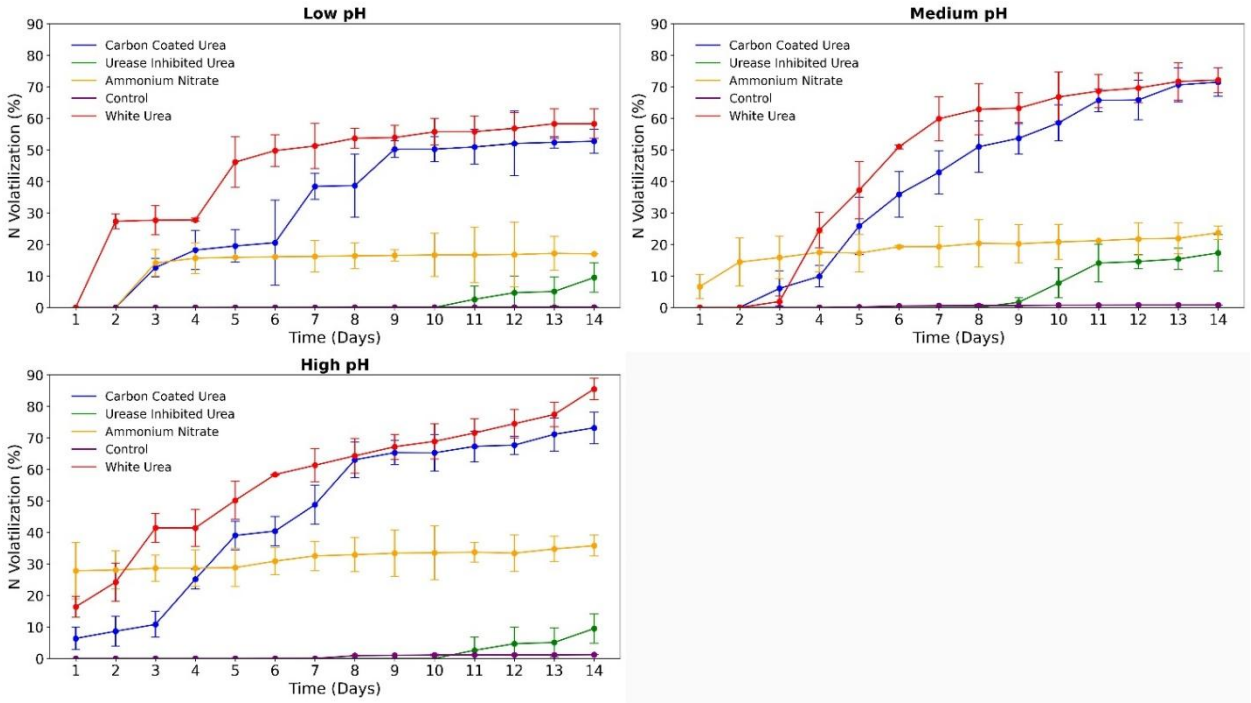


Figure 2. Volatilisation loss (%) of fertilisers at a low (a), medium (b) and high (c) pH over 14 days

Effect of soil texture (clay content) on volatilisation

The soil texture also significantly affected the volatilisation losses ($F=143.75$; $p<0.001$). The average losses of all the fertilisers were inversely related to the clay content, with high-clay soils (greater than 35% clay) averaging a 18.16% loss, compared to 23.21% in medium-clay (15- 35% clay) and 24.11% in low-clay soils (less than 15% clay). Across all textures, the ranking of fertilisers by loss remained as follows: white urea > carbon-coated urea > ammonium nitrate > urease-inhibited urea (Figure 3).

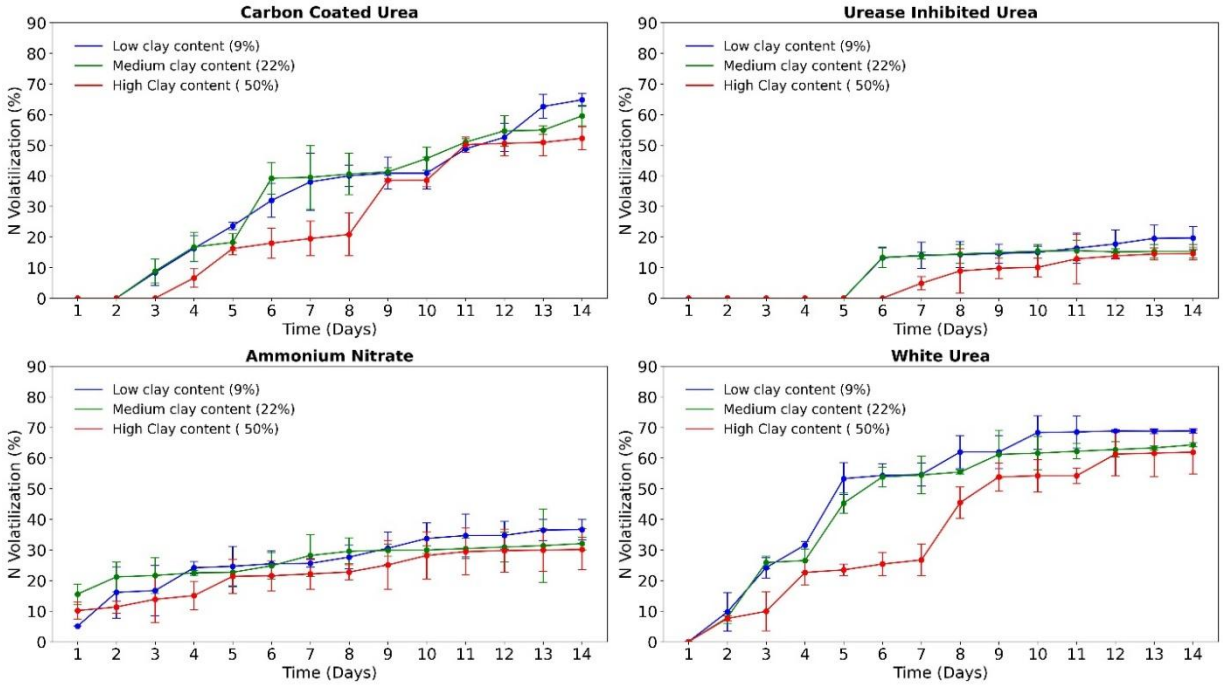


Figure 3. Effect of texture on ammonia volatilisation

High clay soils retain more moisture and have a higher Cation Exchange Capacity (CEC), which enhances their ammonium ion retention and reduces NH_3 volatilisation (Barakan & Aghazadeh, 2020). In contrast, sandy soils with a low clay content have a lower buffering capacity, a greater pore space and a lower water retention, which increases their susceptibility to volatilisation.

The findings contrast with field-based studies, like Rochette *et al*. (2013), who reported 2.8-11.6% ammonia emissions when using wind tunnels. The differences in the volatilisation rates can be attributed to the environmental variability, leaching, plant uptake, as well as other field processes that are absent under controlled laboratory conditions.

The fertiliser type had the most pronounced effect on the nitrogen loss ($F=2550.18$; $p<0.001$). The mean cumulative losses were highest for white urea (43.99%), followed by carbon-coated urea (30.97%), ammonium nitrate (25.09%) and urease-inhibited urea (8.73%). The control treatments consistently showed minimal losses (0.34%).

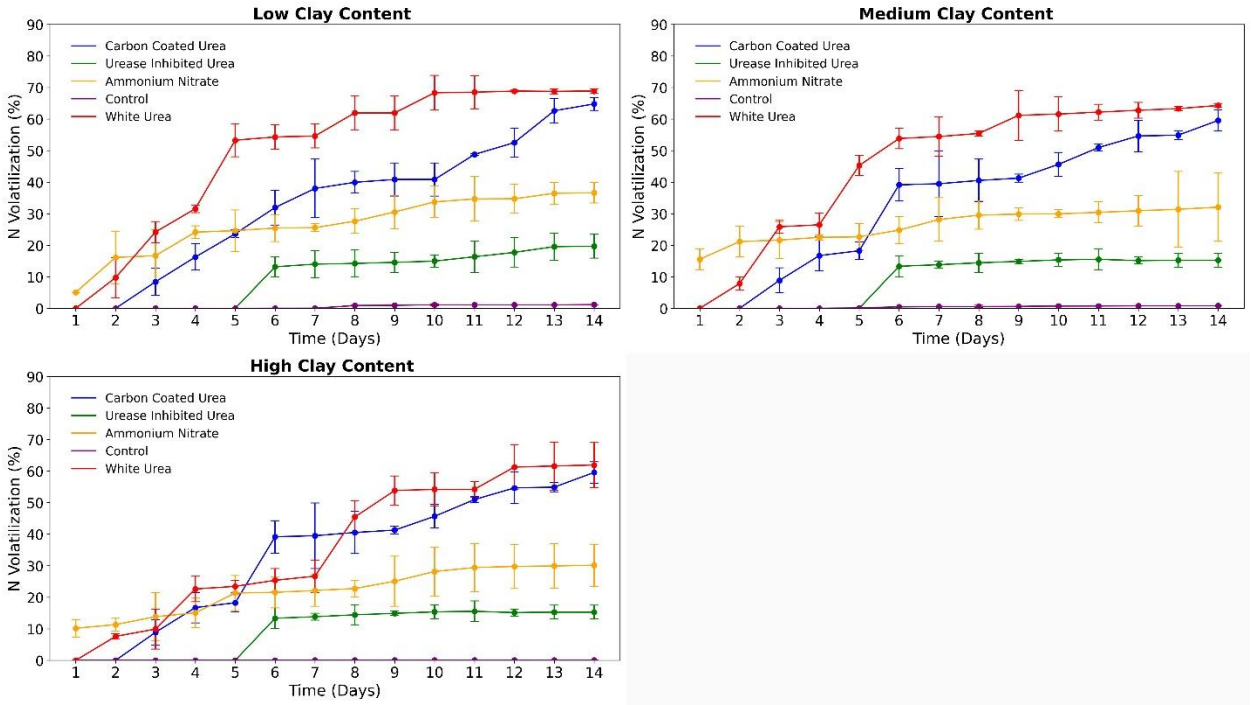


Figure 4. Volatilisation (%) of fertilisers over 14 days in soils with a low-, medium- and high-clay content

A significant interaction between the fertiliser type and clay content ($F=18.42$; $p<0.001$) further emphasised the role of the soil texture. White urea losses were highest under all conditions. Similar trends were observed for carbon-coated urea. Urease-inhibited urea consistently showed lower losses across all textures (14-19%). Control treatments remained stable, with negligible losses (Figure 4).

This interaction underscores the importance of matching the fertiliser type to specific soil characteristics. Stabilised fertilisers, like urease-inhibited urea, are particularly effective in reducing nitrogen losses in both alkaline and coarse-textured soils, where uncoated urea products would otherwise lead to significant inefficiencies.

Conclusion and Recommendations

Nitrogen loss through ammonia volatilisation was strongly influenced by the soil pH, the clay content and the fertiliser type. The losses were highest in alkaline soils and in soils with a low clay content. White urea consistently showed the highest volatilisation, while urease-inhibited urea recorded the lowest losses across all conditions. The use of stabilised fertilisers, such as urease-inhibited urea, can significantly reduce the nitrogen losses, especially in high-pH or sandy soils.

It is recommended that fertiliser selection be guided by the soil properties, in order to improve their nitrogen-use efficiency. Avoiding the surface application of untreated urea on alkaline or coarse-textured soils can help to minimise the losses. These findings offer a practical basis for

improving the fertiliser recommendations and for guiding nitrogen management in sugarcane production. Future studies must look at the effects of temperature and moisture, as they have not been included in this study (kept constant).

References

Beretta AN, Silbermann AV, Paladino L, Torres D, Bassahun D, Musselli R and García-Lamohte A (2014). Soil texture analyses using a hydrometer: modification of the Bouyoucos method. *Int J Agric Nat Resour* 41: 263-271.

Boschiero BN, Mariano E, Torres-Dorante LO, Sattolo TM, Otto R, Garcia PL, Dias CT and Trivelin PC (2020). Nitrogen fertiliser effects on sugarcane growth, nutritional status and productivity in tropical acid soils. *Nutrient Cycling in Agro-ecosystems* 117(3): 367-382.

Chikazaza L, Rambwawasvika H and Mutatu W (2022). Status of micronutrient composition in cultivated and uncultivated soils in the Zimbabwe sugar industry. *Proc S Afr Sug Technol Ass* 94: 102-117.

Clowes MJ and Breakwell WL (1998). Zimbabwe sugarcane production manual. Zimbabwe Sugar Association Experiment Station, Chiredzi, Zimbabwe 1: 102-106.

Degaspari IAM, Soares JR, Montezano ZF, del Grosso SJ, Vitti AC, Rossetto R and Cantarella H (2020). Nitrogen sources and application rates affect emissions of N2O and NH3 in sugarcane. *Nutr Cycling* 116: 329-344.

du Preez CC and Burger RDT (1987). Laboratory measurements of ammonia volatilisation from five nitrogen-containing fertilisers after surface application at different rates on a neutral to alkaline soil. *S Afr J Plant Soil* 4: 17-20.

FAO (2021). Standard operating procedure for soil nitrogen – Kjeldahl method. FAO, Rome, Italy Available at: https://openknowledge.fao.org/server/api/core/bitstreams/17a0e476-f796-4608-a869-295a367c0b56/content.

Meyer JH, Schumann AW, Wood RA, Nixon DJ and van den Berg M (2007). Recent advances to improve nitrogen use efficiency of sugarcane in the South African sugar industry. *Proc Int Soc Sugar Cane Technol* 26: 238-246.

Mthimkhulu SS and Miles N (2017). The fertility status of soils of the South African sugar industry – 2012 to 2016: An overview. *Proc S Afr Sug Technol Ass* 90: 92-103.

Oliveira BG, Lourenço KS, Carvalho JLN, Gonzaga LC, Teixeira MC, Tamara AF, Soares JR and Cantarella H (2023). New trends in sugarcane fertilisation: Implications for NH_3 volatilisation, N_2O emissions and crop yields. *J Environ Manage* 342: 118233.

Rochette P, Angers DA, Chantigny MH, Gasser MO, MacDonald JD, Pelster DE and Bertrand N (2013). NH3 volatilisation, soil concentration and soil pH following the sub-surface banding of urea at increasing rates. *Can J Soil Sci* 93: 261-268.

Sigurdarson JJ, Svane S and Karring H (2018). The molecular processes of urea hydrolysis in relation to ammonia emissions from agriculture. *Rev Environ Sci Biotechnol* 17: 241-258.

Titshall LW, Naicker N and Mdlambuzi T (2023). An overview of the soil fertility status of the South African sugarcane industry from 2017 to 2022. *Proc S Afr Sug Technol Ass* 95: 193-209.

Yang J, Jiao Y, Yang WZ, Gu P, Bai SG and Liu LJ (2018). Review of methods for the determination of ammonia volatilisation in farmland. *IOP Conf Ser Earth Environ Sci* 113: 012022. IOP Publishing.

POSTER SUMMARY

THE INTEGRATION OF SOYBEAN INTO SUGARCANE FARMING SYSTEMS: ENHANCING SOIL FERTILITY AND WEED CONTROL

Phiri JS

Department of Agriculture, Illovo Dwangwa Estate, Malawi

jsphiri@illovo.co.za

Abstract

The sugar industry is increasingly focused on sustainable farming practices that enhance productivity, while minimising the use of resources (González & Pérez 2020). This study investigates the integration of soybean (Glycine max) into sugarcane farming systems to improve the soil fertility, reduce herbicide use and manage weed pressure. A field trial was conducted at the Illovo Dwangwa Estate (Field No. 5132), with two treatment plots, namely: (1) soybean for biomass incorporation, and (2) a plot without soybean. A Randomised Complete Block Design (RCBD) with two treatments and four blocks was used. The results indicated that soybean incorporation increased the soil nitrogen by 27%, and it reduced weed infestation by 65%. This research suggests that integrating soybean into sugarcane farming systems offers significant agronomic benefits, with the potential for broader implementation in other regions.

Keywords: Sugarcane, soybean, soil fertility, weed suppression, integrated farming, crop diversification

SHORT COMMUNICATION

A DATA-DRIVEN APPROACH TO SUPPORT THE ON-FARM MANAGEMENT OF SUGARCANE VARIETIES IN THE KWAZULU-NATAL MIDLANDS REGION

Hoffman, N[1], Clark, D [1,2], Kadwa, M[3], Paraskevopulos, A[1], van Heerden, PDR[1,4], Wilkinson, D[1] and Botha, P[1]

[1]South African Sugarcane Research Institute, Durban, South Africa
[2]University of KwaZulu-Natal, Pietermaritzburg, South African
[3]South African Cane Growers Association, Durban, South Africa
[4]University of Pretoria, Pretoria, South Africa

Natalie.Hoffman@sugar.org.za

Abstract

In the KwaZulu-Natal Midlands, older, well-established sugarcane varieties are traditionally grown on a 24-month cycle. Newer varieties, with enhanced growth characteristics and high yield potential, are prone to lodging under favourable conditions, necessitating earlier harvesting. This shift in harvest cycle has created challenges when managing mixed crop cycles and harvest timing, affecting farm operations, cane supply and replanting strategies, highlighting the need for strategies to optimise economic outcomes. This study aimed to develop a decision support approach for optimising variety management in the Midlands, focusing on variety selection, harvest timing and yield. The approach involved statistical analyses of commercial harvest data to assess the impact of variety type, harvest age and timing on Recoverable Value (RV) yield. Harvest data were obtained from eight farms in the northern and nine in the southern Midlands regions over five seasons. Statistical analyses informed optimal harvest ages, based on peak RV yield for the different region × variety type × harvest age × harvest timing combinations. Results were then evaluated economically, by considering lodging, harvest-to-mill operations and crop management costs. This study represents the first robust evaluation of commercial Midlands variety performance under real-world conditions, revealing clear statistical differences in cane yield and quality across key agronomic factors. Findings indicate that while a 24-month cycle remains common for older varieties, earlier harvesting is necessary for newer varieties in order to maximise yield and economic returns. The novel decision support approach developed in this study leverages commercial data to evaluate trends, and assesses economic feasibility, to inform variety management strategies. It can be customised for specific scenarios, thereby providing valuable insights across different agronomic conditions. With potential applications across the sugarcane industry, this methodology enables informed decision-making on variety deployment, harvest scheduling and crop management, ultimately supporting improved operational efficiency and whole-farm profitability.

Keywords: Commercial data, variety management, harvest age, recoverable value yield, decision support, economics

Introduction

In recent years, sugarcane growers in the KwaZulu-Natal Midlands have expressed uncertainty regarding the optimal management of new and old varieties. Traditionally, older varieties (e.g. N12, released in 1979) are harvested at a crop age of approximately 24 months. Newer varieties (released since 2007, following N48) with enhanced growth characteristics, produce high yields but are prone to lodging under favourable conditions, necessitating earlier harvesting (≤ 18 months) which may impact cane quality. Ramburan (2015) noted declines in

optimal harvest age over time, from 25 months for N12 to 19 months for N48, reflecting breeding and selection shifts. These changes have increased variation in crop cycles and harvest timing, thereby complicating on-farm management, cane supply and replanting strategies. This highlights the need for decision support strategies to optimise variety selection and harvest age to enhance yield, quality and economic outcomes across production conditions. The study aimed to develop a decision support approach for optimising the management of varieties in the KwaZulu-Natal Midlands, focusing on variety selection, harvest timing, crop yield and economic returns.

Methodology/Approach

The study applied statistical analysis of commercial harvest data to identify optimal harvest age ranges under various agronomic conditions. These were then assessed through economic analysis to evaluate their potential impact on farm-level outcomes.

Statistical analysis of commercial data

Harvest data were obtained from eight farms in the northern Midlands (n = 2790 fields) and nine farms in the southern Midlands (n = 2345 fields) regions, respectively, spanning five harvest seasons (2019-2023) and representing ~14% of the area under cane in each region. Data were filtered to exclude unrealistic yields and harvest ages, mixed or unidentified varieties, incomplete records and statistical outliers (using the interquartile method). Varieties were grouped according to the rate of canopy development (slow/fast) and susceptibility to lodging (low / average / severe) as per the SASRI Variety Guide (https://sasri.sasa.org.za/pls/sasri/variety/r/sasri-variety-guide). The three variety groupings with sufficient datapoints were: SlowLow (N12), and newer Midlands varieties, FastAvg (N16, N31, N37, N39, N42, N45, N48, N50, N58, N59, N62, N66) and FastSev (N36, N52, N54, N55, N61). Data were further grouped by harvest age (in five four-monthly increments, from 12 to 31 months) and harvest period (early / middle / late season). Although data indicating soil potential were available for some fields, the number of observations was insufficient to support robust statistical analysis of its effects on annualised RV yield, and soil type could therefore not be included as a factor in the analysis. Furthermore, while weather conditions are a key driver influencing crop productivity, such effects are difficult to isolate in commercial datasets. These effects were minimised by including multi-season data.

Statistical analysis (p=0.05) of annualised recoverable value yield (ATRV, t / ha / annum) was conducted separately for each region x variety group x harvest period combination, using Restricted Maximum Likelihood (REML) analysis in Genstat® v.22 to identify optimal harvest age ranges, based on peak ATRV.

Economic analysis

Economic analysis of optimal harvest ages was conducted using a simple Excel model. Gross margins (R / ha / annum) were calculated using region-specific costs from the SA Cane Growers' Association: (1) April 2024 RV price; (2) ratoon management costs; (3) Eldana spraying costs; (4) cane extraction (harvest-to-mill) costs, factoring in mill distance, and (5) additional extraction costs for lodged cane. The evaluation focused on the agronomic scenarios identified in the statistical analysis, excluding full crop-cycle economics, to assess the harvest timing outcomes for individual crops under actual on-farm conditions.

Results and Discussion

Statistical analysis of commercial data

Statistical analysis of commercial data from the Midlands North showed significant differences in ATRV between harvest age groups for most time of season x variety group combinations (Figure 1). In N12 (SlowLow), ATRV peaked between 12 and 23 months, depending on harvest timing (early / mid / late), suggesting that harvesting earlier than the conventional 24-month cycle may be beneficial. New varieties (FastAvg, FastSev) showed significant differences in ATRV across harvest age groups in most cases, peaking at 16-19 months in the early season and 12-19 months in mid- and late-season crops, highlighting their suitability for earlier harvesting as compared to N12.

In the Midlands South region, early-season N12 crops showed no significant differences in ATRV between harvest age groups, suggesting that there is no clear benefit to deviating from the conventional 24-month cycle. In the mid-season crops, N12 achieved peak ATRV at 20-23 months, while late season crops peaked at 20-27 months. New varieties showed significant differences in ATRV across harvest ages and time of season, peaking at 16-19 months in early-season, 12-15 months mid-season, and 12-15 months (FastSev) and 20-23 months (FastAvg) in the late-season crops.

Economic analysis

The economic analysis estimated that optimal harvest ages for various region x time of season x variety group combinations (Figure 2) generally aligned well with the optimal crop age ranges identified with statistical analysis of ATRV. For example, in the Midlands North early-season harvest, N12 showed peak ATRV between 16-23 months, with no significant difference between the 16-19- and 20-23-month groups (Figure 1). Economic analysis showed that within this range, gross margins were higher when harvesting at 16-19 months (Figure 2). For new varieties harvested early in the season, the optimal harvest age of 16-19 months, based on peak ATRV, also corresponded with the highest gross margins. In late-season crops, FastAvg varieties showed no significant differences in ATRV between harvest age groups, but harvesting at 20-23 months maximised gross margins. For FastSev varieties, both the peak ATRV and the highest gross margins were achieved at 12-15 months.

The only exception to the close alignment between optimal ATRV and optimal economics occurred in the Midlands North, where FastSev varieties in the mid-season showed peak ATRV at 12-19 months (Figure 1). Despite the increased cane extraction costs associated with lodging with age, the additional cane yield gained by extending the harvest to 20-23 months resulted in a higher overall income (Figure 2). Notably, in all cases, optimal harvest ages based on economic evaluation remained unaffected by the mill distance (data not shown).

In the Midlands South, N12 consistently achieved the highest gross margins when harvested at 20-23 months, regardless of the time of season, generally aligning well with peak ATRV. For new varieties, peak ATRV consistently aligned with the highest gross margins across all harvest periods: 16-19 months for early-season harvest, 12-15 months for mid-season, and 20-23 months (FastAvg) and 12-15 months (FastSev) for late-season harvests.

Overall, this integrated analysis approach demonstrated that statistical analysis can effectively determine optimal harvest age ranges based on peak ATRV, while economic analysis further refined this by identifying the most economically advantageous harvest age.

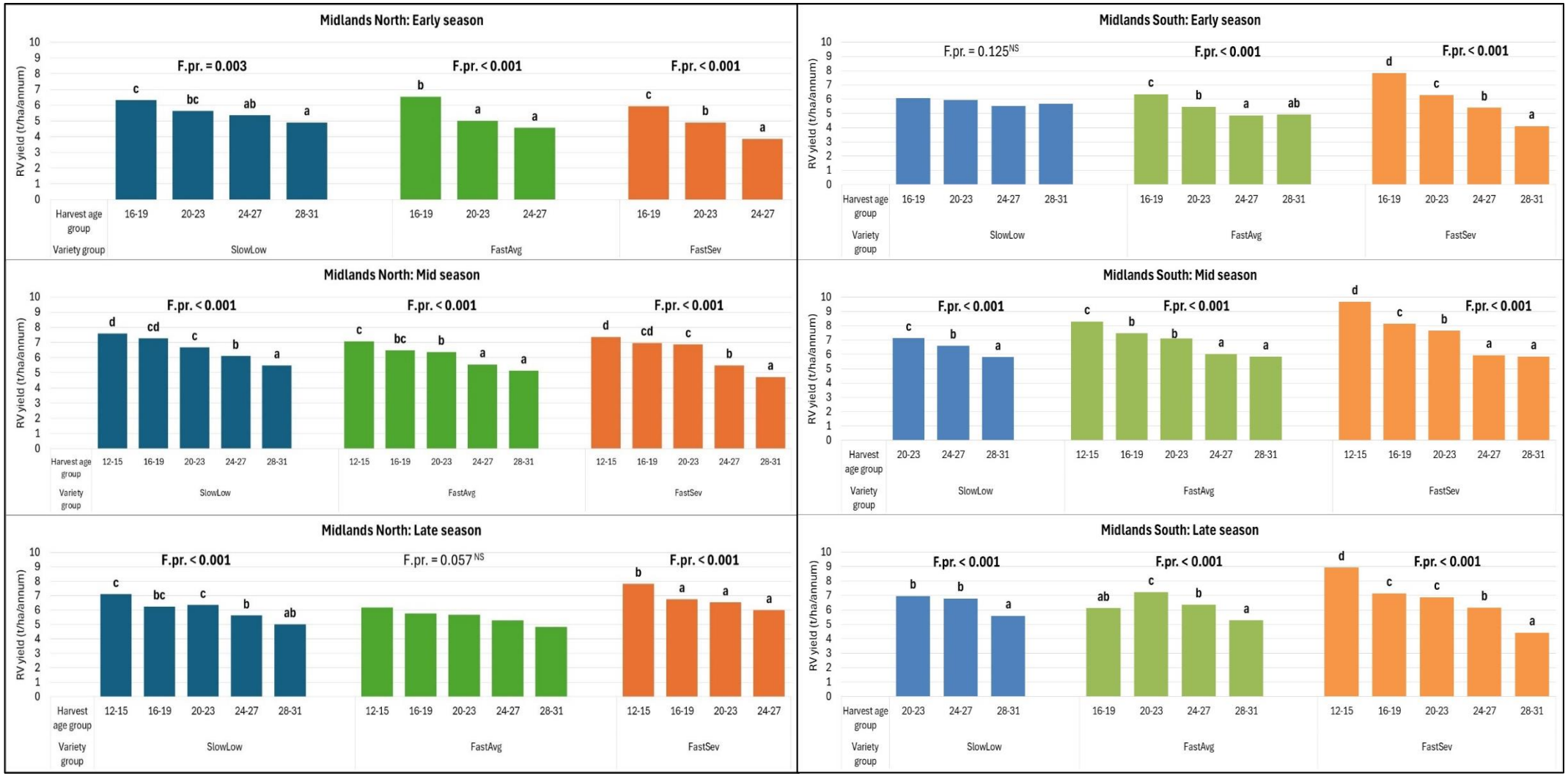


Figure 1. Annualised Recoverable Value (RV) yield measured in the Midlands North (left) and South (right) regions at different times of the harvest season (early/middle/late) and at different harvest ages (four monthly increments, from 12-31 months), for groups representing old (SlowLow) and new (FastAvg or FastSev) sugarcane varieties. F.pr. values at p=0.05 are given (NS=not significant), and bold letters above the bars indicate statistical differences between harvest age groups.

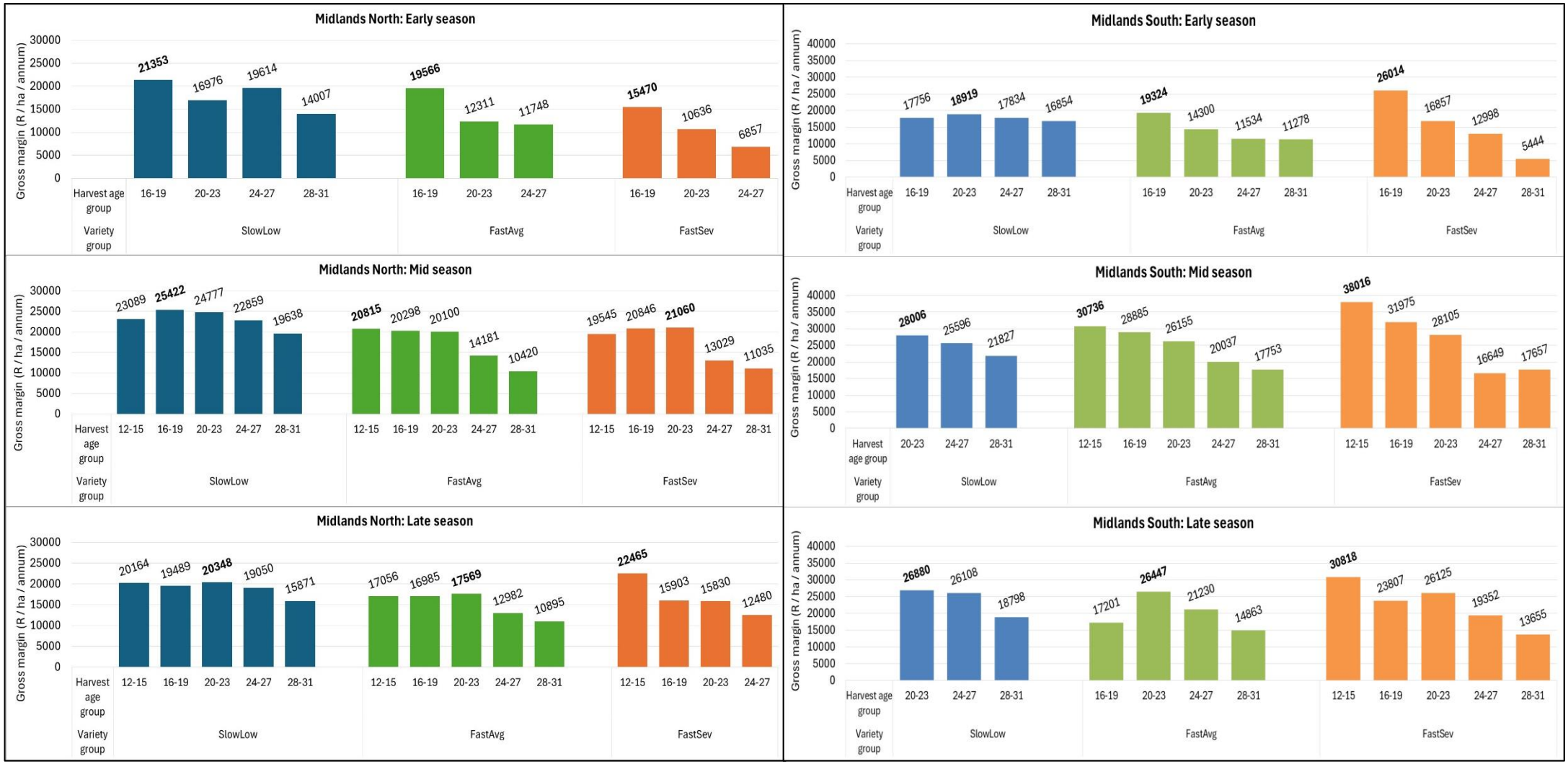


Figure 2. Gross margins estimated from economic analysis of commercial harvest data measured in the Midlands North (left) and South (right) at different times of the harvest season (early/middle/late) and at different harvest ages (four monthly increments, from 12-31 months), for groups representing old (SlowLow) and new (FastAvg or FastSev) sugarcane varieties. Bold values highlighted in each variety group indicate the highest gross margin.

Conclusions

The study successfully developed a data-driven decision support approach using commercial harvest data and economic analysis to assist growers in optimising sugarcane variety management in the Midlands region. The study provided critical insights into the performance of new and old varieties in different production scenarios, by identifying the optimal harvest timing to maximise cane yield, quality and economic outcomes. The approach could have broad potential across the South African sugarcane industry. Future research will apply this framework to grower-specific agronomic systems, enabling whole-farm analyses that account for field-level variability in soil potential, productivity and economic feasibility, and its application could be expanded to other regions to support region-specific decision-making.

Acknowledgments

We gratefully acknowledge the growers in the Midlands North and South regions for providing commercial harvest data which provided the foundation for this research. We also thank SQR Software for their assistance in extracting harvest data from the growers' CanePro databases on the growers' behalf.

References

Ramburan S. 2015. Interactions affecting the optimal harvest age of sugarcane in rainfed regions of South Africa. *Field Crops Research* 183: 276-281.

SHORT COMMUNICATION

EFFECTS OF HARVEST SEASON AND SOIL TYPE ON SUGARCANE RATOON YIELD DECLINE

Dlamini NE[1] and Zhou M[2,3]

[1]Eswatini Sugar Association Technical Services, Simunye, Eswatini
[2]South African Sugarcane Research Institute, Mount Edgecombe, South Africa
[3]Department of Plant Breeding, Faculty of Natural and Agricultural Sciences, University of the Free State, Bloemfontein, South Africa

njabulod@esa.co.sz, Marvellous.Zhou@sugar.org.za

Abstract

A sugarcane-growing environment is constituted of a combination of the harvest season (early-season, ES; mid-season, MS; and late-season, LS) and the soil type (well-drained soil, WDr; moderately-drained soil, MDr; and poorly-drained soil, PDr). Sugarcane yields are known to decline with successive ratoon crops, a phenomenon which is termed Ratoon Yield Decline (RYD). The objective of this study was to assess the impact of the harvest season and soil type on the RYD for the Tons Cane per Ha per Annum (TCHA) and the Tons Sucrose per Ha per Annum (TSHA). Fifteen-year yield data from four commercial sugarcane growers in the Eswatini sugar industry were analysed using the linear mixed model, with a focus on the first eight crops (the plant crop plus seven ratoons). The harvest seasons had significantly ($p<0.0001$) different linear slopes across the ratoon crops for both TCHA and TSHA, while the soil types were significantly ($p=0.0034$) different only for TSHA. The ES harvests had the largest rate of yield decline (-3.33 TCHA and -0.33 TSHA), followed by the LS harvests (-2.30 TCHA and -0.32 TSHA), and the MS harvests had the least decline (-1.98 TCHA and -0.26 TSHA). The PDr soils had the largest rate of decline (-2.92 TCHA and -0.38 TSHA), compared to the MDr soils (-2.30 TCHA and -0.28 TSHA) and WDr soils (-2.43 TCHA and -0.25 TSHA). The nine environments (harvest seasons x soil types) were grouped into three distinct mega-environments (high-, moderate- and low-potential yields). It is envisaged that these results will inform - sugarcane yield forecasting models, selection of genotypes for environment specific adaptation, identification of profitable ratoon crop numbers for each environment, as well as timely scheduling of sugarcane replant programmes.

Keywords: Harvest season, environments, ratoon, soil type, yield decline

Introduction

Several factors are responsible for the decline in yield as the number of ratoon crops grow, and these include soil type and harvest season. Many sugarcane-producing areas globally have diverse soil types and harvesting seasons. For example, in Eswatini and South Africa, sugarcane soils are classified into three groups, depending on their hydraulic properties: well-drained soils (WDr), moderately-drained soils (MDr) or poorly-drained soils (PDr). WDr soils are well-structured, deep and freely-draining. PDr soils are poorly-structured duplex soils that are characterised by prolonged waterlogging after heavy rainfall or irrigation. The characteristics of MDr soils are generally between those of the WDr and PDr soils. In the Eswatini and South African industries, the harvesting of sugarcane happens over a nine-month period. This period is classified into three parts: April to June (early season, ES); July to September (mid-season, MS); and, October to December (late season, LS).

Different soil type and harvest season combinations constitute the sugarcane-growing environment. While it is known that the soil type and harvest season impact the yields of

sugarcane, there is no evidence of any in-depth study being undertaken to systematically and collectively quantify their effects on the yields of ratoon crops. The objectives of this study were therefore, (i) to determine the effects of the harvest season and soil type on the RYD, and (ii) to classify the sugarcane-growing environments according to their yielding potential and RYD, by using commercial data.

Material and Methods

The data used for this study spanned a 15-year period (2000 to 2014) and were sourced from four large-scale sugarcane growers of the Eswatini sugar industry. Together, these growers supply the three sugar mills of Eswatini (Big Bend, Mhlume and Simunye) with approximately 62% of sugarcane milled annually. Their sugarcane fields cover a large area, with diverse soil types, and they supply cane to the mills throughout the milling season, from April to December. These growers have comparable climatic conditions and management practices; therefore, any variation in the crop yields can be attributed to the soil type and harvest season. Furthermore, these growers were chosen for this investigation because of the availability of credible and comprehensive field data.

This analysis considered only the cane (Tons Cane per Ha, TCH) and sucrose yield (Tons Sucrose per Ha, TSH). Sugarcane in Eswatini is harvested 12 months after planting, or after harvesting the previous crop. For a meaningful comparison across years, the productivity data (TCH and TSH) were annualised, i.e. they were extrapolated to represent a yield at 12 months. The annualised TCH and TSH were expressed as Tons Cane per Hectare per Annum (TCHA) and the Tons Sucrose per Hectare per Annum (TSHA), respectively. For the analysis, only the first eight crops (plant cane and seven ratoons) across the 15 years (2000-2014) were considered.

The data were subjected to a simple linear regression to estimate the intercepts and slopes of the two yield traits across ratoon crops. [The intercepts represent the plant cane yields, while the slopes represent the decline in yield across ratoon crops]. Using the intercepts and slopes, graphs were then drawn to compare yield trends for the harvest season, the soil type and the environment (harvest season x soil type).

Results and Discussion

The ES harvests produced a larger plant cane yield (118.60 TCHA) than the MS (111.69 TCHA) and LS (101.97 TCHA) harvests (Figure 1A). However, due to the larger cane yield decline rate of the ES harvest (-3.33 TCHA) than that of the MS (-1.98 TCHA) and LS (-2.30 TCHA) harvests, the MS harvests had a larger cane yield than the ES harvests after the fifth ratoon crop. The larger cane yield decline for the ES and LS harvests, compared to the MS harvests, is largely attributed to soil compaction, as harvesting occurs during the rainy period in these two seasons. ES harvesting happens during the autumn rains, a period which normally follows the heavy summer rains, while LS harvesting occurs at the start of spring/summer rains. As a result, the harvesting machinery cause soil compaction, while being driven through the wet fields during these seasons. Previous studies (Humbert, 1959; van Antwerpen *et al*., 2000; Kingston, 2003; Meyer & van Antwerpen, 2010) have also reported a significant yield decline from soil compaction due to heavy machinery traversing wet fields during harvesting. To counter the effects of soil compaction on fields harvested in the ES and LS, several suggestions have been made. These include the following: controlled infield-traffic (Taylor, 1983); the development of tyres and wheel axles that are configured to minimise compaction (van Antwerpen *et al*., 2000); wider inter-row spacing, with tramline rows to keep the tractor wheels in-between the rows (Meyer & van Antwerpen, 2010); as well as inter-row cultivation and subsoiling/ripping (Ricaud, 1977; Ricaud & Arceneaux, 1986; van Antwerpen & Stranack, 2021).

On the other hand, MS harvesting occurs during the driest period of the year (July to September), hence the low effects of soil compaction. These dry conditions help the harvesting and milling operations to proceed seamlessly, which leads to higher efficiency and minimal soil compaction on the sugarcane fields. Sugarcane is a perennial crop; hence, gaining an understanding of the effect of harvest season on the performance of ratoon crops is crucial, if economically-rewarding yields are to be sustained over the longer cycles. Furthermore, this knowledge is critical for making informed decisions aimed at optimising cane supply to the mills, as well as the mill operations. Growers and millers are therefore strongly encouraged to maximise milling capacity during the MS period, in order to reduce cane volumes crushed during the unfavourable periods.

The LS harvests produced a consistently lower TCHA than those of the other seasons, across the eight crops. This is largely due to the occurrence of favourable conditions (i.e. high temperature, radiation and water availability) for vegetative growth of sugarcane when the crop is still young (i.e. the establishment stage); hence, it cannot utilise these climatic resources effectively and efficiently. For the ES and MS harvests, the stalk elongation period (which is an important cane-growing phase that determines yield) occurs when these conditions are favourable for cane growth. The period of stalk elongation for the LS harvests coincides with the time when these conditions are unfavourable (i.e. at their lowest). Low temperatures are known to slow down photosynthesis, thereby reducing stalk elongation and eventually also the cane yield (Zhou & Shoko, 2011). Moreover, van Heerden *et al*. (2010) reported the 'reduced spring growth' phenomenon, which is the inability of sugarcane harvested in the LS to resume normal growth, even when the favourable conditions are restored following reduced growth initiated by low temperatures in winter.

The MS harvests produced a consistently higher sucrose yield (intercept: 16.57 TSHA; slope: -0.26 TSHA) than the ES (intercept: 16.12 TSHA; slope: -0.33 TSHA) and LS (intercept: 14.27 TSHA; slope: -0.32 TSHA) harvests across the eight crops (Figure 1B). This is largely attributed to the fact that the MS harvests benefit from both the favourable summer conditions, which favour vegetative growth, and the winter conditions, which promote natural cane ripening (di Bella *et al*., 2009). This therefore emphasises the importance of ensuring that more cane is milled in the MS than during the ES and LS, since it is the time when both the growers and millers can realise a higher return on their investment.

Figures 2A and 2B show that the WDr and MDr soils had consistently higher cane and sucrose yields than the PDr soils across ratoon crops. For the cane yield, WDr soils had an intercept of 117.76 TCHA and a slope of -2.43 TCHA, MDr soils had an intercept of 113.65 TCHA and a slope of -2.30 TCHA, while PDr soils had an intercept of 100.89 TCHA and a slope of -2.92 TCHA. For the sucrose yield, WDr soils had an intercept of 16.24 TSHA and a slope of -0.25 TSHA, MDr soils had an intercept of 16.08 TSHA and a slope of -0.28 TSHA, while PDr soils had an intercept of 14.65 TSHA and a slope of -0.38 TSHA. These results emphasise the effects of the soils' hydraulic properties on yield. PDr soils have a shorter profitable crop cycle than WDr and MDr soils, due to the low yields associated with the larger declines across ratoon crops. Other studies (Chapman *et al*., 1992; Henry & Ellis, 1996; Kingston, 2003) have reported a larger yield decline rate for PDr soils than for WDr and MDr soils. Hence, more attention needs to be directed towards improving the productivity of PDr soils, rather than that of the other soil types. PDr soils are characterised by prolonged waterlogging, which often leads to salinity and sodicity problems. Subjecting sugarcane plants to waterlogged conditions reduces their growth and increases plant mortality (McDonald *et al*., 1999). In addition, the accumulation of salts in the root zone because of poor drainage limits the growth and development of roots (Hurney & Schroeder, 2013). To improve productivity or resuscitate PDr soils, the following practices have been suggested: the installation of subsurface drainage pipes; the application of gypsum [calcium sulphate] (Henry & Ellis, 1996); improved irrigation practices (Nixon & Simmonds, 2004); as well as fallowing and green manuring (Nixon, 1992).

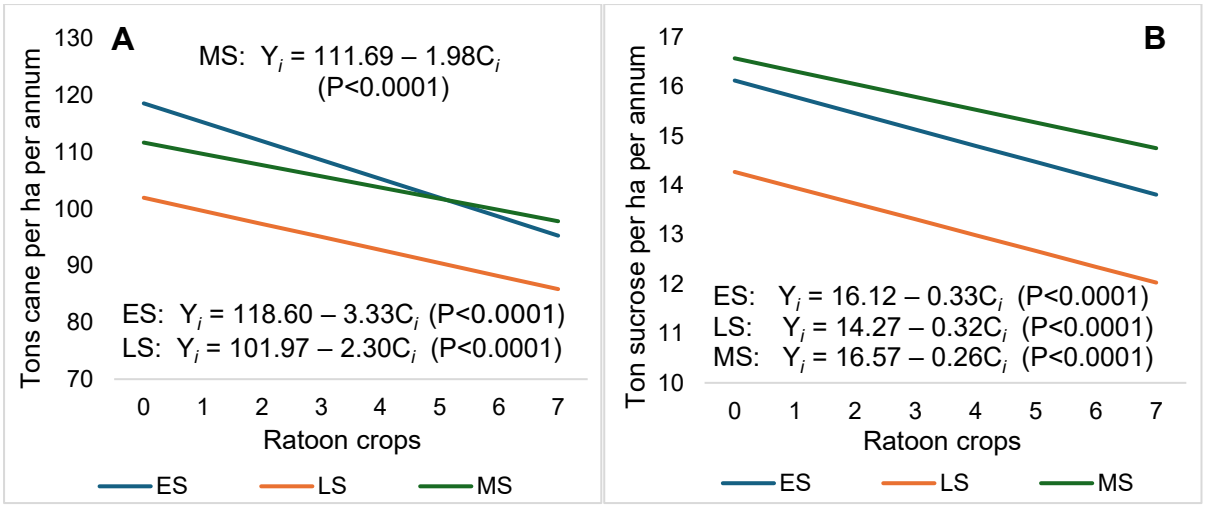


Figure 1. Predicted cane (A) and sucrose (B) yields of sugarcane grown in three different harvest seasons as a function of ratoon crop numbers. (ES: early-season harvest; LS: late-season harvest; MS: mid-season harvest; 0: plant crop; 1 to 7: first to seventh ratoon crops). Y_i is the estimated yield at the *i*th ratoon crop (*i* = 0, 1, 2 … 7), and C_i is the *i*th ratoon crop

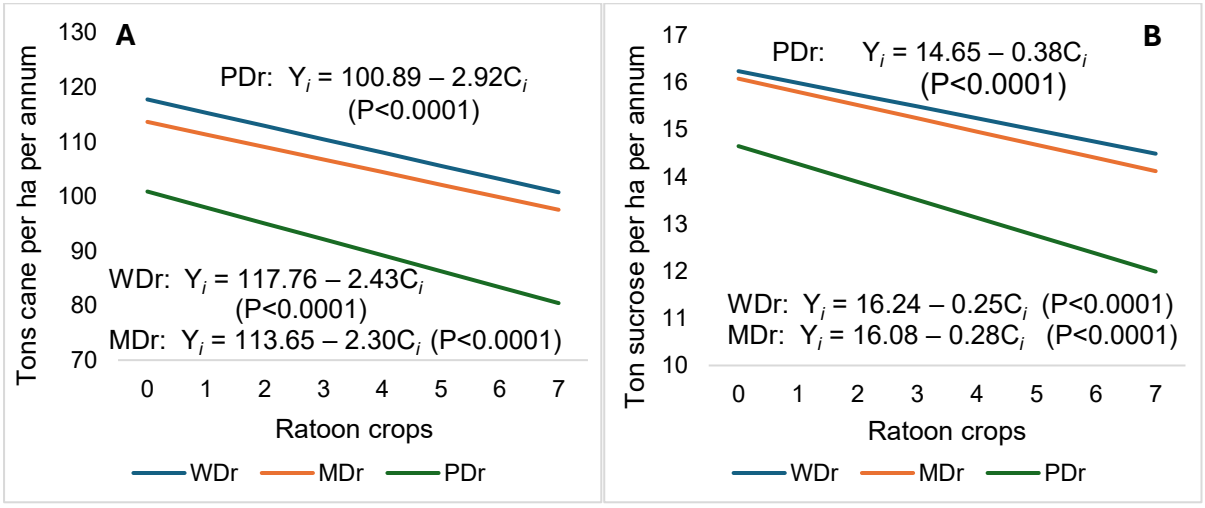
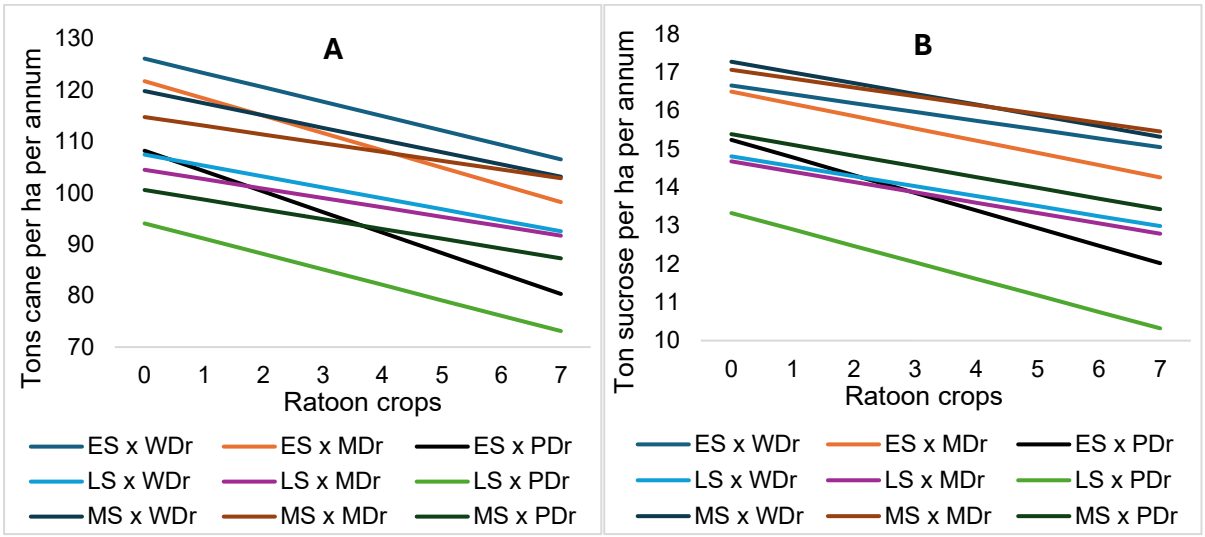


Figure 2. Predicted cane (A) and sucrose (B) yields of sugarcane grown at three different soil types as a function of the ratoon crop numbers. (WDr: well-drained soil; MDr: moderately-drained soil; PDr: poorly-drained soil; 0: plant crop; 1 to 7: first to seventh ratoon crops). Y_i is the estimated yield at the *i*th ratoon crop (*i* = 0, 1, 2 … 7), and C_i is the *i*th ratoon crop

Figure 3 shows that the environments (season x soil type) were separated into three distinct mega-environments for both cane (Figure 3A) and sucrose (Figure 3B) yields. Within each mega-environment, the environments had different intercepts and slopes, which suggests the complexity that is associated with the sugarcane yield. The first mega-environment, which was comprised of the top-four cane and sucrose yield-producing environments across the ratoon crops, were ES x WDr, MS x WDr, ES x MDr and MS x MDr. In this mega-environment, the ES x MDr environment had the largest cane (-3.36 TCHA) and sucrose (-0.32 TSHA) yield decline. The second mega-environment which consisted of environments with average yields, and they were MS x PDr, ES x PDr, LS x MDr and LS x WDr. In the second mega-environment, the ES x PDr environment had the largest cane (-3.98 TCHA) and sucrose (-0.46 TSHA) yield decline. The third mega-environment was comprised of one environment, LS x PDr, which was

consistently the lowest in both cane and sucrose yields across ratoon crops. These mega-environments can be broadly classified as high-yield potential (first mega-environment), moderate-yield potential (second mega-environment) and low-yield potential (third mega-environment). Therefore, sugarcane varieties and other crop husbandry practices can be adopted and tailor-made to maximise production for each mega-environment.



ES x WDr: $Y_i = 126.11 – 2.80C_i$ (P<0.0001)	ES x WDr: $Y_i = 16.66 – 0.23C_i$ (P=0.0002)
ES x MDr: $Y_i = 121.72 – 3.36C_i$ (P<0.0001)	ES x MDr: $Y_i = 16.50 – 0.32C_i$ P<0.0001)
ES x PDr: $Y_i = 108.19 – 3.98C_i$ (P<0.0001)	ES x PDr: $Y_i = 15.24 – 0.46C_i$ (P<0.0001)
LS x WDr: $Y_i = 107.44 – 2.13C_i$ (P<0.0001)	LS x WDr: $Y_i = 14.81 – 0.26C_i$ (P<0.0001)
LS x MDr: $Y_i = 104.48 – 1.83C_i$ (P<0.0001)	LS x MDr: $Y_i = 14.68 – 0.27C_i$ (P<0.0001)
LS x PDr: $Y_i = 94.05 – 2.99C_i$ (P<0.0001)	LS x PDr: $Y_i = 13.33 – 0.43C_i$ (P<0.0001)
MS x WDr: $Y_i = 119.80 – 2.38C_i$ (P<0.0001)	MS x WDr: $Y_i = 17.28 – 0.28C_i$ (P<0.0001)
MS x MDr: $Y_i = 114.74 – 1.70C_i$ (P<0.0001)	MS x MDr: $Y_i = 17.07 – 0.23C_i$ (P<0.0001)
MS x PDr: $Y_i = 100.56 – 1.90C_i$ (P<0.0001)	MS x PDr: $Y_i = 15.39 – 0.28C_i$ (P<0.0001)

Figure 3. Predicted cane (A) and sucrose (B) yields of sugarcane-growing environments (harvest season x soil type) as a function of the ratoon crop numbers. (ES x WDr: early-season harvest x well-drained soil; ES x MDr: early-season harvest x moderately-drained soil; ES x PDr: early-season harvest x poorly-drained soil; LS x WDr: late-season harvest x well-drained soil; LS x MDr: late-season harvest x moderately-drained soil; LS x PDr: late-season harvest x poorly-drained soil; MS x WDr: mid-season harvest x well-drained soil; MS x MDr: mid-season harvest x moderately-drained soil; MS x PDr: mid-season harvest x poorly-drained soil). Y_i is the estimated yield at the *i*th ratoon crop (i = 0, 1, 2 … 7), and C_i is the *i*th ratoon crop

Conclusion

This study indicated that the harvest season and soil type significantly affect sugarcane yields across ratoon crops, which emphasises the importance of taking these factors into consideration when making farm plans. The segregation of the nine sugarcane-growing environments into three mega-environments (yielding abilities) presented an opportunity to adapt agricultural practices suited to each mega-environment, to optimise the use of production resources and to enhance farm yields and profitability.

References

Chapman LS, Ferraris R and Ludlow MM (1992). Ratooning ability of cane varieties: variation in yield and yield components. *Proc ASSCT* 14: 130-138.

Di Bella LP, Stringer JK, Wood AW, Royle AR and Holzberger GP (2009). What impact does time of harvest have on sugarcane crops in the Herbert River district (in Australia)? *Sugar Cane Int* 27(4): 143-148.

Donaldson RA, Redshaw KA, Rhodes R and van Antwerpen R (2008). Season effects on productivity of some commercial South African sugarcane cultivars, I: Biomass and radiation use efficiency. *Proc S Afr Sug Technol Ass* 81: 517-527.

Henry PC and Ellis RD (1996). Soil as a factor in sugarcane ratoon yield decline on an irrigated estate in Swaziland. *Proc ISSCT* 22(2): 84-91.

Humbert, RP (1959). Soil as a factor in varietal yield decline. *Proc ISSCT* 10: 51-62.

Hurney, AP and Schroeder BL (2013). Does prolonged green cane trash retention influence nitrogen requirements of the sugarcane crop in the wet tropics? *Int Sugar J* 115(1371): 212-218.

Kingston G (2003). Ratooning and ratoon management in overseas cane-sugar industries. Final report – SRDC project BSS110. Bureau of Sugar Experiment Stations, Australia.

McDonald L, Wood A and Muchow R (1999). A review of the effect of the harvest time on sugarcane productivity. *Proc ASSCT* 21: 177-184.

Meyer JH and van Antwerpen R (2010). Advances in sugarcane soil fertility research in southern Africa. *S Afr J Plant Soil* 27(1): 19-31.

Nixon DJ (1992). The impact of fallowing and green manuring on properties and the productivity of sugarcane in Swaziland. Doctoral dissertation, University of Reading, United Kingdom.

Nixon DJ, Workman M and Glendinning PJ (1986). Soil and land classification in Swaziland. *Proc S Afr Sug Technol Ass* 60: 219-222.

Nixon DJ and Simmonds LP (2004). The impact of fallowing and green manuring on soil conditions and the growth of sugarcane. *Exp Agric* 40 (1): 127-138.

Ricaud R (1977). Effect of subsoiling on soil compaction and yield of sugarcane. *Proc ISSCT* 16:1039-1048.

Ricaud R and Arceneaux A (1986). Some factors affecting ratoon cane yield and longevity in Louisiana. *Proc ISSCT* 19: 18-24.

Taylor JH (1983). Benefits of permanent traffic lanes in a controlled-traffic crop production system. *Soil Tillage Res* 3: 385-395.

Van Antwerpen R, Meyer J and Meyer E (2000). Soil compaction in the South African sugar industry - a review. *Proc S Afr Sug Technol Ass* 74: 101-108.

Van Antwerpen R and Stranack RA (2021). Soil conservation practices used in the South African sugarcane industry over the past 80 years – a review. *Proc S Afr Sug Technol Ass* 93: 172-186.

Van Heerden PDR, Donaldson RA, Watt DA and Singels A (2010). Biomass accumulation in sugarcane: unravelling the factors underpinning reduced growth phenomena. *J Exp Bot* 61 (11): 2877-2887.

Zhou MM and Shoko MD (2011) Seasonal and varietal effects on tiller population development of sugarcane (*Saccharum officinarum* L.). *S Afr J Plant Soil* 28(1): 11-16.

FULL PAPER

RISING GROUNDWATER LEVELS IN SUGARCANE FIELDS AND THEIR IMPACT ON IRRIGATION WATER MANAGEMENT

Mabaya G[1], Nkala P[2] and Gumindoga W[3]

[1]*Zimbabwe Sugar Association Experiment Station, Chiredzi, Zimbabwe*
[2]*Bindura University of Science Education, Bindura, Zimbabwe*
[3]*University of Zimbabwe, Harare, Zimbabwe*

gmabaya@zsaes.org.zw, prospernkala001@gmail.com, w.gumindoga@eng.uz.ac.zw

Abstract

This study investigated the impact of elevated groundwater levels on water management in irrigated sugarcane agriculture. We examined the variations in Effective Rooting Depths (ERDs) affected by increased groundwater levels and their implications for irrigation scheduling. We measured the groundwater levels, ERDs and Total Available Moisture (TAM) in 31 sugarcane fields at the Zimbabwe Sugar Association Experiment Station. An analysis indicated that 55% of the fields had water table depths of less than 1 m from the soil surface, with furrow-irrigated fields being significantly impacted, where 69% showed shallow water tables under 1 m. We found that the ERD values were 13% lower than the current irrigation scheduling assumptions. This therefore implies that a reduction in irrigation application depths and an increase in irrigation frequency is required. More than 80% of Zimbabwe's 50 000 ha of sugarcane irrigation depends on furrow irrigation systems, which has revealed considerable challenges across the industry. The consistent monitoring of the groundwater levels and measuring the ERDs during plough-outs is crucial for adjusting the irrigation schedules and sustaining crop productivity. We recommend, at the design stage, careful system selection and the matching of irrigation application depths to specific soil properties, along with the implementation of subsurface drainage systems, particularly for furrow-irrigated fields, in order to enhance the plant water-use efficiency and to increase the overall sugarcane yields.

Keywords: Groundwater levels, irrigation scheduling, effective rooting depth, sugarcane cultivation, Zimbabwe

Introduction

Rising groundwater levels in agricultural fields have become a global concern, with profound implications for crop production, particularly in sugarcane farming. In the Indo-Gangetic Plains of India, elevated water tables have led to waterlogging and declining yields in the sugarcane and rice systems (Sanghera & Jamwal, 2019). Similar challenges have been reported in Brazil's São Paulo region, where shallow rooting, due to high water tables, has reduced the plant nutrient uptake and compromised sugar recovery (Monteiro & Sentelhas, 2014). Sugarcane is a high-water-demand crop, and fluctuations in the water table influence its Effective Rooting Depth (ERD) and Total Available Moisture (TAM), both of which are critical for irrigation scheduling and overall crop productivity (Singh *et al*., 2021). The increasing prevalence of high groundwater levels is attributed to multiple factors, including the changing weather patterns, such as floods, intense storms and poor irrigation management, as well as an inadequate drainage infrastructure (Pathak & Sinha, 2019). These factors contribute to waterlogging, soil saturation and reduced ERD and TAM, which ultimately affect the plant health and yield potential.

ERD plays a crucial role in determining the ability of sugarcane to access water and nutrients from the soil, in both irrigated and rainfed systems. When the groundwater levels rise

excessively, the ERD is restricted, which limits the water and nutrient uptake and reduces plant resilience (Moyo & Mashonjowa, 2021). The reduction in ERD directly affects the TAM. Prolonged exposure to elevated groundwater levels can limit the ERD, reducing the volume of soil accessible for water uptake (Nyamugafata *et al*., 2022). Research has shown that reductions in the ERD weaken the plant structures, reduce crop resilience and contribute to yield losses of up to 30% in severely affected areas (SRI, 2021).

Globally, rising groundwater levels have been linked to declining sugarcane yields. In India, over 60% of sugarcane-growing areas - approximately 2.3 million hectares - experience waterlogging due to elevated groundwater levels, which exacerbates the production challenges (Ministry of Agriculture, India, 2022). Similarly, in Brazil, 15-20% of sugarcane fields are affected by the rising water tables, which has led to a 30% reduction in yields (SRI, 2021). In South Africa, the water table has risen by 1-2 m over the past decade, and it has impacted 25% of sugarcane fields in KwaZulu-Natal (AgriSA, 2023). Elevated groundwater levels in sugarcane fields also exacerbate the soil salinity through capillary rise, which transports dissolved salts from the saline groundwater into the root zone as the surface moisture evaporates, thereby impairing the plant growth and reducing the yield potential (Corwin *et al*., 2017; Monteiro & Sentelhas, 2014). While the extent of the issue in Zimbabwe has yet to be quantified, sugarcane farmers are already reporting increased salinity concerns, which may be associated with the persistently high groundwater levels.

Zimbabwe's sugarcane sector covers approximately 50 000 hectares, with furrow irrigation being the dominant method of water application (Mabveni *et al*., 2024). Given the increasing prevalence of high groundwater levels in Zimbabwean sugarcane fields, this study investigates their impact on the irrigation water management practices. Specifically, the study aims to assess the effect of the rising water tables on ERD, to evaluate the resulting reduction in TAM and to analyse how these changes influence the irrigation cycle frequency. In addition, it explores strategies for optimising agricultural water management in sugarcane fields that are affected by rising groundwater levels. The findings of this study will provide valuable insights for policymakers, farmers and agricultural water management professionals in mitigating the negative effects of groundwater fluctuations on sugarcane production.

Methods and Materials

Description of study area

The study was conducted at the Zimbabwe Sugar Association Experiment Station (ZSAES) in Chiredzi, which is located in the south-eastern Lowveld of Zimbabwe. This study site falls within Natural Region V, Zimbabwe's driest agro-ecological zone, which is characterised by semi-arid to arid climatic conditions. Annual rainfall varies between 300 and 600 mm, with high variability and frequent droughts. Temperature extremes are common, with summer temperatures exceeding 35°C, whereas winters remain relatively mild. Despite these harsh conditions, year-round sugarcane cultivation is sustained through irrigation-based agriculture.

Sugarcane is the primary crop grown. It is rotated at plough-out with sugar beans, soybeans, and sun hemp as break crops, to enhance the soil fertility and reduce the pest build-up. The fields are managed under different irrigation systems, with the hectare distribution being as follows: traditional furrow irrigation with open channel feeder canals: 40 ha; improved furrow irrigation supplied with lay-flat pipes: 15 ha; centre-pivot irrigation: 4 ha; and semi-portable sprinkler irrigation: 10 ha. The total area under sugarcane cultivation at ZSAES is 68 hectares, which is comprised of 36 irrigated fields. As shown in Figure 1, 31 fields were selected for groundwater measurements and Effective Rooting Depth (ERD) assessments.



Figure 1. ZSAES fields where groundwater fluctuations were investigated

Groundwater level measurement

In order to evaluate the impact of the rising water tables on sugarcane production, the groundwater levels were systematically monitored across 31 field locations, using observation pits. These pits were excavated immediately after the harvesting of sugarcane in fields that had undergone a dry-off period exceeding three weeks. To ensure comprehensive spatial coverage, three pits were strategically dug along a diagonal transect in each field, with each pit measuring 1 m in length, 1 m in width and 1.2 m in depth.

In south-eastern Zimbabwe, the Effective Root Depth (ERD) of sugarcane in optimal soil conditions typically ranges between 1.0 m and 1.5 m (Mabveni *et al*., 2024). In instances where the excavation process encountered an impermeable layer, such as parent rock, before reaching the intended depth of 1.0 m, further digging was discontinued, and the depth of the restrictive layer was recorded. To enhance the accuracy of the groundwater level assessments, the excavation sites were carefully selected, to avoid atypical areas, such as anthills and isolated gravel patches.

The groundwater levels were determined through direct field measurements that were conducted during pit excavation. In fields where groundwater seepage or saturated soil conditions were observed at depths shallower than 1.0 m, the excavation was halted, and the depth at which water was encountered was recorded as the water table level. Conversely, in fields where no groundwater was detected up to the maximum excavation depth, the groundwater level was classified as being greater than 1.2 m. In each case, the recorded groundwater level was considered to be representative of the entire field.

Spatial groundwater mapping

Groundwater level mapping in QGIS commenced with systematic data collection, wherein field measurements of the groundwater levels were obtained from direct observations at the designated field locations. To ensure spatial accuracy, each measurement was georeferenced by using GPS coordinates. The collected data were subsequently imported into QGIS as a point shapefile, or a CSV file, incorporating key attributes such as elevation and the water table depth.

To generate a continuous groundwater level surface, an appropriate spatial interpolation technique, known as Inverse Distance Weighting (IDW), was applied using the 'Interpolation' tool. This process facilitated the estimation of groundwater levels across unsampled areas by leveraging the spatial correlation of the observed data points. The resulting raster dataset was then visualised by using classified symbology, namely, employing a colour gradient to depict the groundwater level variations, thereby enhancing its interpretability.

Finally, the map was refined and formatted for presentation by using the 'Print Layout' tool, which ensured the inclusion of essential cartographic elements, such as a legend, north arrow, scale bar and coordinate grid. These elements contributed to the map's readability and scientific accuracy, which facilitated the effective spatial analysis and interpretation of groundwater distribution.

Effective Rooting Depth (ERD) determination

The same field observation pits that were used to observe the water table depths after the sugarcane harvest were used to determine the Effective Rooting Depth (ERD). ERDs were assessed within measured unsaturated soil depths by using a targeted soil coring approach. Soil samples were taken by using an auger at intervals of 0.2 m within each pit, from the surface down to where the roots stopped growing. The root density and penetration were evaluated through manual root assessments, which enabled the identification of the depth at which the root activity had significantly declined. Although the exact number of roots, such as the root length or biomass density, was not measured, the study visually checked for root activity to confirm that roots were present, and the decline was defined as the depth where fewer than 10% of roots were found in all samples taken from the field. This approach was aligned with the agronomic understanding that 85%-90% of sugarcane roots are typically concentrated in the ERD (Nzima *et al*., 2022). A favourable estimate of ERD in the south-eastern Lowveld of Zimbabwe is 1.0 m (Nzima *et al.,* 2022). If elevated groundwater or an obstruction of hard rock or sudden increase/decrease in clay content occurs within this depth, then the ERD was measured to the depth of the obstruction. The authors recognise that obstructions can also happen because of soil compaction, salinity or aluminium toxicity (Nzima *et al*., 2022), but this study only focused on the obstructions caused by high groundwater levels, hard rock and a sudden, noticeable increase in the clay content. It is acknowledged that this lack of comprehensive soil constraint analysis is a limitation of the study, as it may underestimate the influence of non-hydrological root barriers.

The newly determined ERDs for each field were analysed to ascertain whether they exceeded the 1.0 m agronomic threshold that is typically applied in local irrigation scheduling practices, which represents the minimum ERD required for optimal sugarcane growth in well-structured soils (Nzima *et al*., 2022). The measured ERD values were then compared to typical irrigation scheduling expectations to see how much the ERD was reduced by, due to the higher groundwater levels. This comparison gave important clues about the potential impact of fluctuating water table depths on root development and crop productivity (Moyo & Mashonjowa, 2021).

Computation of new Total Available Moisture (TAM) values

The relationship between Total Available Moisture (TAM) and Effective Rooting Depth (ERD) was analysed to evaluate the impact of the rising groundwater levels on the sugarcane irrigation requirements. The $TAM_{existing}$ was calculated using the formula:

$$\mathrm{TAM}_{\mathrm{existing}} = (\mathrm{FC} - \mathrm{PWP}) \times \mathrm{ERD} \qquad (1)$$

where FC represents the Field Capacity, and PWP denotes the Permanent Wilting Point. The assumption of the study is that the available moisture content (FC-PWP), which is closely

related to soil type characteristics, such as the soil structure, soil texture, clay percentage and organic matter content, has remained unchanged over the 20-year period, thus not affecting the soil's water-holding capacity. During the initial TAM assessment 20 years ago, $TAM_{existing}$ values were determined when the ERD values across all fields was 1.0 m. However, with the newly observed ERD values, corrected TAM values were computed in proportion to the changes in the ERD. The revised TAM for each field was determined by using the following equation:

$$\mathrm{TAM}_{\mathrm{corrected}} = \mathrm{TAM}_{\mathrm{existing}} \times \frac{\mathrm{ERD}}{1.0} \qquad (2)$$

This approach ensures that variations in the ERD, influenced by fluctuations in the groundwater levels, are accurately reflected in the revised total moisture availability estimates for effective irrigation planning.

Irrigation scheduling analysis

The impact of rising groundwater levels on irrigation management was assessed by evaluating the irrigation depth and frequency across 31 fields, using measured Effective Rooting Depths (ERDs) and corrected Total Available Moisture values ($TAM_{corrected}$). In Zimbabwe, surface and sprinkler irrigation schemes for sugarcane production are typically irrigation scheduled at 50% depletion of the total available moisture. Accordingly, the existing and corrected net irrigation depths (D_{net}) were computed as 50% of $TAM_{existing}$ and $TAM_{corrected}$. The Irrigation Frequency (IF) was determined by using peak crop evapotranspiration (Peak ET_{crop}), which occurs in November at full canopy. With an average reference evapotranspiration (ET_o) of 10 mm/day and a full crop coefficient (K_c) of 0.9, the peak ET_{crop} was fixed at 9 mm/day. The IF was then calculated for both the existing and corrected scenarios as:

$$IF = \frac{\mathrm{Dnet}}{\mathrm{Peak\ ETcrop}} \qquad (3)$$

The comparison between the corrected and existing irrigation schedules at peak revealed the extent to which groundwater fluctuations influence irrigation practices, which provided insights into optimising the water use efficiency and maintaining ideal soil moisture conditions for sugarcane production.

Results

Groundwater map of sugarcane fields

The groundwater mapping of sugarcane fields at ZSAES, as shown in Figure 2, highlights significant spatial variations in the water table depths, which are primarily influenced by the irrigation method that is used. Although other factors, like the soil type and topography, could affect the groundwater levels, they were assumed to have no significant influence on the study area. Overhead-irrigated fields generally exhibit deeper water tables (1.0-1.2 m); these are indicated by the green zones on the map, which suggests that there is a more controlled infiltration rate that prevents an excessive rise in the groundwater. In contrast, furrow-irrigated fields display shallower water tables (<1.0 m, the red and orange zones), which are likely due to higher deep percolation losses along the furrows and inadequate drainage, which leads to localised groundwater accumulation. All furrow-irrigated fields with subsurface drainage systems show moderate water table depths (0.90-1.0 m), which means that these drainage systems are important for managing changes in the groundwater levels.

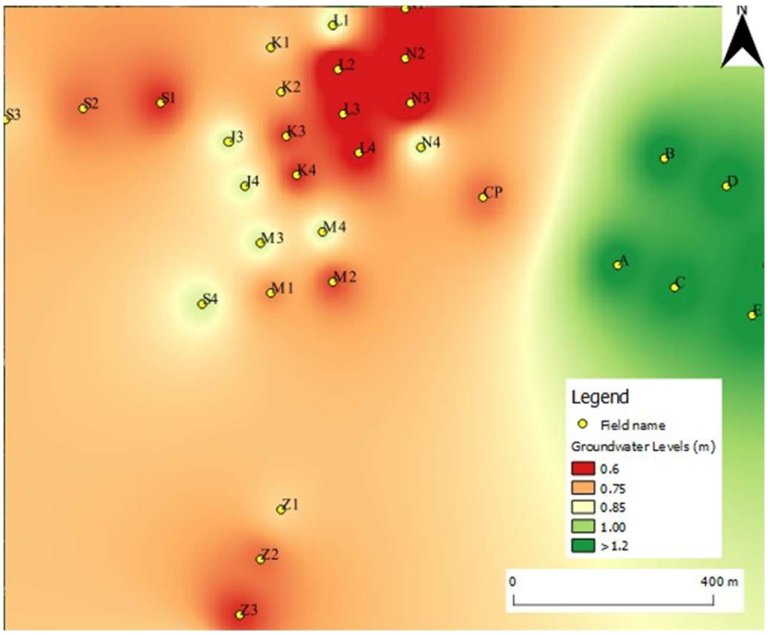


Figure 2. Spatial groundwater map of ZSAES sugarcane fields

Effective Rooting Depths (ERD)

The measured ERD of sugarcane fields at ZSAES exhibit significant variability, as shown in Figure 3. Notably, 55% of the fields fall below the ZSAES-recommended agronomic ERD threshold of 1.0 m (Mabveni *et al.*, 2024). Fields that meet or exceed this threshold (≥1.0 m) are predominantly located in areas with deeper groundwater tables. In contrast, fields with ERDs of less than 1.0 m indicate restricted root development, due to the elevated water tables. Shallow rooting limits the crop's ability to extract irrigation water from the soil profile, and this results in the excess water percolating beyond the root zone. This downward movement contributes to a further rise in the water table, which, in turn, exacerbates the root zone saturation and inhibits further root penetration, which creates a self-reinforcing feedback loop.

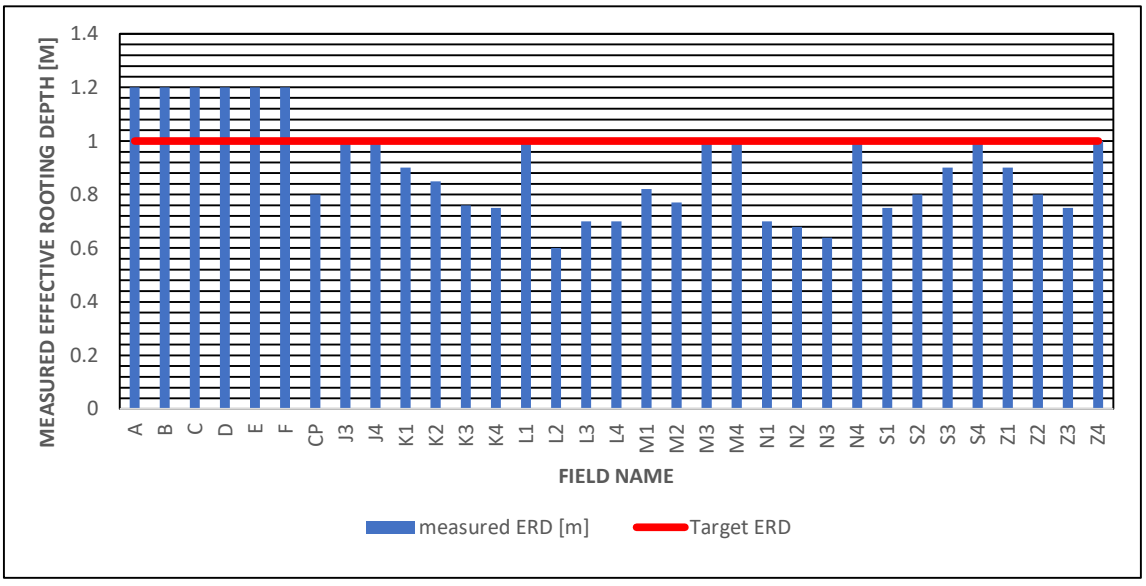


Figure 3. Measured effective rooting depths of ZSAES fields

Effect of reduced ERDs on the Total Available Moisture (TAM)

The measured Effective Rooting Depths (ERD) directly influenced the Total Available Moisture (TAM) in sugarcane fields, as shown in Figure 4, as shallower root systems reduce the crop's access to soil water. The results indicate that 55% of fields experienced a 13% reduction in TAM, with the most significant declines observed in furrow-irrigated fields.

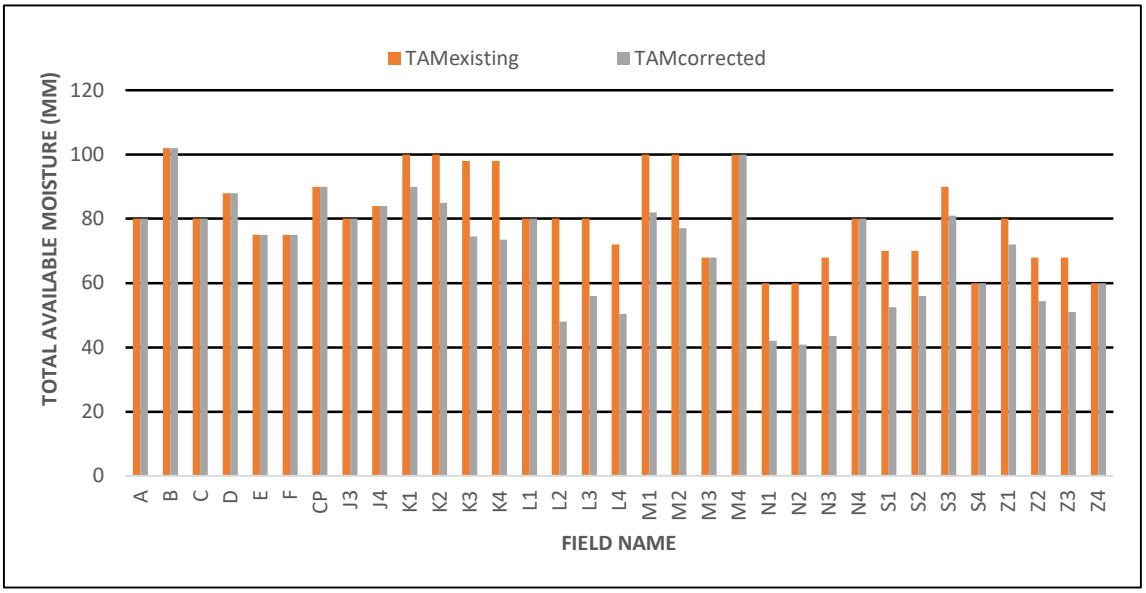


Figure 4. Existing TAM values ($TAM_{existing}$) previously used for irrigation scheduling and corrected TAM values ($TAM_{corrected}$) of ZSAES fields

Influence of TAM reductions on the irrigation water management of the sugarcane crop

A summary of the existing and corrected irrigation schedules at peak crop evapotranspiration (Peak ET_{crop}) across 31 sugarcane fields at ZSAES, under varying irrigation systems, including semi-portable sprinklers ($sprinkler_{s-p}$), centre pivot, open channel furrow ($Furrow_{_oc}$), open channel furrow with subsurface drainage ($Furrow_{_oc+ssd}$) and furrow irrigation supplied with lay-flat pipes ($Furrow_{_LF}$) is shown in Table 1.

Sprinkler and centre-pivot systems showed no changes in their net application depth (Dnet) and Irrigation Frequency (IF), which indicated consistent root zone conditions. In contrast, 69% of furrow-irrigated fields have notable reductions in Dnet and a shortened IF, due to TAM reductions. However, fields with furrow systems incorporating subsurface drainage systems (like J4, M4, N4) retained a stable Dnet and IF, which highlights the importance of maintaining the water table levels in sugarcane fields below the root zone depths. Overall, the findings indicated that furrow-irrigated fields with no subsurface drainage are more prone to shallow rooting and that they require smaller irrigation applications more frequently to meet the crop water needs and minimise the loss of water. Current irrigation practices, based on the $TAM_{existing}$ values, have led to continuous over-irrigation, which has contributed to the rising groundwater levels. Adjusting irrigation schedules to reflect the $TAM_{corrected}$ values would lead to a reduction in irrigation application depth and shorter irrigation intervals, to compensate for the lower soil volumes resulting from the reduced ERDs, due to the shallow water tables.

Table 1. Existing and corrected irrigation schedules at peak crop evapotranspiration (Peak ET_{crop}) in terms of the net application depth (D_{net}), and irrigation frequency (IF) across study fields with different irrigation types at ZSAES

Field Name	Irrigation type	TAM [mm]		Peak ETcrop [mm/day]	Dnet [mm]		Peak IF [days]	
		Existing	Corrected		Existing	Corrected	Existing	Corrected
A	$Sprinkler_{s-p}$	80	80	9	40	40	4	4
B	$Sprinkler_{s-p}$	102	102	9	55	55	6	6
C	$Sprinkler_{s-p}$	80	80	9	40	40	4	4
D	$Sprinkler_{s-p}$	88	88	9	44	44	5	5
E	$Sprinkler_{s-p}$	75	75	9	38	38	4	4
F	$Sprinkler_{s-p}$	75	75	9	38	38	4	4
CP	Centre-pivot	90	90	9	45	45	5	5
J3	Furrow_oc+ssd	80	80	9	40	40	4	4
J4	Furrow_oc+ssd	84	84	9	42	42	5	5
K1	Furrow_oc	100	90	9	50	45	6	5
K2	Furrow_oc	100	85	9	50	43	6	5
K3	Furrow_oc	98	74	9	49	37	5	4
K4	Furrow_oc	98	74	9	49	37	5	4
L1	Furrow_oc+ssd	80	80	9	40	40	4	4
L2	Furrow_oc	80	48	9	40	24	4	3
L3	Furrow_oc	80	56	9	40	28	4	3
L4	Furrow_oc	72	50	9	36	25	4	3
M1	Furrow_oc	100	82	9	50	41	6	5
M2	Furrow_oc	100	77	9	50	39	6	4
M3	Furrow_oc+ssd	68	68	9	34	34	4	4
M4	Furrow_oc+ssd	100	100	9	50	50	6	6
N1	Furrow_oc	60	42	9	30	21	3	2
N2	Furrow_oc	60	41	9	30	20	3	2
N3	Furrow_oc	68	44	9	34	22	4	2
N4	Furrow_oc+ssd	80	80	9	40	40	4	4
S1	Furrow_oc	70	53	9	35	26	4	3
S2	Furrow_oc	70	56	9	35	28	4	3
S3	Furrow_oc	90	81	9	45	41	5	4
S4	Furrow_oc	60	60	9	30	30	3	3
Z1	$Furrow_{LF}$	80	72	9	40	36	4	3
Z2	$Furrow_{LF}$	68	54	9	34	27	4	3
Z3	$Furrow_{LF}$	68	55	9	34	26	4	3
Z4	$Furrow_{LF}$	60	60	9	30	30	3	3

Discussion

Influence of the irrigation method on groundwater dynamics

Spatial variations in the water table depths across sugarcane fields in the study area were primarily influenced by the irrigation method employed. Maintaining a water table depth of at least 1.0 m is widely regarded as critical for maximising the sugarcane yield and avoiding productivity losses, due to excessive soil moisture (Skaggs *et al*., 1994; Kendy *et al*., 2003).

Overhead irrigated fields exhibited comparatively deeper water tables, whereas furrow-irrigated fields consistently recorded shallower levels. A related study by Nhiwatiwa *et al*. (2017) reported that furrow-irrigated sugarcane fields in Zimbabwe's Lowveld often experience groundwater tables below 1.0 m, primarily due to excessive deep percolation and inadequate drainage, thereby increasing the risk of waterlogging. Similar patterns have been observed in other sugarcane-producing regions, such as Santa Isabel, Puerto Rico, where furrow irrigation contributed significantly to the groundwater recharge, resulting in elevated water tables and increased waterlogging hazards (Hollinger & McHugh, 2010).

Furrow irrigation systems are designed to apply large volumes of water often to the point of soil saturation, to ensure adequate infiltration along the length of the furrows. While effective for field coverage, this practice increases the likelihood of overirrigation and uncontrolled deep percolation losses (University of Nebraska–Lincoln, 2023). Persistently high-water tables pose a significant threat to a crop's performance, as they impair root aeration, reduce yields and promote salinity accumulation in the root zone (Ayers & Westcot, 1985; Singh *et al*., 2020). Poor drainage in furrow-irrigated systems exacerbates these issues even further, by limiting root expansion and reducing the plant's water-use efficiency (Moyo & Mashonjowa, 2021). In contrast, overhead irrigation systems, such as sprinklers and centre-pivots are engineered to deliver smaller, more frequent, applications that are tailored to the soil's water-holding capacity and the crop's evapotranspiration demand. This precision enhances the water use efficiency and minimises water losses through runoff or deep percolation (Chaudhary *et al*., 2023). Furrow-irrigated fields in the study area that were equipped with subsurface drainage systems maintained more stable water table depths, typically around 1.0 m. This highlights the importance of a well-designed subsurface drainage infrastructure, with optimised depth and lateral spacing, for regulating the soil moisture conditions and supporting optimal sugarcane growth (Halbac-Cotoara-Zamfir *et al*., 2022).

These findings underscore the need for an integrated irrigation and drainage approach that not only combines the optimal water application strategies with effective drainage management to maintain groundwater tables within recommended thresholds, but it also emphasises the critical importance of properly-designed furrow irrigation systems, making sure that the application depths are already matched to the soil's drainage capacity in the design stage. Furrow irrigation may be inappropriate in poorly drained soils, or where the soils are unsuited to infrequent large applications.

Future efforts should prioritise the continuous monitoring of water table fluctuations and they should promote the adoption of efficient irrigation systems, such as overhead and drip technologies, to enhance sugarcane productivity, while mitigating the long-term adverse effects of rising groundwater on the soil and water quality by investing in subsurface drainage systems.

The effect of groundwater levels on the ERD and TAM

The Effective Rooting Depth (ERD) of sugarcane fields at ZSAES is greatly limited in areas where the groundwater is high, with more than 55% of fields having ERDs of less than the agronomic threshold of 1.0 m. This limitation truncates the soil water that is accessible to roots, which directly reduces the Total Available Moisture (TAM) and impairs the crop's capacity to buffer against water deficits. The reduced TAM disrupts the soil-plant-atmosphere continuum, which leads to a diminished soil water storage capacity and which, under furrow irrigation systems, results in rapid saturation and deep percolation losses.

Analysis of 31 irrigated fields revealed that TAM has often been overestimated by up to 13%, which leads to systematic overirrigation. This has associated negative outcomes, including an elevated water table, the loss of soil structural integrity and the development of reductive soil conditions (Hodgson & Chan, 1982; Singh *et al*., 2020; du Preez *et al*., 2022). These effects collectively reduce the irrigation efficiency and undermine the long-term health of the soil.

Furrow irrigation, which accounts for approximately 80% of Zimbabwe's irrigated sugarcane fields (FAO, 2020), contributes to spatial and temporal variability in the ERD and TAM, due to the associated over-irrigation and the resultant rise in the water table. Its inflexible and larger application depths frequently exceed the field capacity of shallow-rooted zones, which causes a substantial proportion of the irrigation water to bypass the crop root zone and to recharge the groundwater table. Resende *et al.* (2022) have documented this self-reinforcing hydrological feedback loop, where elevated groundwater levels further suppress the rooting depth. Over time, this cycle intensifies root zone saturation, reduces oxygen diffusion in the rhizosphere, and impairs root respiration and nutrient uptake, thereby suppressing the crop vigour (Meyer & van Antwerpen, 2001; Obade & Lal, 2023).

On the other hand, studies using AquaCrop (Mortel & Madramootoo, 2023) show that increasing the Effective Rooting Depth (ERD) by 10-20% can improve irrigation efficiency by as much as 18%, especially in soils with a fine texture. Deeper rooting not only increases the temporal and spatial buffering capacity of the soil profile, but it also allows for longer irrigation intervals and more precise scheduling. In contrast, shallow ERDs require more frequent applications and intensify the inefficiencies that are inherent in furrow systems, further diminishing the crop's water-use efficiency and reinforcing the cycle of reduced TAM.

The necessity of TAM-corrected irrigation scheduling

The decrease in TAM, caused by shallow ERDs, requires a complete change in how irrigation is scheduled in sugarcane fields, especially those using furrow irrigation. This study found that TAM was overestimated by as much as 13%, which resulted in habitual overirrigation. The consequences include deep percolation, a rising water table, soil oxygen deficits and reduced structural integrity, issues that are well-documented in southern African sugarcane systems (du Preez *et al*., 2022; Obade & Lal, 2023). In this study, 69% of furrow-irrigated fields required adjustments in the net application depth and irrigation frequency when schedules were recalibrated by using corrected TAM values. Fields with subsurface drainage retained stable intervals, which underscores the benefits of controlled water table management (Siyal & Skaggs, 2020). Shallow ERDs reduce the root zone's capacity to store water, necessitating smaller, more frequent applications to maintain optimal soil moisture conditions for plant water uptake (van Genuchten, 1980; Silva *et al*., 2017). Aligning the irrigation depth and frequency with the actual root-accessible profile, as emphasised by Kendy *et al*. (2003) and Obade and Lal (2023), is fundamental for improving water use efficiency, avoiding groundwater rises and promoting resilient sugarcane production.

This configuration is, however, more suited to the overhead and drip irrigation methods. Furrow irrigation, despite its widespread use, is ill-suited to such conditions. Its large and imprecise applications, combined with challenges in measuring the infiltration depth, exacerbate its inefficiencies under reduced TAM scenarios (Raes *et al*., 2021). Water applications often exceed the soil's storage capacity, which leads to runoff, drainage losses and groundwater recharge (Bastos *et al*., 2020; Bąk *et al.,* 2023). A more holistic water-soil management strategy is thus essential. Suggested actions for furrow irrigation systems include setting up subsurface drainage systems to help the roots to grow deeper, breaking up compacted soils and adding organic matter, to improve the soil structure.

Conclusion and Recommendations

The findings from this study highlight the critical impact of furrow irrigation practices on the groundwater levels, Effective Rooting Depths (ERDs) and Total Available Moisture (TAM) in sugarcane fields. The predominance of furrow irrigation has contributed to shallower water tables (<1.0 m), reduced ERDs and a 13% decline in the TAM, which lead to continuous overirrigation, waterlogging and an increased drainage demand. The overestimation of the TAM in irrigation scheduling has exacerbated the groundwater to rise further, which has

negatively affected root development, crop resilience and soil productivity. To address these challenges, it is essential to adjust the irrigation scheduling by using corrected TAM values, which will lead to a reduction in irrigation depth and a corresponding increase in the irrigation frequency, in order to optimise the soil moisture availability and prevent a further groundwater rise. In addition, integrating subsurface drainage, deep tillage and precision irrigation techniques will enhance root penetration, improve the water-use efficiency and mitigate the long-term risks of soil salinity and waterlogging. Future research should focus on continuous groundwater monitoring and adaptive irrigation strategies to develop sustainable water management solutions for Zimbabwe's sugarcane industry, as well as other irrigated agricultural systems that are facing similar groundwater challenges.

Acknowledgements

The authors acknowledge the support of ZSAES and its funding of the research facilities. The authors also thank the ZSAES's Department of Agricultural and Industrial Chemistry for the analysis of samples.

References

AgriSA (2023). Water table rise and its effects on KwaZulu-Natal's sugarcane industry: A decade-long assessment. AgriSA Publications.

Ayers RS and Westcot DW (1985). Water quality for agriculture. FAO Irrigation and Drainage Paper 29 Rev. 1.

Bąk A, Kowalski P and Zieliński J (2023). Biogas plant equity returns in EU countries: A comparative analysis. *Energies* 16(1): 31. https://doi.org/10.3390/en16010031

Bastos FL, Martins DCF and Anjos LHC (2020). Water depths and nitrogen rates on sugarcane growth and biomass accumulation. *Journal of Crop Science* 14(7): 1048-1054.

Chaudhary JN, Li H, Jiang Y, Pan X, Hussain Z, Javaid M and Rizwan M (2023). Advances in sprinkler irrigation: A review in the context of precision irrigation for crop production. *Agronomy* 14(1): 47. https://doi.org/10.3390/agronomy14010047

Corwin DL, Scudiero E, Šimůnek J and Skaggs TH (2017). Soil salinity and hydrology in agricultural landscapes: Assessment, implications, and management. *Science of the Total Environment* 577: 477-490. https://doi.org/10.1016/j.scitotenv.2016.10.110

Du Preez K, Keeping M and Snyman HA (2022). Soil regenerative agriculture in South African sugarcane industry. *South African Sugar Journal* 35: 306-318.

FAO (2020). Irrigation Manual: Planning, development, monitoring and evaluation of irrigated agriculture with farmer participation. Food and Agriculture Organization of the United Nations.

Halbac-Cotoara-Zamfir R, Farias-Ramirez AJ, de Miranda JH, Moreno-Pizani MA, Duarte SN, Paredes-Trejo FJ, Salvati L and Halbac-Cotoara-Zamfir C (2022). Simulation of subsurface drainage in the sugarcane crop under different spacing and drain depths. *Land* 11(5): 626. https://doi.org/10.3390/land11050626

Hodgson AS and Chan KY (1982). The effect of waterlogging on the growth and yield of sugarcane. *Field Crops Research* 5(4): 287-296.

Hollinger SE and McHugh TF (2010). Effects of changes in irrigation practices and aquifer development on groundwater availability in the Santa Isabel area, Puerto Rico. U.S. Geological Survey Scientific Investigations Report 2010–5022. https://pubs.usgs.gov/sir/2010/5022/SIR_2010_5022_Report.pdf

Kendy E, Zhang Y, Liu C and Steenhuis TS (2003). Groundwater table dynamics under different irrigation methods in the North China Plain. *Agricultural Water Management* 60(3): 181-198.

Mabveni ARS, Mutatu W, Chibarabada TP, Zvoutete P and Mabaya G (2024). Zimbabwe Sugarcane Production Manual. Zimbabwe Sugar Association.

Meyer JH and van Antwerpen R (2001). Soil management and sugarcane production. *Proceedings of the South African Sugar Technologists' Association* 75: 185-194.

Ministry of Agriculture, India (2022). Waterlogging in sugarcane fields: Impact and mitigation strategies. Government of India.

Monteiro JEB and Sentelhas PC (2014). Impact of water deficits on sugarcane yields in São Paulo, Brazil. *Irrigation Science* 32(3): 241-252. https://doi.org/10.1007/s00271-014-0434-5

Mortel J and Madramootoo CA (2023). Improving water use efficiency of surface-irrigated sugarcane using AquaCrop in Guyana. *Frontiers in Water* 5: 1278306. https://doi.org/10.3389/frwa.2023.1278306

Moyo P and Mashonjowa E (2021). Influence of groundwater fluctuations on irrigation scheduling in southern Africa's sugarcane industry. *Water Resources Management* 35(5): 1734-1752.

Nhiwatiwa T, Makurira H, Mhizha A and Mhizha S (2017). The impact of irrigation return-flows on groundwater quality and quantity in the Lowveld of Zimbabwe: A case study of Chiredzi sugarcane estates. *Physics and Chemistry of the Earth* 100: 1-9.

Nyamugafata P, Jiri O and Chitata T (2022). Groundwater table dynamics and their impact on sugarcane production in Zimbabwe. *Journal of Agricultural Hydrology* 57(3): 112-130.

Nzima M, Nyati C, Mudima K, Jemwa W and Lecler N (2022). Zimbabwe Sugarcane Irrigation Manual – A practical, science, and knowledge-based guide to efficient irrigation management. Zimbabwe Sugar Association Experiment Station.

Obade VO and Lal R (2023). A standardized soil quality index for diverse field conditions. *Communications in Soil Science and Plant Analysis* 54(16): 2171-2184. https://doi.org/10.1080/00103624.2023.2215062

Pathak H and Sinha S (2019). Root zone water dynamics in sugarcane under varying irrigation and drainage conditions. *Irrigation Science* 37(4): 321-334.

Raes D, Steduto P, Hsiao TC and Fereres E (2021). AquaCrop Reference Manual: Version 7.0. FAO Land and Water Division.

Resende RS, Cintra, F L D, Pacheko, E D, de Amorim J R A, Gomes R S B, da Silva S M(2022). Soil penetration resistance and sugarcane rooting under sub-surface drip irrigation levels. *Sugar Tech* 24: 1237-1245. https://doi.org/10.1007/s12355-022-01186-4

Sanghera GS and Jamwal JK (2019). Waterlogging in sugarcane fields of the Indo-Gangetic Plains causes 15-45% yield and sugar losses. *Journal of Agricultural Science and Technology* 21: 103-110.

Silva MA, Oliveira JB and Coelho EF (2017). Sugarcane yield and soil moisture dynamics under subsurface drainage conditions. *Water Resources Management* 31(10): 3173-3185.

Singh A, Sharma P and Bhardwaj AK (2020). Impact of waterlogging and salinity on sugarcane yield in semi-arid regions. *Irrigation Science* 38(2): 167-179.

Singh K, Sharma P and Patel R (2021). Optimizing water use in sugarcane farming: Strategies for mitigating waterlogging effects. *Sugarcane Research Journal* 48(2): 87-102.

Siyal AA and Skaggs RW (2020). Modelling drainage water salinity in sugarcane fields under different leaching fractions. *Agricultural Water Management* 233: 106058. https://doi.org/10.1016/j.agwat.2020.106058

Skaggs RW, Brevé MA and Gilliam JW (1994). Hydrologic and water quality impacts of agricultural drainage. *Critical Reviews in Environmental Science and Technology* 24(1): 1-32.

Sugarcane Research Institute (SRI) (2021). Impact of rising groundwater levels on sugarcane yield and productivity. SRI Technical Report.

University of Nebraska–Lincoln (2023). Irrigation Management for Furrow Irrigated Corn. UNL Extension Publications. https://extensionpublications.unl.edu/assets/html/g1338/build/g1338.htm

van Genuchten MT (1980). A closed-form equation for predicting the hydraulic conductivity of unsaturated soils. *Soil Science Society of America Journal* 44(5): 892-898.

FULL PAPER

THE HIDDEN COSTS OF OVER-DESIGNING BOILER BACK-END EQUIPMENT

Mienie B[1] and Dauvellier R[1]

[1]Rheinmetall Resonant South Africa 9, Uitzicht Office Park, 1 Bellingham St, Highveld, Pretoria, 0157

barend.mienie@rheinmetall-resonant.com, ronnie.dauvellier@rheinmetall-resonant.com

Abstract

Accurately determining a representative design basis is a critical factor in the engineering and optimisation of process equipment, particularly in the sugar industry. Overestimating key design parameters, without proper testing or a thorough understanding of the actual process conditions, can lead to significant inefficiencies in resource utilisation.

This paper examines the implications of overestimating the design inputs, including the flow rates, pressures, temperatures, particle size distributions., and inlet dust loads, on utility consumption, with a focus on power and water usage in back-end equipment, such as scrubbers. Overestimating flow rates can lead to excessive power and water consumption. Furthermore, overestimating the inlet dust load and particle size distribution requires increased pressure loss across the scrubber throat. Modelling scenarios are analysed to quantify the operational inefficiencies caused by over-design, such as increased energy demands, excessive water usage., and elevated operational costs.

The study assumed a base case of critical design parameters and found that overestimation can lead to a power consumption increase of up to 158% and a 488% increase in the water requirements. The water increase in this study is related to the evaporation losses in the scrubber. Although a constant water flow rate was used across all cases, the actual water demand may rise if the gas volume or temperature is overestimated, to maintain the required liquid/gas ratio. This would necessitate larger pumps and it would increase the power usage further. The findings highlight the value of accurate design inputs in improving equipment efficiency and reducing utility consumption, which aligns with the industry's sustainability goals.

Keywords: Over-design, utility consumption, process testing, sustainable engineering, operational efficiency, boiler back-end equipment, wet scrubbers

Introduction

The sugar industry requires boilers for steam generation, and these boilers might be bagasse-fired only or dual-fired boilers. With dual-fired boilers, bagasse and coal are used as the fuel during steam generation. The burning of these fuels will lead to the generation of particulate matter, which, by law, should be collected in a particulate matter capture device. This paper will focus on wet scrubbers as the chosen particulate matter collection device; in particular, the cyclonic type of wet scrubber.

This paper will present the historical data collected from various sources, which were used to calculate the requirements to achieve the regulatory emission levels. In this case, the outlet particulate emission was designed to 50 mg/Nm^3. This paper investigates the effect of varying

input parameters on the design of wet scrubbers, and it specifically examines their influence on the equipment sizing, power requirements and system efficiency.

Improving the accuracy of the design basis will lead to a reduction in capital cost, as well as the operational utility costs, such as power and water, which can lead to significant economic benefits and sustainability in the sugar production process. This study indicates that an over-estimation of crucial design parameters can lead to an increase of 158% in power consumption and an increase of approximately 488% in water consumption, from the base case-defined parameters. The increase in water is mostly linked with evaporation losses in the scrubber, due to higher temperatures. It should be noted that an over-estimation of the flue gas volumes will lead to more water requirements for the actual scrubbing of the flue gas, which might lead to an increase in the pump size and power consumption.

Approach

The information gathered in this paper is collected from historical data received from the Original Equipment Manufacturers (OEMs) of the boiler and its customers. Only bagasse-fired boilers will be used in the calculations, but coal and other fuels are expected to have a similar result, as the scrubber design and working principles remain the same.

The variables used in the calculations are as follows:

- Particle Size Distribution (PSD);
- inlet dust load;
- inlet gas temperatures; and
- inlet pressure

The historical data were used to determine a minimum, average and maximum case for each variable listed above. These values were used to design a scrubber for the three cases. The PSD range and dust load were used to determine the required differential pressure over the scrubber throat. The required differential pressure would then indicate the type of scrubber that is to be used.

Historical data compilation

Particle Size Distribution (PSD)

Historical client data for the various Particle Size Distribution (PSD) were collected and can be observed in Figure 1 below:

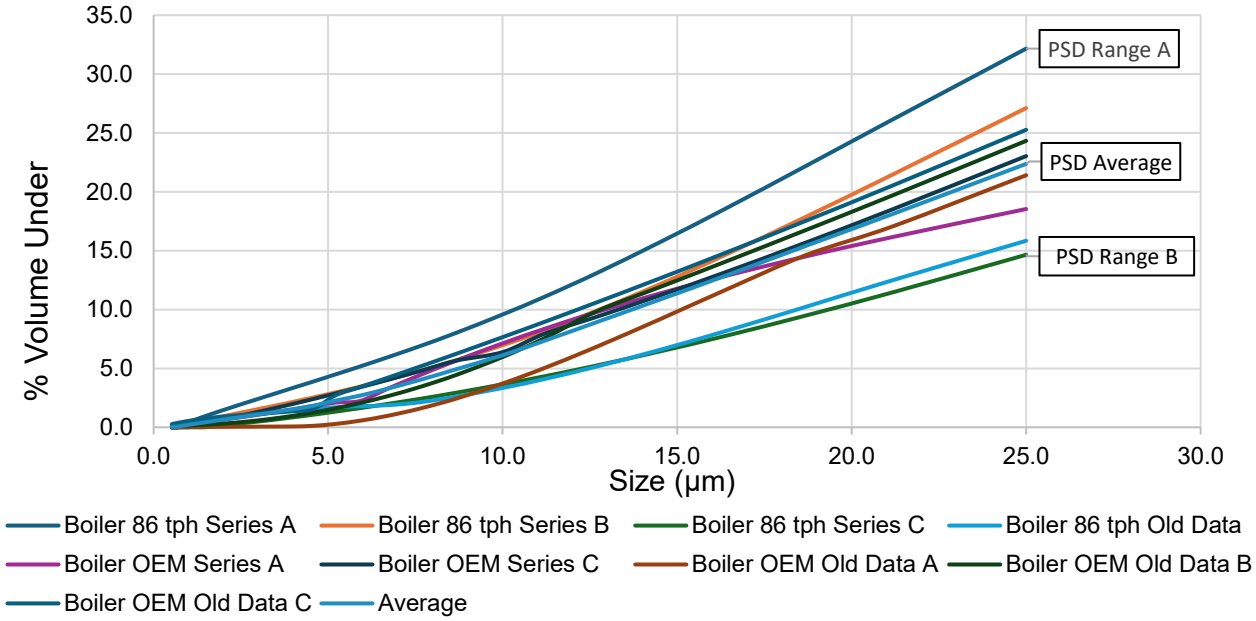


Figure 1. Numerous historical PSD ranges

The PSD data, shown in Figure 1, are collected from historical data, with the average (PSD Average), the finest (PSD Range A) and the coarsest (PSD Range B) being specifically highlighted in Figure 2 below:

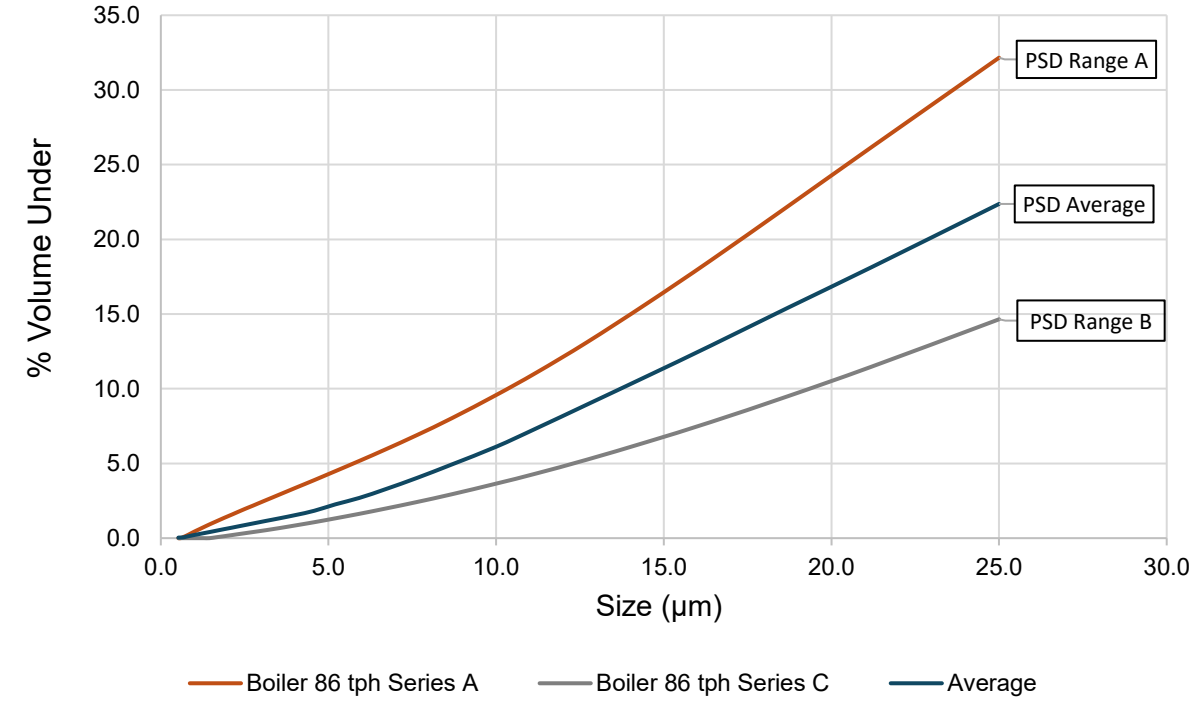


Figure 2. PSD graph for finest, coarsest and average

As indicated in Figure 2, the PSD data are tabulated in Table 1.

Table 1. PSD data table

Size (um)	Fine %volume under	Coarse %volume under	Average %volume under
1	0.44	0.00	0.21
5	4.49	1.33	2.27
10	9.58	3.65	6.12
20	26.18	11.48	18.14
30	41.02	19.77	29.07
40	52.20	27.20	38.84
50	63.39	35.96	51.47

Inlet dust load

The collected dust loads obtained from the historical data are tabulated in Table 2.

Table 2. Historical dust loads

Dust Load (g/Nm³)	
Maximum	**20**
	18.9
	17
	15
	14.5
	12
Minimum	**5***
Average	**16.23**

*The 5 g/Nm^3 value from Table 2 was collected from an old enquiry document and is no longer applicable to industry standards; hence, it has been excluded from all calculations.

The dust loads vary between 12 and 20 g/Nm^3. For this paper, the maximum, minimum and average data were used as a design basis during the scrubber design.

Inlet gas temperatures

Temperature variations are important in the scrubber calculations, as they impact the evaporation rate from the scrubbers, as well as the volume of the gas entering the scrubber. The historical scrubber inlet temperature data are summarised in Table 3.

Table 3. Scrubber inlet temperature variations

Scrubber inlet temperature (°C)	
Maximum	**200**
	181
	178
	173
	171
	162
	162
	156
	150
Minimum	**149**
Average	**168.2**

The data in Table 3 represent the scrubber inlet temperature where the boiler is equipped with an air-preheater and an economiser.

Inlet pressure

The scrubber inlet static pressure collected from historical data is tabulated in Table 4. The inlet static pressure into the scrubber will influence the actual gas volume through the scrubber, as well as the size of the fan motor required.

Table 4. Scrubber inlet static pressure

Economiser Outlet Pressure (Pa)	
Maximum	**-707**
	-1 134
	-1 179
	-1 344
	-1 351
	-1 480
	-1 483
	-1 560
Minimum	**-1 778**
Average	**-1 335.1**

The scrubber inlet pressure varies between – 707 Pa and - 1,778 Pa. The maximum, minimum and average pressure, as highlighted above, are further used in the scrubber design calculations.

Type of scrubber to be used

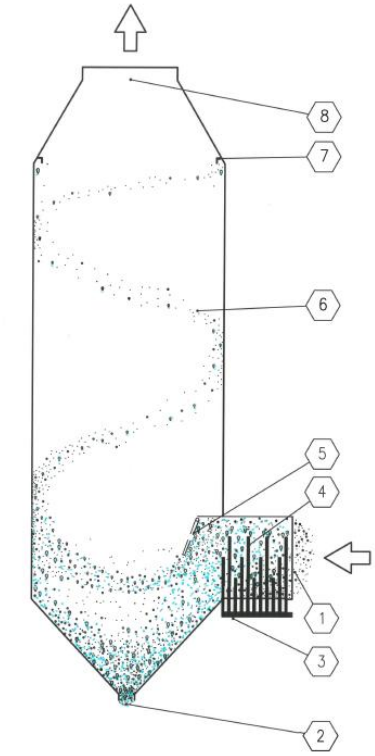
We have selected the cyclonic scrubber, as this is commonly used on bagasse-fired boilers. The differential pressure required for a dual-fired boiler is higher, as the PSD range is finer, and a Venturi scrubber would be more suitable.

Bagasse-fired boilers usually have a coarser PSD, when compared to coal-fired boilers. Therefore, the pressure drop across the throat can be reduced. Cyclonic scrubbers typically

operate at a lower differential pressure across the throat than Venturi scrubbers, and a Cyclonic scrubber would be a sufficient particulate collection device.

The Cyclonic scrubber functions on the following principles:

- Gas enters the lower section of the cylinder tangentially;
- The inlet is equipped with multiple fan spray nozzles for wetting the inlet gas and quenching the gas below the saturation temperature; and
- Entering the cyclonic separator, the modulating damper blade controls the differential pressure to a controlled set-point at varying boiler loads.



Legend

1. Bottom inlet section
2. Slurry outlet
3. Water supply header
4. Flat spray nozzles
5. Throat damper blade
6. Cyclonic separator
7. Anti-creep ring
8. Scrubber clean gas outlet

Figure 3. Sectional view of a Cyclonic scrubber



Figure 4. Cyclonic scrubber for a 150 tph bagasse-fired boiler

Case Study 1 – Cyclonic scrubber

Table 5. Specifications & Performance: South African Cyclone Scrubber.

Boiler MCR Capacity	80 tph with Bagasse Fuel
Boiler fuel	Bagasse and Coal fired
Gas Volume – Bagasse (MCR)	175 083 Nm^3/hr
Gas Volume – Coal (MCR)	91 650 Nm^3/hr
Inlet Dust Load - Bagasse	8.5 g/Nm^3
Inlet Dust Load - Coal	5.0 g/Nm^3
Outlet emission - Bagasse	120 mg/Nm^3
Outlet emission - Coal	120 mg/Nm^3
Collector	Cyclonic Scrubber
Collector size	Ø5 350 mm
Scrubber water requirement	215 m^3/hr
Pressure drop – Bagasse (MCR)	2 000 Pa
Pressure drop – Coal (MCR)	2 600 Pa
Emission – Bagasse (Tested)	20 mg/Nm^3
Emission – Coal (Tested)	110 mg/Nm^3



Figure 5. Scrubber inlet section

Case Study 2 – Cyclonic scrubber

Table 6. Specifications & Performance: South African Cyclone Scrubber

Boiler MCR Capacity	150 tph with Bagasse Fuel
Boiler fuel	Bagasse and Coal fired
Gas Volume – Bagasse (MCR)	253 829 Nm^3/hr
Gas Volume – Coal (MCR)	159 041 Nm^3/hr
Inlet Dust Load - Bagasse	10.0 g/Nm^3
Inlet Dust Load - Coal	7.0 g/Nm^3
Outlet emission - Bagasse	120 mg/Nm^3
Outlet emission - Coal	120 mg/Nm^3
Collector	Cyclonic Scrubber
Collector size	Ø6 680 mm
Scrubber water requirement	312 m^3/hr
Pressure drop – Bagasse (MCR)	2 000 Pa
Pressure drop – Coal (MCR)	2 600 Pa
Emission – Bagasse (Tested)	
Emission – Coal (Tested)	

Scrubber selection specification (assumed)

A typical scrubber RFQ data sheet has been created, as can be observed in Table 7. The boiler that was selected was a 100 tph bagasse-fired boiler.

The scrubber inlet gas mass flow of 71.1 kg/s, or a 59 Nm^3/s volume, was assumed and fixed. The historical data, as described in the sections above, were associated with three different cases:

- Case A represents the minimum values for the variables and the finer PSD range;
- Case B represents the average PSD and other historical data; and
- Case C represents the maximum values for the variables and the coarser PSD range.

The three cases will highlight the difference in design, and the results from each design will highlight the influence of each variable on the scrubber size. The water supplied to the scrubbers was fixed for all three cases at 55 L/s.

Table 7. Scrubber design RFQ data sheet

RHEINMETALL RESONANT				
CUSTOMER:	SUGAR MAN (Pty) ltd			
PLANT:	1 X 100 TPH BAGASSE FIRED BOILER			
REFERENCE:	COLD FACTS			
BY:	SIXTO DIAZ RODRIGUES			
DATE:	MARCH 1970			
GENERAL INFORMATION:				
Altitude	m.a.s.l	**50**		
Barometric Pressure	kPa	**100.7**		
Boiler Fuel		**BAGASSE**		
DESIGN PARAMETERS:				
Boiler Type		**Bi-Drum Boiler**		
Type of Scrubber Required		**Cyclonic Scrubber**		
Gas Constituents (Economiser Outlet)		**Volume %**	**Mass %**	
	CO_2	11.20%	18.20%	
	N_2	43.00%	44.60%	
	O_2	0.00%	0.00%	
	H_2O	29.50%	19.70%	
	H_2	0.00%	0.00%	
	SO_2	0.00%	0.00%	
	Air	16.30%	17.50%	
SCRUBBER INLET PARAMETERS:		**CASE A**	**CASE B**	**CASE C**
Gas Volume (Actual)	Am^3/s	92.4	97.2	104.7
Gas Volume (Normal)	Nm^3/s	59.0	59.0	59.0
Gas Mass Flow	kg/s	71.1	71.1	71.1
Gas Temperature	°C	**149.0**	**168.2**	**200.0**
Gas Pressure	Pa	**-707.0**	**-1 335.1**	**-1 778.0**
Dust load	g/Nm^3	**12.0**	**16.2**	**20.0**
Particle Size Distribution		**PSD Range B**	**PSD Range Average**	**PSD Range A**

Scrubber calculated results

The design results for the three cases are summarised in Table 8 and discussed below:

Table 8. Scrubber design results

RHEINMETALL RESONANT				
CUSTOMER:	SUGAR MAN (Pty) ltd			
PLANT:	1 X 100 TPH BAGASSE FIRED BOILER			
REFERENCE:	COLD FACTS			
BY:	SIXTO DIAZ RODRIGUES			
DATE:	MARCH 1970			
SCRUBBER SPECIFICATIONS				
		CASE A	**CASE B**	**CASE C**
Diameter of Cyclonic Scrubber	m	5.43	5.53	5.65
Calculated Throat Differential Pressure	kPa	0.88	1.66	2.74
Inlet Water Temperature	°C	35	35	35
Water Consumption	L/s	55	55	55
Liquid to gas ratio	L/Am^3	0.73	0.71	0.67
Mass of scrubber casing	kg	22 400	23 100	24 200
Outlet Emissions	mg/Nm^3	50	50	50
SCRUBBER RESULTS				
		CASE A	**CASE B**	**CASE C**
Saturated Gas Volume (Actual)	Am^3/s	75.2	78.0	81.6
Saturated Gas Volume (Normal)	Nm^3/s	58.5	59.4	60.7
Gas Mass Flow	kg/s	70.7	71.4	72.5
Gas Temperature	° C	67.95	68.23	68.9
Gas Pressure at Outlet of Scrubber	Pa	**-1 941**	**-3 349**	**-4 869**
Evaporation Rate	L/h	**1 297**	**-1 121**	**-5 041**
Evaporation Percentage	%	**0.66%**	**-0.57%**	**-2.55%**
Gas Constituents %V/V				
	CO_2	11.29%	11.13%	10.88%
	N_2	56.16%	55.37%	54.13%
	Ar	0.15%	0.15%	0.15%
	O_2	3.44%	3.39%	3.32%
	H_2O	28.96%	29.96%	31.52%
	H_2	0.00%	0.00%	0.00%
	SO_2	0.00%	0.00%	0.00%
Fan Motor Absorbed Power	kW	**219**	**390**	**593**

Some of the main observations are noted below:

Gas volume

As the gas volume in the scrubber increases, the scrubber diameter must also increase, in order to maintain the desired upward gas velocity. The scrubber is typically sized, based on this velocity, to ensure effective separation performance. However, if the gas volume is underestimated due to improper testing, the actual velocity during operation will be higher than intended. This can result in particulate and water carry-over to the fan, potentially causing premature wear and the early replacement of the fan.

Another important factor influenced by the gas volume is the Liquid-to-Gas ratio (L/G). If the L/G ratio is too low, dry zones may develop within the scrubber, which lead to elevated outlet gas temperatures. Dry zones in the scrubber will lead to the gas being unsaturated, which reduces its scrubbing efficiency and increases the particulate emissions.

Overestimating the gas volume leads to oversized scrubbers, which unnecessarily increase the Capital Expenditure (CAPEX) of the project. In addition, maintaining the desired L/G ratio for a larger gas volume requires more water, which necessitates larger pumps and motors, which further increases both the initial and operational costs.

Throat differential pressure

The differential pressure across the scrubber throat is a function of the gas acceleration through the throat section. As the acceleration increases, the pressure drop increases. Finer Particle Size Distributions (PSDs) require more acceleration through the throat to ensure that the finer particles are collected in the scrubber.

When the PSD shifts toward finer particles (PSD Range A), the pressure drop across the throat increases. This elevated pressure drop results in greater system resistance, which the fan must overcome. Since pressure is a key factor in determining the fan's absorbed power, an increase in the system’s resistance leads to a higher power demand and, potentially, a larger fan motor size.

Overestimating the concentration of particles in the gas stream can result in an unnecessarily high pressure drop design, which can lead to increased fan shaft power requirements. Conversely, underestimating the amount of fine particulate matter can reduce the scrubber collection efficiency, resulting in excessive emissions and non-compliance with environmental regulations.

Scrubber size

As the scrubber inlet gas volume increases, the size of the scrubber should increase, to maintain the desired upward velocity in the scrubber and to avoid any carry-over of particulates and moisture to the fan. Since the water in each case remained fixed, the saturated volume increased, due to the gas being at higher saturation temperatures.

An undersized scrubber would lead to excessive particulate matter carry-over to the fan. Over-sized scrubbers will lead to ineffective scrubber efficiencies, due to the dry areas in the scrubber.

Scrubber inlet dust load

The inlet dust load has a significant impact on the differential pressure across the scrubber throat. Along with the Particle Size Distribution (PSD), it is one of the most critical factors that influence the throat pressure-drop and, consequently, the fan’s power consumption.

Overestimating the inlet dust load can result in the design of a scrubber system with unnecessarily-high throat differential pressure requirements, which will lead to an increased fan power demand and higher operational costs. On the other hand, underestimating the dust

load can compromise the scrubber's performance and result in excessive particulate emissions and potential non-compliance with environmental standards.

The importance of site-specific process testing

Thorough process testing, particularly isokinetic and flow testing, is essential for establishing a realistic and robust design basis when developing a Request for Quotation (RFQ) for a new or retrofit scrubber system on the existing boilers. These tests must be conducted under representative operating conditions and they must always include a record of the boiler load at the time of testing, as some field tests are performed below the Maximum Continuous Rating (MCR). Designs based on non-representative or unverified data risk serious technical and financial consequences, including non-compliance, underperformance and costly retrofits.

Isokinetic sampling delivers vital information, such as dust loading and the Particle Size Distribution (PSD) of the boiler outlet gas stream, both of which are critical for selecting appropriate scrubber technologies and predicting removal efficiencies. Meanwhile, flow testing ensures the accurate determination of the flue gas volumetric flow rate, temperature and pressure, all of which are necessary for sizing scrubbers and the associated Induced Draft (ID) fans.

Process testing should be conducted on the boiler with varying boiler loads. As the boiler is turned down from MCR conditions, the PSD shifts towards the fine side of the curve. As discussed in this study, this might require higher pressure drops across the scrubber. Boiler testing should also be conducted in different seasons, as the wet or dry climate might have an influence on the dust load into the scrubber.

Conclusion and recommendations

This study underscores the substantial operational and financial consequences of over-designing boiler back-end equipment, which often stem from the use of inaccurate or assumed input parameters. In the absence of detailed site-specific process testing, particularly isokinetic sampling and accurate flow measurements, designers tend to apply overly-conservative safety margins. While being well-intentioned, this practice frequently results in unnecessarily large equipment, inflated Capital Expenditure (CAPEX), and elevated Operational Expenditure (OPEX), particularly relating to power and water consumption.

The modelling scenarios presented in this study demonstrate the impact of this approach: overestimating the design inputs can lead to a 158% increase in power consumption and a 488% increase in water usage, compared to a well-founded base case. These inefficiencies translate directly into a higher energy demand, oversized mechanical systems and increased operational complexity. We therefore strongly recommend that:

- process testing should be conducted before RFQ development, or in the early stages of the design phase;
- process testing should be completed at varying boiler loads, a minimum, a maximum (MCR) and an intermediate point;
- the boiler load should be logged during testing, in order to contextualise the data;
- isokinetic and flow test results should be used directly in the design calculations; and
- conservative margins should be applied only after verifying the actual process conditions.
- By prioritising accurate, on-site testing data, project teams can develop boiler back-end systems that are cost-effective, technically appropriate, and future-proofed against operational variability.

OPERATIONAL PAPER

CONTROLLING BOILER SWELL AND SHRINK

Wannenburg E

Babcock Ntuthuko Engineering, Johannesburg, South Africa

etienne.wannenburg@babcock.co.za

Abstract

The steam drum level is one of the main causes of boiler trips on industrial boilers. As it is affected by the phenomenon of swell and shrink, it is a difficult parameter to control accurately. Babcock conducted a study to determine the advantages of using different control configurations (single-, two- and three-element control) to mitigate the effects of the swell and shrink phenomena. The testing was conducted on two identical boilers that were connected to a common header, which allowed for a comparison of the different control strategies with the same load change. It was found that the single-element control is simple, but it performs poorly. The two-element control improves the performance and is easy to install. The three-element control offers the best performance, but it is complex and requires careful engineering. Both configurations improve stabilisation after the shrink or swell reactions, but they do not mitigate the initial reaction.

***Keywords*:** Boiler, steam, swell, shrink, control, level control

Introduction

The steam drum level is one of the major contributors of boiler trips and down-time. As it is affected by a specific phenomenon (swell and shrink), it is difficult to control the drum level optimally. Babcock conducted tests to determine the best configuration for controlling the steam drum level and how to optimise it.

It was found that the single-element control is simple in construction, but it offers the poorest performance of the three configurations. The two-element control improves the performance and is easy to install, requiring only the addition of a cascade controller and the re-tuning of the loop. The three-element control provides the best performance, but it is more complex, although it can be derived from the two-element configuration. It requires careful engineering during its implementation and start-up. While it improves control after the shrink reaction, it does not fully mitigate the initial reaction of shrink or swell reactions.

Boiler circulation

In natural circulation boilers, the steam drum is used to separate the steam from the water by using mechanical scrubbers and other mechanical equipment. Once the steam is separated, it flows to the superheater and main steam equipment, with the outflow replenished by adding feed water to the steam drum.

Natural circulation within the boiler causes the feed water to flow from the steam drum through the downcomers to the boiler furnace. When the water reaches saturation temperature, it flows back to the steam drum due to a change in density. The steam and water are then separated in the steam drum, and the cycle continues. Figure 1 indicates a basic representation of the natural circulation within a boiler circuit.

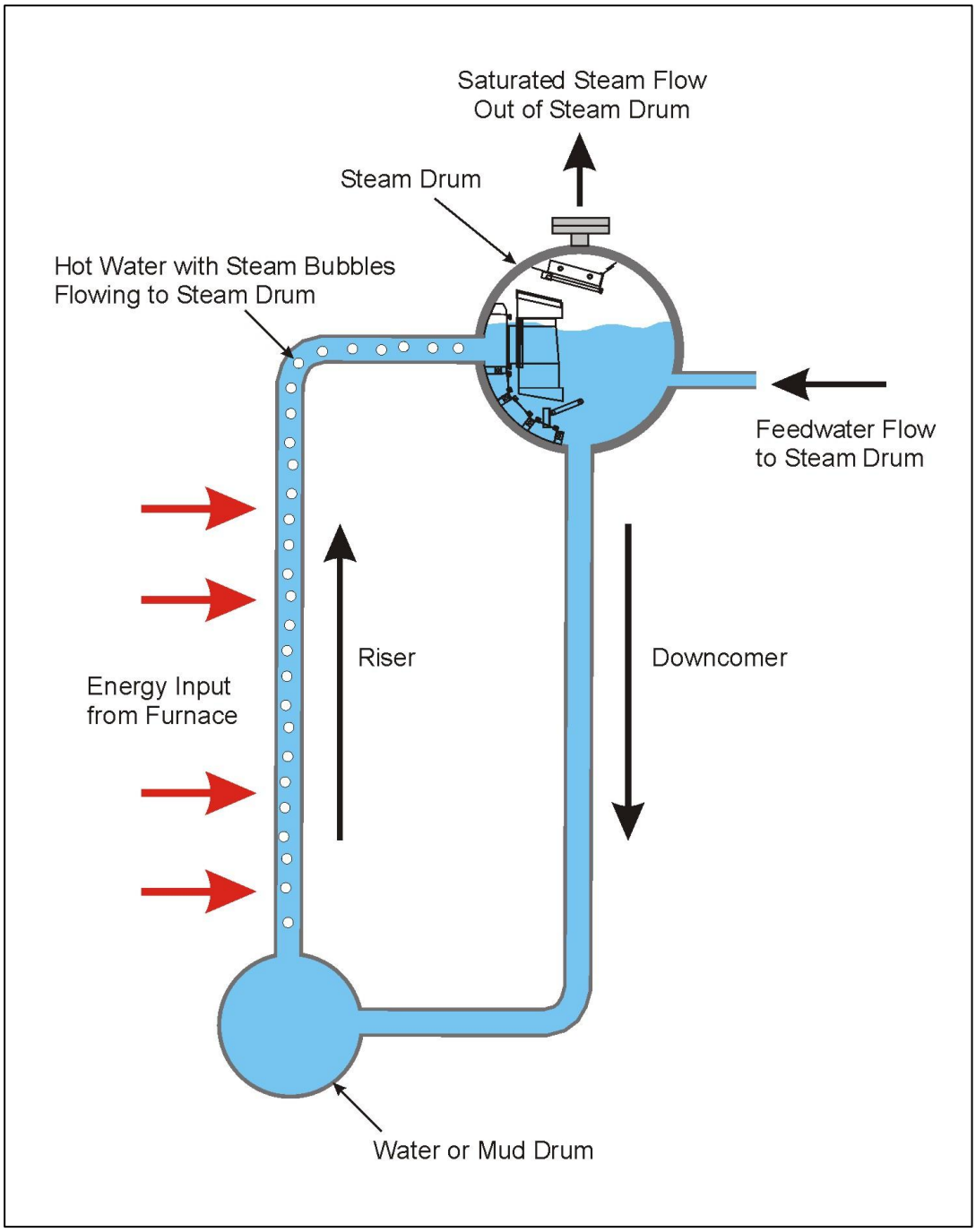


Figure 1. Basic representation of natural boiler circulation

Swell and shrink reaction

As indicated above, during normal operation, a water-tube boiler contains a mixture of water and entrained steam bubbles. The system is considered to be in a steady-state condition when the rate of steam generation equals the feedwater input, and the heat input and losses remains constant.

A change in the boiler pressure or input energy alters the average density of the water-steam mixture and the steam generation. For example, when the boiler load is increased, the concentration of steam that is entrained in the water must increase. The result is that the volumetric proportion in the water-steam mixture changes and the average density of the mixture decreases, which increases the steam drum level. If this is conducted suddenly, it will

rapidly increase the steam drum level i.e. swell. Inversely, a sudden loss of energy input will increase the average density, which will result in a decrease of the steam drum level, i.e. shrink. However, in both instances, some adjustment needs to be considered for the pressure changes (Dukelow, 1991).

Similarly, if the energy input remains constant, but the steam pressure is changed rapidly, this will also cause a swell-and-shrink reaction. A rapid increase in pressure causes the average density of the water-steam mixture to increase and it also lowers the steam generation, which will collapse the steam drum level i.e. shrink. Conversely, a sudden pressure drop leads the average density of the steam-water mixture to decrease and it also increases the steam generation, which will raise the steam drum water level i.e. swell.

The magnitude of the swell-and-shrink reactions is also dependent on the boiler load, as the water-steam mixture contains more steam at higher loads, and it will therefore have a larger impact on the average density.

Drum level control configuration and testing

The objective of the control loop is to maintain the water level at ±50% of the steam drum capacity. Water in the steam drum must not be allowed to deviate from the specified minimum and maximum trip limits, as this could cause damage to the boiler and downstream equipment.

The trip limits of a boiler are determined during the design of the steam drum, and they are derived from the boiler size, the boiler type, the scrubbing equipment and the position of the down-comer tubes. The steam drum is designed to be as small as possible (due to the high cost of the pressure vessels), which thus leads to stringent trip limits.

If the water level increases above the high trip limit, water will carry over into the steam line and super-heater systems, and if it decreases below the low trip limit, the water tubes can run dry and cause damage to the boiler.

The drum level, feed water flow and steam flow are the main parameters that are used in traditional steam drum level control systems. A combination of cascade and feed-forward methods are employed to control the steam drum level, with single-, two- and three-element control being the most common configurations.

Babcock conducted a study to determine the advantages of using two and three-element configurations in a steam drum level application. The testing was conducted on two identical 55 t/h Babcock waste heat boilers that were connected to a common header, which supplies steam at 66 Barg 490°C to a single turbine unit. Boiler 1 was used as the baseline for the testing. The steam drum level configuration on Boiler 1 was left on the single-element control configuration during the test period and compared to Boiler 2, which was configured with the two- and three-element control configurations.

The following section explains the control loop configurations and performance testing of the different control methods.

Single-element control

The single-element control loop is indicated in Figure 2. The steam drum level signal is used as the process variable, and the output of the controller is used to control the feed water flow to the steam drum. The set-point of the controller is configured to ± 50% of the drum level capacity. The steam drum pressure is used for the density correction of the drum level measurement.

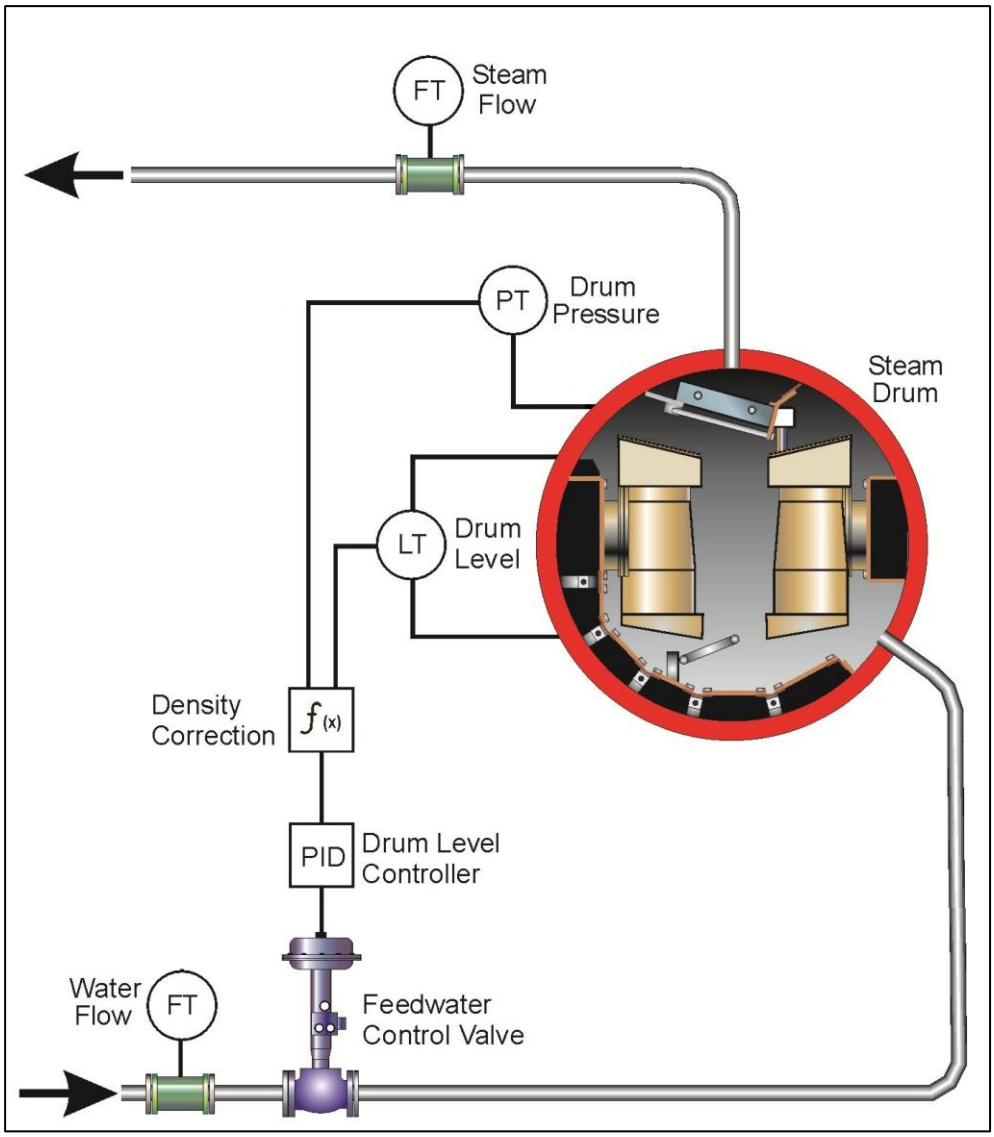


Figure 2. Single-element control

A standard open-loop step change was used to analyse the process response. The control loop was placed in manual, and the feed-water valve was opened with a step change. The test data were analysed, and fast proportional and integral settings were selected for the control loop.

In order to evaluate the tuning values, the controller was placed in automatic, and a change was induced on the set-point signal. The test results that are shown in Figure 3 indicate that the fast-tuning settings were optimal for the controller. The single-element control philosophy was installed on Boiler 1 as the base line.

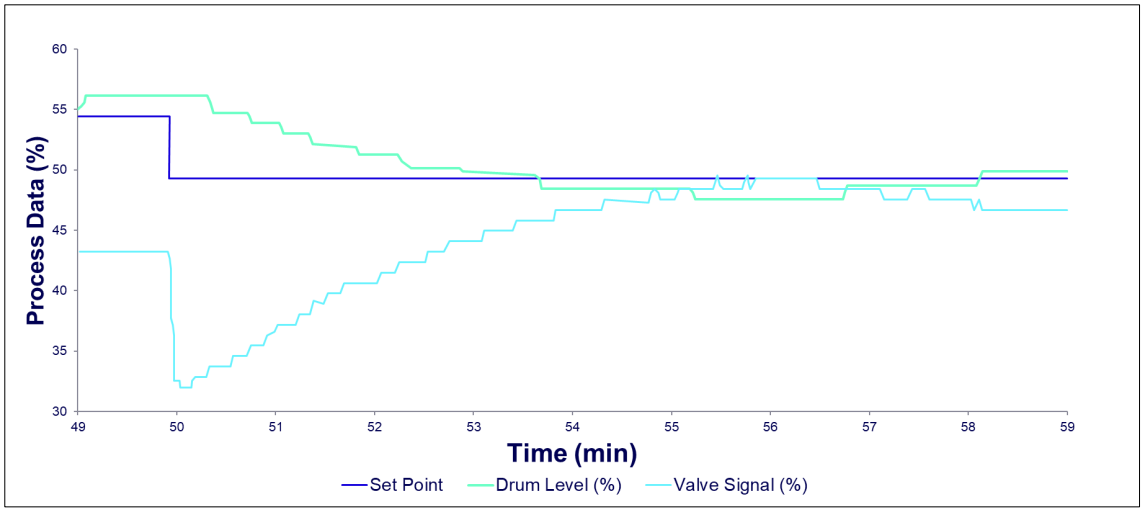


Figure 3. Single-element performance testing

Two-element control

The standard two-element controller is shown in Figure 4 and includes a feed water controller in cascade to the drum level controller. The drum level controller output is the feed water controller set point. The feed-water flow into the steam drum is the process variable for the secondary control loop.

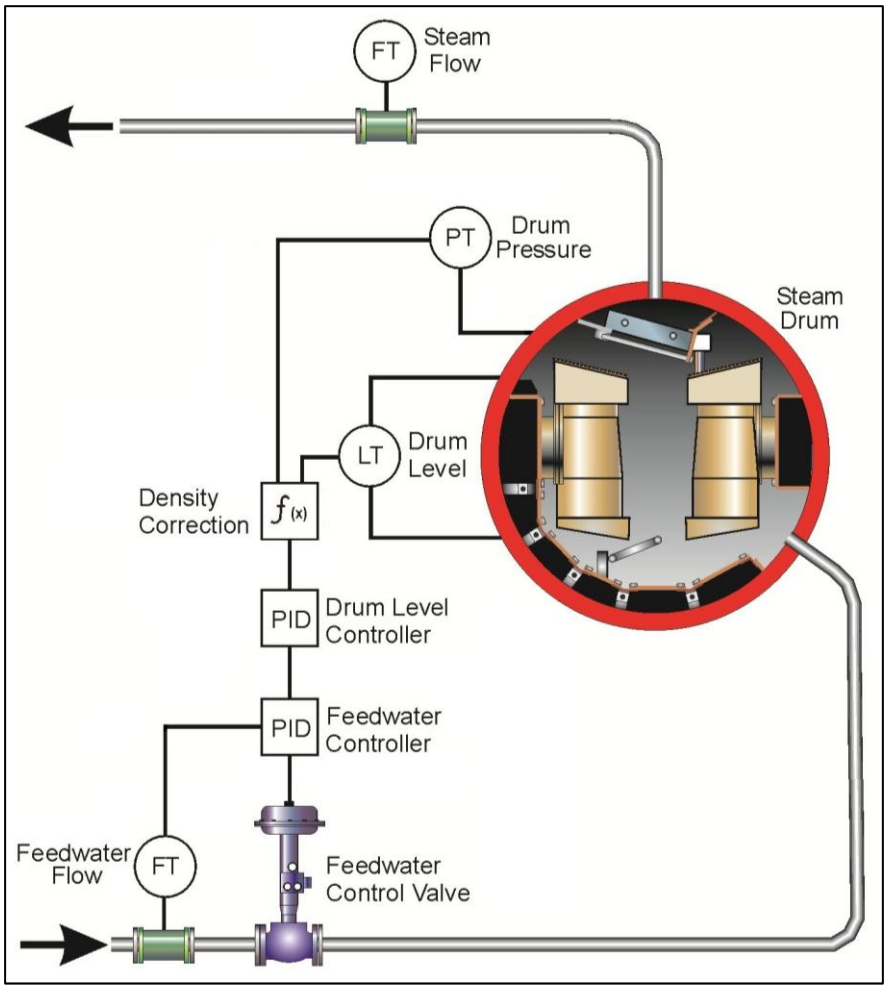


Figure 4. Two-element control

Tuning optimisation started with the secondary (feed water control) loop. Step changes were induced on the feed-water valve and the feed-water flow was recorded. The data from the results were analysed, and fast proportional and integral settings were selected for the flow loop.

After the tuning parameters were obtained, the flow controller was updated with the new values and the tuning was done on the primary (level control) loop.

The primary loop had to be re-tuned, due to the addition of the cascade flow controller. The flow loop was set to automatic and the drum level loop was set to manual. A step change was introduced to the output of the drum level controller and the drum level was recorded. The data were re-analysed, and the tuning values were updated with the new proportional and integral settings.

The two-element control was then placed in operation and exceptional control was achieved, as can be seen in Figure 5.

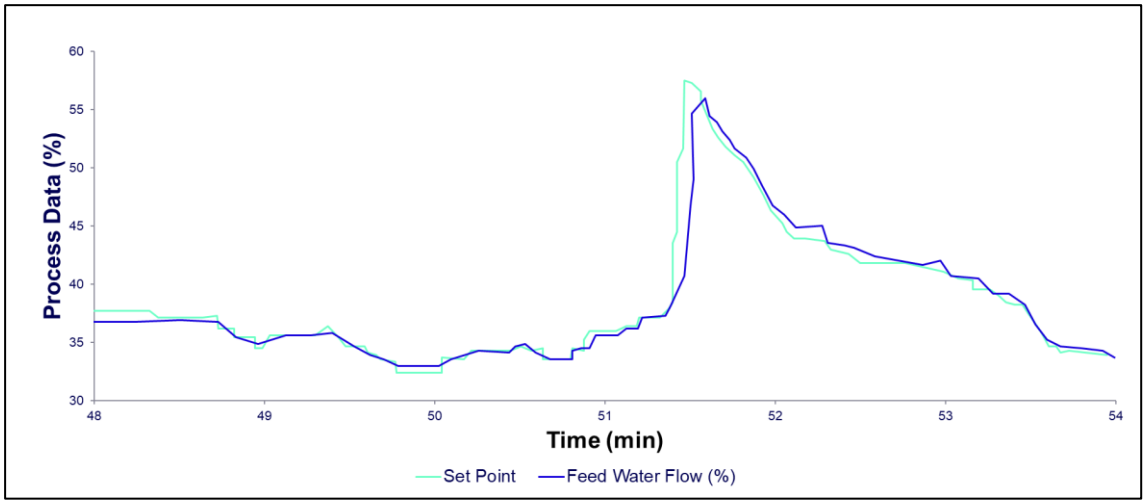


Figure 5. Flow controller response

Performance testing

After the two-element control was made operational on Boiler 2, a load change was recorded on the boilers when the common turbine, which was supplied by the two boilers, tripped. The trip was caused by a turbine fault, thus the boilers did not trip and remained in service.

During the turbine trip, the steam supply valve is closed, and the turbine by-pass line is opened. The turbine supply valve closes quicker than the by-pass valve can open, and thus the steam flow is stopped momentarily during the change-over. The turbine trip caused an upset in the boiler steam drum levels, as indicated in Figure 6.

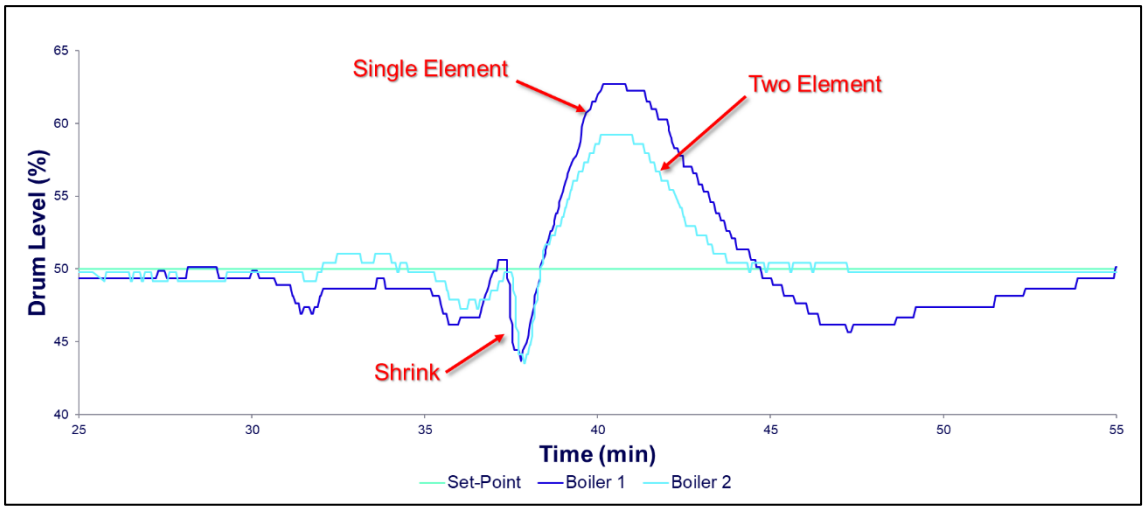


Figure 6. Single- versus two-element performance testing

The results indicated that the two-element configuration provides an improved reaction response and the stabilisation of the drum level, when compared with the single-element configuration Table 1 summarises the reaction of both boilers.

Table 1. Boiler reactions

Control Configuration	Max	Min	Settling Time
Boiler 1 (Single-element)	66%	42%	18 min
Boiler 2 (Two-element)	62%	42%	10 min

A comparison of the two reactions shows that the low-level points are identical, but there are notable differences in the maximum levels and settling times. The two-element control on Boiler 2 stabilised 8 minutes before the single-element control on Boiler 1. The load change confirmed that the two-element control configuration reduces the settling time and reaction magnitude more than the single-element configuration.

Three-element control

The three-element configuration is formed by cascading the drum level and feed water controllers with the addition of the steam flow in a feed-forward configuration. The steam flow signal is added to the drum level controller's output. Figure 7 indicates the basic three-element configuration.

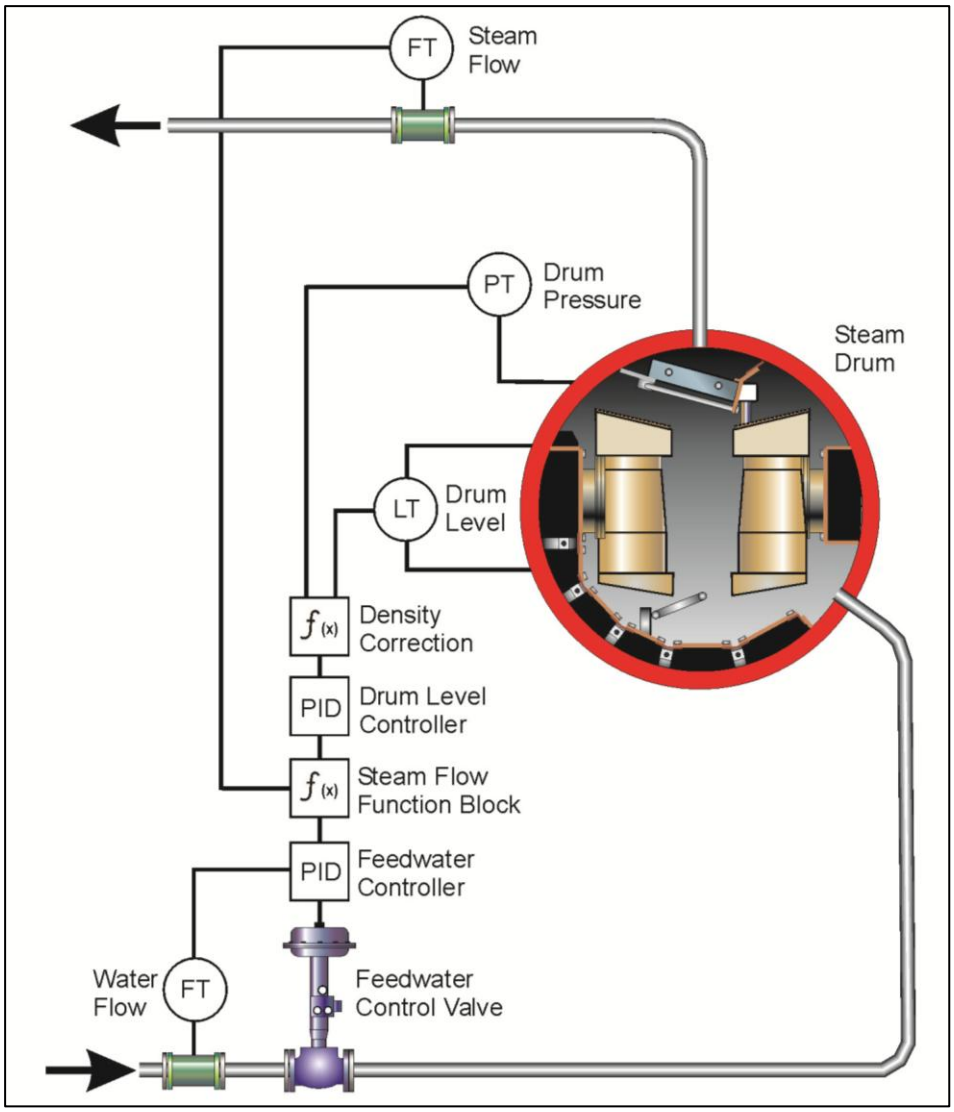


Figure 7. Three-element control

The principle of the three-element configuration is to control the mass balance of the steam drum. If steam is removed from the boiler circuit, the loss of steam must be replaced with an equal mass of feed water.

The feed water and steam mass balance cannot be used independently to control the drum level, as it is difficult to obtain a precise measurement of the steam and water flow. Furthermore, the boiler is normally not a closed circuit. The steam drum blow-down and sootblower steam take-off will affect the boiler mass balance. Thus, the drum level control is retained in the configuration to resolve the problems experienced by the mass balance control, and it will be used as a trim function.

A function block is used to introduce the steam flow signal to the drum level controllers' output and to manipulate the steam flow signal. A steam flow influence magnitude adjustment is used to change the controller from a two- to a three-element control. When the value is adjusted to 100%, the full magnitude of the steam flow will be used in the control loop.

The function block also contains a drum level controller bias signal. The bias signal is used to correct the operating range of the drum level controller's output. In a steady state condition, the steam flow will equal the water flow. If this mass balance maintains the drum level at 50%, the output of the drum level controller will be reduced to zero, which is not ideal. The bias signal will correct the drum level output signal to operate close to 50% under steady-state conditions.

Switching from two- to three-element control

Unlike the single- and two-element configurations, the three-element configuration cannot be used from start-up, as the steam flow is unreliable. When sufficient steam pressure and temperature is achieved after start-up and a reliable steam flow is maintained, the drum level control can be switched to the three-element configuration.

The three-element configuration uses the same controller that is used in the two-element configuration, thus retuning of the controllers is not required. The steam flow signal magnitude is just increased until the full signal is used.

During this increase, the drum level output signal will reduce as the steam flow signal is increased. The bias signal must be adjusted in proportion to the steam flow signal, in order to maintain the correct drum level output signal.

The steam drum mass balance requires the water and steam flow to be equal, and thus no gain is placed on the steam flow signal. The raw value derived from the process is used directly in the control configuration.

Figure 8 shows a 10% increase in the steam flow magnitude signal. It indicates that the set-point of the feed water controller is increased, without the drum level controller's output increasing. The feed-water flow is increased due to the change in set-point of the feed-water controller, which is followed by a decrease in the drum level controller output.

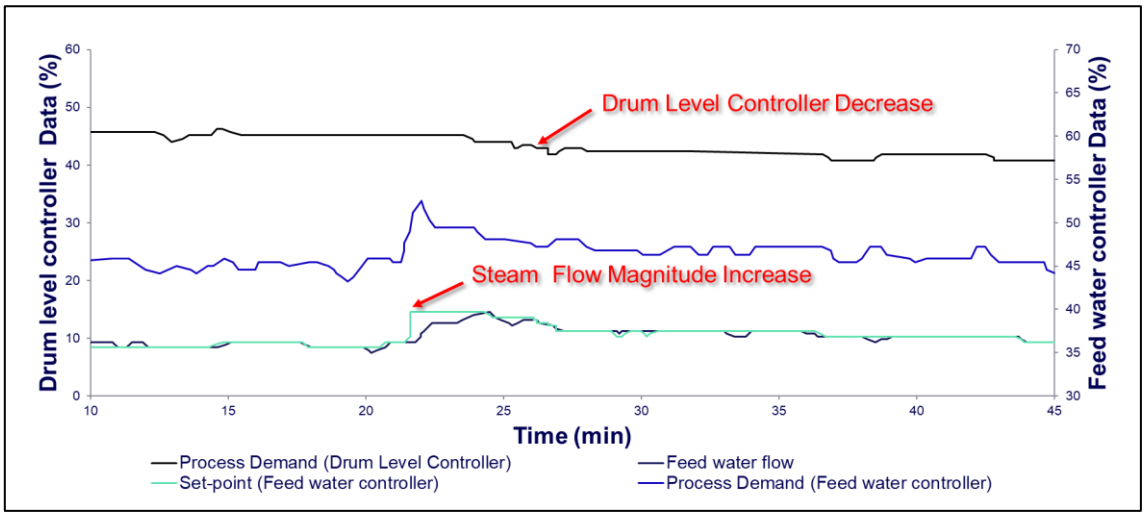


Figure 8. Three-element change-over

Three-element performance test

During the implementation period of the three-element controller, set-point changes were introduced to establish the performance of the configuration. Figure 9 indicates where the drum level set-point was increased from 50% to 54%.

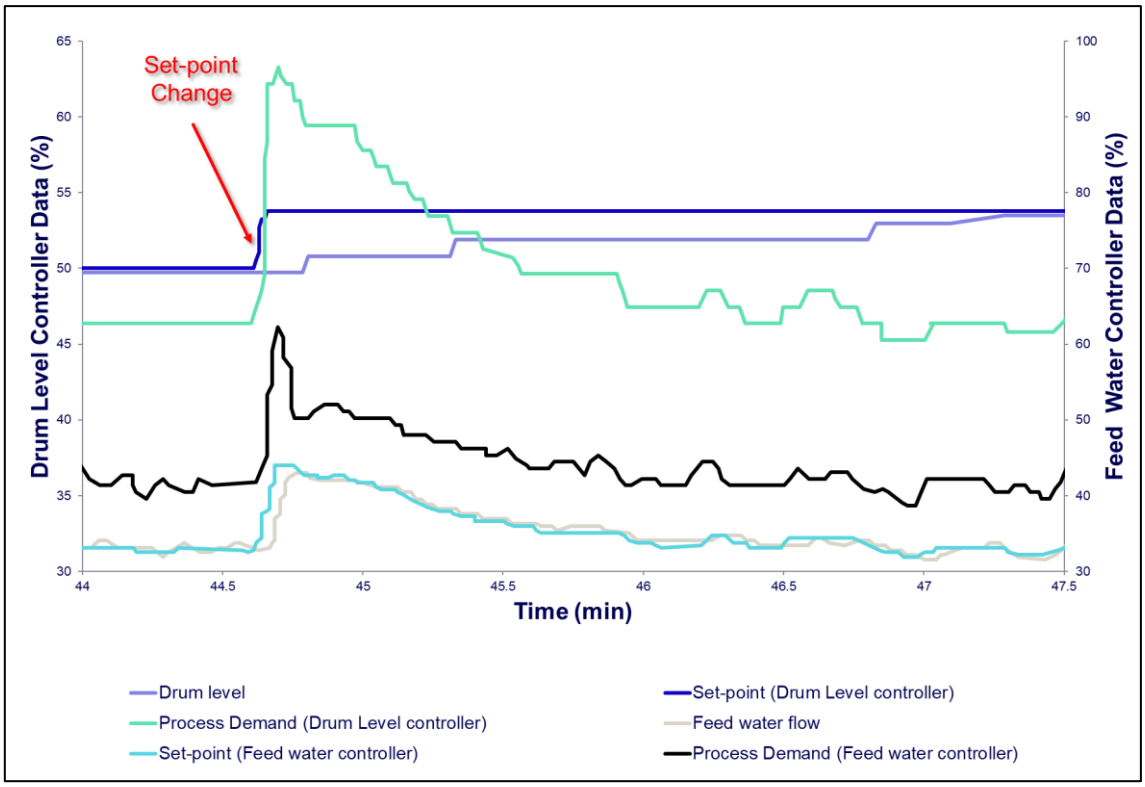


Figure 9. Three-element set-point change performace test

At the instant of the test, the magnitude influence signal from the steam flow was maintained at 40%. The set-point test indicated that the controllability of the configuration did not deteriorate by the addition of the steam flow signal.

The same type of load change that were experienced during the two-element configuration testing, was also experienced after the implementation of the three-element configuration. The common turbine supplied by the two boilers, tripped. Figure 10 indicates the reaction on both the drum levels caused by the turbine trip. The steam drum pressure and steam flow for Boiler 2 are also indicated.

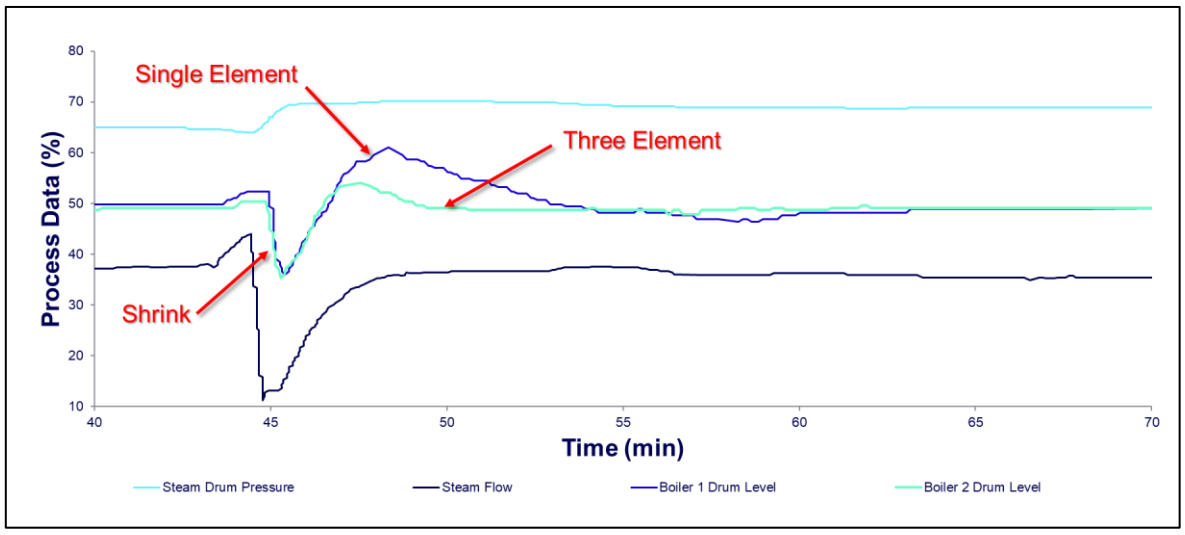


Figure 10. Single- versus three element performance testing

The change-over to three-element control was not fully completed at the time of the turbine trip, the steam flow influence signal was set at 70%. Even without the complete steam flow signal, the load change response indicated an improved performance, compared to the single-element control.

Table 2. Boiler reaction

Control Configuration	Max	Min	Settling Time
Boiler 1 (Single-element)	62%	33%	18 min
Boiler 2 (Three-element)	54%	32%	11 min

The recording indicated that the load change was more severe than the previous trip and the that the drum level experienced a dramatic shrink. Both boilers activated the low drum level alarm. After the shrink reaction, Boiler 1 overshot the set-point significantly more than Boiler 2. The three-element control on Boiler 2 also stabilised 7 min faster than the single-element control on Boiler 1.

Conclusion

The single-element control functioned well and has a simple construction; however, it offered the worst performance of the three configurations.

The two-element control offers an improved performance, compared to the single-element, and it is simple to install. On most boiler plants, only the addition of the cascade control and the re-tuning of the loop is required, to obtain two-element control.

The three-element offers the best performance of the tested configurations. The configuration is the most complicated, but it is simple to derive from the two-element model. Engineering considerations are, however, required during its implementation and start-up.

The control configurations were not observed to fully mitigate the shrink and swell reaction, specifically the initial reaction. As indicated above, the addition of the steam flow signal will close the control valve during a shrink reaction. This is directly the opposite required to maintain the drum level at set-point during the shrink reaction. However, closing of the valve is required to stabilise the process after the shrink reaction. Thus, the addition of the steam flow signal improves the control only after the shrink reaction, and it will not obviate the initial shrink or swell reaction.

References

Dukelow SG (1991). *The Control of Boilers.* 2nd ed. The Instrumentation, Systems and Automation Society, United States of America. pp 184.

FULL PAPER

BOILER EQUIPMENT: TYPICAL ANOMALIES AND THEIR EFFICIENCY CONSEQUENCES

Wilke CD[1] and Marais F[1]

[1]John Thompson, a Division of ACTOM (Pty) Ltd, Cape Town, South Africa

CharelW@johnthompson.co.za, FrancoisM@johnthompson.co.za

Abstract

Boiler and power plant efficiency is significantly impacted by equipment anomalies that result from inadequate maintenance. These anomalies can lead to reduced reliability, increased operational costs and even unplanned plant shutdowns. This paper examines common boiler equipment anomalies and their effects on the overall plant efficiency, with an emphasis on case studies that use thermal performance modelling to quantify these impacts.

Typical anomalies include damaged or missing refractory, tramp air ingress from defective ducting and air heater seals, bypassing economiser elements, missing superheater tubes, as well as inadequate insulation in key areas. The case studies demonstrate that such defects result in efficiency losses, increased fuel consumption and higher operational expenses, particularly in dual-fuel plants that utilise both bagasse and coal. For instance, missing refractory and air leaks reduce the combustion efficiency, while defective economisers and air heaters contribute to heat losses. In addition, missing superheater elements and compromised steam line insulation lower the steam temperatures, which negatively affects the turbine performance and power output.

By identifying and quantifying these anomalies, this paper highlights the importance of preventive maintenance strategies. Addressing these issues can enhance boiler efficiency, reduce fuel costs and optimise power production. The findings emphasise the need for proactive maintenance, in order to ensure cost-effective and reliable plant operation.

Keywords: Boiler, power plant, efficiency, turbine, thermal modelling

Introduction

The efficient, reliable and safe operation of the boiler is crucial in the sugar industry, in order to produce sugar at the lowest operational cost and of the highest quality, thereby remaining competitive. Any deficiencies in the boiler performance - whether due to faults in the boiler itself, or its auxiliary equipment - result in direct economic losses. Bagasse-fired boilers rely on a consistent supply of bagasse from the sugar mill, while the mill, in turn, depends on a minimum quantity of steam from the boilers. If the boilers are unable to supply the required steam, this interdependence is disrupted, which necessitates the co-firing of boilers with coal as a supplementary fuel, in order to maintain the steam production. Since coal incurs a direct cost, this leads to additional economic losses.

Co-generation plants are even more severely impacted. These plants supply electricity not only to the sugar factory but also, in some cases, to the national grid under power purchase agreements. The failure to meet these contractual obligations may result in significant penalties, which compels the plant to co-fire bagasse-fired boilers with coal, in order to ensure compliance.

To prevent unplanned shutdowns and optimise boiler performance, sugar mills follow a strict annual maintenance programme. This typically includes comprehensive boiler inspections during the annual off-crop period. It is common practice to involve the boiler's Original

Equipment Manufacturer (OEM) in these inspections. During this process, all boiler components are thoroughly examined, and a formal inspection report is issued. This report identifies equipment anomalies and defects, it provides recommendations for corrective action, and it may also include suggestions for enhancing the boiler performance.

The typical component failures have been categorised in Figure 1, based on the frequency with which they occur across the multiple boilers that were inspected and reported on, over several years. The most common defects are general tube failure and corroded tubes, which account for 20% of all the issues. These are followed by air and gas leaks (15%), refractory and structural damage (15%), combustion and fuel distribution issues (10%), as well as superheater and economiser tube failures (10%). Air heater failures make up 8%, while steam drum issues represent 7% of the total. The remaining 20% includes various other defects, such as problems with the grit collectors and scrubbers, draught fan issues, as well as general wear-and-tear and operational inefficiencies.

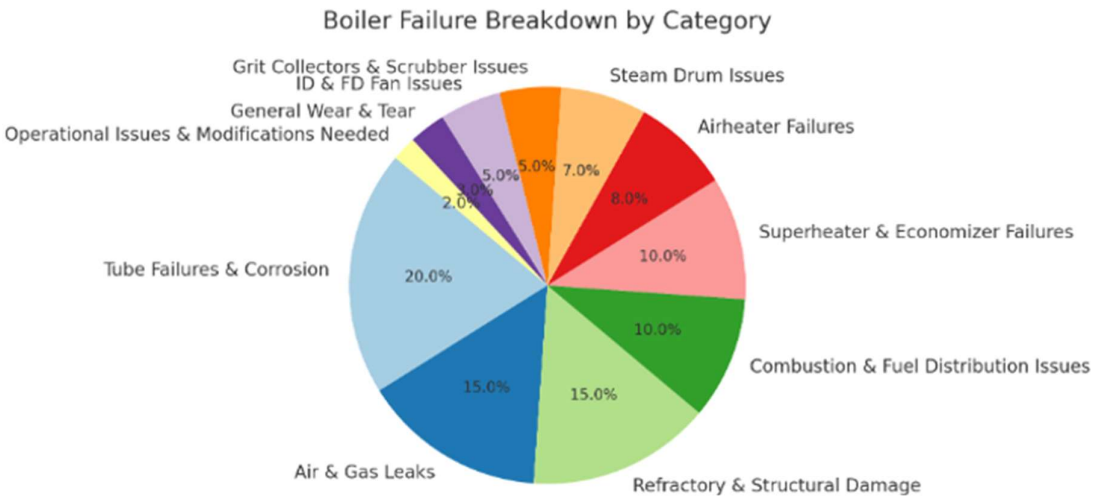


Figure 1. Boiler failures categorised, based on years of OEM inspection reports

This paper focuses on seven common equipment anomalies that are frequently identified during boiler inspections and that fall within the above-mentioned defect categories. These anomalies typically lead to a reduced boiler efficiency. As noted earlier, such reductions often necessitate supplementing the bagasse with coal, in order to maintain the required steam production. The impact of these anomalies on boiler efficiency can be quantified by using a lumped thermal analysis, which allows for the calculation of the additional coal that is required to sustain the steam output to the mill.

The seven identified equipment anomalies are presented, in no particular order, as follows:

1. **Damaged main bank refractory**, which results in elevated boiler gas outlet temperatures.
   (Category: Refractory damage)
2. **Tramp air ingress** at the back-end ducting and air heater, due to corroded tubes and failed rope seals. This increases the final flue gas flow and reduces boiler efficiency.
   (Category: Air heater failures, air & gas leaks)
3. **Blanked-off superheater elements** caused by previous tube failures, which lower the steam temperatures and reduce turbine power generation.
   (Category: Superheater failure)

4. **Partially blanked-off economiser elements** due to prolonged corrosion and erosion, which leads to decreased boiler efficiency.
   (Category: Economiser failure)
5. **Missing casing, lagging and cladding** from the boiler outlet ducting, much of the heat recovery tower ducting and the hot air duct, which contributes directly to heat losses and reduced boiler efficiency.
   (Category: General wear and tear)
6. **Missing lagging and cladding on the main steam line**, resulting from inadequate maintenance. This reduces steam temperature entering the turbine, which leads to decreased power generation.
   (Category: General wear and tear)
7. **Partially-open bypass damper on the air heater**, which lowers under-grate air temperatures and reduces combustion efficiency.
   (Category: Air and gas leaks)

Methodology and Modelling Approach

The basic methodology and thermal modelling approach that is followed here is the same as described by Rawlins *et al*. (2024). Their modelling approach employs simplified mass, energy and momentum balance equations to simulate the boiler and plant performance. Key components - including the furnace (modelled by using the projected method), heat exchangers (via tube bank and LMTD analysis) and balance-of-plant systems - are integrated with system-specific fluid properties and site-calibrated parameters. This enables the evaluation of thermal efficiency, steam utilisation and power generation in industrial applications.

Only natural convection was assumed for the heat-loss calculations in the case studies that involved missing lagging and cladding at the ducting or piping surfaces Cengel *et al*. (2015) give simple empirical correlations for the average Nusselt number for natural convection over various geometries, including flat horizontal, inclined and vertical surfaces, as well as horizontal and vertical pipe surfaces. For natural convection, the Nusselt numbers are typically a function of the Raleigh number, which can be viewed as the ratio of the buoyancy forces and the thermal and momentum diffusivities (Cengel *et al*., (2015)).

Table 1. Empirical correlations for the average Nusselt number for natural convection over surfaces

Geometry	**Characteristic Length (L_c)**	**Range of Rayleigh number (Ra)**	**Nusselt number (Nu)**
Vertical plate	Plate length (L)	10^4 - 10^9	$Nu = 0.59Ra_L^{1/4}$ **(1)**
Inclined plate	Plate length (L)		Use vertical plate equations for the upper surface of cold plate and the lower surface of a hot plate. Replace g by gcosθ for $0 < \theta < 60°$. (Note g is the gravitational acceleration constant) **(2)**
Horizontal plate: (a) Upper surface of a hot plate	Plate surface area (A_s) / plate perimeter (p)	10^7 – 10^{11} 10^5 – 10^{11}	(a) $Nu = 0.1Ra_L^{0.33}$ **(3)** (b) $Nu = 0.27\ Ra_L^{0.25}$

(b) Lower surface of a cold plate			(4)
Vertical cylinder	Cylinder length (L)		Treated as a vertical plate
Horizontal cylinder	Diameter (D)	$Ra_D < 10^{12}$	$Nu = \{0.6 + \frac{0.387\ Ra_L^{1/6}}{[1+(0.559/Pr)^{9/16}]^{8/27}}\}$ (5)

The Raleigh number (Ra_x) is defined as follows:

$$Ra_x = \frac{g\beta(T_s - T_{amb})L_c^3}{\nu^2} Pr \quad (6)$$

where β is the coefficient of volume expansion, T_{amb} is the ambient temperature, Pr is the Prandtl number and ν is the kinematic viscosity. Note that all the fluid properties are evaluated at the film temperature ($\frac{1}{2}(T_s + T_{amb})$)).

The Nusselt number (Nu) relates to the heat transfer coefficient (h) as follows:

$$h = \frac{NuL}{k} \quad (7)$$

where k is the thermal conductivity. Using Equation (7) the convection heat loss to ambient can be calculated as follows:

$$Q = hA_s(T_s - T_{amb}) \quad (8)$$

For radiational heat loss calculated over pipes, the general radiation loss equation is used:

$$Q_{rad} = \varepsilon\sigma\ A_s\ (T_s^4 - T_{amb}^4) \quad (9)$$

Where ε = 1 (outer surface of the pipe is approximated as a black body), σ = 5.67e-8 W/m^2K^4 and T_s is the average pipe surface temperature.

To compare the anomalies and associated supplementary coal consumption, the same coal specification is used throughout the case studies and is given as follows:

Table 2. Coal specification

Description	**Value**
Coal Type	Peas Gr A
Moisture % (wt/wt)	3.33
Ash % (wt/wt)	12.94
Carbon % (wt/wt)	70.59
Hydrogen % (wt/wt)	3.39
Sulfur % (wt/wt)	0.74
Oxygen % (wt/wt)	7.3
Nitrogen % (wt/wt)	1.7

GCV %	27,670
NCV %	26,849

The cost of coal delivered to the site is measured in Rands per month and it varies, depending on the location of the sugar mill, in relation to the coal source. For example, the average cost of Peas Gr A coal delivered to a mill in the Mpumalanga region is approximately R1 815 per ton, whereas the same coal delivered to a coastal mill can cost around R2 700 per ton. In each of the case studies presented, this range of the coal costs will be considered monthly, using an average month length of 30.4 days, for consistency in the calculations.

Case Study 1 – Damaged mainbank refractory

The boiler specific to this case study is a bi-drum water tube boiler with the following characteristics:

- final steam condition 17.2 Barg, 277°C, 220tph when firing bagasse;
- screened pendant superheater;
- three-pass main generating bank;
- single-pass air heater; and
- single-bank economiser.

The original boiler flue gas outlet temperature is 385°C at the Maximum Continuous Rating (MCR), but due to a local mainbank castable refractory failure in the superheater cavity (refer to Figure 2), the flue gas temperature increased considerably across the boiler outlet duct.

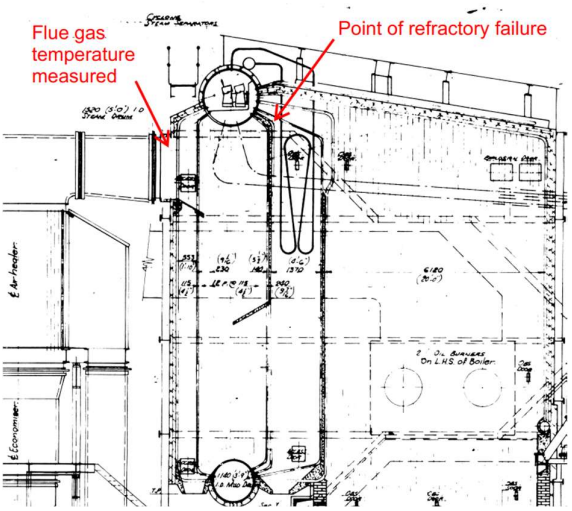


Figure 2. Boiler arrangement showing the location of refractory failure

In Table 3 below, the design case with no defects in the mainbank is compared with the load case where the mainbank refractory has failed:

Table 3. Boiler performance compared with and without refractory failure

	Boiler steam load	Flue gas temperature at boiler outlet	Boiler efficiency (GCV)	Supplementary coal consumption	Cost of coal range
Unit	tph	°C	%	kg/hr	Rand per month
No defect in mainbank refractory	189	380	66.93	None	None
Failed refractory	189	432	65.96	433	R573,704 - R853,444

Case Study 2 – Tramp air ingress

This case study focuses on tramp air ingress that occurs from the boiler back-end through to the economiser, based on the boiler described in the first case study. The tramp air ingress was deduced from visual inspection findings, which included failed expansion joints, worn rope seals, as well as other compromised sealing surfaces across the air heater, with a lesser extent noted across the economiser bank. Figures 3, 4 and 5 illustrate the failure of the air heater casing, the degraded rope seals and the corroded tubes at the bottom of the air heater, which all contribute to the ingress of tramp air.

Tube corrosion in the air heater typically occurs during boiler start-up, due to dew point condensation at the coldest part of the air heater tubes, particularly when the air heater bypass is not engaged. The lowest metal temperatures are found at the cold air inlet side, near the bottom of the air heater, where the flue gas temperatures are also at their lowest. When the tube metal temperature falls below the flue gas dew point, condensation forms on the tubes, which leads to progressive corrosion.

In cases where coal is used as a supplementary fuel, the risk of corrosion increases. The tube metal temperatures at these cold spots can fall below the sulphuric acid dew point, which results in sulphuric corrosion over time. This degrades the tube integrity further and contributes to the reduced boiler efficiency and increased maintenance requirements.

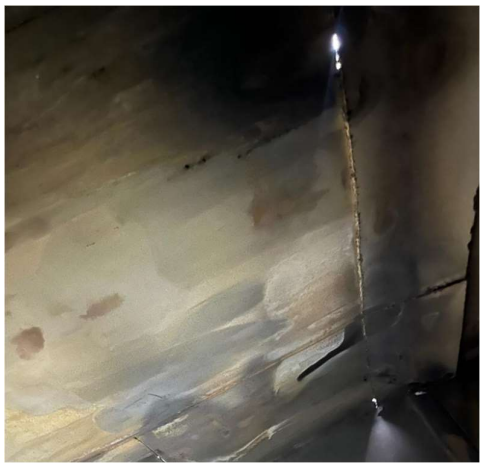


Figure 3. Failed air heater casing



Figure 4. Defective air heater rope seal



Figure 5. Corroded air heater tubes

Table 4 summarises the flue gas parameters that are measured across the air heater and economizer, and it compares them to the original design case with no back-end defects.

Table 4. Boiler performance with normal and excessive tramp air ingress

	Boiler steam load	**O_2 content increase across backend**	**Boiler GCV efficiency**	**Final flue gas temperature**	**Supplementary coal consumption**	**Cost of coal**
Unit	tph	% (wt/wt)	%	°C	kg/hr	Rand per month
Backend - No defects	189	0.26	66.93	199	None	None
Excessive tramp air ingress across air heater	189	2.56	66.29	193	221	R292 814 – R435,591

Case Study 3 – Missing superheater elements

The boiler and turbine specific to this case study is a bi-drum water tube boiler and condensing turbine with the following characteristics:

- final steam condition 45 Barg, 440°C, 90tph when firing coal;
- screened pendant superheater;
- three-pass main generating bank;
- steam air heater;
- dual-bank economiser; and
- connected to 21.7 MW Thermodyne pass out and condensing TA set.

Upon the examination of the superheater outlet header during the annual boiler inspection, five missing superheater elements were identified (see Figure 6). These elements had been removed and blanked off, due to the previous tube failures that had occurred over several years. Such failures are common in pendant-type superheater tubes and are often attributed to rapid boiler start-ups.

Typically, superheater tube failures occur when steam condenses inside the tubes during start-up and shut-down, and it collects at the elbows near the bottom of the tubes, which is a common phenomenon in non-drainable superheaters. Under normal start-up conditions, this condensed water has sufficient time to evaporate, which allows steam to flow through and cool the tubes, as they are exposed to increasing radiative and convective heat flux from the flue gases. However, during a rapid boiler start-up, the water collected in the elbows may obstruct the steam flow, which prevents proper cooling. As a result, the tube metal is exposed to high flue gas heat flux without adequate internal cooling, which causes the metal temperature to rise above the tube's design limit.

This temperature elevation leads to metal creep - a permanent deformation of the metal under sustained high temperature and stress - which eventually results in tube failure. The repeated occurrence of this failure mechanism necessitates the removal and blanking off of the affected superheater elements.



Figure 6. Missing superheater elements visible at the steam outlet header

The reduction in the superheater tube heating surface has led to lower steam temperatures being delivered to the condensing turbine, which subsequently impacts the power output.

Table 5 compares the original design performance of the boiler and turbine with the current performance, considering the reduced superheater heating surface, at the same steam load.

Table 5. Boiler and turbine performance with and without five superheater elements

	Boiler steam load	**Superheater steam exit temperature**	**Power generated**	**Supplementary coal consumption**	**Cost of coal**
Unit	tph	°C	kW	kg/hr	R per month
No defects in superheater	84	435	15,895	None	None
Missing superheater elements	84	425	15,635	None	None
Missing superheater elements	85.43	425	15,895	84	R111,296 – R165,564

Case Study 4 – Missing economiser elements

The boiler specific to this case study is a bi-drum water tube boiler, which includes:

- final steam condition 32 Barg, 400°C, 150tph when firing bagasse;
- radiant pendant superheater;
- single-pass main generating bank;
- single-pass air heater; and
- single bank H-fin economiser.

During an annual boiler inspection, it was observed that 6 of the 16 economiser elements were heavily corroded and subsequently blanked off by the mill, to prevent further leaks during operation. The corrosion of economiser elements typically occurs at the bottom economiser feedwater inlet (in this case, the economiser was of a counter-flow arrangement) during start-up, when the flue gas temperature is at its lowest. This results in lower tube metal temperatures and, subsequently, dewpoint corrosion on the external surface. Over time, the tube wall thickness fails to meet the minimum design criteria, which leads to premature tube failure. Refer to Figures 7 and 8 for illustrations of the condition of the economiser and tubes. With supplementary coal firing, sulphuric dewpoint corrosion can also result in tube failure, as well as erosion, due to high ash- and sand- loading in the flue gas.



Figure 7. Economiser with six elements blanked off

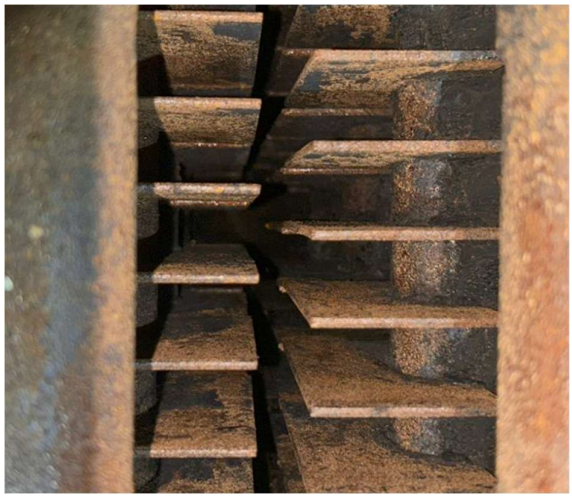


Figure 8. Corroded economiser elements

Table 6 compares the original performance of the boiler with all the installed economiser tubes, to the existing thermal performance of the boiler with the six economiser tubes blanked off.

Table 6. Boiler performance with and without the six elements

	Boiler steam load	**Boiler GCV efficiency**	**Final flue gas temperature**	**Supplementary coal consumption**	**Cost of coal**
Unit	tph	%	°C	kg/hr	R per month
No defects with economiser	150	64.82	247	None	None
Economiser elements blanked off	150	63.26	284	695	R920,841 – R1,369,847

Case Study 5 – Missing hot air and gas ducting lagging and cladding

The boiler specific to this case study is a bi-drum water tube boiler, which includes:

- final steam condition 32 Barg, 400°C, 140tph when firing bagasse;
- radiant pendant superheater;
- single-pass main generating bank;
- two-stage counter flow air heater; and
- dual-bank H-finned economisers.

It is standard practice to replace any missing boiler duct lagging and cladding, especially on hot air ducts from the air heater outlet to the boiler under-grate, or across the back-end, from the boiler flue gas outlet to the last heat recovery equipment. The insulation limits convective heat losses from the hot duct and casing surfaces to the ambient air. Convective heat loss to the ambient air reduces the boiler efficiency, which results in increased supplementary coal firing.

Table 7 illustrates the surfaces identified during an annual inspection that was not insulated.

Table 7. Ducting surfaces not covered with insulation

Location	Type of surface	Surface area (m²)	Surface Number
Boiler gas outlet ducting to air heater inlet	Horizontal surface (Facing Upwards)	57	1
	Vertical surface	38	2
	Inclined surface (45 degrees)	23	3
Air heater air side second pass	Vertical surface	93	4
	Horizontal surfaces (Facing Upwards)	23	5
Air heater air side first pass	Vertical surface	97	6
	Horizontal surface (Facing Downwards)	27	7
Air heater gas outlet to economiser gas outlet	Vertical surface	132	8
	Horizontal surface (Facing Upwards)	4	9
	Horizontal surface (Facing Downwards)	3	10
	Inclined surface (45 degrees)	13	11
Hot air ducting	Vertical surface	198	12
	Horizontal surface (Facing Upwards)	52	13
	Horizontal surface (Facing Downwards)	68	14

Table 8 summarises the heat loss to ambient, as per the surface areas 1 to 14:

Table 8. Heat loss per duct surface as referenced in Table 7

Surface Nr	Ra	Nu	h (W/m²K)	Q (kW)
1	1.55E9	115.8	5.15	88.3
2	1.55E9	117.1	5.21	59.6
3	1.10E9	107.4	4.77	33.1
4.1	2.46E9	60.15	2.15	85.7 (avg)
4.2	1.72E9	120.1	4.97	
5.1	2.46E9	135.0	4.84	21.4 (avg)
5.2	1.72E9	119.8	4.95	
6	2.46E9	131.4	4.71	34.0
7	2.46E9	60.2	2.15	4.3
8.1	2.45E9	131.3	4.80	103.8 (avg)
8.2	2.87E9	136.6	4.58	
9.1	2.45E9	134.8	4.93	3.3
9.2	2.87E9	142.1	4.76	
10.1	2.45E9	60.1	2.20	1.1
10.2	2.87E9	62.5	2.09	
11.1	1.73E9	120.4	4.4	9.4
11.2	2.03E9	125.2	4.2	
12	1.72E9	120.1	4.97	226.0
13	1.72E9	119.8	4.95	51.2
14	1.72E9	119.8	4.95	77.4

Table 9 compares the boiler performance with insulation and without insulation.

Table 9. Boiler performance with and without gas- and air-duct insulation

	Boiler steam load	**Boiler GCV efficiency**	**Final flue gas temperature**	**Supplementary coal consumption**	**Cost of coal**
Unit	tph	%	°C	kg/hr	R per month
Boiler with insulation	140	64.30	166	None	None
Missing insulation	140	63.86	165	156	R206,692 – R307,476

Case Study 6 – Missing main steam lagging and cladding

The boiler specific to this case study is a bi-drum water tube boiler with the following characteristics:

- final steam condition 45 Barg, 440°C, 80tph when firing coal;
- radiant pendant superheater;
- single-pass main generating bank;
- single-bank H-fin economisers;
- two-stage counter-flow air heater; and
- connected to 18.8 MW ABB pass out and condensing TA set.

This case study examines the impact of missing main steam lagging and cladding on the steam temperature entering the turbine and the subsequent underperformance of the turbine, in terms of power generation. During a boiler inspection, it was found that missing insulation on the main steam line accounted for 30% of the entire pipe length, from the boiler outlet to the turbine inlet. The main steam line under investigation is a 300NB Schedule 40 pipe, 74.7m long, with 19.5 m vertical sections and 8 elbows. The uninsulated vertical pipe sections comprised 10% of the total vertical pipe length, while the uninsulated horizontal pipe sections comprised 20% of the total horizontal pipe length.

The convective heat loss for the main steam line is calculated in Table 10, based on the equations described in Table 1. The reduction in steam temperature across the main steam line is less than 5°C, and the assumption of a constant pipe wall temperature across the entire length of the pipe is considered to be valid.

Table 10. Main steam pipe losses (convective and radiant heat)

Main steam surface	**Pr**	**Ra**	**Nu**	**h (W/m²K)**	**Q (kW)**
Horizontal pipe section – Convection	0.6954	2.21E7	35.8	4.34	3.5
Vertical pipe section - Convection	N/A	2.21E7	40.4	0.81	0.7
Horizontal pipe section - Radiation	N/A	N/A	N/A	N/A	207.0
Vertical pipe section - Radiation	N/A	N/A	N/A	N/A	27.7

Table 11 compares the turbine performance and the power that is produced, with the main steam line insulated and uninsulated:

Table 11. Boiler and turbine performance with and without main steam heat loss

	Boiler steam load	**Steam temp. at boiler outlet**	**Steam temp. at turbine inlet**	**Power produced**	**Supplementary coal consumption**	**Coal cost**
Unit	tph	°C	°C	kW	kg/hr	R per month
Fully insulated main steam pipe	72	440	440	16,452	None	None
Partially uninsulated main steam pipe	72	440	435	16,321	None	None
Partially uninsulated main steam pipe	72.54	440	435	16,452	68	R90,097 – R134,028

Case Study 7 – Partially by-passed air heater

This case study focuses on the same boiler, as specified in Case Study 6. A partially-open bypass damper (10% open) was noted during the boiler inspection, which will result in an uncontrolled amount of air by-passing the air heater at a lower under-grate air temperature. The type of damper fitted on this boiler is a twin-bladed parallel flow damper. The inherent flow characteristics of a parallel blade damper is given in Figure 9 (Johnson Controls (1991)).

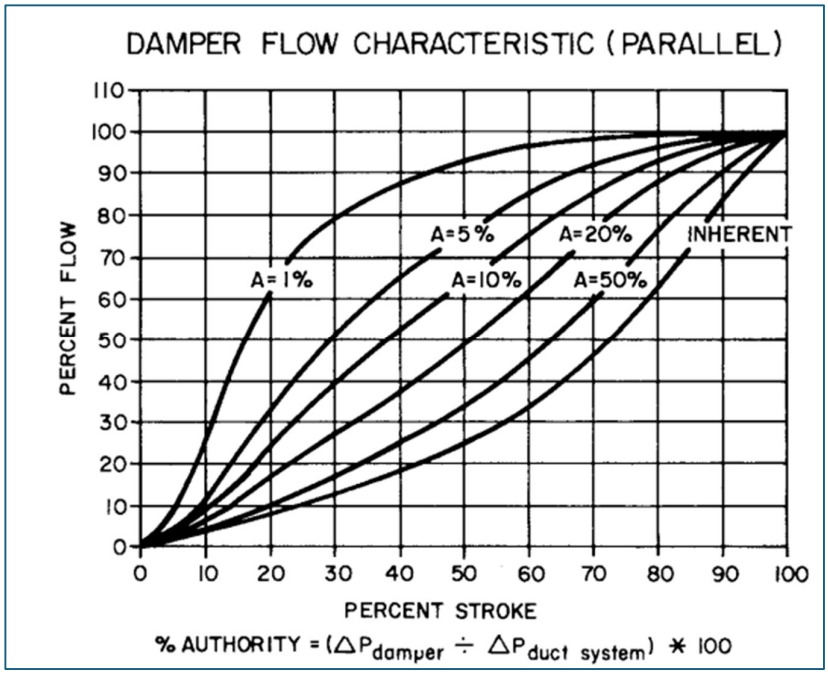


Figure 9. Damper flow characteristics for a parallel flow damper

The damper authority is determined as a percentage of the pressure drop across a wide-open damper, relative to the total pressure drop across the entire duct system, from the forced draught fan to the boiler under-grate inlet.

% Authority = (ΔPdamper / Δ*P*system)

(10)

In this case, the pressure-drop across the air side dampers is less than 152 Pa, as per the original design, compared to the overall air duct losses of 1286 Pa, which results in a damper authority of less than 12%. Based on Figure 9, the percentage flow through the bypass damper is approximately 10%. Table 12 compares the boiler performance when the damper is fully closed to when it is 10% open, which allows 10% of the total under-grate air to bypass the air heater. The results emanate from the thermal model of the case study boiler system.

Table 12. Boiler performance with the air heater damper fully-closed and partially-open

	Boiler steam load	**Total under-grate air flow**	**Bypassed air flow**	**Under-grate air temp.**	**Supplementary coal consumption**	**Coal cost**
Unit	tph	kg/hr	kg/hr	°C	kg/hr	R per month
Damper fully closed	72	79,087	None	134	None	None
Damper 10% open	72	79,249	7,925	129	18	R23,849 – R35,478

Conclusion

This research has thoroughly investigated the impact of common boiler equipment anomalies on the efficiency of co-generation power plants, with a particular focus on operations within the sugar industry. By applying thermal modelling techniques and cost evaluations, this paper has quantified the performance deficits that are associated with seven key anomalies that range from refractory and insulation failures to air heater bypass and economiser degradation.

Each anomaly, while varying in its direct effect on the thermal efficiency, invariably contributes to an increased supplementary coal consumption and, therefore, higher operational costs. The findings demonstrate a consistent correlation between the presence of equipment anomalies and the need for coal co-firing, even under optimal bagasse combustion conditions. For instance, a damaged refractory was shown to increase the flue gas outlet temperature and reduce the boiler efficiency, which led to a coal cost of up to R853,444 per month. Similar efficiency penalties were observed across all the other studied cases, which underscores the cumulative financial and operational impact of neglecting boiler maintenance.

The case studies reinforce the critical importance of comprehensive and proactive maintenance regimes, particularly those involving OEM-guided annual inspections. Preventative maintenance not only mitigates the risk of unplanned down-times, but it also safeguards against the erosion of operational efficiency and contractual penalties in the power purchase agreements.

In conclusion, this paper emphasises that it is essential to pay meticulous attention to boiler integrity and component performance, in order to optimise the thermal efficiency, to reduce the fuel costs and to ensure reliable power generation. Investing in routine inspections and prompt anomaly resolution is not merely a maintenance strategy, but it is also a fundamental requirement for sustainable and profitable plant operation.

References

Cengel YA and Ghajar AJ (2015). Heat and Mass Transfer Fundamentals & Applications, 5th ed. McGraw-Hill.

Johnson Controls (1991). Damper and Actuator Manual p 268

Rawlins BT, Marais F and van den Berg CS (2024). A holistic approach to the optimisation of industrial co-generation plants. *South African Sugar Technologists' Association* (96): 320-329.

FULL PAPER

CFD STUDY ON BAGASSE SPREADER AIRFLOW AND DEFLECTOR PLATE CONFIGURATIONS: IMPACTS ON FUEL DISTRIBUTION AND BOILER PERFORMANCE

Rawlins, BT[1], Marais, CFP[1] and de Villiers, E[1]

[1]John Thompson, a division of ACTOM Pty Ltd, Cape Town, South Africa

bradr@johnthompson.co.za, francoism@johnthompson.co.za, etienned@johnthompson.co.za

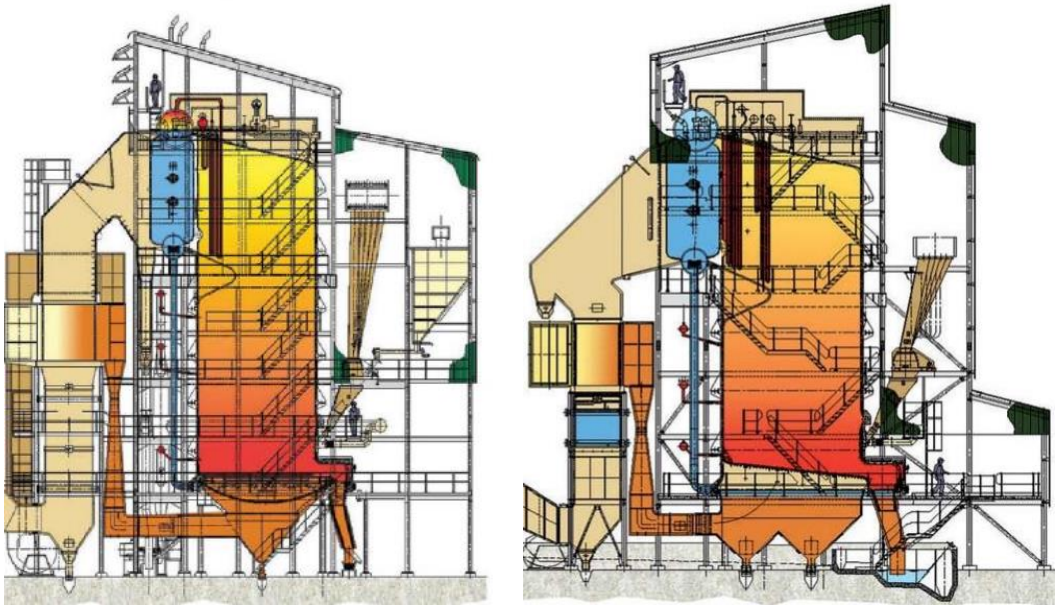
Abstract

Achieving optimal bagasse distribution in grate-fired boilers is critical for efficient combustion and operational reliability. This study focuses on the influence of spreader airflow profiles and deflector plate positioning, relative to the air slot. Using Computational Fluid Dynamics (CFD), several key scenarios are analysed, including oversized air slots, airflow blockages and improper deflector plate placements. The results indicate that deviations, such as obstructed, or excessively wide air slots create uneven fuel trajectories, which cause poor distribution across the grate with high-density zones near the side and rear walls of the furnace. Furthermore, the incorrect positioning of the deflector plate can lead to the poor distribution of bagasse on the grate and it increases the likelihood of chute blockages occurring. By comparing these configurations to an optimal setup, where the spreader air pressure is maintained and the deflector plate is correctly aligned, this study provides valuable insights into the design and operational parameters that influence the distribution of fuel on the grate.

***Keywords*:** Grate-fired boilers, bagasse distributions, deflector plate positioning, Computational Fluid Dynamics

Introduction

The most common types of grate-fired boilers in the South African sugar industry are Continuous Ash Discharge (CAD) stoker and the pin-hole grate-fired arrangements Each configuration offers distinct advantages, particularly when firing bagasse, which is a fibrous by-product of sugarcane-processing that is widely used as fuel in these boilers. Regardless of the grate type, both systems rely on the pressurised distribution air to achieve effective fuel delivery and combustion within the furnace (Laubscher & de Villiers, 2021). Figure 1 below illustrates the general arrangement of a CAD stoker and a pin-hole grate boiler, which are typically found in South African sugar mills.



a.) Typical CAD grate. b.) Typical pin-hole grate.

Figure 1. Typical arrangement of a a) CAD stoker and b) pin-hole grate boiler

Effective fuel distribution is essential for promoting stable and efficient combustion on the grate. A critical factor influencing the bagasse distribution is the configuration of the spreader system. This system depends on the distribution air slot profile and strategically-positioned deflector plates to ensure the uniform dispersion of bagasse into the furnace (Laubscher & van der Merwe, 2021). Deviations in these elements, such as oversized air slots or incorrectly-positioned deflector plates, can result in poor fuel trajectories, which lead to uneven distribution, localised fuel piling on the grate, and increased unburnt carbon losses, all of which can degrade the overall boiler reliability (Rousseau *et al*., 2023).

This study employs Computational Fluid Dynamics (CFD) to investigate the effects of spreader airflow profiles and deflector plate positioning on the bagasse distribution over the grate. The simulated configurations are based on observations from recent boiler inspections, which highlighted common issues, such as incorrectly-aligned deflector plates and warped or oversized air slots.

These real-world deviations formed the basis for the load cases analysed in this work. By identifying the key parameters influencing the fuel spread, the study provides practical insights into maintaining the optimal spreader configurations. The findings serve as a valuable guide for boiler operators, offering recommendations that align with the Original Equipment Manufacturer (OEM) specifications. Implementing these best practices can enhance combustion efficiency and improve the overall reliability of grate-fired boiler systems.

Methodology/Approach

Boiler configuration

The study focuses on a Continuous Ash Discharge (CAD) stoker boiler with a steam generation capacity of 100 tons per hour (tph) and a steam-to-fuel ratio of 2.1. The boiler is equipped with the latest deflector plate configuration and spreader arrangement. The outcomes of this study are expected to provide practical insights for operators seeking to

improve the fuel dispersion in similar grate-fired boiler systems, such as a pin-hole grate boiler.

CFD modelling methodology

A two-part CFD approach was employed to evaluate the effect of air slot configuration and deflector plate positioning on the bagasse spread. The computational domain was split into two independent regions, as described below:

1. The *distribution air ducting domain*, which models the airflow through the air slots; and
2. The *furnace domain*, which simulates the bagasse injection and distribution, using velocity profiles patched from the ducting simulations.

This approach allowed for a decoupled, yet representative, evaluation of the influence of air slot geometry and deflector plate configurations on particle trajectories. The ducting domain was solved separately for multiple air slot geometries (OEM, oversized and warped), with simulations conducted at a constant operational inlet pressure of 4500 Pa. This constant pressure represents the typical operating pressure. The resulting velocity profiles at the air slot outlets were extracted and patched into the furnace domain as inlet boundary conditions. Figure 2 below highlights the two independent computational domains.

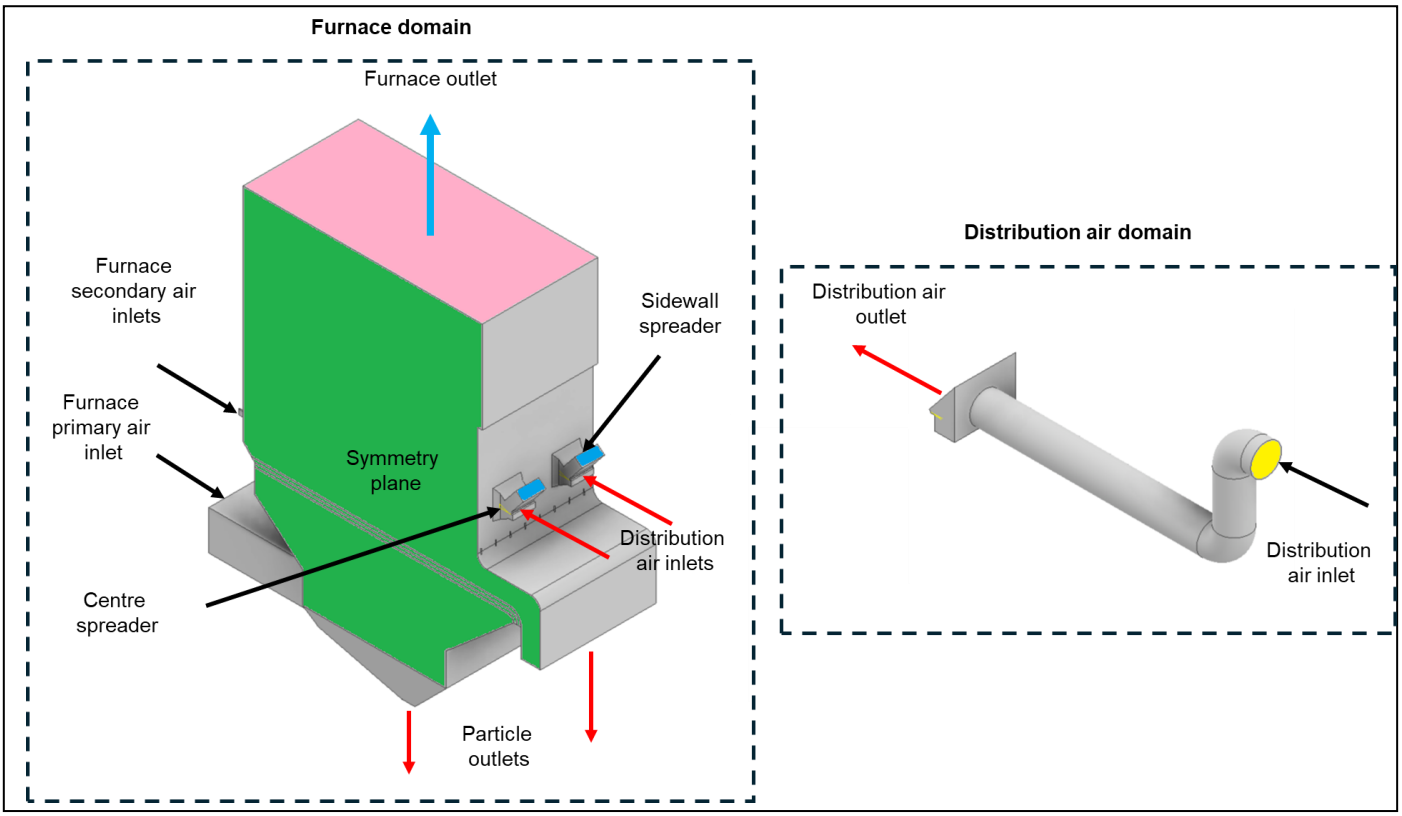


Figure 2. CFD computational domain of the furnace and distribution air ducting

Within the furnace domain, the spreader system and deflector plates were modelled in detail. The primary air and secondary air were modelled as velocity inlets, with the air temperatures being set to the respective operational combustion air temperatures. The furnace domain was modelled on a symmetry plane located on the centreline of the boiler to reduce the computational requirements, while maintaining a sufficiently-detailed representation of the

spreader and fuel distribution system. While it is acknowledged that full-scale bagasse-fired boilers exhibit complex flow behaviour near the sidewalls, including crossflow and swirling, the use of a symmetry boundary is justified in this study for several reasons. Firstly, the investigation focuses on the dispersion and landing patterns of bagasse particles on the grate, rather than on the detailed modelling of solid-phase combustion or wall heat transfer. Secondly, the fuel spreader system is typically mounted symmetrically, with respect to the furnace geometry, and the furnace itself is designed to promote a uniform flow in the central region, where the bulk of combustion occurs. Although asymmetries near the sidewalls may influence the local flow fields, these effects are considered secondary for the purposes of evaluating the initial particle distribution trends. The limitations of the symmetry assumption are acknowledged, and future studies may incorporate the full furnace geometry to resolve wall-induced flow deviations more explicitly.

Bagasse particles were introduced on inlet planes above the air slots (see Figure 3), using the discrete phase modelling approach (ANSYS, 2022) to simulate the particle-laden flow that interacts with the continuous phase (i.e. air flow profiles). A non-spherical correlation for the drag force coefficient was utilised to correctly capture the higher drag forces cylindrical particles experience (Laubscher & van der Merwe, 2021). A Rosin-Rammler particle size distribution was used in modelling the bagasse particle size distribution into the domain. Table 1 below highlights the particle size distribution parameters.

Table 1. Rosin-Rammler particle distribution parameters

Size distribution parameter	Value	Unit
Mean particle diameter	1.43	mm
Maximum particle diameter	9.146	mm
Minium particle diameter	0.189	mm
Spread parameter	0.8379	-

Solid-phase combustion was not included, as the study focuses solely on the aerodynamic and geometric influences that affect the bagasse dispersion and distribution onto the grate.

Mesh, solver and boundary conditions

To ensure grid-independent results, a mesh refinement study was conducted for the baseline (Load Case 1) scenario. Three mesh densities were evaluated: coarse (400 000 cells), medium (800 000 cells), and fine (1.6 million cells). Particle landing profiles and flow field characteristics were compared across these mesh levels, in order to assess convergence. The results showed a negligible variation between the medium and fine meshes, confirming that the medium mesh provided sufficient resolution for accurate predictions, while maintaining computational efficiency. This mesh was subsequently adopted for all the load cases, with local refinements applied, when necessary, to accommodate for the geometry variations. To maintain the numerical stability and mesh quality, the aspect ratio was restricted to below 20, and the mesh orthogonality was kept above 0.2 throughout the domain.

All CFD simulations were performed by using ANSYS FLUENT 2024 R1 with the pressure-based solver. The realizable k-e model was used to capture the turbulent effects. The pressure–momentum coupling was handled by using the SIMPLE algorithm. The momentum and turbulence equations were discretised by using second-order upwind schemes to enhance the solution accuracy, while the discrete phase equations utilised a first-order scheme for the solution stability. The pressure equation was solved by using the standard discretisation method.

Load case definitions

A total of eight load cases were simulated to evaluate the impact of the geometric deviations commonly observed during boiler inspections. These cases are summarised in Table 1. Load Cases 1 to 6 vary the deflector plate configuration, while maintaining the OEM air slot profiles. Load Cases 7 and 8 evaluate the impact of the air slot deviations (i.e. a larger air slots) using the OEM deflector configuration. Table 2 below summarises the simulated load cases for the various air slot and deflector plate configurations.

Table 2. Load Cases 1 to 8 for various air slot and deflector plate arrangements

Load case No.	Air slot configuration	Deflector plate configuration
1	Standard	Standard deflector plate.
2	Standard	Deflector plate with no chevrons.
3	Standard	Deflector plate with large chevrons.
4	Standard	Standard deflector plate tilted to the maximum downward position.
5	Standard	Standard deflector plate tilted to the maximum upward position.
6	Standard	Standard deflector plate offset from air slot – older configuration.
7	Larger air slot	Standard deflector plate.

Further clarification of the load case setup is shown in Figure 3 (a to c). Figure 3(a) illustrates the standard configuration of the deflector plate and air slot. Figure 3(b) and (c) illustrate the configuration of the centre and sidewall deflector plates, highlighting the different chevron arrangements, respectively.

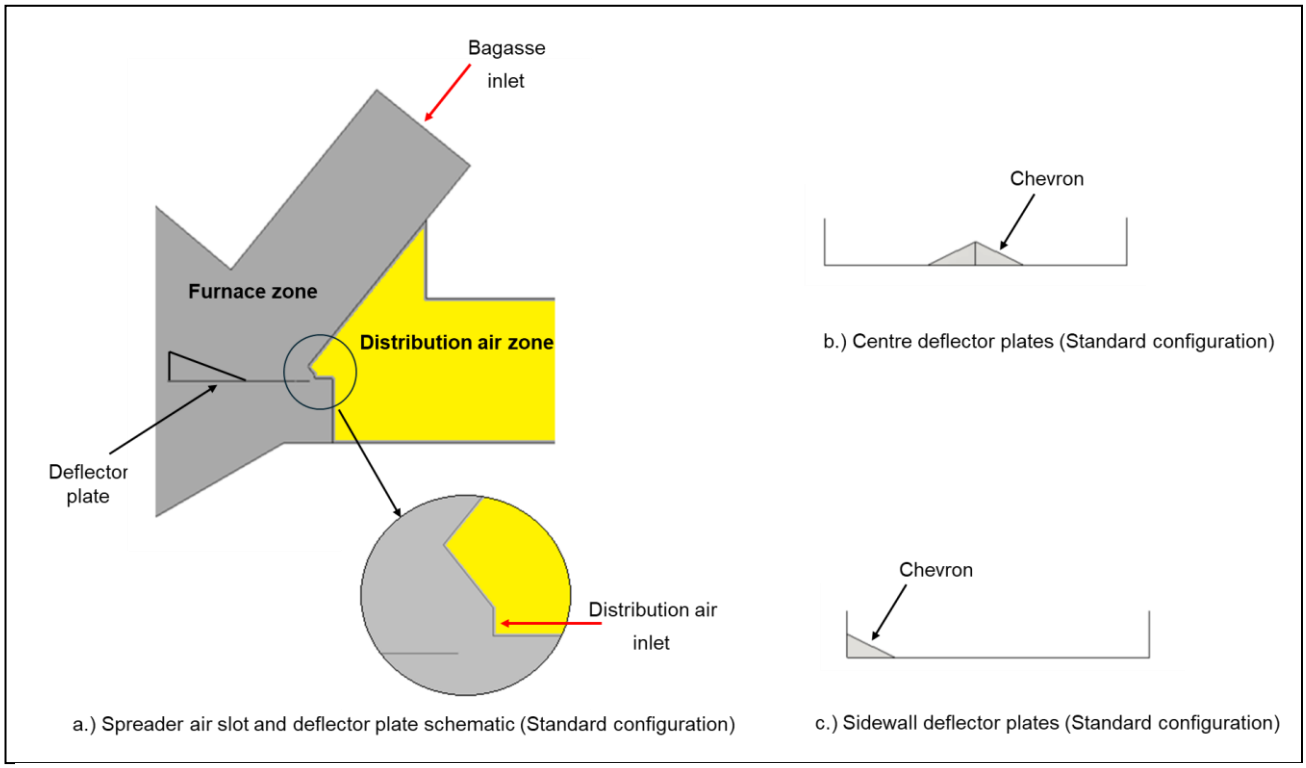


Figure 3. Standard configuration of the (a) air slot and deflector plate, (b) centre spreader deflector plate, and (c) side-wall deflector plate

To improve clarity for readers who are unfamiliar with bagasse spreader systems, the key terms used in the manuscript are defined and illustrated in Figure 4. A chevron in this context refers to the V-shaped plate positioned on the deflector plate/s to guide and distribute the falling bagasse across the combustion surface (see Figure 3). The term 'offset' describes an earlier configuration in which the deflector plate was positioned significantly off-centre, relative to the air slot. In the current design, this offset has been substantially reduced to improve the alignment and spreading performance. 'Warped' refers to the deformation of the air slot over time, due to prolonged exposure to thermal and mechanical stresses.

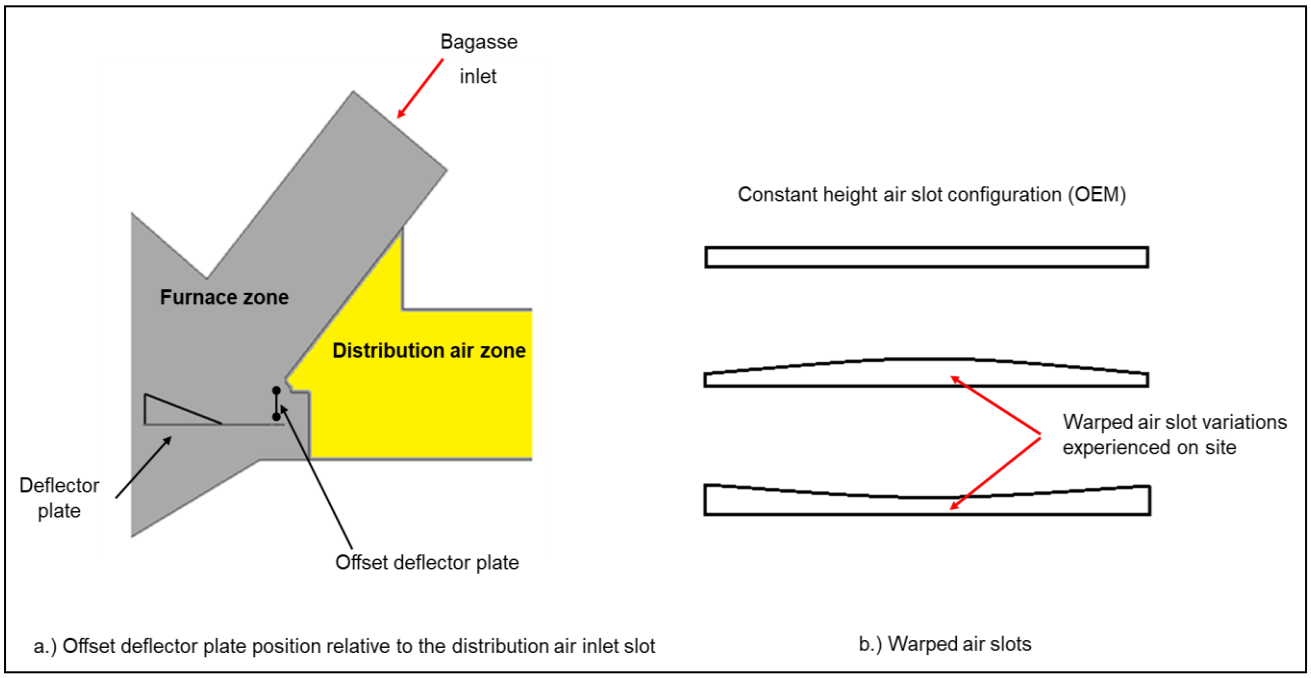


Figure 4. Load case schematic aids for (a) an offset deflector plate configuration and (b) warped air slot illustrations

Results

Previous studies have shown that for a bagasse-fired boiler, approximately 20 to 30% of the bagasse ends up burning on the grate (dependent of the fuel moisture content) (du Toit & Meyer, 2015), with the remainder burning in suspension. This finding highlights the critical role of the initial particle distribution in influencing combustion efficiency, burn-out rates and ash formation. Since a significant portion of the fuel remains on the grate for combustion, ensuring that the particles are evenly spread is essential for optimal grate combustion. Figure 5 below illustrates the distribution of dominant combustion species mass fractions within the furnace.

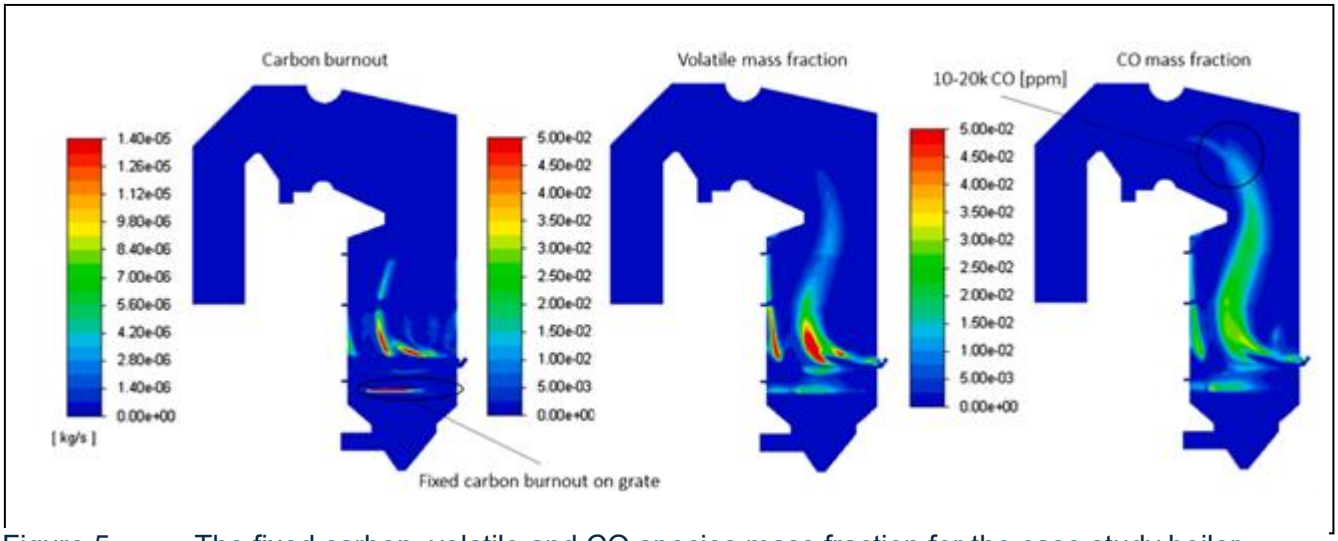


Figure 5. The fixed carbon, volatile and CO species mass fraction for the case study boiler (Laubscher & van der Merwe, 2021)

The ideal particle distribution should have most of the particles distributed within the first third of the grate, taken from the rear wall, to liberate any reminiscent moisture, and subsequently, the volatiles left in the particle. In John Thompson boilers, the rear third of the grate are typically designed to encourage a highly-turbulent and oxygen-rich zone to achieve the initial phases of solid fuel combustion (i.e. moisture evaporation and devolatilisation) before the onset of char burnout on the grate, as seen in Figure 5).

Thus, Figure 6 illustrates the ideal particle distribution on the grate, whereby particle concentrations are skewed towards the rear of the grate, with minimal concentrations occurring near the rear wall and the sidewalls (i.e. to prevent piling near the walls).

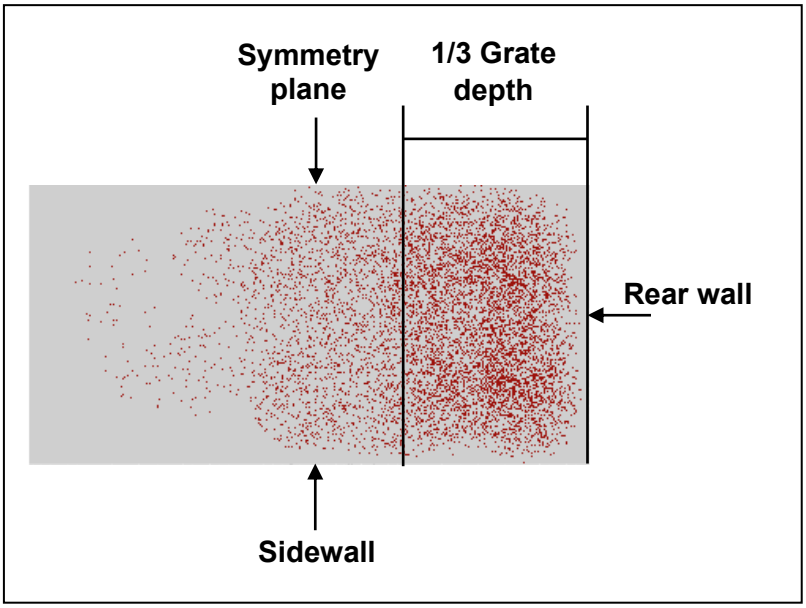


Figure 6. Ideal particle distribution on the grate

Load Case 1

Load Case 1 considers the OEM air slot configuration and the standard deflector plate configuration (as per Figure 3). Figure 7 highlights the resultant particle distribution across the grate.

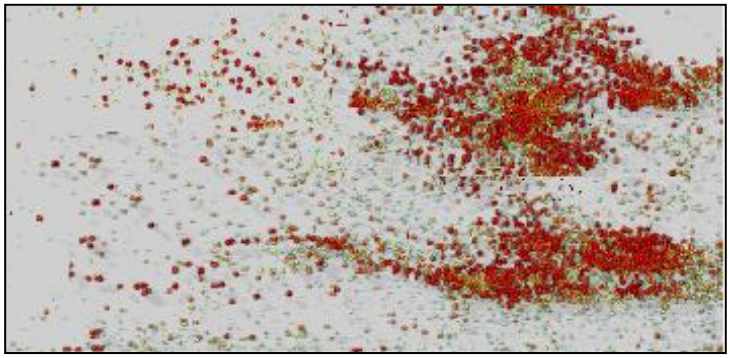


Figure 7. Particle distribution for Load Case 1

The standard OEM configuration results in a reasonably good fuel distribution compared to the ideal case shown in Figure 6, with the majority of particles settling on the rear third of the grate. Minimal particle accumulation is observed near the side and rear walls, reducing the risk of fuel piling in those regions.

Load Case 2

The simulation of Load Case 2 considers the results of having no chevrons on the deflector plate. The centre deflector plate chevrons were designed to promote adequate spreading across the width of the grate, whereas the sidewall chevrons were designed to mitigate the likelihood of bagasse piling on the sidewalls.

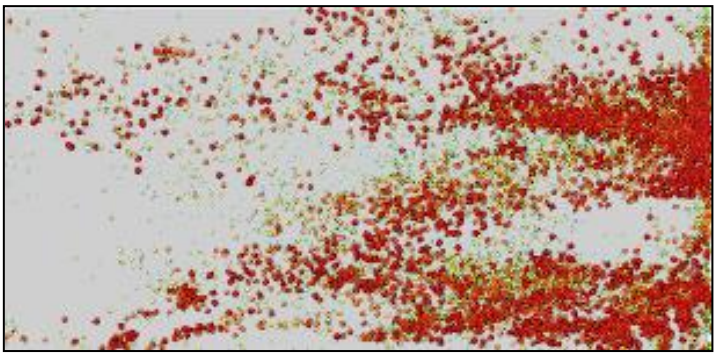


Figure 8. Particle distribution for Load Case 2

Figure 8 highlights the resultant particle distribution on the grate. Much higher concentrations of particles are observed closer to the side wall and rear wall, in comparison to Load Case 1. Continued operation, even on a CAD stoker, increases the likelihood of piling occurring in those areas, since less primary air can propagate through to aid in combustion. The use of chevrons on the deflector plates does promote a more uniform distribution of fuel on the grate, whereas their absence results in particle trajectories that are less governable, resulting in uneven fuel distribution, with localised concentrations near the walls.

Load Case 3

Considering the importance of chevron on the deflector plate, the same can be said for chevrons that are over-/undersized, with the latter more likely to emulate the results of Load Case 2. Load Case 3 addresses a defect, which involves the use of a significantly larger fabricated chevron. Figure 9 provides an example of an oversized chevron being used on site. For this, both the centre and sidewall deflector plates were modelled with chevrons double in size, in comparison to the OEM deflector plate chevrons.



Figure 9. Example of both chevron plate deviation from the OEM design and an example of deflector plate tilted in the upmost direction

The fuel distributions are presented in Figure 10. Larger chevron angles cause heavier fuel particles to settle nearer to the spreaders, shortening their time on the grate and likely increasing unburnt fuel and carbon losses.

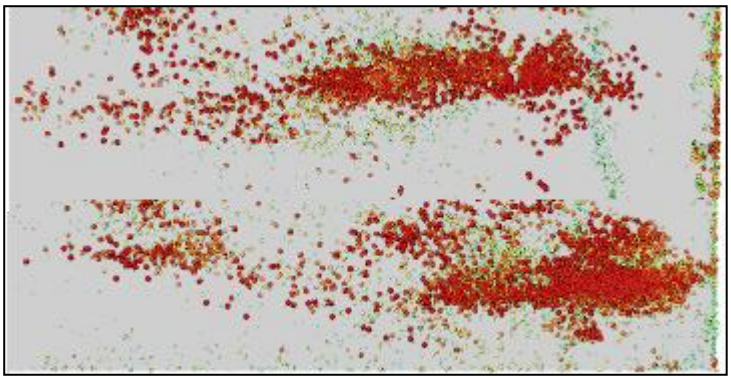


Figure 10. Particle distribution for Load Case 3

Load Case 4

Load Case 4, considers the deflector plate tilted to the maximum downward configuration. Examples of this configuration are provided in Figure 11 (a) and (b), which emanate from recent visual inspections highlighting the poor configurations that deflector plates can be subjected too.



(a) Example 1 - Downward tilt and large



(b) Example 2 - Downward tilt.

Figure 11. Industrial examples of downward angled deflector plates

The resultant particle distribution of Figure 12 showcases the poor distribution across the grate. Particles are concentrated closer to the spreader, which would result in an increase in unburned fuel losses and could lead to most of the primary air bypassing the main fuel zone location on the grate. This configuration results in the poorest particle distribution and should be avoided during operation.

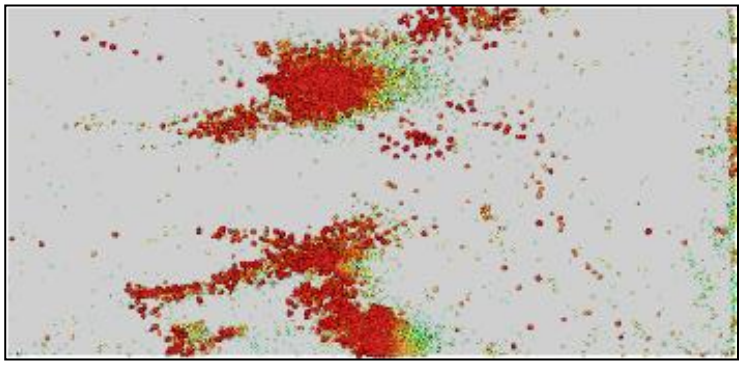


Figure 12. Particle distribution for Load Case 4

Load Case 5

For this load case, the deflector plate is simulated for a deflector plate inclined to the steepest angle. Industrial examples are shown in Figure 9 and Figure 11(a). Figure 13 highlights the fuel distribution across the grate. A reasonable distribution is achieved, in comparison to the ideal case.

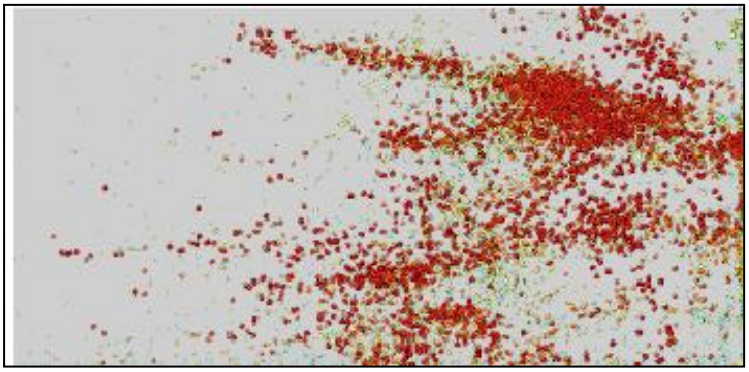


Figure 13. Particle distribution for Load Case 5

However, this configuration has been known to lead to fuel choking, due to the fuel building and wedging itself between the deflector plate and the air slot inlet. Thus, this configuration is not recommended for continued operation.

Load Case 6

Load Case 6 considers a deflector plate that is offset downwards in relation to the inlet air slot (consider Figure 3Figure 4(a)), which is an older deflector configuration. Figure 14 illustrates a fuel distribution on the grate further away from the rear walls, when compared to that in Figure 7 (representing the current deflector to air slot configuration).

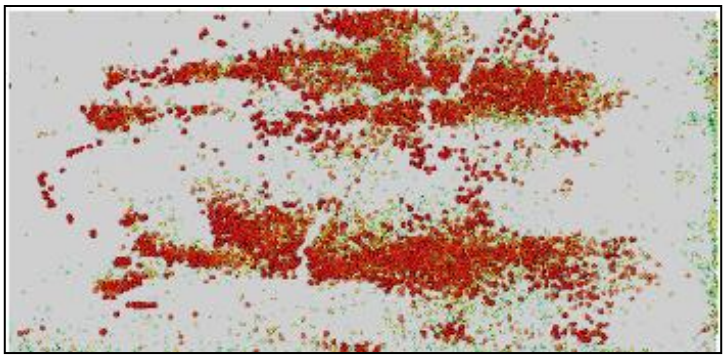


Figure 14. Particle distribution for Load Case 6

Due to the offset, a larger percentage of the fuel particles lack the momentum, provided by the distribution air inlet, to penetrate deeper into the domain. The operation of such deflector plates are prone to choking, due to the build-up of fuel between the air slot and deflector plate, because of the higher recirculation that occurs in the said zone, as illustrated in Figure 15.

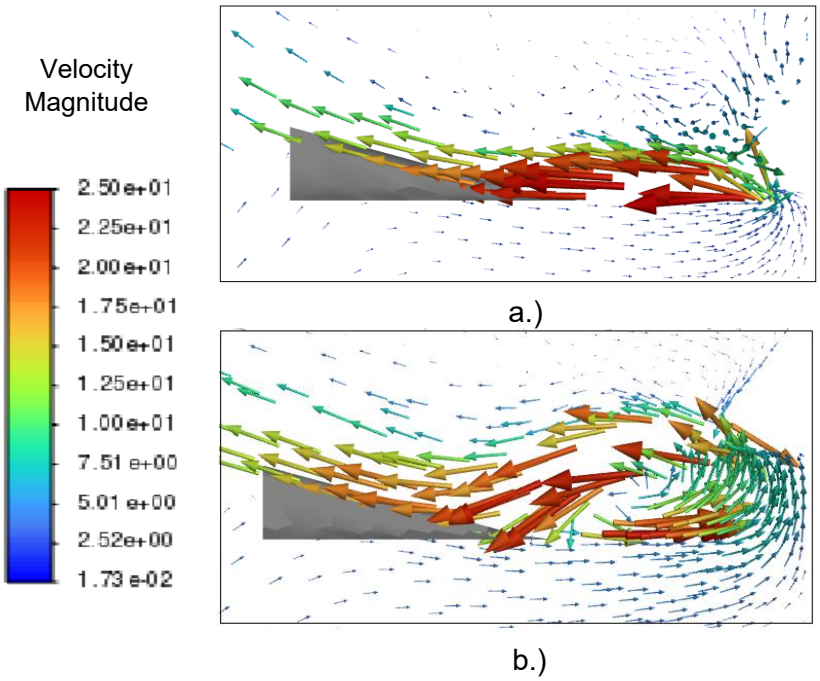


Figure 15. Velocity vector fields for (a) OEM deflector plate and air slot arrangement and (b) the offset deflector plate and air slot configuration

Load Case 7

The final load case that this study considered was the variation of the air slot area. A typical example is presented in Figure 16 (consider Figure 3Figure 4(b)), which shows a badly-maintained air slot that is in need of attention.



Figure 16. Industrial example of large and deformed air slots

Figure 17 presents the fuel distribution on the grate because of the larger air slot. A fair fuel distribution is achieved in the rear third of the boiler, with higher concentrations of fuel being located nearer to the rear and side walls, when compared to the ideal case of Figure 6 and Load Case 1.

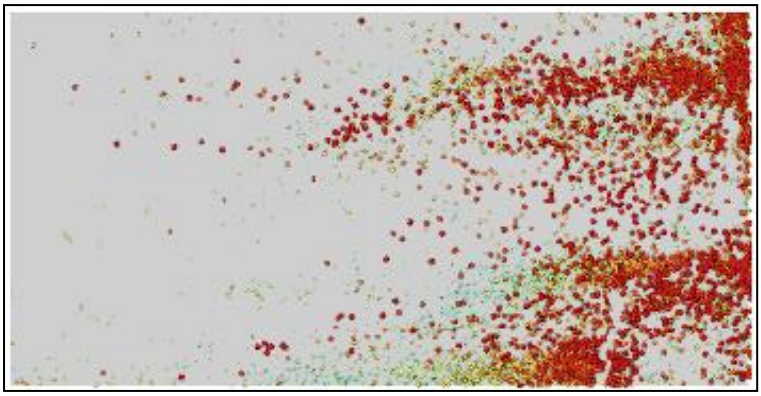


Figure 17. Particle distribution for Load Case 7

However, a larger air slot for the same inlet pressure conditions results in the mass flow of distribution air increasing by 20%. This can adversely affect combustion by introducing excess cold air. While it may be tempting to adjust the inlet pressure damper to reduce the flow through the oversized slot, this approach is not recommended, as the damper typically controls the distribution of the air supplied to all spreaders. Reducing the overall pressure to compensate for one faulty spreader may impair the performance of the others, which may lead to inadequate spreading, uneven fuel distribution and poor combustion conditions. Instead, it is recommended that oversized or warped air slots should be restored to the Original Equipment Manufacturer (OEM) specifications, which will ensure a balanced flow across all the spreaders and it will enable a fine-tuned, uniform operation.

Discussion

To support the graphical results in the comparative analysis, the percentage of fuel mass landing on the rear third of the grate has been extracted for each load case and summarised in Table 1 below. This metric is an important indicator of the fuel burn-out potential, as it reflects the ability of the system to transport fuel deep into the grate area, where the residence time is maximised.

Table 3. Mass percentage landing on the rear third of the grate

Load Case	Description	% Mass on Rear Third
1	OEM air slot & standard chevron	61%
2	No chevrons	56%
3	Oversized chevrons	48%
4	Deflector tilted steeply downward	22%
5	Deflector inclined steeply upward	55%
6	Offset deflector (older design)	48%
7	Oversized air slot (20% flow increase)	58%

Load Case 1, which represents the OEM configuration, performs best with 61% of fuel reaching the rear third, therefore closely matching the ideal case. Load Case 2, in which the chevrons are removed, shows a drop to 56%; however, the lack of directional control allows more fuel to accumulate near the rear and sidewalls. In contrast, Load Case 3's oversized chevrons cause heavier particles to settle near the front of the grate, reducing rear-third coverage to 48%.

The steep downward deflector in Load Case 4 exhibits the poorest performance, with just 22% of the fuel reaching the rear. Load Case 5, where the deflector is steeply inclined upward, performs better (55%), although it introduces the risk of physical obstruction and fuel choking, as well as the increasing risk of fuel carry-over occurring. The outdated Load Case 6 configuration (offset deflector) also demonstrates a reduced penetration, with only a 48% rear-third coverage. Lastly, Load Case 7, which simulates an oversized air slot, achieves a 58% coverage, but introduces other operational challenges that must be carefully managed.

These results reinforce the importance of maintaining OEM-specified geometries and they highlight the influence that small design deviations have on overall grate fuel loading.

Conclusion

This study demonstrates the critical impact that deflector plate configurations and air slot geometries have on bagasse distribution in grate-fired boilers. CFD simulations of various real-world deviations, drawn from field inspections, highlighted how even minor misalignments or oversized components can significantly disrupt the fuel trajectories. These disruptions lead to poor combustion conditions, such as fuel piling, a reduced residence time and increased unburnt losses. Of all the scenarios, the OEM configuration consistently yielded the most uniform fuel spread, which underscores the importance of adhering to the original design specifications. By maintaining the proper alignment and sizing of the deflector plates and air slots, operators can enhance combustion performance, improve thermal efficiency and reduce maintenance frequency. The findings offer actionable guidance to boiler operators, and they reinforce the value of routine inspections and corrective maintenance to uphold an optimal fuel distribution in biomass-fired systems.

References

ANSYS (2022). *ANSYS Fluent Theory Guide*, 20th ed.; Ansys Inc.: Canonsburg, PA, USA.

du Toit P and Meyer C (2015). *The development and validation of a computational fluid dynamics model of an industrial water-tube boiler burning bagasse.* Master's Thesis, Stellenbosch University.

Laubscher R and de Villiers E (2021). Integrated mathematical modelling of a 105 t/h biomass fired industrial water-tube boiler system with varying fuel moisture content. *Energy*, Volume 228, 120537, https://doi.org/10.1016/j.energy.2021.120537

Laubscher R and van der Merwe S (2021). Heat transfer modelling of semi-suspension biomass fired industrial water-tube boiler at full and part-load using CFD. *Thermal Science and Engineering Progress,* Volume 25, 100969, https://doi.org/10.1016/j.tsep.2021.100969

Rousseau P, Laubscher R and Rawlins BT (2023). Heat transfer analysis using thermos-fluid network models for industrial biomass and utility scale coal-fired boilers. *Energies,* 16(4), 1741, https://doi.org/10.3390/en16041741

Yin C, Rosendahl L, Clausen S and Hvid SL (2011). Characterizing and modelling of an 88 MW grate-fired boiler burning wheat straw: Experience and lessons*. Energy,* Volume 41, Issue 1, pages 473-482, **https://doi.org/10.1016/j.energy.2012.02.050**

FULL PAPER

SHAFT-MOUNTED PLANETARY MILL DRIVE FOR FACTORY EXPANSION AND MILL PERFORMANCE IMPROVEMENT

Patil M[1], Carroll B[2] and Kristensen P[3]

[1]Sales Director Industrial and Sugar Division Dinamic Oil SPA Italy
[2]Product Support - Sugar: BMG South Africa
[3]Director Business Development Dinamic Oil SPA Italy

m.patil@dinamicoil.com, brettc@bmgworld.net, p.kristensen@dinamicoil.it

Abstract

As global demands for energy, food security and renewable biomass grow, sugarcane becomes an essential alternative to fossil fuels, especially in bioenergy production. Meanwhile, sugar mills worldwide are shifting from long crushing seasons to shorter, high-efficiency periods that are focused on maximum sucrose recovery. This shift has led to increased production capacity targets, which are often constrained by the high capital costs of traditional expansion. A major expense in mill expansion is the drive system, which includes motors, variable-speed drives, civil foundations, as well as the related infrastructure.

In response, this paper explores the strategic application of shaft-mounted planetary drive systems as compact, efficient solutions that enable mills to modernise with minimal structural modifications and a lower capital investment. These systems can serve as auxiliary drives or complete replacements, which makes them suitable for both retrofitting existing mills and new constructions. Using case studies from India and Central America, as well as performance data from global installations, the paper reports the following key results: a 24% reduction in power consumption, a 4.5% increase in bagasse extraction and the maintenance of bagasse moisture levels below 49%. The simple design eliminates components like pinions and tail bars, which decreases the mechanical stress by up to 50%, thereby reducing the inventory needs and prolonging the lifespan of mill parts.

This research confirms that shaft-mounted planetary drives are more than mechanical upgrades; they also support sustainable, cost-effective and scalable milling operations. Their adoption enhances operational efficiency and aids strategic cost control, which is vital in today's competitive and energy-conscious industry. In addition, the paper offers practical insights from Dinamic Oil's retrofit projects, by providing mill operators with proven methods to reduce expansion costs, to decrease energy use and to optimise the overall milling performance.

Keywords: Shaft-mounted planetary drives, sugarcane bioenergy, mill retrofitting, energy efficiency in milling, capital expenditure optimisation

Introduction

As the global sugar demand grows and the pressure for sustainable and energy-efficient methods increases, sugar mills must make vital decisions when they are expanding or upgrading. The key is to choose the right juice extraction technologies and their drive systems. Although many

technological options exist, they vary in how well they meet the rising demand for cost efficiency, energy savings, operational reliability and capital investment (Huges, 1964; Hugot, 1986).

Expanding an existing sugar mill - usually a brownfield site with spatial, structural and power limitations - demands a well-balanced engineering and strategic plan. Mill operators need to evaluate a wide array of technical and economic factors, including the following:

- project timelines and overall capital expenses (CAPEX);
- compatibility with the existing milling infrastructure;
- minimising disruptions to the current operations;
- system simplicity and operational ease;
- low civil and structural modification requirements;
- high reliability, with minimal maintenance costs;
- efficient integration of legacy equipment and modern technology; and
- the highest extraction efficiency with the lowest power and steam consumption.

These considerations are not just engineering choices—they significantly impact the Return on Investment (ROI), operational resilience, and long-term competitiveness. Many mills still use adequate existing roller sizes. Still, projects often face delays due to the high CAPEX that is linked to outdated systems, such as the need for extensive civil works and complete drive-train replacements (Gomez *et al*., 1996; Gardener, 1964).

The drive system typically represents the most significant cost and the main technical challenge during mill expansion. Traditional single-foot-mounted gear technologies, which were once reliable, now exhibit limitations in their flexibility, efficiency, maintenance and scalability. In addition, hydraulic independent drives, which have been standard since the 1990s, also have issues, such as high maintenance costs and a reliance on the oil quality and pressure for performance (Kharbanda *et al*., n.d.). In this changing industrial landscape, a new approach is emerging with pinion-less, shaft-mounted planetary drive systems (Kent & McKenzie, 2001). These eliminate the mechanical inefficiencies found in older technologies, which marks a significant improvement in their performance, cost efficiency and sustainability. By removing the crown pinions, tail-bars and complex gear trains, shaft-mounted drives significantly reduce mechanical stress, down-time, energy losses and maintenance needs, while enhancing the torque control and uniform extraction.

This paper offers a strategic and comparative overview of the current and emerging drive technologies in sugar milling. It explains why the choice of drive system is now a critical factor, and not just a minor detail, in modern mill performance. Through a detailed analysis, real-world case studies and data on transmission efficiency, the discussion shows how advanced planetary systems, especially those that are shaft-mounted, help mills to increase their throughput, lower their power use, cut the maintenance costs and improve the ROI.

As it is aligned with industry sustainability and resource efficiency, this review provides technical insights and strategic guidance for sugar mills that are involved in expansion, modernisation or retrofitting. It convincingly argues that upgrading power transmission systems is more than a technical upgrade; it is a crucial investment in the future of sugar production.

Limitations of the single-foot-mounted technology
(Rodriquez *et al*., 2023)

These limitations include the following:

- a massive civil foundation requirement for gearbox installation;
- a big base frame and support is required;
- assembly skills are required for alignment;
- a large-sized gearbox, hence long delivery;
- huge inventory costs for spares like bearings/carriers;
- no flexibility of independent speed;
- limitations in a mill setting;
- power transmission efficiency loss due to pinion/tail bar/rope coupling;
- no flexibility during expansion, as power and drive capacity are bottlenecks;
- no easy replacement possibilities during shutdown;
- limitation during shock load;
- high down-time for replacement, if the pinion, tail bar or rope coupling fails; and
- limitation during shock load.

Hydraulic independent-drive technology

This technology has been running since the late 1990s. Many factories are still following this technology, but it shows some limitations and disadvantages, for example:

- a high start-up investment;
- high maintenance costs;
- efficiency depends upon oil quality and pressure;
- limitations on speed variations;
- limitation of performance during specific operation parameters; and
- highly-skilled maintenance and operation staff required.

Development of a pinion-less mill

A conventional mill that is driven by an electric motor or turbine, through a set of foot-mounted reduction gearing, tail bar/rope coupling and crown pinions, has the following disadvantages:

- In conventional mills, all the power is transmitted through the square end of the top roll, which drives the bottom rolls via a set of crown pinions. Therefore, very high stress levels develop at the square end and on the crown pinion teeth, and this becomes the primary cause of shaft and pinion failures;
- Pinion reactions at one end of the roller shaft cause an asymmetrical roll lift, which hinders the uniform compression of the cane blanket and thus reduces the efficiency of pol extraction. The inefficiencies, which have been long acknowledged in conventional designs, are emphasised in the seminal research by Hugot (1986), and are further elaborated in mill torque distribution analyses by Kent and McKenzie (2001);
- Throughputs must be limited to prevent excessive stress on the mill headstock and the drive-side top-roll bearing; and
- Wear and the subsequent need to repair the pinions, the tail bar and top roll bearings after each crushing campaign, is a significant issue that the mill engineer must address year after year (Gomez *et al*., 1996).

Extensive market research and observations of the sugar industry's operations have provided valuable insights into the areas that need improvement. Our findings indicate that traditional systems are inefficient and could benefit from upgrades.

Optimising power transmission for sustainable competitiveness: a strategic assessment of drive systems in industrial sugar milling

In the field of industrial manufacturing, especially in energy-intensive sectors, such as sugar milling, transmission efficiency has become a vital performance indicator. As mills aim for operational excellence, cost savings and sustainable development, choosing the right drive system is essential for impacting the energy use and initial investment costs. Mechanical power transmission systems, often neglected in the broader discussions, can significantly affect the reliability of equipment, maintenance needs and profit margins over time. This section compares various drive technologies, and it offers insights into their real-world application, their economic implications, and how they support modernisation efforts to improve a plant's performance.

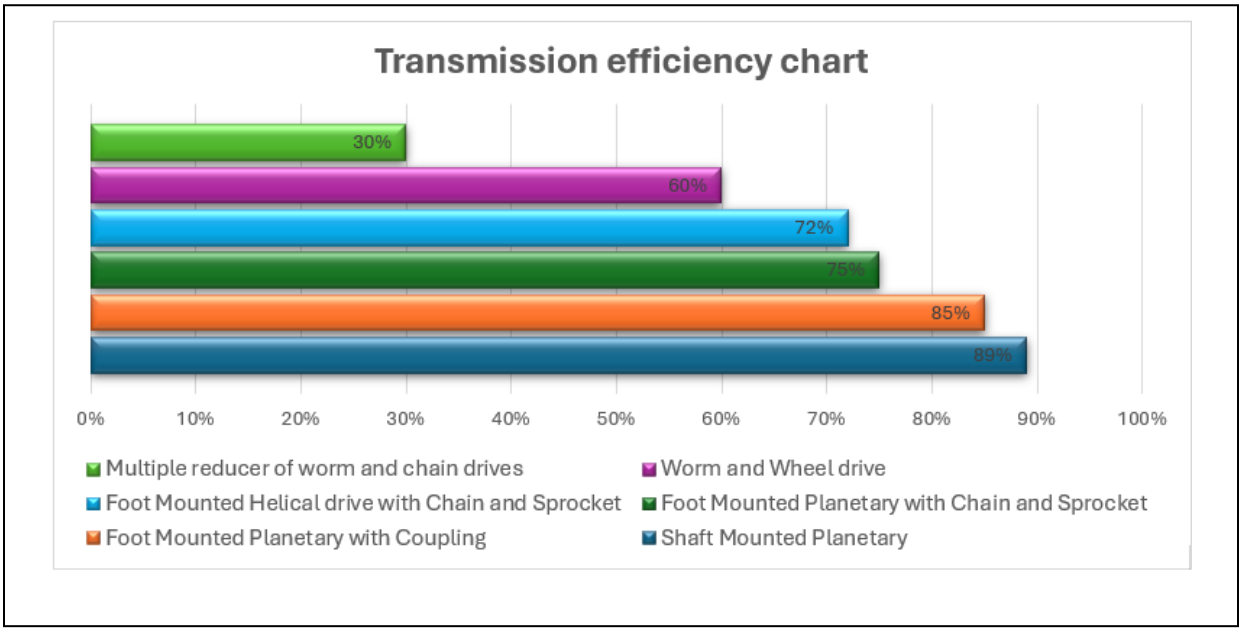


Figure 1. Transmission efficiency chart (Source: Own presentation developed from research by Machado Rodriquez *et al*., 2023)

Figure 1 illustrates a Transmission Efficiency Chart that compares the various drive systems employed in an industrial environment, such as sugar mills. It demonstrates how well each system transmits power, which is represented by the percentage of input power that reaches the output shaft, as guided by Rodriquez *et al*. (2023).

The chart (Figure 1) illustrates the differences in efficiency among various drive mechanisms, and it emphasises the importance of choosing the right transmission system in an industrial setting. Recognising the impact of each configuration is vital for stakeholders who aim to improve their performance, to reduce energy waste and to lower both their capital and operational costs. The following sections systematically review each drive type shown in the chart, which are listed from

the least efficient to the most efficient. These sections detail the efficiency, operational mechanism and practical relevance of each system for modern sugar mills and industrial applications.

Multiple reducer of worm and chain drives (30%)

- Efficiency: Very low (30%).
- Explanation: This set-up uses several stages of power transfer, often involving worm gears and chain drives. Each stage incurs mechanical losses, such as heat, friction and misalignment, which accumulate and significantly reduce the overall efficiency.
- Implication: Outdated and inefficient, this set-up is only appropriate when the cost surpasses energy efficiency. This is likely to result in high operating expenses and increased maintenance costs.

Gardener (1964) and Gomez *et al*. (1996) have previously identified the relative inefficiencies of worm- and chain-based systems, hence endorsing the transition to compact, high-torque alternatives, such as shaft-mounted planetary systems.

Worm and wheel drive (60%)

- Efficiency: Moderate (60%).
- Explanation: Worm gears involve a sliding motion that causes high friction losses. They provide high reduction ratios in small spaces, but their energy losses are considerable.
- Use Case: Commonly employed in low-speed, high-torque scenarios, although they are being gradually replaced in energy-conscious settings.

Foot-mounted helical drive with chain and sprocket (72%)

- Efficiency: Fair (72%).
- Explanation: Uses helical gears, which are more efficient than worm gears, combined with a chain and sprocket system. While this set-up is more efficient than worm drives, the chain still introduces tension and misalignment losses.
- Note: Helical gears are durable and quiet but incorporating chain systems lessens the overall efficiency gain.

Foot-mounted planetary with chain and sprocket (75%)

- Efficiency: Good (75%).
- Explanation: The planetary gear system is recognised for its compact size, its effective load distribution and its high efficiency. Despite this, incorporating a chain and sprocket can lead to some mechanical losses.
- Advantage: It slightly surpasses helical systems that use chains, and it provides an improved power density and load capacity.

Foot-mounted planetary with coupling (85%)

- Efficiency: High (85%).
- This set-up eliminates the chain and sprocket by using a direct coupling. Since couplings typically transmit power more efficiently than chains, this results in a higher overall system efficiency.

- Advantage: The outcome includes reduced mechanical losses and better energy utilisation.

Shaft-mounted planetary (89%)

- Efficiency: Very high (89%).
- Explanation: This compact, integrated drive connects directly to the shaft, which eliminates the need for extra components, such as foundations, couplings or alignment structures. Its direct contact reduces energy loss.
- Benefits include the following:

    - reduced capital expenses (no need for extra foundation or alignment tools);
    - lower maintenance;
    - perfect for retrofits or expansions with space and budget limitations; and
    - highly--recommended for high-efficiency setups, such as in modern sugar mills that are focused on lowering their energy costs and minimising the down-time.

Key insights

- Trend: There is a clear correlation between drive compactness and transmission efficiency.
- Design implication: Transitioning to shaft-mounted planetary systems yields the most energy-efficient setup.
- Capital and operational efficiency: Compact planetary drives not only decrease operational power use, but they also cut capital costs, which is significant in large-scale mill expansions, where managing the expenses is vital.

Strategic recommendation (contextualised for mill operations)

For sugar mills that want to expand their capacity or retrofitting, the data show that investing in shaft-mounted planetary drives is beneficial due to their higher transmission efficiency, their reduced infrastructure needs and the long-term cost savings. Moving from traditional worm or helical-chain drives to advanced planetary systems is a modernisation step that aligns with their sustainability goals and boosts competitiveness.

The comparative analysis of drive systems in this section highlights a key strategic insight, namely, that transmission efficiency is more than just a technical detail; it is essential for industrial competitiveness, energy efficiency and long-term financial stability. In modern sugar milling, where energy consumption, mechanical reliability and cost management are critical, outdated systems such as worm and chain drives pose significant operational risks. Their high energy losses and maintenance demands increase the operational costs, reduce the up-time and limit the throughput. Conversely, the data clearly show a preference for more efficient solutions and emphasise the need for modernisation with compact planetary drive systems, especially shaft-mounted types. These systems achieve the highest energy transfer efficiency at 89%, and they offer lower capital costs for infrastructure elements, including the foundations, alignment tools and couplings. They also enable modular upgrades, which are vital for brownfield expansions and process intensification, without disrupting existing operations. Their adoption provides measurable benefits, including reduced lifecycle costs, a lowered Total Cost of Ownership (TCO) and an increased Return on Invested Capital (ROIC) (Rodriquez *et al*., 2023). Therefore, forward-looking mill operators and project stakeholders should view planetary drives, especially the shaft-

mounted types, as more than just mechanical improvements; they are strategic assets that foster operational excellence and sustainability.

Case Studies

As sugar mills worldwide face the increasing pressure to boost their efficiency, to cut operational costs and to optimise resource use amid rising energy and sustainability demands, targeted upgrades in drive systems and process improvements are becoming essential. This section highlights real-world results from a multi-year case study of a leading sugar mill in South Maharashtra, India, which is often referred to as the 'Sugar Bowl of India'. Facing throughput limits, power shortages and high capital costs, the mill aimed to expand its crushing capacity without replacing its core infrastructure. The study demonstrates how a strategic retrofit with a shaft-mounted planetary drive system resulted in measurable improvements in key areas, including the crushing rate, reduced stoppages, moisture content in the bagasse and sucrose recovery.

Performance Improvement Analysis: Maharashtra Sugar Mill (2021-2024)

A factory located in South Maharashtra, India, is known as the 'Sugar Bowl of India'. The management aimed to expand, while retaining all its existing mill components, and they did not intend to install a new mill. The current tandem includes a zero-mill 38" x 78" and four mills measuring 33" x 66". These mills are top roller-driven through electric drives, and the bottom rollers are driven through crown pinions from the top rollers. The client wants to increase its crushing capacity from 145 to 200 Tons of Cane crushed per Day (TCD). Analysing the previous year's data, it was found that the tandem reached a peak capacity of 3 500 TCD; however, the average seasonal throughput was only 2 900 TCD, due to several constraints, including cane feeding and preparation issues, drive breakdowns caused by over-use, and insufficient overall installed power.

Dinamic Oil SPA evaluated the situation and found that reaching the plant's capacity goals depended on fixing the power shortages. Replacing the existing drives was deemed to be too expensive and capital-intensive, so an economical alternative was necessary. Based on the calculations, the absorbed power data and the predictive analysis, we determined that an additional 110 kW would be enough to achieve the desired throughput and mill performance. Consequently, the total power capacity was set at 510 kW.

This was achieved through a specialised load-sharing programme, where the main electric motor functions as the master, and the auxiliary drive motor functions as the slave. The ratio of installed power to the power absorbed by the main motor served as the reference, and this ratio was maintained for the auxiliary drive. The auxiliary motor was interlocked with the main drive, with the start commands only being issued to the main motor. The gear ratio of the auxiliary drive was chosen to match the reduction ratio of the existing open gear train, which ensured that the final speed of the auxiliary drive matched that of the crown pinion.

Table 1. Performance results at Maharashtra sugar mill in India

.

Parameter	**units**	**2021-2022**	**2022-2023**	**2023-2024**
Average crushing rate	TCD	3150	3950	4680
Stoppages	%	3.9	1.42	0.39

Bagasse moisture	%	51.3	49.3	48.4
Bagasse Pol	% of cane	2.21	2.1	1.96

Source: Own research at sugar mills

Over the three years, from 2021-2022 to 2023-2024, the Maharashtra Sugar Mill exhibited significant improvements in its operational performance, which were driven by enhanced mechanical efficiency, better process controls, and most likely the modernisation of key equipment, such as the milling drive systems. The average crushing rate increased significantly from 3,150 TCD to 4,680 TCD, which was a 48.6% rise, and notable gains were reflected in the throughput and capacity utilisation. This improvement corresponds with the infrastructure upgrades and enhanced asset reliability. The stoppage time, as a share of operational hours, dropped from 3.9% to just 0.39%, a ten-fold reduction, which indicates substantial progress in the system's up-time, maintenance practices and reliable engineering, which are usually linked to adopting more efficient drive technologies and predictive maintenance. The moisture content decreased from 51.3% to 48.4%, which indicated a more effective juice extraction and less residual moisture, which signifies improved milling performance and enhanced energy recovery in the downstream processes, such as cogeneration. The sucrose content declined from 2.21% to 1.96%, which suggests that there was an improved sucrose recovery and extraction efficiency, which are key financial and technical indicators for sugar mills.

These results show a clear trend towards greater efficiency, lower losses and increased operational resilience. Improvements in the crushing rate and fewer stoppages directly lead to a higher daily throughput and lower down-time costs. Meanwhile, a better bagasse quality enhances both the sugar yield and energy co-generation efficiency. Overall, this performance improvement strongly indicates the effects of targeted investments in plant modernisation, which may include the adoption of high-efficiency shaft-mounted planetary drive systems and other optimisations, such as data-driven maintenance, energy savings and resource maximisation.

This case provides a strong benchmark for other mills that are seeking to enhance their competitiveness, operational stability and energy efficiency within a constrained capital environment.

Post-installation performance gains: Central American Sugar Mill (2021-2024)

The client has an existing mill line with a 33" x 66" mill and wishes to upgrade the mill by installing a new, larger mill that measures 40" x 80". The customer requires a new mill with a reduced civil footprint, due to space constraints and the relocation of many pipelines. In addition, the existing material handling system must be able to accommodate the required weight of the drive. Based on these requirements, the customer, the Engineering and Procurement Contractor (EPC) and the Original Equipment Manufacturer (OEM) agreed on a proposal to install all shaft-mounted drives for the mill. The new drives are designed to accommodate for future expansion of up to 8 000 TCD, while delivering the desired mill performance. They are equipped with 160 kW individual drives; two on the top roller and one on each bottom roller. The initial target is to achieve a capacity of 6 000 TCD.

The following results (see Table 2) have been achieved after the installation of the drive:

Table 2. Performance results in Central America

Parameter	units	2021-2022	2022-2023	2023-2024
Average crushing rate	TCD	4430	4980	5850
Bagasse moisture	%	50.72	48.8	47.5
Bagasse Pol	% of cane	2.24	2.04	1.90
Average Absorbed Power	KW/TCH	1.4	1.1	1.05

Source: Own research at sugar mills

After the installation of the new drive system, the Central American sugar mill exhibited consistent operational enhancements across all key performance indicators, over three consecutive crushing seasons (2021-2024). The average crushing rate rose from 4 430 TCD in 2021-2022, to 5 850 TCD by 2023-2024, which indicates a 32.1% increase in the throughput capacity. The observed improvement reflects an enhanced mechanical efficiency and torque management, which has been enabled by the newly-implemented shaft-mounted planetary drive system and has resulted in more reliable and continuous operations.

The quality of the bagasse improved significantly. The moisture content was reduced from 50.72% to 47.5%, thereby increasing its value as a biofuel for cogeneration and lowering the handling costs in the subsequent processes. The Bagasse Pol content, which is indicative of the sucrose loss, decreased from 2.24% to 1.90%. This reduction indicates an improved sugar recovery in milling, an essential element for revenue generation and process efficiency.

The energy efficiency improved significantly. The average absorbed power per ton of cane handled (kW/TCH) decreased from 1.4 to 1.05, which represents a 25% reduction in specific energy consumption. The reduction is strategically important in energy-intensive milling operations, especially in areas that face increasing power costs or sustainability regulations.

These results highlight the strategic importance of focused capital investment in contemporary drive technologies. Compact, shaft-mounted planetary drive systems have resulted in measurable improvements in the throughput, energy efficiency and sucrose recovery. The outcomes enhance the operational resilience of the mill, reduce the carbon intensity and improve its cost competitiveness, which are essential in a sustainability-oriented global sugar market.

Comparative performance analysis: Maharashtra vs Central America

The two case studies from Maharashtra, India, and Central America demonstrate how targeted drive system interventions can significantly improve the operational performance of sugar mills across different geographic, economic and infrastructure contexts. Both facilities faced common challenges, such as a limited capital, suboptimal energy use and mechanical inefficiencies; yet both achieved substantial performance improvements through the implementation of modern shaft-mounted planetary drive systems that were customised to their specific operational conditions.

Table 3. Comparative Performance Improvement Analysis – Maharashtra vs Central America Sugar Mills (2021-2024)

Performance Indicator	**Units**	**Maharashtra (India)**	**% Improvement (2021–2024)**	**Central America**	**% Improvement (2021–2024)**
Average Crushing Rate	TCD	3,150 → 4,680	+48.6%	4,430 → 5,850	+32.1%
Stoppages	%	3.9 → 0.39	−90.0%	N/A	N/A
Bagasse Moisture	%	51.3 → 48.4	−5.6%	50.72 → 47.5	−6.3%
Bagasse Pol (Losses)	% of cane	2.21 → 1.96	−11.3%	2.24 → 1.90	−15.2%
Average Absorbed Power	kW/TCH	N/A	N/A	1.40 → 1.05	−25.0%
Drive Upgrade Strategy		Load-sharing assist drive added (110 kW)	Capital-efficient retrofit	Shaft-mounted planetary drives (4 x 160 kW)	Full drive modernisation
Modernisation Constraints		Retained existing mill structure	Capex-limited expansion	Reduced civil footprint & retrofit space	Space-constrained expansion
Scalability Potential		Moderate – limited by existing structure	Up to 5,000 TCD achievable	High – designed for 8,000 TCD	Future-ready infrastructure

Source: Own research at sugar mills

Key insights and strategic lessons

Throughput gains:
Both mills boosted their crushing capacity, with Maharashtra gaining 48.6%, due to infrastructure optimisation, and Central America gaining 32.1% due to a scalable setup.

Efficiency:
Central America switched to shaft-mounted planetary motors, which improved its energy efficiency (25% reduction in kW/TCH) and bagasse Pol recovery.

Operational reliability:
Maharashtra experienced a 90% decrease in stoppages, which indicates an increased up-time from better drive synchronisation and load-sharing.

Modernisation approach:
Maharashtra employed assist drives to cut costs and retrofit, while Central America used progressive, scalable system architecture, with integrated planetary drives

Strategic alignment**:**

Central America's modular drive configuration and energy footprint reduction assists future expansion, decarbonisation and digitalisation.

Drive modernisation solutions can improve the operations of capital-constrained and greenfield sugar mills, as seen in this comparison. Maharashtra is resourceful, but Central America is scalable and high-performing, following global best practices.

Power-saving comparison in the Indian mill with a conventional and shaft-mounted system

The comparison of the absorbed power in the 400TCH mill for conventional and planetary drive systems is shown in Figure 2. The existing mill has 1 200 kW of installed power, by utilising a traditional steam turbine and a shaft-mounted multiple-reduction system. The tandem was upgraded by installing four 250 kW shaft-mounted motors.

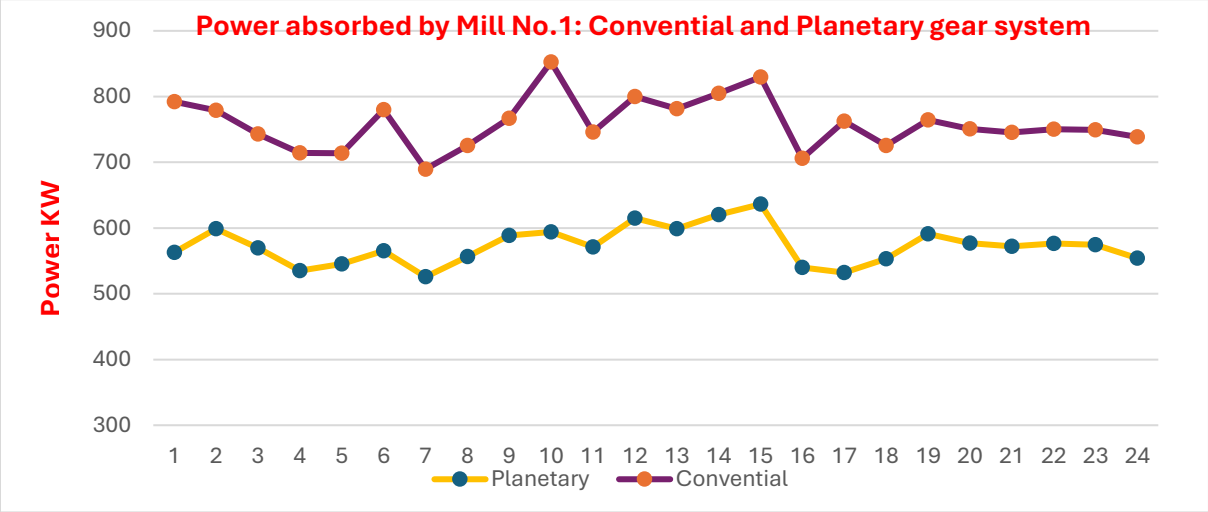


Figure 2. Power absorbed by Mill No. 1: Conventional and planetary gear system (Source: Own research at sugar mills)

This data indicate that approximately 24% of power is saved when switching from an old foot-mounted planetary gear, with a turbine and tail-bar, to a shaft-mounted planetary gearbox for the same crushing rate, which echoes similar findings by Kharbanda *et al*. (n.d.), who indicated that such designs minimise the mechanical losses and enhance the operational reliability. The preparation index, feeding arrangement, roller speed and hydraulic settings were maintained in nearly the same way (the data are based on the daily average absorbed power from the turbine chest pressure and power meter readings for the motor).

The planetary set-up shows a more stable power consumption, while the conventional set-up fluctuates more noticeably, which indicates an inconsistent demand or higher inefficiency (Figure 2). The planetary mill consistently uses less power, which implies a better energy efficiency. Although the conventional mill might offer other mechanical benefits, it consumes more energy and could result in higher operational costs, due to its variability. This trend probably arises from improvements in mechanical design or how power is transmitted in the planetary systems. If reducing energy use is a priority, whether for cost savings, sustainability or system optimisation. the planetary mill is the better choice.

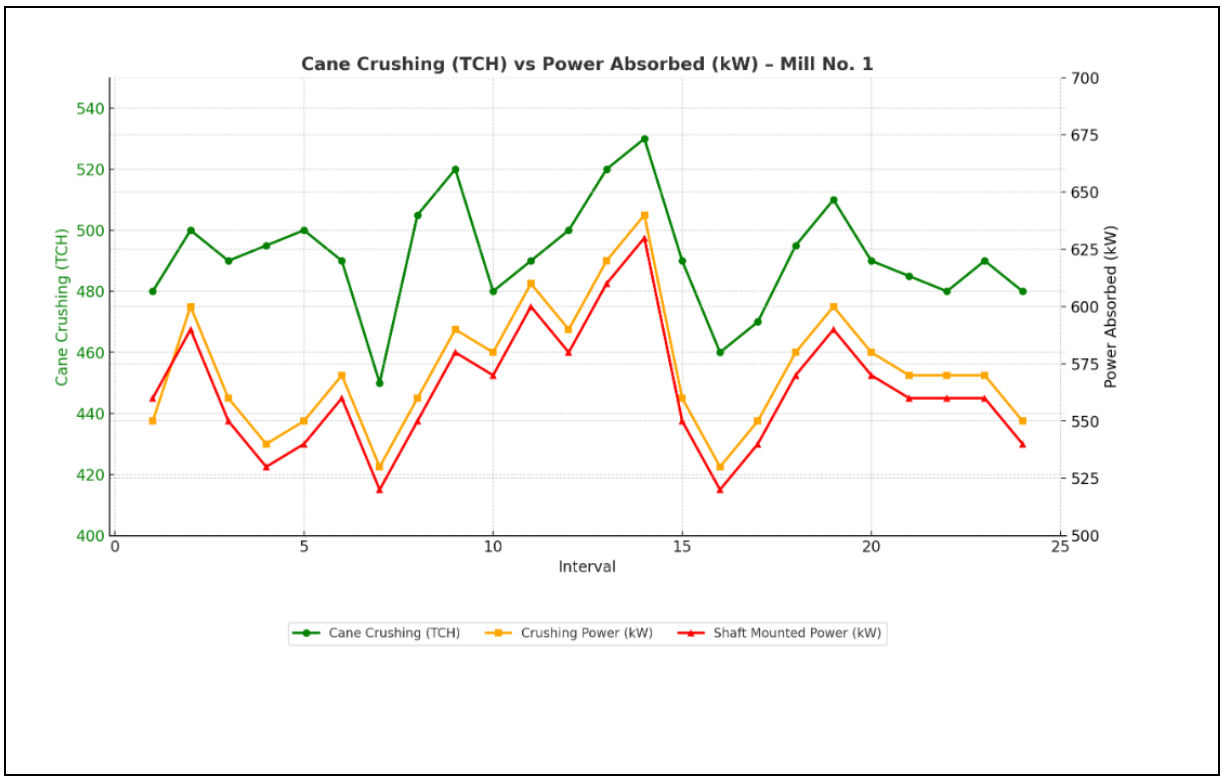


Figure 3. Cane crushing and power absorbed by Mill No. 1 (Source: Own research at sugar mills)

Figure 3 shows that the power absorbed by the mill is in a linear proportion, approximately 1.1 kW/t/h, which is less than 25% of the power required for the same crushing rate with the foot-mounted turbine. The primary mill Brix extraction was recorded during the observation period, and it was observed that there was an average rise of 4.5% in the primary Brix extraction after the installation of the shaft-mounted drive. During crushing, the hydraulic load was kept the same, in order to determine the precise impact. The bagasse pol was reduced, on average, by 0.38 units, and the moisture was reduced by 0.30%. We have tried to maintain the operating parameters consistently to evaluate the effectiveness of the drive installation.

Conclusions

This assessment highlights that shaft-mounted planetary drives provide a transformative edge for sugar mills, by boosting their performance, efficiency and long-term competitiveness. Compared to traditional foot-mounted gearboxes and hydraulic systems, these drives cut the power consumption by around 24%, with an average power intake of only 1.15 kW/TCH, which surpasses the conventional systems.

The operational benefits extend beyond energy savings: mills with shaft-mounted drives achieve a 4.5% increase in their primary bagasse extraction, while maintaining moisture levels below 49%, which is vital for the downstream processes, like cogeneration. The maintenance costs also decline significantly, due to the elimination of components such as pinions, tail-bar couplings and large foundations, which reduce the mechanical stress and inventory needs. These improvements

simplify the plant design, lower the down-time, and they can extend the lifespan of the key components by up to 50%, due to reduced stress, as posited by Machado *et al.* (2023).

Case studies from Maharashtra and Central America demonstrated that targeted, cost-effective retrofits can enhance the throughput, reduce the energy expenses and improve the extraction rate without complete overhauls. As the emphasis on power export, energy efficiency, and cost optimisation grows, now is the perfect time for sugar mills to adopt high-efficiency, shaft-mounted drives. These systems are not just mechanical upgrades; they are also strategic investments that drive operational excellence, financial gains and sustainability. Such outcomes align with the technical frameworks developed by Hughes (1964) and Hugot (1986), who laid the early groundwork for evaluating the resilience of drivetrain components. Moreover, this approach reaffirms the findings of Goel (2013) regarding the energy-saving potential and increased extraction efficiency when using compact, integrated drive systems.

Acknowledgements

The authors thank the management of Dinamic Oil SPA for allowing the publication of this article. They also acknowledge the staff of Dinamic Oil SPA for their assistance in preparing the article and collecting valuable data. Gratitude is extended to our distributor and channel partner for the sub-Saharan region, BMG, for their support and collaboration with the SASTA team. We also thank our clients who provided valuable data and images that are essential to this work. Finally, we appreciate the SASTA conference organising committee for granting us the time to publish and present this article on an important topic.

References

Gardener A (1964). Comparison of various electrical drives suitable for cane-crushing mills. *Proceedings of the South African Sugar Technologists' Association, 74-81*

Goel DK (2013). *Technical presentation on 'Innovative energy efficient milling train'*. XXVIII ISSCT Congress, Sao Paulo, Brazil.

Gomez AL, Ortiz JJ and Reyes M (1996). Measurement of power sharing in a conventional three-roller mill. *Proceedings of the International Society of Sugar Cane Technologists, 19:850-859*

Hughes DL (1964). *Sugar mill drives*. Proceedings of the South African Sugar Technologists' Association, 66-73

Hugot E (1986). *Handbook of Cane Sugar Engineering*. Amsterdam: Elsevier. 1-872

Kent GA and McKenzie NJ (2001). The distribution of torque in a three-roll mill. *Proceedings of the International Society of Sugar Cane Technologists, 24:220-225*

Kharbanda JK, Ingale R and Vasanthan KP. (n.d.). *Innovative solutions for upgradation of mills*.

Machado Rodríguez ÁS, Hernández Vargas WJ, Chagoyén Méndez CA, García del Pino G, Hernández Battez AE and Moya Rodríguez JL (2023). *Trends in mechanical design for power transmissions in sugarcane mills*. 4th International Scientific Convention UCLV 2023, Central University “Marta Abreu” of Las Villas

SHORT COMMUNICATION

THE RETROFITTING OF BOILER-INDUCED DRAFT FAN ROTORS TO INCREASE EFFICIENCY AND THE ASSOCIATED ENERGY SAVINGS

Frost MC

Universal Fans (Pty) Ltd, 26 Industry Road, Clayville, Olifantsfontein, 1666

mike@universalfans.co.za

Abstract

Boilers, gas cleaning equipment and fans are critical components in the processing of sugar, with fans being considered as the heart of the system. The poor performance and efficiency of fans leads not only to high energy costs, but it also directly impacts the efficiency and performance of the boiler and gas-cleaning equipment. There are a multitude of factors that influence and contribute to underperforming fans; for example, high initial safety margins, changing operational requirements, inferior quality fuel, system leaks, ageing equipment, etc., to mention but a few. Retrofitting the impeller (rotor) is a cost-effective, verifiable and tangible solution for increasing and improving its performance, static efficiency, cost savings and reliability. Simply, a rotor retrofit is the replacement of the impeller, shaft and inlet cone, while still utilising the fan's static components i.e. the casing, bearing centers, bearing size, civils, drive motor, etc. In most cases, a new rotor will allow the fan to increase its performance, to achieve a boiler MCR at, or close to, its best efficiency, and to allow for a lower power consumption at a higher static efficiency, which will translate into cost savings and which, in all cases, will contribute to a project's payback in a relatively short period. An engineering study and analysis of the installed fans will confirm if a retrofit is feasible and, if so, the current operational duties are determined by means of performance measurements, vibration readings and power consumption, which are compared to the new performance requirements. The results demonstrate that, when performing a retrofit, the new design yields a significant improvement in its static efficiency, which results in reduced energy consumption and stable operational performance.

Keywords: boiler efficiency, impeller retrofitting, fan static efficiency, fan reliability, energy cost savings

Introduction

This paper focuses on boiler-induced draft fans and presents a high-level overview alongside a real-world case study, which showcases the benefits of a rotor retrofit. The case study highlights the notable improvements in static efficiency, the reduced power consumption and stable operational conditions, which translate into efficient energy use and cost savings.

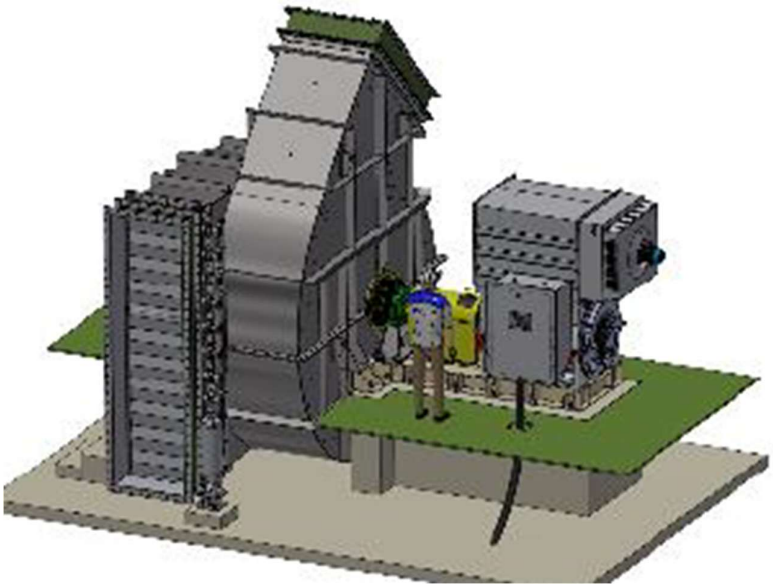


Figure 1. Typical boiler-induced draft fan

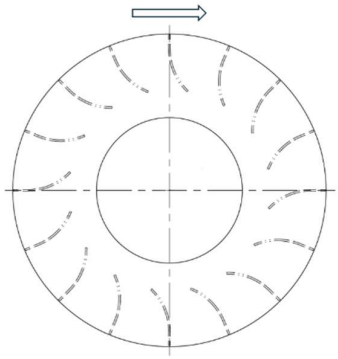


Figure 2. Typical boiler-induced draft fan impeller profile (forward-curved and radially-tipped)

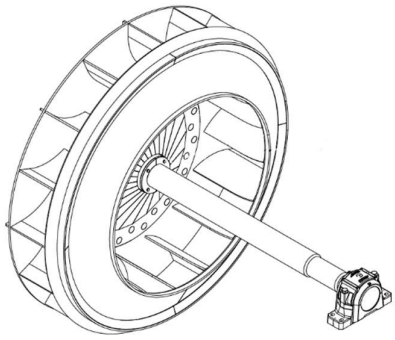


Figure 3. Typical boiler-induced draft fan rotor

Methodology/Approach

A rotor retrofit involves replacing the impeller, shaft and inlet cone, while attempting to retain and re-use the static components, such as the fan casing, bearing bases, bearing pedestals, coupling and motor base. In most cases, the only modification required is adjusting the fan casing cut-off to maintain optimal clearance between the impeller tip and the casing cut-off, in order to ensure maximum efficiency.

In simple terms, the casing cut-off (see Figure 6) is a round bar that is located between the fan side-plates, and where the logarithmic casing spiralling scroll starts. The placing and location of the casing cut-off is of great importance, as it has a direct impact on:

1. Efficiency: A well-designed casing cut-off can improve the fan's efficiency by minimising the losses and optimising the airflow.
2. Performance: The casing cut-off affects the fan's pressure and flow characteristics, which influences its overall performance.
3. Noise: The design of the casing cut-off can impact the noise levels, with some configurations reducing noise generation.

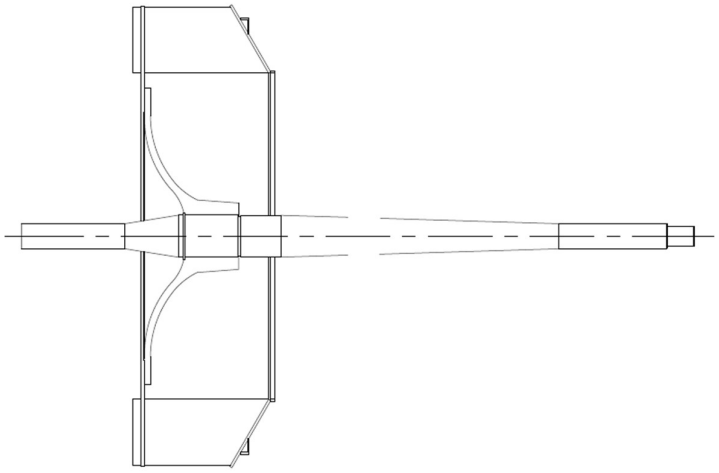


Figure 4. Typical induced draft fan rotor

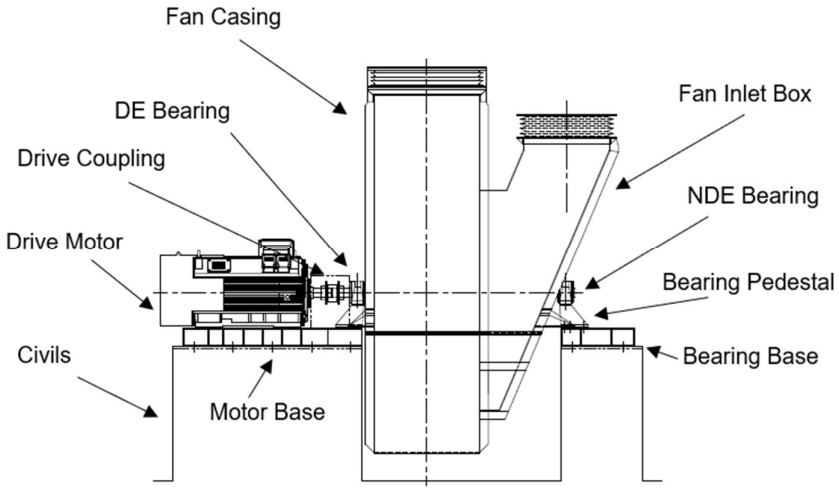


Figure 5. Typical boiler-induced draft fan components to be re-used

In most cases, the only modification required is for the fan casing cut-off to be moved upwards or downwards, to ensure that the gap between the impeller tip and the casing cut-off is maintained. This gap is all-important in maintaining the fan's efficiency.

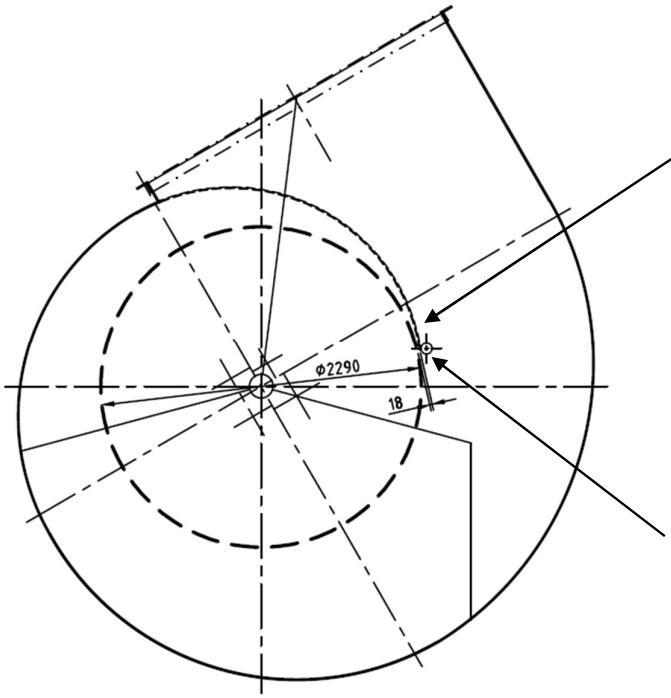


Figure 6. Casing with existing Ø2290mm impeller

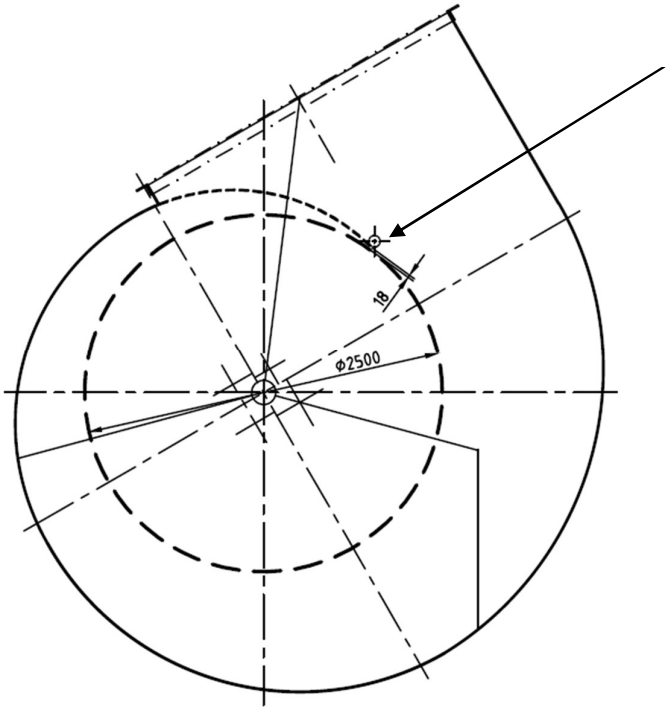


Figure 7. Casing with retrofitted Ø2500mm impeller

A new inlet cone would be required to accommodate the wider or narrower impeller, as well the impeller inlet eye, which ensures that the intended higher static efficiency is maintained.

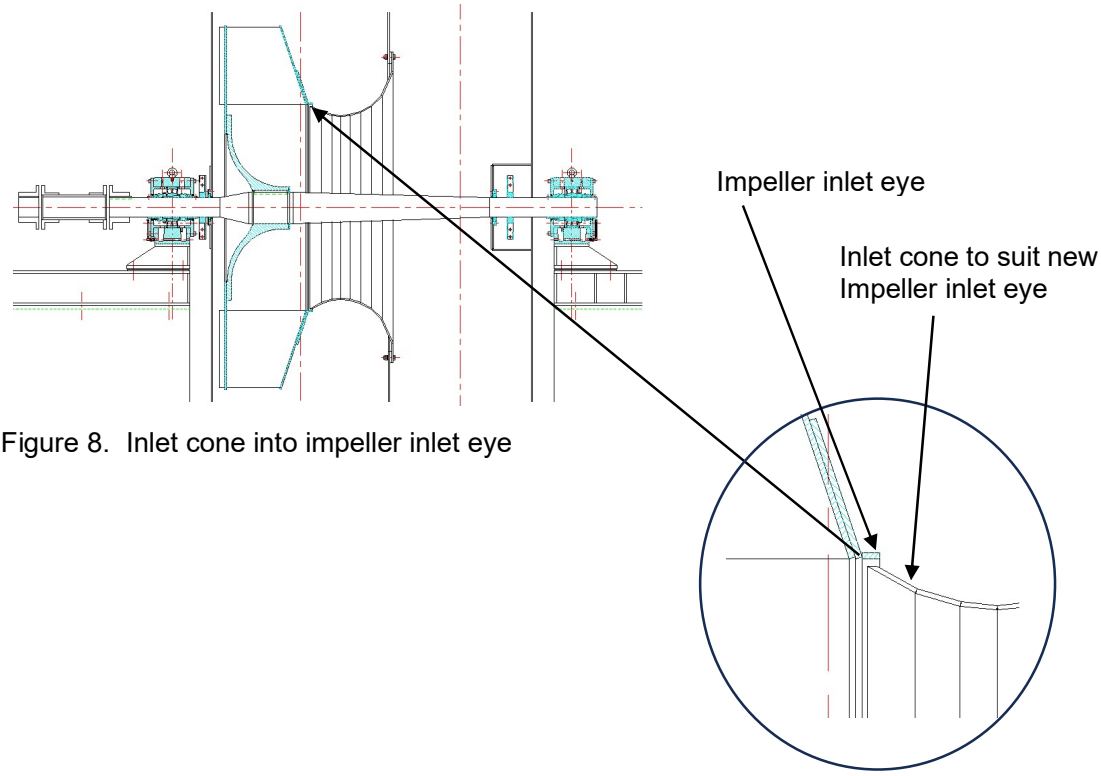


Figure 8. Inlet cone into impeller inlet eye

It is important to clarify upfront what the intended retrofit is expected to achieve:

- to maintain the current fan's performance at an increased static efficiency, while operating in a smooth, reliable and stable condition.
- to increase the fan's performance to achieve the process requirements, while increasing the static efficiency and operating in a smooth and stable condition.

In most, if not all, cases, performing a rotor retrofit to increase the static efficiency is possible and, in general, it presents no great engineering challenges.

However, when an increase in the fan's performance is required, with either an increased volume or increased static pressure, or both, there are several engineering challenges. Increasing the volume will require a wider impeller, and increasing the static pressure will require an impeller with a larger diameter, both of which translate to larger impellers overall.

Fitting the larger impeller into the existing fan casing will be determined in the engineering study carried out by our Team.

The current performance of the installed fan will be determined in consultation with the client and, together with a variety of testing methods, the final data will be agreed upon. This will be an opportune time to discuss any excessive wear that the impeller is being exposed to, and it will include placing suitable wear liners into the new impeller.

Further consultation will be required with the client and, if required, the boiler and gas cleaning manufacturers will be included, to determine what the fan should be generating, in order to achieve the process and system requirements under efficient, reliable and stable operational conditions.

The required increase in performance is unitised to select, applicate and engineer a new fan rotor that achieves the required increase in static efficiency, static pressure and volume, in order to achieve the desired results The new impeller is then compared to the installed fan installation to ensure that the new impeller can be accommodated in the casing, with minor modifications to the casing being cut off by either moving it upwards, for a larger impeller, or downwards, for a smaller impeller. The increase or decrease in the impeller size will increase or decrease the rotor mass and may alter the radial and axial loads on the fan bearings. The required bearing centres and bearing sizes will be compared to the current installation, which ensures that no modifications or changes are required in keeping the installed bearing sizes and centres that were installed. A new inlet cone will be designed to take up the narrowing or widening of the impeller.

On the completion of the retrofit, new flow measurements are performed by noting the volume, static pressure and current drawn. These demonstrate an increase in the fan's performance, at a greatly reduced power consumption, which translates to direct energy cost savings. It is these energy savings that contribute to the cost of the project and the retrofit. The payback period will depend on the increase in static efficiency and the decrease in absorbed power. The greater the increase in static efficiency, the greater the savings in power. At the same time, this will result in an increase in the fan's performance, which will achieve for it a Boiler Maximum Continuous Rating (MCR), and it will operate with increasing stability and reliability.

A working case study example

Universal Fans completed a typical retrofit at a large paper mill, where significant energy savings were made in a multi-million Rand project, which paid for itself within the first year, mainly through the increase in its static efficiency and reduced energy consumption.

The replaced impeller was a straight radial-bladed type, with a diameter of Ø2890mm over the blades and an overall width of 580mm, and the new build applicated and engineered impeller is a forward-curved, radially-tipped type with a diameter of Ø2692mm over the blades and an overall width of 786mm. A new inlet cone was fitted to accommodate the wider impeller and the new impeller inlet eye dimensions. Forward-curved, radially-tipped impellers are used extensively as boiler-induced draft fans within the sugar industry.

The client requested that we offer two options, namely:

- a new build rotor retrofit – to the current and original fan's performance, with an increase in static efficiency; and
- a new build rotor retrofit – with an increase in static pressure of 600Pa and existing volume, with an increase in static efficiency.

➢ **Original fan's performance with a 2200 kW installed motor**

Duty	**100%**	**120%**	**140%**
Volume per fan – Am³/sec	81.5	89.22	118.79
Static pressure at operating altitude at temperature – Pascal	4500	6490	8840
Power absorbed at fan shaft at operating altitude and temperature	±595 kW	±1093 kW	±1795 kW
Original static efficiency	**±61.8%**	**±52.9%**	**±58.5%**

➢ **Anticipated fan's performance – retrofitted rotor at original fan's performance**

Duty Volume per fan – Am³/sec	**100%** 81.5	**120%** 88.77	**140%** 118.64
Static pressure at operating altitude at temperature – Pascal	4500	6490	8840
Power absorbed at fan shaft at operating altitude and temperature	490.1 kW	767.4 kW	1383.7
Static efficiency	70.7%	70.9%	70.7%
INCREASE IN STATIC EFFICIENCY	**±8.9%**	**±18%**	**±12.2%**
EXPECTED POWER SAVINGS	**±104.9 kW**	**±325.6 kW**	**±411.3 kW**

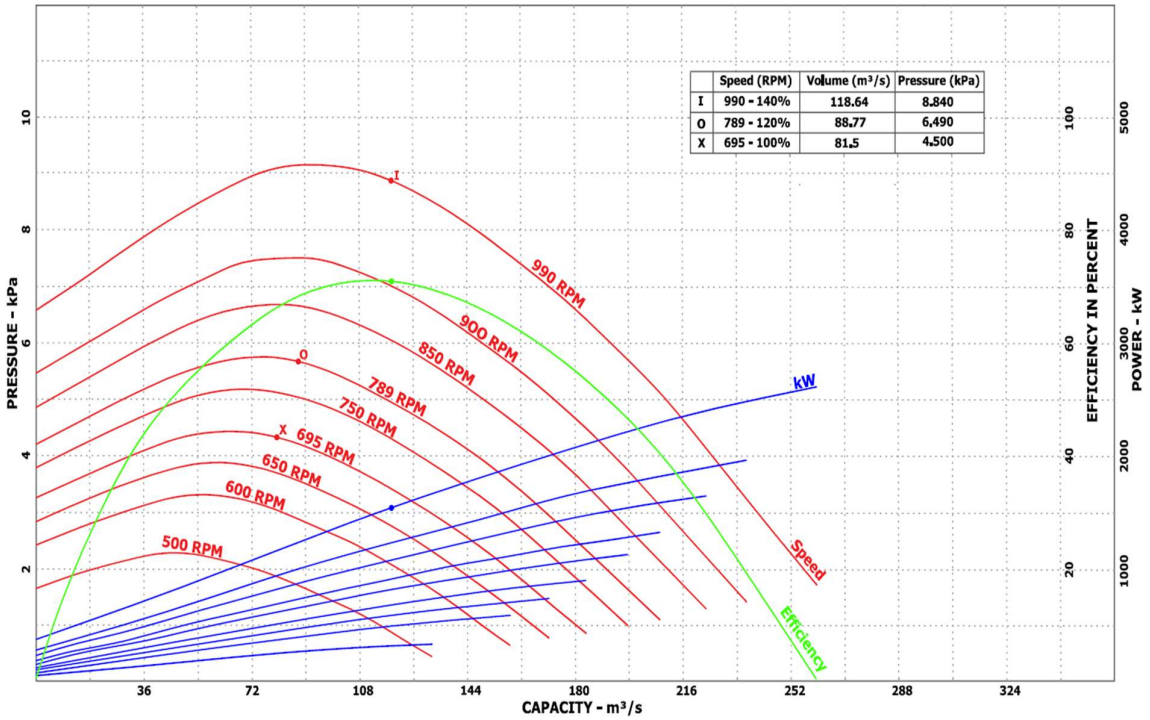


Figure 9. Fan's performance curve – retrofit rotor original fan's performance

➢ **Anticipated Fan Performance – Retrofitted Rotor with 600Pa Static Pressure Increase**

Duty Volume per fan – Am³/sec	**100%** 81.5	**120%** 88.77	**140%** 118.64
Static pressure at operating altitude at temperature – Pascal	5100	7090	9440
Power absorbed at fan shaft at operating altitude and temperature	586.8 kW	883.1 kW	1551.3 kW
Static efficiency	67.7%	67.4%	67.6%
INCREASE IN STATIC EFFICIENCY	**±5.9%**	**±14.5%**	**±9.1%**

EXPECTED POWER SAVINGS	**±8.2 kW**	**±209.9 kW**	**±243.7 kW**

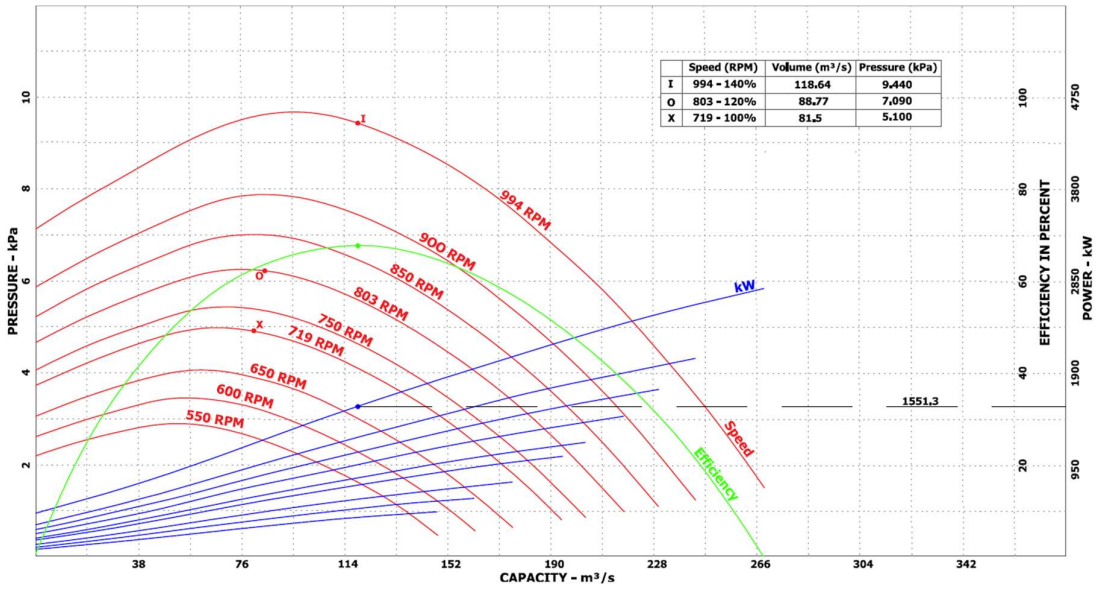


Figure 10. Fan's performance curve – retrofit rotor increased static pressure +600Pa

Summary

Original absorbed power	±595 kW	±1093 kW	±1795 kW
Original static efficiency	**±61.8%**	**±52.9%**	**±58.5%**
Absorbed power at same fan duties	490.1 kW	767.4 kW	1383.7 kW
Static efficiency	70.7%	70.9%	70.7%
INCREASE IN STATIC EFFICIENCY	**±8.9%**	**±18%**	**±12.2%**
EXPECTED POWER SAVINGS	**±104.9 kW**	**±325.6 kW**	**±411.3 kW**
Absorbed power at increase +600Pa	586.8 kW	883.1 kW	1551.3 kW
Static efficiency	67.7%	67.4%	67.6%
INCREASE IN STATIC EFFICIENCY	**±5.9%**	**±14.5%**	**±9.1%**
EXPECTED POWER SAVINGS	**±8.2 kW**	**±209.9 kW**	**±243.7 kW**

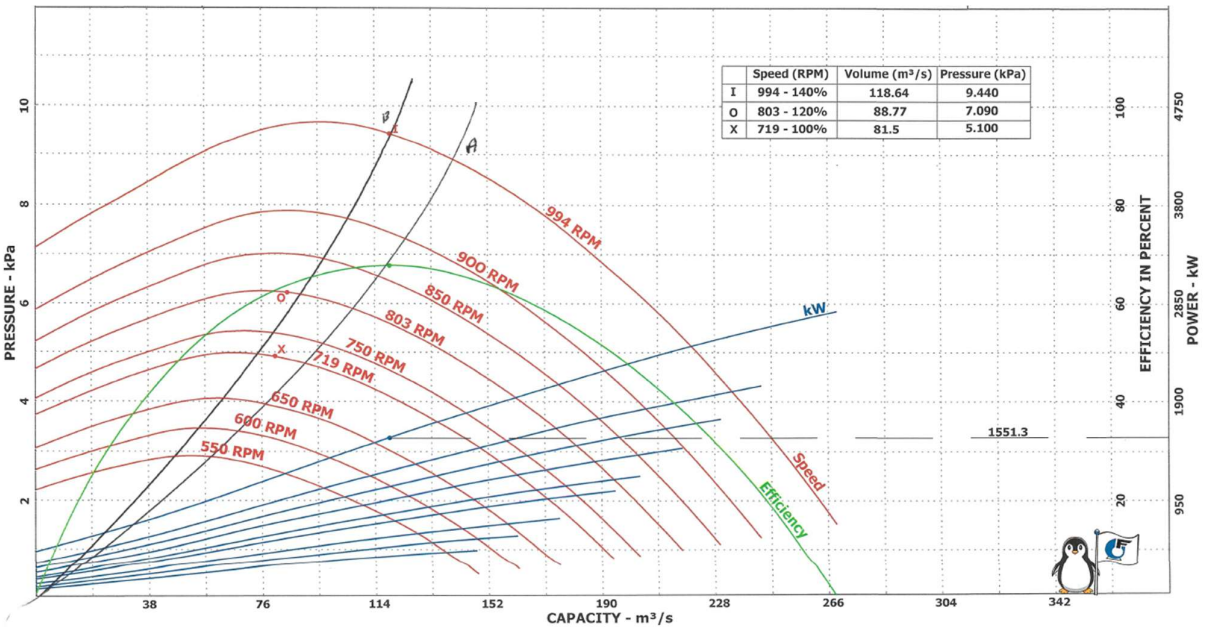


Figure 11. The fan's performance curve (A: retrofit rotor original fan duty; B: increased static pressure +600Pa)

Conclusion

The option to increase the static pressure by 600Pa was chosen by the client, and substantial savings were made through the higher production outputs, an increase in the static pressure and the reduced absorbed power. Furthermore, additional savings will be made with the fan operating at a stable and reliable point, which translates to less, or no, unplanned outages.

This fan operates 24 hours per day, with one- or two-day planned shuts and a two-week planned shut on an annual basis.

Allowing for the above planned shuts, the installation operates for approximately 8 436 hours annually. The saving of approximately 210 kw per hour translates to a substantial savings.

The results confirm that retrofitting fan rotors is a highly effective method of enhancing efficiency and achieving cost savings in the boiler operations of the sugar industry. The approach provides a relatively short payback period, while ensuring a reliable and stable performance. By using careful engineering assessments, organisations can optimise the performance of their fans, reduce their energy consumption and extend the lifespan of their equipment.

FULL PAPER

ENERGY SAVINGS UTILISING DIMPLE TUBE TECHNOLOGY

Bezuidenhoudt D[1], Yeo W[1], Stevens M[1], Gokool M[1]

[1]Bosch Projects, South Africa

bezuidenhoudtd@boschholdings.co.za; yeow@boschholdings.co.za; stevensm@boschholdings.co.za; gokoolm@boschholdings.co.za

Abstract

Steam economy is a critical factor in today's sugar industry, due to the rising fuel and electrical energy costs and the increased need for cogeneration. The recently developed and commercialised dimple tube technology has been shown to increase batch and continuous vacuum pan performance considerably, in terms of throughput, and it has been well-received in the industry for this reason. During the previous experimental tests, trials conducted to determine real-world throughput/capacity benefits and commercial operation, the dimple tube technology showed a significant improvement in heat transfer coefficients in vacuum pans due to the turbulence created on the tube surfaces. Through rigorous experimentation and analysis, this paper quantifies the impact of dimple tube technology on energy savings and its potential for overall process efficiency. This work applies specifically to sugar factories or refineries, where energy efficiency could be improved by taking advantage of the improved heat transfer coefficients and operating vacuum pans on lower-grade steam.

Keywords: Vacuum pan, tubes, heat transfer, co-generation, continuous vacuum pan, batch vacuum pan, dimple tubes, energy savings, sugar industry, steam economy, process efficiency

Introduction

As factories aim to expand their operations, or reduce their energy consumption, it becomes a common requirement to modify their vacuum pan capacity and operations. The significant investment that is associated with installing new vessels, reallocating existing vessels, as well as the need for additional ancillary services and support structures, often make capacity expansion or energy reduction modifications economically unfeasible. In response to this challenge, the new innovative dimple tube has been developed and commercialised, and is proving to be a cost-effective solution for the improvement of vacuum pan capacity (Bezuidenhoudt *et al.*, 2023).

Since the development of these tubes was finalised, several vacuum pans have been retrofitted, in order to improve the capacity of these vacuum pans, and the desired results have been achieved. The measured and observed increases in evaporation rates (and the resulting capacity) exceed the increase in heating surface area due to an improvement in heat transfer coefficient that is caused by the increase in turbulence on the tube surfaces. Full-scale industrial testing has been conducted to show the potential for energy savings by utilising the dimple tubes, and theoretical calculations have been used with comparative results. A 'typical' cane sugar factory scenario is considered to quantify their potential for steam savings.

There are a few factors to consider during sugar crystallisation in a vacuum pan, such as the crystal content and size, as well as the syrup/molasses brix, for example. However generally, the more heat that is transferred in the vacuum pan, the faster the vacuum pan boiling time. The new dimple tubes have a positive impact on both the heat transfer coefficient and the surface area, and thus, they create opportunities to improve pan operations. Previous performance verification tests proved the improvement in heat transferred (Bezuidenhoudt *et*

al., 2023). This paper presents a comprehensive analysis of the performance characteristics, it quantifies the performance variation in relation to steam temperature, and it goes on to detail the retrofitting advantages of the new dimple tube technology.

Performance Testing

Previous work on the development, testing and implementation of dimple tube technology was published in 2023, and several vacuum pans having been retrofitted since then, with excellent results. The outcome of the laboratory testing and full-scale industrial trials is summarised briefly in the following section, in order to demonstrate the potential for energy savings, as well as the throughput benefits that have already been established.

Laboratory testing

The initial prediction of the performance of the dimple tube technology was demonstrated in extensive laboratory tests that were conducted at the Sugar Milling Research Institute NPC in South Africa, using A-massecuite in a pilot plant batch vacuum pan (Rahiman *et al*., 2023; Bezuidenhoudt *et al*., 2023).

The results demonstrated improvements across all phases of the batch vacuum pan cycle, with the overall batch vacuum pan cycle time improved by over 30%, which enables a significant enhancement in pan-floor throughput. The results of the trials are graphically represented in Figure 1, where the smooth-walled tubes are compared with the dimple tubes.

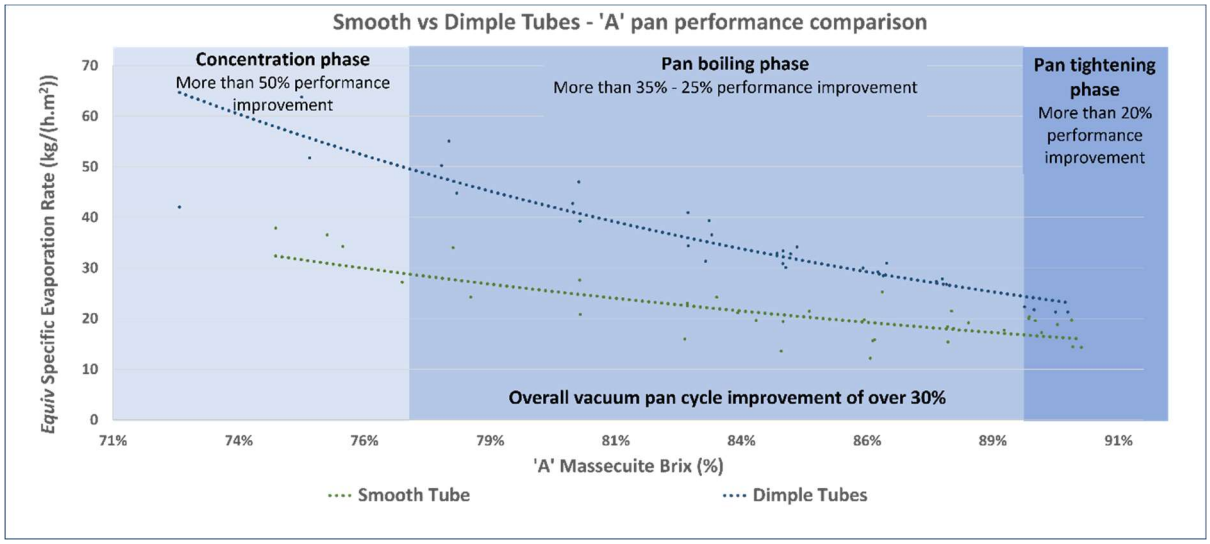


Figure 1. Dimple tube vs smooth-wall tube performance on A-massecuite (pilot plant)

Industrial trials and performance results

Following on from the pilot plant testing, full-scale/industrial tests were then conducted at the Umfolozi Sugar Mill. The ‘A’ batch vacuum pan, on which the initial industrial trials were conducted, was completely retubed using dimple tubes before the start of the 2023 season. The data collected from this vacuum pan at the Umfolozi Sugar Mill was analysed, and a comparison of the 2022 (standard tubes) and 2023 (dimple tubes) operational data of the same vacuum pan can be seen in Figure 2 below.

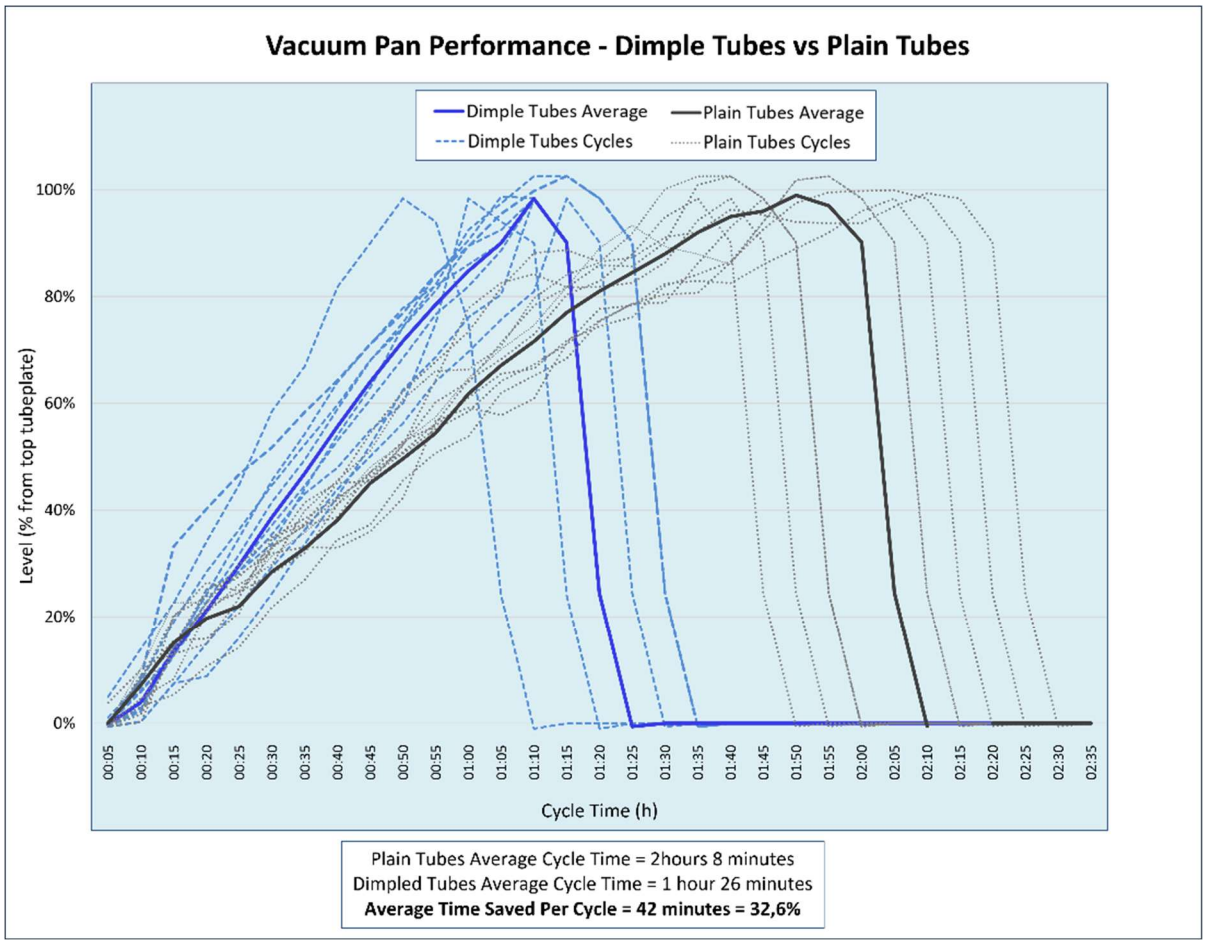


Figure 2. Comparison of dimple tubes and standard tubes in a full-scale vacuum pan

The performance of the vacuum pan after fitting dimple tubes showed a significant reduction in the cycle time, compared to the control tests that were recorded in 2022 with plain tubes. Figure 2 compares the data collected over a nine-week period in each season, it analyses 525 individual vacuum pan cycles from the same pan, and it shows that the 2023 cycle time improved by an average of 32.6% across the full cycle, compared to 2022. These results validate, and exceed, the improvements that were predicted by the pilot plant tests shown in Figure 1.

At the time of writing of this text, seven vacuum pans have been retrofitted with the new dimple tube technology, and considerable performance improvements have been reported since obtaining the results for the first vacuum pan. This new technology offers a notable enhancement in the performance of vacuum pans. More detailed reporting on the previous trials and test results can be found in Bezuidenhoudt *et al*. (2023).

Dimple tube vacuum pan performance prediction with a reduction in the steam vapour grade

As described above, whilst several factors affect vacuum pan throughput, generally a higher rate of heat transfer, results in a faster boiling time and more effective circulation of massecuite in the vacuum pan.

From the above summary of previous work, which describes the pilot plant and industrial trial tests and results, and from the analyses of the subsequently retrofitted vacuum pans, we know that the dimple tubes provide an additional 32.6% improvement in the performance of vacuum

pans. From the geometry of the dimple tubes, we know that the additional heating surface area is approximately 16.5%, compared with a standard vacuum pan tube. The remainder of the improved performance can be attributed to the increased overall heat transfer coefficient, due to the turbulence on both the internal and external tube surfaces of the dimple tubes.

The overall increase in HTC, due to turbulence when using dimple tubes, is calculated simply by dividing the overall average improvement in the boiling time, and hence the heat transfer rate, considering that all the other parameters were equal, by the increase in the heating surface area.

$$Q_1 = Q_2$$

$$U_1 \times A_1 \times dt_1 = U_2 \times A_2 \times dt_2$$

Accounting for the additional area and improved performance, with the change in temperature in both scenarios remaining the same:

$$Q_1 = 1.326Q_2$$

$$A_1 = 1.165A_2$$

$$dt_1 = dt_2$$

The above equations can then be rewritten as:

$$U_1 \times 1.165A_2 = 1.326 \times U_2 \times A_2$$

$$U_1/U_2 = 1.326/1.165 = 1.14$$

This provides the calculated improvement of the heat transfer coefficient of 14%, when using dimple tubes over plain tubes.

Where:

Q_1 = total heat transfer with dimple tubes; U_1 = heat transfer coefficient with dimple tubes; A_1 = heat transfer area with dimple tubes; dt_1 = temperature differential with dimple tubes; Q_2 = total heat transfer with plain tubes; U_2 = heat transfer coefficient with plain tubes; A_2 = heat transfer area with plain tubes; dt_2 = temperature differential with plain tubes.

The following simple formulae illustrate that dimple tubes may be utilised to reduce the steam temperature requirements, whilst maintaining the same rate of heat transfer, and therefore, vacuum pan productivity. This will allow sugar factory and refinery operators to reduce energy consumption by repurposing the higher-grade steam to be utilised beneficially elsewhere, or through a reduction in fuel demand.

Straight wall tubes

For comparative purposes, for straight wall tubes, we assume an overall heat transfer coefficient (HTC) of one for parity (1 kW/m²K), the surface area of one for parity (1 m²), the calandria steam grade vapour 1 (V1), with a temperature of 108.2 °C and pressure of 135 kPa(a), and a massecuite strike temperature of 75°C.

Heat transferred (Q) = Heat transfer coefficient (U) x surface area (A) x temperature differential (dt)

$$Q_{st} = 1 \times 1 \times (108.2\text{-}75)$$

$$Q_{st} = 33.2 \text{ kW}$$

Dimple technology tubes

From both the experimental data and the factory-validated data, it is clearly determined that the dimple tube pan conversion increases the HTC by a factor of 1.14 and the heating surface area by a factor of 1.16. Should Vapour 2 (V2) at 102.3°C and 110 kPa(a) be utilised, with a massecuite strike temperature of 75°C, the following equations show how the overall heat transfer is affected by a reduction in the temperature differential.

Heat transferred (Q) = Heat transfer coefficient (U) x surface area (A) x temperature differential (dt)

$$Q_{dt} = 1.14 \times 1.16 \times (102.3-75)$$

$$Q_{dt} = 36.1 \text{ kW}$$

Despite the use of a lower vapour grade, the overall rate of heat transfer is theoretically still 8.7% higher in a vacuum pan fitted with dimple tubes utilising V2 vapour, when compared to a vacuum pan fitted with straight wall tubes utilising V1 vapour.

The above comparison serves to simply show that, due to the increased overall HTC and heating surface area when utilising dimple tubes, a typical factory could convert their vacuum pans to use a lower-grade vapour, whilst maintaining (or slightly exceeding) the productivity or throughput of the vacuum pan. The use of lower-grade vapour would then lead to improvements in the overall factory steam efficiency.

In-factory tests: vacuum pan performance tests using a lower vapour grade

The theoretical analyses of the data, as well as the results collected during the previous work, show that it is possible to utilise a lower-vapour grade steam on a vacuum pan equipped with dimple tubes and to achieve the same throughput. This theory was then tested at the Umfolozi Sugar Mill. The same ‘A’ batch vacuum pan that was used for the first set of industrial trials, was run by using steam at a lower pressure of 110 kPa(a), to simulate typical V2 conditions. This was carefully controlled by constantly monitoring the calandria steam pressure and temperature during these trials.

The process data (the feed and discharge crystal size, the feed and discharge massecuite brix, the feed and discharge purities) were compared and found to be very similar. Several V2 vapour supply cycles were run, and the cycle time data was compared to V1 vapour cycles with plain tubes, as well as with V1 vapour cycles with dimple tubes.

V2 vapour pressure averaged 110 kPa(a), with a corresponding temperature of 102.3°C. V1 vapour pressures at the same factory, during this period, averaged 135 kPa(a) with a corresponding temperature of 108.2°C. The cycle times were plotted and compared, and the data is shown in Figure 3.

It is acknowledged that the simulation of V2 operating conditions was implemented by regulating the vapour feed valve, which resulted in a slight degree of steam superheat. This superheat was quantified as 4.4°C, based on the application of the Joule-Thomson effect. In the context of total heat transfer, comprising both sensible heat and the latent heat associated with condensation, the contribution of this superheat was calculated to be approximately 0.4% of the total heat transferred. As such, its influence on the experimental results was deemed to be negligible.

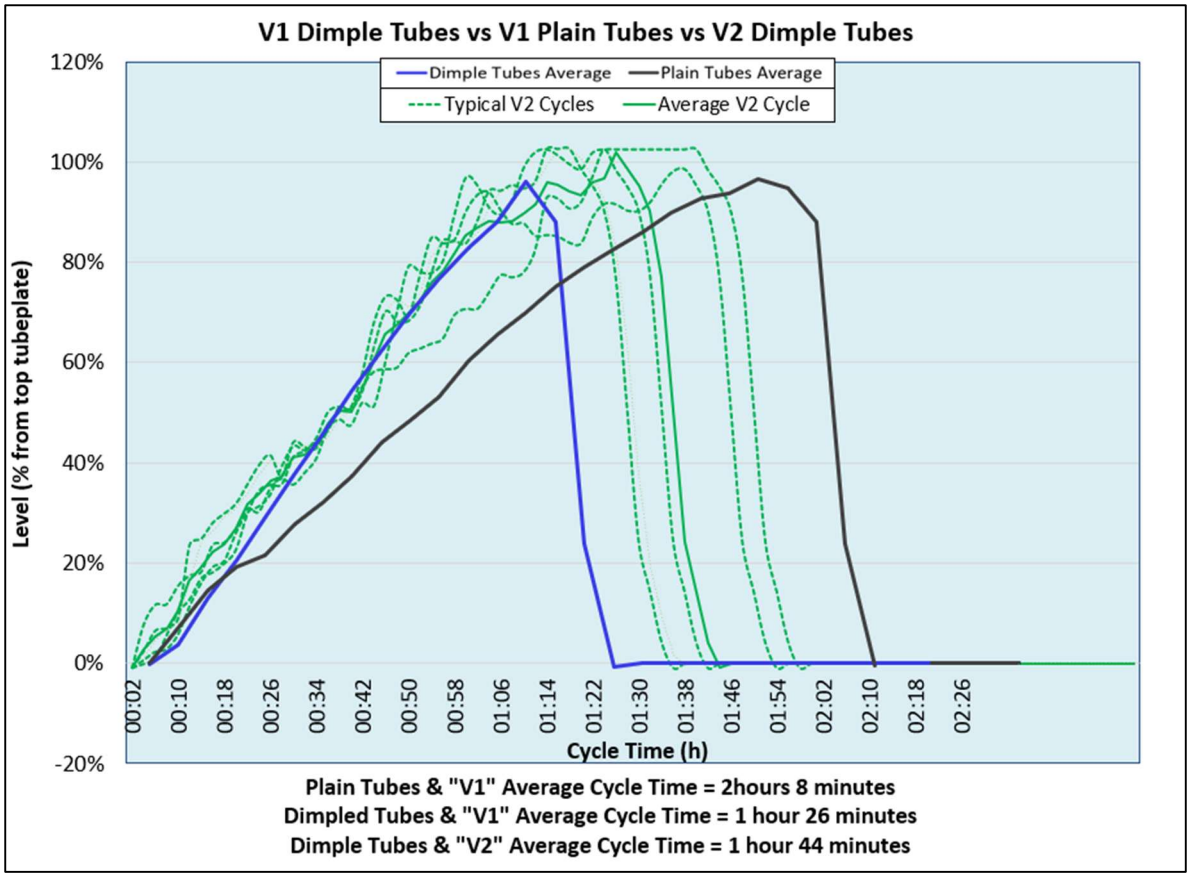


Figure 3. Vapour 2 cycle times

The cycle time plot shows an improvement in the cycle time, as expected based on the theoretical analysis, when utilising dimple tubes and a reduced vapour grade, when compared with the standard vacuum pan tubes and a higher vapour grade. This full-scale factory trial therefore confirms the theoretical comparison and shows that vacuum pans can be comfortably converted to operate on lower vapour grade steam by utilising dimple tubes, whilst the throughput/productivity of the vacuum pans is not affected.

Retrofitting energy cost savings

Benefit to a sugar factory

A theoretical comparative Energy and Mass Balance (EMB) was run of a raw sugar factory running at 300 TCH and that is reliant on coal and characterised by a high V1 bleed. This was used to investigate the equivalent coal savings by using dimpled tubes on all 'A' batch vacuum pans and changing the heating medium from V1 to V2 steam. This is graphically shown in Figures 4a-d. While compiling the model to quantify a fuel cost saving, there is the appreciation and acknowledgement that each application will differ, as no sugar factory is the same as the next. The benefits are especially recognised with regard to sugar factories that need to use supplementary alternative fuel, that intend to export power or that are incentivised by carbon tax credits.

The results of this hypothetical analysis show that the use of dimple tubes on 'A' batch vacuum pans running on V2 vapour would reduce the factory process steam on cane by 2.2%. Considering a typical 300 TCH sugar factory that only utilises back pressure turbo-alternator sets, this process steam saving will amount to a 5 040 metric ton reduction in coal usage, or the equivalent of 1 680 metric tons of coal per 100 TCH, for a 35-week season.

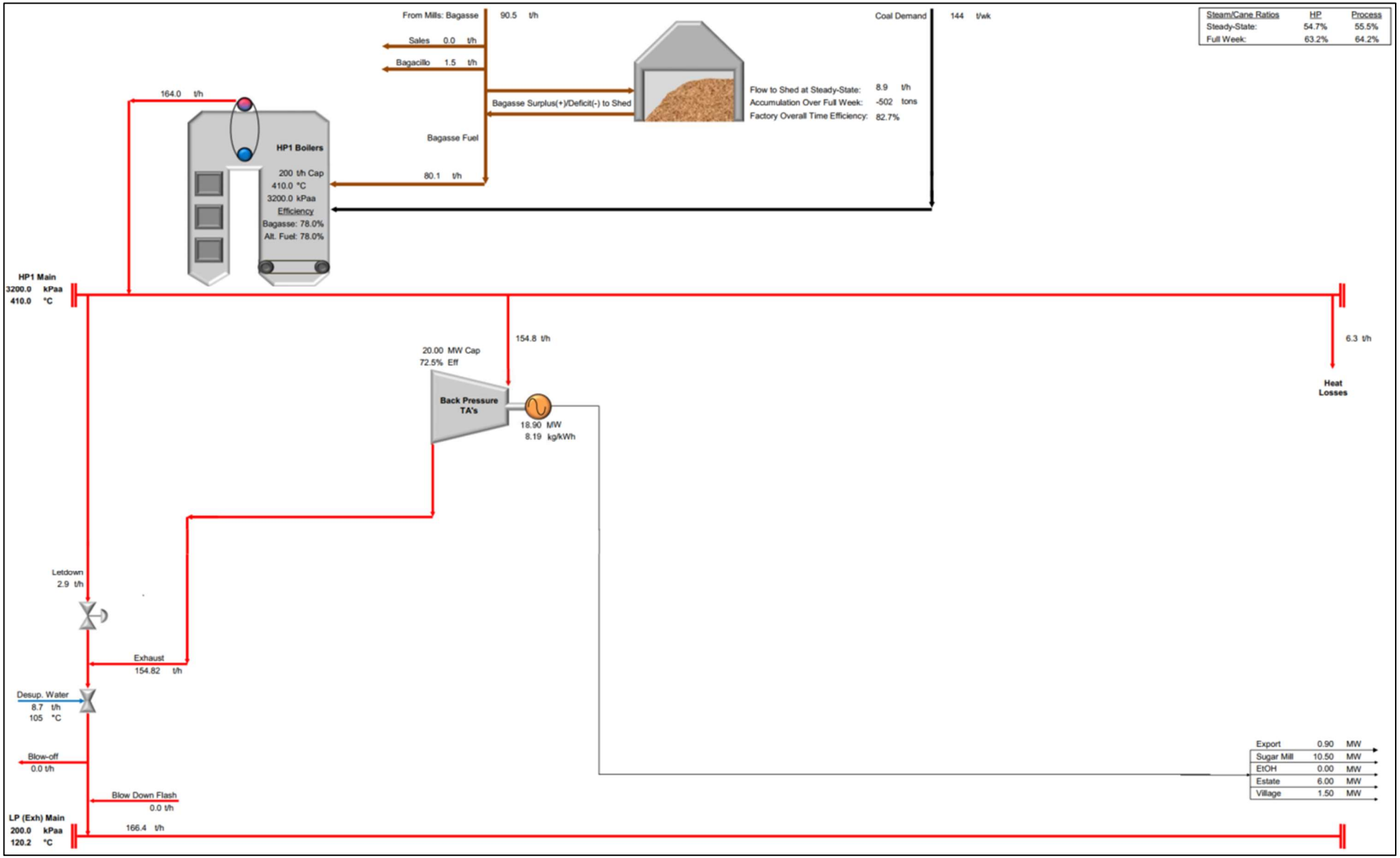


Figure 4a. Excerpt from coal usage factory EMB typical steam and powerhouse

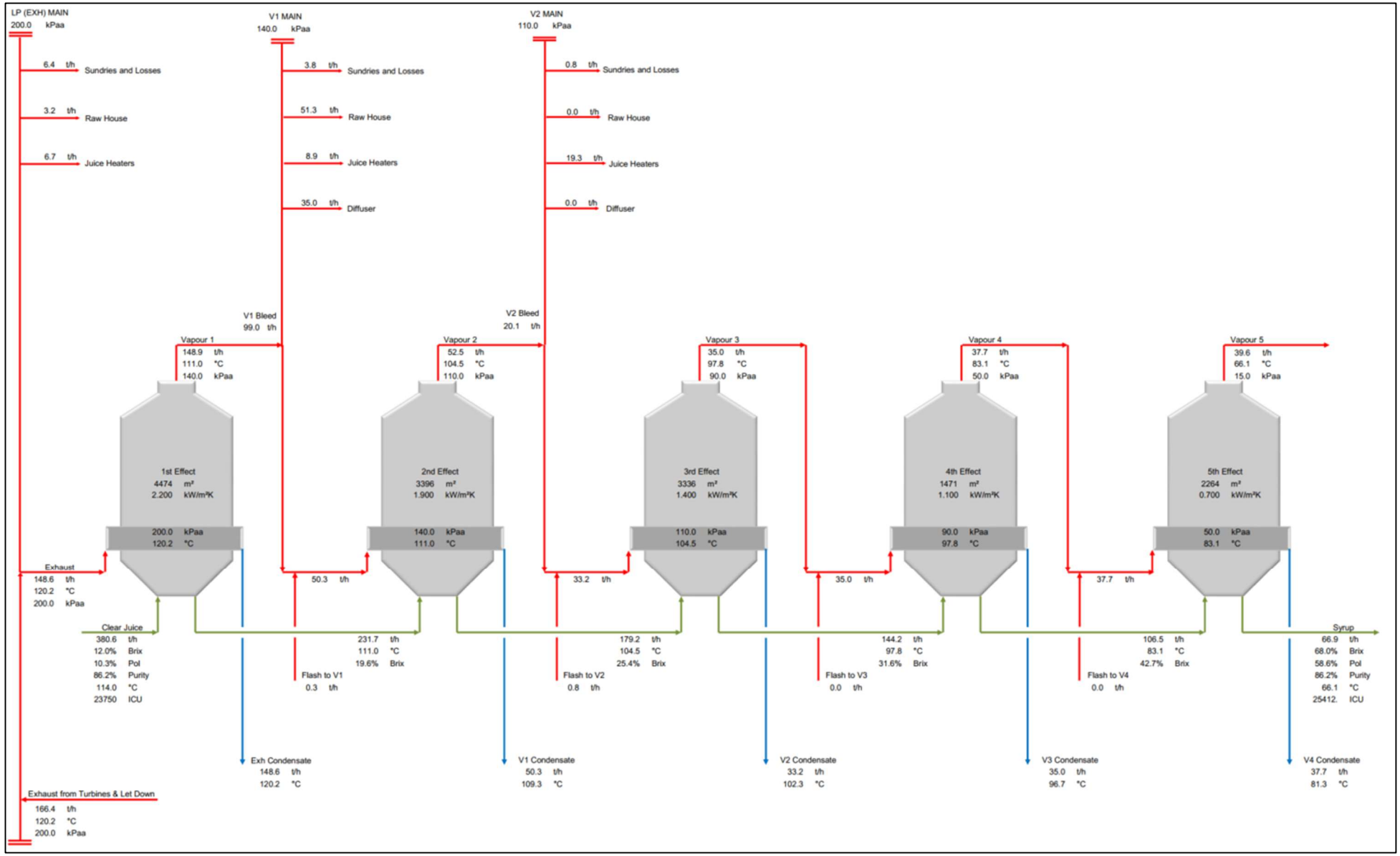


Figure 5b. Excerpt from a coal usage factory EMB evaporator station

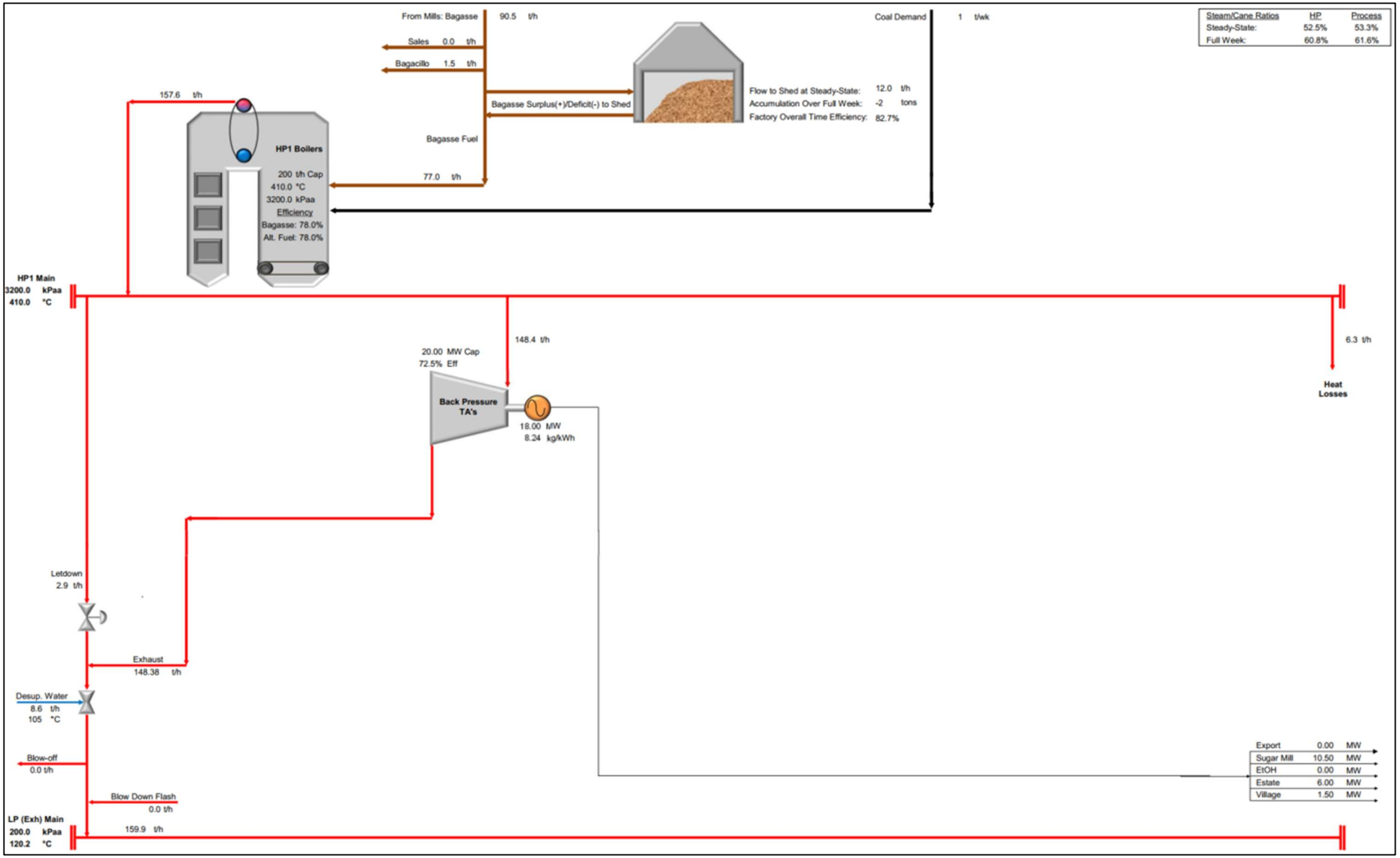


Figure 4c. Excerpt from dimple tube factory EMB typical steam and powerhouse

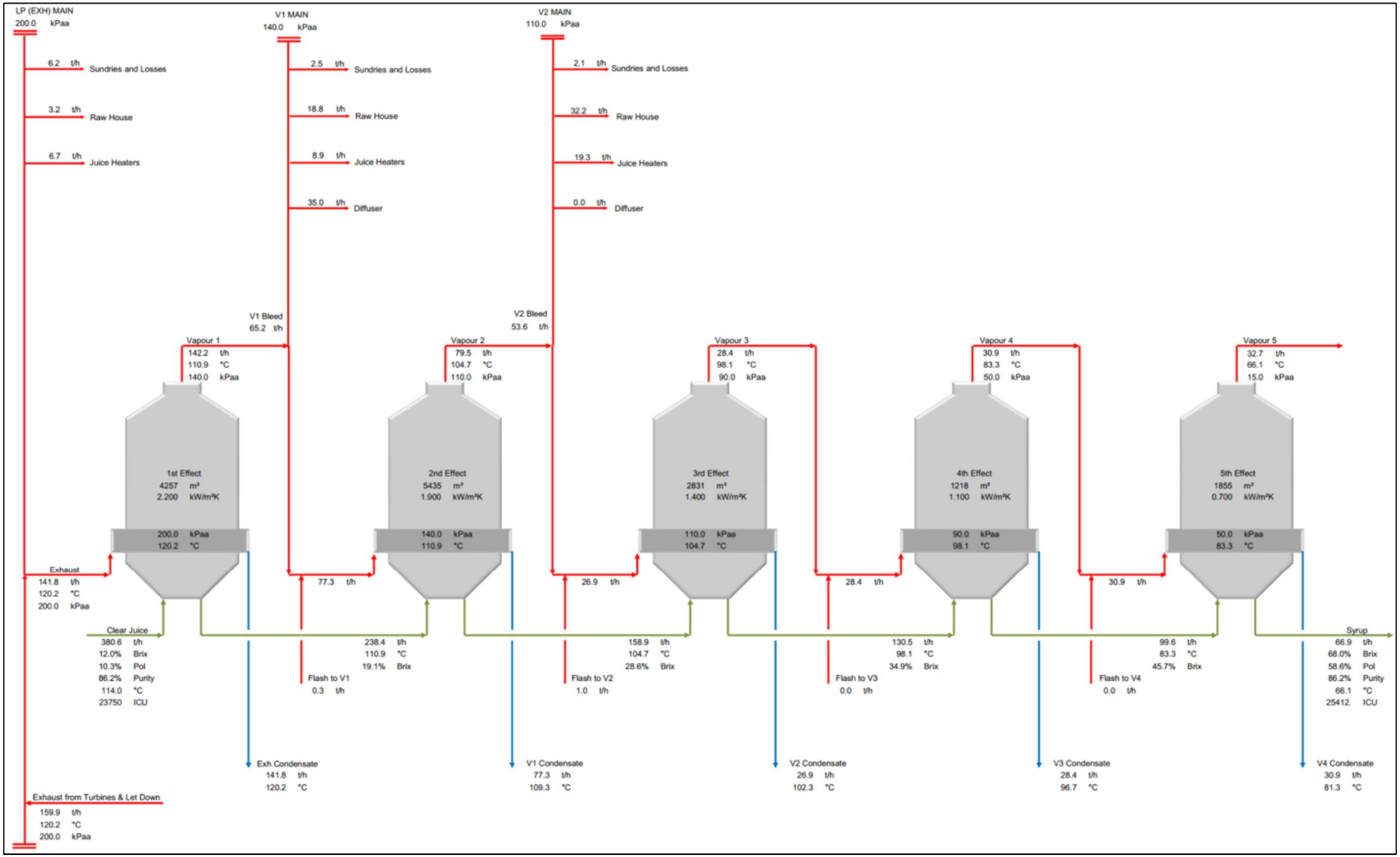


Figure 4d. Excerpt from dimple tube factory EMB evaporator station

Cost-saving conclusion

The Internal Rate of Return on investment (i.e. IRR) will differ from factory to factory. The example above illustrates the potential for fuel savings by using these parameters and the costs of converting a 'typical' 300 TCH raw sugar factory's 'A' vacuum pans only, and by utilising the coal price of approximately USD100/metric ton at the time of writing. This yields a pay-back period of less than 6 months. Of the raw vacuum pans, converting the 'A' vacuum pans to dimpled tubes will have the greatest impact on steam utilisation, but converting the 'B' and 'C' vacuum pans will also benefit the sugar factory, in terms of the steam economy and performance/throughput. Further benefit will be realised if back-end refinery vacuum pans are also converted to dimple tubes.

Retrofitting advantages

One of the key advantages of the dimple tube technology is the ease with which the existing vacuum pans can be retrofitted. The retrofit process is as simple as the conventional retubing of the pan, where the plain tubes are replaced with dimple tubes. This retrofit capability eliminates the need for costly and time-consuming vessel modifications and recertification, which are required by the alternative options.

Sugar manufacturers and refiners can increase the capacity of their existing batch or continuous vacuum pans by up to 30%, or save energy by dropping a vapour grade in the steam supply, without compromising or interrupting the ongoing operations for extended periods. At the time of writing this paper, seven batch vacuum pans have been completely converted to operate using dimple tubes.

Market impact

The commercialisation of dimple tube technology represents a significant advancement in vacuum pan operations, with major implications for both capacity enhancement and energy efficiency in the crystallisation stage of a sugar factory or refinery. While other options or technologies focus primarily on increasing the throughput, the unique contribution of the dimple tube lies in its ability to reduce energy usage by enabling operations at lower steam temperatures, without sacrificing performance.

One of the most impactful findings from the factory trials and theoretical analyses is that vacuum pans fitted with dimple tubes can operate effectively on a lower grade of steam, while maintaining, or even improving, the boiling performance, compared to conventional vacuum pans running on higher-grade steam. This reduction in the steam quality requirement will translate directly into a lower factory-wide steam demand, which will free up high-grade steam for other uses, such as electricity generation or process heating, in other parts of the plant. In coal-dependent sugar mills or refineries, this shift can lead to a measurable decrease in coal consumption.

The ability to retrofit existing pans without modifying the vessel structure further, amplifies the advantages of the technology. This straightforward replacement of plain tubes with dimple tubes minimises the down-time and avoids the costly capital expenditure that is associated with the alternatives, like complex calandria replacement or mechanical stirrers.

In terms of market positioning, dimple tube technology uniquely offers both throughput gains and quantifiable energy reductions, which makes it particularly attractive for sugar producers who are facing increasing fuel costs, or are needing to expand their factories. As decarbonisation efforts accelerate globally, the opportunity to enhance the steam economy, without sacrificing productivity, provides a valuable competitive edge.

In summary, beyond its well-demonstrated capacity enhancements, dimple tube technology introduces a significant change in how vacuum pans utilise thermal energy, which enables sugar factories and refineries to do more with less energy, to reduce their operational costs and to take advantage of further energy savings. Table 1 compares various options for improving the vacuum pan capacities, with a summary of some of the advantages and disadvantages of each.

Table 1. Comparison of the options for vacuum pan capacity-increase projects

Description	**Relative cost (factored to cost of dimple tubes)**	**Performance benefit**	**Comments**
Mechanical circulators	3 to 3.5	Varies, +20 to +30%	Electrical energy requirement Complexity of vacuum leaks Requires stirrer drive access and infrastructure Often requires roof and structural modifications Additional maintenance
Calandria replacement or honeycomb-type calandrias – increased heating surface area	3 to 4	+15%	Vacuum pan calandria rebuild Longer operational interruptions Susceptible to weld leaks High installation costs Increases graining volume
New vacuum pans and pan floor reconfiguration	Project Specific 10+	Project specific	On a case-by-case basis Major project/intervention and operational changes required Often not feasible
Dimple tube upgrade	1	+30%	Simple installation No change to the vessel for tube installation Bespoke design to suit each vacuum pan No issues with leaks Energy benefit due to reduced vapour grade options

Conclusion

This study set out to assess the performance characteristics of dimple tube technology, and to analyse and quantify its performance advantages with respect to the potential for energy savings, due to the improved heat transfer coefficients that are experienced.

Previous work showed that laboratory-scale testing, using A-massecuite, demonstrated a >30% reduction in the batch vacuum pan cycle time, while full-scale industrial trials at the Umfolozi Sugar Mill confirmed these results, with an average cycle time improvement of 32.6%. The geometry of the dimple tubes contributes an additional 16.5% increase in the heating surface area, while turbulence induced by the dimple geometry leads to a calculated 14% increase in overall heat transfer coefficient.

Thermal modelling showed that dimple tubes can achieve equal, or improved, heat transfer by using lower-grade steam, compared to standard tubes operating using V1 steam, which results in a theoretical 8.7% increase in heat transfer, even with a reduced temperature differential. This was verified by factory trials in which vacuum pans fitted with dimple tubes operating on V2 vapour achieved equivalent, or improved, cycle times, compared to those operating on V1 steam and plain tubes.

A theoretical mass and energy balance conducted for a 300 TCH sugar factory predicted a 2.2% reduction in the process steam on cane, which translates to an estimated equivalent of 5 040 metric tons of coal saved per season. With coal priced at approximately USD 100/ton, this equates to a potential fuel cost saving of over USD 500 000 per season. The resulting payback period for retrofitting ‘A’ pans was calculated at under six months, with an even greater benefit possible by extending the retrofit to ‘B’ and ‘C’ vacuum pans. Of particular interest would be the benefits that would be gained from retrofitting the dimple tubes to refinery vacuum pans.

In addition to performance and energy savings, the retrofitting process is simple and cost-effective, and it requires only a standard tube replacement, with no need for vessel modification or recertification. This contrasts with the alternative options, such as mechanical circulators or calandria rebuilds, which often cost three to four times more, require structural alterations and cause extended down-times.

In conclusion, dimple tube technology delivers a verified and replicable improvement in the vacuum pan capacity and thermal efficiency. It enables sugar factories and refineries to reduce their dependence on high-grade steam, to lower their fuel consumption and to significantly improve their steam economy, all with a minimal capital intervention and an excellent return on investment.

Acknowledgements

We would like to thank the Sugar Milling Research Institute, Warren Lawlor from RCL Foods and Umfolozi Sugar Mill for their assistance with the trials and operations during the development and testing of the dimple tubes.

References

Bezuidenhoudt D, Gokool M, Rosettenstein S and Stevens M (2023). The new dimple tube - a technology to improve vacuum pan performance. *Proc S Afr Sug Technol Assoc* 95: 366-374.

Rahiman SN, Mbuthuma Y, Love DJ and Davis SB (2023). Installation of a steam-heated pilot pan at the Sugar Milling Research Institute. *Proc S Afr Sug Technol Assoc* 95: 349-365.

OPERATIONAL PAPER

WHY GRID CODES MATTER FOR EMBEDDED GENERATORS – COMPARING UTILITY VS FACTORY PERSPECTIVES

Ahlschlager R[1], Seebran P[1] and Gent R[1]

[1]Zutari (Pty) Ltd, La Lucia, South Africa

richard.ahlschlager@zutari.com, prasun.seebran@zutari.com, roy.gent@zutari.com

Abstract

Sugar companies, their factories and their estates are under significant pressure, in terms of their financial sustainability; this has been caused by many factors such as international competition, local taxes, escalating utility costs and land-use competition.

Cogeneration in sugar mills, especially those using bagasse as fuel, offers a compelling synergy between sugar production and electricity generation. However, balancing these dual outputs introduces several technical, operational and economic challenges, some of which can be highlighted as follows:

- Fuel supply variability - bagasse availability is tied directly to the sugarcane crushing schedules. Seasonal fluctuations and an inconsistent cane supply can lead to an unreliable fuel input, which affects the continuity of power generation.
- Steam demand – there is typically a conflict between consistent steam requirements for sugar processing and the steam requirements of turbines for exporting power.
- Technology issues – the older mills use inefficient boilers and back-pressure turbines. Upgrading them to condensing extraction turbines and high-pressure boilers is capital-intensive.
- Grid integration issues – many mills lack a robust interconnection infrastructure and are impacted by voltage fluctuations and synchronisation problems that impact a stable grid export.

A challenge (and frustration) to many in the sugar industry is the grid code. It stands as a barrier to the net power export and the associated income from power sales.

This paper attempts to demystify the grid code, to explain its purpose and to offer guidance on key considerations before exporting power. It outlines the importance of grid stability and the role of the grid code in achieving it. Protection requirements and network studies are examined, with the focus on their impact on sugar factories. Two scenarios are presented, based on examples from the southern African sugar industry.

***Keywords*:** Grid code, generation, power, export, stability

Introduction

The past 10 years has seen increasing pressure being placed on the sugar industry in southern Africa. Prior to the introduction of the sugar tax, the South African industry was selling around 1.55 million tons of sugar, but since then, the consumption of sugary drinks has decreased by 30% (Minnaar, 2024). Coupled with this, there has been significant volatility in the reliability of the local utility electrical supply (loadshedding and shortage of capacity in

RSA, Malawi and Zambia, to name a few), which has had a particular impact on the demand costs and production in the agri-zone (Cronje, 2020; MOE, 2024; Nyasa Times, 2024).

With the availability of factory-based embedded generation, several large sugar corporations have grasped the opportunity afforded by the supply shortages and have seriously considered, or embarked on, the expansion of their facilities to become exporters of electrical power. Electricity is a commodity, as the Mauritian sugar industry has demonstrated by contributing 10% to the country's energy mix (EDBmauritius, 2023).

From the authors' experience, several barriers are faced by the sugar industry when developing or converting their facilities for power export, namely:

- the existing facilities have been developed for self-generation, behind-the-meter and islanding configurations, but not for power export; and
- there is a general lack of experience and knowledge relating to utility operations, transactions and technical design requirements.

A recurring theme in industry discussions is a persistent 'fear' of the grid code, which has been driven mainly by concerns over the compliance costs and the potential loss of their licenses. Ironically, due to the evolving standards and policies, many existing facilities are already non-compliant. Each country interprets and enforces their grid code differently, based on its regulatory maturity.

The current approach adopted by many companies that have historical co-generation facilities seems to be the 'don't poke a sleeping lion' approach. Based on the experience in South Africa, in particular, there may be serious merit in this. Any attempt to change the current operational model usually results in the following two drastic outcomes:

- a triggering of the renegotiation of the Distribution Use of System Agreement (DUOSA), with major implications relating to tariffs and possible technical requirements; and
- an in-depth evaluation of areas of the code non-compliance (based on plants installed over 30 years ago, with little supporting documentation).

In the RSA context, the local distributors for the DUOSA (Eskom and Municipalities) tend to be significantly more pragmatic on compliance than the national GCC Technical Evaluation Committees. A key constraint is that the GCC struggles to appropriately differentiate between a 765 MW utility scale base generation unit at a coal-fired power station and an embedded 5 MW cogeneration steam Turbo-Alternator (TA) at a sugar factory. This has not been appropriately resolved over the past two decades.

Furthermore, there is a requirement that any licensed generator must re-evaluate its GCC compliance every 6 years, but this generally does not trigger an 'event', unless there has been a change to the facility generation, which is a fortunate loophole for the industry.

Regardless, whether it is for power export or a compliance triggering event, this paper aims to demystify the grid code and provide some practical rationale and guidance for navigating compliance. The paper aims to minimise the technical jargon and explain why this often-feared regulation ultimately benefits all stakeholders.

Methodology/Approach

Dynamic (unstable) network theory

An electrical network is inherently unstable! What this means is that there is a fine balance that needs to be maintained between the supply and demand (Vargas, 2023). This is measured by monitoring the system frequency. Historically, power is largely generated by rotating machines. As they become overloaded, they slow down, and hence, there is a change in the grid frequency. If a machine rotates too slowly, it generates stress on the mechanical parts; and if it is too fast, heating and over-loading occur (Ibe & Oguejiofor, 2024). Should this happen, units will start to trip and isolate themselves from the electrical grid. This results in less generating capacity being available, with the remaining units becoming more overloaded, and thus tripping out. This is termed as a cascading event. The grid must either shed its load (within 2-3 seconds) to balance the remaining generation, or there is a national black-out. Restoration, after a national black-out, can take up to two weeks, based on the generation mix (BusinessTech, 2023). The economic losses to a nation are catastrophic (Cronje, 2020). The extended black-outs in the Iberian Peninsula in April 2025 are a very recent illustration of this – a cascading event caused 60% of Spain's generating capacity to be lost within 5 seconds (Carbonbrief, 2025)

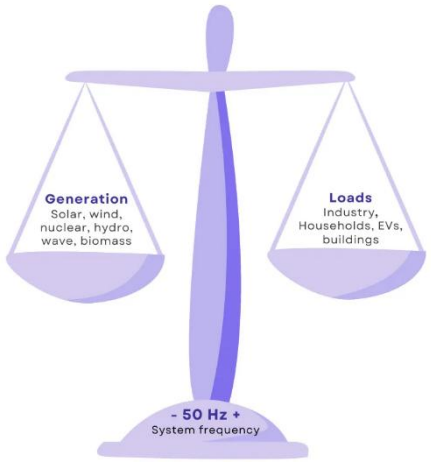


Figure 1. Power system frequency balance (Source: Vargas, 2023)

Why Frequency Hertz? – the purpose of a grid code

A grid code has a very necessary purpose and aims to achieve many different things (Next, 2025). From a system perspective, embedded generation within a sugar factory impacts everyone on a national grid (via the concept of the butterfly effect). However, the impact is related to its scale:

- Safety – protection for all parties, for people and plants (as well as third parties – utility customers);
- Reliability – minimise the impact of internal and external network events on all parties on the network;
- Planning – the utility needs to understand what is happening on the networks as it is serving multiple customers, some locally affected by the embedded plant; and
- Fairness – it creates a standardised framework for all assets that wish to connect to the grid, setting a level playing field for all participants.

Layperson's overview of the grid code

The grid code, irrespective of country, will generally covers the following key aspects (next, 2025):

- the connection requirements regarding the voltage quality and the delivery of active and reactive power;

- the behaviour of the system in the event of failures in the power grid, also with regard to its islanding and black start capability;
- protection of the power grid in case of technical defects on the part of the connected generator;
- the technical requirements on the part of the generator, which allow the grid operator to remotely control (and curtail) power generation in case of turbulences in the power grid or for safety reasons;
- the specifications for the provision of system services (ancillary services) by the connected power generator;
- the tasks of the network operator in relation to the grid capacity and grid architecture; and
- organizational matters of daily operations e.g. the nomination of forecasted power generation, the metering and billing of generated electricity, the scheduling of maintenance works and the resulting down-time, etc.

Theoretically, the requirements for compliance will vary, based on the size and scale of the facility in relation to the general stability of the grid. However, many small rooftop PV units that are summed up can create a massive impact, an issue experienced in Australia (ABC News, 2025).

PPP – Protection for People, Plant and Performance

Protection 101 is firstly about protecting people. Human tissues, especially blood, muscles and nerves, contain a lot of water and ions, which make us susceptible to electricity flow. The consequences are numerous, such as cardiac arrest, thermal damage, involuntary muscle contraction and organ failure. The skin's resistance is only around 100 ohms, with an approximate 80V insulation threshold. Furthermore, it only takes 8 mA to cause the heart to fibrillate (IEEE, 2015). The largest challenge with protection is that electricity (and hence the threat) is unseen, and professional engineers are trained on the concept of earthing, insulation, touch-potential and step-potential.

Secondly, the sustainability of the facility (and shareholder interest) is built on the availability of the plant. Suffice it to say that an electrical plant failure can be catastrophic, depending on the criticality. The repair/replace lead times of a few key items, such as large transformers (8 months), primary HV/MV boards (4 months) and TAs (6 months), excluding transport, installation and commissioning, are measured in months.

What is often not adequately considered in protection, is the impact of performance and reliability. Protection is like a form of 'band-aid' that can be used to stop the bleeding. This is illustrated below, using a KPI called SLI:

Supply Loss Index (SLI):

$$\text{SLI} = \sum(\text{MVA Interrupted} \times \text{Interruption Duration})$$

Consider a simple network in Figure 2 with four loads of 1 MVA each. A fault occurs on L3 for 10 hours. If the L3 breaker operates, we have a SLI of 10 MVA hrs. However, if L3 does not operate and S1 operates instead, the SLI becomes 40 MVA hrs (400% greater impact). This becomes even more important if L2 was a critical service to, say, a boiler. Let us apply a system perspective and say that L3 is the cogenerating facility, and L1, L2 and L4 are grid customers; however, up to L20 customers exist on the node, instead of four customers. Suddenly the perspective changes and the reliability of the L3 breaker (termed the Point of Utility Connection PUC breaker) becomes a very important issue, from a utility perspective.

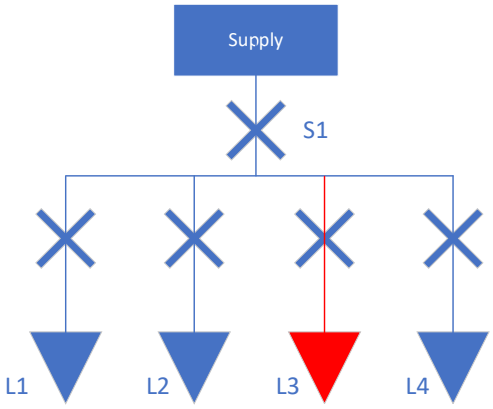


Figure 2. Simple Network to Illustrate Reliability

Protection is both a science and an art, with the key criteria being selectivity, discrimination, sensitivity and speed. It is a central part of a grid code that is aimed at protecting all the affected parties.

Stability – plant and grid

A key aspect of the grid code is to maintain the network stability. A power grid is a complex real network and it obeys certain complex laws (Holland, 2014). Although a network obeys physical laws (primarily Maxwell's equations, Ohm's law, Kirchoff's current law, etc.), the electrical flow is dynamic. Furthermore, networks are subject to both external environmental and internal factors that range from extreme weather, an inadequate design, lightning, a sudden load loss, human error, etc. The aim of the grid code is to maintain the stability of the network, whilst keeping certain operating criteria (the voltage, current and frequency limits) within the design and regulatory requirements. When the operating criteria threaten to step outside of these requirements, protection, and possible cascading, steps in. The national black-outs in Spain in April implies that their grid code application or philosophy had failed (assuming that, at the time of writing, it was not a cyberattack).

What studies inform projects (grid stability, fault, load, etc)

My colleagues and I have been fortunate in being able to assess multiple scenarios across many different countries in Africa (South Africa, Zambia, Nigeria, Eswatini, Malawi, Mozambique and Botswana, to name a few). A key danger for both agents and engineers is to think simplistically, which can manifest itself in several ways i.e.

- by assuming that a facility (factory or agricultural estate) is a closed system, and ignoring that it is embedded in part of a larger system (the national grid), which is embedded in part of a larger system (the Southern African Power Pool); and
- by assuming that the system is complicated and not complex. What is meant by complex is that changes or incidents in one part of a system can result in unforeseen consequences elsewhere. Behaviour can be hard to predict, due to the number of components and interactions, and these systems are not always adaptive (Kunjir, 2024).

This simplistic thinking is often driven by several factors, such as a lack of knowledge or competency, expediency and time constraints, as well as the difficulties involved in engaging with other stakeholders.

Studies are generally separated into static modelling and dynamic modelling. Static models are good for simulating and determining the status of system variables at a point in time. Generally, the network is simulated as a system of interconnected nodes that are linked by networks. Plant and system parameters are assigned to simulate scenarios (what is and what could be), in order to compare various parameters against the plant ratings. These parameters include power and thermal loading, load current and fault current, as well as over- and under-voltages. Static models are good, cheap and give quicker risk assessments to determine whether a project is viable. For instance, they can be used if a sugar factory wants to install a new 20 MW TA and needs to determine whether the internal and external system can accommodate the change (thermal loading, current, fault current and voltage step change for the sudden loss of supply or load).

Dynamic modelling is generally a requirement for most grid codes in larger plants (>10 MW). It looks at the real-time behaviour of the system to changes in the micro-second, milli-second and second range. The level of detail for building a realistic model can be onerous, as the expected accuracy of the model is extremely high by some bodies (i.e. in South Africa). The dynamic studies look at how the various control equipment will perform under various conditions. The equipment control could be the dynamic response of governors, excitation control, voltage regulation and inverter behaviour. The key question to answer is whether they can react appropriately and fast enough to dampen the consequences of an event, in order to prevent it from escalating or cascading.

These issues will be illustrated by considering some scenarios below:

Scenario 1 – Small export vs large export

Facility A has an embedded generation capacity of 20 MW. The capacity is the determining factor, in terms of contributing to the overall system impact. The system does not consider that the facility may already be using all, or 90%, of the power for self-generation and that it may only be exporting a maximum of 2 MW. This is because the embedded generation will still have an impact on both the facility system and the broader grid system. The critical system considerations are as follows:

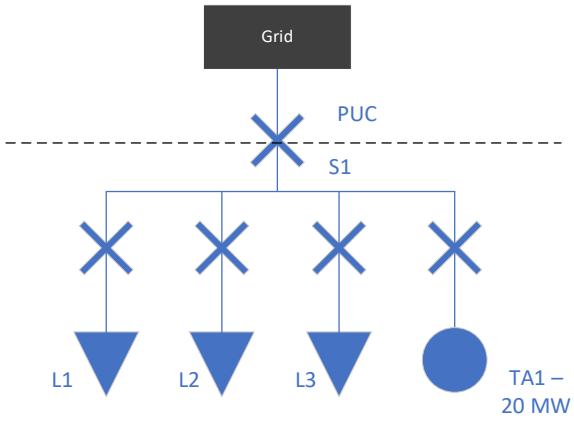


Figure 3. Facility with embedded generator

- The embedded generation contributes to the fault current, which has an impact on the fault current ratings of the existing equipment. The authors have encountered numerous industrial facilities that have ‘evolved’ over time. System considerations are often omitted within the scope of work, and it may emerge over time that the equipment is underrated, that the facility does not comply with safety considerations, and that the cost of rectification is significant. The fault current contribution feeds back to the utility equipment ratings. It may transpire that the utility switchgear is now under-rated for its fault capacity, which poses a risk for the utility operators, such as exploding MV panels.

- Embedded generation changes the thermal loadings of the plant, primarily the networks (cables and lines) and transformers. Under different operating configurations (generally contingencies), it is not unknown for a plant to become thermally overloaded, which leads to it either becoming damaged (if protection is inadequate), or it may result in thermal tripping, which creates a cascading loss of production.

Scenario 2 – Weak vs strong networks

- While still considering the same Facility A of 20 MW embedded generation, there are some considerations regarding the strength of the network. What does that mean exactly? Strength can be a very technical term that incorporates system impedance, installed capacity, robust design and the inertia of an 'infinite' grid. Typically, it refers to the ability of the local grid to remain stable during system events, such as faults (voltage or current). Some of the factors affecting the connection to a network are explained below: Dynamic stability – A key constraint with a 'weak' network is that it cannot hold its frequency or voltage during a system event. There is a fundamental difference between the 4 GW of installed high-speed (3000 rpm) steam turbines and the 4 GW of a mixed hydropower (1000 rpm) and coal generation plant. High speed turbines have serious inertia, and when they are stacked together, it allows for a very stable network in terms of maintaining the frequency and voltage. Small TAs and hydropower units are generally much slower and have lower inertia, which means that they will change speed easily and cannot hold up the voltage during faults. So why is this important? Imagine a scenario where the facility is exporting or generating 30 MW in a country where the installed capacity is only 300 MW, and suddenly the facility's TA trips. The grid needs to respond to the sudden supply loss of 10% of available capacity within 2 seconds or risk a black-out. It must either dispatch power (via battery energy storage systems BESS or hydro) or shed the load quickly. Compare this with the 30 MW loss against that of 3 GW or 30 GW (for South Africa), and the issue of network stability for weak networks becomes apparent.
- Location, location, location – Even for South African facilities that are deeply embedded in a 'strong' network, such as the Eskom grid, this does not guarantee a solution. If the facility is assessing the viability of large power export, there are practical power transfer limits to the current infrastructure on the grid system that can set upper limits to project development. There is a major difference in the network capacity and considerations between trying to export 20 MW adjacent a 132/22 kV high-voltage substation, compared to being fed from a 22 kV or 11 kV medium voltage line 20 km away substation. Lower voltages in the MV range constrain the power export thermally and drive the power losses up significantly. For instance, it would be a poor investment if 5% of a new TA's power is lost to heat losses.

Key challenges with GCC planning and approval

From the authors' experience across the sub-continent, the following observations have been made. Each country manages GCC differently, in terms of rigour and expectations (realistic or otherwise). The following are a list of the considerations, without naming and shaming the utilities:

1. Some countries apply an unrealistic, legalistic approach to the GCC. The reality is that many facilities and co-generation TAs are +30 years old. The required plant

characteristics are not available, and the facilities were never designed with GCC in mind (as it did not exist at that time). There may be an exemption process; however, it can be inconsistently applied, and unfortunately, utility thinking is often applied to industrial facilities. The irony is that many of these facilities have been happily grid-tied with large-scale embedded generation for +30 years, without any major issues. If a facility wishes to move from net zero to a positive export of say 500 kW with 20 MW of TA installed based on existing plant, the facility is expected to fully comply, over time, to the utility level requirements, with the associated costs (refer also to Table 1 for the key technical issues).

2. A minor change in operations and infrastructure that is triggered within a project, can have significant unforeseen regulatory and economic ramifications. When applying for a change in the operating regime, opportunistic utilities may use the opportunity to trigger a change to the status quo, i.e. the technical requirements for Distribution System Use, tariff restructuring, etc. This can have major unforeseen consequences on the viability of current operations or on the project, in terms of cost and/or timelines. Although it may come across as cynical, some cash-strapped utilities use (or abuse) non-technical or unsuspecting developers to pay for deferred plant upgrades within their own systems, which have already been charged as embedded allocations within the current tariff.
3. Some utilities have made strategically inappropriate decisions regarding new energy mix and the dispatchability of power, which place the grid at risk. This presents both a constraint and an opportunity. For example, a significantly high level of solar PV, although comparatively economical to develop, is non-dispatchable and creates a network stability risk. The utility cannot call up a solar farm and demand a further 20 MW of power to address supply constraints. These networks are potentially weak and vulnerable to system disturbances (i.e. a cloud coming over a large PV facility, which triggers a rapid supply loss). It is unlikely that utilities will allow sugar factories to develop further PV facilities to support their energy mix; however, there could be a significant appetite to leverage the cogenerating facility upgrades with preferential tariffs, for both the base supply power export and dispatchability (based on facility constraints).
4. There are utilities with institutional challenges; for example, the utility may not have the capability or capacity to model and adequately simulate the planned facility for grid code compliance. As illustrated earlier, it can be tempting to ‘chance’ it and assume that the facility will behave as planned within the grid. However, an unstable generation node impacts all the stakeholders. The costs are reasonably small and, therefore, the developer should find the appropriate partners to determine the reasonable technical compliance, in order to identify and mitigate the risk to all parties.

Technical considerations and issues for the sugar plant

Based on several years of experience, we have identified the following list of the more common shortcomings, with respect to brownfield installations and the grid code.

Table 1. Typical issues between cogeneration within sugar facilities and the grid code

Grid code Item	Challenge
Power system stabilisers	The code requires that all Co-generators have PSS installed. This should not apply to existing generators, especially those with smaller generation plants. This should be dependent on the Co-generator size and position relative to the transmission system.
Short circuit test	Short circuit testing poses many risks; care needs to be taken when performing the tests, to ensure that no damage is done to the machines. Ideally, these tests should be carried out by the OEM to ensure that they are done within the machine limits. The OEM also then carries all the risks and not the Co-generator. However, many of the cogeneration machines are old, and the OEMs, when in existence, will not carry out the tests and carry all risks, transferring the risk to the Co-generator.
Excitation tests	The required excitation testing comes at a high cost, due to the technical expertise and external measuring equipment. Modern AVRs offer built-in testing tools, which should be allowed to demonstrate compliance; this reduces the cost and saves time. In addition, some excitation tests pose a risk to the units themselves, with one example being the ceiling limit test, which requires the excitation system to have a minimum excitation limit of 1.6pu rotor current. Testing this capability within the cogeneration environment, especially with ageing machines and limited OEM data, is a risk.
Remote control of reactive capabilities	The code calls for the remote control of the cogeneration units. This is not aligned with the SA OHS Act. The SO/NSP is not an authorised person to operate equipment in a cogeneration facility. Further to this, adjustments to the reactive power output of the machines affect the voltage control in the cogeneration plant. In general, this should be an ancillary service.
High & low frequency response	The required frequency range, and the associated time to be able to withstand these changes, are a risk to cogeneration units. Cogeneration plants prioritise both the electrical and steam stability and island themselves under abnormal external grid conditions to prevent a plant black-out. In general, the frequency withstand requirements should be revised, taking into account the machine's capability and plant process steam requirements.
Information exchange	OEM data for most existing cogeneration facilities is not available or limited. Further to this, information requirements are aligned to what is typically provided for modern Gx units, which would not have been available for older units. Proving this OEM data is a serious challenge for most existing plants and should be limited to minimum testing, where they are not available. To provide all the required data would require intrusive testing with the associated risks in an environment that is not conducive for what would typically be type tests.

Considerations at project inception

Should a sugar factory wish to explore a transition to power export, the following can be useful considerations:

- Assemble the appropriate team – It will require a mix of facility and utility competency and experience. Country specific knowledge is preferable. Why? Not all the information is readily available, and experienced practitioners can make informed assumptions, which will reduce the risk.
- Phase the assessment – Power export conversion and feasibility assessments can be phased appropriately. Static studies are faster and cheaper than dynamic studies and can point to system constraints that will affect the decision making. At current prices, a feasibility assessment can cost in the range of R300-500k, whereas a detailed pre-COD (Commercial Operations Date) dynamic modelling is in the range of R1-1.5 million.
- Fail quickly – Determine the economic parameters up-front. The margins in this type of project are narrow, and sometimes a donkey cannot be transformed into a racehorse with a coat of paint. Upgraded grid connections can be expensive (at scale, consider R40 million for a new substation and R3 million per km for network). However, if it is time to upgrade the boilers, or plant efficiencies have created excess steam, then opportunity knocks.

There are no quick and easy solutions. Each facility has evolved and is unique and should be evaluated within its unique context. Do not fall for simplistic thinking but consider the broader context and the impact on others, outside the facility perimeter fence.

Conclusion

The primary objective of this paper is to sensitise practitioners in the sugar industry to grid code compliance. The paper has illustrated how the grid code exists to regulate generation expansion, to level the playing field for those wanting to expand, and to address various technical and safety considerations. The code is applied inconsistently, which can be challenging, and projects that are aligned to a change between parties could trigger unforeseen consequences. Energy is a commodity and opportunities do exist to take advantage of this. However, engineering around large embedded generation is a complex undertaking, and developers should equip themselves with an appropriate team, they should phase their approach and be agile in their decision-making.

Acknowledgments

The authors wish to acknowledge Associated British Foods plc (ABF), Illovo Sugar Africa and Illovo Sugar South Africa for providing the opportunities over many years to partner, practise, explore and innovate around transforming traditional sugar operations in the area of energy production and power export.

References

ABC News (2025). ‘Overabundance of rooftop solar threatens to overload energy grid’, *ABC News*, 18 February. Available at: https://www.abc.net.au/news/2025-02-18/overabundance-of-rooftop-solar-threatens-to/104951632 (Accessed: 26 March 2025).

BusinessTech (2023). *Eskom has 6 ‘barriers’ to prevent a total black-out in South Africa*, *BUSINESSTECH*. Available at: https://businesstech.co.za/news/energy/705371/eskom-has-6-barriers-to-prevent-a-total-black-out-in-south-africa/ (Accessed: 26 March 2025).

Cronje J (2020). *Load-shedding cost SA economy at least R59bn in 2019 - CSIR*, *Fin24*. Available at: https://www.news24.com/fin24/Economy/Eskom/load-shedding-cost-sa-economy-at-least-r59bn-in-2019-csir-20200122 (Accessed: 12 August 2020).

Carbonbrief (2025). 'Q&A: What we do – and do not – know about the black-out in Spain and Portugal'. Available at: https://www.carbonbrief.org/qa-what-we-do-and-do-not-know-about-the-black-out-in-spain-and-portugal/ (Accessed: 30 April 2025).

EDBmauritius (2023). 'Energy Sector in Mauritius'. *Sustainability – the emerging business model – opportunities and challenges*, May. Available at: https://ibcmauritius.org/wp-content/uploads/Renewable-Energy-PRESENTATION.pdf (Accessed: 26 March 2025).

Holland JH (2014). *Complexity: A Very Short Introduction*. OUP Oxford.

Ibe UJ and Oguejiofor VC (2024). 'Under frequency in generating units, effects and mitigations'. *International Journal of Research and Publication* 3(5): 130-140.

IEEE (2015). 'IEEE Guide for Safety in AC Substation Grounding'. IEEE. Available at: https://doi.org/10.1109/IEEESTD.2015.7109078.

Kunjir A (2024). 'Exploring the applications of complex adaptive systems in the real world: A review', in *Artificial Intelligence, Machine Learning and User Interface Design*. Bentham Science Publishers, pp. 136-160. Available at: https://www.benthamdirect.com/content/books/9789815179606.chapter-7 (Accessed: 21 April 2025).

Minnaar K (2024). 'Trouble for sugar in South Africa', October. Available at: https://businesstech.co.za/news/finance/792944/trouble-for-sugar-in-south-africa/ (Accessed: 26 March 2025).

MOE (2024). 'Press statement on the electricity situation in Zambia'. Zambian Ministry of Energy. Available at: https://www.moe.gov.zm/wp-content/uploads/2024/06/PRESS-STATEMENT-ON-THE-ELECTRICITY-SITUATION-IN-ZAMBIA-AT-GOVERNMENT-COMPLEX-12.06.2024.pdf (Accessed: 26 March 2025).

Next (2025). 'What is the Grid code?', *The Power of Many*. Available at: https://www.next-kraftwerke.com/knowledge/what-is-the-grid-code (Accessed: 26 March 2025).

Nyasa Times (2024). 'Malawi: Prolonged black-outs return as Escom is overwhelmed by surge in stormy weather electricity faults', *Nyasa Times*, 28 November. Available at: https://allafrica.com/stories/202411280259.html (Accessed: 26 March 2025).

Sky News (2025). *Spain and Portugal black-outs latest: Power cuts not caused by cyber attack, Spanish grid says - but investigation launched*, *Sky News*. Available at: https://news.sky.com/story/spain-portugal-power-outage-latest-large-parts-of-countries-affected-with-traffic-lights-not-working-and-phone-lines-down-13357538 (Accessed: 30 April 2025).

Vargas B (2023). 'Power grid stability issues. Power grids are critical infrastructure', *Medium*, November. Available at: https://medium.com/@brandonvar/power-grid-stability-issues-aaeb41865718 (Accessed: 26 March 2025).

OPERATIONAL PAPER

KILLING-THE-JOULE: ENHANCING ENERGY EFFICIENCY THROUGH STRATEGIC AND PRACTICAL INITIATIVES AT THE HULETT SUGAR REFINERY

Reddy J, Rambukus Z and Maharaj N

Hulett Refinery, 444 South Coast Road, Rossburgh, 4072, South Africa

jesita.reddy@tongaat.com zyven.rambukus@tongaat.com nishan.maharaj@tongaat.com

Abstract

The Tongaat Hulett White Sugar Refinery, which is located in Rossburgh, Durban, is the largest stand-alone refinery in South Africa, with a rated throughput capacity of 80 tons/hour. In recent years, manufacturing entities have shifted their focus from solely achieving throughput targets to doing so in an energy-efficient manner. As climate change and global warming continue to receive heightened attention, they have become pivotal considerations for the long-term sustainability of businesses. In pursuit of sustainable manufacturing, the refinery has launched an integrated energy-efficiency programme under the initiative 'Killing-the-Joule'. Improving energy efficiency not only enhances environmental sustainability, but it also positively impacts a company's financial performance by reducing its coal consumption. In alignment with this objective, the refinery has implemented several initiatives that are aimed at boosting energy efficiency. The key areas of focus included the front-end (decolourisation) operations, particularly focusing on stabilising the dissolved solids concentration (brixes) through melt brix control and lime density stabilisation, as well as the back-end (crystallisation) operations and the boiler plant operations. This paper also introduces a parallel initiative – the Vapour Recovery Project, which captures previously-wasted flash vapour to heat carbonated liquor, thereby achieving additional steam savings and reducing the dependency on coal even further. The emphasis was placed on enhancing the reliability of the equipment and optimising the recovery of energy through capital projects that are aimed at energy savings. This paper presents an overview of the various projects and initiatives that were undertaken at the Rossburgh refinery. It highlights the effects of the continuous improvements, which demonstrates that it is a robust model for energy management in sugar refining.

***Keywords*:** Energy efficiency, sugar refinery, sustainability, operational optimisation, decolourisation, vapour recovery, boiler interventions

Introduction

The Rossburgh Sugar Refinery, which is recognised as South Africa's largest stand-alone sugar-processing facility, refines approximately 450 000 tons of sugar annually and has a name-plate capacity of 600 000 tons per annum. Unlike integrated sugar mills that typically utilise bagasse - a fibrous by-product of sugarcane - as a renewable fuel source, the refinery relies exclusively on coal for its thermal energy needs. This dependence on coal not only constitutes the second-highest cost component, but it also represents one of its most significant cost drivers. Consequently, improving energy efficiency has emerged as both a strategic necessity for its economic sustainability and an environmental imperative, in the context of the global and national decarbonisation efforts.

Traditional methods of energy optimisation include waste heat recovery from low-grade vapours for process-heating purposes (Mbohwa, 2013), multiple-effect evaporation and boiler efficiency optimisation through economisers, preheaters and air-to-fuel ratios and good operational control on the furnace conditions, as well as the elimination of rogue water into the processes that drive up the evaporation requirements (Elwardany, 2024; Lavarack *et al*., 2004). Some more exotic technologies incorporated within industrial processes include heat pump technologies that are used to step-up low-grade vapour (Chua *et al*., 2010); however, the total exergy dynamics of electrical and thermal energy must be considered for its economic viability. Lastly, a popular method that has also been used at the Hulett Refinery is the pinch technology, to optimise the heating requirements across a system (Tayfield & Hoekstra, 1998).

This paper examines the strategic and operational measures that were undertaken by the refinery to enhance the thermal efficiency of its refining processes. Commencing in the 2020/21 operational season, the refinery initiated a comprehensive turnaround strategy that encompassed the key focus areas, such as yield optimisation, energy management, digital transformation through information systems, workforce development and organisational culture enhancement. The outcomes of the various energy efficiency interventions that have been implemented since 2021 are presented below.

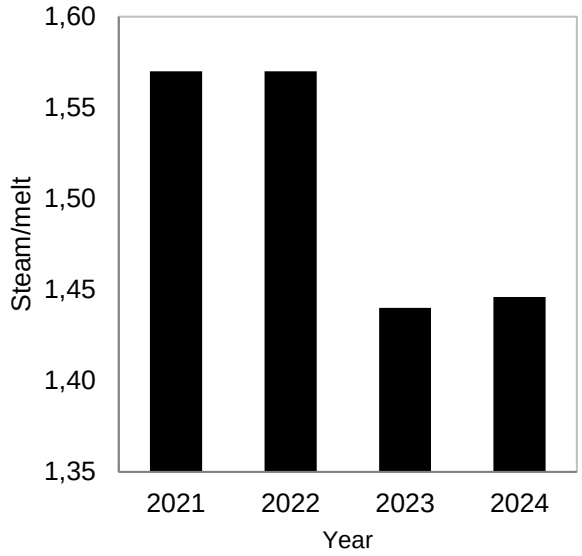


Figure 1. Steam-to-melt ratio – a reduction of 8.3% basis points from 2021

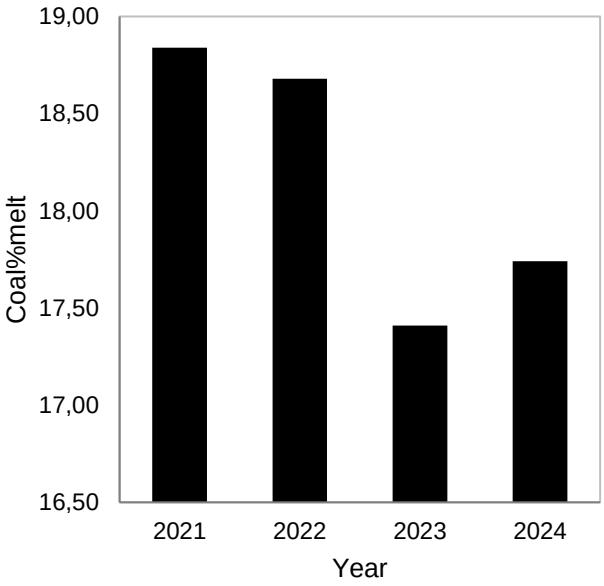


Figure 2. Coal%melt - a reduction of 6.3% basis points from 2021

Refining and energy flowsheet description

The refinery employs a conventional four-boiling scheme and has more recently integrated a fifth boiling stage into the local market blend for white sugar production. The run-off syrup from the pan house undergoes further concentration in a three-boiling partial remelt recovery system, in which the remelt is redirected to the main melting process. Thermal energy for the refining operations is supplied by two 31-bar boilers and a series of 14-bar Babcock boilers. A significant portion of steam is expanded through a turbine to facilitate electricity generation. Despite these efforts, the refinery remains a net importer of electricity to meet its complete energy demands. The performance of the process is evaluated by using a set of efficiency metrics, which are outlined below:

Steam to melt – This is the ratio of the total steam tonnage raised at the boiler plant to the total amount of raw sugar melted.

Steam to coal – this is the ratio of the total steam that is generated at the boiler plant, relative to the coal input to the boiler.

Coal % melt – this is the 'bottom line' metric for energy efficiency at the refinery. This measures the amount of coal used per ton of melt, and the goal at the refinery is to drive it as low as possible.

Figure 3 is a simplified flow sheet for refining and the energy demands per unit operations, with details given in Table 1.

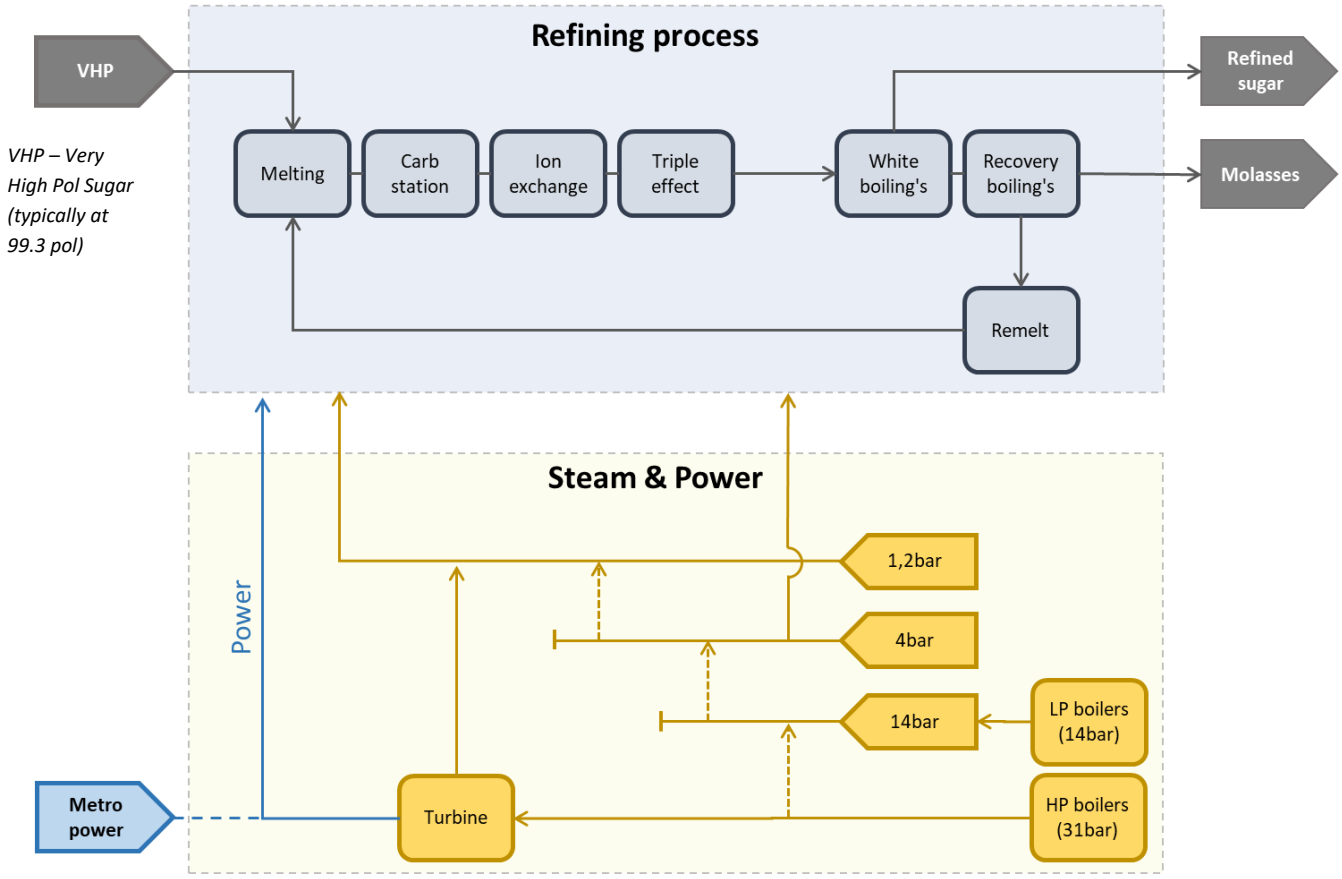


Figure 3. Simplified refining, steam and power flowsheet for the Tongaat Hulett refinery

Table 1. Unit operation's theoretical steam demand (both 120 kPa and 400 kPa) with a melt basis of 60 tph

Unit Operations	Exhaust - Ton/hr	% on melt	% Utilisation	Comment
Melting	0	0	0%	Heat of dissolution - V1 & V3 bleed from evaporators
Carbonatation & ion exchange	5	0,08	6.94%	Heating of carbonated liquor & hot-water heating
Evaporation	8	0,13	11.11%	Concentration to fine liquor
White pan house crystallisation	45	0,75	62.5%	5-boiling scheme
Recovery house crystallisation	10	0,17	13.89%	3-boiling scheme with partial remelt
Deaerator - boilers	4	0,07	5.56%	Boiler feed water
	72	**1,20**	**100%**	

A shifting operating paradigm

The operational experience accumulated over several years has demonstrated that an optimal performance in both the yield and energy efficiency is achieved when the refinery operates at, or near, its name-plate capacity of 600 kilo-tons per annum (ktpa), which is equivalent to approximately 80 tons per hour. This correlation is illustrated in Figures 5 and 6.

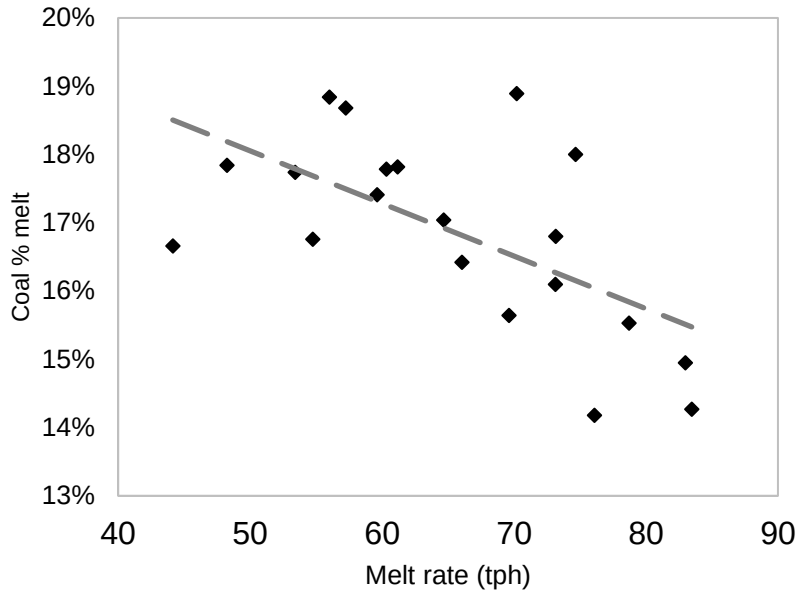


Figure 5. Long-term regression analysis of energy efficiency for the period 2005-2024

The short-term trend (Figure 6) covering a four-month period in the 2023 period also confirms a similar dynamic, i.e. poor energy efficiency results in low throughputs.

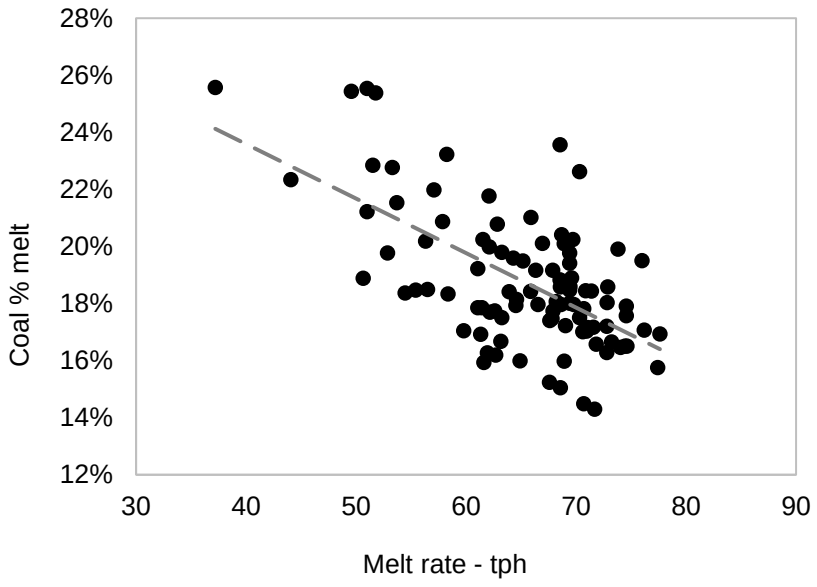


Figure 6. Short-term regression analysis for April to July 2023 – case study approach to energy efficiency for various melt rates

An analysis of Figures 5 and 6 suggests the presence of both fixed and variable loss components that influence the refinery's energy efficiency. Fixed losses may include factors such as radiant heat losses, extended residence time, which results in liquor cooling, and a consistent proportion of recycled solids (sweet water), relative to a reduced melt rate. Consequently, it can be inferred that optimising the throughput in relation to these fixed losses can significantly improve the overall energy efficiency.

This correlation between energy efficiency and throughput introduces a critical operational challenge, particularly in the context of the declining market demand for refined sugar, which is attributed to increased imports and shifting consumer attitudes towards sugar consumption. Currently, production hovers around 450 kilo-tons per annum, which is well below the refinery's name-plate capacity. In response, a key strategic priority for the refinery's leadership is to enhance energy optimisation across varying throughput levels and to develop a 'variable refining strategy' that aligns more closely with the market demand dynamics and that is energy-efficient at different market demand points.

A practical framework to manage energy

In developing a deeper understanding of the refinery's energy dynamics, the following model (Figure 7) reflects the myriad factors that directly and indirectly influence the energy efficiency performance paradigm. The following section highlights the various practical strategies implemented at the refinery.

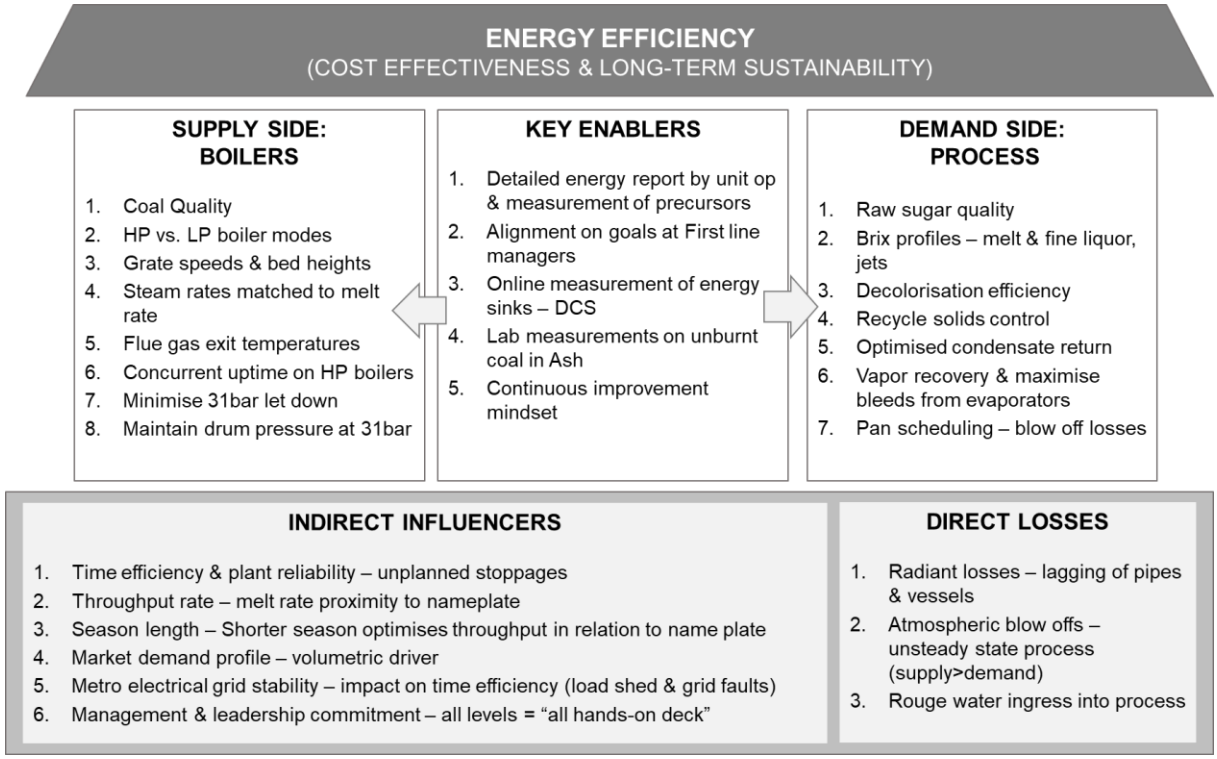


Figure 7. Working framework for energy efficiency at refinery

Practical interventions

Melt brix optimisation: driving energy efficiency at the source

Background

In sugar refining, the concentration of dissolved solids in the melter, which is commonly referred to as brix, plays a critical role in determining the energy demand of the subsequent evaporation stages. The initial stage of the refining process involves combining raw sugar with water in a four-compartment melter and applying heat to produce the 'melt solution'. Operating the melter at elevated brix levels minimises the volume of excess water that must be evaporated during the downstream processing, prior to the recrystallisation phase. This reduction in the water-load directly translates into decreased steam consumption. These findings are consistent with those of previous research, which demonstrated that the optimisation of melter operations can yield substantial energy savings (Bodija *et al*., 2020)

For the 2023/24 season, the average main melter brix was 67.4%. For the 2024/25 season, this increased to 68.7%. This 1.3% increase resulted in the evaporator station's steam consumption reducing from 9.36 tph to 7.95 tph, which was a 15% saving.

The means by which this was achieved is highlighted below:

Melter brix control enhancement

To achieve precise control over melter brixes, advanced instrumentation and control strategies are essential (Lorenz, 2008). Previously, the refinery utilised a Coriolis meter to control the brix of the melter. Based on the brix reading, the amount of water would be varied to achieve the brix set point. This Coriolis meter was installed on a slip-stream line from the outlet of the first compartment of the melter. The Coriolis meter was prone to blockages and it would frequently require intervention to unblock the lines (during which the melter brix would not be controlled). These instabilities would result in inaccurate melter brix readings and ultimately affect the downstream processes and energy efficiency. The instrumentation improvements included installing a microwave probe directly into the first compartment of the melter, thus alleviating the challenge of blockages.

Energy implications

Following the change of the brix measurement instrumentation from a Coriolis meter to a microwave probe, a high-brix melting trial was carried out to determine the optimum level of brix, which allowed for energy-efficient operations, whilst not hindering the throughput. The melter brix set point was increased to 72ºBrix which would effectively reduce the amount of water entering the evaporation stage and resulted in lower steam requirements.

The optimum brix that was achieved was 71%; anything above this resulted in flow issues being experienced downstream.

The quality of the incoming raw sugar played a crucial role in allowing the implementation of the high brix trial. During the 2021/22 season, the high dextran and low pol sugar resulted in increased flow and throughput restrictions.

Maintaining a consistent brix of 71ºBrix is the next step for improving the energy efficiency across the factory, as process instabilities have a cascading effect on the melter brix control.

Fine liquor brix optimisation

A major initiative aimed at optimising the energy consumption was the installation of a falling film triple-effect evaporator station downstream of the ion exchange units. Prior to this upgrade, the fine liquor was concentrated by using a double-effect Robert evaporator system, typically achieving a final brix of approximately 72ºBrix. With the implementation of the new system, the fine liquor brix supplied to the first boiling now consistently ranges between 76% and 78%. This significant increase in pre-concentration markedly reduces the energy required in the fine pans to bring the liquor to the graining point - approximately 83ºBrix - thereby improving the overall thermal efficiency in the crystallisation process. An effective 53% reduction in evaporator steam savings (% on melt) was achieved by using this intervention (Figure 8).

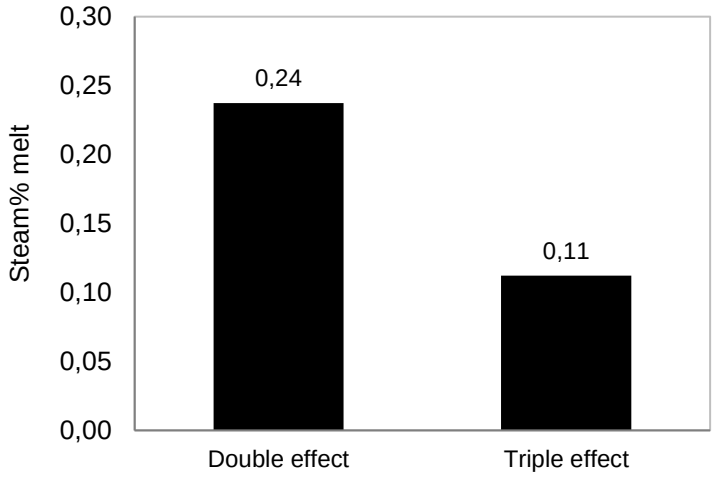


Figure 8. Reduction in steam requirements from the double effect to a falling film triple effect at fine liquor brix of 78% on 60 tph melt basis

Decolourisation optimisation

One of the critical factors in optimising the energy efficiency within the refinery is the reduction of reject sugar via the off-specification (off-spec) stream, which is commonly referred to as ‘wet recycle solids’. Every ton of sugar rejected to the main melter effectively undergoes the entire refining process again, thereby re-consuming energy at multiple stages. In the 2019/20 season, the refinery implemented a third stage of ion exchange by using styrenic resin. This enhancement, in conjunction with an intensified effort to reduce the raw sugar colour from the supplying mills, resulted in a marked improvement in the fine liquor colour profile. The colour is measured in units of ICUMSA (International Commission for Uniform Methods of Sugar Analysis) and the improvement resulted in a drop in colour from approximately 450 ICUMSA to below 300 ICUMSA, thus enabling the consistent production and packaging of fifth boiling sugar, which contributes to a 3.2% reduction in recycle solids and an associated 3 percentage point decrease in the energy consumption, relative to the baseline.

Lime slaking optimisation

Background

Lime slaking is a critical process in sugar refining that involves the preparation of the lime slurry used in the carbonatation process (the first decolourisation step). A consistent lime quality is paramount for efficient impurity removal and for maintaining the efficiency of the process (Moodley *et al*., 2002). One of the feeds into the carbonatation process is slaked lime. Dry lime (CaO) powder is slaked (mixed with water) to yield milk of lime (a suspension of hydrated/slaked lime ($Ca(OH)_2$) in water. The water and lime are mixed to achieve a density that is usually between 1080 and 1100 kg/m^3. Density is an important factor, as a lower density will result in unnecessary melt dilution, whilst a higher density may result in pumping and handling difficulties. The density of the milk of lime is achieved by controlling the flow rate of water to the lime slaker. The combination of CaO and water is an exothermic process and, therefore, the density of slaked lime is achieved by indirectly controlling the temperature of the slaker. Water at approximately 65°C is required to achieve the desired slaked lime temperature of 90°C, and hence the density of the slaked lime. Samples of the milk of lime are tested in the laboratory to measure the density by simply dividing the mass of the sample by the volume of the sample. To achieve the right temperature, the flow-rate of the water is controlled via a control valve on the water line to the lime slaker. However, the temperature of this water was not constant, due to upstream process instabilities.

Slaked lime density control

Automating a heated water make-up stream to achieve the desired temperature of 65°C of water in the lime slaker ensures a consistent slurry density and temperature. Having a stable water temperature could lead to an improved reaction efficiency (Rein, 2007). The water temperature control into the lime slaker was automated by using a temperature-regulated control valve. This stabilised the slaked lime density within the target of 1080–1100 kg/m³, improving the First Time Yield from 54% to 88%. The First Time Yield is a key performance metric that measures the proportion of units that are produced correctly and that meet the quality standard the first time, without needing to be reworked. This is shown in Figure 9. The consistent lime quality also improved the downstream process stability and brix control.

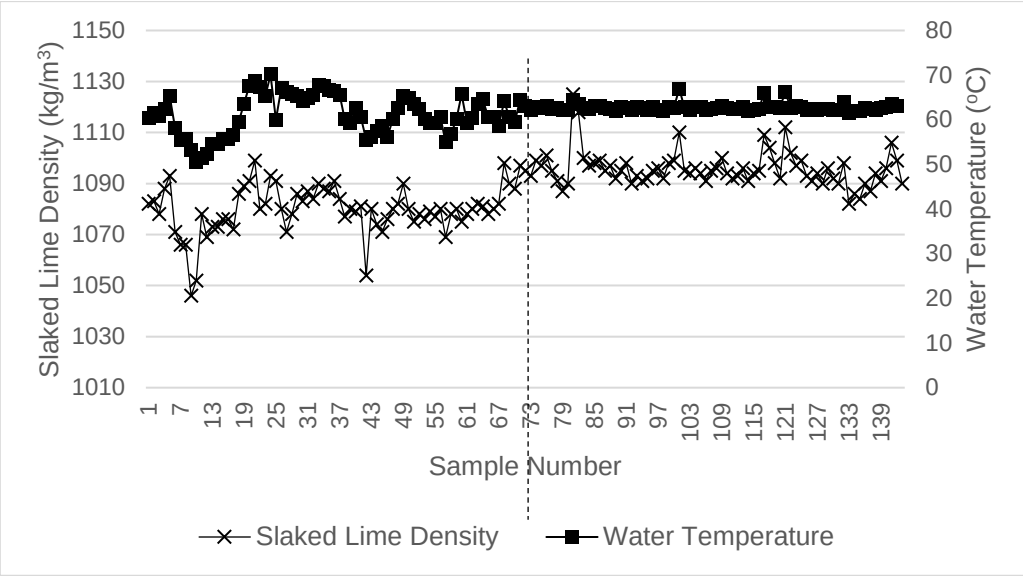


Figure 9. Slaked lime density and water temperature before and after automated control (indicated by the dotted line)

The vapour recovery project: capturing untapped energy and the application of pinch analysis

Background

In many industrial processes, including sugar refining, waste heat recovery presents a substantial opportunity for energy conservation. At the refinery, flash condensate vapour (from the pans and evaporators), which are often vented to the atmosphere, represents a loss of potential energy that can be harnessed for process heating. Implementing a vapour recovery system can capture this energy, which will lead to the improved overall efficiency and reduced coal consumption (Lavarack *et al*., 2004).

Process design

The vapour recovery project at the refinery involves redirecting this flash vapour from the condensate-receiving flash tank to heat carbonated liquor in a repurposed Robert evaporator. The heating of carbonated liquor was previously carried out in a saturator with a tubular calandria (known as the C-saturator) by using exhaust steam from the boilers. The Robert evaporator was decommissioned in 2018, when it was replaced by a triple-effect falling film evaporator.

This process therefore utilises the existing equipment, which has been retrofitted with new piping and control systems, to facilitate the efficient heat exchange. By utilising this flash vapour to heat carbonated liquor, the amount of exhaust steam that is required is reduced. The exhaust steam is thereafter only used as a top-up in the C-saturator, to heat the carbonated liquor to the desired temperature. This integration illustrates the process integration techniques that are aimed at minimising the energy demand by optimising the heat recovery (Figure 10).

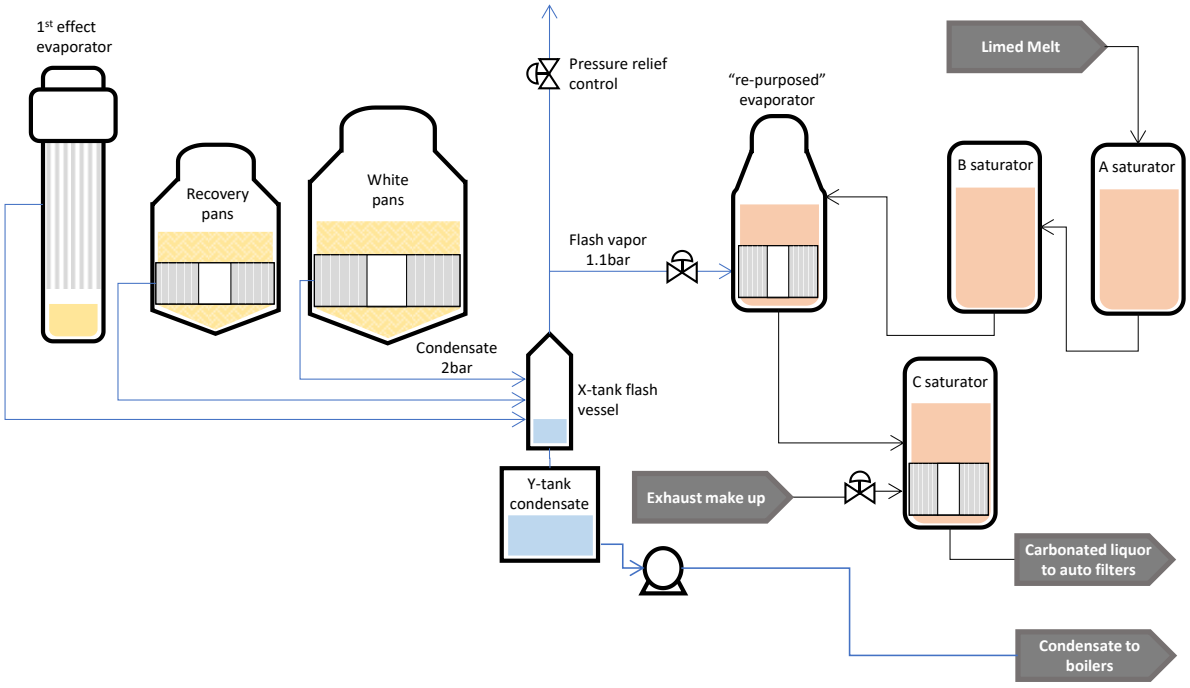


Figure 10. Schematic of the refinery waste heat recovery system

Control philosophy

Effective control strategies are critical for the success of the vapour recovery system. The implementation of control valves, temperature and pressure transmitters and automated control loops ensures that the system operates within the designated parameters. Supervisory controls are established to handle deviations, such as excessive liquor temperatures or pressure drops, thereby maintaining the system's integrity and safety.

Outcomes and savings

The implementation of the vapour recovery system has led to a significant reduction in steam demand within the C-saturator, which translates to considerable cost savings and a decrease in coal consumption. Prior to the vapour recovery project, the steam usage in the C-saturator averaged 3.95 tons/hour. After the implementation of the project, this figure dropped to 1.84 tons/hour.

To exemplify the drop in steam usage, the exhaust steam to the C-saturator, as a fraction of the total steam supply, is indicated in Figure 11. As illustrated, this figure dropped from 0.05 in the 2023/24 season to 0.03 in the 2024/25 season (after the implementation of the project).

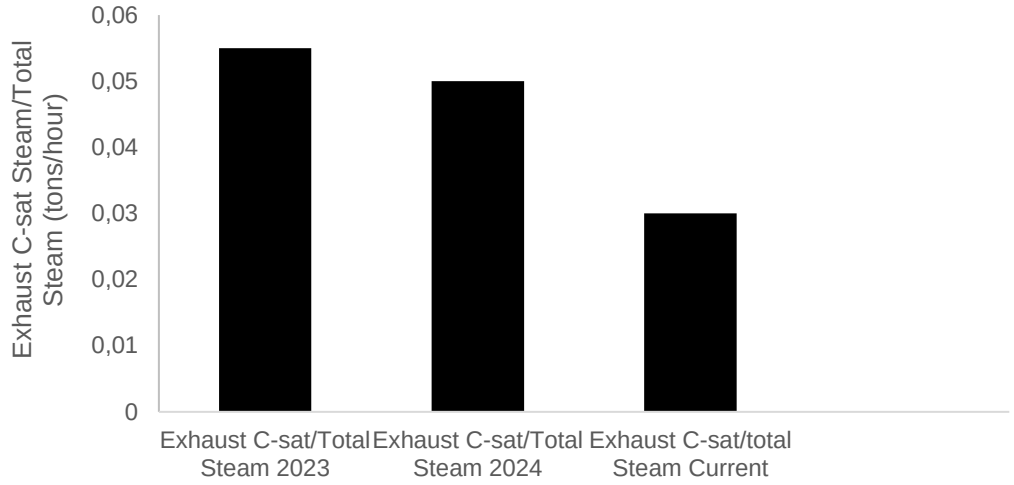


Figure 11. Exhaust steam to C-sat as a ratio of the total steam supplied – a comparison before and after the vapour recovery project

Boiler plant interventions

The boiler plant represents the supply aspect of the thermal supply chain and is an integral key success factor for refinery optimisation. The following aspects were optimised and remain the key focus area:

Reinstating economisers

This will be achieved by reintroducing an additional bank of economisers in the refinery's HP boiler, provided that there is a guaranteed improvement in thermal efficiency of the boilers.

Optimisation of the concurrent run-time of the two HP boilers

Traditionally, the most effective energy performance is obtained via the HP boilers (31-bar) as opposed to the 14-bar small Babcock boilers. The HP boilers further support the maximum power generation by the existing Turbo Alternator (TA) set, which limits the electrical power imports. The typical HP boiler run-time cycle used to be 4 weeks, after which the boiler would be decommissioned, cooled, cleaned and the essential maintenance rendered, prior to returning it to service. In recent times, a 'back to basics' programme was implemented, which involved the detailed process of upskilling the vendors responsible for cleaning and a focused approach to inspections and buy-offs, prior to returning it to service. This detailed and focused approach with key quality inspection gates has seen the boiler run-time cycle increase from 4 weeks to 8 weeks.

Optimisation of 'unburnt coal' in ash

The refinery boilers are designed to combust A-grade coal and the typical unburnt coal fraction in the ash can range from as low as 10% to as high as 20%, depending on the quality of the coal and operational factors. Much focus and attention to detail has recently been deployed in this regard. Some of the key interventions in this aspect are as follows:

- All operational staff have been trained to spot unburnt coal, by using visual sampling methods on the ash belt;
- Shift samples are composited and tested for unburnt coal with a target of <10% set;

- The grate speed and bed heights have been through an extensive trial-and-error approach, to optimise the burn-off and to maintain these key parameters, together with the steady state operations (avoiding stop/starts); and
- Incoming quality monitoring and partnering with the mining suppliers has ensured that A-grade standards are maintained and deviations from key parameters, i.e. volatile and fixed carbon, are addressed timeously.

Broader energy management system implementation

Developing a comprehensive energy management system involves a systematic approach to monitoring, analysing and optimising the energy use throughout the refinery. An Energy Dashboard and reporting system is used to monitor the energy use within the refinery. The key components include real-time monitoring, which uses meters to collect data on energy consumption across the various processes and unit operations. To ensure continuous improvement, corrective actions are implemented, based on the data insights. Future work involves using analytical tools to identify the patterns, inefficiencies and further opportunities for improvement (e.g. the usage of grey water in non-potable areas, as well as repurposing the flue gas and ultrasonic leak detectors).

Future work

The refinery's future work will revolve around the optimisation of the vapour bleeds from the evaporators and condensate systems, in order to maximise the application of hot-water heating within the process and integrating cooling crystallisation into the white boiling systems.

The refinery is in the process of phasing out the 4-bar ribbon calandrias in the white house pans, and it will migrate into a single-range 1.2-bar exhaust, thus simplifying the steam process control logic and maximising power generation. This will also uncouple the refinery's electrical grid from the metro grid, thus enabling an island operation.

Mixed fuel options are also being evaluated and, most recently, woodchips have been blended into the HP boilers; the early results show that a low blend option (<10% woodchips) may be possible. Woodchips exhibit adequate energy properties and a high volatile content, which is therefore favourable for combustion in boilers. Furthermore, woodchips are a renewable energy source and, therefore, they have the potential to reduce the reliance on fossil fuels and subsequently to reduce the environmental impacts. These trials continue to be explored, together with the option of the torrefaction of bagasse from the mills. Possible impacts, such as increased slagging and fouling, will also be investigated.

In the long-term, the strategy of decommissioning the recovery house facility that relies on traditional evaporative crystallisation, in favour of chromatographic techniques, represents a substantial paradigm shift. This transition is anticipated to markedly enhance both the energy efficiency and the product yield.

Conclusion

The energy efficiency initiatives undertaken by the Rossburgh Sugar Refinery demonstrate the tangible benefits of process optimisation and waste heat recovery. By focusing on key areas, such as melter brix optimisation, lime slaking and the recovery of waste heat, the refinery has achieved substantial energy savings. These efforts have not only enhanced its operational efficiency, but they have also contributed to environmental sustainability by reducing fossil fuel consumption and the associated emissions. The strategies that have been implemented serve as a model for other similar areas in the factory that aim to improve their energy efficiency and to ultimately *kill-the-joule*.

References

Bodija YO, Akinwonmi AS, Oladokun AS and Kolawole AA (2020). On the efficient utilization of energy in a sugar refinery. In: I Joseph and O Aluko (Eds.), Re-invigorating Nigerian Universities for Sustainable Development: Festschrift in Honour of Rt. Rev'd Prof. Dapo Asaju (pp. 97-106). Ajayi Crowther University.

Chua KJ, Chou SK and Yang WM (2010). Advances in heat pump systems: A review. *Applied Energy* 87(12): 3611-3624. https://doi.org/10.1016/J.APENERGY.2010.06.014

Elwardany M (2024). Enhancing steam boiler efficiency through comprehensive energy and exergy analysis: A review. *Process Safety and Environmental Protection* 184: 1222–1250. https://doi.org/10.1016/J.PSEP.2024.01.102

Lavarack BP, Hodgson JJ, Broadfoot R, Vigh S and Venning J (2004). Improving the energy efficiency of sugar factories: Case study for the Pioneer Mill. *International Sugar Journal* 106(1266): 337-342.

Lorenz F (2008). Improving energy efficiency in sugar processing. Handbook of Water and Energy Management in Food Processing: 885-903. https://doi.org/10.1533/9781845694678.6.885

Mbohwa C (2013). Energy Management in the South African Sugar Industry. World Congress on Engineering (WCE): 3-5 July, 2013, Imperial College London, London, U.K. *Proceedings of the World Conference on Engineering* 1: 2249.

Moodley M, Schorn PM, Walthew DC and Masinga P (2003). Optimising the carbonatation process. *International Sugar Journal* 105(1249): 24-28**.**

Rein P (2007). *Cane Sugar Engineering* (2nd ed.)*.* Bartens

Sanadi AG and Khot SA (2024). Design and analysis of multiple effect evaporator for the sugar industry. *African Journal of Biomedical Research* 24 (4S): 1444-1455. https://doi.org/10.53555/AJBR.V27I4S.3846

Tayfield D and Hoekstra R (1998). Energy efficiency improvements to the Huletts Sugar Refinery. *Proceedings of the Annual Congress - South African Sugar Technologists' Association 72*: 192-197.

OPERATIONAL PAPER

THE BENEFITS OF INSTALLING MUD BELT FILTERS IN THE SIMUNYE SUGAR MILL IN THE 2024/25 SEASON

Dlamini M, Dlamini M, Kunene T and Kugara R

Royal Eswatini Sugar Corporation, Simunye Sugar Mill, Simunye, Eswatini

Mduduzi.dlamini6@res.co.sz (lmcdlamini@gmail.com),mfanasibili.dlamini@res.co.sz, thembinkosi.kunene@res.co.sz, robert.kugara@res.co.sz

Abstract

The extraction of pol from sugar cane mud through filtration is a fundamental process for boiling house recovery of a sugar mill. The Royal Eswatini Sugar Corporation's Simunye mill had been experiencing high losses of pol in the filter cake between 2020 to 2022, reaching a maximum of 4.76%. The mill had four rotary Dorr Oliver filters at the mud filtration station. As part of its continuous improvement initiatives, an investigation was undertaken, with the objective of arresting the high losses in pol through equipment optimisation and process improvements.

Before the start of the 2024/25 crushing season, the mill procured and installed two Córdoba-type mud belt filters to replace two Dorr Oliver filters. The combined capacity of the belt filters is 400 tons of filter cake per day, i.e. 200 t/day for each unit. The filters were sized based on a filtration area of 0.3 m^2/per ton of cane. By the end of the crushing season, the mud belt filters decreased the filter cake pol losses by close to 40% and reduced the moisture % filter cake by 3%. This improvement resulted in improved boiling house recovery of the mill, as well as the reduction of filter cake transportation costs by more than 60% of the previous season.

However, the high volume of wash water from the belt filters is a challenge. This has had a serious impact on the crush rate at the mill, due to the increased hydraulic loading on the evaporators. Currently the mill installed a wash water recirculation tank, which has improved the crushing rate.

Keywords: boiling house recovery, rotary vacuum filters, mud belt filters, moisture % filter cake, wash water recirculation tank

Introduction

The Simunye sugar mill, one of the three cane mills in Eswatini, produces about one-third of the country's sugar. The mill has relied on conventional Rotary Vacuum Filters (RVFs) for the recovery of sucrose in mud filtration. For decades, the traditional RVFs have proven to be robust and efficient in maximising the recoveries. The mill had previously installed four rotary vacuum filters with a capacity of 0.4 m^2 per ton of cane. However, the limitations of the RVFs have driven the Simunye factory to consider alternatives for optimising sugar recoveries. The RVFs failed to cope with the high mud volumes, due to the high rainfall between 2020 and 2022, and this resulted in high sucrose losses in the filter cake. The filter cake pol was as high as 4.76 % and the moisture % filter cake was above 70%. The high rainfall was a result of the La Niña triple dip, which affected the southern African region for three consecutive years, from 2020 to 2022.

Ng Lung Kit *et al*. (2023) also highlighted the fact that the clay soil type exacerbated the operating conditions at the filter station. The cane fields of the Simunye estate are dominated by clay soil, which is generally characterised by its low permeability. The resultant filter cake

is not easily scraped and requires manual scraping by the filter operators. During wet conditions, the resulting high volumes of mud affected the throughput from 440 to 397 tons cane per hour (tch), which led to an extended crop season of 39 weeks (Lung Kit *et al*., 2023). Alternative technologies, such as the decanter, were considered by the mill, but proved to be unsuccessful. The decanter operates by using centrifugal force for solid-liquid separation. The decanted juice is collected continuously through a central opening. The settled solids are discharged by a scroll towards the narrow end of the decanter. One of the advantages of the decanter is that it has a high solids retention, which means that juice clarification improves, due to less solids recirculated. In addition, the moisture and pol of the filter cake is considerably less, when compared to the rotary vacuum filters (Joshi *et al*., 2016). However, one of the disadvantages of the decanter is the high usage of flocculant for mud preparation.

The solid bowl decanter centrifuge (prototype 450 mm × 1100 mm) was loaned to the Simunye mill in 2018.The decanter operates at a high speed of about 2000 rpm, with a design gravity factor of 1000. The recoveries at the filtration station improved, and the moisture % filter cake was reduced to 60.2 %, compared to 73.1% in the RVFs. In addition, the usage of bagacillo was no longer needed in the mud decanter. The only chemical cost was the high dosage of various flocculants on the feed, namely 23 ppm to 50 ppm. Nonetheless, the high operational costs were not economical for the mill, and hence the decanter was discarded (Ng Lung Kit *et al*., 2023).

Vacuum Press Filters (VPFs), also known as mud belt filters, were also considered by the mill. The first reported studies of belt filters in sugar industry were at Maidstone sugar mill in South Africa. The results of the pilot scale plant were positive, even though this had little influence on the sugar industry (Kruger, 1984). In 2009, the Bois-Rouge sugar (refinery) mill in Reunion upgraded the filtration with a single belt filter from the manufacturer, Technopulp. Later, in 2010, an additional two vacuum belt press filters were installed by the Bois-Rouge mill, due to the positive impact of the first unit that had been installed (Petit, 2014). However, the low filtrate brix that was recycled into the raw mixed juice had a serious impact on the energy balance of the mill (Petit, 2014). Despite this, the Bois-Rouge mill reported good recoveries, due to the belt filters. Hence, the Simunye sugar mill investigated the possibility of installing mud belt filters to replace the conventional rotary vacuum filters.

In 2024, the Simunye mill installed two Córdoba vacuum press filters to solve the challenges of the high pol losses at the mud filtration station. The performance and robustness of the belt filters has vastly improved the mill recoveries at the filter station; decreasing disposal costs of filter cake; reducing electricity and maintenance costs. However, the mill also had issues with low filtrate brix (screen wash water) which could not be sent back for imbibition due to high traces of pol, was directed to the weighed juice tank. Similarly to Bois-Rouge mill, this impacted the mill crush rate, resulting in reduced throughput for the whole of the 2024/25 crushing season. As a quick solution, the mill designed a wash water recirculation tank that had a high-water retention, to allow for the settling of the suspended mud in the wash water. Only the settled mud is automatically purged from the recirculation tank to the weighed juice tank. This set-up was commissioned during the last off-crop and significant results have been achieved, with the mill now operating at its design capacity.

Operation of mud belt filters at the Simunye mill

The mud-belt filters (from the manufacturer Córdoba) were installed at the beginning of the 2024/25 crop season. The belt filters replaced two rotary vacuum filters (with a total filter area of 136 m^2). The two remaining rotary vacuum filters are currently not in use, but have been kept as a contingency, in case of breakdown on the belt filters. In total, the mill had four rotary vacuum filters with filter area of 167 m^2 before installation of the two Cordoba filters. The production capacity of the mill is 10 560 tons of cane per day. Each belt filter is specified at a minimum capacity of 200 tons of filter cake/day.

Figure 1 below shows the process flow diagram of the belt filter installed in Simunye sugar mill.

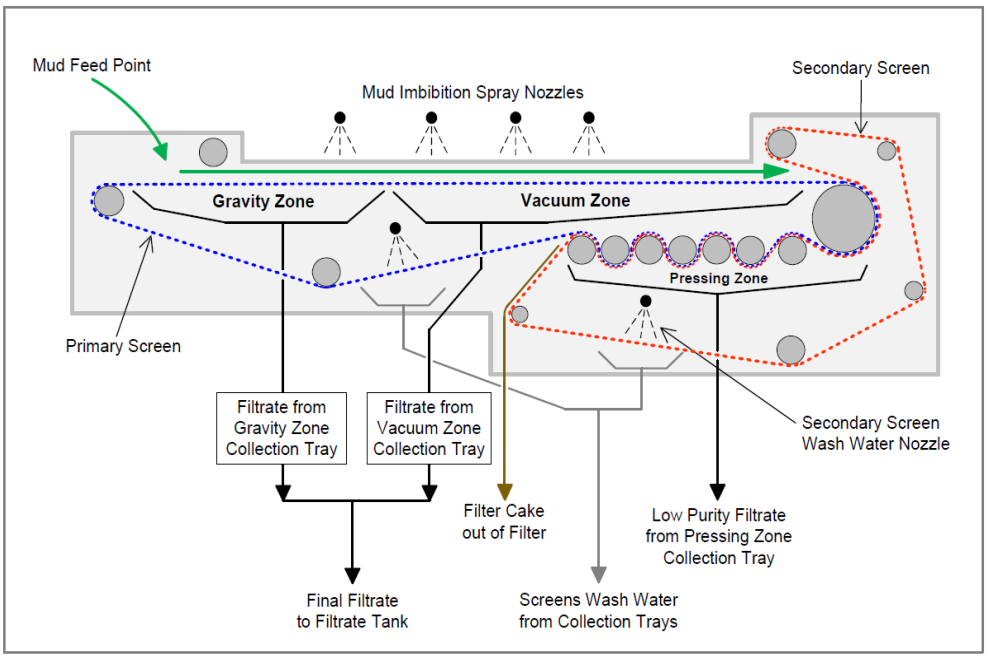


Figure 1. Process flow diagram of a belt filter.

Mud pumps

Mud is pumped to the dynamic mixer, which feeds the two belt filters, by one of the two installed progressive cavity pumps on the variable speed drive (VSD), each having the capacity to deliver a maximum flow rate of 60 m^3/hr. One pump is on standby. A milk of lime is dosed at the delivery side of the pumps.

The lime, which is drawn from the existing lime tank, is adjusted in a dedicated filters' lime preparation tank to a concentration of 5º to 7º Baumé, as recommended by the equipment manufacturer. The lime dosing pumps are on the VSD to allow for controlled lime dosing.

Mud preconditioning

The limed mud is preconditioned in the dynamic mixer by the addition of a polymer. The mixer has a horizontal stirrer/agitator for the homogeneity of the polymer in the mud. This mixer has no steam injection points, since steam is added to the old mud mixer for the RVFs.

The polymer that is currently in use is LT27 AG (anionic high molecular weight polyacrylamide flocculant), which was recommended by the filter manufacturer. The polymer is prepared in the polymer preparation tank to a concentration of 0.1% on a w/v basis (1 kg of polymer per m3 of water). The mixing of the polymer salt/powder and water is done through air sparging. This was chosen over a conventional agitator mixer, to maintain the quality of the polymer.

Once the polymer has been mixed and matured, it is transferred to the polymer dosing tank by gravity. From the dosing tank, the polymer is pumped to the dynamic mixer by a dosing pump on the VSD, to control the feed. This pump is also a progressive cavity type that is suitable for pumping sheer-sensitive polymers.

The quality of the preconditioned mud influences the performance of the mud belt filters. The higher the concentration of solids, the less residual sucrose there is in the filter cake, and the less wash water is used. Overdosing of the polymer (and lime) is not only uneconomical, but it can affect the performance of the filters. Correctly 'flocculated' mud improves the drainage in the filter's feed supply box.

The concentration of the polymer dosed into the mud mixer is controlled between 2.5 to 5 ppm. The adjustment of the polymer concentration is made to achieve the required solids concentration of > 45% in the mixer. On the other hand, the pH of the mud is carefully monitored between 7 and 9 for the mud quality and the preservation of the belt screens.

The ratio of mud, lime and polymer mixture is achieved by adjusting the speed of the pumps for the three respective process streams on the VSDs through the Distributed Control System (DCS) interface, since the pumps are classified as positive displacement pumps. However, maintaining a balance of the three for a sustained period is difficult, due to the varying process conditions, such as the concentration of mud from clarification. Therefore, regular visual inspections are carried out at the mud feed box at the end of the filters mud feed pipes from the dynamic mixer (the filter supply box in Figure 2).

The use of bagacillo in the mixer is currently limited; it is not required, since the preconditioning of the mud with polymer and lime improves the porosity of the filter cake.

As the preconditioned mud enters the top of the filters from the feed box, it is spread across the width of the belt screens by a homogeniser (levelling) roller, to maintain a uniform cake thickness across the belt's screen surfaces, as seen in Figure 2.

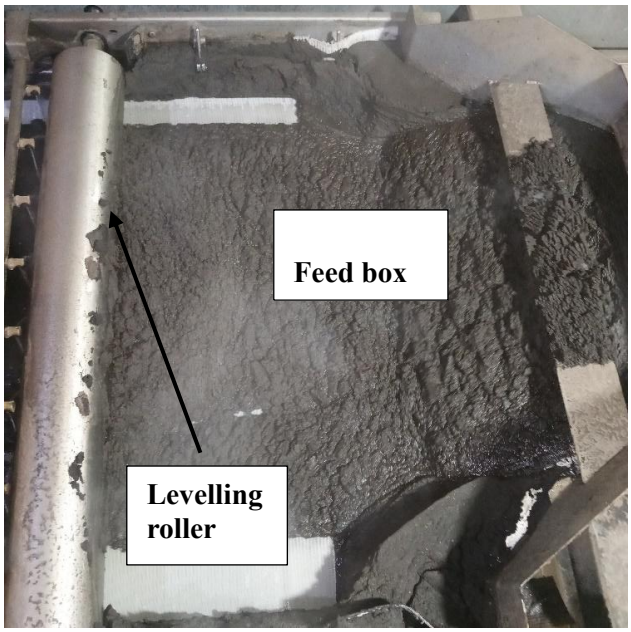


Figure 2. Feed box of the mud belt filter.

Primary and secondary screens

Two screen belts are used in the belt filter, namely, the primary and secondary screens. The screen sizes are shown in Table 1. The speed of the belts is adjusted, depending on the pol % filter cake and clarifier mud levels. The primary screen transfers the mud from the feed area through to the vacuum box of the filter. The filtrate collected is the high brix filtrate (gravity filtrate) in the feed box. This filtrate is almost similar to the clear juice obtained from

clarification. The turbidity of the gravity filtrate is dependent on good mud preconditioning. The vacuum box collects the second filtrate in the vacuum zone before the mud is transferred to the secondary screen. The primary and secondary screens intersect between a series of rollers, to press the last remaining filtrate (press filtrate) in the filter cake. After pressing the filter cake, it is discharged into a filter cake discharge conveyor. Scrapers are found below the manifold of the unit to remove any filter cake that sticks to the screens.

The screens are washed by using pressurised water (5 bar for the Simunye mill) at the sections, after separating at the discharge of the filter cake. This wash water gravitates to a wash water tank.

Table 1. Screen sizes for belt filters.

Screen	Size
Primary belt	1400 ×13400 mm
Secondary belt	1400 × 10500 mm



Figure 3. Clear juice from clarifiers (two test tubes on the left) and gravity filtrate (test tubes on the right).

Table 2 compares the brix, purity and reducing sugars ratio between the clear juice and filtrate for the Simunye mill.

Table 2. Comparative data for clear juice and filtrate from the mud-belt filters.

	Clear Juice	Filtrate	Mixed Juice
Brix	13.4	7.6	13.8
Purity	87	85.2	87.63
RSR	5.1	4.4	-

The belt filter is operated at maximum speed to counter the high clarifier mud levels during wet conditions, even though this increases the filter cake pol losses. The mill has planned to install another belt filter to increase the filter station's capacity and to reduce the pol loss in the filter cake during high-rainfall seasons.

A photograph (Figure 4) of the belt filters station with the dynamic mixer and vacuum generators is also shown below:

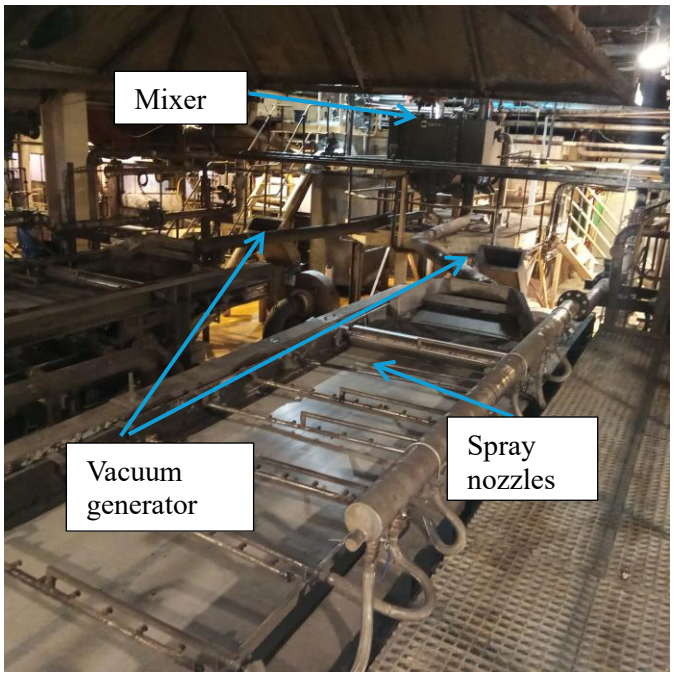


Figure 4. The mud belt filter station at Simunye sugar mill.

Imbibition water and screen wash system

Hot wash water is added in the vacuum zone to increase recoveries of sucrose through a series of nozzles. The wash water is pumped at a high-pressure (5 bar) with a centrifugal pump from the mill supply tank. The water is filtered through a water filter before pumping it to the distribution manifold of the filters. About 15 to 30 m^3/hr of wash water is used on the filter cake for each unit. Separate nozzles are also used for cleaning the screens, with one set for each screen. The cleaning nozzles deliver 10 to 15 m^3/hr of water to the screens. The total water usage on the belt filters is 25 to 45 m^3/hr.

The wash water for the belt is stored in a wash water tank, before recycling it back to the weigh juice tank. The mill had attempted several options to manage the wash water from the screens, and reduce filtrate returns to the weigh juice tank, including:

- to use the water as imbibition water for the milling tandem; and
- to use the wash water in the dynamic mixer to precondition the mud, instead of using flocculant.

Both attempts were unsuccessful, due to the residual pol in the wash water. The first option increased the pol factor of the mill, as the water had traces of sugar in it. The second option increased solids concentration in the mud mixer, which affected the filtration operation, as the mud was very ‘slack’ and flooded the drainage table. Eventually, the mill recycled the wash water to the weighed juice tank.

Vacuum generator

The filter unit requires a vacuum of -15 to -20 kPa(g) that is generated with a vacuum generator (centrifugal fan type). The generator is linked to the manifold of the unit (below the vacuum box). Each unit also has a vacuum receiver that connects to the final filtrate tank.

Troubleshooting the vacuum loss in such a unit is less complex. The loss of a vacuum in the belt filters is mainly affected by a high solids concentration in the final filtrate tank. Applying a vacuum on the belt filter reduces the flooding on the screens.

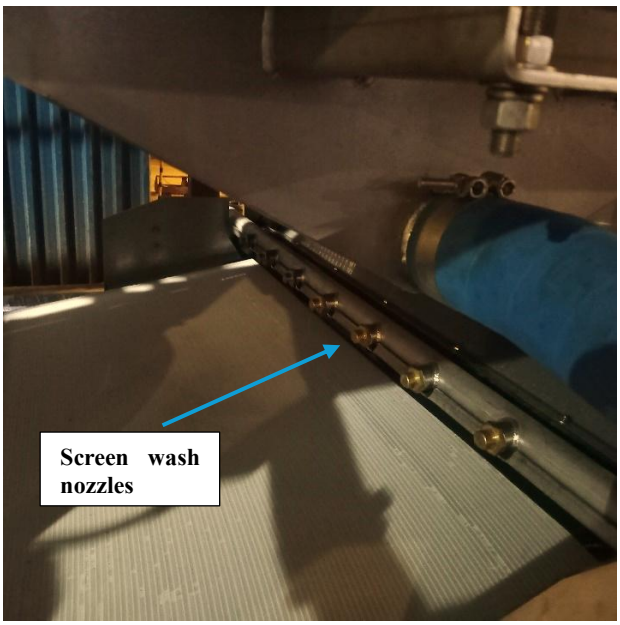


Figure 5. Primary screen wash water spray nozzles.

Final filtrate tank

The gravitational, vacuum and press filtrate are collected in the final filtrate tank. The design of the tank is such that it has an overflow section for solid-liquid separation before the filtrate is pumped to the weighed juice tank. The solids are drained from the tank on stop-days, as this may cause clogging in the barometric columns and it may compromise the vacuum system. Once the vacuum of the system is compromised, the filter cake porosity is reduced, and the drainage on the table is very poor. If this happens, the filter station is stopped immediately, as pol is lost in the filter cake.

The operating conditions of the mud belt filter

The operating conditions of the mud belt filter are summarised in Table 3 below**:**

Table 3. Operational parameters for the mud belt filters.

Parameter	**Target Value**	**Simunye (Typical actuals)**
Brix of filtrate juice	>7.0	8.2
pH mud in dynamic mixer	7 to 9	8.5
pH of the imbibition water	> 7.0	8.0
Cake thickness	8 to 12 mm	10 mm
Water hardness for polymer solution	< 30 ppm	18 ppm
Mud temperature	> 85 ºC	90 ºC
Minimum air pressure for operation under load	>5.0 bar	5.0 bar

The benefits for the 2024/25 crushing season

Data was gathered from factory balance software for the 2024/25 crop season. The data for the 2023/24 crushing season was sourced from SAP system that had been in use the previous season. The Key Performance Indicators (KPIs) of interest included the filter cake pol, moisture % filter cake, filtrate brix, Overall Recoveries (OR) and the Boiling House Recovery (BHR). The data were analysed on Excel, by using statistical methods.

Filter cake pol

The mill target pol for filter cake is specified at 1.5%. The data for the filter cake pol were gathered for the 2023/24 and 2024/25 crushing seasons. The average pol % filter cake for mud belt filters is relatively closer to the target pol of 1.5%. On analysis, higher sucrose recoveries are anticipated from the mud belt filters.

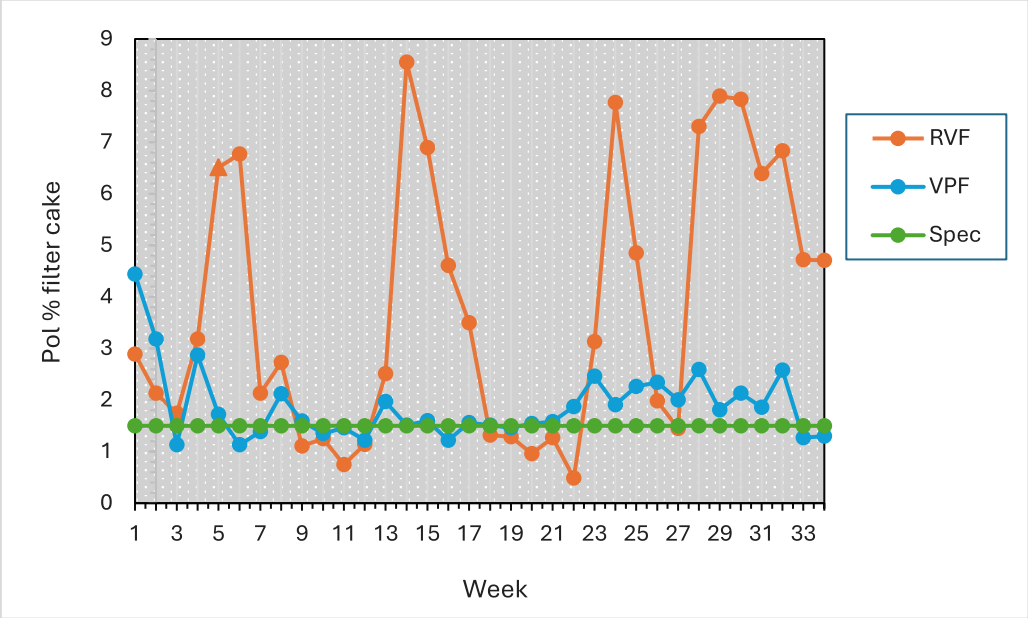


Figure 6. Weekly filter cake pol for crop RVF (2023/24) & VPF (2024/25).

Filter cake moisture

The average weekly moisture of the Oliver filters ranged between 63 and 78%. Compared to the mud belt filters the average was between 60.9 and 73.3% from the trends in 2024/25. The trends, as depicted in Figure 7 showed that there was a significant improvement with the belt filters. The moisture decreased by 3% from the previous season. The lower limit and upper limit for the moisture content was 65% and 70%, respectively. The reduction in moisture content of the filter cake, decreased filter cake disposal costs which significantly benefitted the business. The trend is shown in Table 5 below.

Table 4 also shows the season-to-date figures of the mill for moisture % filter cake and pol % filter cake.

Table 4. Summary of year-to-date values for parameters.

Year	Moisture % filter cake	Pol % filter cake
2023/24	72.2	3.8
2024/25	69.4	1.9

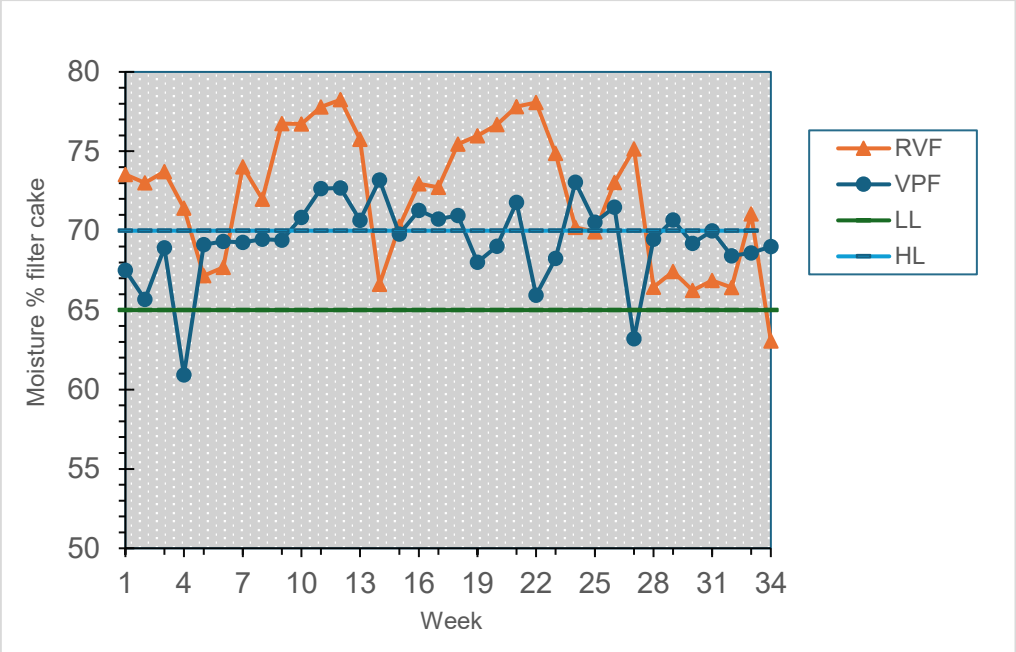


Figure 7. Weekly averaged moisture % filter cake for 2023/24 and 2024/25 seasons.

Filter cake disposal cost

In 2024/25, the mill saved 62.37% of the previous season's filter cake disposal costs. Table 5 below shows the transportation costs of the filter cake that were incurred in 2023 and 2024.

Table 5. Transportation cost of filter cake comparison between the filters for the 2023/24 and 2024/25 financial years (in Rand).

Month	2023	2024	Variance
April	370,350	176,651	193,698
May	898,557	526,734	371,823
June	701,484	169,315	532,169
July	791,222	168,824	622,398
August	1,142,553	255,041	887,512
September	651,304.	300,659	350,645
October	939,223	220,707	718,516
November	592,182	472,675	119,507
Total	6, 086, 875	2,290,606	3 796 268

Overall recoveries and boiling house recovery

The improvement in the filter cake pol has contributed to a better overall recovery and boiling house recovery for the mill. The effect of the drop in performance of the Oliver filters (in 2022 to 2023) on overall recovery and boiling house recovery is also shown in Table 6.

Table 6. Overall recoveries and boiling house recoveries for the Simunye sugar mill between 2022 and 2024.

Year	Boiling house recovery	Overall recovery
2022	86.57%	83.47%
2023	88.48%	85.22%
2024	90.76%	87.38%

Power savings and reduction in bagacillo usage

The belt filters are currently operated with no bagacillo. The additional bagacillo is available for power generation in the mill. Furthermore, the belt filters require less power for vacuum generation than the rotary vacuum filters.

Table 7. Installed power on vacuum and bagacillo usage.

	Rotary vacuum filters	Mud belt filters
Power required/installed on vacuum system	477 kW	150 kW
Total bagacillo [tons]	7 000*	Currently not in use

*Bagacillo usage from 2020 to 2023.

Improved hygiene and housekeeping

The Oliver filter station was prone to bacterial degradation, due to a drop in temperature in the mud boot (Ng Lung Kit *et al*., 2023). It was difficult to maintain good hygiene, especially during rainy conditions. As shown in Figure 8, the assistant filter operator is scraping the mud on the drum to improve the filter capacity. The filter cake spillage can be seen on the walkway grating between the Oliver filters.



Figure 8. Oliver filters in operation at Simunye sugar mill.

The effect of high filtrate returns

Throughput

The mud belt filters have filtrate returns as high as 82 m^3/hr, due to the high volumes of wash water for cleaning the screens. The mixed juice flow rate is normally 500 m^3/hr (mixed juice % cane of 115%) at the maximum crushing capacity of 440 tons of cane/hr for the mill. Hence, the maximum mixed juice flow to the clarifiers is 583 m^3/hr. The Simunye mill has two Dorr clarifiers that are designed for a maximum mixed juice flow of 560 m^3/hr. An additional 23 m^3/hr of mixed juice flow has been added, due to filtrate returns from the belt filters. The hydraulic loading increased in the evaporators, which resulted in a low syrup brix and a drop-in the crush rate during the 2024/25 crushing season.

The mill crush rate for the 2024/25 crushing season was 402 TCH, on average, against a baseline target of 440 TCH. On average, the mill stops amounted to 11.62 hours, due to the high volume of filtrate returning into the weigh juice tank. The total water usage on the mud belt filters is summarised in Table 8 below.

Table 8. Total water usage for the mud belt filters.

Description	Maximum Flow [m^3/hr]
Water in Lime	0.8
Water in Flocculant (and to clean the tank)	22.0
Wash water for filter cake	30
Belt wash water	30

The maximum total water usage on the mud belt filter is 82.8 m^3/hr. This implies that an additional 5.1 tons/hr of steam is required at the evaporator station, based on the quintuple effect.

Filtrate brix

The filtrate brix indicates that there is a high usage of water on the mud belt filters. A significant amount of the water is used for washing the belts, to prevent the clogging of the screens. For each screen belt, the spray nozzles can deliver between 15 and 30 m^3/hr of wash water, as mentioned earlier. This high water usage has increased the hydraulic loading on the evaporators, which caused a drop in the syrup brix and which, in turn, has had a negative impact on the crush rate.

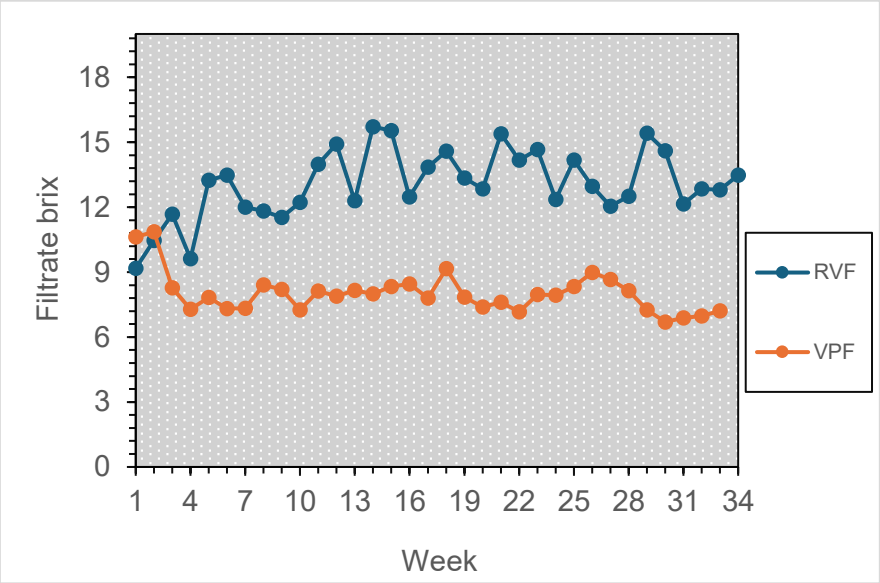


Figure 9. Filtrate brix for the belt and rotary vacuum filters.

Table 9. Comparison of the filtrate brix and wash index of rotary vacuum filters and mud belt filters (season-to-date).

Parameter	Rotary vacuum filters	Mud belt filters
Filtrate brix	13.1	8.0
Wash index	92.3	99.8

Although retention of solids is not considered by the mill in the analysis of the filtrate, the reported figures from the literature studies indicate high figures for the belt filters, in comparison to the conventional rotary vacuum filters (Petit, 2014). A high retention of solids benefits clarification and filtrate turbidity.

Increased cost and usage of flocculant

The belt filters require the addition of flocculant, to precondition the mud before filtration. This has increased the flocculant usage at the clarification and filtration station, and subsequently, also the operational costs of the belt filter station. Table 10 shows the data extracted from the 2024/25 season for Weeks 18 to 21.

Table 10. Weekly flocculant usage for clarification and the belt filter unit.

	Week 18	Week 19	Week 20	Week 21
Tons of cane crushed	66 694	59 941	57 829	66 096
ppm flocculant per ton cane[1]	3.4	3.8	4.3	3.8
ppm flocculant per ton cane[2]	5.3	5.8	5.2	4.5
Cost of flocculant R/ton cane[1]	0.35	0.39	0.45	0.39
Cost of flocculant R/ton cane[2]	0.65	0.71	0.64	0.55

[1]Without belt filter flocculant usage. [2] Includes clarifiers and filters.

Discussion

The results above show that the mill has benefited from the installation of the mud belt filters. This is because of the filter cake pol, which decreased significantly from 4.76 % during the La Niña period (2020 to 2023) to 1.91% in 2024. The figure is still marginally above the target of 1.5%, but it is expected to improve, since it was compromised during high mud-level conditions. The wash water for the screens and the filter cake were reduced to a minimum, especially during dry conditions, when recoveries were favourable. This was done to improve the mill crush rate by reducing the filtrate returns to the mixed juice tank. The filter speeds were increased when the filter capacity was exceeded under wet conditions. When it rains, the mud levels tend to be high in the clarifiers, which necessitates high speeds in the filters to prevent carryover and which, in turn, can affect the clear juice quality.

However, the operational costs have increased, due to the high usage of flocculant to precondition the mud. This has been offset by the reduction in the filter cake disposal costs and the reduced power consumption from the belt filters.

The mill is in a better position to manage mud volumes, due to the belt filters. The disadvantage of the mud belt filter has been the high filtrate returns that are recycled into the mixed juice tank. The mill has designed and installed a recirculation tank for the wash water used on the primary and secondary screens. The recirculation tank was installed during the 2025 off-crop season; and it was designed as a settling tank with three compartments, in which the solids are purged to the mixed juice stream. The purging is done through a timer which opens or closes on/off valves installed in the three compartments.

Currently, the mill crush rate has improved with a season-to-date throughput at 424 TCH, due to the installation of this settling tank. Filter cake pol recoveries have also improved from 1.9% to 1.7%, as shown in Table 11. The effects of the high rainfall between 2020 to 2023 can also be seen in Table 11. It is also anticipated that the mill will add a third belt filter, for redundancy at the filter station.

Table 11. Comparison data for filter cake pol between 2019 to 2025.

Season	2019	2020	2021	2022	2023	2024	2025*
Filter cake % cane	4.02	4.5	4.62	4.87	4.69	2.92	2.58
Pol % filter cake	1.23	2.52	2.41	4.76	3.72	1.91	1.71
Filter cake pol loss [tonnes]	916	2150	1960	3754	3013	802	303
g pol in filter cake/ton cane	0.49	1.13	1.17	2.32	0.17	0.50	0.32

*Season-to-date values.

Conclusion

The implementation of mud belt filters at Simunye sugar mill has greatly improved the filter cake pol and moisture of the filter cake. This improvement has contributed to increasing the overall recoveries of the mill to about 90.76% (pol-based). In the previous season, the mill struggled to achieve the filter cake pol and moisture % filter cake targets, due to the high rainfall received during the La Niña triple dip period. The filter cake transportation costs have also decreased significantly due to the reduction in the filter cake moisture. Hence, the overall benefits of the belt filters outweigh the drawback of increased operational costs, due to the additional flocculant and lime usage. With optimisation, the mill can reduce the wash water usage on the belt filters even further, to improve the mill crush rate and to increase the recoveries at the filter station.

Acknowledgments

A special thanks to the following individuals who contributed to the compilation of this paper:

- *Production Manager (T Kunene)*
- *Area Production Manager (M Dlamini)*
- *Projects Electrical Engineer (R Kugara)*
- *Process Engineer (H Dlamini)*

References

Coughlan KJ, McGarry D and Smith GD (1986). The physical and mechanical characterization of Vertisols. In: *First Regional Seminar on Management of Vertisols under Semi-arid Condition* (pp. 89-106).

Joshi C, Bhave A and Giramkar A (2016). Two-stage decanter operation for treatment of muddy juice. *Proceedings of the International Society of Sugar Cane Technologists* 26: 181-190.

Kruger G (1984).The application of a horizontal vacuum belt filter to smuts dewatering and cane mud filtration. *Proceedings of the South African Sugar Technologists Association* Citeseer 8: 34-38.

Petit A (2014). Application of vacuum belt press filters for cane mud filtration and performance comparison with rotary filters. *Zuckerindustrie. Sugar industry* 139: 298-301.

Ng Lung Kit H, Myeni P and Dlamini H (2023). Rotary vacuum filter operation under rainy conditions at Simunye. *Proceedings South African Sug Technologists Association* 95: 271-284.

REVIEW PAPER

A REVIEW OF SUCROSE SOLUBILITY IN IMPURE CANE SUGAR SOLUTIONS USED IN RAW SUGAR FACTORY PAN STATIONS

Rahiman SN[1], Mbuthuma Y[1], Love DJ[1] and Davis SB[1]

[1]Sugar Milling Research Institute NPC, c/o University of KwaZulu-Natal, Durban, 4041, South Africa

srahiman@smri.org, ymbuthuma@smri.org, dlove@smri.org, sdavis@smri.org

Abstract

Crystallisation is a crucial step in the production of crystalline sucrose within raw sugar factories, and this is typically achieved in multiple stages across a factory's pan station. The majority of the crystallisation occurs in vacuum pans and it is widely accepted that the main driving force during crystallisation is the supersaturation of the mother liquor. Therefore, optimal control of the mother liquor supersaturation in vacuum pans is essential to achieve the highest crystallisation rates while minimising the risk of false grain formation. Hence, it is vital to understand both the solubility at saturation and the metastable zone supersaturation limit of the mother liquor being processed, which are strongly influenced by the nature and quantity of impurities. However, limited sucrose solubility data is available for South African raw syrups and molasses. Consequently, there is a large reliance on factory-scale trial-and-error solubility experimentation in vacuum pans and pan boiler experience to adapt pan boiling procedures to variations in impurity levels resulting from varying sugarcane quality throughout the crushing season, which is not ideal.

In 2024, the Sugar Milling Research Institute NPC (SMRI) upgraded its steam-heated 50 l pilot pan by equipping it with an online pan microscope (ITECA SOCADEI CrystObserver), which presented an opportunity to utilise this equipment for solubility measurements. This paper provides a comprehensive review of the available sucrose solubility data, outlining the common methods for measuring the saturation and metastable solubility limits of impure cane sugar solutions, and the potential application of the fully-equipped SMRI pilot pan as a tool for solubility assessment.

Keywords: Crystallisation, solubility, saturation, metastable limit, pan boiling, pilot pan

Introduction

Crystallisation is a necessary recovery and purification step in raw sugar factories for producing crystalline sucrose (or sugar) of the required quality. Crystallisation typically occurs in multiple steps in a raw sugar factory and involves the use of evaporative crystallisation (or pan boiling) and cooling crystallisation. The majority of the crystallisation is performed during pan boiling and this process generally utilises batch vacuum pans, or a combination of batch and continuous vacuum pans. The objectives of pan boiling include (1) recovering the maximum amount of crystalline sucrose efficiently, (2) production of massecuite crystals of the required size and a narrow size distribution for efficient separation in the centrifuge station and (3) production of sugar that meets the customer quality specifications. South African raw sugar factories typically employ the partial-remelt pan boiling scheme (see Figure 1) to produce very high pol (VHP) sugar.

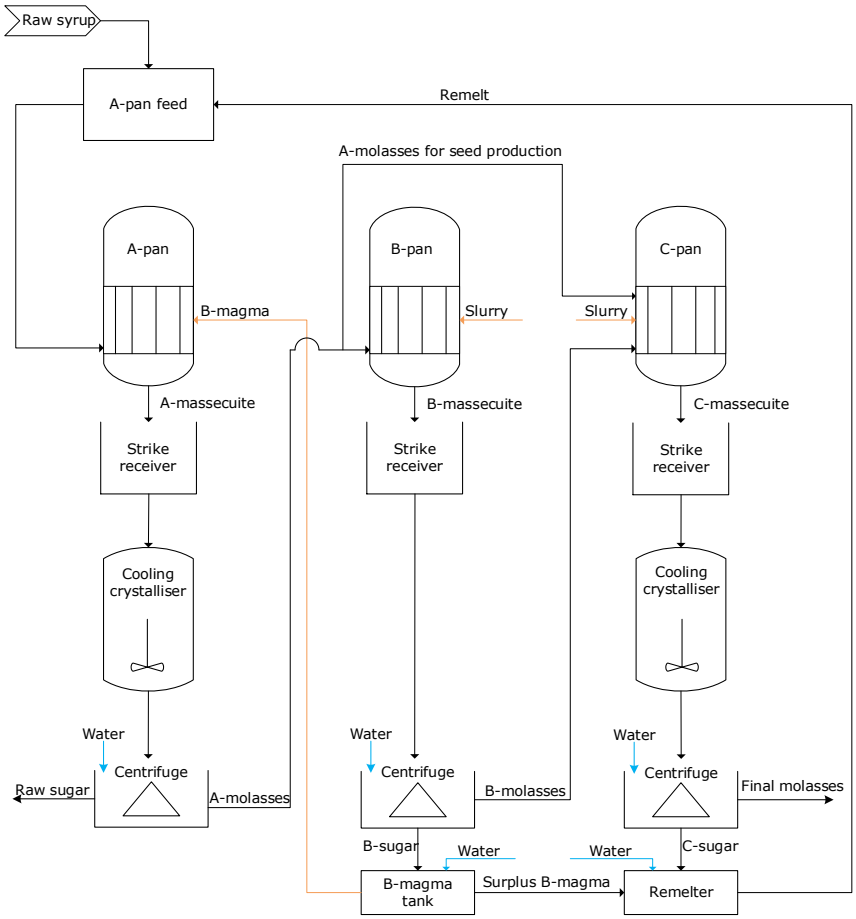


Figure 1. Process flow diagram of the partial-remelt boiling scheme (Rein, 2007)

In this boiling scheme, the A-pans are typically seeded with B-magma, while the B-pans and C-pans are seeded with ball-milled slurry (i.e. finely-milled refined sugar suspended in alcohol). Pan boilers strive to achieve true seeding (i.e. only the seed crystals grow into product crystals and there is no crystal dissolution nor spontaneous crystal formation) during pan boiling as this feeds into Objective (2) of the process.

Good pan station performance largely depends on controlling the mother liquor supersaturation which is the main driving force during pan boiling. Therefore, objectives (1) and (2) of pan boiling ideally require a sound knowledge of the solubility of sucrose in impure cane sugar solutions. This ensures that pan boiling proceeds at the fastest rate while reducing the risk of forming new crystals (or false grain). There is a large variation in the solubility data for impure cane sugar solutions (Rein, 2007) and very limited data for South African cane sugar process streams (i.e. raw syrup, A-molasses and B-molasses) is available. Therefore, pan boilers have limited information with which to adjust the concentration of the mother liquor. There is therefore a large reliance on trial and error and pan boiler experience to adjust pan boiling control to accommodate for cane quality changes throughout the crushing season. Consequently, there is a risk of long boiling times, production of poor quality massecuite and increased usage of energy that adversely affects factory throughput, boiling house recovery and energy efficiency, respectively. There is certainly a need to generate reliable solubility data for South African impure cane sugar solutions as this may assist with optimisation and automation of the pan boiling process, and the upskilling of pan boilers, especially when there is poor succession planning between pan boilers.

The Sugar Milling Research Institute NPC (SMRI) owns a fully-instrumented 50 l pilot pan capable of simulating industrial pan boiling behaviour (Love and Walthew, 2002 and Rahiman *et al*., 2023). The pan is equipped with an ITECA online pan microscope that may potentially be used for generating solubility data similar to the visual technique reported by Chen (1985) and Honig (1959). The objective of this paper is to critically review the available solubility literature for impure cane sugar solutions and the common methods used to measure solubility. This paper also discusses the assessment of the technical viability of using the SMRI 50-l pilot pan to generate solubility data.

Available solubility literature for cane sugar solutions

Understanding how the solubility of sucrose in aqueous solutions changes with temperature and dissolved impurities is the foundation of sucrose crystallisation. Raw sugar factory boilings are typically performed between 60 and 70°C (Penklis and Wright, 1963 and Rein, 2007) and the boiling temperature is typically reduced from the A-pans to C-pans to slow down the undesirable Maillard reaction. Rein (2007) states that the Maillard reaction thrives under high dissolved solids, high temperature and low purity conditions, and therefore recommends boiling temperatures of <63°C particularly for the C-pans.

Solubility of pure sucrose solutions

Sucrose is highly soluble in water as about two thirds by mass of sucrose can dissolve in onethird by mass of water at room temperature (25°C – Anon, 1985). The solubility of pure sucrose in aqueous solutions primarily depends on the temperature of the solution. Mathlouthi and Cedus (1995) provide a comprehensive review of the solubility of pure sucrose solutions showing that the solubility of sucrose increases with temperature (i.e. more sucrose can dissolve in a unit mass of water at higher temperatures). A saturated aqueous sucrose solution is a solution that is in a state of equilibrium with its undissolved solid sucrose phase, and as such, it contains the maximum amount of dissolved sucrose at a given temperature.

The sucrose solubility review by Mathlouthi and Cedus (1995) stated that the Charles (1960) and Vavrinecz (1962) empirical solubility correlations for a pure sucrose solution were recommended by the International Commission for Uniform Methods of Sugar Analysis (ICUMSA – Heitz, 1974), which is in agreement with Rein (2007). The Charles (1960) correlation (Equation 1) is applicable for a temperature range from 0 to 86°C whereas the temperature range of the Vavrinecz correlation (Equation 2) is from -13 to 100°C. Rein (2007) states that the Charles (1960) correlation may be used up to a temperature of 90°C, and this is in agreement with the South African Sugar Technologists' Association (SASTA) manual (Anon, 1985). Equations 1 and 2 assume that the dissolved solids are equivalent to the refractometric brix (B) of the pure solution. Both the SASTA manual and Rein (2007) recommend the use of Equation 1.

$$B_{sat} = 64.397 + 0.07251T + 2.0569 \times 10^{-3}T^2 - 9.035 \times 10^{-6}T^3 \quad \text{..... Equation 1}$$

$$B_{sat} = 64.447 + 0.08222T + 1.6169 \times 10^{-3}T^2 - 1.558 \times 10^{-6}T^3 - 4.63 \times 10^{-8}T^4 \quad \text{..... Equation 2}$$

Where B_{sat} is the saturation brix of the solution (°Bx) at a given temperature, T (°C).

Supersaturation and supersaturation coefficient

Crystallisation of sucrose can only be achieved in a supersaturated sucrose solution, which is a solution that contains more dissolved sucrose than at its equilibrium state at the same temperature. Supersaturated solutions in sugar factories may be produced by increasing the concentration of sucrose at a given temperature through evaporation of water (via pan boiling) or by cooling a saturated solution (via cooling crystallisation). Supersaturation is the main

driving force in crystallisation and the extent of supersaturation is referred to as the supersaturation coefficient (SSC). The SSC of a sucrose solution may be determined by using Equation 3.

$$SSC = \frac{\frac{S}{W}}{\left(\frac{S}{W}\right)_{sat}} \quad \text{..... Equation 3}$$

Where S is the mass percent of sucrose (%), W is the mass percent of water (%) and the subscript 'sat' refers to saturation (i.e. the S/W ratio at saturation at a specific temperature). Hugot (1960) proposed the following equation to determine the SSC of a solution at a given purity and temperature.

$$SSC = \frac{\frac{B}{100-B}}{\frac{B_{sat}}{100-B_{sat}}} \quad \text{..... Equation 4}$$

Equation 4 is a convenient form as it utilises brix and may be used with Equation 1 to determine the SSC of a pure sucrose solution.

Figure 2 was constructed using Equations 1 and 4, and shows the three zones of supersaturation (Chen, 1985, van der Poel *et al*., 1998 and Love *et al*., 2016) that are described as follows:

- Metastable zone (1.0<SSC<1.2) – only crystal growth occurs in this zone.
- Intermediate zone (1.0<SSC<1.3) – new crystals form in the presence of existing crystals.
- Labile zone (SSC>1.3) – new crystals form spontaneously in this zone.

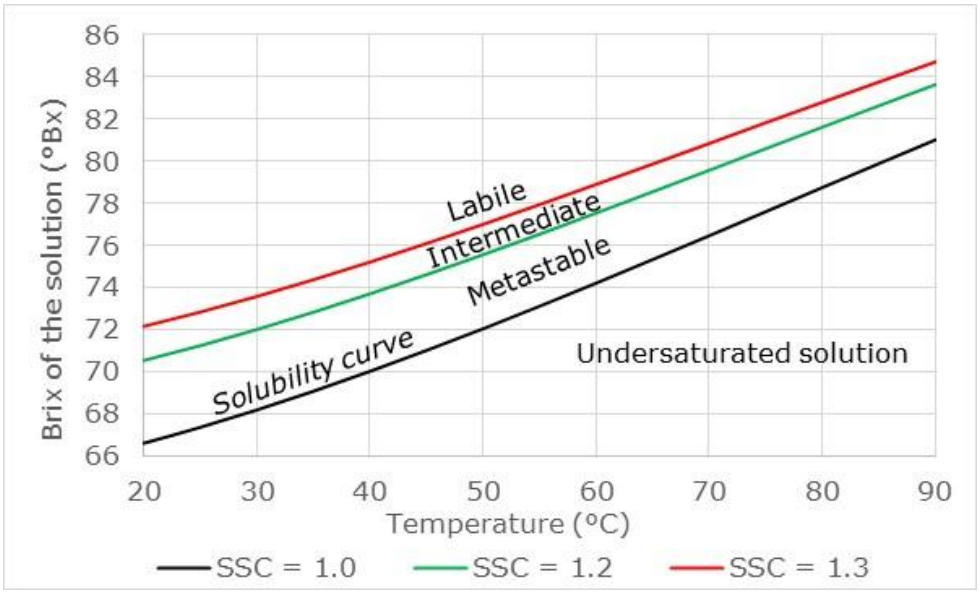


Figure 2. Solubility and zones of supersaturation for a pure sucrose solution

It is desirable for pan boilers to operate at the upper region of the metastable zone so that the crystallisation rate is maximised without the risk of false grain formation.

Solubility of sucrose in impure cane sugar solutions

The non-sucrose content of cane sugar syrups and molasses is the difference between the total dissolved solids and the sucrose contents. Non-sucrose alters the solubility of sucrose in water, and the effect of non-sucrose depends on the type and quantity that is present (van der Poel *et al*., 1998 and Rein, 2007). The effects of non-sucrose are complicated and the type of non-sucrose may be different in various regions of South Africa and may change with sugarcane varieties. Therefore, having a good understanding of the effect of non-sucrose on raw sugar factory syrups and molasses, particularly in South Africa, is of great practical importance during crystallisation.

Mathlouthi and Cedus (1995) and van der Poel *et al*. (1998) provide good reviews of the key aspects of the solubility of sucrose in impure beet and cane sugar solutions. According to Mathlouthi and Cedus (1995), the non-sucrose in cane sugar solutions may affect sucrose solubility by either binding water and/or sucrose molecules. Rein (2007) states that the reducing sugars (i.e. fructose and glucose) typically decrease the solubility of sucrose in water and van der Poel *et al*. (1998) states that Vavrinecz (1978/79) shows that the effect of reducing sugars increases with decreasing temperature. The ions present in cane juice, specifically, the potassium, sodium, calcium and magnesium cations, increase the solubility of sucrose. There are differing opinions on which cation is the most melassigenic: van der Poel *et al*. (1998) reports on the experimental data from Vavrinecz (1978/79) and shows the melassigenic effect of the following cations in descending order:

$$K^+ > Na^+ > Li^+ > Ca^{2+} > Mg^{2+}$$

Sahadeo (1998) showed the melassigenic effect of the following cations in descending order using South African raw sugar factory molasses:

$$Na^+ > Ca^{2+} \text{ and } Mg^{2+} > K^+$$

Interestingly, sodium was found to be the most melassigenic cation on a mg/kg dry solids in molasses basis; however, potassium is expected to create more molasses as it is the most abundant in molasses (Sahadeo, 1998). The cations (and anions) are typically measured collectively as conductivity ash in raw sugar factories. Generally, the reducing sugars and ash are grouped as the reducing sugar to ash (RS/Ash) ratio when considering their impact on solubility (Rein, 2007). Although it may be considered convenient to use the RS/Ash ratio given the limited analytical capability of sugar factories for analysing ions, the ash composition may change from region to region and/or season to season, and therefore it may be appropriate to focus on specific ash components, particularly if the analysis can be done rapidly.

The effect of non-sucrose on sucrose solubility is typically expressed as the Solubility Coefficient (SC), as defined by Equation 5.

$$SC = \frac{\left(\frac{S}{W}\right)_{sat,impure}}{\left(\frac{S}{W}\right)_{sat,pure}} \quad \text{..... Equation 5}$$

It is clear from Equation 5 that the sucrose-to-water ratio of an impure solution at saturation may be determined if the solubility coefficient and the sucrose-to-water ratio of a pure solution at the corresponding temperature are known. The value of SC strongly depends on the Non-Sucrose to Water (NS/W) ratio and is defined mathematically by Lionnet and Rein (1980) as follows:

$$\frac{NS}{W} = \frac{DS\left(1-\frac{P}{100}\right)}{100-DS} \quad \text{..... Equation 6}$$

Where DS is the total dissolved solids (%) and P is the true purity (%). Lionnet and Rein (1980) showed that the solubility coefficient for C-massecuite crystallisation was strongly-dependent on the NS/W and RS/Ash ratios, and a regression analysis revealed that the two parameters were significant at a 95% confidence interval. Other sources of literature (Mathlouthi and Cedus, 1995, van der Poel *et al*., 1998 and Rein, 2007) mainly show the dependence of SC on the NS/W ratio and the standard form (Rein, 2007 and Rosza, 2000) of the equation that relates these two parameters is as follows:

$$SC = m \times (NS/W) + b + (1-b) \times e^{-c\times\left(\frac{NS}{W}\right)} \quad \text{..... Equation 7}$$

Where m, b and c are constants. The constant 'm' is at times referred to as 'a' in earlier literature (Mathlouthi and Cedus, 1995 and van der Poel *et al*., 1998); however, m was chosen as this symbol as it is typically used to denote the gradient of a straight line. It is clear from Equation 7 that the SC vs NS/W ratio curve is made up of a straight line and an exponential term (see Figure 3). Figure 3 was constructed using the recommended SC constants from Rein (2007) and a RS/Ash ratio of 0.97 (the South African industry average value for the 2023 season). Furthermore, note that an increasing NS/W ratio corresponds to a decreasing purity, starting at 0 (100% purity) and increasing to 6 (C-boiling purity range). Therefore, using the SC vs purity trend reported by Rosza (2000), Figure 3 shows the approximate ranges for the various types of boilings in sugar factories.

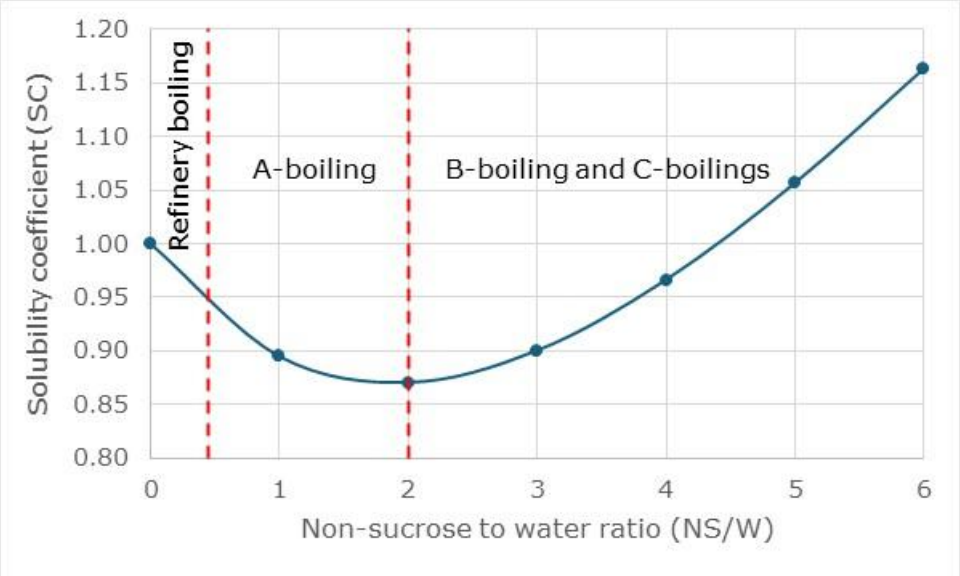


Figure 3. SC versus NS/W ratio for cane sugar solutions

Generally, the shape of the SC vs NS/W ratio curve is similar to Figure 3 in most of the cited literature (Mathlouthi and Cedus, 1995, van der Poel *et al*., 1998 and Rein, 2007). The non-sucrose tends to reduce the solubility of sucrose at low NS/W ratios (<2) and increases the solubility of sucrose at high ratios (>3). However, Rosza (2000) reports a deviation from the general SC versus NS/W curve using the comprehensive Thieme solubility data for cane sugar solutions (Hugot, 1960). Rosza (2000) reports that the cane sugar solutions that were used by Thieme behaved differently from beet solutions with a general linear decline in the SC from a NS/W ratio of zero. The RS/Ash ratio seems to have a profound effect on the SC when considering the SC correlation proposed by Rein (2007), and it is possible that Thieme's data

was obtained at high RS/Ash ratios (>2) as Chen (1985) implicitly reported a similar SC vs NS/W graph (at a RS/Ash ratio of 2.42) to that reported by Rosza (2000).

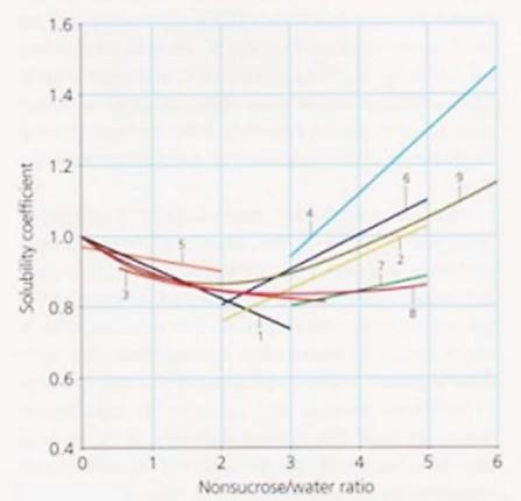
There has been some contention in literature about the impact of temperature on the solubility coefficient. Van der Poel *et al*. (1998) reports that Wiklund (1946) discovered that the solubility coefficient was independent of temperature and there seems to be a consensus in literature about the validity of this discovery (Vavrinecz, 1978/79, Lionnet and Rein, 1980, Chen, 1985 and Mathlouthi and Cedus, 1995). However, Steindl *et al*. (2001) report that the SC constants (m, b and c) are affected by the temperature of the cane sugar solution. Love (2002) conducted solubility experiments that indicated minimal variation in the solubility coefficient of cane syrups within a temperature range of 60 to 70°C, up to a NS/W ratio of approximately 2.5. However, data for NS/W values exceeding 2.5 suggest that the solubility coefficient increases with rising temperature. It remains unclear whether the observed differences at higher NS/W ratios fell within the method's uncertainty as the relative standard deviation for the data points was not provided. Table 1 is a summary of the m, b and c constants from a range of authors.

Table 1. Summary of m, b and c solubility coefficient constants

Reference	**m or a**	**b**	**c**	**NS/W range**	**T (°C) range**	**RS/Ash range**
*van der Poel *et al*., (1998) – Grut's data	0.178	0.820	2.1	0.3 to 3.0	20 to 90	n/a
*Mathlouthi and Cedus (1995) – Vavrinecz average data	0.292	0.691	1.80	0.2 to 7.0	20 to 98	n/a
Rosza (2000) – based on the corrected and extended Thieme's data	-0.063	0.982	-2.1	0 to 2.6	70 to 80	n/a
Steindl *et al*. (2001)	0.011+ 0.00046T	0.670 + 0.0021T - 0.007(RS/Ash)	0.540 + 0.0049T	0 to 5.0	40 to 60	0.5 to 1.0
**Rein (2007)	0.14	0.45 – 0.2(RS/Ash)	0.4	0.5 to 7.3	34 to 65	0.6 to 1.7

*The solubility coefficients from these authors are applicable to the beet sugar factory products.
**The NS/W, temperature and RS/Ash ranges were not explicitly mentioned by Rein (2007), the ranges were obtained by considering all the references quoted by the author (see Figure 4).

Figure 4 has been extracted from Rein (2007) and shows the variability of solubility coefficient data in literature. Furthermore, it is uncertain whether the solubility data presented is applicable to raw syrup and molasses currently being processed in South African raw sugar factories. Therefore, given the above-mentioned concerns with the existing solubility data, there is certainly a need to perform solubility tests to confirm the applicability of the constants detailed in Table 1 or to propose a revised set of constants.



Correlations proposed by different investigators for the solubility coefficient in cane sugar solutions (where the correlation equations require it, temperature is specified as 50 °C and $q_{MS/A}$ or $q_{NS/A}$ = 1.0).
1 *Batterham* et al. (1974); 2 *Maudarbocus* and *White* (1978); 3 *Broadfoot* and *Steindl* (1980); 4 *Lionnet* and *Rein* (1980); 5 *Rouillard* (1980); 6 *Rouillard* (1980); 7 *Broadfoot* (1984); 8 *Steindl* et al. (2001); 9 Equation (18.5)

Figure 4. Summary of SC vs NS/W curves (Rein, 2007)

The metastable supersaturation limit of impure cane sugar solutions

During pan boiling, it is imperative that there is a good understanding of the metastable zone's upper supersaturation limit so that pan boilers can avoid false grain formation during crystallisation. The absence of false grain is required if the boiling is expected to approach full seeding and the size distribution of the crystals is to be kept at an acceptable level [i.e. a sieve analysis size coefficient of variation <35% (Rahiman *et al*., 2023)]. Furthermore, it is desirable to maximise the rate of crystallisation without the risk of false grain formation, and therefore, operating near the upper level of the metastable region is necessary to ensure that pan throughput is kept at an optimum.

The metastable limit for pure sucrose solutions is widely accepted as 1.20 SSC (Chen, 1985, van der Poel *et al*., 1998, Pan boiling, 2015 and Rein, 2007). However, the limit of 1.20 SSC may not be applicable to impure cane sugar solutions. Hugot (1960) and Broadfoot and Wright (1972) report that the metastable limit increases as the purity of the cane sugar solution decreases. Broadfoot and Wright (1972) performed experiments using a laboratory vacuum pan to determine the metastable limit of cane syrup over a true purity range of 65 to 100%, a temperature range of 50 to 70°C, a crystal content (CC) range of 0.3 to 20% and at different rates of syrup concentration (range not specified). It was found that the true purity and CC showed a statistically significant effect on the secondary nucleation point, and the relationship was described by Equation 8.

$$\mathrm{SSC_m} = 2.864 - 3.516\left(\frac{\mathrm{S}}{\mathrm{S+NS}}\right) + 1.81\left(\frac{\mathrm{S}}{\mathrm{S+NS}}\right)^2 - 0.00177\mathrm{CC} \quad \text{..... Equation 8}$$

Where SSC_m refers to the metastable supersaturation limit and the term S/(S+NS) is essentially the true purity expressed as a fraction. Equation 8 suggests that the purity of the mother liquor is the major variable that influences the supersaturation limit. However, Broadfoot and Wright (1972) did mention that a standard error of ±0.036 SSC was obtained during this test due to the difficulty in reproducing the point of nucleation.

If slurry-seeding is considered, the crystal surface area after injection of the slurry crystals is negligible, and therefore the CC content term in Equation 8 may be omitted. Table 2 provides a summary of the metastable zone upper limit data obtained from Hugot (1960) and that obtained via Equation 8 (assuming negligible CC). It was assumed that the purity reported by Hugot (1960) was the true purity of the cane sugar solution.

Table 2. Summary of metastable zone upper limit data

True purity (%)	Hugot (1960)	Broadfoot and Wright (1972)
60	1.55	1.41
70	1.30	1.29
80	1.25	1.21

The metastable zone limits shown in Table 2 are substantially different, particularly for mother liquor purities of 60% and 80%. Broadfoot and Wright (1972) cited Davies and Yearwood (1944) from the data presented by Honig (1959), and state that the metastable limits were found to be 1.20 (determined by extrapolation) and 1.30 for pure sucrose solutions and 70% purity cane syrups, respectively. These results are close to the 70% purity metastable limit results detailed in Table 2; however, the results from Broadfoot and Wright (1972) implicitly suggest that the metastable limit for a pure sucrose solution is <1.20 (specifically 1.16 SSC). Clearly, there is large variation in the available metastable limit data for impure cane sugar solutions, and therefore, there is scope for exploring the metastable limit for South African cane syrups and molasses.

Methods of measuring the solubility of sucrose in impure cane sugar solutions

This section details some of the common analytical and optical methods described in literature to determine the saturation and metastable limit data for impure sugar solutions.

Determination of the solubility of syrups and molasses

The Polish test

A rapid method used for measuring the solubility of sucrose in impure solutions, particularly in the beet sugar industry, is the Wagnerowski method (or the Polish test) and this method is detailed by van der Poel *et al.* (1998). Samples of syrups or molasses are typically diluted or concentrated (under vacuum) to give NS/W ratios in the range of 1.6 to 3.0. After adjustment of the NS/W ratio, the samples are added to a vessel containing a mechanical stirrer and a predetermined amount of coarse sugar is added to the vessel and allowed to mix at a constant temperature for at least three hours (at this point the mother liquor is presumed to be saturated). McGillivray *et al*. (2003) used a temperature of 80°C and allowed the mixture to saturate for 24 h. It is expected that the minimum time to reach saturation would depend on the saturation temperature and the degree of mixing in the saturation vessel, and therefore the minimum time to reach saturation should be determined experimentally. The coarse sugar contains 8000 crystals in 1 g of sugar and this corresponds to crystals that have an average sieve aperture size of about 1.00 mm (Bubnik and Kadlec, 1992). The NS/W ratio of the saturated solution is not expected to change assuming that the coarse refined sugar used to saturate the mother liquor has negligible moisture content. Once the mother liquor is saturated, the mixture is filtered through a glass filter and the sucrose content and dry substance are determined. These analytes may then be used to determine the true purity and the NS/W ratio. Adequate data points are required at different NS/W ratios to assist with determining the m, b and c constants. The Polish test relies on the dissolution of sugar in an undersaturated solution to reach saturation as this occurs faster than the crystallisation of sucrose from a supersaturated solution to reach saturation. Since the solubility coefficient is independent of

temperature, which is the basis of the Polish test, equations 1, 5 and 7 may be used to determine the solubility of an impure solution at the desired temperature range.

Adaptation of the Polish test for the sugarcane industry

Love (2002) adapted the Polish test to determine the solubility coefficients of cane sugar factory molasses at various NS/W ratios. He showed the time benefit of approaching equilibrium via dissolution as opposed to crystallisation. The rate of dissolution is substantially faster than the rate of crystallisation as observed in Figure 5 (Wright, 1983). The abbreviation I/W refers to the impurity-to-water ratio which is the same as the NS/W ratio. It is clear from Figure 5 that at the pan boiling temperatures typically experienced in a raw sugar factory, the rate of dissolution is faster than the rate of crystallisation for the same level of oversaturation (defined as SSC-1), particularly as the purity of the mother liquor decreases (a negative oversaturation value implies that the solution in undersaturated). Interestingly, Figure 5 also shows that at NS/W ratios ≥2, the rate of crystallisation is almost independent of oversaturation and is close to the zero mm/h crystallisation velocity line (i.e. the red dashed line). This suggests that it may take a long while before the solution achieves saturation by crystallisation. Love's (2002) review of sucrose solubility reinforces this observation as the conclusions from the saturation tests reported by Charles (1960) for a pure sucrose solution at approximately 15°C revealed that reaching saturation by dissolution took approximately 45 min, whereas reaching saturation by crystallisation took about 75 h.

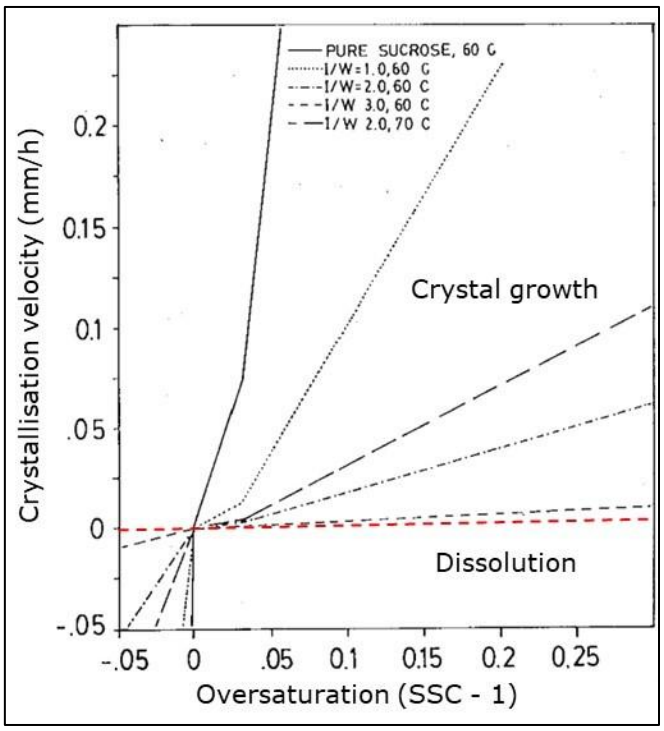


Figure 5. Dissolution and crystallisation rate of cane syrups at various NS/W ratios temperatures (Wright, 1983)

Love acknowledged that the temperature at which the Polish test is typically performed (80°C) may not be suitable for cane syrups and molasses as the non-sucrose components (particularly the reducing sugars) are prone to thermal degradation, especially via the Maillard reaction (Rein, 2007). Therefore, saturation tests would need to be conducted in the 60 to 70°C range that is typically used in raw sugar factories.

Love (2002) used the experimental set-up shown in Figure 6 to perform the saturation experiments. Six brass-jacketed pots, each with their own paddle stirrer operating at 62 rpm,

were connected to a temperature-controlled water bath to maintain the temperature of the syrup or molasses at the desired level. The pot design is the same as that used for the boil-down test performed at the SMRI. A summary of the procedure detailed by Love (2002) is provided in Appendix A.

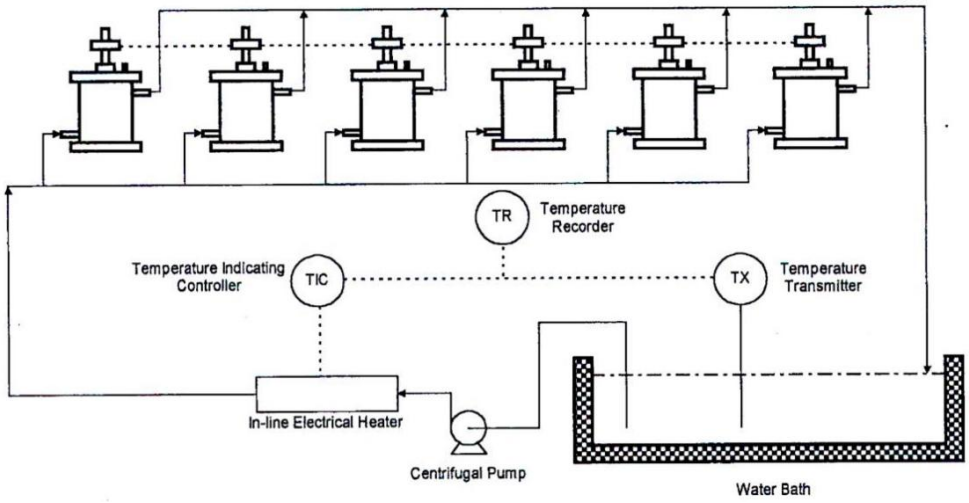


Figure 6. Six-pot saturation set-up used by Love (2002)

Love (2002) recommended that changes to the non-sucrose composition be assessed in future solubility work as it is undesirable to change the non-sucrose matrix during the saturation tests.

Solubility methods described by Honig (1959)

Honig (1959) discussed several methods to determine the solubility of sucrose in impure cane sugar solutions. The two methods that have fundamentally different approaches for determining the saturation limit are summarised below:

- *Kelly's (1954) method:* This method involves the saturation of pure or impure sugar solutions by the dissolution of crystalline sucrose. This method is similar to the Polish test; however, it typically involves the use of tightly-sealed tubes into which the mixture of crystals and mother liquor is poured and thereafter held in a constant temperature water bath. The water bath has to be equipped with a mechanism to rotate the tubes at a speed of at least 4 rpm. Approximately 20% more crystals than what is required to saturate the mother liquor should be added and the crystals should be in the size range of 0.8 to 1.0 mm. The method involves a saturation time of 14 days; however, this may be shortened if mixing conditions are improved. Furthermore, Honig (1960) reported that saturation temperature did affect the saturation time and it is expected to decrease as the saturation temperature increases. It is preferable to place a glass rod in the tubes containing viscous solutions to assist with mixing. After saturation, samples are allowed to stand in the constant temperature water bath for at least 24 h to allow the crystals to settle and thereafter the supernatant is decanted for analysis. Alternatively, pressure filtration may be used especially in the case of very viscous mixtures. Saturation by dissolution via Kelly's method may potentially be achieved using the crystallisation water bath system as reported by Rahiman and Mbuthuma (2023).

- *Harman's (1932) method*: This method is also referred to as the saturascope technique and employs microscopic examination of sugar crystals in molasses. The saturation cell is either jacketed or electrically-heated to provide good temperature control. A

sample of molasses of known composition is placed on a cover glass and the temperature of the molasses and saturation cell is such that the molasses is supersaturated. Finely-milled sugar is added to the molasses and a suitable microscope objective is used to observe the edge of the crystals as the temperature is increased at a rate of 1°C per minute. The temperature at which the edges of the crystals start to erode is recorded as the saturation temperature. Typically, the test is repeated at a slower rate of temperature increase (i.e. 0.33°C per minute) starting about 5°C away from the initially recorded saturation temperature to assist with accurate determination of the temperature. This technique is typically suited for syrup purities of ≤60% as the rate of crystallisation is slow and therefore the finelymilled seed crystals are not expected to significantly affect the mother liquor composition. by Honig (1960) also reported a variation of the saturascope technique by Taylor (1947) where a minimum of two large crystals (0.5 to 0.25 mm in size) were used to check erosion of the crystal edge and carefully calibrated thermocouples were used to increase the temperature at a rate of 0.02°C per minute. A further variation of the Harman method, known as the photometric saturation temperature method, is reported separately below as this method was not detailed by Honig (1959).

The photometric saturation temperature method

Wright (1978) detailed a variation of the Harman method in an attempt to reduce operator-dependency in determining the point at which crystal edges start to dissolve. This method (i.e. the photometric method) was used for determining the saturation temperature of cane sugar syrups and molasses across a wide purity range (45 to 99% true purity). The author noted that the Harman method was advantageous over the equilibrium test methods (such as the Polish test and the Kelly's method) as a small quantity of sample was required (approximately five grams of syrup or molasses) and that it could be easily incorporated as part of process control in sugar factories; however, the technique's major drawback was its operator-dependency. The photometric method detailed by Wright (1978) relies on the change in light transmission through a sample when dissolution occurs to assist with determining the saturation temperature, instead of relying on the operator's eye to determine the point when the crystal edges begin to round. The apparatus used to perform the photometric saturation test primarily comprised of two 13 mm (diameter) slide cover slips that were separated by a 13 mm metal washer permanently attached to one coverslip, a Gallenkamp MF 350 microscope hot stage (i.e. a temperature-controlled microscope stage) that controlled the temperature of the sample sandwiched between the two cover slips, a steady light source that provided light beneath the sample and a light-sensitive sensor (such as a photovoltaic cell or a phototransistor) that converted the transmitted light to an electrical signal that was presented by an x-y recording system. The apparatus was subsequently modified so that it was more compact than its precursor, and the light sensor electronics were optimised so that there was automatic regulation of the light source intensity. Appendix B provides details on the equipment and procedure used in the photometric method.

Initially there was a gradual rise in the recorder output voltage as the sub-sample temperature increased and this was followed by a steep decline in the voltage once the temperature exceeded the saturation point. According to Wright (1980), given the circuitry used in the equipment (see Appendix B - Figure B2), the steep fall in the voltage can be explained by the dissolution of the fine crystals whilst the gradual rise in the recorder output voltage was suggested to be due to the slight pre-crystallisation and/or tendency of the light transmission of the molasses sub-sample to decrease with a rise in temperature. Further investigation is required to understand exactly why the light transmission through the sample decreases as the temperature increases towards the saturation temperature point.

According to Wright (1978), initial scans were typically done at about 5 to 10°C per minute followed by repeat scans performed at 1 to 2°C per minute for high purity solutions (90 to 99%

true purity), and 0.5 to 1°C per minute for low purity solutions (45 to 58% true purity). Wright (1978) equilibrated molasses samples using excess sugar in a constant temperature water bath and then performed the photometric analysis of the sample to determine the saturation temperature. The saturation temperature results reported by Wright (1980) were in close agreement with the equilibration bath temperatures: temperature differences of 0.50 to 0.65°C for a 99% pure sucrose solution at 60.0 and 51.2°C equilibrium bath temperatures were achieved, respectively. The standard deviation of the temperatures from the repeat photometric scans ranged from 0.1°C to 0.3°C. These results are promising; however, the work done by the author seems to implicitly suggest that high temperature saturation tests (>50°C) require saturation of the samples using excess sugar in a constant temperature water bath before the photometric measurement and therefore adds to the analysis time as per the procedure mentioned above.

Qin and Wright (1992) further developed the photometric technique by using an infrared light source instead of an LED light source. The authors provided a detailed assessment of some of the factors that affected the accuracy of the saturation temperature measurement such as enhanced solubility of the sample due to the size of the seed crystals, pre-crystallisation of the sample, temperature lags and random errors that may arise from the analogue to digital conversion of the light transmission and temperature signals. It was concluded that the use of good equipment and technique may result in an uncertainty in the supersaturation measurement of as low as ±0.0015 SSC. Inaccuracies due to the stability of the infrared light source and photodetector, the presence of air bubbles and the effect of the seed dispersant were not quantified but were acknowledged. Furthermore, the authors considered the use of the photometric method as an online method to determine the saturation conditions during batch pan boiling; however, careful attention would need to be given to the factors affecting the accuracy of the measurement, the operating pressure of the sample being measured and the possibility of introducing fines into a vacuum pan.

Determination of the metastable zone limits of impure cane sugar solutions

A study detailing the method of determining the metastable limits of Australian syrup and molasses was reported by Penklis and Wright (1963). Raw syrups and molasses (apparent purity range of 55 to 80%) were used in a stirred laboratory vacuum pan and boiled at temperatures of 60 and 71°C. Raw sugar was added to the syrup or molasses of a certain purity such that the crystal content ranged from 2 to 35%. The evaporation rate was controlled above the saturation point such that the SSC increased at 0.004 per minute. Samples were taken using the pan's proof stick until a high concentration of fine grain was observed. These samples were centrifuged to determine the crystal content and obtain the mother liquor purity. Once a high concentration of fine grain was visible, the temperature was recorded and the mother liquor brix was measured followed by the determination of the supersaturation (i.e. using Equation 4). It is important to note that dry solids is a true indication of total dissolved solids and is generally equal to refractometric brix for pure solutions. However, according to Honig (1959), the dry solids of molasses that has a gravity purity of 40% is typically to 2 to 4 units lower than brix. Therefore, when using Equation 4, it is important to understand the dry solids and brix relationship, particularly for the mother liquor purities experienced in the B-station and C-station of a raw sugar factory.

Penklis and Wright (1963) discovered that the metastable zone limit increased steeply as the molasses purity decreased, and the oversaturation approximately doubled as the apparent purity decreased from 80% to 60%. Furthermore, there was not much alteration in the metastable zone limit over a crystal content range of 10 to 30%.

Factory-scale solubility and metastable width tests

Chen (1985) reported on the determination of the saturation and metastable limits in a full-scale pan. To determine the saturation point for raw syrup or molasses of a certain purity, coarse crystals that have sharp edges are added to a proof stick and exposed to the syrup or molasses in the pan during the concentration phase. As soon the crystal edge ceases to become round and begins to sharpen, saturation has been reached.

The metastable limit is obtained by concentrating massecuite to the point where new crystals begin to form. The massecuite is sampled and filtered, and the Nutsch molasses is analysed for dissolved solids and sucrose content. Pan boilers cannot afford to spend large amounts of time determining the saturation and metastable points as there are throughput and/or energy targets to be met. Instead, pan boilers rely on experience and existing solubility data to guide them during crystallisation. Therefore, there is certainly a benefit in determining and making available reliable solubility data that applies to South African syrups and molasses.

Potential use of the SMRI steam-heated pilot pan as a solubility measurement tool

The SMRI has a fully-instrumented 50 l steam-heated vacuum pan (Figure 7) capable of simulating industrial pan boiling (Rahiman *et al.*, 2023). The pilot pan is equipped with an online pan microscope (the ITECA SOCADEI CrystObserver) that is capable of detecting crystals as small as four microns (i.e. the size of ball-milled slurry crystals) and provides real time crystal growth and product quality data (i.e. the crystal mean aperture, size coefficient of variation and % fines in the massecuite). In addition to the real time crystal size results, the pan microscope system also records a video of the boiling which may allow the user to easily troubleshoot problems and/or optimise the process accordingly.

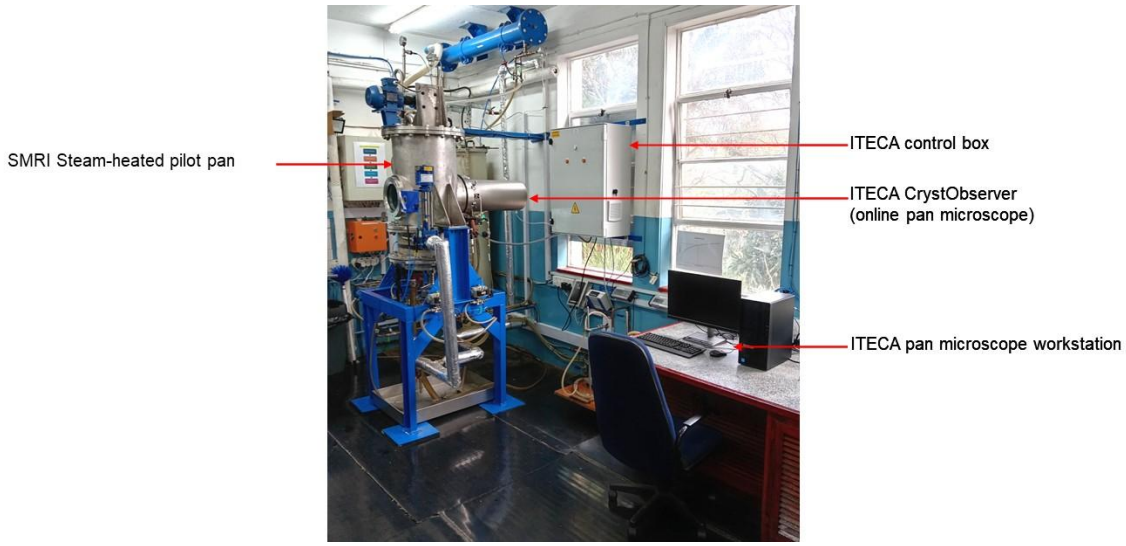


Figure 7. SMRI steam-heated pilot pan equipped with an online pan microscope

The pan microscope system may be used in a similar way to a saturascope, to determine the saturation limit of impure cane sugar solutions. In the case of the pan, the vacuum pressure may be held constant such that the raw syrup or molasses boils within the typical raw sugar factory pan temperature range (60-70°C) and it should be allowed to reach a state of supersaturation. The mother liquor supersaturation in the pan is controlled by maintaining the brix of the mother liquor and this is inferred from the Boiling Point Elevation (BPE) measurement. The BPE of the mother liquor is maintained at a constant value by adding water into the pan such that it matches the evaporation rate of the vapour exiting the pan. Thereafter, coarse sugar crystals (>0.5 mm) are added to the pan and the BPE reduced gradually until

the crystal edges begin to round. The massecuite in the pan is then sampled and filtered using a Nutsch filter so that the mother liquor dissolved solids and sucrose content can be measured. This may be done at various NS/W ratios by starting with C-molasses (40% purity) and thereafter adding pure sucrose solution to the C-molasses to change the NS/W ratio so that the range achieved is from 0.5 to 5. As mentioned in the above section, determination of the point of saturation by visual inspection by the operator may be subjective particularly when observing the roundness of the crystal edges. It would be convenient if the image analysis performed by the online pan microscope could determine the circularity of the particle using Equation 9 (Balter, 2017) to reduce subjectivity from analyst to analyst.

$$C = \frac{4 \times \pi \times A}{P^2} \quad \text{..... Equation 9}$$

Where C is the circularity (dimensionless), A is the crystal area (μm^2) and P is the crystal perimeter (μm). The circularity for a circle, square and rectangle (with length two times width) are 1.000, 0.785 and 0.698, respectively. A circularity real time trend could potentially be monitored to assist with determining the saturation point (i.e. the circularity of the sugar crystal is expected to increase with time when the mother liquor is undersaturated but should remain the same if the mother liquor concentration is increased to the saturation point). Secondly, to determine if the saturation point was determined correctly using the pilot pan system, the tests conducted using the pan would need to be validated using the Love's (2002) adapted Polish test or by the Kelly's (1954) method.

As mentioned above, the metastable supersaturation limit of cane syrup or molasses may be determined using the method described by Penklis and Wright (1963). The detection of false grain can easily be achieved since the SMRI pilot pan is equipped with a microscope capable of measuring crystals as small as four microns and can track the number of crystals throughout a pan boiling.

Conclusions

The literature review highlights the following key findings in summary form:

Pure sucrose solutions

- The solubility of sucrose in pure aqueous solutions is well understood and is dependent on the temperature of the solution. The two solubility correlations accepted by ICUMSA include the Charles (1960) and Vavrinecz (1962) equations of which the recommended equation for South African sugar factories is the Charles (1960) correlation. The Charles (1960) correlation is applicable across a temperature range from 0 to 86°C, however, Rein (2007) and the South African Sugar Technologists' Association (Anon, 1985) suggest that the equation may be extended to 90°C.

Impure cane sugar solutions

- The solubility of sucrose in impure cane sugar solutions depends on the temperature, and type and quantity of non-sucrose in the solution.
- The solubility of sucrose in impure cane sugar solutions is typically determined from the Solubility Coefficient (SC). The SC is the quotient of the S/W ratios of a saturated impure solution and saturated pure solution at the same temperature.
    - The SC is mainly dependent on the Non-Sucrose-to-Water (NS/W) ratio of the solution and the widely accepted SC correlation typically includes an exponential and linear term, the general form of equation is below:

      $$SC = m \times (NS/W) + b + (1 - b) \times e^{-c \times \left(\frac{NS}{W}\right)}$$

      Where m, b and c are constants. Some sugar technologists include the effect of the type of non-sucrose, mainly the reducing sugar and ash components, on the b constant in the above-mentioned equation.

  - There is contention in literature about the temperature dependence of the SC, majority of the literature suggests that the solubility coefficient is independent on temperature, however, it was found that one source includes temperature dependence.

- The literature on the solubility coefficient for cane sugar solutions was limited for South African raw sugar factory streams, and there is a large variation in the data across the same NS/W range. Furthermore, there is uncertainty as to whether the available solubility data is applicable to South African raw syrups and molasses being processed today.
- The metastable supersaturation limit data for impure cane sugar solutions was also found to be substantially different from one source to another and the data provided was not based on experiments using South African raw sugar syrups and molasses. However, there was agreement in literature that the metastable supersaturation limit of impure cane sugar solutions increased as the true purity of the solution decreased.

Common methods used to measure the saturation and metastable limits of sucrose in impure cane sugar solutions:

- There are various methods used to measure the saturation point of sucrose in impure cane sugar solutions and these methods may be broadly classified into two groups. Group 1 typically involves the saturation of impure cane sugar solutions at the different NS/W ratios by dissolution of crystalline sucrose at constant temperature. Whereas Group 2 involves observing a physical change in the sample to determine the saturation point (such as the slight rounding of the existing crystal edges when the mother liquor is close to the saturation point).
- The SMRI 50 l steam-heated pilot pan, equipped with ITECA online pan microscope, falls under Group 2 of the methods, and may be used to determine saturation data by observing the rounding of the crystal edges. Furthermore, the pan microscope can also detect new crystals and therefore is ideal for also determining the metastable supersaturation limit of impure cane sugar solutions.
- The Kelly's solubility technique (Honig, 1959) falls under Group 1 and the equipment required for this technique is readily available at the SMRI. Therefore, this technique may be an attractive option of potentially validating the saturation data obtained using the pilot pan.
- The review suggests that the SMRI pilot pan is an attractive tool for determining both the saturation and metastable limit data for impure cane sugar solutions, however, exploratory research will need to be conducted to practically determine the technical viability of using the pilot pan system, particularly for obtaining saturation limit data.

Future work

It is recommended that exploratory experiments be performed to practically assess the viability of using the SMRI pilot pan as a solubility measurement tool using the proposed method of determining the saturation and metastable limit data of impure cane sugar solutions.

Furthermore, it would be beneficial to perform solubility experiments to determine the effect of temperature on the solubility coefficient, preferably within the true purity (40 to 85%) and temperature (60 to 70°C) ranges used in a raw sugar factory station.

Acknowledgments

Special thanks are due to SMRI Advisory Research Committee for approving the time for this review.

References

Anon (1985). *Laboratory manual for South African sugar factories*. South African Sugar Technologists' Association, 3rd edition, Mt. Edgecombe, pp 403.

Balter A (2017). How to calculate circularity. https://sciencing.com/calculate-circularity-5138742.html (Accessed on 19 September 2024).

Broadfoot R and Wright PG (1972). Nucleation studies. *Proc Queensland Soc Sug Cane Technol* 39: 353-362.

Bubnik Z and Kadlec P (1992). Sucrose crystal shape factors. *Zuckerindustrie* 117: 345-350.

Charles DE (1960). Solubility of pure sucrose in water. *Int Sug J* 62: 126-131.

Chen JCP (1985). *Cane sugar handbook*. 11th edition. John Wiley and Sons, New York, pp. 290-353.

Davies JG and Yearwood RDE (1944). *Trop. Agri. London* 31(3): 43 (this article was not accessible).

Harman RW (1932). Determination of the saturation temperature of sucrose solutions and its use in finding coefficients of saturation and of supersaturation. *Proc Int Soc Sug Can Technol* 6: 1-8.

Heitz F (1974). Subject 25, Crystallizing qualities of sugar solutions. *Proc Int Commission Uniform Methods Sug Anal Session* 25: 343-354.

Honig P (1959). *Principles of sugar technology*. Vol. 2. Elsevier Publishing Company pp. 68-74 and 137-138.

Hugot E (1960). *Handbook of cane sugar engineering*. Elsevier Publishing Company. New York, pp. 460-464.

Kelly FHC (1954). *J Appl Chem London* 4: 401 (this article was not accessible).

Lionnet GRE and Rein P (1980). Pilot plant studies on the exhaustion of low grade massecuites. *Proc Int Soc Sugar Cane Technol* 17: 2328-2350.

Love DJ (2002). Dynamic modelling and optimal control of sugar crystallisation in multi-compartment continuous vacuum pan. PhD Thesis. University of Natal, Durban, pp 2:5 to 2:12, 5:1 to 5:12.

Love DJ and Walthew DC (2002). A pilot scale batch pan. *Proc S Afr Sug Technol Ass* 76: 383-395.

Love DJ, Rahiman SN, Madho S and Davis SB (2016). Continuous production of seed crystals using sound-induced nucleation. *Proc Int Soc Sugar Cane Technol* 29: 199-212.

Mathlouthi M and Cedus PRC (1995). *Sucrose properties and applications*. Chapman and Hall, London, pp, 100-116.

McGillivray T, Heggeness J and Groom DR (2003). Determination of the coefficient of Wagnerowski equation for extract derived molasses. *Zuckerindustrie* 128: 600-604.

Pan boiling *in SMRI ten week course in sugar engineering notes* (2015). Sugar Milling Research Institute NPC, Durban, South Africa, pp: 6-7.

Penklis P and Wright PG (1963). Nucleation in sugar boiling. *Proc Queensland Soc Sug Cane Technol* 30: 177-182.

Qin GF and Wright PG (1992). Infrared photometric measurement of the saturation temperature and supersaturation of syrups. *Proc Int Soc Sugar Cane Technol* 19: 671-687.

Rahiman SN and Mbuthuma Y (2023). Validation of the alternative crystal counting technique. *Sugar Milling Research Institute NPC Technical Note* No. 01/23 RC, 9 February 2023, 12 pp.

Rahiman SN, Mbuthuma Y, Love DJ and Davis SB (2023). Installation of a steam-heated pilot pan at the Sugar Milling Research Institute. *Proc S Afr Sug Technol Ass* 95: 349-365.

Rein P (2007). *Cane sugar engineering*. Verlag Dr Albert Bartens, Berlin, pp 353-354, 363-367, 455-457, 539-540.

Rosza L (2000). Sucrose solubility in impure cane sugar solutions. *Int Sug J* 102: 230-235.

Sahadeo P (1998). The effect of some impurities on molasses exhaustion. *Proc S Afr Sugar Technol Ass* 72: 285-289.

Steindl RJ, Broadfoot R and Miller KF (2001). Development and application of a model for low-grade cooling crystallisation. *Proc Int Soc Sugar Cane Technol* 24: 116-123.

Taylor M (1947). *J Chem Soc*: 1679 (this article was not accessible).

Van der Poel PW, Schiweck H and Schwartz T (1998). *Sugar Technology: Beet and Cane Sugar Manufacture*. Verlag Dr Albert Bartens, Berlin, pp 650-651, 660-661, 683-687.

Vavrinecz G (1962). Neue tabelle über die löslichkeit reiner saccharose in wasser. *Zuckerindustrie* 12: 481-487.

Vavrinecz G (1978/79). The formation and composition of beet molasses: The equation for solubility. *Sug Technol Rev* 6: 117-129.

Wiklund O (1946). *Socker Handl*. 2: 65-140 (this article was not accessible).

Wise WS and Nicholson EB (1955). *J Chem Soc*: 2714 (this article was not accessible)

Wright PG (1978). The determination of the saturation temperature of sugar syrups by a photometric method. *Int Sugar J* 80: 40-44.

Wright PG (1980). The photometric saturation temperature method. *Int Soc Sugar Cane Technol* 15: 2264-2278.

Wright PG (1983). Pan and pan stage control. *Sug Technol Review* 10: 39-85.

Appendix A

Below is a summary of the procedure employed by Love (2002) to determine the solubility limit of impure cane sugar solutions:

- The base molasses (A-, B- or C-molasses), water and sucrose (starch-free icing sugar) were added together to obtain the desired NS/W ratio such that the concentration approximates saturation at the desired temperature (this was determined using an appropriate solubility coefficient correlation).
- The sucrose was dissolved in the molasses by heating using a microwave oven.
- The conditioned molasses was placed in the stirred jacketed pot to equilibrate at the desired temperature.
- Thereafter, large sugar crystals (between a mean aperture size of 550 and 880 µm) were heated to the same temperature as the molasses and were added to the pot. The mass of sugar was approximately 40% of the mass of the conditioned molasses used for saturation.
- The mixture of crystals and molasses was then heated to about 10°C higher than the saturation temperature to dissolve fines. The mixture was then cooled to 20°C lower than the saturation temperature so that sucrose may be exhausted from the mother liquor. Mixing at the temperature 20°C below saturation was performed for about 30 to 60 min. This was to ensure that when the temperature was raised to the desired saturation temperature, the mother liquor would be undersaturated and therefore saturation would occur by dissolution.
- The mixture of crystals and molasses was held at the saturation temperature for about 16 h and thereafter the mother liquor was separated by pressure filtration.
- A sample of the crystals in the mixture was analysed using a microscope to check that rounded crystal edges were obtained, thus confirming saturation by dissolution.

Appendix B

Figures B1 and B2 illustrate the assembly diagram of the hot stage and the light sensor set-up, and the general arrangement of the photometric apparatus used by Wright (1980), respectively.

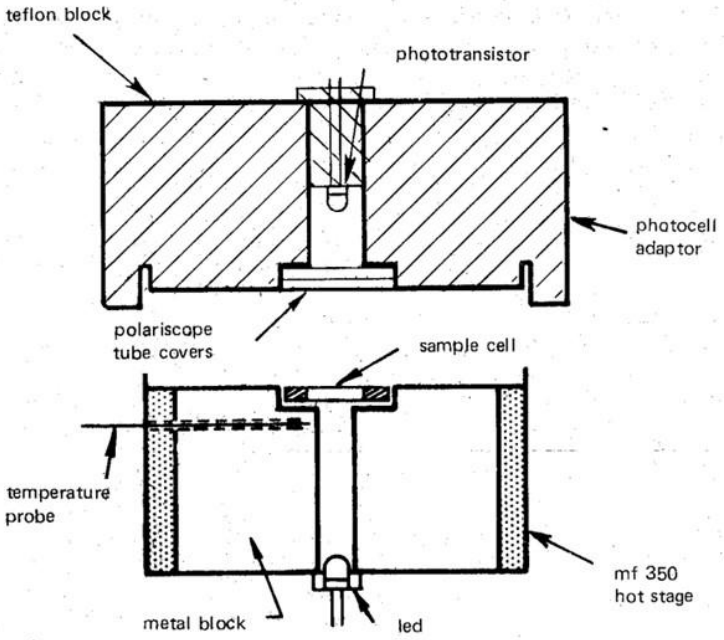


Figure B1. Assembly diagram of the hot stage and the light sensor set-up (Wright, 1980)

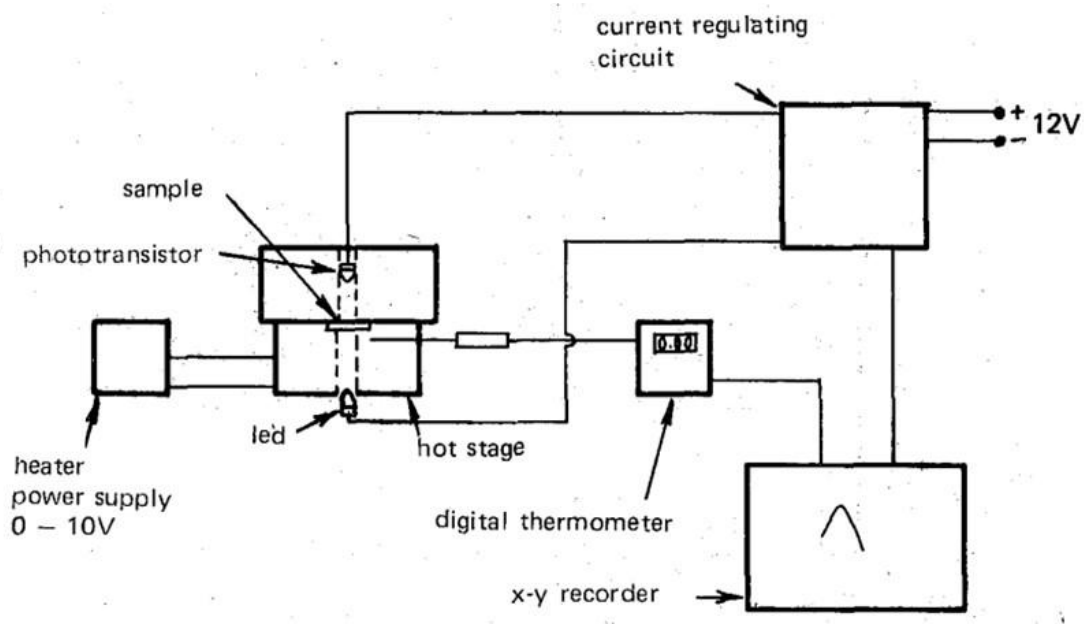


Figure B2. General layout of the photometric saturation temperature apparatus (Wright, 1980)

The procedure that was used to determine the saturation temperature was as follows (Wright, 1980):

- The molasses sample was preheated in a microwave oven to dissolve any crystals.
- The heated sample was removed from the microwave and stirred, and a sub-sample of approximately five grams was transferred onto a ceramic plate.
- The sub-sample was naturally cooled on the ceramic plate and thereafter about 250 to 500 mg of slurry crystals were added to the sub-sample and the mixture was stirred. The slurry was obtained by centrifuging conventional ball-milled slurry, the thick white paste left over after decanting the alcohol was used.
- Viewing slides were prepared using the molasses-slurry mixture. Careful attention was required in this step to minimise the presence of air bubbles in the sub-sample as this would interfere with the light transmission through the viewing slide.
- The metal block temperature (Figure B1) was controlled such that it was 10 to 20°C below the expected saturation temperature.
- The viewing slide (or sample cell) was placed in the photometric apparatus as shown in Figure B2, to be scanned, and the heating rate was adjusted based on the purity of the sample being processed. Note, it was desirable to scan the viewing slides shortly after the slides were prepared.
- The recorder generates a voltage versus temperature trace that may be used to locate the saturation temperature (i.e. the peak of the curve).
- Repeat analysis was performed by replacing the photocell adaptor shown in Figure B1 with a copper block to rapidly cool the hot stage to the initial temperature value. Thereafter, the procedure starting from the sixth bullet point was followed. Approximately six scans may be completed in an hour. It was recommended that each sample prepared for measurement be scanned once.

FULL PAPER

THE USE OF SUPERSATURATION FOR CRYSTALLISATION CONTROL

Muir BM[1] and Rózsa JS[2]

[1]Tereos Corporate Technology Centre, Aalst, Belgium
[2]Zutora, Budapest, Hungary

barbara.muir@tereos.com, jakab.rozsa@zutora.com

Abstract

Sucrose crystallisation is the final and definitive purification process in every sugar factory, be it the cane raw house, refinery or beet factory. In addition to the purification of sucrose, crystallisation is instrumental in maximising the overall sucrose yield, while at the same time producing a good quality sugar crystal. All of this must be achieved with minimum recycling, energy and water usage.

The driving force of crystallisation is the supersaturation of the system, which is achieved by increasing the dissolved solids content above the saturation value of the solution. Since the solute concentration at saturation is an empirical value that is unique to the exact conditions and the purity of the solute, it cannot be measured directly. Many measurement devices have been used to provide inferred information about the supersaturation during crystallisation, and some of these can be used for control purposes.

This paper describes a system that was developed for advanced process control to calculate the supersaturation of a system in real time. The basic assumptions and required information are discussed. The use of the measurement to control crystallisation for the optimisation of the crystal quality is demonstrated, as used in several beet and raw cane sugar factories. The effects on sucrose recovery, crystal quality, sucrose recycling, as well as energy and water usage, are discussed.

Keywords: Solubility, supersaturation, crystallisation, advanced process control, seeding point, automation

Introduction

Crystallisation is one of the key steps in the sugar process. It is the final and definitive purification step in every sugar factory. It has been used in some way or another for centuries to isolate pure sucrose from (almost) everything else around it, and yet it remains one of the more difficult parts of a factory that is often in need of some optimisation. This is partly due to the changing nature of the raw material and partly due to the changing nature of the operators and their tools that are operating the factory. The industry is experiencing an increasing turnover in human capital and the predicted skills gap has now become a reality. While automation and simulation has been used for decades to support crystallisation, it has still been seen as an art, until very recently.

One part of the technical literature of the industry has been quite cautious in providing well-defined instructions and data regarding the operating conditions that are to be used during the industrial-scale crystallisation of sugar. In most cases the views of the ‘artisan’ pan-man are reflected in the publications (Price, 1997; Mahrholz *et al.*, 2018; Thelwall, 2002).

The other part of the literature is more academic and relies on high-level models and simulations of the process of crystallisation. These are based on material, energy and crystal

population balance equations with inevitable simplifications and sometimes incredible results. Their use in actual practise on the pan floor is rather limited (El-abdein *et al.*, 2009; de Azevedo *et al.*, 1993). Again, this is also valid for the major reference handbooks (Rein, 2017; van der Poel *et al.*, 1998; Hugot, 1986; Asadi, 2007; Chen and Chou, 1993). Some of the most useful papers on the topic are those of Rózsa (2008), Ziegler ([1]unpublished), Rein (2003), Broadfoot *et al. (*2023) and Rhoten (2013).

The key performance indicators for crystallisation are arguably: 1) the purity of the crystal product (including associated properties such as solution colour) and 2) the particle size distribution of the crystal population. The desire to produce pure and uniform crystals by using a modest crystallisation rate is in direct conflict with the desire for fast throughput, since growing of a fixed number of uniform crystals requires care and precise control of the exact conditions during the entire process. This becomes more difficult under the conditions of fast crystallisation. Poor crystal size distribution is unfortunately still a common issue that leads to higher recirculation rates, increased energy and water consumption, lower yield and problems with centrifuge operation.

Supersaturation is the driving force of crystallisation. It determines the rate at which the sugar crystal will grow, multiply or dissolve, and therefore also the outcome of the process, in terms of quality and compliance to product criteria, yield, throughput, recycling, losses and energy demand. Since throughput has often been the most important performance indicator in a factory, the tendency would be to push the supersaturation as high as possible, to obtain a higher throughput. However, if the supersaturation is too high, the consequences could be devastating. Not only will this slow down or stop some of the unit operations, but it could also result in a sub-standard product that has to be diverted or even reprocessed.

Batch pan boiling

The successful use of the batch crystallisation process requires the execution of a number of sequential steps in a more-or-less consistent way from one batch to the next, to produce a uniform product with consistent quality and yield, at an optimal energy usage and acceptable throughput. According to Rhoten (2013), there are several requirements for performing the batch crystallisation in an optimal way. Firstly, it requires an in-depth understanding of the nature of the various steps, in relation to the control strategy that is used. Secondly, there needs to be ample provision within the control strategy for adjusting to the exact processing conditions (e.g. raw material quality and purity) and the typical variation in process parameters (absolute pressure, feed syrup density, evaporation rate, etc.) that are normally encountered during the batch control cycle, in a consistent and reliable manner.

The minimum measurements required for operating a modern pan are:

- the level in the pan;
- the vacuum (absolute pressure);
- the massecuite temperature; and
- the heating steam pressure.

The steps of the semi-batch crystallisation sequence are typically comprised of the following:

- filling the pan with feed liquor to just above the calandria (pan footing);
- starting the boiling (concentration) process by opening the steam and vacuum valves just enough to achieve the desired boiling rate and temperature (generally around 70°C);

[1] *Sugar boiling - the syrups in the vacuum pans; Sugar boiling - some facts and some fancies; Sugar boiling - some useful strategies.* https://www.zieglerassociates.com/about (accessed 10/04/2025): 8 pp; 12 pp; 10 pp.

- concentration of the footing liquor to the right supersaturation (generally around 1.1);
- seeding of the pan with a fixed number of fine sugar particles (8-10 µm) suspended in a sucrose-saturated or non-polar solvent;
- allowing the grain to establish and grow to the point of visibility with the naked eye (*ca.* 50 µm);
- starting the feeding sequence in which feed liquor is fed into the pan in accordance with the rate of evaporation of water and the rate of crystallisation, so that the concentration of the mother liquor in the pan is within an acceptable level of supersaturation;
- stopping the feeding when the pan volume reaches a certain level;
- continuing the steam and vacuum for a bit longer, thus tightening of the brix to maximise crystal content to 50-55% and to fully exhaust the mother liquor in the pan;
- emptying of the pan; and
- cleaning of the pan.

Saturation and supersaturation

A solution is said to be saturated when no more solute can be dissolved in the solvent at a specific temperature and pressure. If undissolved solute is present, the solution will be in equilibrium with the rate of dissolution of the solute being equal to the rate of crystallisation, so that the mixture of liquid and solids will at least appear to be dormant. If more solvent is added the solution, it becomes undersaturated, and if some solvent is removed, the solution becomes supersaturated. A solution cannot become over-saturated by adding more solute, since the solute will no longer dissolve at the given temperature, or at least not at a rate any faster than it would again be dissolved. In the same way, if the temperature is increased, the solution becomes (in most cases) undersaturated, and if the temperature is decreased, the solution becomes (in most cases) over-saturated. Over-saturation can therefore only be achieved by either decreasing the temperature or by the removal of the solvent (e.g. by evaporation). Another option is to increase the pressure of the system, although this only finds application if the solvent is in the gas phase.

If a solution is only slightly supersaturated and in the absence of crystals, the probability of the formation of new crystals (nucleation) is negligible. Note that sucrose is quite extreme, in terms of the supersaturation levels that can be achieved without any spontaneous nucleation, compared to other organic molecules. This is due to a high level of hydration and hydrogen bonding in the water medium (Mathlouthi and Genotelle, 1998). In the presence of sucrose crystals, the supersaturation acts as a driving force for crystallisation. On a typical sucrose solubility curve (Figure 1) this range is known as the metastable zone, which is indicated here in blue. On the same graph, as the supersaturation increases, there comes a point where the likelihood of spontaneous nucleation in the presence of sucrose crystals (secondary nucleation) becomes significant, and the metastable zone migrates into an intermediate zone. Finally, the intermediate zone migrates into a labile zone, where the supersaturation is high enough to result in spontaneous nucleation, even in the absence of sucrose crystals (primary nucleation).

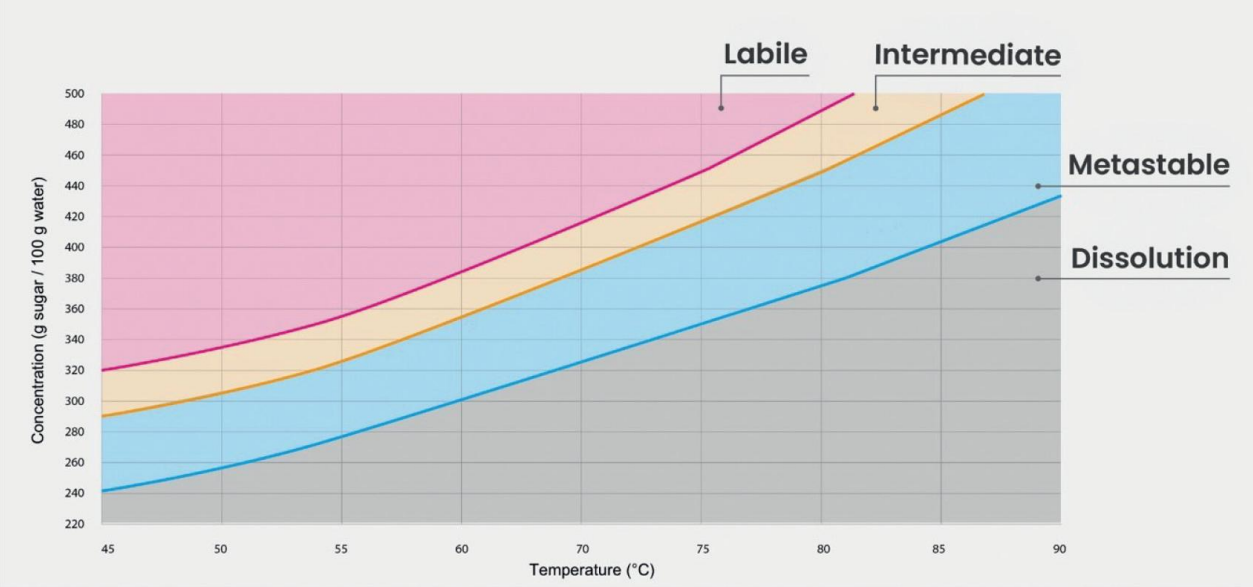


Figure 1. The supersaturation zones of a pure sucrose solution

The most important consideration for the sugar process engineer is to know the upper limit of the metastable zone, in order to avoid operating too close to the edge (risk of nucleation) while remaining close enough to optimise crystal growth, and therefore, throughput. The upper limit is different for almost every syrup, as it depends on the temperature, purity and crystal content. Broadfoot *et al.* (2023) built on the empirically-derived supersaturation nucleation limits from previous work conducted in Australia (see Broadfoot and Wright, 1972), and proposed updated equations to describe the supersaturation nucleation limit (SSNuc) for A- and B-massecuites (high purity, Equation 1) and for C-massecuites (low purity, Equation 2). They noted that the original correlations were limited in scope and not fully representative of industrial pan conditions.

$$SSNuc = 1 + \frac{(SSpandrop - 1)}{0.9} \qquad \text{Equation 1}$$

Equation 1 assumes that the supersaturation at pan drop is approximately 90% of the critical supersaturation.

$$SSNuc = 0.958 + 1.712\left(\frac{I}{S+I}\right) + \left(-3.130 + 0.0154 \times (T + 7.1)\right)\left(\frac{I}{S+I}\right)^2 \qquad \text{Equation 2}$$

where

I = mass of impurities

S = mass of sucrose

T = temperature in °C

Of course, supersaturation is not constant inside the pan, as the temperature tends to have a gradient from the bottom of the pan to the top of the calandria, where the temperature is the highest and the supersaturation the lowest. This gradient needs to be taken into consideration when deciding on the setpoints in the pan, in order to manage the risk of spontaneous nucleation.

Measurement of supersaturation

Supersaturation cannot be measured directly. It is a multivariable function of several parameters of the liquid phase only (syrup or mother liquor). There is therefore no single parameter that could provide the required information needed to know the supersaturation. It can only be calculated based on acquired data, as shown in Equation 3 (van der Poel *et al.*, 1998).

$$Supersaturation\ (SS) = f(C_l, Q_l, T, m, b, c) \qquad \text{Equation 3}$$

where

C_l: syrup or mother liquor concentration (%)

Q_l: syrup or mother liquor purity (%)

T: temperature (°C)

m, b, c: syrup quality coefficients

It has been shown that the concentration (C_l) has the strongest effect on supersaturation (Rózsa, 2003, Figure 2). For example, a 1% change in syrup or mother liquor concentration has roughly a five times bigger effect on supersaturation compared to a 1% change in syrup purity, or 1°C change in temperature. These ratios, however, are not constant, due to the strong non-linear nature of the function.

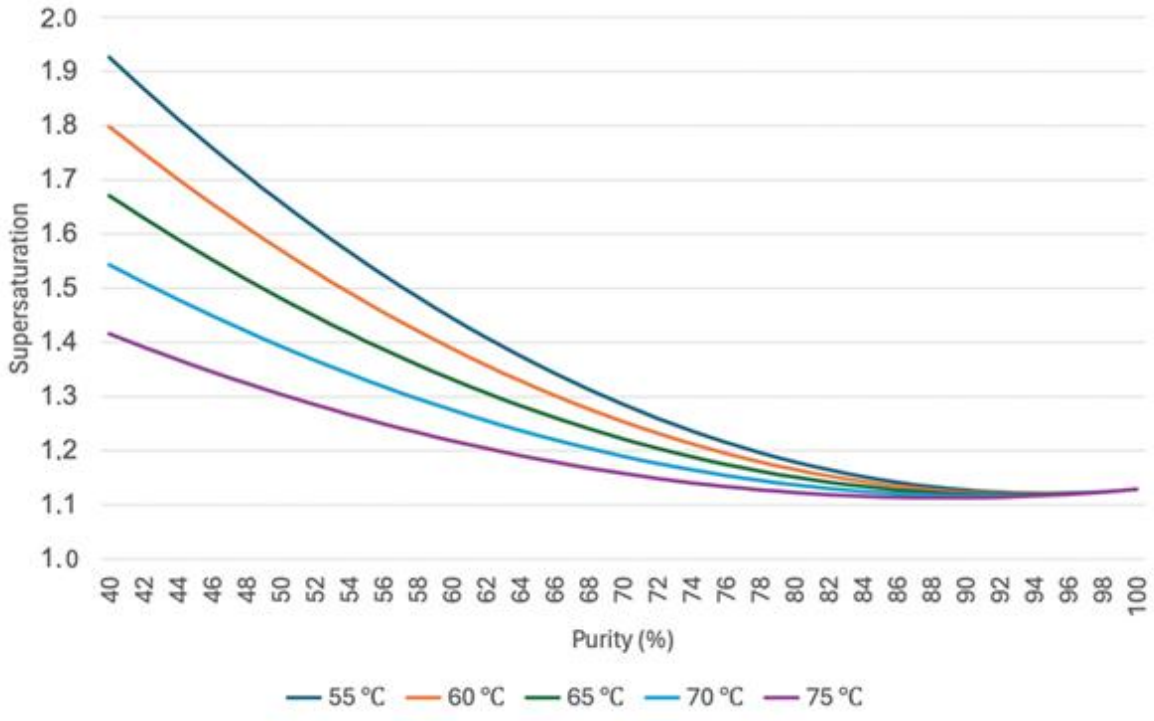


Figure 2. The effect of temperature and purity on the upper limit of the metastable zone (Broadfoot and Wright, 1972)

The concentration of the syrup, or mother liquor, should be measured by an appropriate sensor that operates reliably and accurately during the complete a boiling cycle, and which is undisturbed by physical phenomena, such as increasing crystal content or vapour bubbles. The purity of the liquid phase can also change considerably. Starting from the purity of the feed syrup, the mother liquor purity drops consistently during the strike (for example, for beet sugar: from 94% to 88% at a 50% crystal yield). Neglecting this drop in purity, which is done quite often when claiming the on-line calculation of supersaturation, can result in serious errors.

In Equation 3, the m, b and c terms are empirical coefficients that signify the quality parameters of the syrup, as expressed in Equation 4 (Tuzhilkin *et al.*, 2021; Broadfoot *et al.*, 2023). These factors have been studied well for both cane and beet and are understood to have a significant effect on supersaturation. The parameters can only be determined in the laboratory by using standard laboratory tests. During a campaign, the values should be determined every other week, or at least once a month. If these are not available, typical data can be used, but with some caution.

$$SC = m \times \frac{NS}{w} + b + (1 - b) \times e^{-c \times \frac{NS}{W}} \quad \text{Equation 4}$$

where

SC = supersaturation coefficient

m, b, c = syrup quality coefficients

NS = mass of non-sucrose

W = mass of water

Nucleation or seeding

For a long time, the pan-man typically used the labile zone at the start of the pan cycle, in order to afford spontaneous nucleation through shock seeding. The control of exactly how many crystals were forming and maintained was entirely up to the master pan boiler. This particular skill typically took about a decade to transfer to a new person, as it requires careful observation, tactile testing, experience and intuition, as well as a deep understanding of the effect of the changing nature of the feed material.

Today, full seeding is practised by most factories by using a carefully-determined amount of a seed slurry and by seeding the pan at a much lower supersaturation in the middle of the metastable zone, to eliminate spontaneous nucleation. As its name implies, in the ideal case, the number of crystals in the end-product is exactly the same as in the slurry that was used for seeding. Today almost all factories assume that they are using full seeding, but almost all factories are mistaken. In reality, every time the concentration of the mother liquor goes above the metastable zone limit in any part of the pan, even for a short period of time, new crystals form.

By and large, the impact of purity on crystallisation is to make the metastable zone even wider, thus making the process more forgiving (at least as far as supersaturation control is concerned) (Blecher, 1999).

Crystal content

While supersaturation remains the most critical parameter in crystallisation, the crystal content also plays a key role (Thelwall, 2002). Once seeding is complete, the crystal size and mass increase within the supersaturated solution via crystallisation. The rate of mass growth is proportional to the crystal surface area, or the square of the crystal size, which means that the syrup must be fed into the pan at a controlled rate, in order to sustain this growth. Consequently, having an indication of the crystal content is valuable, although it is not as critical as the parameters that are used for real-time supersaturation monitoring. The accuracy requirements for sensors measuring the crystal content are therefore lower than those for monitoring supersaturation.

Since crystal mass growth depends on the surface area, precise syrup feed management is essential for achieving the desired crystal size and distribution. A higher crystal content increases the massecuite viscosity, which impacts circulation and leads to uneven

supersaturation distribution, which can compromise the product quality. Excessive supersaturation promotes the formation of fine crystals and conglomerates, which necessitates the use of additional water to lower supersaturation and which prolongs the boiling time and increases energy consumption. Ziegler ([2]unpublished) argues that water washing to eliminate fine grain in a pan is a myth, as the supersaturation during the growth phase will never be low enough to allow the dissolution of any sucrose crystals, no matter how small. In contrast, Mahrholz *et al.* (2018) uses the early detection and dissolution of spontaneous nuclei to determine the upper limit of the metastable zone empirically. It is likely that unstable nuclei could go back into solution by a slight lowering of the supersaturation. However, once the new crystals have been established, they will persist to the end of the pan cycle, forming a secondary crystal size distribution crop.

Crystallisation control relies on sensors that measure various parameters, but their accuracy and reliability vary, which makes it challenging to obtain consistent supersaturation data throughout the strike. Viscosity and flow behaviour can be assessed by using different methods, including monitoring the power consumption of a stirrer motor that drives a propeller within the pan.

Online instrumentation used for process control

Understanding of the supersaturation at the seeding point is critical in establishing a fixed number of grains in either full seeding or spontaneous seeding. A number of instruments can give accurate information about the seeding point, provided that the purity of the feed syrup is known (Blecher, 1999; Rein, 2003, Rózsa, 2003).

However, for the control of the feeding phase, independent from the principle of operation, the readings of the sensors mentioned below will increasingly be influenced by the crystal content after seeding:

1. **Electrical conductance, or conductivity probes**: These sensors operate at low or radio frequencies and measure electrical properties, such as conductivity, resistance or capacitance. The probes operate by assessing the ability of the syrup or mother liquor to conduct an electrical current. The measured data is expressed as a multivariable function that can be correlated to the syrup concentration, crystal content, ash content and temperature (Mitra *et al.*, 2009). Note that sucrose in solution does not conduct electricity, so that this is really a measure of the ionic non-sucrose impurities.

2. **Consistency probes**: Consistency probes are sensors that measure the power consumption of a small electric motor that drives a propeller intruded into the pan. The power consumption is directly related to the viscosity of the massecuite, which is a mixture of the sugar crystals and mother liquor. As the viscosity increases, the motor requires more power to drive the propeller through the thick mixture. Viscosity is closely correlated to the concentration of the syrup or mother liquor, and by measuring the power consumption, the consistency probe provides data that can be used to infer the concentration of the liquid phase. However, viscosity is also influenced by temperature and non-sugar content, which must be taken into account when interpreting the data from the consistency probe. After seeding, the contribution of the crystal content to the measured consistency increases sharply, making the viscosity of the mother liquor almost negligible towards the end of the strike. This means that, based on the consistency data, no information on mother liquor concentration, and therefore on supersaturation, can be extracted. Despite these challenges, consistency probes can be used to determine the approximate crystal content and to control the syrup feed,

[2] *Sugar boiling - the syrups in the vacuum pans; Sugar boiling - some facts and some fancies; Sugar boiling - some useful strategies.* https://www.zieglerassociates.com/about (accessed 10/04/2025): 8 pp; 12 pp; 10 pp.

and they are commonly used to signal the end of the strike, due to their excellent sensitivity. In many cases the stirrer motor will do the same job.

3. **Nuclear radiation attenuation probes**: These sensors use nuclear sources to measure the attenuation of nuclear radiation, which is translated into the density, or solids content, of the massecuite. Density data can provide reliable information on the syrup concentration only until seeding is completed. After seeding, density depends on both mother liquor concentration and crystal content, which makes it impossible to get selective information on supersaturation. At the end of the last century, these probes were a revolutionary solution to a tricky (sticky) problem of measuring Brix in high-Brix solutions and they were extremely popular were at the time. This is no longer the case, due to the safety and regulatory issues associated with the radioactive components.

4. **Microwave radiation probes**: Microwave probes operate by transmitting microwave radiation through the massecuite and measuring the attenuation and phase shift of the microwaves, as they pass through the medium. These measurements are influenced by the density and dielectric properties of the massecuite, which are affected by both the dissolved sucrose and the crystal content. As a result, the Brix measurement obtained from microwave probes reflects the overall concentration of the soluble solids in the massecuite, including the contribution from the sugar crystals. After seeding, the density depends on both the mother-liquor concentration and the crystal content, which makes it impossible to get selective information on supersaturation. Since it is blind to the presence of the sucrose crystals, it is extremely useful in controlling the feeding phase of the pan.

5. **Boiling Point Elevation (BPE) sensors**: BPE (Ziegler, [3]unpublished; Saska, 2002; Rein, 2003) refers to the difference between the temperature of a boiling solution and the temperature of pure water boiling at the same pressure. When sucrose is dissolved in water, it increases the boiling point of the solution compared to pure water. This effect is proportional to the concentration of sucrose in the solution: the BPE decreases as the temperature decreases, and it increases as the sucrose concentration decreases. At a given density and temperature, the BPE is proportional to the solids dissolved per 100 parts of water. By knowing the BPE at saturation, it is possible to determine supersaturation quite accurately, by dividing the measured BPE by the BPE at saturation. However, the BPE also increases with the decreasing purity (increasing non-sucrose), which makes accurate measurement difficult over the feeding phase of the pan. Devices that are based on BPE have therefore not found wide acceptance in cane sugar factories.

6. **Refractive index sensors**: These sensors are identical to the laboratory instruments that measure the refractive index of solutions, which depends on the concentration and temperature. When light passes from one medium to another, such as from air into a liquid, it changes speed and bends, a phenomenon known as refraction. The refractive index quantifies the extent of this bending. Typically, a sample of the liquid is placed on the refractometer's prism, and the angle at which a light that is directed through the sample is refracted, is measured. Modern digital process refractometers are robust instruments with a high accuracy and built-in temperature compensation. They are immune to the presence of crystals and vapour bubbles and have found widespread use in sugar crystallisation applications to measure the solids content of the mother liquor phase of the massecuite. As with most other instruments, the refractive index is also affected by decreasing purity (increasing non-sugar), which adds some uncertainty to the measurement of the sucrose content of the liquor, as the purity varies during a crushing season.

---

[3] *Sugar boiling - the syrups in the vacuum pans; Sugar boiling - some facts and some fancies; Sugar boiling - some useful strategies.* https://www.zieglerassociates.com/about (accessed 10/04/2025): 8 pp; 12 pp; 10 pp.

7. **Ultrasonic sensor:** Blecher (1999) described the use of ultrasound to determine the density of the massecuite, with the purpose of crystallisation control. The system operated based on the propagation speed of an ultrasound wave through the liquid medium. The time taken for the ultrasound wave to travel from the emitter to the receiver is used to calculate the speed of sound in the medium, which is directly proportional to the density of the solution.

Only the boiling point elevation and digital process refractometer (5 and 6 above) are therefore able to provide information on the concentration of the liquid phase without interference from the crystals, which is one of the important parameters in the calculation of supersaturation. However, the measurement of boiling point elevation (5) to track changes in the mother liquor concentration, is less practical and convenient than the refractive index sensor.

Ideal of sucrose crystallisation

The ideal end-product from strike to strike consists of well-formed single crystals of the same required size and number in a unit volume. Unfortunately, this aim is impossible to achieve consistently. Crystal size distribution, the number of fine crystals and conglomerates, and colour are important parameters, when talking about product quality.

The benefits of good supersaturation control include:

- the usage of water to dissolve fine crystals can be avoided, thus shorten boiling time and less energy utilisation;
- fine crystal and conglomerate content will be decreased, resulting in better crystal quality (size distribution and colour); and
- the amount of re-circulated (re-melt and re-crystallised) fine crystals and conglomerates will be reduced, increasing the yield of good quality crystals; less re-circulated sugar and a better yield translates into the increased effective rate of production and lower costs.

There are cases, especially in the beet sugar industry, where the speed of production is of highest priority. Typically, these sugar producers operate their pans at high supersaturation levels, yielding high throuhgput but inferior crystal quality. For such operators, introducing a proper supersaturation-based control could potentially come at the cost of longer boiling times. This, however, would be amply compensated for by the time that is gained, due to the positive effects that are listed above.

Supersaturation control during the seeding phase

The most important part of the crystallisation process, as far as product quality is concerned, is the seeding point. This paper will only consider full seeding, as this is common practice today. For more information on the different types of seeding systems, see van der Poel *et al.* (1998) and Rein (2017). In full seeding, an undersaturated syrup is evaporated until it reaches the middle supersaturation region of the metastable zone. This is the safest place to add seed crystal, while avoiding both spontaneous nucleation (intermediate and labile zones) and the dissolution of crystals (undersaturated). Of course, the evaporation of the syrup is not a start-stop process and there is always a delay in the stopping of the evaporation process to allow seeding and the final supersaturation that is reached. This is adequately illustrated in one of the examples later in this paper. Caution is always advised to ensure the final seeding point supersaturation is still within the metastable zone. Of course, it is only possible with online monitoring (and/or control).

Supersaturation control during the feeding phase

It is not enough to only use supersaturation during the seeding phase. While this certainly has the biggest effect, the good results from a proper seeding point could be entirely annihilated if

the supersaturation is not kept under control during the feeding phase. Since higher supersaturation results in faster crystallisation, and throughput is one of the primary directives in a sugar factory, conditions in the pan are often at risk of forming false grain and/or conglomerates, due to supersaturation that is too high.

Unfortunately, the costs associated with these risks are mostly hidden and therefore not always obvious to the financial controllers. The first cost is in the use of water to dissolve, or rather to condition, the false grain or to support the purging of the small crystals during centrifugation. Any water that is used needs to again be evaporated and this will cost approximately one tonne of steam per one tonne of water used.

In addition, the time it takes for this washing to be done takes away time from effective sugar production. A third cost, that is most often overlooked, is the effect of recycling. To demonstrate the consequences, consider two scenarios: idealised conditions (0% recycling) and realistic conditions (15% recycling). Let us assume that we have a crystallisation station where 1 t of dissolved sugar in the A-pan feed is crystallised to produce 0.6 t of a perfect-quality product, while 0.4 t sugar leaves the station dissolved in A-molasses (K or yield = 0.6). In this case there is no recycled crystallised sugar and the product yield is 60% (Figure 3).

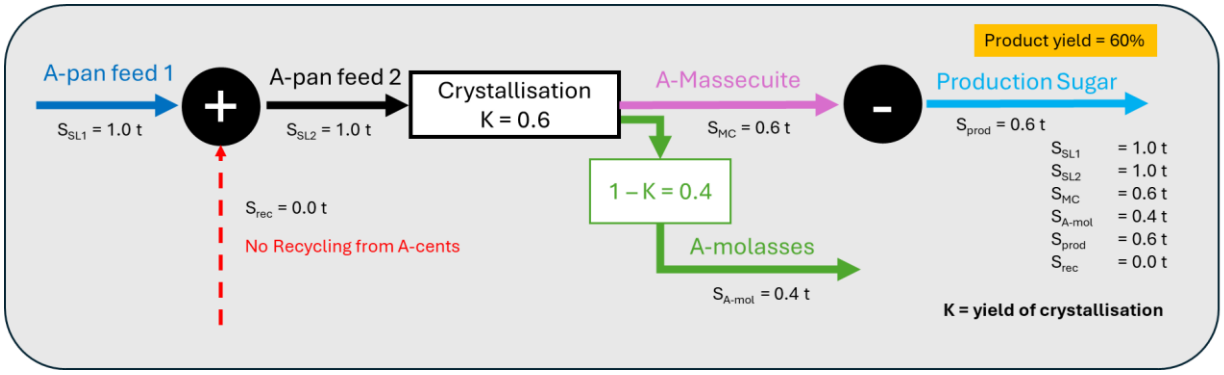


Figure 3. Material balance in an idealised sugar factory

Under these conditions, recycled sugar could result from:

- small crystals escaping through the centrifuge screen; and
- fines and conglomerates removed by screening.

The sugar removed by screening will be collected and dissolved in the syrup and added to the A-pan feed. Assume this amounts to 15% (rate of recycling R = 0.15) of the full number of crystals produced (typical industry value for beet sugar in Europe). While the yield of crystallisation remains unchanged (K = 0.6), the material flow diagram and data valid for this case are illustrated in Figure 4.

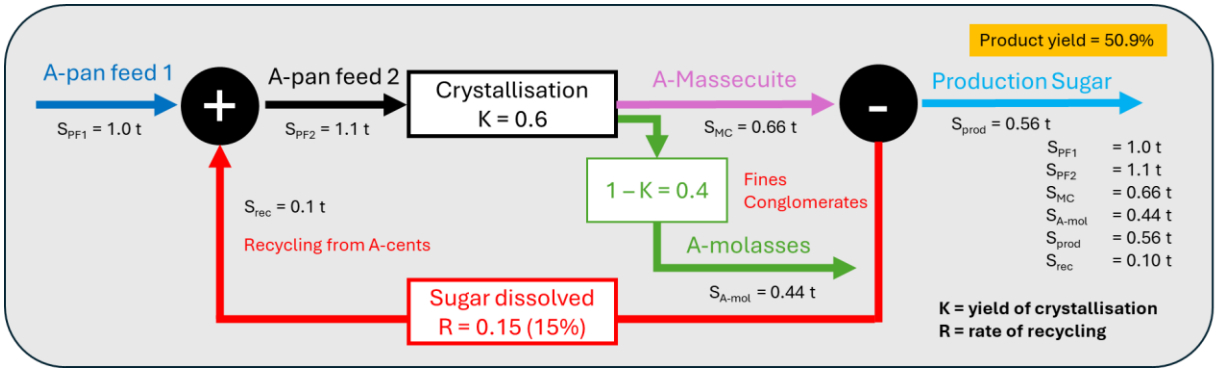


Figure 4. Material balance in a realistic sugar factory

In this scenario, the crystalliser station has a 10% increase in sugar input, compared to the ideal case. In reality there is of course no 1st and 2nd A-pan feed, but it is separated here, to illustrate the effect of recycling of B-magma and C-sugar, depending on the boiling scheme, compared to the additional recycling of A-sugar lost during the process. Despite maintaining an identical crystallisation yield (K), the final product output decreased by 6.67% (0.04 t), resulting in the accumulation of A-molasses. Consequently, the product yield (Yp) reduces by 9.09%. This situation would lead to the increased consumption of water and energy, prolonged boiling times and a reduction in the actual product output, which ultimately escalate the production costs.

Assuming the same amount of dissolved sugar in the A-pan feed (1.0 t) from the evaporator station, it is informative to compare some of the data of the two cases, as shown in Table 1.

Table 1. Comparing the ideal process and a realistic process in terms of sugar recycle

	Ideal process	**Realistic process**	**Change**
Recycled crystal sugar (S_{rec}) (t)	0.0	0.1	+ 0.1
Sugar input to crystallisation (S_{PF2}) (t)	1.0	1.1	+ 10%
Yield of crystallisation (K) (%)	60	60	–
Recycling of fines / conglomerates (R) (%)	0	15	–
Amount of product (S_{prod}) (t)	0.60	0.56	- 0.04 (- 6.67%)
Dissolved sugar in A-molasses (S_{mol}) (t)	0.40	0.44	+ 0.04 (- 10%)
Product sugar yield on pan feed (Yp) (%)	60%	50.91%	- 9.09

This example is obviously exaggerated; however, it is the experience of the authors that it is sometimes surprisingly and unfortunately close to the truth. You can only know if you measure.

Online measurement of supersaturations

Ziegler

The first real supersaturation measuring device was manufactured by Ziegler Associates, USA, and worked on the principle of boiling point elevation (Ziegler, [4]unpublished). The late J. Ziegler himself was a well-known name, not only as a pioneer in automation control, but also for the significant contributions that he made to sugar crystallisation control, which are held in high regard.

The latest version, Model 970-M Monitor, is designed to measure the supersaturation of sugar syrups boiling in vacuum pans. It defines a term ‘oversaturation’, which is expressed between 0% to 100% corresponding to supersaturation coefficients of 1.0 to 2.0. The sensor is adjustable for both cane and beet syrups over the range of purities from 70 to 100% in beet and 50 to 100% in cane, as is typically encountered in sugar boiling. It is compensated for by the absolute pressure variations between 13-33 kPa(a).

The principle of operation is a pair of matched resistance thermometer bulbs that are housed in a compact assembly. One sensor measures the temperature of the vapour exiting the vacuum pan, which is the coldest point in the massecuite and thus the zone of highest supersaturation, while the second sensor records the temperature of pure water boiling at the same pressure. The instrument compares these two readings to calculate and display the

[4] *Sugar boiling - the syrups in the vacuum pans; Sugar boiling - some facts and some fancies; Sugar boiling - some useful strategies.* https://www.zieglerassociates.com/about (accessed 10/04/2025): 8 pp; 12 pp; 10 pp.

oversaturation level directly, based on the purity selected and the known boiling point elevation under the conditions. This method provides a real-time indication of massecuite concentration at the pan's upper surface.

SeedMaster

The SeedMaster (Rózsa, 1998) was developed specifically to address the challenges of supersaturation measurement in sugar crystallisation, not only during seeding, but also during the feeding and final phases of the pan. The system integrates with sensors and measurement devices on the pan, such as process refractometers, microwave probes, as well as level and vacuum pressure sensors.

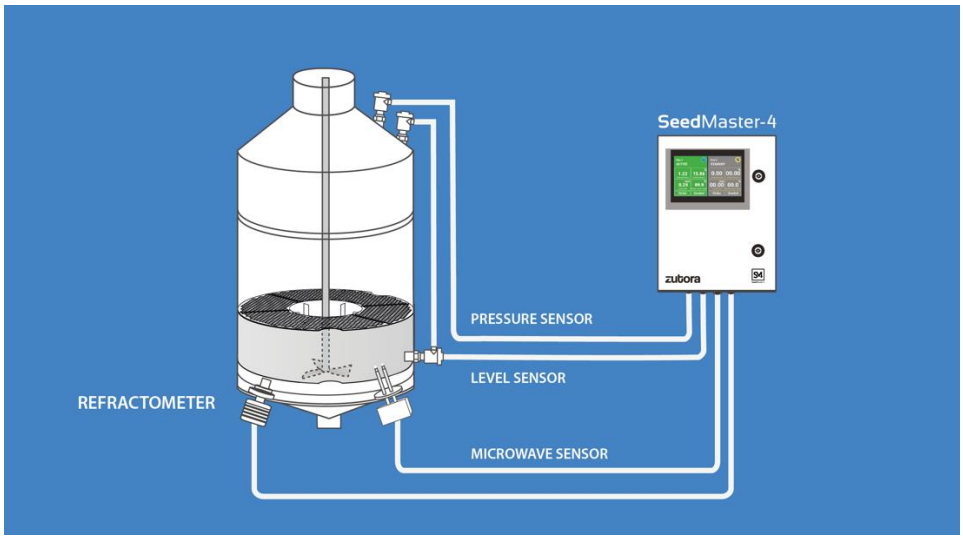


Figure 5. In-line sensors connected to the SeedMaster

The SeedMaster system is designed for use with batch vacuum pans and cooling crystallisers, where it continuously monitors key variables, such as supersaturation, crystal content, crystal size and mother liquor purity. The latest model, the SeedMaster-4 (SM4), employs proprietary algorithms to calculate supersaturation in real time. This value can either be retransmitted to existing control systems or used directly by the SeedMaster to manage the entire crystallisation process. Versions equipped with control functionality are capable of maintaining the supersaturation coefficient of the mother liquor within the metastable zone throughout the batch. This is achieved by precisely regulating both the concentration and temperature of the mother liquor, typically by adjusting the calandria steam valve to control evaporation and using vacuum to manage the temperature.

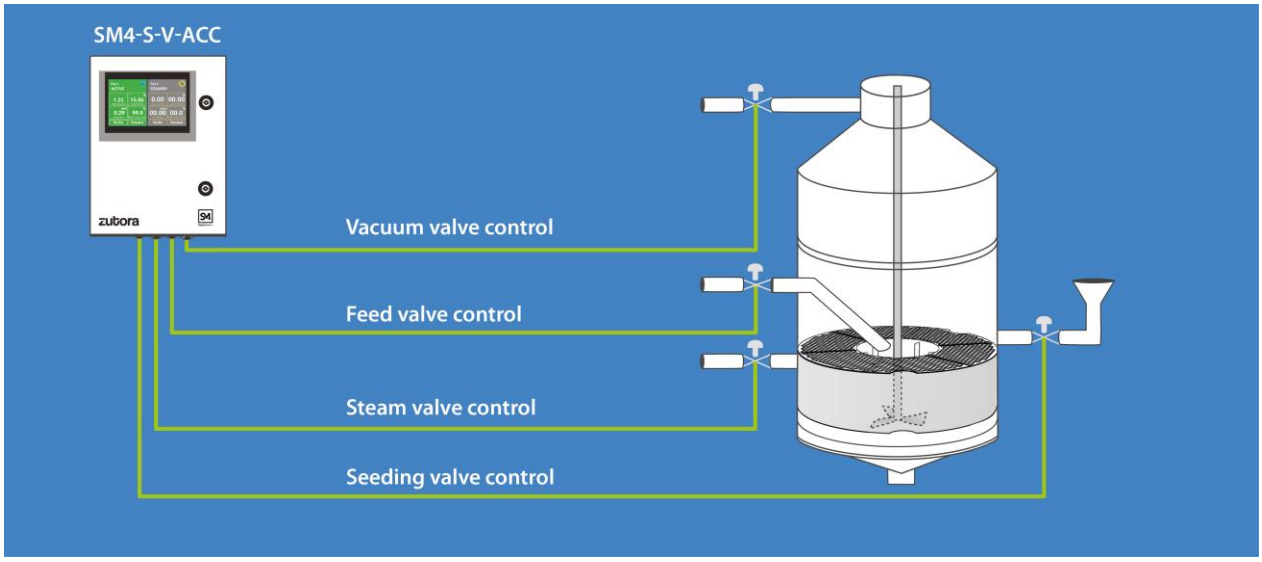


Figure 6. Control valves managed by the SeedMaster

For the accurate determination of crystal content within the massecuite, best practice involves the concurrent use of a microwave probe and a process refractometer. The microwave probe quantifies the total solids content of the massecuite, and it encompasses both the dissolved and crystalline phases, whereas the refractometer selectively measures the concentration of dissolved solids in the liquid phase. The differential between these two readings provides a reliable estimate of the crystal content. Prior to seeding, when no crystals are present, both instruments yield equivalent concentration values, thereby validating the calibration and sensor alignment.

Since seeding at the correct conditions plays a critical role in the overall quality of a batch, it can also be automated by using this system, be it with seed slurry or with magma (Ròzsa, 2003).

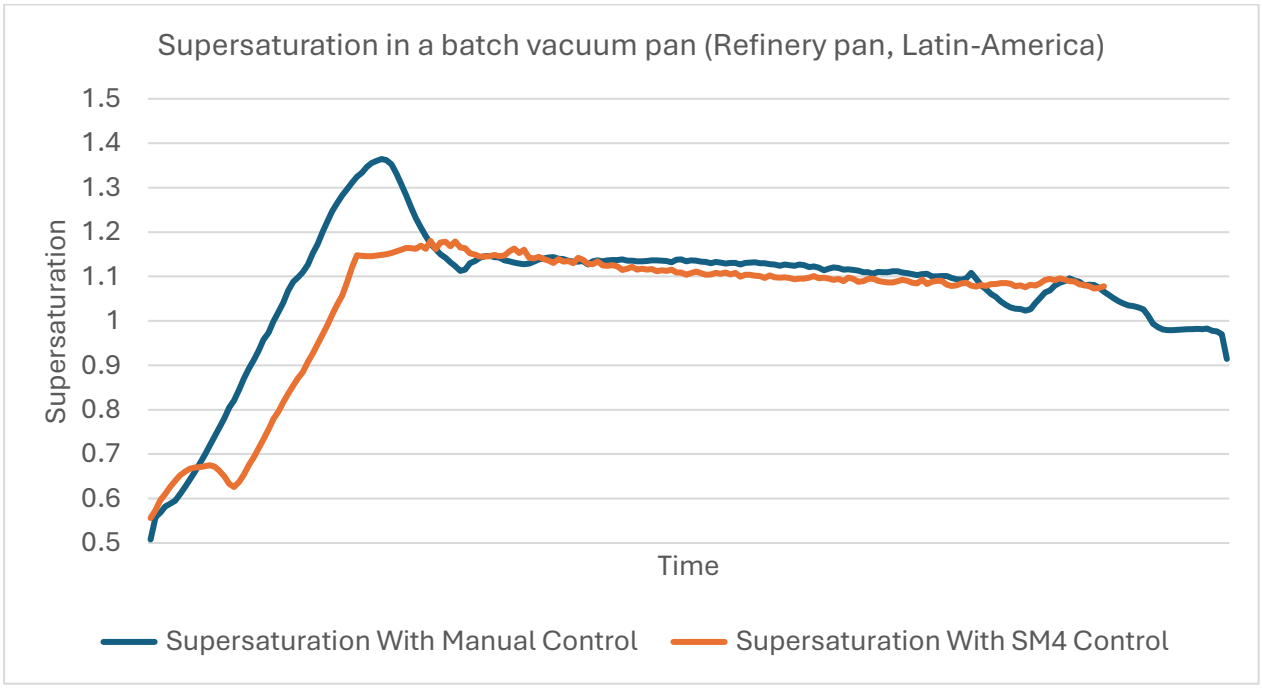


Figure 7. Supersaturation curves with manual vs SM4 control

Case Study 1
Thailand, reducing steam consumption by eliminating water addition

The sugar cane factory in Thailand uses the Double Einwurf (three-boiling) scheme where C-magma is used as seed and the starting point of crystallisation. The quality of the C-pan is therefore of key importance for the performance of the crystallisation station. It also determines the C-molasses exhaustion, and therefore, the yield. The initial focus was therefore on this pan ([5]Rukavina, unpublished). To this end, the SM4 was installed on a C2 batch vacuum pan with a 60 t capacity. The pan is seeded with 0.01 mm wet milled slurry to produce magma of 0.22 mm (target size) which is fed to a horizontal continuous vacuum pan.

Instrumentation for supersaturation-based control

The C2 pan was already equipped with a microwave probe and level sensors. A process refractometer was installed in the W-shaped bottom (Figure 8) for the measurement of the liquid phase concentration and temperature. A flexible tube was added for - automatic refractometer prism wash, using hot condensate. The SM4 was connected to the factory's Distributed Control System (DCS) and given access to the control valves of the pan through an industrial protocol Modbus/TCP. The SM4 was therefore able to make decisions during the pan boiling and/or to take over control, in the case of unexpected scenarios.



Figure 8. Process refractometer installed on the batch pan bottom

Comparison of the traditional and the SeedMaster control

Once the SM4 system was up and running, the first three pan cycles were run in the normal operational mode, while the SM4 monitored the supersaturation for each cycle. The pan was then switched over to SM4 control and a fourth batch cycle was completed. The feed syrup purity (Q = 68%) from the laboratory determination was manually entered by using the Human Machine Interface (HMI). Figure 9 shows the pan levels and Figure 10 shows the supersaturation of the three first pan cycles, together with the SM4-controlled cycle (indicated in green each time).

[5] Rukavina, M. C-seed crystallization - high quality crystals without water. https://www.zutora.com/blog/c-seed-crystallization-high-quality-crystals-without-water (accessed 10/07/2025).

It is evident from Figure 9 that traditional control resulted in stepwise level changes, due to the periodic feeding of syrup and water. In contrast, the SM4 was able to provide a smooth feeding profile of the 68° Brix syrup throughout the entire boiling phase.

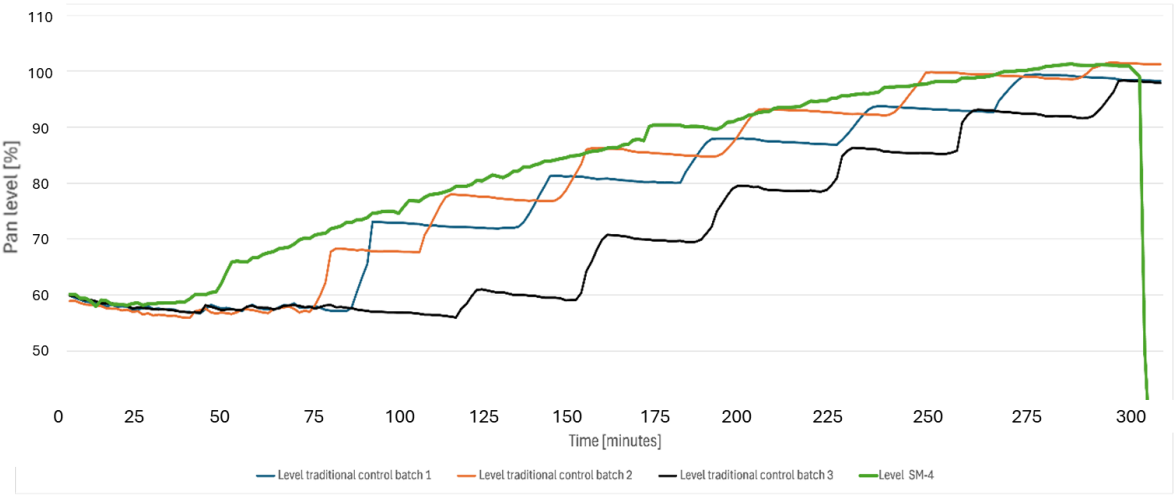


Figure 9. Pan level curves with traditional control (x3) and SM4 control (green)

Similarly, Figure 10 shows that supersaturation under traditional control attained extreme values in the initial phase of the batch, often entering the labile zone and leading to spontaneous nucleation. It is also worth noting that under the traditional control system, water was intermittently added to wash the fine crystals - a practice that significantly increased the steam consumption and reduced the thermal efficiency.

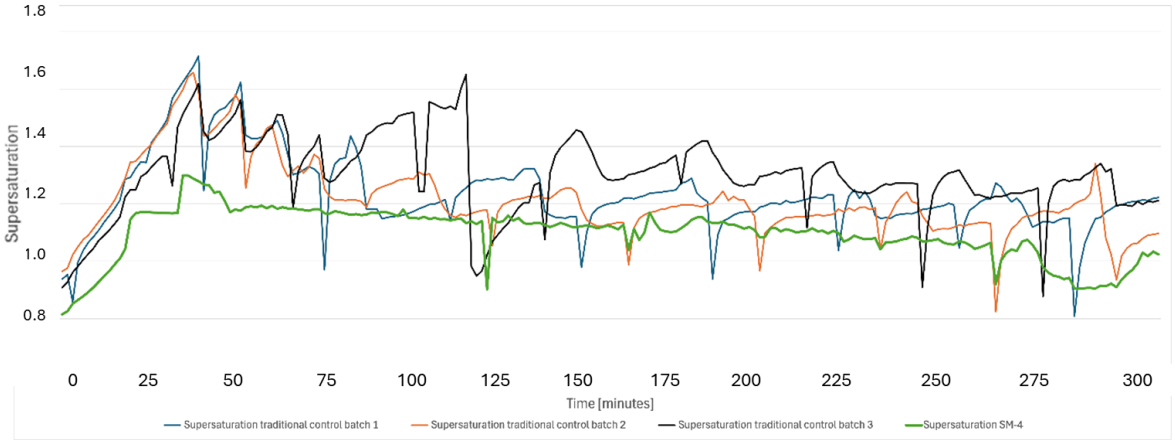


Figure 10. Supersaturation curves with traditional control (x3) and SM4 control (green)

Condensate flow measurement

To accurately track the amount of condensed vapour within the calandria, the factory installed a condensate flow meter, which was integrated into their DCS for continuous monitoring. Under the traditional control setup, the condensate outflow typically ranged between 41 and 53 m³ per batch. However, after implementing the SM4 control system, this range dropped to between 27 and 31 m³ (Figure 11). This reduction translates to an average saving of 18 m³ of condensate per batch, and a 38.3% decrease in steam consumption. Such a substantial improvement not only reflects an enhanced thermal efficiency, but also indicates a more stable and controlled crystallisation process, with less reliance on corrective water additions and a reduced steam demand.

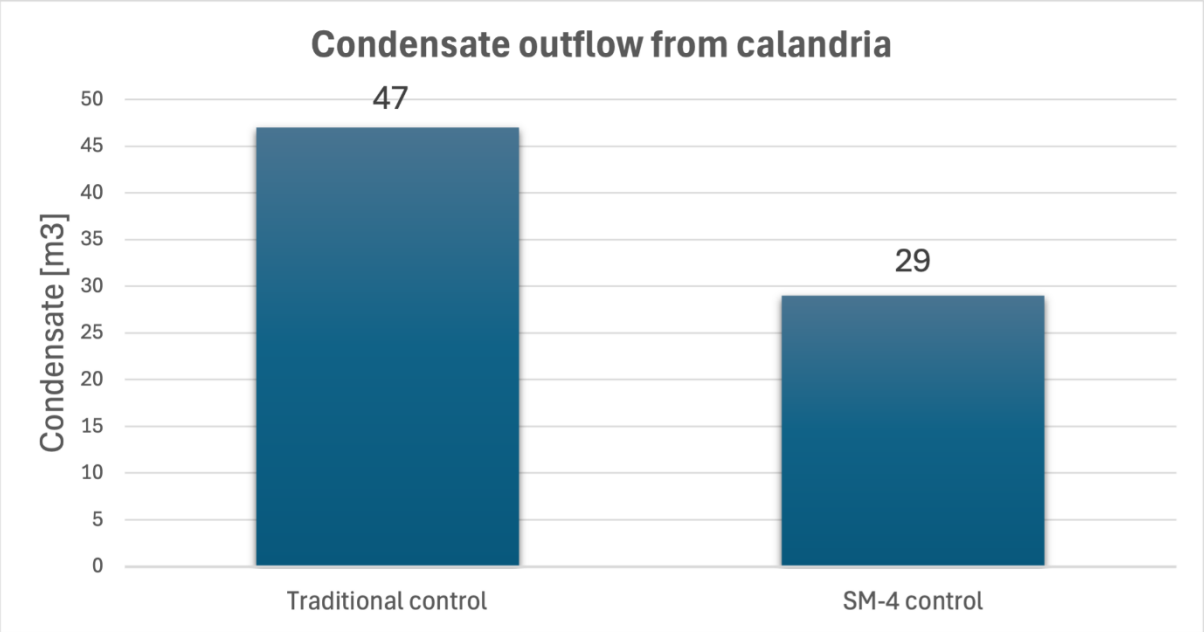


Figure 11. Condensate flow with the traditional vs SM4 control

Crystal size and uniformity

During and after each batch, massecuite samples were taken from the C2 crystalliser and observed under a microscope. Figures 12 and 13 show photographs of the C-seed at the end of the crystallisation process for a traditional and a SM4-controlled pan, respectively. For the SM4-controlled sample, the crystals appear more uniform in size, with a notable absence of very large crystals, compared to the traditional control image.

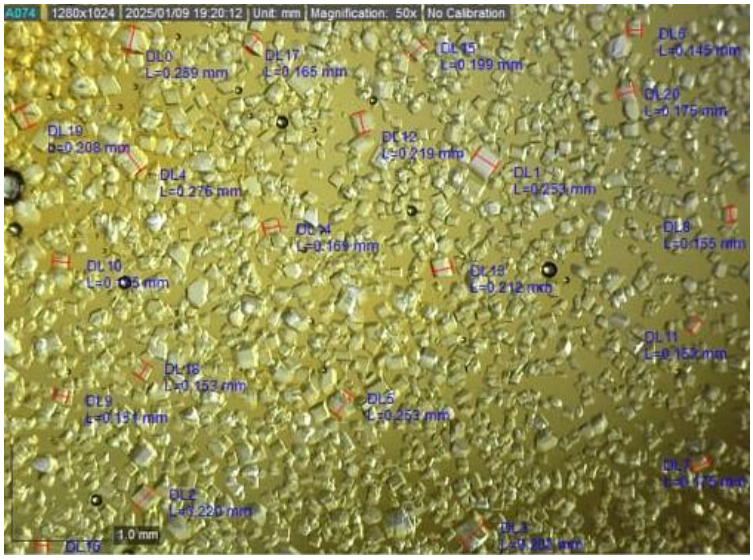


Figure 12. C magma crystals produced by traditional control

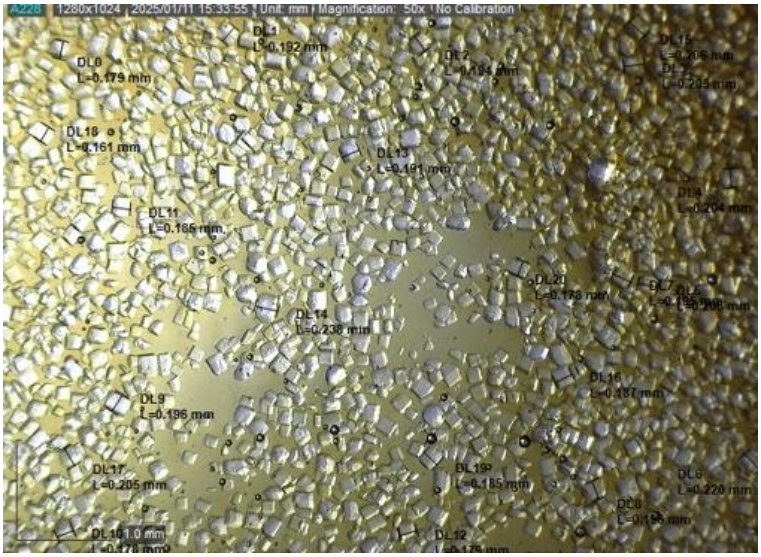


Figure 13. C magma crystals produced by SM4 control

Case Study 2
Dobrovice, Adjusting the seeding point of the mother pan

Established in 1931, the Dobrovice factory holds the distinction of being the oldest continuously-operating beet sugar facility in the world. The factory employs a mother-daughter configuration of batch vacuum pans for the production of A-sugar. The objective of this study was to enhance the quality of A-sugar crystals produced in the daughter pans by optimising the crystallisation dynamics of the footing magma that was generated in the mother pan.

The crystallisation system comprises one mother pan with a capacity of 120 tonne and a heating surface of 320 m², alongside five daughter pans, each with a capacity of 90 tonne and a heating surface of 500 m². Notably, the instrumentation and control systems of the daughter pans remained unchanged throughout the study; instead, the intervention focused exclusively on upgrading the control strategy of the mother pan.

In this context, crystal size distribution was assessed solely on the final product crystals, as the direct measurement of the footing magma crystals was not feasible. Initially, the advanced control system governing the mother pan was evaluated to determine its influence on the granulometric properties and the overall quality of the product crystals. Following the implementation of the SM4 control system, granulometry data from multiple strikes were collected and systematically compared against the historical data obtained under the traditional control regime, which enabled a robust assessment of the impact of the upgraded crystallisation control.

Instrumentation for supersaturation-based control

The mother pan was already equipped with a microwave probe and a level transmitter. In addition, the factory installed a process refractometer to measure the liquid phase concentration and massecuite temperature. The SM4 was installed adjacent to the seed pan. As mentioned before, the system integrates signals from the microwave probe, refractometer and level sensor via standard 4-20 mA analogue channels, while the calculated supersaturation output is transmitted directly to the DCS.

The traditional control system

Initially, the traditional control system was used according to the steps shown below:

1. the pan is filled up to seeding level with 78% Brix syrup (purity 95%);
2. the syrup is concentrated to the seeding point as fast as possible;
3. seeding is performed with slurry at the target microwave Brix; and
4. after seeding, 74% Brix syrup (purity 95%) was used for feeding.

For the first few strikes, the traditional control system was used, while monitoring the supersaturation with the SM4. Some interesting observations were made, as follows:

- in each case, the pan was seeded too late: supersaturation was already above 1.20 (sometimes above 1.25) when the seeding was done; at this purity, secondary nucleation will already start at around 1.13;
- for the duration of the pan, the supersaturation was quite low, on average around 1.05; this value is lower than what is needed for the optimal crystal growth rate; and
- the temperature was generally too high, around 78°C; at this level, there is a risk of colour formation, and it contributes to the low supersaturation.

Technological bottlenecks

Normally, the initial strategy to increase the supersaturation during the boiling phase would be to increase the vacuum. The resulting reduction in boiling temperature by just a few degrees could have shifted the system into a more favourable supersaturation range. However, the vacuum system was already operating at full capacity, with the mother pan's vacuum valve almost consistently open at 100%. This constraint was imposed by the existing infrastructure. As a result, no further optimisation of the vacuum could be achieved.

An alternative strategy involved intensifying of evaporation to increase the concentration of the mother liquor, thereby increasing the supersaturation. This option also proved unfeasible, as the factory's steam supply was already fully utilised. These limitations suggested the need for a more sophisticated control approach, one that is capable of optimising crystallisation conditions within the existing thermal and mechanical constraints.

Changes in the control

Because of the limited availability of vacuum and steam, the boiling phase control could not be modified. The consequences of this are longer pans and the increased risk of colour formation. Instead, efforts were concentrated on the most critical part of the strike: the seeding point. The low supersaturation in the boiling phase resulted in longer strikes. However, the excessive supersaturation around the seeding point resulted in the formation of false grain and thus, poor product quality with a high recirculation rate.

In order to improve the mother pan crystal size distribution and yield, the control was changed as follows:

- seeding was to be performed at a target supersaturation, instead of a target Brix;
- after seeding, a period of time was allowed for the seed crystals to grow, before feeding commenced;
- the length of this period was based on supersaturation measurement;
- a supersaturation setpoint was used to determine the feeding rate; and
- the system was switched to the traditional control during the boiling phase.

Granulometry analysis

As mentioned, it was not possible to sample and measure the quality of the mother massecuite; evaluation was therefore based on the quality of the final product. To reiterate, the new control system was only installed on the seed pan that produced the magma for the A-sugar daughter

pans. The daughter pans themselves were not changed. Any improvement in the quality of final product crystals was therefore only due to the improvements in the mother seed pan.

Granulometry data of 87 A-sugar strikes was obtained from the factory laboratory for the evaluation: 39 with the traditional control and 48 with the SM4 control. The granulometry date contains the crystal size distribution results that were obtained by sieving (Anon, 2007). Figure 15 shows the average crystal size distribution before and after the installation of the SM4 on the mother pan.

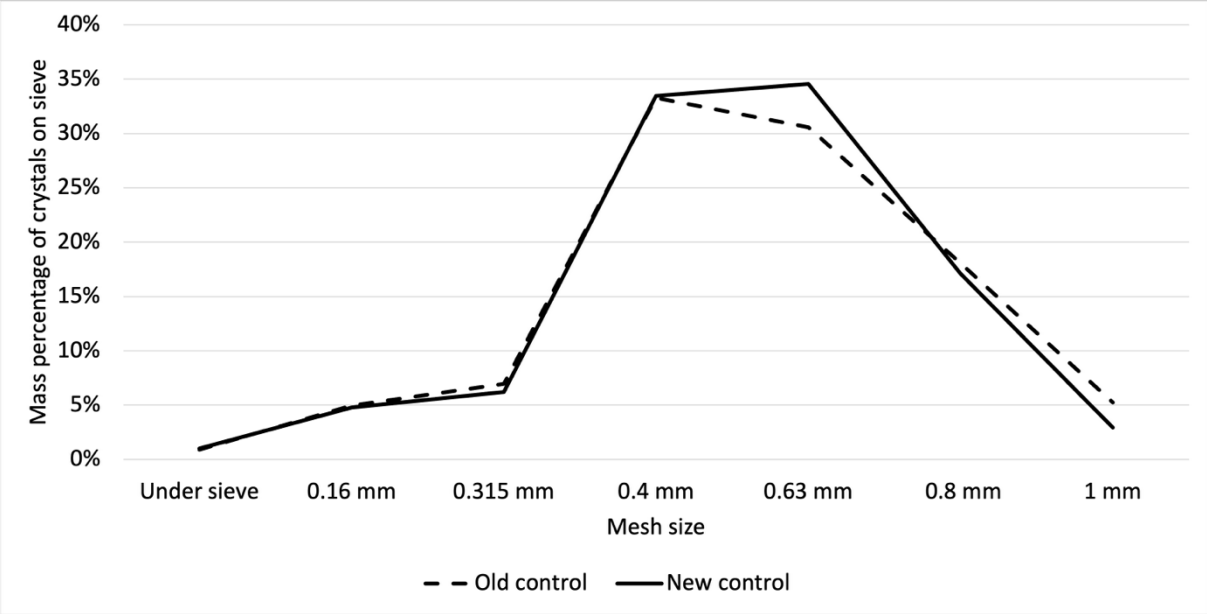


Figure 15. The average crystal size distribution with the old and the new control, based on the granulometry data of 87 strikes

The percentage of crystals retained on the target sieve (0.63-0.8 mm) for each strike is shown in Figure 16.

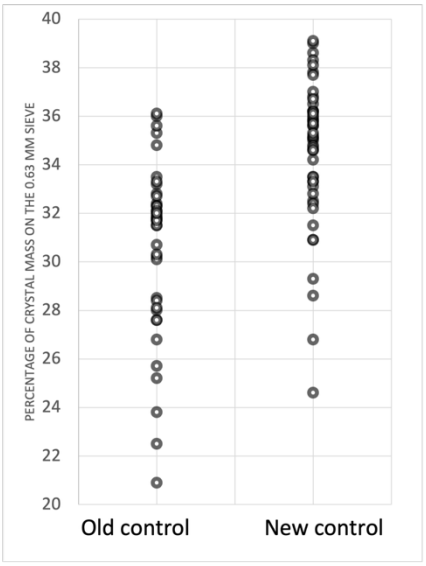


Figure 16. The percentage (%) of crystals retained on the target sieve (0.63-0.8 mm) with and without SM4 control. Each dot represents one strike

The Coefficient of Variation (CV) was calculated for each strike. CV values are shown on Figure 17.

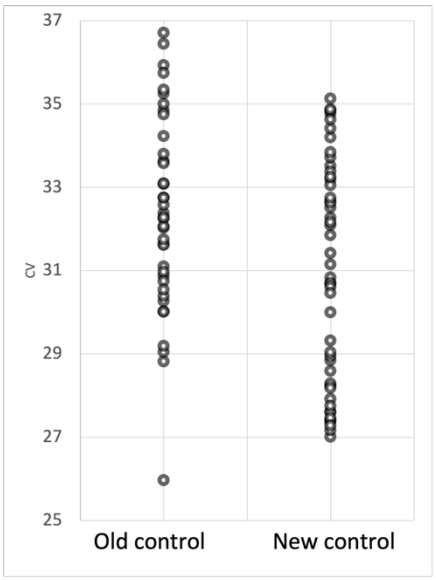


Figure 17. The Coefficient of Cariation (CV) of the crystal size distribution with and without SM4 control. Each dot represents one strike

Numerous studies have demonstrated that supersaturation-based control can significantly enhance both the crystal yield and quality, as reflected in the key metrics, such as MA and CV (de Azevedo *et al.*, 1993; Broadfoot *et al*., 2023; Mahrholz *et al*., 2018). In the present case, the advanced control system was applied exclusively to the mother pan responsible for producing footing magma, while the daughter pans - where final crystal growth occurs - remained under traditional control.

To evaluate the impact of this intervention, the granulometric data from multiple strikes were analysed. The dataset was divided into two groups: the first comprising the strikes initiated with

the footing magma produced under the legacy control system, and the second comprising the strikes that used magma generated under the new, supersaturation-based control.

The sieving analysis revealed an improvement in the product's crystal quality. The proportion of target-sized crystals (0.63 mm) increased from 30.6% to 34.6%, a statistically significant enhancement (Bootstrap two-sample t-test, 1000 replications, two-tailed P=0.011). Furthermore, the proportion of strikes achieving a CV below 30% increased from 10% under the old control, to 38% with the new system, which is a highly-significant improvement (P=0.001).

Operator observations corroborated these findings further. For example, instances of seed crystal dissolution following seeding, which was previously reported under the old control regime, were eliminated. Similarly, the occurrence of 'dusty' strikes, characterised by excessive fine sugar accumulation on the product conveyor, was no longer observed. Weekly reports of large conglomerates in the sugar separator (post-drum dryer) also ceased, following the implementation of the new control strategy.

To reiterate, only the initial phase of the crystallisation process (up to a crystal size of approximately 0.2 mm) was subject to the new control regime. The subsequent growth to the target size of 0.63 mm occurred in the daughter pans under unchanged conditions. Despite this limitation, the targeted optimisation of the footing magma crystallisation phase yielded substantial improvements in the final product's crystal size distribution, which underscores the critical influence of early-stage control on the overall product quality.

Conclusions

This study has demonstrated that real-time, supersaturation-based control represents a transformative advancement in industrial sugar crystallisation. By integrating precise online measurement technologies with intelligent control algorithms, it is now possible to maintain supersaturation consistently within the metastable zone, where optimal crystal growth occurs without the risk of spontaneous nucleation.

The implementation of such advanced control systems across both beet and raw cane sugar factories has yielded measurable improvements in the crystal size distribution, product uniformity, sucrose recovery and resource efficiency. Notably, these gains have been achieved without requiring major changes to downstream equipment, which demonstrates the power of targeted intervention at the earliest stages of crystallisation.

As the sugar industry continues to grapple with increasing variability in the feedstock quality and a widening skills gap among its operators, the adoption of robust, automated control strategies is no longer optional - it is essential. Supersaturation control not only enhances the stability of the process and the quality of the product, but also contributes to the broader goals of sustainability and cost reduction.

The findings presented here suggest that the future of crystallisation lies in data-driven, precision-controlled systems. Continued innovation in this domain will be critical for unlocking further efficiencies and for ensuring the long-term competitiveness of sugar manufacturing in an evolving industrial landscape.

Acknowledgments

The authors would like to acknowledge the work and dedication of the Dobrovice factory in the Czech Republic and the factory in Thailand.

References

Anon (2007). The determination of the particle size distribution of white sugar and plantation white sugar by sieving – Accepted. *ICUMSA Method GS2/9-37.* 3 pp.

Asadi M (2007). Beet-Sugar Handbook. Chapter 3, Section 16: Syrup crystallisation. John Wiley and Sons. pp 345-387.

Blecher D (1999). Technological and operational aspects of measuring instruments in the control of crystallization. *Zuckerindustrie* 124(5): 388-394.

Broadfoot R and Wright PG (1972). Nucleation studies. *Proc. 39th Conf. QSSCT*: 353-362.

Broadfoot R, Fraga L and Luiz G (2023). Increasing our understanding of supersaturation and the use of massecuite dry substance in pan control - Part 1. *Proc Australian Soc Sug Cane Technol* 44: 322-339.

Chen JCP and Chou CC (1993). Cane Sugar Handbook: A Manual for Cane Sugar Manufacturers and their Chemists (12th ed.). John Wiley and Sons. pp 226-312.

de Azevedo SF, Chorão J, Gonçalves MJ and Bento SM (1993). On-line monitoring of white sugar crystallisation through software sensors. *Proc Sug Int Technol* 646: 217-250.

El-abdein OZ, Tmerek YM, Abdullah ID and Ferweel ST (2009). Design and evaluation of a full control program for sucrose crystallization based on the soft sensor approach. *Proc Sug Int Technol* 1026: 43-71.

Hugo E (1986). *Handbook of Cane Sugar Engineering,* 3rd Ed, Elsevier Science Publishing Company, Amsterdam. pp 689-690.

Mahrholz J, Lehnberger A and König M (2018). Improved industrial crystallisation by automation. *Proc AVH Symposium* 25: 9.

Mathlouthi M and Genotelle J (1998). Role of water in sucrose crystallization. Carbohydrate Polymers 37: 335-342.

Mitra SK, Kumar V and Sanyal P (2009). Conductometric studies and its significance during cane sugar manufacture. *Sugar Tech* 11(4): 324-329.

Price CJ (1997). Take some solid steps to improve crystallization. *Chemical Engineering Progress* 93(9): 34-43.

Rein P (2003). Some fundamental considerations of crystallisation and their implications for the control of sugar boiling. *Proc Sug Int Technol* 902A: 13.

Rein P (2017): *Cane Sugar Engineering*, 2nd ed. Chapter 15: Crystallisation. Verlag Dr. Albert Bartens KG, Berlin: 407-456. DOI: 10.36961/cse.

Rhoten CD (2013). An innovative approach to self-optimizing batch evaporating crystallizer control. *Sugar Industry* 138(7): 475-481.

Rózsa L (1998). The Seed Master device for on-line supersaturation measurement and automatic crystallizer seeding. *Int. Sugar Journal* 100(1200): 601-607.

Rózsa L (2003). Sensor selection: Still an issue in sugar crystallization control. Prod. Philippine Sugar Technologist's Convention, Bacolod City, Philippines. 11 pp.

Rózsa L (2008). Sugar crystallization: Look for the devil in the details – Part 1, *Int Sugar J* 110(1315): 403-413; Part 2, Int Sugar J 110(1320): 729-739.

Saska M (2002). Boiling point elevation of technical sugarcane solutions and its use in automatic pan boiling, International Sugar Journal 104(1247): 500-507.

Thelwall JC de C (2002). Discussion on batch and continuous boiling techniques. *Proc Sug Int Technol* 817: 14.

Tuzhilkin VI, Balykhin MG, Petrov SM, Podgornova NM, Lukin ND and Kovalyonok VA (2021). Mathematical description of the isobaric vaporizing crystallization of sucrose. *Journal of Food Engineering* 306(110614): 12.

van der Poel PW, Schiweck H and Schwartz T (1998). *Sugar Technology*. Chapter 12. Verlage. Dr A Bartens, Berlin. 649-828.

POSTER SUMMARY

THE ANALYSIS OF LIME ON MELT BY DOUBLE ALKALINITY TITRATION

Naicker A, Ngcobo S, Naidoo Y, Walthew D and Myeza M

Sugar Milling Research Institute NPC, c/o University of KwaZulu-Natal, Howard College Campus, Durban South Africa 4041

anaicker@smri.org, lnaidoo@smri.org, dwalthew@smri.org, mpume.myeza@tongaat.com

Abstract

The quantity of calcium carbonate that is formed during the carbonation process in sugar refining is critical for the successful removal of impurities. In order to achieve this, it is essential for factories to monitor the amount of calcium added to the melt that is available to react with the carbonic acid, to form a calcium carbonate precipitate, which is often referred to as the 'available lime'.

This study investigates the adoption of a double alkalinity titration method for the quantification of the available lime in the melt. The method distinguishes between the available lime (calcium hydroxide) and calcium carbonate by employing a strong acid titration to determine the first and second end-points, using phenolphthalein and bromocresol green indicators.

Compared to the complexometric and instrumental methods, this technique offers simplicity, cost-effectiveness and minimal sample preparation, which makes it highly practical for routine application in sugar refineries.

Keywords: Available lime, calcium hydroxide, calcium carbonate, double alkalinity titration

REVIEW PAPER

A REVIEW OF THE PHYSICAL PROPERTIES OF A-MASSECUITE THAT AFFECT BATCH CENTRIFUGAL OPERATIONS

Munsamy SS

[1]Consulting Sugar Technologist, [2]JA van Wyk Consulting
70 St Andrews Drive, Durban North, South Africa 4051

Stanleymunsamy1@gmail.com

Abstract

The function of the centrifugal is to efficiently separate the sugar crystals and molasses from the A-massecuite. Small quantities of steam and water are used to wash the remaining molasses from the surface of the crystal and to improve the Polarization (Pol) of sugar. There is a linear inverse relationship between the sugar Pol and colour. In the washing process, a degree of crystal dissolution and loss in exhaustion takes place. A-exhaustion plays an important role in sugar recovery and colour recirculation in the factory. At some factories, up to 20% of the exhaustion gained in the vacuum pan is lost in the batch centrifugal.

The two important physical properties of A-massecuite that affect the batch centrifugal operations are the viscosity of the mother liquor and the Coefficient of Variance (CV) of the crystals. The viscosity of the mother liquor is a function of its non-sucrose content, the total dissolved solids (brix) and the temperature. Small crystals and bagacillo affect purging by blocking the voids in the bed of crystals inside the centrifugal basket. The centrifugal will experience high vibration if the molasses cannot drain rapidly during the spinning cycle. The vibration can lead to damage and sometimes to the catastrophic failure of the centrifugal, which poses a risk to the operator.

The effect of the mother liquor viscosity is more pronounced when producing a high Pol, low colour sugar. Since the refining process is essentially a colour-removal process, back-end refineries, without the affination stage, can benefit from the low sugar colour.

The type and concentration of the non-sucrose is not in the hands of the factory personnel. Factories can improve the operation of the batch centrifugal by producing good quality crystals and by optimizing the fugalling characteristics of the massecuite, by adjusting the brix and temperature throughout the season, as the type and concentration of the non-sucrose changes.

Keywords: A-massecuite viscosity, batch centrifugal performance, sugar quality, mother liquor viscosity, loss across batch centrifugal, fugalling behaviour

Introduction

In this paper, ‘mother liquor’ refers to the liquid fraction of massecuite, and ‘molasses’ refers to the mother liquor after it has been diluted with steam and hot water in the centrifugal. A sample of the mother liquor is extracted for analysis purposes by using a Nutsch pressure filter. The sugar colour is measured by using the ICUMSA 420 method and it will be referred to as ‘colour’. Pol refers to the polarization of sugar measured as °Z, and it will be referred to as ‘Pol’. Brix refers to the total dissolved solids measured as °Brix. The Mean Aperture (MA), Coefficient of Variance (CV) and % fines of the crystals are calculated as per the official methods (SASTA Laboratory Manual). The difference in purity between the massecuite and the mother liquor is a convenient way of measuring the exhaustion at each stage in the crystallisation process. ‘Centrifugal’ refers to the batch centrifugal.

The South African export requirement of 99.35 Pol and 1500 colour is generally easy to meet, for most of the crushing season. The introduction of Very High Pol (VHP) sugar has resulted in South African refineries dispensing with the affination process as the first step in colour removal. These refineries can benefit from high-Pol, low-colour sugar.

VHP and affinated sugar colours

The batch centrifugal is used to produce both raw and affinated sugars. When the molasses coating from the crystal surface is completely stripped way, the sugar is referred to as 'affinated sugar'. If affination is done correctly, about 85% of the impurities can be removed from the raw sugar (Watson & Nicol, 1975). El-Syiad *et al.* (2020) compared the impurity levels of raw and affinated sugars in the Egyptian sugar industry. Their results showed that the dextran, ash and reducing sugars decreased by 55%, 83% and 47% respectively by increasing the sugar Pol from 99.45 to 99.62. However, there was no removal of starch, which indicated that the starch was occluded inside the crystal. Davis *et al*. (2013) presented the VHP and affinated sugar colours for South African raw sugar for the period 2003 to 2013. This trend is shown in Figure 1.

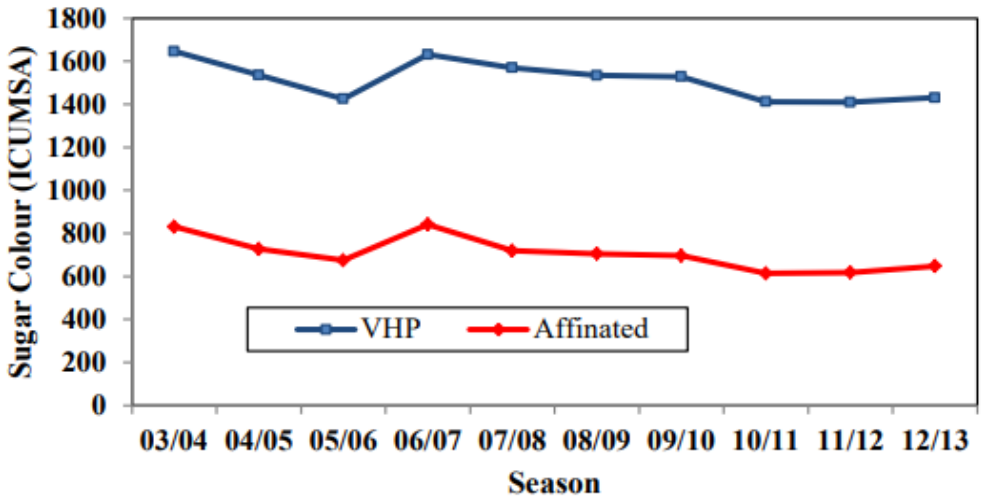


Figure 1. VHP and affinated sugar colours for the period 2003 to 2013 (Davis *et al*., 2013)

By eliminating affination as the first step in colour removal, South African refineries have increased the impurity/colour loading on the other colour removal processes.

Sugar Pol and colour

The Pol and the colour reflect the purity of the sugar. There is a linear inverse relationship between sugar Pol and colour. The data shown in Figure 2 were collected from several sugar factories in southern Africa in the 2022/23/24 seasons, as well as from various publications across the global sugar industry, and they include data from refined, mill white and Australian very low colour sugars.

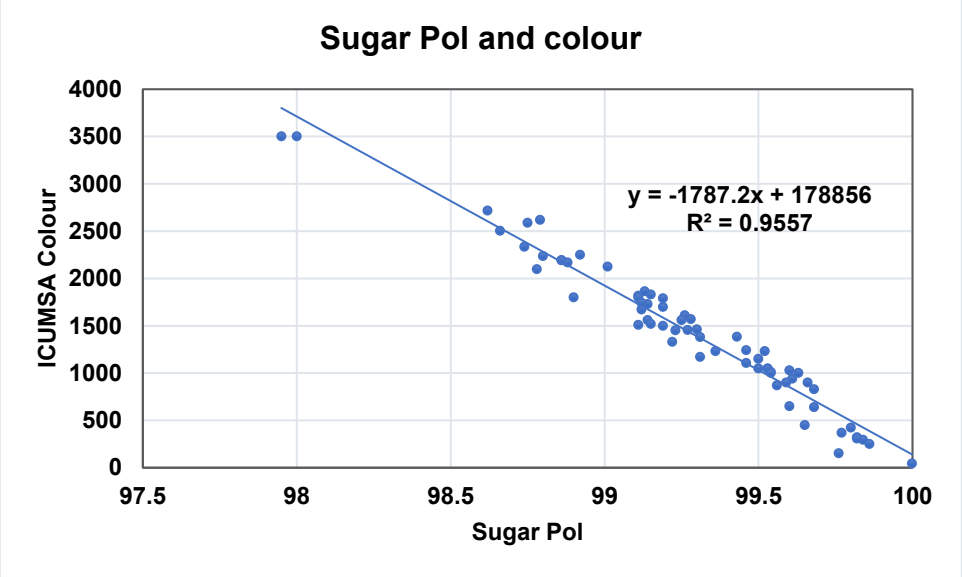


Figure 2. The relationship between Pol and colour

Irrespective of the type of colour removal process that is employed, there is a linear relationship between the Pol and colour. Jullienne (1983) found a similar relationship: "the level of impurities in A-sugar was found to decline linearly with the sugar purity". The South African affinated sugar colour of around 700 can be achieved with a sugar Pol of around 99,68.

A-exhaustion

Ninela and Rajoo (2006) demonstrated the importance of A-exhaustion in improving factory sugar recovery. Booysen and Davis (2019) and Naidoo *et al*. (2024) showed the importance of high A-exhaustion in reducing colour recirculation in a sugar factory. Data on A-station exhaustion, expressed as 'purity drop/rise', is shown in Table 2. The vacuum pan is the biggest contributor to A-exhaustion and the centrifugal is the biggest 'thief' of exhaustion, with about 20% of pan exhaustion being lost in the centrifugal.

Table 1. The purity drop/rise across the vacuum pans and crystallisers, and the purity rise across the centrifugals

Purity drop/rise across:	Nielson (1992) *	2023/24 season**
A-Pan	-20.34	-19.98
A-Crystalliser	-2.85	-1.73
A-Centrifugal	4.22	4.23

*Average of 5 season **average of 6 factories in South Africa

Some technologist, believe that producing a higher Pol sugar will result in a lower A-exhaustion, as extra 'washing' is required in the centrifugal. However, this does not have to be the case if the physical properties of A-massecuite are such that the molasses and crystals separate easily in the batch centrifugal with the minimum of wash water. Naidoo *et al*. (2024) showed that a factory can produce a VHP of 967 colour and still achieve 69.75% exhaustion, if good sugar technology principles are followed in the factory. Naidoo *et al.* (2024) focused on low boiling temperatures to minimise the Maillard reaction.

Molasses flow in a batch centrifugal

The separation process in a batch centrifugal is essentially a filtration process through a packed bed of sugar crystals, assisted by the inertial effects of the rotation motion, which is commonly referred to as the 'centrifugal force'. The mother liquor has a difficult flow path in the centrifugal and must move through the crystal bed of about 150 mm wide, as well as the working screen and the backing screen, and then through small drainage holes in the basket. According to Grimwood *et al*. (2003), the resistance to flow is dominated by the crystal bed. It is important to note that the crystal bed in a batch centrifugal is stationary, relative to the screen, whereas in a continuous centrifugal, a thin bed of crystals is moving up the screen.

Hedley (1937) found "that when the temperature of the centrifuged massecuite is high, a much higher purity of sugar is obtained, as a result of the better elimination of the molasses that results from the reduction of its viscosity"

Broadfoot and Miller (1996) investigated the fugalling behaviour of high-grade massecuites in Australia. They found that of all the variables that influence the fugalling performance, the mother liquor viscosity had the strongest influence on the composition of the purged sugar. The influence of the molasses viscosity on the fugalling performance is more pronounced when producing higher polarization sugar. The viscosity of the mother liquor has a significant effect on the drainage time of the liquid in the centrifugal. Of the granulometric properties determined by the usual sieving procedures, the Coefficient of Variation (CV) of the size distribution was the variable with the strongest influence. The above authors recommend the following actions to reduce mother liquor viscosity:

- Increase the A-massecuite temperature by decreasing the vacuum just before striking the pan
- Reheating or diluting the massecuite before centrifugalling.

The Australian sugar industry does not use cooling crystallisers on A-massecuite because the industry prefers to centrifugal the massecuite while it is hot.

A collaboration study was conducted by researchers from various Universities (viz. the UK, Australia and RSA) and the South African Sugar Industry. The Industry was represented by Richard Loubser and Steve Davis, in response to difficulties that the industry was experiencing at the centrifugal station. The study was entitled 'Liquid flow in a sugar centrifugal', and it modelled the behaviour of molasses in a batch centrifugal (Please *et al.*, 2012). Since the drainage time is a function of the viscosity of the mother liquor, researchers used hot water, hydrogen peroxide and steam in their trial to decrease the viscosity. They found that "by far, a better way to remove the remaining molasses is to heat the molasses by spraying with steam. Spraying with steam can reduce, by half, the volume of the molasses remaining on the crystals". The practical implication of this finding is that steam addition will increase the centrifugal capacity for a given sugar quality, or the sugar quality can be improved for a given cycle time.

Massecuite and molasses viscosity

Honig (1959) stated that: "The dominant factor in crystallisation technology is viscosity... Since viscosity varies extensively with the composition of the non-sucrose constituents, optimum operating procedures are attained by adjusting the principal variables, temperature and solids content, in order to reach the desired viscosity ranges. No closely-defined specifications can be set up due to the uncontrollable variations in composition of the molasses. Each factory, therefore, must investigate its own situation with regard to the effect of the variables, temperature, supersaturation and viscosity".

Shah *et al.* (2017) referenced the work of several researchers and showed that the viscosity of massecuite was highly-dependent on the viscosity of the mother liquor. Mother liquor

viscosity is dependent on dry substance and temperature, as shown by Rouillard and Koenig (1980). Love (2002) proposed the following correlation between Dry Solids (DS), brix and pol.

$$DS = Brix\left(1 - 0.00066\,(Brix - Pol)\right) \quad \ldots \quad (1)$$

The biggest effect on dry solids is the brix, and increasing the brix will increase the viscosity of the mother liquor. Jullienne (1994) found a linear relationship between the brix of A-massecuite and the brix of the mother liquor. Increasing the A-massecuite brix, for example, from 91° to 93° Brix, will increase the mother liquor from 81° to 83° Brix. A good 'rule of thumb' is that the mother liquor brix is 10 units lower than the A-massecuite brix.

Genotelle (1978) produced the following equation for the viscosity of a pure sucrose solution:

$$\log_{10}\mu_{solution} = 22.46N - 0.114 + \ (30 - T) \times \frac{(1.1 + 43.1N^{1.25})}{91 + T} \quad \ldots \quad (2)$$

$$Where \qquad N = \frac{B}{1900 - 18B} \quad \ldots (3)$$

$$\mu = dynamic\ viscosity\ in\ mPa.s\ ;\ B = \ brix\ as\ \%\ ;\ and\ T = \ temperature\ as\ ℃$$

It must be noted that the above equation is for pure sucrose solutions, and that the viscosity will increase as impurities are introduced into the solution. The viscosity will increase further by the Maillard reaction, if gases are introduced into the massecuite. Impurities, like dextran, will also increase the viscosity. South African massecuites are known to have high levels of dextran and other polysaccharides in the rainy season.

The above equation was used to model the effect of brix and temperature on the mother liquor viscosity. The effect of temperature and mother liquor brix is shown in Figures 3 and 4.

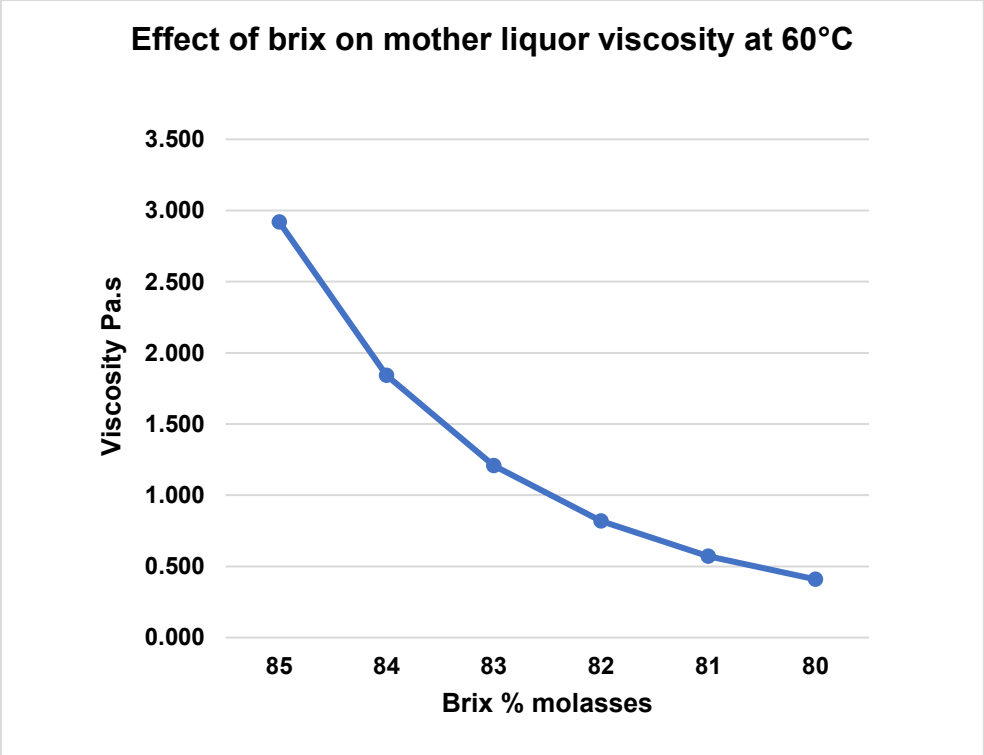


Figure 3. Effect of brix on mother liquor viscosity

In Figure 3, the temperature of the mother liquor was kept constant at 60°C. The mother liquor brix, in typical South African A-massecuite, ranges between 80° and 82°Brix. Decreasing the brix from 82° to 80°Brix decreases the viscosity from 0.818 to 0.409 Pa·s, a reduction of 50%.

Honig (1959) states that the viscosity of factory molasses almost doubles, for each increase of 0.8% in the total solids.

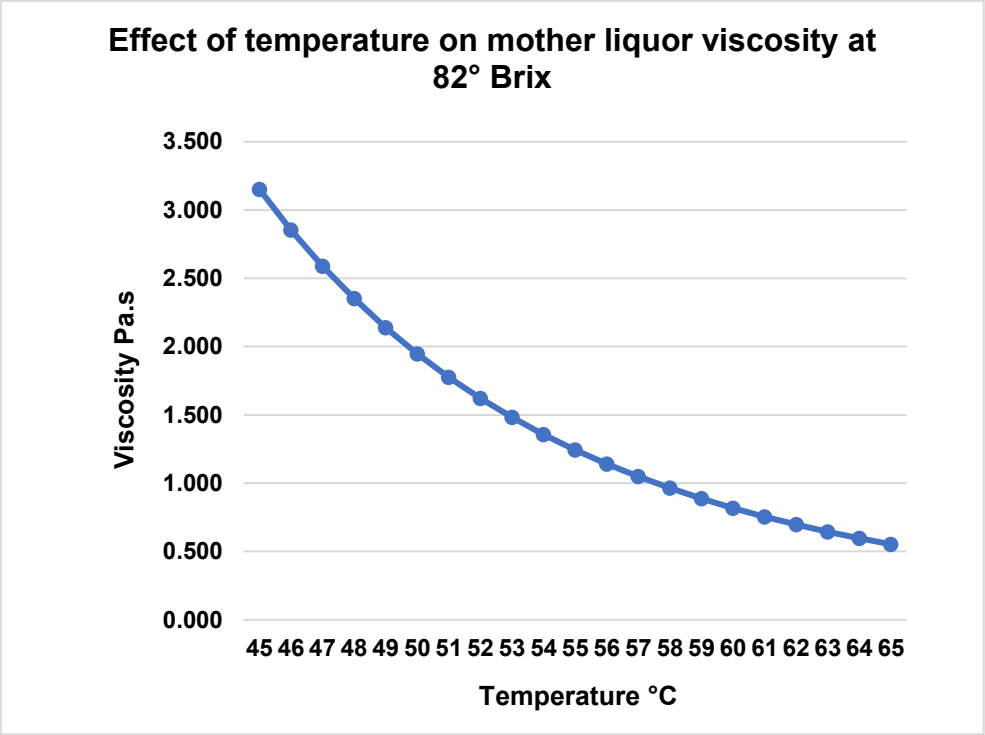


Figure 4. Effect of temperature on the mother liquor viscosity

In Figure 4, the mother liquor Brix was kept constant at 82°Brix. Increasing the mother liquor temperature from 50° to 60°C, decreases the viscosity from 1.948 to 0.818 Pa·s, which is a decrease of 42%. Rein (2007) referenced the work of several researchers and proposed a two-fold change in massecuite and molasses viscosity with a temperature difference of 9°C.

The data presented in Figures 3 and 4 show that both the Brix and temperature have a strong influence on the viscosity of the mother liquor for pure sucrose solutions. Although the viscosity will be higher for factory molasses, it is assumed that the shape of the graph will be the same. As the viscosity of the mother liquor decreases, the drainage time in the crystal bed will also decrease, which means that a shorter time will be required to spin off the molasses in the centrifugal basket.

The effect of the crystal content on massecuite viscosity has been discussed by Honig (1959) and Rouillard and Konig (1980). According to Honig (1959), as the crystal content approaches 45%, the mobility of the massecuite is severely restricted. Some South African factories achieve high crystal contents of up to 54% in the vacuum pan. However, this might not be the crystal content that enters the centrifugal, due to dilution in the crystallisers. Robertson *et al.* (1979) proposed pre-curing as a method of decreasing the viscosity, by decreasing the crystal content of the massecuite in the A-crystallisers. By pre-curing a part of the strike massecuite without water or steam addition, the undiluted A-molasses was returned to the A-crystalliser to decrease the crystal content. This method allowed a higher pan brix without the inhibiting effect of crystal content on the massecuite viscosity and damage to the crystalliser stirrers (and to the centrifugal). The proposal was not adopted on a large scale due to the fact that 25%-30% of the massecuite was pre-cured and resulted in a sugar with a low Pol and high a colour.

Crystal quality and bagacillo

Although smaller crystals increase the rate of crystallisation in the pan, the limiting factor towards smaller crystal size is the ability of the centrifugal to remove the molasses (Honig, 1959). Watson and Nicol (1975) highlighted the importance of the Specific Grain Size (SGS) on the affination process. A mixture of grain sizes negatively affects the affination process. This is the reason that South African export sugar needs to conform to certain granular properties like MA, CV and percentage fines.

Watson and Nicol (1975) also found that dust (bagacillo) behaved like fine crystals. Smith *et al.* (2000) found that a syrup flotation clarifier removed up to 88% of the bagacillo from the syrup. Although there has been anecdotal evidence that syrup clarifiers improve A-exhaustion, the science is not clear. The blockage of voids in the packed sugar bed by bagacillio explains how bagacillo can affect A-exhaustion. Blom and Munsamy (1994) found that certain juice flocculants had a higher affinity for bagacillo than others. Again, there was anecdotal evidence that some flocculant types improved A-exhaustion. It is therefore important that flocculant trials should include bagacillio removal as one of the selection criteria. Bagacillo in clear juice will find its way into the A-massecuite, in the absence of syrup clarification. Wind-borne bagacillo and other foreign matter will also enter the A-crystalliser if it is not covered.

Some factories believe that ‘slurry graining’ the A-massecuite will improve the crystal quality. Bux and Munsamy (1989) conducted trials at a sugar factory and assessed several sugar quality parameters. They found no significant difference between ‘slurry graining’ and ‘B-magma footing’ with the MA, the CV, percentage fines and affinated colour of the two methods. However, a smaller grain size produced a higher percentage of fines in both methods. It is important that factories stay within the export specification of ≤35% fines.

Grimwood *et al*. (2003) state that the typical open area between the crystals in a sugar cake in a batch centrifugal is around 42% of the total volume of the cake. Unlike those in a continuous centrifugal, not all the fine crystals are lost in a batch centrifugal. Fine crystals, which are commonly referred to as false grain, are trapped in the crystal bed, thus decreasing the open area in the cake bed. If the occurrence of false grain is severe, the factory operations can come to a halt, as the A-massecuite will not purge. The build-up of molasses in the crystal bed can cause severe vibrations and put the centrifugal out of balance. If the centrifugal is not protected with vibration/gyration switches, the unit can be damaged and cause injury to the operator. Grimwood *et al.* (2002) stated that a 1.2 m diameter basket spinning at 1200 rpm generates energy equivalent to a family car travelling at 280 km/h. Centrifugal basket diameters have increased to a 2.0 m diameter, with 1200 rpm speeds resulting in higher energy generation. Good general maintenance and regular checking of the safety devices are essential for the safe operation of centrifugals. The structure supporting the centrifugal must be strong and rigid, and the regular inspection of the structure should be part of the planned maintenance.

Dissolution of sugar during washing in the centrifugal

Small quantities of steam and water are used in the centrifugal to produce the different grades of sugar. Jullienne (1983) studied the dissolution of sugar in batch A-centrifugals at two factories in South Africa. His test data are shown in Table 2.

Table 2. Crystal dissolution and A-molasses purity rise at different A-sugar purities (Jullienne, 1983)

A-sugar purity	% crystal dissolution		Molasses purity rise	
	Darnall	Umzimkulu	Darnall	Umzimkulu
98.9%	0.7	1.6	0.4	0.7
99.4%	2.3	4.2	1.2	2.3

99.6%	3.7	6.0	2.0	3.2

The average CV for both the Darnall and Umzimkulu sugar was 37 and the average massecuite temperatures were 62°C and 55°C, respectively. The effect of washing time on sugar purity is shown in Figure 5.

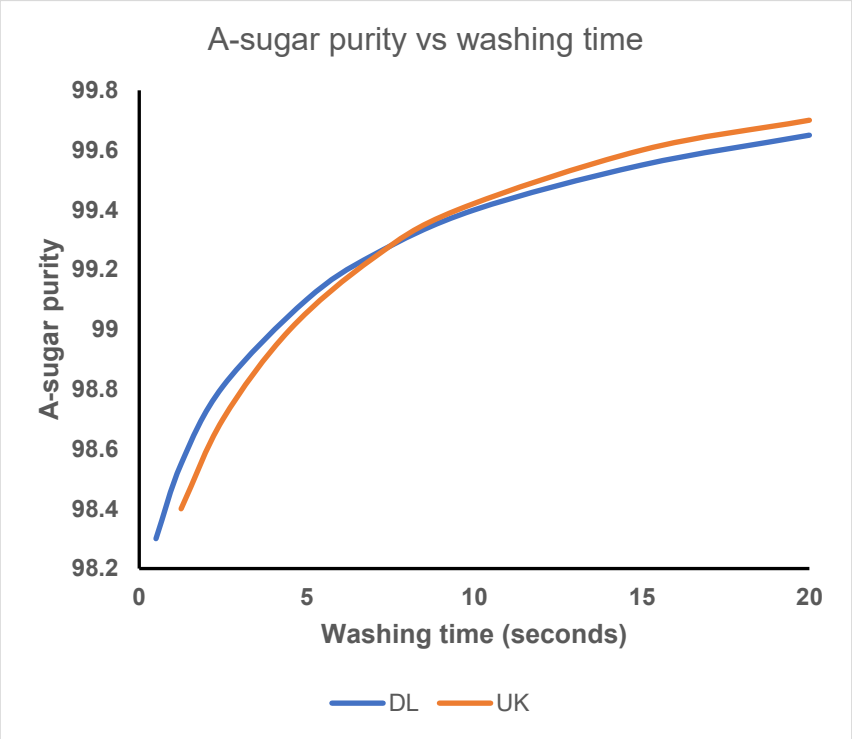


Figure 5. The effect of washing time on A-sugar purity (Jullienne,1983)

Figure 5 shows that the South African export specification of 99,35 Pol sugar can be obtained with 10 seconds of washing.

Handling massecuites of high viscosity in batch centrifugals

At certain times in the crushing season, the juice is contaminated with dextran and other polysaccharides, due to long burn-to-crush delays. These contaminants increase the viscosity of the massecuite to a point where it does not cure easily, or not at all, in the batch centrifugal. Until the introduction of the continuous centrifugal, A, B and C-massecuites were cured in batch centrifugals. The low-grade massecuites were 'conditioned' by reheat and/or dilution before centrifugalling. Beckett and Munsamy (1994) adopted this methodology when faced with drought-affected viscous A-massecuite that was difficult to purge and that caused excessive vibration in the centrifugal. The A-massecuite temperature before purging was increased to 55°C by bypassing 50% of the crystallisers and introducing hot water in the cooling coils. In addition, the massecuite brix was lowered to around 90°Brix. The batch centrifugal was loaded to about 75%, to decrease the flow path in the crystal bed. These interventions resulted in the centrifugal operating 'quietly' without vibration. In addition, defoamers (vegetable oil and commercial defoamers) and sodium hydrosulphite (Blankit) was used to improve the evaporation in the pan. Although there was anecdotal evidence that these additions improved pan boiling and purging in the centrifugal, no qualitative evidence was available for A-massecuite. In summary, when faced with massecuites of high viscosity, factory personnel can try the following:

- Increase the temperature of the massecuite
- Decrease the brix of the massecuite in the pan
- Dilute the massecuite before centrifugalling

The factory massecuite piping is configured for end-of-season liquidation, so the facility to bypass the crystallisers and increase the temperature already exists.

Summary and Recommendations

The centrifugal requires a massecuite from which crystals and molasses will separate easily.

- The viscosity of the mother liquor is the single parameter that has the greatest influence on the final sugar purity and the wash-time required to reach the required purity. Since the viscosity also varies with the composition of non-sugars, it is difficult to prescribe the optimum brix and temperature for a factory. The A-massecuite should have sufficient fluidity to fill the centrifugal basket in about 10 seconds. If this target is not met, then the massecuite temperature and brix will need to be adjusted. A word of caution; massecuites that are too fluid can overfill the centrifugal basket, which is dangerous.
- The massecuite brix, which is very important for crystallisation in the pan, must also meet other operational requirements. Factories that produce A-massecuite in continuous vacuum pans must select a brix that will minimise encrustation and fouling inside the pan. For batch pans, a predetermined striking time should determine the brix of the massecuite (Jullienne,1984). The striking time is a good indication of the viscosity (fluidity) of the massecuite. A rapid rate of brixing will increase the crystal colour. Jullienne (1984) found that about 40% of the crystal colour was occluded in the final 30 minutes of the brixing stage, when the crystallisation rate was rapid. Lionnet (1998) found that the impurity transfer rate was totally dependent on the rate of sucrose crystallisation and the concentration of impurity in the feed liquor. Therefore, from a colour perspective, a very high brix in the pan and consequent dilution of the massecuite for mobility, is counterproductive. A rapid rate of brixing will also increases the chance of false grain formation, which has a negative effect on the purging efficiency of the centrifugal.
- The steam cycle should commence early, to heat the mother liquor and lower its viscosity, and the hot water should be around 80°C. The top covers of the centrifugal must be closed to avoid ambient air from entering the basket and cooling the massecuite.
- Even if raw sugar factories supply their own refineries, the granular quality of the crystals is very important for centrifugal operations. A sieve analysis must be conducted regularly and pan boiling techniques must be adjusted to produce a low CV and percentage fines below 30%. Action must be taken to lower the bagacillo content of A-massecuite.
- It is important that there is good communication between the centrifugal operator and the pan-boiler, and that the pan-boiler adjusts the massecuite properties to meet the target settings in the centrifugal, and not *vice versa*.
- A high level of ‘equipment sympathy’ is required to protect this expensive and critical equipment from vibration and damage. A long spin cycle must not be used to compensate for poor dryer performance. The long spin time will harden the sugar cake and make it difficult to plough the sugar. The dryer performance should be investigated and rectified.

References

Beckett J and Munsamy SS (1994). Experiences with processing very low purity cane. *Proc S Afr Sugar Technol Ass* 68: 101-104.

Booysen KC and Davis SB (2019). Colourant behaviour during sugarcane processing. *Proc S Afr Sugar Technol Ass* 92: 358-371.

Broadfoot R and Miller KF (1996). Fugalling characteristics of high-grade massecuites. *Proc Aust Soc Sugar Cane Technologists*: 350-360.

Genotelle J (1978). Expression de la viscosité des solutions sucrées. *Ind Aliment Agric* 95: 747-755.

Hedley EP (1937). The crystallisation of massecuites. *Proc S Afr Sugar Technol Ass* 11*:* 68-81.

Honig P (1959). Principles of Sugar Technology, Volume 2: Crystallisation. *Elsevier Publishing Company, Amsterdam.*

Grimwood C, Thewlis J and Thompson P (2002). Observations on centrifugal operations – Part 1. *International Sugar Journal* 104: 1248.

Grimwood C, Thewlis J and Thompson P (2003). Observations on centrifugal operations – Part 2. *International Sugar Journal* 105: 1253

Jullienne LMSA (1983). Washing sugar in batch A-centrifugals. *Proc S Afr Sugar Technol Ass* 56: 42-45.

Jullienne LMSA (1984). Exhaustion and colour investigations in A-massecuite. *Proc S Afr Sugar Technol Ass* 57: 42-46.

Lionnet GRE (1998). Impurity transfer rates during the crystallisation of sucrose. *Proc S Afr Sugar Technol Ass* 72: 261-268.

Naidoo S, Mncube F, Ndlovu V and Ninela M (2024). Improvements in sugar colour and boiling house recovery at the Maidstone mill. *Proc S Afr Sugar Technol Ass* 96: 264-271.

Ninela M and Rajoo N (2006). Practical steps taken at Tongaat-Hulett sugar factories to achieve low target purity difference. *Proc S Afr Sugar Technol Ass* 80: 448-461.

Please CP, Fowkes DP, Mason DP, Khalique CM, Hutchinson A and Rademeyer MC (2012). Liquid flow in a sugar centrifugal. *Report on Mathematics in Industry Study Group, South Africa Meeting, Africa Institute of Mathematical Studies, Muizenberg, January 2012.*

Rein P (2007). Cane Sugar Engineering. *Berlin. Vertrag Dr Albert Bartens KG:* 406-407

Rouillard EEA and Koenig (1980). The viscosity of molasses and massecuite. *Proc S Afr Sugar Technol Assoc* 54: 89-92.

Smith GT, Davis SB, Madho S and Achary M (2013). Eighty-eight reviews of the milling season in southern Africa (2012-13). *Proc S Afr Sugar Technol Ass* 86: 339-365.

Smith IA, Schumann GT and Walthew DC (2000). Some developments in floatation clarification. *Proc S Afr Sugar Technol Ass.*70: 263-266.

Shah S, Lokhat D and Peacock SD (2017). An investigation into the viscosity of C-massecuite using a pipeline viscometer. *Proc S Afr Sugar Technol Ass* 90: 339-365.

Watson JA and Nicol WM (1975). Raw cane sugar quality in relation to refining requirements. *Sugar Technol Rev* 3: 69-126.

OPERATIONAL PAPER

OPTIMISATION OF THE BACK-END OF A STAND-ALONE REFINERY

Dlamini EM[1], Maharaj N[2] and Rambakus Z[3]

Tongaat Hulett, Durban, South Africa

Ephraim.Dlamini@tongaat.com; Nishan.Maharaj@tongaat.com; Zyven.Rambakus@tongaat.com

Abstract

One of the advantages of a back-end refinery is the recycling of the final run-off back into the boiling house. In a stand-alone refinery, the final run-off is boiled further at the recovery station to recover the remaining sucrose. The performance of this recovery station affects the overall refinery yield. In the Huletts Refinery, the recovery house utilises a 3-boiling scheme to boil down the final run-off. The sugar from the first two boilings is sent to the main raw sugar melter, while the third boiling sugar is melted and recycled into the return syrup. The high colour in the first two boilings increases the colour-loading into the refinery. The third boiling sugar has a risk of both colour and ash recirculation, which will affect the performance of the refinery. Good manufacturing practices, plant modifications, automation and the repurposing of equipment are some of the steps that were taken to optimise the recovery house of the Huletts Refinery. This has resulted in an improved refinery yield, due to the reduction in the final molasses loss-on-melt.

Keywords: Recovery house, optimisation, refinery yield, molasses loss-on-melt

Introduction

The Huletts Refinery (Hulref) measures the overall performance by using the yield, unlike the overall recovery, which is used in sugar mills. The similarity of these two figures is the fact that molasses loss affects them both. The higher the loss, the lower is the yield or recovery, and vice versa. It is also common for the molasses loss to be the biggest loss, in both sets of factories. The main disadvantage of back-end refineries is the complexity of their performance calculations. Schorn (1995) mentioned some complexities when the Malelane sugar mill first separated the raw house and refinery into separate business units.

Compared to the back-end refineries, the stand-alone refinery carries with it the advantage of precise performance calculations. The reported molasses loss in Hulref is based purely on the recovery house performance, where the return syrup or Jet 4 from the white pan house is the only raw material. The optimised performance of the recovery house improves the refinery yield. Over and above dealing with the biggest loss (molasses), some other physical and chemical losses were addressed to improve the performance. This optimisation was done mainly through plant modifications, automation and improving the manufacturing practices.

Over the past few years, a lot of work has been done to improve the performance of the recovery house. Mncube *et al.* (2012) did exceptional work in this plant, which was evident from the improvement in its performance. However, this work was followed by the partial closure of the recovery house, due to some business dynamics, which resulted in the loss of skills. A poorly-performing recovery house affects not only the refinery yield, but also the throughput. It therefore

became imperative to turn this plant around. This paper reports on the practical steps that were taken to optimise the plant, as well as their respective impacts.

Team alignment

After the reopening of the recovery house, some manufacturing practices were not effective. This included both operations and maintenance. Finding the product on the floor had become a norm, either as a result of tank overflows or leaks. This had contributed massively to the ash and/or non-pol recirculation, especially in the third-crop station, where the concentration is high. When tackling this problem, it was very important to align the team members, because it involved a change in culture.

The cane-yard personnel and effluent operators in a sugar mill are often despondent because they feel isolated and not part of the main team ([1]Personal communication). This was the same feeling in the recovery house and a few of team members were verbal about being neglected ([2]Personal communication). In order to take the whole team on a journey of change, it was very important to communicate openly and honestly with them. A lot of verbal and written communications were used to effect a change of culture.

The 5S component of leam manufacturing ('Sort', 'Set', 'Shine', 'Standardise' and 'Sustain') was employed to address the issue of non-pol recirculation, as a result of the product on the floor. 'Sort' (the first S component) was simply communicated as 'no product on the floor'. Often, the sump that contained different products would be pumped into the third-crop station. Addressing the leaks and overflows ensured that everything goes where it is meant to go, which is the 'Set' component (the second S). The recovery house was washed from top to bottom, using high-pressure washing machines. After washing, the electrical department fixed the old lights and installed new ones. The whole plant must 'Shine', (the third 'S'). When the place is clean and shining, everyone notices what it is like. Everyone gets to know the minimum 'Standards' (the fourth 'S'), and no-one wants to let it get worse than that. Avoiding a drop in the 'Standards' leads to 'Sustainability' (the fifth 'S'), which is what happened in recovery house, and credit is given to both the maintenance and operations teams.

The repurposing of equipment

Mncube *et al.* (2012) clearly mention the recovery house pan sizes and boiling scheme as an original set-up. As mentioned earlier, a lot of work was done to improve the performance of the recovery house. Dlamini (2018) suggested the reallocation of the heating surface area in the pans ([3]unpublished data). The suggestion was to exchange the first and third-crop massecuite boiling from the original set-up, i.e. a bigger stirred pan to boil the first crop and small pans to boil the third crop. The reason was simply based on the improvement of the throughput. A pan equipped with a stirrer has a few advantages over an unstirred pan, one of which is capacity (Bachan & Webb, 1985).

This de-bottlenecking exercise was done within the maintenance budget, as it only required minor modifications on the pipe network. Feed pipes were altered for the small pans (A and B-pans) to change over from the return syrup feed to the second-crop molasses. In essence, these pans would change duty from the first-crop to the third-crop massecuite boiling. The D-pan, which was initially boiling the third-crop massecuite, would change to the first crop. The return syrup feed to

[1] Main author observed this from various mills in a SADC region.

[2] This was mentioned by a few recovery-house operators

[3] Internal Memo by EM Dlamini, Optimisation Engineer, Technology Group, Tongaat Hulett Sugar SA

this larger pan was already in place for high-purity graining; therefore, no modifications were required on the feed.

More work was required downstream of the pans to align the sugar outlets and molasses run-offs to the respective pan duty. The modification allows the first and second sugar to be combined, remelted and recycled into the main raw sugar melter. The third sugar is melted and recycled into the return syrup. All the run-off syrups are properly separated in a centrifugal station and have dedicated tanks, as per the original set-up.

Changes in the pan duty improved the throughput of the recovery house, which was evident in the return syrup intake. Prior to this modification, the main pan house would often stop pumping the return syrup into the recovery house, due to a full return-syrup tank. An accumulation of return syrup in the white pan house would also result in a throughput reduction for the whole refinery.

Decluttering of the first and second crop feed lines into pans

One of the recovery pan-boilers pointed out the difficulty of having to batch feed the second- and third-crop massecuite pans ([4]Personal communication). It was established that when the pan feed modification was done, the first- and second-crop syrups were tied-in on a common line. In order to avoid mixing these materials, the pans were fed in batches. There was a huge risk of mixing the boilings, due to human error, which would affect the purity profile of the whole recovery house. This needed urgent attention. Figures 1 and 2 below show the common feed and the modification, respectively.

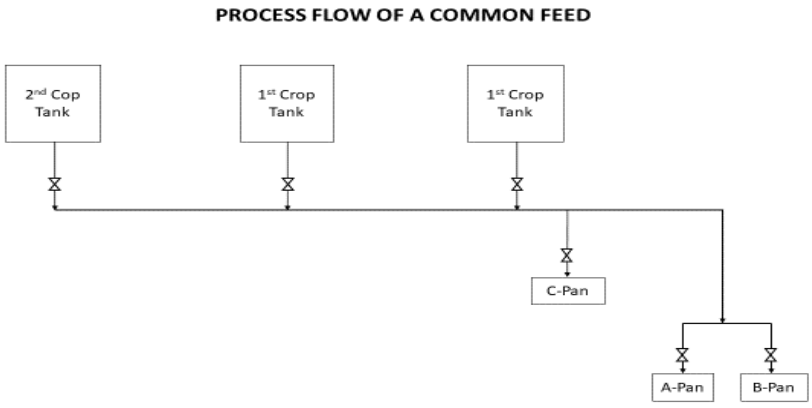


Figure 1. Feed system on a common line

[4] Mark Saunders Recovery House Pan-boiler

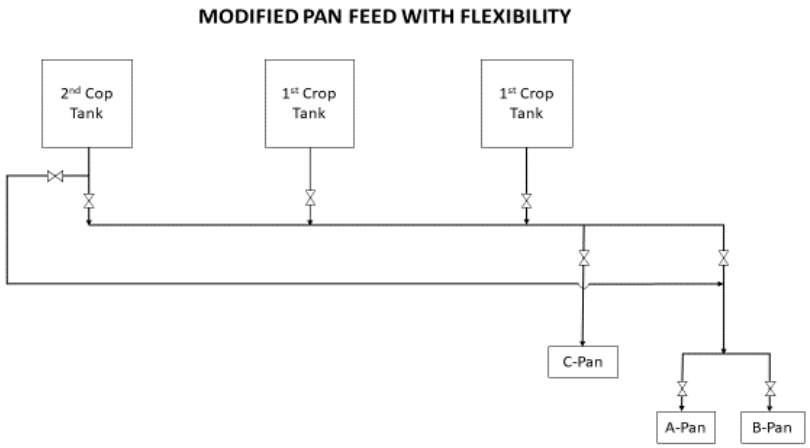


Figure 2. Modified feed system

After improvements on the first-crop boiling, the next bottleneck was the batch feeding of the second- and third-crop pans. The modification significantly improved the overall throughput in the recovery house, and the flexibility of changing the boilings amongst these pans was left in place.

Improvements on HTM production

Other than being a normal boiling house, the recovery house often makes High-Test Molasses (HTM) (Mncube *et al.*, 2012). However, this product is not regularly produced and it is made only on request. The preparation of HTM requires a stirred pan. This means taking a big pan out of its normal duty of boiling massecuite. In the past, it used to take very long to make a single batch of HTM. At times, it would take up to twenty hours. An assessment of this issue revealed that many problems were just related to the pumps, as these were undersized for this duty. It would sometimes take well over ten hours to pump a required amount into the pan. Preparing a batch of HTM suppressed the already stretched boiling capacity.

Inefficiencies in this process could not be accommodated. The pumps had already been stripped and serviced, but there had been no improvement. One pump was then upgraded by increasing the impeller diameter and motor size. No civil work was required. The upgraded pump now takes just below two hours to deliver the raw material, which is a significant improvement from a process that used to take almost two shifts.

It was also established that other delays involved the sampling and calculation of the ingredients. The pan-boilers were required to ‘break’ the pan vacuum, in order to be able to take samples and restart the pan after sampling. This also had a risk of entraining the pan, when restarting. Sampling is done at least twice for a batch of HTM. To address this delay, D-pan slurry funnel was slightly modified to allow for a double-valve system. That has enabled the sampling of HTM at any point during boiling, without having to ‘break’ the vacuum. Previously, the calculation of the ingredients was manual, by using a sophisticated formula; however, the calculation has since been computerised, with quicker results.

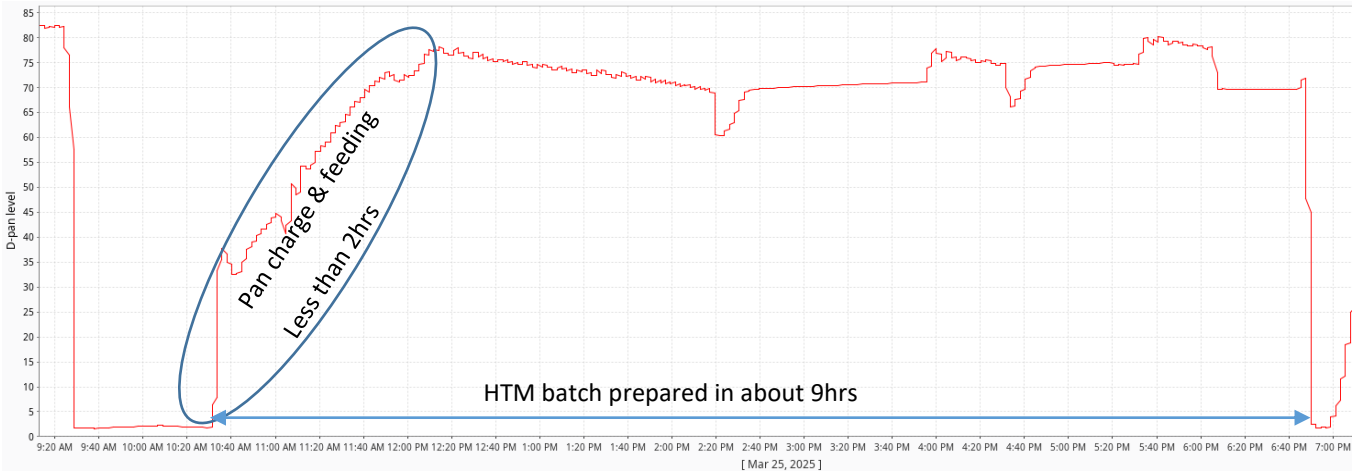


Figure 3. Improved pan cycle for HTM preparation

Figure 3 above shows the improved pan cycle for HTM production. The pan feed has been reduced to less than two hours, by using the upgraded pump. With these improvements, each batch can now be done in eight hours, as opposed to the previous 18-20 hours.

Pan control system upgrade

The recovery house was using a stand-alone system for the pan control. The system had difficulty with automation, data logging, general troubleshooting, etc. The unavailability of spares was also a problem and this was a risk to the plant. The system was therefore changed to DCS. The new system enabled the addition of more control loops. More points that highlight the issues with the previous system versus the new are mentioned in Appendix A ([5]Personal communication).

This system upgrade allowed for the full automation of the D-pan boiling cycle, with a view to implementing it on all pans. A new pan curve was developed by using a quadratic equation. The curve controls the brix and the level during the pan feeding stage and the brix-to-strike part. The automation has taken away the risk of human judgement and improved the consistency and quality of the massecuite. One cannot overemphasise the importance of consistent pan-boiling. There is enough literature on the work that has been done on pans over the years, and the dominating reasons have been either to achieve a consistent performance or to improve the energy. Figures 4 and 5 below show the difference in the boiling trends, before and after automation.

[5] Thanda Msane, Instrument Trainee Engineer at Hulref

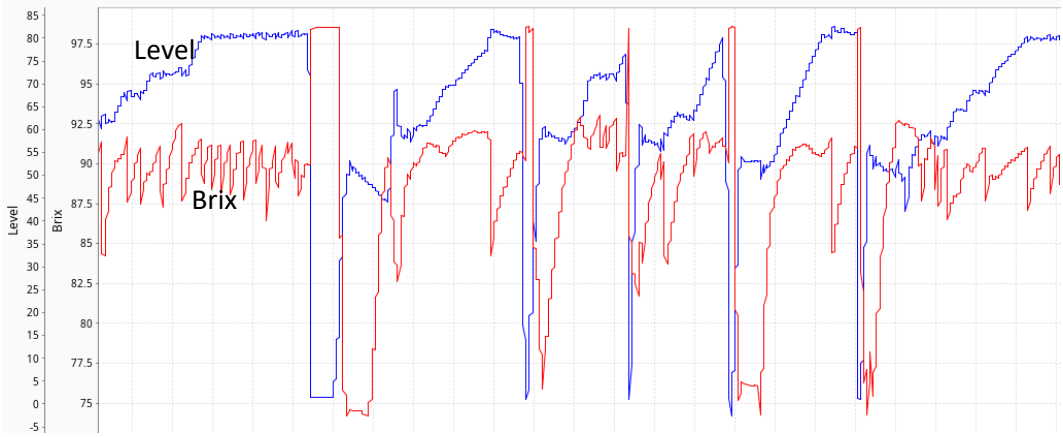


Figure 4. Brix and level trends before automation

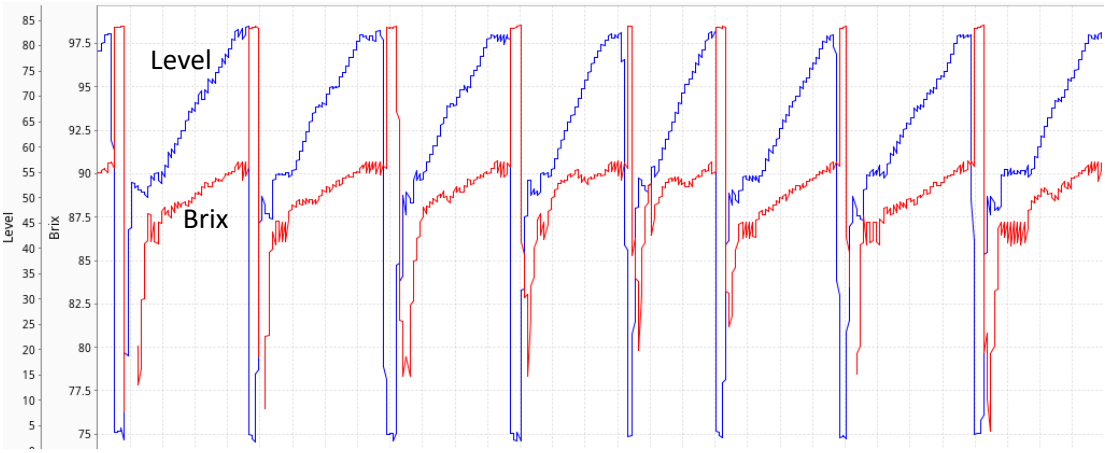


Figure 5. Brix and level trends after automation

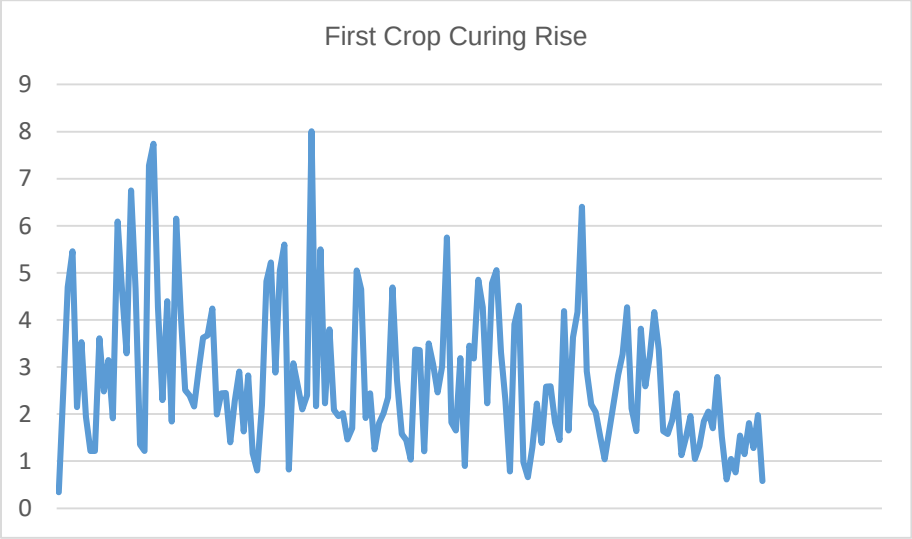


Figure 6. First crop curing rise for 2024/25 season

Figure 6 above illustrates the curing rise in the first-crop for the entire 2024/25 season. There is a noticeable drop in the curing rise towards the end of the season, which coincides with pan automation.

Linking the small crystallisers

Third-crop cooling crystallisation was done in batches, by using four crystallisers. Over the years, batch crystallisers have been replaced by the continuous type (Rein, 2006); however, the batch-type vessels had remained at Hulref. Rein (2006) mentions the disadvantages of batch crystallisers, one of which is the increased labour requirements. This operation was found to be labour-intensive and it was risky, in terms of safety. In addition, curing from these vessels followed a first-in, first-out method which was based on operator manual records. These records were not always accurate, which would affect the massecuite retention time and therefore, the exhaustion. Massecuite spillage was another problem with this type of operation. It was therefore decided to link these crystallisers and convert them into a continuous type.

These crystallisers are installed very close to each other, with a gap of about 300 mm. This made it easier to cut windows and installed overflow chutes, in order to link the flow of massecuite from the receiving crystalliser to the next one. The chutes in each crystalliser (inlet and outlet) have different depths, to allow a gravity flow from crystalliser to crystalliser. Baffle plates were also installed in the centre of each crystalliser, to force a plug-flow of the massecuite. This modification is illustrated by Figures 6, 7 and 8 below:

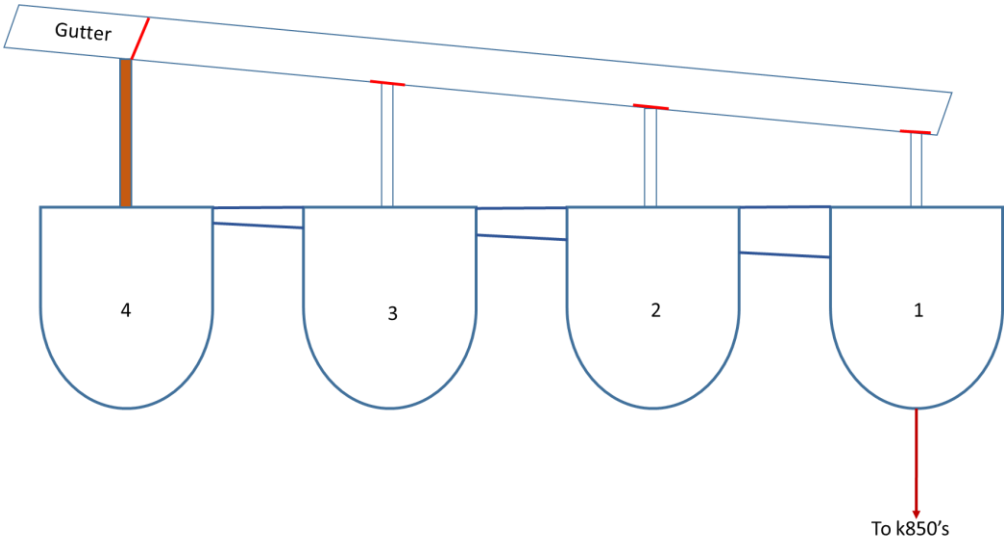


Figure 7. Front view of crystalliser

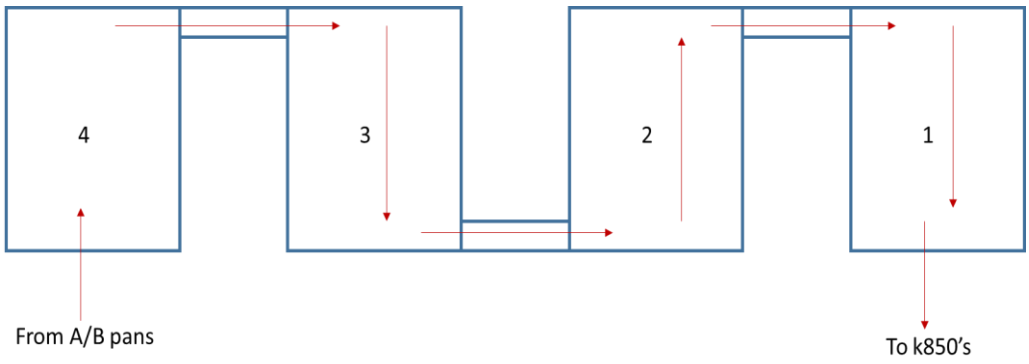


Figure 8. Top view of crystallisers

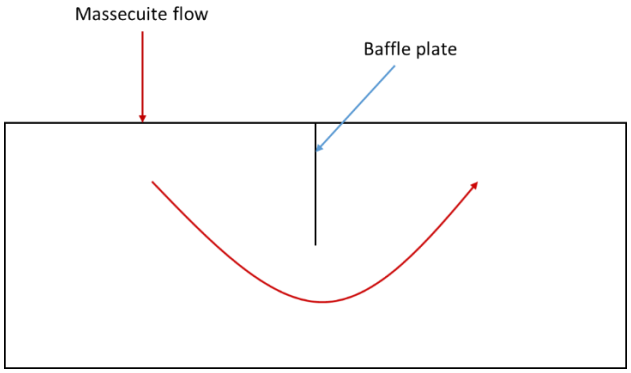


Figure 9. Side view of the crystalliser

Other interventions

Molasses seals

The centrifugation process utilises BMA K850 machines across all crops. These machines have rubber seals just under the tip of the basket, to eliminate the escape of molasses into the sugar chamber. As expected, the rubber wears away and requires replacement. Regular inspections of these seals need to be done, and they must be replaced as and when required. The chamber itself also needs to be inspected for leaks. Molasses escape onto the sugar not only increases the colour, but it also comes with ash recirculation, especially on the third crop. The practice of seal inspection and replacement has since been put in place, through scheduled maintenance.

Centrifugal screens open area

First-and second-crop massecuite curing was done with a 14% Open area (OP) screen whilst the third crop was done with a 7% screen. When investigating the difference on both screens, it was established that the difference was the slot length. 7% screens have a slot length of 2.67 mm versus 1.82 mm for 14% screens. The width is the same, at 0.06 mm. However, the 14% screen has a greater number of slots, and hence a higher open area. The test was then conducted by installing different screens in two machines and curing the same massecuite. Wash water was

shut in both machines, whenever molasses sampling took place. A 14%-screen produced high brix molasses and the purity was a unit lower than its counterpart. The 7%-OA screen has since been discontinued and only the 14% screen is used.

Centrifugal screen checks

In raw sugar mills, screen changes are usually time-based. This practice might lead to waste in the recovery house operations, since the machines are alternated. The run times are not equal amongst these machines. Routine inspections are therefore paramount. Previously, inspections were conducted by the maintenance staff only, but now the operational staff have been trained to check the screens. The screens can now be checked in between the pan strikes.

Slurry containers

A few common mistakes are made with the slurry operations, i.e. from preparation, to handling and injecting it into the pan. All of these can easily affect the quality of the slurry. The good work done on pans could be in vain, if the slurry quality is not kept constant. In this case, the prepared slurry was decanted into 20-litre containers. Pan-boilers would then take the required amount for graining from the 20-litre container after ‘shaking’ it. The effectiveness of shaking of a 20-litre container is subjective to each Pan-boiler, and therefore the possibility of inconsistent quality of slurry is high. These containers were removed and replaced with 5-litre containers which are easy to handle. An improvement was evident, even in the white-pan house, as the MA and CV became more consistent. These parameters are not measured in the sugar from the recovery house; however, a consistency in the grain size was witnessed after the intervention on slurry handling.

Summary of the performance

The overall performance of the refinery had once been high in the past. This performance had dropped over the years, for many industrial reasons. However, Hulref needed to adjust internally, in order to absorb the external factors. A few other interventions were carried out across the factory to improve the overall yield. There is no doubt that the improved performance of the recovery house contributed to the refinery yield. Table 1 below shows a 3-year history of the recovery house performance.

Table 1. A 3-year history of the recovery house performance

Year	2022/23	2023/24	2024/25
Molasses%melt	4.19	2.94	2.50
Molasses Purity	62.94	60.35	60.55
Pol loss%melt	2.01	1.41	1.21

The drop in molasses percentage on melt translates into the higher exhaustions achieved in the recovery house. The pol loss, as a percentage in melt, also confirms a greater recovery of sugar. Over the years, the molasses purity has dropped from the mid-60s to just below 61%. This is not abnormal for a stand-alone refinery. Moodley *et al.* (1996) specified the difficulties involved in reducing the refinery molasses to below 74%.

Furthermore, the visible change in the plant is evident e.g. the additional storage of the return syrup in tanks that were allocated for other products (invert cisterns), as a result of the tank filling up, has been eliminated. Only allocated factory tanks are now used. In addition, there has been a notable drop in the number of centrifugal machines that are used. The second and third crops are consistently using one machine each, and the first crop uses the second machine intermittently. Dry floors are also evidence of a well-performing plant. The performance of the recovery house has improved, mainly based on the back-to-basics approach mentioned by Dlamini (2016).

Conclusion

Turning around the performance of a plant is not a one-man-show, but it requires the whole team to be involved. This was also not just a short-term project, but a long-term project, with short- and medium-term milestones. Each milestone that is reached does not translate into an overall achievement, but there is a continuous improvement. All milestones are celebrated to ensure that the team remains motivated.

Acknowledgements

The authors of this paper would like to thank the management of Tongaat Hulett Sugar South Africa for approving this work for publication. Many people were involved in this work. The authors also thank all teams involved in this work i.e. maintenance, laboratory and operations (mainly Senzo Gwabuzela and Mark Saunders). Their support has been amazing.

References

Bachan L and Webb B (1985). Assessment of a stirrer installed in a low-grade pan at Noodsberg. *Proc S Afr Sug Technol Ass* 85: 39-42.

Dlamini EM. (2016). Vicious cycles in factory operations. *Proc S Afr Sug Technol Ass* 89: 416-423.

Mncube FS, Rambukus Z and Muzzell D (2012). Optimisation of recovery house operation at the Hulett Refinery. *Proc S Afr Sug Technol Ass* 85: 378-387.

Moodley M, Schorn PM and Singh I (1996). Off-crop refining at Malelane. *Proc S Afr Sug Technol Ass* 70: 189-194.

Rein P (2006). *Cane Sugar Engineering*. Verlag Dr A Bartens KG, Berlin, Germany.

Schorn PM (1995). The splitting of Malelane factory into separate raw-house and refining operations. *Proc S Afr Sug Technol Ass:* 177-180.

Appendix A

Summary of points supporting DCS upgrade

Before DCS Automation

- Each Yokogawa controller operated independently, with no central monitoring or coordinated control of pans.
- It was difficult to apply advanced control mechanisms such as interlocking, sequencing, or batch management.
- There was no centralized historical data logging or trending for crucial process parameters including level, brix, vacuum, and temperature.
- Troubleshooting process issues was difficult due to a lack of recorded operational history.
- Operators were required to monitor local indications and manually adjust setpoints and valves.
- Increased likelihood of human error and delayed responsiveness to process disruptions.
- Operators needed to be physically present at each pan's controller or pneumatic panel to make adjustments.
- Inefficient personnel use, particularly during crucial tasks such as pan boiling or discharge.
- Pneumatic control lacked accurate, automated timing and sequencing which affected product quality and compromised safety.

After automation

- All pans and loops are now controlled and monitored using a single control room interface.
- Improves pan-operational coordination, optimizes workforce usage, and enables faster response to process conditions.
- Enhances process consistency, product quality, and operational safety.
- Continuously record vital parameters for trending, analysis, and troubleshooting.
- Identifies process irregularities early and supports performance optimization.
- Automated setpoint control and valve actuation reduce human error.
- Operators prioritize supervision and exception management over routine adjustments.
- Centralized alarm system provides prioritizing, logging, and operator instruction.
- Improved situational awareness under normal and abnormal settings.
- The DCS console allows operators to remotely control pans, alter setpoints, and acknowledge alarms.
- Automated sequences, such as door discharge, can reduce operating risks.
- Interlocks and permissive controls can avoid harmful operations, (e.g. opening a pan door under vacuum).
- Integrated control and data availability facilitate optimization and energy-saving strategies.

POSTER SUMMARY

DESIGN AND OPTIMISATION OF A BATCH REACTOR FOR THE DIGESTION STAGE IN THE PRODUCTION OF POTASSIUM SULPHATE FROM STILLAGE AT A PILOT SCALE

Nyemba, T[1], Mutanda, P[2], Rambwawasvika, H[3] and Mutatu, W [3]

[1]National University of Science and Technology, PO Box 939, Ascot, Bulawayo
[2]Hippo Valley Estates Mill, PO Box 1, Chiredzi
[3]Zimbabwe Sugar Association Experiment Station, Private Bag 7006, Chiredzi

tnyemba35@gmail.com, PardonSimbarashe.Mutanda@tongaat.com, rambwawasvika2016@gmail.com, wmutatu@zsaes.org.zw

Abstract

Stillage is a liquid waste that is released during the production of ethanol, and it contains an appreciable amount of potassium. Preliminary laboratory-scale investigations indicated the technical viability of recovering potassium from ethanol stillage. However, directly scaling up this process for commercial deployment involves various hurdles and uncertainties that must be addressed further. This study aimed to design and optimise a batch reactor for the digestion stage in the production of potassium sulphate. The digested stillage had its physical properties measured, as they were important for the design of the reactor and for the selection of the materials needed for construction. The mass of potassium sulphate that was expected to be produced at this pilot scale was 10 kg. For this mass of potassium sulphate, about 612 L of stillage was required to be mixed with 30.6 L of 98% sulphuric acid. The reaction between the stillage and sulphuric acid was exothermic, with toxic fumes being released. A wet scrubber was also designed to manage the amount of toxic fumes released into the atmosphere. Stainless steel 316 was the material selected for the reactor because of its resistance to corrosion and its lower cost, when compared to the other materials with a high corrosion resistance. Calculations were carried out to determine the dimensions of the reactor that could accommodate the reagents safely. The volume of the reactor was 917 L, with a height of 1.3 m and an inside diameter of 1 m.

Keywords: Stillage, design, optimisation, reactor, potassium, digestion

POSTER SUMMARY

THE SMRI FACTORY LABORATORY CERTIFICATION SCHEME: ENSURING CREDIBLE AND RELIABLE LABORATORY RESULTS

Ngema M, Naidoo Y, Mbuyazi M and Pillay V

Sugar Milling Research Institute NPC, University of KwaZulu-Natal, Durban, 4041, South Africa

mngema@smri.org, lnaidoo@smri.org, mmbuyazi@smri.org, vpillay@smri.org

Abstract

The Board of the Sugar Milling Research Institute NPC (SMRI) highlighted an urgent need for the SMRI to consider how it could best extend its influence to help improve the performance of factory-based laboratories. The SMRI Factory Laboratory Certification Scheme (Scheme) was developed to address this need. The primary objective of the Scheme is to ensure confidence in the analytical results generated by its laboratories, and to produce valid and credible results to support the factory control operations.

The laboratories will achieve certification by demonstrating their competence in various areas. These will be assessed by the SMRI by means of the following:

- audits of the laboratory and factory figure procedures.
- training; and
- ongoing competency assessments.

This poster describes the process of the cyclic three-year Scheme, which consists of a full laboratory and factory figure audit during the first year, as well as two surveillance audits during the two subsequent years. Parallel to the audits, the laboratory analysts and managers undergo two training programmes, and the ongoing competence of the mill laboratory staff is assessed. The poster highlights the benefits, the major findings and the challenges experienced during the first year of the Scheme's inception in 2024.

Keywords: Audit, training, laboratory certification, factory control, ongoing competency assessment

OPERATIONAL PAPER

THE SMRI FACTORY IMPROVEMENT INITIATIVE

Mbuyazi M[1], Ndinisa NV[1] and Schorn P[1]

[1]Sugar Milling Research Institute NPC, c/o University of KwaZulu-Natal, Durban, South Africa

mmbuyazi@smri.org, nndinisa@smri.org, pschorn@smri.org

Abstract

Due to the declining trend in the recovery performance of the South African (SA) sugar factories, the Sugar Milling Research Institute NPC (SMRI) implemented a strategy for assisting factories by identifying areas of opportunity to focus on and to provide recommendations for, how factories could return to the recommended best practices. The factory improvement initiative was conducted across the 2022/23 to 2024/25 seasons. It started with desktop audits, which identified the possible areas for improvement, and these were discussed with the factories via on-line meetings, which was followed by the SMRI team visiting the factories.

This paper discusses the key areas of the operations that were assessed for performance improvements in the various factories. The paper is limited to the deviations from best practice that were most common across the industry, in the different sections, namely: extraction, clarification, mud filtration, evaporation and pan house. The recommendations that were given to the various factories are provided in this paper for shared learning across the entire industry.

The recent performance trends show that there has been an improvement in key performance indicators, such as the overall recovery, extraction, undetermined loss, and target purity difference from 2022/23 to 2024/25. Whilst the SMRI is not claiming sole responsibility for the improvement in performance, this intervention is believed to have had a positive impact on the factory operations.

***Keywords*:** factory, improvement, best practice, intervention, recoveries, financial benefit

Introduction

Historical data shows that the average SA sugar mill performance has declined since the 2006/07 crushing season, and alarming levels were recorded in 2021/22. In order to assess the needs of the SMRI members i.e., the SA sugar mills, online surveys were completed by industry stakeholders, and strategic meetings were held with the leadership of all the SA sugar companies. The loss of technical skills, the inadequate maintenance of equipment, the increasing energy costs, budget constraints and climate change challenges were among the cited causes of the poor performance in the mills. A collective responsibility was agreed upon to address this decline and to improve the sustainability of the sugar industry. It was acknowledged that the sugar companies previously had sizeable technical support teams and therefore, the SMRI had been encouraged to focus its efforts on creating novel technologies and opportunities to bring about step-changes in the industry. However, it became apparent that there was an urgent need for the SMRI to assist the sugar factories to improve their technical performance. This led to the birth of an initial three-year intervention, which saw the SMRI refocusing its resources, in order to fulfil the objective of assisting factories to improve their performance and to recover more saleable sugar.

Methodology

The implementation of the SMRI factory improvement initiative was rolled out in the 2022/23 season and started with desktop study exercises and analyses of factory performance. These entailed the use of data diagnostics to identify the key focus areas (the top five bottlenecks) at each of the 12 SA sugar milling factories. Factory performance data for the past 10 years for each factory was used, and key performance parameters such as extraction, Boiling House Recovery (BHR), Overall Recovery (OR), and Undetermined Loss (UDL) were assessed. These were compared and assessed by taking into account the previous season's performance, the factory's benchmark standard, which was the factory's 10-year best performance, and the industry's average performance over the same period. The major areas of poor performance were then identified from this analysis, and the SMRI team engaged with each factory to share the outcomes of the desktop analysis. Based on the identified areas of concern, the SMRI and the factory leadership then agreed on which areas to focus their attention on and how to best support the given factory. This was followed by a physical visit to each of the mills by a team of SMRI experts on various subjects. Technical discussions took place during the visits, and detailed technical reports containing observations, proposed action plans, and short and long-term recommendations to facilitate the improvements were sent to the mills after the visits. On occasions, and as a result of identifying opportunities for improvement during the mill visits, some mills commissioned the SMRI to conduct additional consulting work in order to assist in the identified focus areas. As a way of following up on the progress and action items for improvement, an update performance review (follow-up audit) was done towards the end of the milling season for each mill. This showed the mills how they had performed throughout the season, compared to the rest of the industry and their previous season's performance. This paper discusses the most common themes that emerged across the 12 SA factories in the different sections, namely: extraction, clarification, mud filtration, evaporation, A-station and C-station. The observations that were made during the factory visits and the recommendations given for improvement are highlighted.

Improvements observed since the intervention

The Mixed Juice (MJ) purity trend depicted in Figure 1, shows that the cane quality was somewhat stable from 2017/18 to 2024/25, whilst the industry Overall Recovery (OR) performance had declined from the 2018/19 to 2021/22 season, which suggests that the decline in recoveries was mostly associated with suboptimal factory operations. However, since 2022/23, the industry's downward performance trend has reversed. The average OR has improved from 80.78% in 2021/22 to 82.41% in 2024/25, which represents 1.63% units of improvement, with OR having improved in 8 out of the 12 factories. Whilst the overall industry trends are showing improvement, some mills improved much more than others and even attained their 10-year best performance. Figure 2 shows that extraction, accompanied by a decrease in imbibition, continued to decrease in 2022/23, but that it has since started to improve, with extraction increasing by 0.23 percentage units from 2022/23 to 2024/25, and imbibition increasing from 292 to 313% over the same period. However, it should be noted that the SA factories focused more on maximising throughput than extraction during the 2022/23 and 2023/24 seasons because of the large amount of carryover cane that required processing.

The trends of the losses, as shown in Figure 3, have also started improving, which is encouraging. The Undetermined Loss (UDL) sucrose in cane decreased from 4.39% in 2021/22 to 3.22% in 2024/25, which represents 1.17% units of improvement. The UDL improved in 9 out of the 12 factories. The TPD and losses to final molasses were lagging behind the other parameters, as they were still increasing in 2022/23. However, it is encouraging to note that the losses to final molasses and TPD decreased from 11.42% and

10.2% in 2022/23 to 10.56 and 8.1% in 2024/25, respectively, and it is hoped that this downward trend will continue.

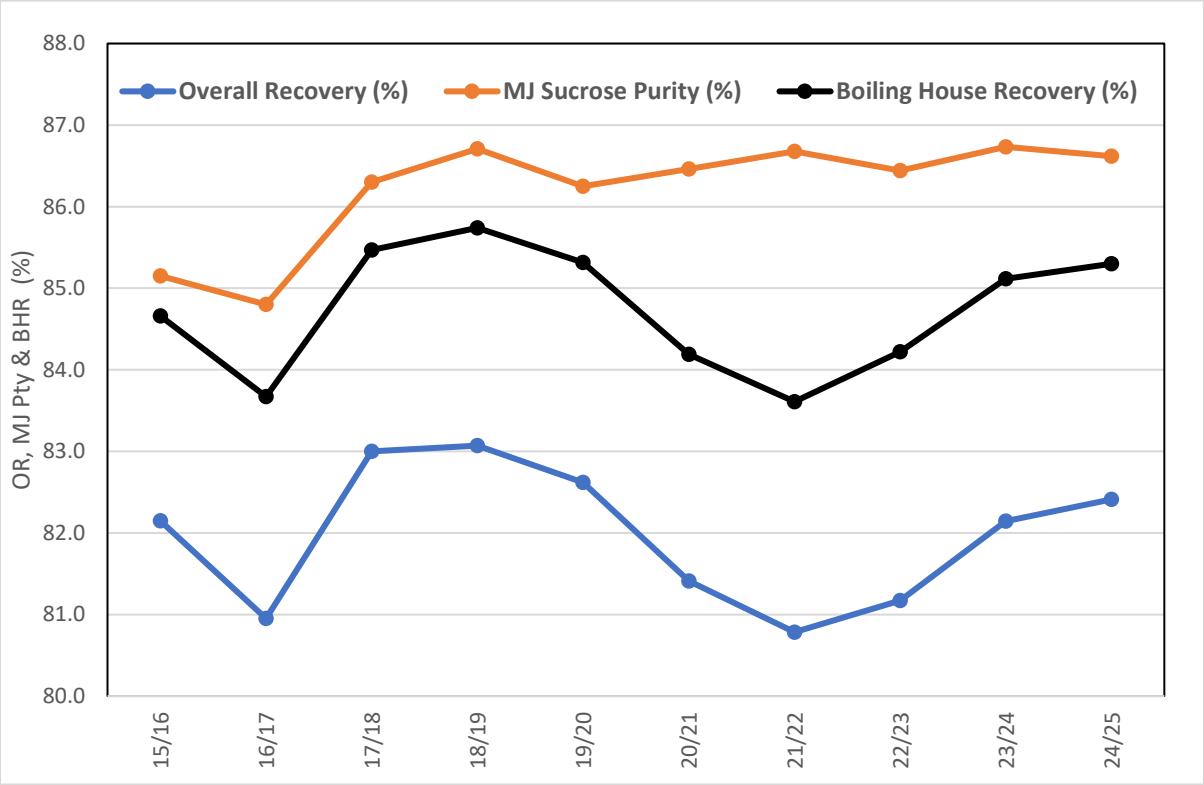


Figure 1. Recent trends of Mixed Juice Purity Boiling House Recovery and Overall Recovery

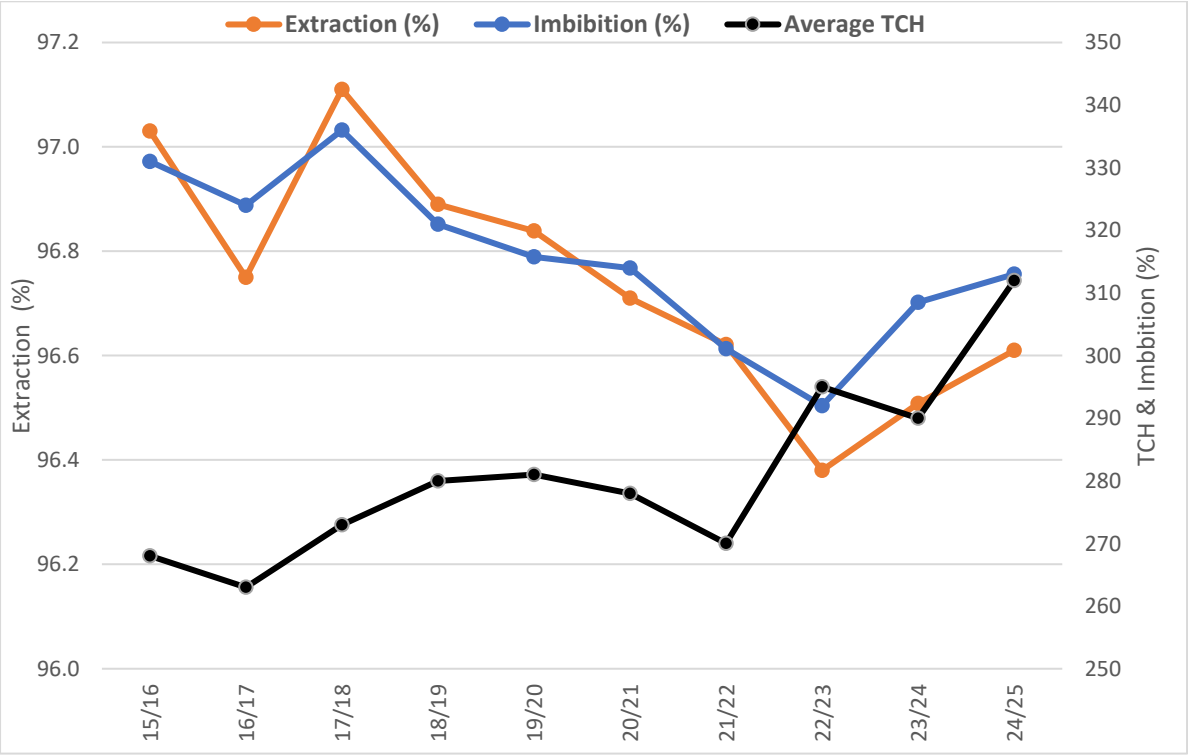


Figure 2. Trends of average TCH, Extraction and Imbibition

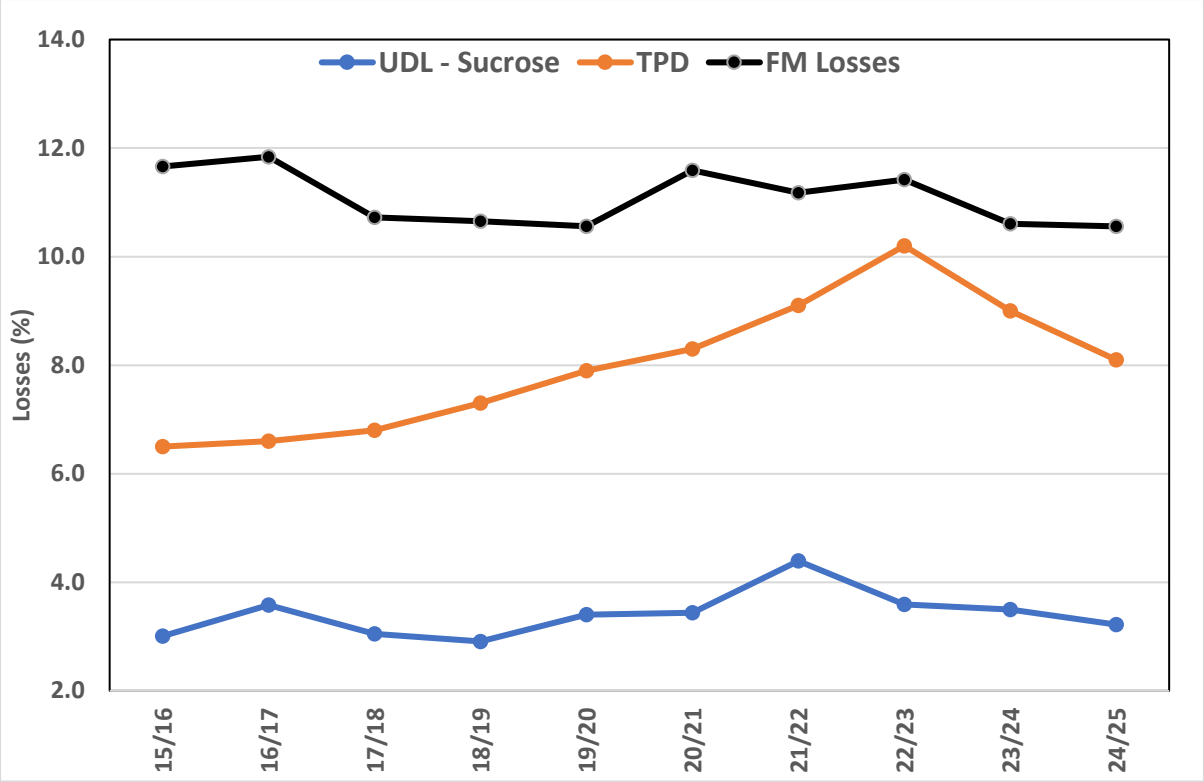


Figure 3. Recent trends of Undetermined Loss, Target Purity Difference, and losses to Final Molasses

The SMRI factory improvement initiative has been running from 2022/23 to 2024/25. The overall aim of this initiative was to assist factories to return to their basic operational practices. Whilst there is evidence that the average technical factory performance of the industry improved over this period, and some factories by a marked amount, it is difficult to gauge how much of the realised improvement in factory performance can be credited to the interventions of the SMRI.

The observations made during the factory visits gave rise to SMRI conducting further investigative work, e.g. evaporator control strategy reviews, continuous pan evaluation, tracer tests, evaporator fouling investigations, diffuser assessments, and factory speed profiling on a contract consulting basis, which no doubt contributed to the improved performance of the factories.

Findings from factory visits and discussions

Extraction

Although the cane throughput and energy management initiatives are the key contributory factors to the reduced extraction performance industry-wide, there are other fundamental areas of operation that the factories can address to obtain better extraction results. Extraction performance, in this context, was limited to diffuser operations where the observations were made. The industry 2024/25 season extraction was 96.61%, with the imbibition % fibre at 313%, an improvement from the 10-year average value of 96.38% and 292 imbibition % fibre. The SMRI team identified the top five most common parameters the factories could rectify to optimise the extraction performance. These are: (1) the low imbibition quantity, (2) the out-of-service bed screws, (3) the low diffuser temperature, (4) the uneven bed level and degree of

bed saturation, and (5) the poor diffuser hygiene. In addition, cane preparation showed mixed performance patterns, where some factories did better than others. It was encouraging to observe the Brix profiles being measured throughout the industry, although these were not being used as an effective monitoring tool.

Low imbibition quantity

Imbibition levels as low as 216% on fibre were recorded at the mills, and this was driven by the 'crush rate is king' strategy. The high crush rates, meeting cane budgets, and completing the available crop took precedence over performance. In 2022/23 and 2023/24, this was more pertinent because of the high levels of carryover cane. If the juice flows are too high or tank levels are high, the imbibition % fibre is generally reduced. Other reasons for reduced imbibition are energy-related. Meadows (2022) recommends a reasonable imbibition value of 300% on fibre when designing a diffuser, and typical values are in the 300% to 375% range in southern Africa. The higher the quantity of imbibition water added, the higher the extraction, as shown in Figure 2.

Malfunctioning bed screws

Frequently, fewer than 50% of the bed lifting screws were found to be in operation during the factory visits. Bed screws play a vital role in preventing the compaction and blinding of the cane bed, and they assist in juice percolation and must therefore be operational. Typically, five out of a set of 11 lifting screws were operational in the mills, the rest of the screws were either completely removed or tilted out of the bed, due to a pin having sheared. It was a usual occurrence to find that all the bed screws, even in the second set, were not working in the factories. The typical condition of the bed screws observed at the factories is shown in Figure 4.



Figure 4. The state of a partly out-of-service set of bed screws, which was a common observation in factories

One of the challenges experienced by the mills was the steam leaks, which prevented maintenance from taking place on the bed screws while the diffusers were in operation (Figure 5). The necessity for bed screws to be lifted out of the bed when a shear pin breaks, makes complete sealing difficult. Ensuring that such steam leaks are repaired during stop days would assist in avoiding the inevitable loss in extraction, due to bed screws being out of action

for long periods. However, it is acknowledged that there were a few mills in which a fair number of bed screws (over 60%) were operational.



Figure 5. A representation of how steam leaks prevented maintenance from being done on the screws, while the diffuser is in operation

Low diffuser temperature

At most mills, the overall diffuser temperature profile was low, with the observed juice stage temperatures averaging approximately 66°C (Figure 6), thus rendering the diffuser susceptible to microbiological activity and reducing its extraction potential. If diffuser temperatures are allowed to drop below 75°C, sucrose loss due to the activity of thermophiles becomes significant (Meadows, 2022). The target temperature to be maintained throughout the diffuser stages is in the range of 80-85°C, with a Draft Juice (DJ) temperature of approximately 65°C. Experience with different diffuser temperatures has confirmed that temperatures higher than this lead to a higher juice colour (Rein, 1995). Even so, it is not considered feasible to operate diffusers at lower temperatures, as losses under these conditions can be severe (Rein,1995). Whilst Scalding Juice (SJ) temperatures are meant to be more than 90°C to heat the cane sufficiently as it enters the diffuser, temperatures ranging between 76-88ºC were observed. Low steam pressure, due to evaporator-related challenges, was a common cause.

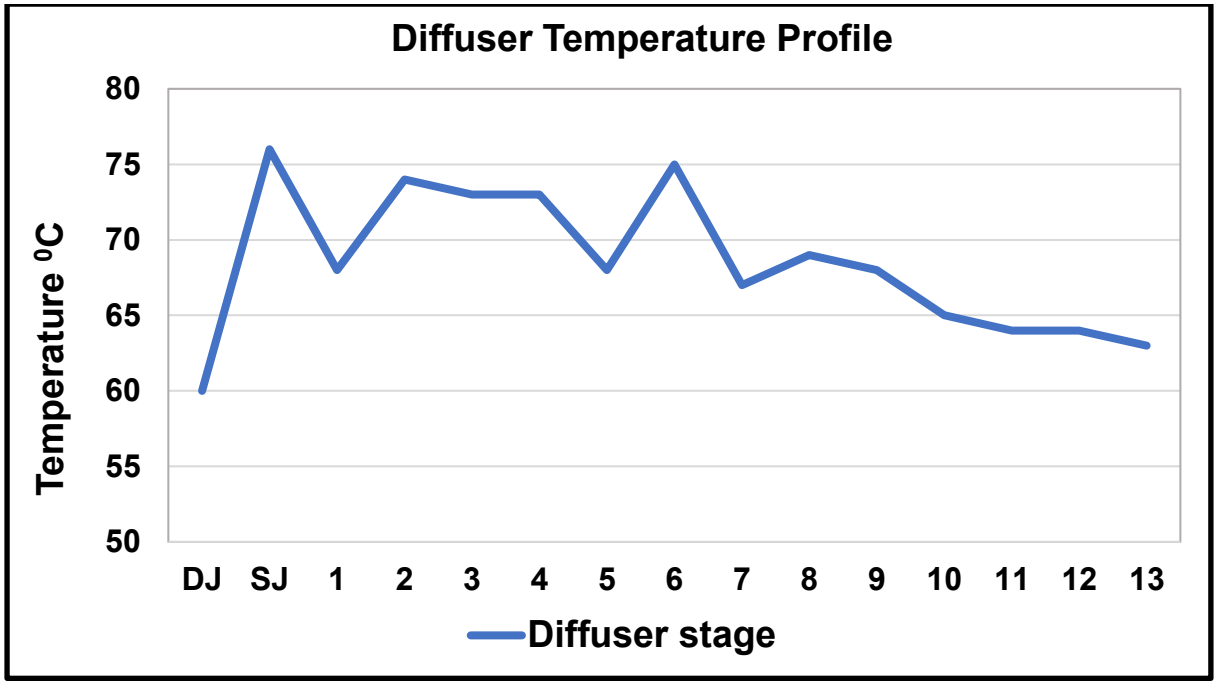


Figure 6. Profile showing a poorly-controlled diffuser temperature, which was typically seen in most factories

Uneven bed and juice level

An uneven bed level across, and along, the length of the diffuser was a common observation in the diffusers throughout the industry. Uneven beds affect the degree of saturation within the bed. The stages observed were either too dry or flooded in the same diffuser. A diffuser bed height should be maintained at a consistent level, and should, in every way possible, be maintained above 1.6 m to increase residence time and extraction. The inconsistency in bed levels, as observed in a factory, is shown in Figure 7.



Figure 7. A combination of photographs taken of one diffuser, showing uneven bed levels with flooded and dry beds, as commonly seen during the visits

In instances where a factory's target bed height is 1.4 m, because of design limitations, the mechanical indicator displayed or diffuser markings indicated even lower levels of 1.2 m across the width of the diffuser. Flooding destroys the Brix profile, whilst a low level of saturation/dry bed reduces extraction. The routine flushing of spray nozzles during stop-days, the checking of stage saturation, and the adjustment of diffuser sprays during operations are recommended. Adjusting diffuser sprays during operations, as recommended by Meadows (2022), helps to advance the spray positions if flooding occurs, and it retards them if the bed is too dry. However, most of the diffusers that were observed did not have adjustable sprays.

Poor diffuser hygiene

Diffuser hygiene is an overlooked best practice driver for good extraction and, as such, is often placed at the bottom of the priority list of where improved performance is sought. This is a mistake, as sucrose loss under these conditions is inevitable. The control of losses, due to lactic acid-producing bacteria, involves keeping the diffuser as clean as possible. The common poor hygiene observations, as shown in Figure 8, included leaking stage pump glands, leaking juice pipes and diffuser troughs, and fermenting sumps in the diffuser bunded area that are left unemptied for long periods. It is important to return the juice to the diffuser as soon as it spills on the floor and to preserve the quality of juice in the sumps.



Figure 8. Juice leak from a front-end pump indicated by the red ring. Poor diffuser hygiene observed in factories during the visits

Cane preparation

It is widely known that cane preparation is the most important variable affecting diffuser extraction and is easily within the factory's control. Preparation determines the 'extractability' of the cane by determining how available the sucrose-containing juice is to the counter-current washing and leaching process that takes place in a diffuser (Meadows, 2022). The better the preparation, the better the extraction. Evidence of coarsely-prepared cane, with large chunks of poorly-shredded cane, was seen in some factories. Meanwhile, reasonably well-prepared long-fibre cane with no apparent unshredded portions of the stalks were observed in other

factories. Figures 9 and 10 depict these differences in the observations made in different factories.



Figure 9. Poorly prepared cane at two different factories



Figure 10. Reasonably well-prepared cane at two different factories

The rapid wearing of shredder hammers, which results in poorly-prepared cane (Preparation Index (PI) less than 90), was attributed to the presence of sand and stones in the cane. For mills where washboard adjustments were scheduled and shredder hammers regularly hard-

faced and weighed, the degree of cane preparation was fair, with a PI of 91, as opposed to a PI of 89 observed in other mills.

Brix curve

Meadows (2022) states that a Brix curve is an essential tool in the management of proper diffuser operation. A good Brix curve should be smooth, as it drops off steeply after the feed and levels towards the discharge end, as shown by the control plot (depicted in blue) in Figure 11. The green trend in Figure 11 shows an offset (about 1 Brix unit over much of the diffuser), and 8 Brix in Stage 3, instead of 4 Brix. A useful rule of thumb has been given by (Meadows, 2022), namely "4 at 3 and 3 at 4", i.e. the Brix should be approximately 4% at Stage 3 and approximately 3% at Stage 4. During the mill visits, the Brix curves were mostly conducted once a day by the mills across the industry. However, this did not enable these to be used effectively to control the diffusers, as the recommended interval for effective monitoring is once per shift. Some Brix curves were representative of the poor diffuser performance; for example, whilst the profile shown in Figure 12 does follow the typical smooth curve showing the steep drop-off in the early stages, the Brix at the last stage ranged from 1.71%-2.17% (indicated by yellow and green trends), where this should ideally be below 1%. Impact issues were amongst the challenges that were reported, e.g. several stage pumps being out of commission, flooding across the bed due to very high juice levels, and the inability to control the position of juice return to the bed, thus affecting juice distribution.

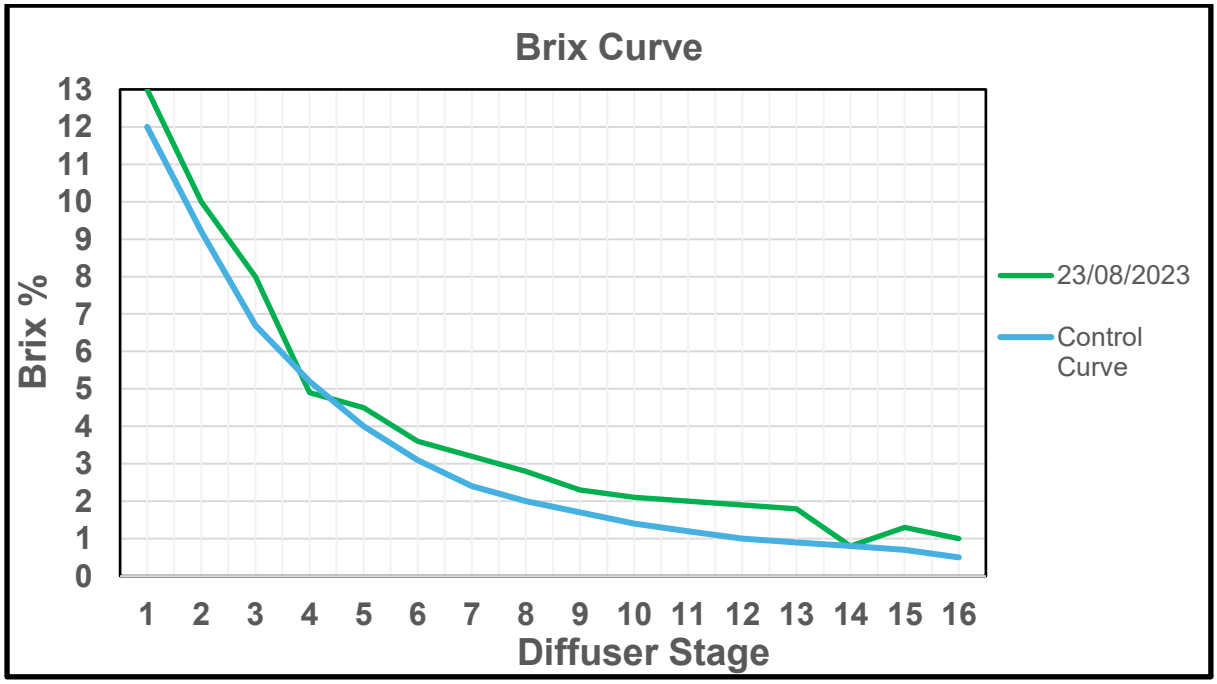


Figure 11. A plot of a Brix profile showing a smooth profile, but with higher Brix values than otherwise required for a good Brix profile

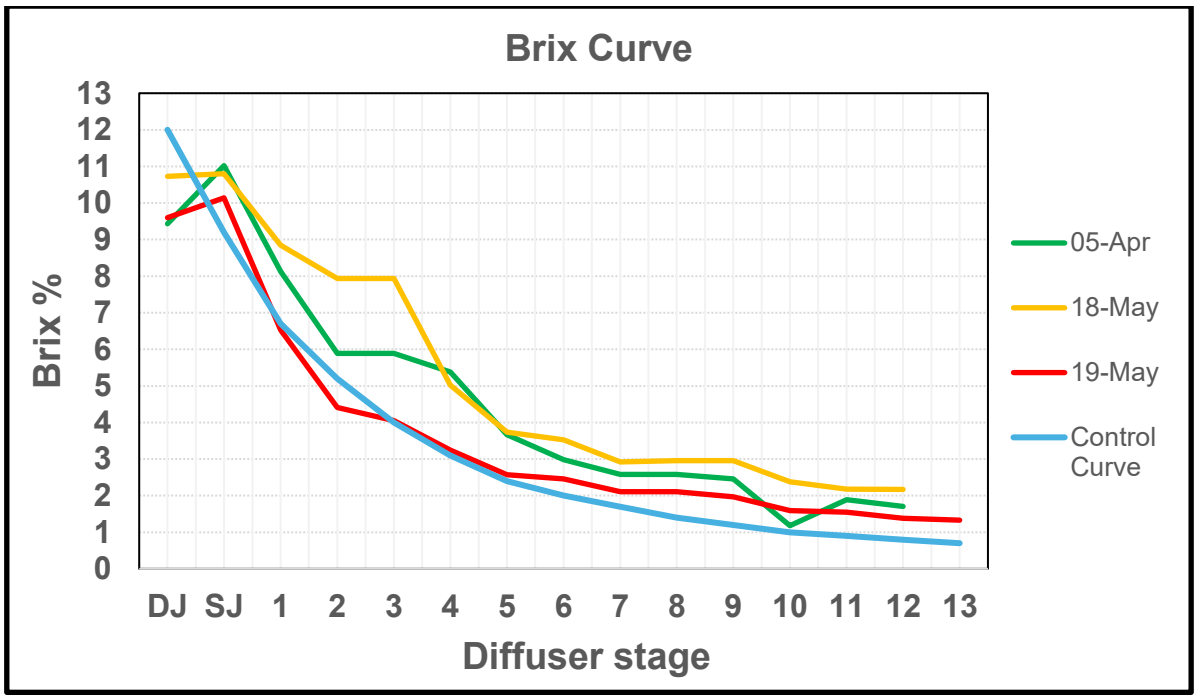


Figure 12. A plot of a poorly operated diffuser showing the Brix profiles across the diffuser stages from a factory

Clarification

The clarification station was an area of focus for seven of the 12 SA factories, which means that in five factories the clarification station was not perceived as an area of opportunity for optimisation. The seven that were audited had mixed performance patterns. The most shared areas of concern, where both good and poor performances were observed, were: 1) the Clear Juice (CJ) quality, 2) the flocculant preparation and quality, and 3) pH control, whilst 4) the juice flow control was generally carried out well across all these factories.

Clear juice quality

The CJ from some of the factory clarifiers looked turbid, with a high level of suspended solids carried over from MJ to CJ (Figure 13). In some factories, the CJ quality was reasonably good, showing a desirable yellow colour.



Figure 13. CJ samples indicating poor quality and the improper settling of mud (left) and good quality (right) observed using a test tube in two different factories

The various reasons for the poor-quality juice included the improper settling of the mud, due to high throughputs, high mud levels, and uneven juice distribution into the clarifiers. Some reasons were simply unknown and needed to be investigated. In addition to aligning the operations with the best practice guidelines, recommendations were made, such as conducting a water-level test for the clarifier launders and conducting a tracer test, to diagnose the causes of the poor performance. Where the recommended standard 'wedge' shown in Figure 14 was used to observe the juice clarity, readings ranging from 12 to 22 were observed. A wedge reading of 15 and above is generally considered to be acceptable (Mbuyazi et al., 2024). In most mills, a clarifier rack for CJ samples was not used. It was recommended that factories also set up a rack of test tubes (preferably tubes with a diameter of 25 mm), with 24 tubes (one for each hour over the day) with a fluorescent light, for the continuous visual monitoring of the CJ quality.



Figure 14. The CJ quality observed using a standard wedge in two different factories, poor (left) and good (right)

Flocculant quality

It was mostly observed that the system used to mix the powdered flocculant into a homogeneous liquid solution was good, but the flocculant solution shown in Figure 15 was full of conglomerates or 'fish-eyes', which indicated the poor mixing of the flocculant. In several factories, this was established to be caused by the stirrer, which appeared to be running very fast for this application, and the choking of the feed eductor (feeder). A low-speed (20 rpm) paddle is recommended for mixing in the flocculant dilution tanks and ageing tanks (Mbuyazi et al., 2024). As a best practice recommendation, the top of the mixing tank, as shown in Figure 16, should be covered to prevent foreign matter from entering the tank, and this was missing in all factories. It was often observed that there was no further dilution of the flocculant in the ageing tank. The recommended practice (Mbuyazi et al., 2024) is first to make the flocculant strength of 0.1-0.2% and then to further dilute the solution to approximately 0.05%, for better dispersion in the limed juice.



Figure 15. A poorly-agitated flocculant solution in a tank with conglomerates 'fish-eyes'



Figures 16. An uncovered mixing tank exposed to foreign matter ingress

pH control

The pH control at all factories was generally good and responded well to the flow changes, although the pH of the CJs was sometimes found to be higher than the recommended target range of between pH 6.9 and 7.2 (Mbuyazi *et al*., 2024). Good pH control is important for efficient juice clarification. During the factory visits, the control appeared to be good (Figure 17) where the Process Value (red = PV) was often seen to be close to the set point (yellow). The pH measurements from the field probe (in the plant) should be constantly verified against the laboratory, instruments, and it is better to have two field instruments, to cross-check against each other.

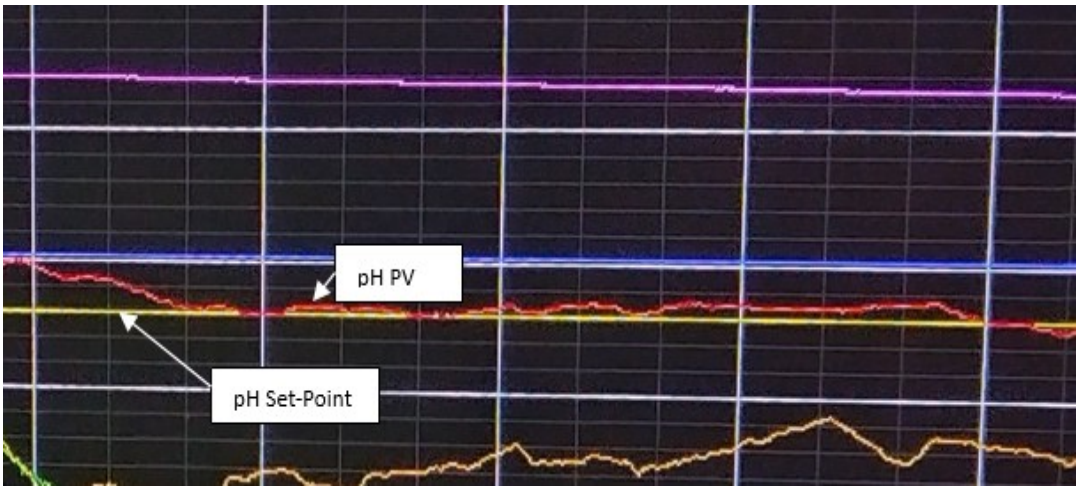


Figure 17. A snapshot of good pH control monitored in a factory control room, typically seen across the industry

Mud filtration

While being mindful of the fact that there are only four factories in SA that still practice mud filtration, it was deemed to be important that this station also be monitored for its performance since it does have an impact, on a bigger scale, on the overall factory performance. The

common areas of concern where recoveries could be realised, amongst these four factories were found to be: 1) the pol% filter cake, 2) the filter vacuum and 3) the drum speed. The mud temperature in the filter boot, which is also a good indicator of long mud retention times, or poor mud extraction, which leads to inversion losses, were also monitored.

Pol % filter cake

Poor cake formation was a common observation in all four factories. The cake formed on all the filter drums was thin and wet, with areas that were patchy and areas that were not covered at all, possibly due to the blocked backing screens. The low quantity of bagacillo that was seen to be entering the mud mixer was a major contributor to the poor cake formation, as well as the inability to effectively apply water onto the filters, to the extent that there would sometimes be no water being used on the filters at the time of the visit. This therefore led to inadequate washing of the cake, resulting in poor recoveries at this station. Several spray nozzles needed aligning, in order to face the filter, and there was evidence of a blockage on some, which resulted in the water not being sprayed across the whole filter. It is known that a bagacillo to mud ratio of 0.4 is a good target for good filter cake formation, and can be calculated as shown below:

$$Bagacillo\ Ratio = \frac{Dry\ bagacillo}{Dry\ mud\ solids} \times 100$$

The reported pol % cake was at its worst and very high up at 8.79%, at a particular factory. The rule of thumb as an indication of good pol % filter cake performance is a figure below 1.5%. Photographs showing a typical filter cake and the condition of filter screens are shown in Figure 18.



Figure 18. Poor filter cake formation with the damaged screen area commonly observed in the factories

Filter vacuum

Most of the filters had poor vacuum readings, which indicated ineffective sealing, as depicted in Table 1. Both the high and low vacuums read well below the required operating vacuums; for example, at one factory, where low and high vacuum should have read -20 kPag and -40 kPag, respectively, they read -15 kPag and -18 kPag. This is an indication of leaks, which could be the reason for the insufficient vacuum. In a well-operated filter station, it is expected that a sufficient vacuum is maintained to efficiently pull the mud onto the drum and draw the filtrate through the cake into the receivers.

Table 1. Records of high and low vacuum readings taken from a factory vs the recommended target values for receivers and filters

Vacuum Readings	**Gauge Readings (kPag)**	
	High	**Low**
Filtrate Receivers	-49	
Receiver Target	-50	-30
No 1 Filter	-23	-18
No 2 Filter	-32	-26
Filter Target	-30	-10

Drum speed

The drum rotational speeds were usually too fast for the minimum and maximum recommended drum speeds, as shown in Table 2. Higher filter speeds must be adjusted to the recommended speed, in order to improve the filter performance. Slower speeds are recommended, as this enables the filter to pick up a thicker layer of cake and to give a longer time to wash out the sugar and dry the cake. This was part of the reason for the inadequate washing of the cake, and hence the high losses at the filter station.

Table 2. An example of high/fast filter speeds observed at a factory

Filter Number	**Minutes/Revolution (Min/Rev)** **Recommended Ranges** **3-5**
2	2.58
4	2.40
5	1.52

Evaporation

The sub-optimal operation of evaporator stations was a problem in several factories, and this was recognised by a prolonged failure to achieve and maintain the desired syrup Brix. The most common problematic operational aspects that were observed by the SMRI team are reported in this section, as well as suggestions on how to improve their performance.

Evaporator feeding systems

In most cases, the feeding arrangements used for Kestners and Robert vessels were not the ideal external feed ring-type arrangements (Figure 19). The feed ring ensures the uniform distribution of the feed around the vessels, which promotes plug flow and good circulation. An external feed ring can be removed easily and cleaned during the stop-days.



Figure 19. Evaporator external feed ring with feed risers

Pressure drop between effects

In several cases, the pressure drop between the last two effects in the evaporator train was quite high. This phenomenon causes high juice velocities into the last effect, as well as a high degree of flashing, which results in entrainment. If this high-pressure drop is persistent, installing a small juice flash tank between the last two effects can help to reduce the amount of flashing into the last effect (Dlamini & Bindoff, 2013).

Incondensable gas removal

Ideally, there should be the separate removal of light and heavy Incondensable Gases (IGs). IG removal is important, as 0.5% air by mass in the steam will reduce heat transfer in the calandria by up to 13% (Allan, 1979). In most cases, the IG was removed by using a single pipe that extended down the calandria. This is not efficient, and the SMRI recommendation is to have separate removal of light and heavy IGs, and these manifolds should have their nozzles facing upwards in the calandria. Where IG are vented into atmosphere, it is important

to regularly check for the quantity and type of fluid coming out of these vents. Liquid can come out through these vents if there is poor condensate drainage in the vessel.

Monitoring of the heat transfer coefficient

It was found that most factories did not have a habit of checking the Heat Transfer Coefficients (HTCs) across the evaporator train on a regular basis. The regular checking of the HTCs is highly recommended, as it is a good way of detecting the poorly-performing evaporators that should be prioritised for cleaning. The installation of condensate flowmeters, coupled with the monitoring of temperatures and pressures, can allow for the online calculation of HTCs and avoid off-line calculations that require some time to implement.

Level and BrixBrix control

There were challenges with evaporator control strategies, in terms of the juice level and Brix. Brix control was unstable in most cases, probably due to the improper tuning of the control loops, or a long dead-time in the control loop (Figure 20). It is recommended that the steam control valve for BBrix control should be located after the last bleed.

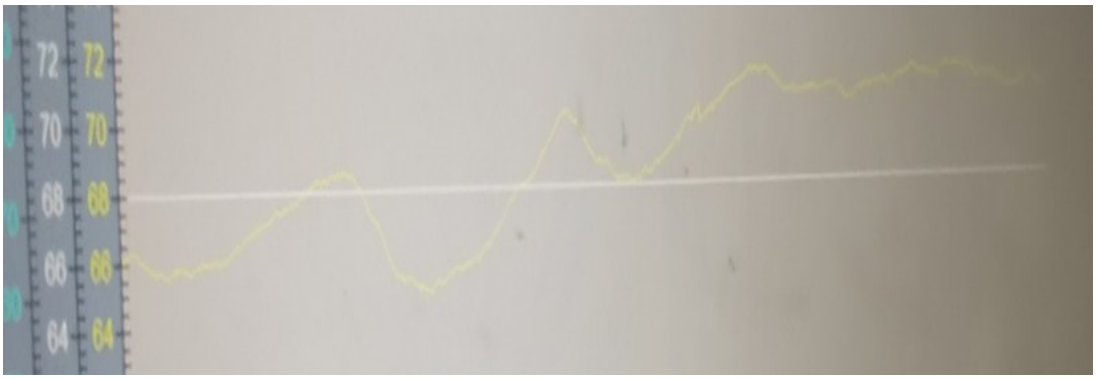


Figure 20. Brix control trend over a 4-hour period (the white line is the set point and the yellow line is the process value)

For Robert vessels, the ideal juice level should be between 30 to 40% of the tube height (Hugot, 1986), but this was not consistently achieved by most factories. Low levels should be avoided as they will cause localised overheating and then spouting.

Entrainment monitoring

Another issue that was encountered was the monitoring of entrainment from the evaporators, which is mostly based on analysing the condensates from the intermediate effects, and so entrainment from the final effect would not be detected. Whilst it was not possible for the SMRI team to examine the entrainment separators during operation, it is strongly recommended that pressure drop monitoring be installed across entrainment separators, especially the Metex screen types, as this would be an easy way of knowing when they start to foul. The use of isokinetic sampling of the vapours is the ideal way of identifying the source of this problem (Beale & Stewart, 1962).

General pan house issues

It is generally believed that there is much greater potential for improvement in the operations of boiling houses than in the extraction plants across the SA industry. The SMRI team visited the factories with this in mind. This section reports on the observations and recommendations that were made for the improvement of BHRs.

Performance targets

In most cases, the basic operating targets, as listed in Table 3, were not achieved, which resulted in poor exhaustions, high losses to molasses and high TPDs.

Table 3. General pan house operating targets

	A-station	B-station	C-station
Massecuite Brix at strike	92 – 94 °Brix	94 – 96 °Brix	97 – 98 °Brix
Purity drop on strike	18 – 20%		
Overall purity drop across all stations	> 50%		
Purity drop on cooling	> 2%		
Purity change on heating			0%
Purity rise on curing	< 2%		
Magma purities		90 – 92%	82 – 84%

It was sometimes reported that massecuite strike Brixes were intentionally slackened to avoid massecuite flow problems in the crystallisers; however, this should not be the case if all the equipment were designed properly. Most factories also did not do purity profiles of the Nutsches, from strike to curing. With the availability of the SMRI Mini-Nutsch filter and the SMRI-NIRS[1] analysis technology, it should be relatively easy and quick to do these purity profiles and they will be informative to improve the exhaustions, in terms of which areas require more focus.

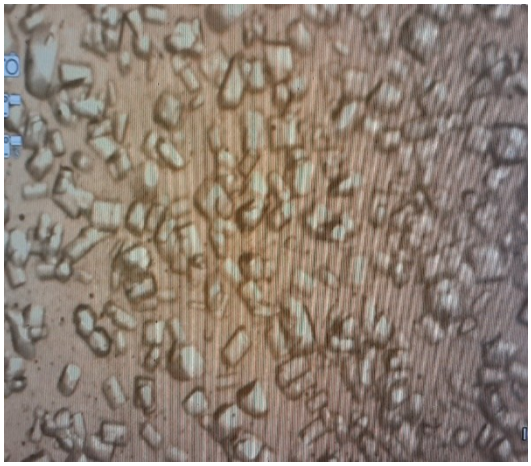
Massecuite crystal quality

Pictures of crystals in samples of the seeds and massecuites showed that their quality was at most not good . The variation in crystal sizes was often huge, with the presence of substantial false grain, as shown in Figures 21 A to D. When the starting seed quality was poor, it usually resulted in poor massecuite. Despite the widespread use of wide monitor casings in the B-station, the quality of the B-magma was not good in some cases, which could have been due to poor quality slurry being used, the use of the wrong slurry addition point in the boiling cycle, and generally-poor boiling conditions in the pan, which allowed the formation of false grain. Another major concern was that these photographs were not viewed by pan boilers and their managers on a regular basis. Ideally these photographs should be reviewed during the morning meetings, to identify the corrective action, where necessary, with regards to how the boilings are conducted.

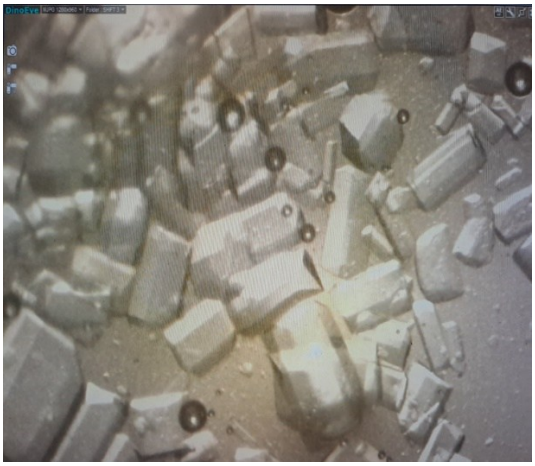
In several cases, it was found that the slurry used was not uniform, because it had been produced under inconsistent conditions (Figure 22). The factories were urged to stick to the approved SASTA method of preparing the slurry (Anon, 2009) and that this operation should be carried out under the quality control of the laboratory. Factories were encouraged to send slurry samples to the SMRI to check that their equipment produces the required quality slurry when the correct procedure is being followed. There were cases where factory microscopes did not have the facility to measure the crystal sizes and these factories were urged to rectify this as soon as possible. Factories were also encouraged to make use of a polarising UV-filter on their microscopes to improve the visibility of false grain on the pictures. The storage of historical crystal photographs in most cases was not good, with no, or limited, historical

[1] Near Infra-red Spectroscopy

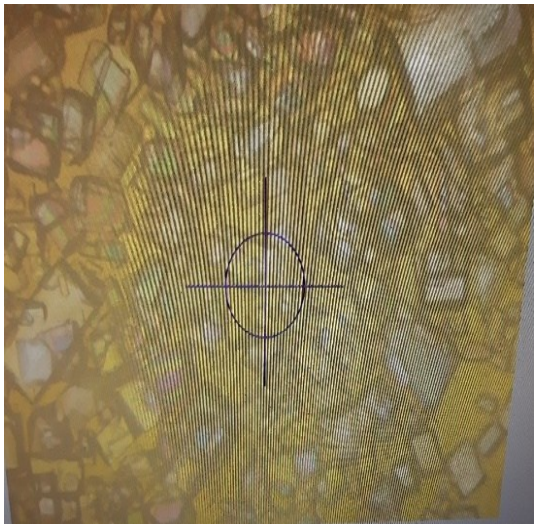
pictures being available. Factories are encouraged to provide for a sufficient capacity for the storage of historical crystal pictures, if they should be required for troubleshooting.



(A)



(B)



(C)



(D)

Figure 21. Pictures of different seeds and massecuites (A) B-magma, (B) A-massecuite, (C) C-seed and (D) C-massecuite

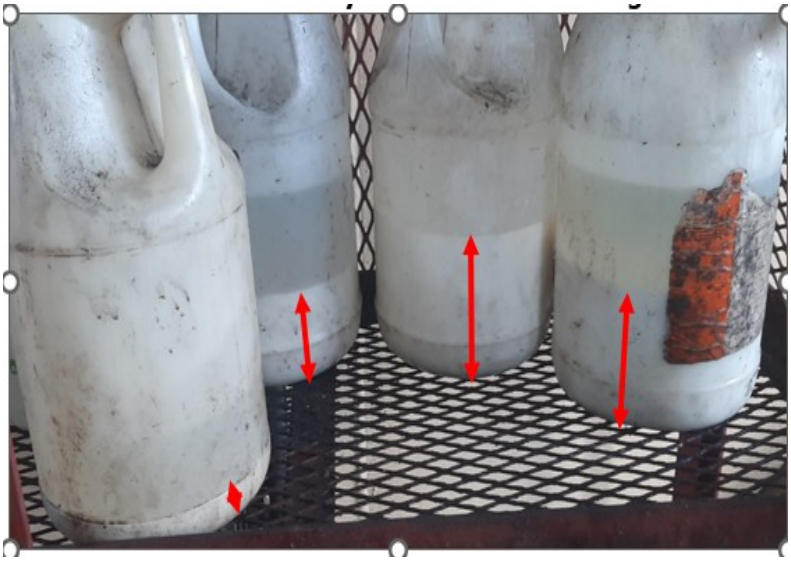


Figure 22. Inconsistent slurry preparation

Manual control of pans

Batch pans are mostly boiled manually due to the inadequate instrumentation available in the pans. The reproducibility of good boilings would be achieved more often with automated boilings than with manual boilings. It is strongly recommended that the pan instrumentation be improved and to allow for the implementation of automated boilings by implementing properly developed boiling recipes. Control loops being put on manual was another problem that was encountered in the continuous pan operations. The following control loops in continuous pans should always be put on automatic mode for consistent operation:

- calandria pressure control;
- evaporation rate control; and
- compartment feed control

The compartment Brix profile in the C-CVPs did not follow the recommended Brix profiles in most pans (Figure 23), as per the SMRI best practice guide (Love, 2023). In addition to the control loops being put on manual, this could also have been caused by the poor quality of the instruments being used for monitoring, as well as some probes being located in inappropriate places in the pans, for example, near internal steel work (proof sticks, ladder rungs, baffle plates etc.) that give noisier signals than other probes, thus causing an offset in the readings. Factories were urged to check for such types of interference during their stop-day inspections. It was also found that the on/off proportional control for feed and water on the continuous pans was sometimes not set correctly, in order to give about a 50% valve open time.

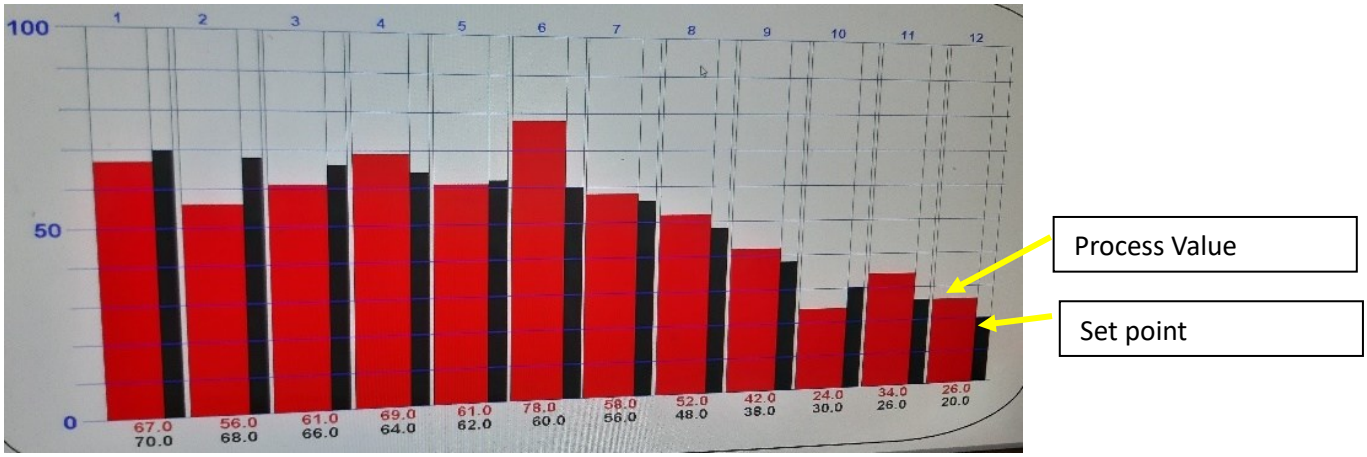


Figure 23. Actual versus set point Brix profile in a C-CVP

General operating issues

With regards to the construction of the pans, the following design issues were often picked up:

- The sight glasses for the entrainment return were located in obscured locations, which makes it difficult for operators to see if there is entrainment occurring.
- Pan steamings being dropped onto the massecuites. These should rather be routed to molasses tanks, remelt or steaming tanks and rateably pumped into a remelter.
- The lack of pan volume indications. These are needed, particularly when cutting over or drawing in magma.

Some operators had a habit of leaving the proof sticks extended, which draws air into the pans and some proof sticks were not sealing properly into the pan. These bad operating practices need to be stopped. With regards to the A- and C-cooling crystallisers, in most cases it was found that there was hardly any further exhaustion of massecuites taking place, despite there being sufficient available capacity. Some of the reasons for the poor performance of crystallisers were:

- no cooling water being used due to leaking elements;
- no cooling water being used due to the reheater being bypassed;
- low operating levels;
- The uncontrolled lubrication of massecuites; and
- broken crystalliser shafts

A-station

On several occasions, the elongation of A-massecuites was encountered, due to the recycling of impurities. In some cases, this was linked with the processing of carry-over cane and long burn-to-crush delays. An A-seed prepared by graining with slurry (rather than by using B-magma) was seen to have substantially less crystal elongation, which indicated that it was the recycled impurities, rather than the impurities in the syrup, that were the likely cause of the crystal elongation. Elongation causes difficulties in curing and it causes the passage of crystals through the screen. The van Hengel (1983) boiling scheme was recommended as a means of dealing with this problem.

The usage of pan movement water was found to be higher than necessary. This was more evident in continuous pans, where the number of compartments held on water was unusually

high. In these instances, pan boilers were encouraged to slow down the evaporation rate in the pan, rather than holding the pan on water, which results in a wastage of steam.

C-station

Evidence of Maillard reactions on the C-massecuite was quite prevalent. The massecuite looked reddish brown, foamy and gassy (Figure 24). The monitoring of the Fructose/Glucose (F/G) ratios across factory streams is usually another good indicator of the existence of Maillard reactions, which is reflected by an increase in the F/G ratio. The Maillard reaction is caused by a high Brix, high temperature, and low purities. Therefore, it is very important to control the boiling temperature of the C-massecuite. Rein (2007) recommends that C-massecuite should exit the pans at no more than 63°C.

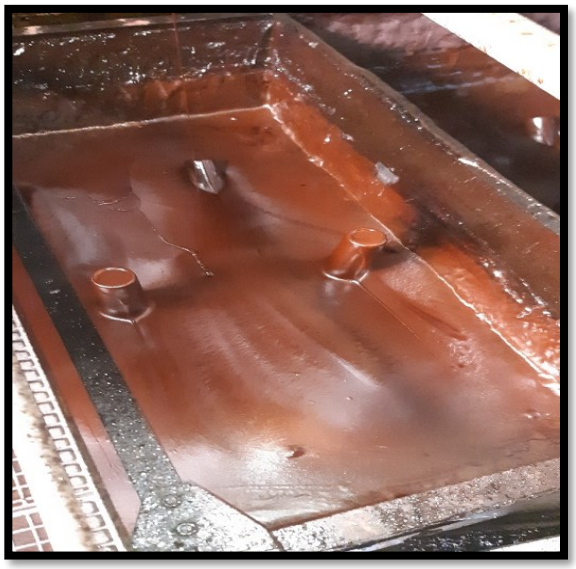


Figure 24. Evidence of the Maillard reaction in C-massecuite in the crystallisers (reddish colour)

The C-massecuite reheater was found to be a problematic unit operation in several factories that resulted in the reheaters being bypassed, which contributed to the high TPDs. The most common problem with reheaters was the leaking tubes, either in the reheaters or in the calorifiers, which suggested that there were problems with the quality monitoring in the water treatment systems. Another problem was that the factories struggled to get massecuite to flow through the reheaters, due to the poor designs. Sometimes C-massecuite Brixes were deliberately kept lower than the ideal, for ease of flow of the massecuite. This was discouraged, as it reduces C-massecuite exhaustion. Rather, the equipment design challenges that are encountered with high Brix massecuites should be properly addressed. In some cases, the high Brix massecuite from the crystallisers was lubricated to reduce the viscosity of the massecuite into the centrifugals. However, it was often found that the lubrication of massecuite was not done in a properly controlled or automated process, and therefore excessive water or molasses was used during the lubrication process, which resulted in the massecuite been too dilute (Figure 25).



(A) (B)

Figure 25. Lubrication of the massecuite with (A) water and (B) molasses

In some instances, the C-massecuite crystal content was found to be higher than the ideal target of 25 to 28% (Love, 2023). This increases the production of C-massecuite and increases viscosity. C-magma purities were mostly found to be on the higher side of the target range of 82 to 84%, due to over-washing in the C-centrifugals, which increases the losses of sucrose to molasses and results in the final molasses Brixes being lower than the recommended minimum target of 82 ^{o}Brix (Rein, 2007).

It was also often found that factories targeted a C-seed purity, rather than a C-massecuite purity. Consequently, the C-massecuite purity just followed the B-molasses purity, as can be seen in Figure 26, which was plotted by using data from a factory. A good practice would be to determine a target C-massecuite purity by using a desired crystal content, which should ideally be in the range of 25 to 28%, and the latest Reducing Sugars (RS) to ash (RS/Ash) ratio in MJ. Figure 26 shows what a targeted C-massecuite purity would have been for this particular factory. Targeting a C-massecuite purity will generally ensure a consistent crystal content, which should result in a better TPD. As found by Ninela and Rajoo (2006), boiling C-massecuite purities higher than the target C-massecuite purities leads to poor TPD results.

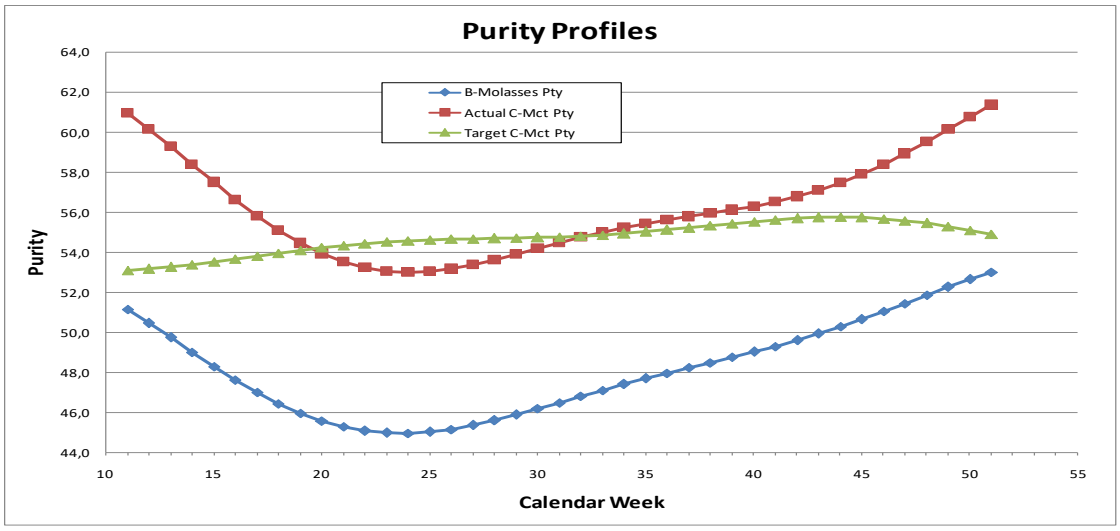


Figure 26. Relationship between B-molasses and C-massecuite purities

Batch centrifugal machines

High purity rises across batch centrifugal machines was a major challenge in most factories. These were caused by factors, such as an excessive amount of water being used for washing in order to achieve the raw sugar specifications, or for the benefit of the downstream back-end refinery. Some of the water spray valves did not close off tightly after washing, which resulted in water dripping into the basket. This is probably not serious while the centrifugal is in the high-spin cycle, but during the plough-out, the water falls onto the sugar being discharged, dissolving some of the sugar and causing lumps. Spray nozzles need to be set at a slight angle, so that there is no overlapping in the spray pattern. Sometimes the water sprays were not aligned properly, or they were bent, resulting in an overlap in the spray pattern and causing excessive sugar dissolution. This was partly caused by using in-house fabricated spray pipes, instead of using the spray pipes supplied by the original equipment manufacturer (OEM).

The plough settings were often not correct, which resulted in sugar being left behind after ploughing, as shown in Figure 27. Therefore, in some cases, the screen wash cycle was disabled in order to improve exhaustions, but this increases the risk of screen blinding. Leaking massecuite valves were sometimes an issue and resulted in massecuite leaking into the sugar.

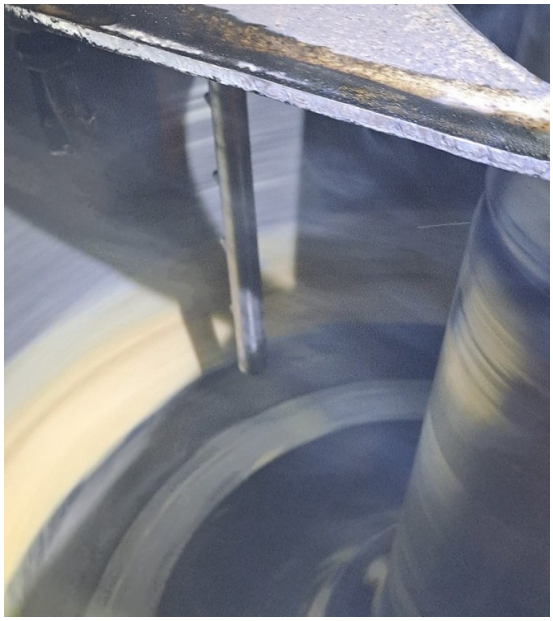


Figure 27. A-Centrifugal – showing sugar left behind after ploughing

The poor grain size distribution in the massecuite is another cause of high purity rises on curing. The small false grain crystals in the massecuite dissolve quickly in the centrifugals and also pass easily through the screen holes. When there is a high purity rise on curing, the molasses should be routinely analysed for crystals, to determine the integrity of the screen.

In most factories, there was no display on the centrifugal floor of the centrifugal wash water temperature and pressures. This is important information for centrifugal operators to know, so that they can halt operations and raise an alarm if these parameters fall outside of the desired range. A water pressure of at least 400 kPa and a temperature above 85ºC is considered to be acceptable for good centrifugal operations (Rein, 2007).

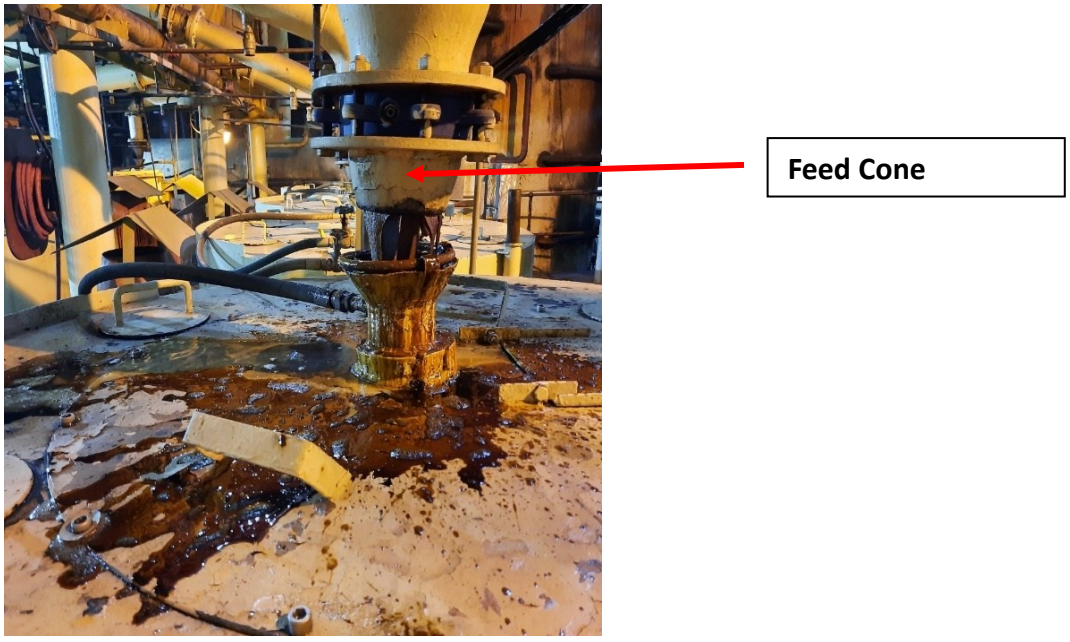
Continuous centrifugal machines

In most cases, lubrication (lube) rods are no longer used due to the discontinuation of iris valves, and because water is added outside of massecuite in the feeding cone. This is inefficient, as there is no proper mixing of the water and the massecuite, which results in the separation of the two as soon as the mixture reaches the spinning basket (Figure 28A). Factories were encouraged to reinstate the use of lube rods. The design and construction of ‘lube rods’ is described in the paper by McEvoy and Archibald (1975).

Butterfly valves (as opposed to iris valves) are now commonly used to feed the centrifugals, therefore appropriately sized feeding cones are necessary to direct the feed into the machine and to contain the water that is added within the resulting ‘rope’ of massecuite. Feeding cones were often found to be either oversized and not yielding a good ‘rope’ of massecuite into the centrifugal, as shown in Figure 28B, or undersized, resulting in the build-up of massecuite in the crystallisers. Often the feed into similarly sized centrifugals was found to be disproportional. In addition, there was no monitoring of the water flow into the various centrifugals, which implied that the ratio of massecuite to that of wash the water would be different for each centrifugal. It was recommended that factories should monitor and control the wash water flow to each centrifugal.



(A)



(B)

Figure 28. (A) C-centrifugal water addition and (B) oversized feed-cone

It was mentioned earlier that factories were encouraged to determine Nutsch purity changes across the various unit operations in the pan house. With the SMRI-NIRS and SMRI Mini-Nutsch it should be possible to do numerous TPD analyses during each shift and for each machine. This practice will indicate the worst-performing machine, which should then be attended to for optimisation.

There are still a few factories that do not use wide monitor casings to produce B-magma. Wide monitor casings are known to minimize crystal breakage, and these factories were encouraged to move towards the use of wide monitor casings.

Summary of recommendations

The ultimate aim of the SMRI factory improvement initiative was to assist the sugar factories to return to well-established operational best practices and, thereby, to improve the technical performance. The most common deviations from best practices that were observed in the different sections of the factories have been discussed in detail in this paper. This section summarises the overall recommendations across the factory sections:

Extraction

- Cane preparation should be closely monitored and adjustments should be made to the cane preparation equipment, when deemed necessary.
- Factories should improve the imbibition levels to 300 to 375% on fibre. Where energy efficiency is a concern, investigations should be done to improve the energy efficiency.
- All lifting screws should be operational.
- Diffuser operating temperature should be between 80 and 85^{o}C across the diffuser stages.
- Instrumentation to monitor and control the bed level should be installed and operational to assist with minimising incidents of flooding in the diffuser.
- Operators should frequently monitor the diffuser and take the necessary steps to mitigate flooding and dry bed conditions.
- The hygiene of the diffuser should be improved e.g. leaks should be repaired quickly and diffuser sumps should be kept empty by using a level control.
- Brix curves should be determined regularly and used effectively to control the diffuser.

Clarification

- Ensure the Juice flow conditions into the clarifiers are not turbulent.
- There should be proportional juice distribution to different clarifiers, based on their operating volumes.
- Flocculant should be prepared under recommended conditions, as per Rein (2007)
- pH measurements from the field probe should be constantly cross-checked against the laboratory instruments, and there should preferably be two field instruments to cross-check against each other.
- The mud level should be monitored frequently and kept at an optimal level.
- The clarity of juice should be monitored frequently by using a standard clarity wedge, and hourly samples should be displayed on a test-tube rack.

Mud filtration

- It should be ensured that the vacuum system is operating correctly, so that the desired low- and high-vacuum pressures can be achieved.
- The filter drums should rotate within the recommended speed range.
- Water sprays should be set properly and be in a good operating condition.
- It should be ensured that there is sufficient bagacillo added to the mud, in order to obtain the desired mud-to-bagacillo ratio.

Evaporation

- A feed-ring type of feeding arrangement is recommended when using Kestners and Robert vessels.
- A juice flash vessel should be installed between the last two effects in the evaporator train, if there is a consistently high pressure drop between these vessels.
- Light and heavy IGs should be removed separately from the calandria and vented to the atmosphere or into a common manifold.
- Factories should monitor HTCs regularly and move towards the implementation of monitoring these online.
- The setpoints for level and Brix controls should be set properly and the control loops should be tuned properly. Factories can consult the SMRI for assistance with improving the evaporator control strategies.
- Isokinetic sampling should ideally be used for the identification of entrainment in vessels.

Pan House

- Factories should strive to achieve the key performance targets, as listed in Table 3.
- The Nutsch purity profiles across the various sections of the pan house should be measured routinely.
- Seed should be prepared correctly, and quality control on slurry production should be in place to provide a good starting point for massecuite production.
- All microscopes should have the facility to measure the crystal size and it is recommended that a polarising UV-filter be used for clear visibility of the false grain.
- Absolute pressure control in the vacuum pans should always be maintained on auto-mode, with the tail-pipe temperature override implemented.
- Factories should move towards the automatic boiling of all batch and continuous pans to achieve the reproducibility of good boilings.
- Compartment Brix profiles in all continuous pans must follow the recommended profiles, as outlined in the SMRI best practice guides for these pans (Love, 2023)
- Entrainment returns in the pans should be located externally and fitted with sight glasses in areas where they are clearly visible.
- Pan steamings should not be dropped onto the massecuites. These should be diverted to a steamings tank and rateably pumped to a remelter.
- There should be clearly-demarcated level indicators on the pans.
- Proof sticks should have a proper seal and should not be left extended.
- Leaking cooling elements in the crystallisers should be repaired as soon as practicable.
- Operating levels in the crystallisers should be as high as possible, and circulation through horizontal crystalliser banks should be such that the massecuite flow does not short-circuit. For example, the massecuite should flow from left to right and top to bottom.
- The lubrication of massecuites should be carefully controlled.
- Crystallisers should be properly maintained.

A-Station

- The use of pan movement water should be monitored carefully and controlled.

C-Station

- C-massecuites should exit pans below 63°C to minimise the onset of Maillard reactions.
- Final molasses should be stored below 40°C to minimise the onset of Maillard reactions.
- The quality of heating water treatment for the reheater should be monitored carefully.
- The lubrication of massecuites should be done by using the first molasses purged from a centrifugal in a classification process before the blow-up tank.
- Rather than targeting a C-seed purity, factories should determine a target C-massecuite purity using a desired crystal content in the range of 25 to 28% and the latest RS/Ash ratio in MJ.

Batch centrifugals

- The over-washing of the sugar should be avoided at all times.
- Water spray valves should be closed tightly.
- Spray nozzles need to be set at a slight angle, so that there is no overlapping in the spray pattern.
- Ploughs should be set properly to avoid sugar being left behind after ploughing.
- Screen wash cycles should not be disabled.
- Massecuite feed valves should close tightly, to avoid massecuite dripping into the sugar.
- Centrifugal wash water temperature and pressure should be prominently displayed on the centrifugal floor.
- Molasses should be routinely checked for crystals, to determine the integrity of the screens.

Continuous centrifugals

- Lube rods should be used for the more effective addition of water into the massecuite.
- Feeding cones should be sized correctly and feeding valves should be set properly, so that there is a roping effect of massecuite into the centrifugal.
- The massecuite should be distributed proportionally across different machines, running in parallel.
- The centrifugal wash water flow should be measured and controlled.
- TPD analyses should be conducted regularly for each C-centrifugal machine.
- Wide monitor casings should be used for the curing of B-massecuite.

Conclusion

The feedback on the first three years of the SMRI factory improvement initiative from the industry stakeholders has been overwhelmingly positive. The expertise, insights and collaborative approach to assisting factories with their improvement goals have been cited as beneficial, and the actionable and relevant recommendations given during the plant visits have been a welcomed success factor in this process. With the support of the SA sugar factories, the SMRI has decided to continue to offer the factory improvement initiative in subsequent seasons. It is acknowledged that factories are unique in their characteristics and that they have different challenges; therefore, going forward, a tailored approach will be used to meet the unique needs of each factory.

References

Allan GN (1979). Investigations into evaporator malperformance. *SMRI Technical Note 2*.

Anon (2009). Laboratory manual for South African sugar factories. South African Sugar Technologists' Association, 5th Edition, Mt. Edgecombe. https://sasta.co.za/laboratory-manual.

Beale RF and Stewart PN (1962). Entrainment Investigations. *Proc QSSCT, 29th Conference,* pp 95-107.

Dlamini BMW and Bindoff A (2013). Felixton mill evaporator station: Final effect partial flash tank. *Proc S Afr Sug Technol Ass* 87: 375-383

Hugot E (1986). *Handbook of Cane Sugar Engineering, Sugar Series 7*. Elsevier, 3rd Edition Amsterdam, The Netherlands.

Love DJ (2022). Best practice guide: A-Continuous vacuum pan. *SMRI Technical Report No. 2383.*

Love DJ (2023). Best practice guide: Operation of C-Continuous vacuum pans. *SMRI Technical Report No. 2421.*

Mbuyazi M, Ndinisa V and Mbuthuma Y (2024). A best practice guide to clarification. *SMRI Technical Report No. 2450.*

Meadows DM (2022). Best practice guide: Diffuser extraction plant. *SMRI Technical Report No. 2374.*

McEvoy MAJ and Archibald RD (1975). Increased capacity of continuous centrifugals on low grade massecuites. *Proc S Afr Sug Technol Ass* 49: 80-85.

Ninela M and Rajoo N (2006). Practical steps taken at Tongaat Hulett sugar factories to achieve low target purity differences. *Proc S Afr Sug Technol Ass* 80: 448-461.

Rein PW (1995). A comparison of cane diffusion and milling. *Proc S Afr Sug Technol Ass* 69: 196-200.

Rein PW (2007). *Cane Sugar Engineering.* Albert Bartens KG, 3rd Edition, Berlin.

Van Hengel A (1983). Modified boiling system for better sugar quality. *Proc S Afr Sug Technol Ass* 57: 38-41.

POSTER SUMMARY

COMPARISON OF NEAR INFRA-RED SPECTROSCOPY (NIRS) AND THE CONVENTIONAL DIRECT ANALYSIS OF CANE (DAC) IN THE DETERMINATION OF CANE QUALITY PARAMETERS

Siyakisa FM, Rambwawasvika H and Mutatu W

Zimbabwe Sugar Association Experiment Station, P/Bag 7006, Chiredzi

siyakisafascinate46@gmail.com, hrambwawasvika@zsaes.org.zw, wmutatu@zsaes.org.zw

Abstract

The use of Near Infra-red Spectroscopy (NIRS) as an analytical tool has several advantages over the conventional methods in the sugar industry. Despite having been adopted for the analysis of products in many sugar-processing factories, some companies are yet to adopt the technology. The Zimbabwe sugar industry has just acquired a transmission NIRS instrument and it is in the process of evaluating the possibility of adopting the technology for use in both mill factory products and for cane quality determination. This study aimed to compare the results of NIRS and the conventional Direct Analysis of Cane (DAC) in determining the cane quality parameters. A total of 749 sugarcane samples were obtained from across the fields, and they were analysed concurrently in the laboratory, by using NIRS and the conventional DAC methods. The results of pol, brix, purity and ERC% cane from the two methods were computed and regressed. The regression R^2 value for the brix, pol, purity and ERC% cane was 0.9834, 0.9733, 0.7065 and 0.9484, respectively. While the majority of the samples showed comparable results between NIRS and the conventional DAC, a few samples that deviated from the trend were also observed, which warrants further investigations.

***Keywords*:** Near Infrared Spectroscopy, Direct Analysis of Cane, polarimeter, refractometer, mixed juice, Brix, pol, sucrose, ERC

OFFICERS 1926-2025

Council of the Association 2024 – 2025

Patron: S NAIDOO and S MABASO-KOYANA

M KADWA (President)
CM BAKER
WK LAWLOR
G NAIDOO
GT SMITH
P MIYA

SJ SNYMAN (Vice-President)
P GOVENDER
S MADHO
NV NDINISA
DL SWEBY
S DAVIS

S RAMGAREEB (Congress Chair)
SV JOSHI
M MBUYAZI
R RHODES
S MCFARLANE

Former Presidents

1926-27	M MCMASTER	1959-60	JPN BENTLEY	1991-92	PW REIN
1927-28	M MCMASTER	1960-61	JL DU TOIT	1992-93	PW REIN
1928-29	HH DODDS	1961-62	JL DU TOIT	1993-94	PW REIN
1929-30	HH DODDS	1962-63	JL DU TOIT	1994-95	PH HEWITT
1930-31	GS MOBERLY	1963-64	JR GUNN	1995-96	PH HEWITT
1931-32	GC DYMOND	1964-65	JR GUNN	1996-97	GB O'REILLY
1932-33	GC DYMOND	1965-66	JR GUNN	1997-98	GB O'REILLY
1933-34	BED PEARCE	1966-67	LF CHIAZZARI	1998-99	TJ MURRAY
1934-35	E CAMDEN-SMITH	1967-68	LF CHIAZZARI	1999-00	TJ MURRAY
1935-36	GC WILSON	1968-69	TG CLEASBY	2000-01	TJ MURRAY
1936-37	GC WILSON	1969-70	TG CLEASBY	2001-02	TJ MURRAY
1937-38	J RAULT	1970-71	TG CLEASBY	2002-03	MS GREENFIELD
1938-39	P MURRAY	1971-72	TG CLEASBY	2003-04	MS GREENFIELD
1939-40	P MURRAY	1972-73	J WILSON	2004-05	KM HURLY
1940-41	EP HEDLEY	1973-74	J WILSON	2005-06	SS MUNSAMY
1941-42	FW HAYES	1974-75	J WILSON	2006-07	PM SCHORN
1942-43	A MCMARTIN	1975-76	JB ALEXANDER	2007-08	PM SCHORN
1943-44	G BOOTH	1976-77	JB ALEXANDER	2008-09	PM SCHORN
1944-45	GS MOBERLY	1977-78	GD THOMPSON	2009-10	PM SCHORN
1945-46	GS MOBERLY	1978-79	GD THOMPSON	2010-11	GT SMITH
1946-47	W BUCHANAN	1979-80	GD THOMPSON	2011-12	GT SMITH
1947-48	W BUCHANAN	1980-81	GD THOMPSON	2012-13	GT SMITH
1948-49	JL DU TOIT	1981-82	GW SHUKER	2013-14	GT SMITH
1949-50	HH DODDS	1982-83	GW SHUKER	2014-15	GT SMITH
1950-51	A MCMARTIN	1983-84	AB RAVNO	2015-16	GT SMITH
1951-52	GC DYMOND	1984-85	AB RAVNO	2016-17	GT SMITH
1952-53	GC DYMOND	1985-86	AB RAVNO	2017-18	GT SMITH
1953-54	GC DYMOND	1986-87	AB RAVNO	2018-19	GT SMITH
1954-55	GC DYMOND	1987-88	PK MOBERLY	2019-20	GT SMITH
1955-56	JB GRANT	1988-89	PK MOBERLY	2020-21	S MADHO
1957-58	JPN BENTLEY	1989-90	PK MOBERLY	2021-22	S MADHO
1958-59	JPN BENTLEY	1990-91	PW REIN	2022-23	M KADWA
				2024-25	M KADWA

Former Vice-Presidents

1926-27	LE ROUILLARD	1958-59	JL DU TOIT	1991-92	PH HEWITT
1927-28	HH DODDS	1959-60	JL DU TOIT	1992-93	PH HEWITT
1928-29	GS MOBERLY	1960-61	J DICK	1993-94	PH HEWITT
1929-30	GS MOBERLY	1961-62	JPN BENTLEY	1994-95	GB O'REILLY
1930-31	GC DYMOND	1962-63	JPN BENTLEY	1995-96	GB O'REILLY
1931-32	AC WATSON	1963-64	LF CHIAZZARI	1996-97	TJ MURRAY
1932-33	AC WATSON	1964-65	LF CHIAZZARI	1997-98	TJ MURRAY
1933-34	GC DYMOND	1965-66	LF CHIAZZARI	1998-99	BS PURCHASE
	E CAMDEN-SMITH	1966-67	TG CLEASBY	1999-00	BS PURCHASE
1934-35	BED PEARCE	1967-68	TG CLEASBY	2000-01	BS PURCHASE
1935-36	E CAMDEN-SMITH	1968-69	JB ALEXANDER	2001-02	MS GREENFIELD
1936-37	J RAULT	1969-70	JB ALEXANDER	2002-03	KM HURLY
1937-38	P MURRAY	1970-71	JB ALEXANDER	2003-04	KM HURLY
1938-39	EP HENDLEY	1971-72	JB ALEXANDER	2004-05	SS MUNSAMY
1939-40	EP HENDLEY	1972-73	M MATIC	2005-06	RA BAILEY
1940-41	FW HAYES	1973-74	M MATIC	2006-07	DL SWEBY
1941-42	A MCMARTIN	1974-75	M MATIC	2007-08	DL SWEBY
1942-43	G BOOTH	1975-76	GW SHUKER	2008-09	DL SWEBY
1943-44	FB MACBETH	1976-77	GW SHUKER	2009-10	DL SWEBY
1944-45	G BOOTH	1977-78	GW SHUKER	2010-11	BM MUIR
1945-46	W BUCHANAN	1978-79	GW SHUKER		KA REDSHAW
1946-47	GC DYMOND	1979-80	GW SHUKER	2011-12	KA REDSHAW
1947-48	GC DYMOND	1980-81	GW SHUKER	2012-13	KA REDSHAW
1948-49	GC DYMOND	1981-82	AB RAVNO	2013-14	KA REDSHAW
1949-50	JL DU TOIT	1982-83	AB RAVNO	2014-15	KA REDSHAW
1950-51	OWM PEARCE	1983-84	PK MOBERLY	2015-16	CM BAKER
1951-52	OWM PEARCE	1984-85	PK MOBERLY	2016-17	CM BAKER
1952-53	K DOUWES-DEKKER	1985-86	PK MOBERLY	2017-18	CM BAKER
1953-54	JB GRANT	1986-87	PK MOBERLY	2018-19	CM BAKER
1954-55	K DOUWES-DEKKER	1987-88	PW REIN	2019-20	CM BAKER
1955-56	GC DYMOND	1988-89	PW REIN	2020-21	CM BAKER
1956-57	WG GALBRATH	1989-90	PW REIN	2021-22	SJ SNYMAN
1957-58	JL DU TOIT	1990-91	GW SHUKER	2022-23	SJ SNYMAN
				2024-25	SJ SNYMAN

Former Congress Organising Committee Chairs

2013-14	DL SWEBY	2017-18	S RAMGAREEB	2021-22	S RAMGAREEB
2014-15	S RAMGAREEB	2018-19	S RAMGAREEB	2022-23	S RAMGAREEB
2015-16	S RAMGAREEB	2019-20	S RAMGAREEB	2024-25	S RAMGAREEB
2016-17	S RAMGAREEB	2020-21	S RAMGAREEB		

Former Treasurers

2013-14	A VAN DER NEST	2017-18	A VAN DER NEST	2021-22	M KADWA
2014-15	A VAN DER NEST	2018-19	A VAN DER NEST	2022-23	NV NDINISA
2015-16	A VAN DER NEST	2019-20	M KADWA	2024-25	NV NDINISA
2016-17	A VAN DER NEST	2020-21	M KADWA		

SASTA GOLD MEDALISTS

1968 AE RABE
1970 CGM PERK
1974 JL DU TOIT
1977 PCG BRETT
1981 JB ALEXANDER
1988 IA BELL
1990 GD THOMPSON
1998 SW UPFOLD
2000 PW REIN
2002 AB RAVNO
2002 K SCHAFFLER
2005 E MEYER
2005 JH MEYER
2005 PG MOREL DU BOIL
2008 KM HURLY
2009 TG CLEASBY
2010 GRE LIONNET
2012 BS PURCHASE
2019 TJ MURRAY

TALBOT-CROSBIE AND KYNOCH/TRIOMF PRIZEWINNERS 1962 TO 2023

Year	Prize Award	Author(s)
1962	Talbot-Crosbie	T COVAS
	Kynoch	JR ANDERSON
1963	Talbot-Crosbie	EJ BUCHANAN, K DOUWES-DEKKER and A VAN HENGEL
	Kynoch	GS BARTLETT
1964	Talbot-Crosbie	AE RABE
	Kynoch	RT BISHOP
1965	Talbot-Crosbie	EJ BUCHANAN
	Kynoch	JM GOSNELL and GD THOMPSON
1966	Talbot-Crosbie	Prize shared by RC TURNER and RP JENNINGS
	Kynoch	AJM CARNEGIE
1967	Talbot-Crosbie	A VAN HENGEL
	Kynoch	J GLOVER
1968	Talbot-Crosbie	J BRUIJN and RP JENNINGS
	Kynoch	G ROTH
1969	Talbot-Crosbie	RCS ROBINSON and RP JENNINGS
	Kynoch	PK MOBERLY
1970	Talbot-Crosbie	IA SMITH
	Kynoch	ME SUMNER
1971	Talbot-Crosbie	GG ASHE
	Kynoch	JM GOSNELL and AC LONG
1972	Talbot-Crosbie	JP MURRAY
	Triomf	FE RICHARDSON
1973	Talbot-Crosbie	B ST C MOOR
	Triomf	H ROSTRON
1974	Talbot-Crosbie	No Winner
	Triomf	JPM DE ROBILLARD and GA IGGO
1975	Talbot-Crosbie	EEA ROUILLARD
	Triomf	PGC BRETT, RL HARDING and RH PAXTON
1976	Talbot-Crosbie	LMSA JULLIENNE
	Triomf	JR PILCHER and G VAN DER MERWE
1991	Kynoch	RA BAILEY and SA TOUGH
1992	Talbot-Crosbie	Prize shared by MGS COX and

Year	Prize award	Author(s)
1977	Talbot-Crosbie	RP SCOTT
	Triomf	J BURROWS
1978	Talbot-Crosbie	PG MOREL DU BOIL and K SCHÄFFLER
	Triomf	DB HELLMANN
1979	Talbot-Crosbie	MR KEDIAN
	Triomf	PR ATKINSON
1980	Talbot-Crosbie	A KOEN
	Triomf	NG INMAN-BAMBER
1981	Talbot-Crosbie	RG HOEKSTRA
	Triomf	KE CACKETT and JJ RAMPF
1982	Talbot-Crosbie	LMSA JULLIENNE
	Triomf	E MEYER and B WORLOCK
1983	Talbot-Crosbie	BS PURCHASE
	Triomf	TMC BOEVEY and TJ MURRAY
1984	Talbot-Crosbie	GPN KRUGER
	Kynoch	PET TURNER
1985	Talbot-Crosbie	PG MOREL DU BOIL
	Kynoch	NB LEIBBRANDT
1986	Talbot-Crosbie	GRE LIONNET
	Kynoch	KM HARBORNE-RUTHERFORD, RA BAILEY and JV DA GRACA
1987	Talbot-Crosbie	RW REIN, MGS COX and G MONTOCCHIO
	Kynoch	TMC BOEVEY and JP FOURIE
1988	Talbot-Crosbie	MJ REID
	Kynoch	BRF GEORGE
1989	Talbot-Crosbie	GRE LIONNET
	Kynoch	JH MEYER, RA WOOD and RL HARDING
1990	Talbot-Crosbie	CMJ DAY-LEWIS and KJ SCHÄFFLER
	Kynoch	NG INMAN-BAMBER and BA STEAD
1991	Talbot-Crosbie	SJ MADAREE, PW REIN and CM WENMAN
2004	Talbot-Crosbie	DJ LOVE, SD PEACOCK and GT SCHUMANN
	Kynoch	PJ THORBURN, HL HORAN,

Year	Prize Award	Author(s)
		P SAHADEO and M MEADOWS and S WADLEY
	Kynoch	SJ SNYMAN, KG BLACK, BI HUCKETT and MP WATT
1993	Talbot-Crosbie	M MOODLEY
	Kynoch	NG INMAN-BAMBER, TL CULVERWELL and MG McGLINCHEY
1994	Talbot-Crosbie	VC STONE
	Kynoch	BL SCHROEDER, JB ROBINSON PET TURNER and M WALLACE
1995	Talbot-Crosbie	DC WALTHEW and LM TURNER
	Kynoch	DB HELLMANN, GG PLATFORD and M WALLACE
1996	Talbot-Crosbie	DC WALTHEW and RW WHITELAW
	Kynoch	R VAN ANTWERPEN, MG McGLINCHEY, NG INMAN-BAMBER AND ATP BENNIE
1997	Talbot-Crosbie	KJ SCHÄFFLER and MTD DE GAYE
	Kynoch	MG KEEPING
1998	Talbot-Crosbie	Prize shared by DM MEADOWS, GT SCHUMANN and S SOJI;
		SB DAVIS, M MOODLEY, I SINGH and MW ADENDORFF
	Kynoch	Prize shared by CRP CRONJE, RA BAILEY and K McFARLANE; E MEYER
1999	Talbot-Crosbie	None
	Kynoch	MJ PARSONS
2000	Talbot-Crosbie	PG MOREL DU BOIL
	Kynoch	EJ SCHMIDT, G NARCISO, P FROST and C GERS
2001	Talbot-Crosbie	N MAGASINER, C van ALPHEN, M INKSON and B MISPLON
	Kynoch	Prize shared by FC BOTHA, J ROHWER; and MK BUTTERFIELD, A D'HONT and N BERDING
2002	Talbot-Crosbie	PB DEVNARAIN, DR ARNOLD and SB DAVIS
	Kynoch	Prize shared by E MEYER and N GOVENDER; and P THORBURN, R van ANTWERPEN, J MEYER and C BEZUIDENHOUT
2003	Talbot-Crosbie	BM SCHOONEES
	Kynoch	S GUYON, JL VOGEL, J OMARJEE, T VAN ANTWERPEN, P CADET and J BALANDREAU
2018	Talbot-Crosbie	PS JENSEN and L SMITH; KM FOXON and M STARZAK
	Kynoch	S RAMBURAN

Year	Prize award	Author(s)
		IM BIGGS and SE PARK
2005	Talbot-Crosbie	L SMITH
	Kynoch	Prize shared by PWL LYNE, E MEYER and R HERBERT; And M VAN DEN BERG and MT SMITH
2006	Talbot-Crosbie	L ECHEVERRI and P REIN
	Kynoch	OL KVEDARAS, MG KEEPING, F-R GOEBEL and MJ BYRNE
2007	Talbot-Crosbie	Not awarded – no Congress
	Kynoch	Not awarded – no Congress
2008	Talbot-Crosbie	R SIMPSON and J OXLEY
	Kynoch	SJ SNYMAN, GM MEYER, M BABASIAK, TL NICHOLSON, T VAN ANTWERPEN, P NAIDOO and JD ERASMUS
2009	Talbot-Crosbie	BM MUIR, G EGGLESTON and B BARKER
	Kynoch	A SINGELS, MA SMIT, M BUTTERFIELD, PDR VAN HEERDEN and M VAN DEN BERG
2010	Talbot-Crosbie	V KOCHERGIN, C GAUDET and M ROBERT
	Kynoch	S RAMBURAN, DM McELLIGOTT and O DE HAAS
2011	Talbot-Crosbie	Y NAIDOO and R SIMPSON
	Kynoch	V HARRACA, J DU PISSANIE, RS RUTHERFORD and DE CONLONG
2012	Talbot-Crosbie	PS JENSEN
	Kynoch	S RAMBURAN, T WETTERGREEN, SD BERRY and B SHONGWE
2013	Talbot-Crosbie	PS JENSEN
	Kynoch	Prize shared by S RAMBURAN; PV RAMOUTHAR, R RHODES, T WETTERGREEN, U PILLAY, MR JONES and R VAN ANTWERPEN
2014	Talbot-Crosbie	PS JENSEN, SB DAVIS, DJ LOVE and A RASSOL
	Kynoch	PDR VAN HEERDEN, MW ADENDORFF, G LAGERWALL, P BOTHA, CPR CRONJE, J VAN DER MERWE, N NEL, P SMITH, E HÖLL, G HYSLOP, V SMITH, A HARRIS, W HARRIS, JB MHLONGO, DM HARRIS, J DHEOPURSAD, T MATTHEWS and P NAIDOO
2015	Talbot-Crosbie	RC LOUBSER and PS JENSEN
	Kynoch	S RAMBURAN
2016	Talbot-Crosbie	M STARZAK and SB DAVIS
	Kynoch	D ELEPHANT and N MILES
2017	Talbot-Crosbie	WK LAWLOR
	Kynoch	N MILES, R RHODES and A WEIGEL
2019	Talbot-Crosbie	K FOXON
	Kynoch	W MAFUNGA, S FERRER, S BOTHA and A STARK

Year	Prize Award	Author(s)	Year	Prize award	Author(s)
2021	Talbot-Crosbie	B BARKER and K FOXON	2021	Kynoch	MW ADENDORFF, A JUMMAN and A PARASKEVOPOULOS
2021	Kynoch	SA McFARLANE, RB ISMAEL AMEER, CJ KISTAN and AC KOCH			
2022	Talbot-Crosbie	D BEZUIDENHOUDT, M GOKOOL, S ROSETTENSTEIN and M STEVENS	2023	Kynoch (Highly Commended)	B SCHROEDER and A WOOD
2023	Kynoch (First)	PDR VAN HEERDEN, TR RAMUSANDIWA, B CHONCO, WL SHELEMBE, SN HLELA, WA GILLESPIE, NE MKHABELA, ME BUTHELEZI and RT MASONDO	2023	Kynoch (Highly Commended)	R VAN ANTWERPEN and PB TWEDDLE
2024	Kynoch (First)	SA MCFARLANE, C KISTAN, A KOCH, and S RUTHERFORD	2024	Kynoch (Highly Commended)	PDR VAN HEERDEN, P BOTHA and B O'NEILL
2024	Talbot-Crosbie	R LOUBSE, B BARKER, N NDINISA and Y MBUTHUMA	2024	Talbot-Crosbie (Highly Commended)	S RAHIMAN, Y MBUTHUMA, D LOVE and S DAVIS

ANNUAL CECIL RENAUD AWARDS 1977-2023

Year	Prize Award	Author(s)
1977	Factory	B ST C MOOR
	Agricultural	RT BISHOP
1978	Factory	RD ARCHIBALD and C MACK
	Agricultural	OP LANDREY
1979	Factory	GG ASHE
	Agricultural	No Winner
1980	Factory	DCM KEIR
	Agricultural	AN MILLS and EH RINGELMAN
1981	Factory	S NORTH-COOMBES, K TAYLER And K KOSTER
	Agricultural	JG HARDY
1982	Factory	P GLAUM and A LANDMAN
	Agricultural	PC WISE
1983	Factory	RAH CHILVERS
	Agricultural	JE LONSDALE
1984	Factory	DJ CARLIELL
	Agricultural	PG BRAITHWAITE
1985	Factory	MA GETAZ
	Agricultural	J CHEDZY and JBR FINDLAY
1986	Factory	RAH CHILVERS and DJ LOVE
	Agricultural	DJ NIXON, M WORKMAN and PJ GLENDINNING
1987	Factory	GF MANN
	Agricultural	CPM SWEET, PW WHITE and GH DODSWORTH
1988	Factory	RP SCOTT
	Agricultural	DAG RALFE
1989	Factory	PM SCHORN, J BECKETT and WS GRAHAM
	Agricultural	TL PEARSE
1990	Factory	DM VAN DEN BERG
	Agricultural	RN STATHAM
1991	Factory	B ST C MOOR
	Agricultural	PJB GARDINER and K CAZALET
1992	Factory	RR SANDERS
	Agricultural	GC SPALDING
1993	Factory	DJ TAYFIELD and EW ANDERSON
	Agricultural	OP LANDREY, GG EICHLER and J CHEDZEY
1994	Factory	C CREBO, L BACHAN and V PILLAY
	Agricultural	PC HENRY and W RHEBERGEN
1995	Factory	M MacNAUGHTON
	Agricultural	D McARTHUR and VW SPAULL
1996	Factory	B MISPLON, H VERBANCK and P McINTYRE
	Agricultural	PA DONOVAN
1997	Factory	Prize shared by M MOODLY, DJ BEKKER, PJ PIENAAR and R PILLAY; M MOODLEY and PM SCHORN; I SINGH, NJ COETZEE and E BURMEISTER; I SINGH, R RILEY and D SEILLIER
	Agricultural	A PRINS, JJ BORNMAN and JH MEYER
1998	Factory	None
	Agricultural	JB CHADWICK
1999	Factory	T DALE and TD KNOETZE
	Agricultural	HR ROSTRON, DWF BUTLER and MD ZWANE
2000	Factory	CRC JENSEN and G GOVENDER
	Agricultural	N LECLER
2001	Factory	M DEBWE
	Agricultural	M HUMM
2002	Factory	I SINGH, H JONES and S GAYAPERSAD
	Agricultural	M ISYAGI and DMW Whitbread
2003	Factory	Prize shared by: LJ MELROSE; And M MOODLEY, M PILLAY, PM SCHORN, G MITCHELL and R GELLING
	Agricultural	Prize shared by: GW MAHER and L SCHULZ; And C PFOTENHAUER
2004	Factory	None
	Agricultural	D ARMSTRONG
2005	Factory	None
	Agricultural	None

Year	Prize Award	Author(s)
2006	Factory	Prize shared by: M REIN, L SMITH, B STRACHAN and R WIRMINGHAUS; and M NINELA and N RAJOO
	Agricultural	Prize shared by: MI LANGTON, JC SMITHERS, CN BEZUIDENHOUT and PWL LYNE; RR FORTMANN, PG BRENCHLEY and AK MATHEW
2007	Factory	Not awarded – no Congress held
	Agricultural	Not awarded – no Congress held
2008	Factory	S RAMA and SS MUNSAMY
	Agricultural	JJ MURRAY
2009	Factory	PM SCHORN, L SMITH, SD PEACOCK, DJ LOVE and DJ MUZZELL
	Agricultural	AT WYNNE, TJ MURRAY and AB GABRIEL
2010	Factory	DJ LOVE
	Agricultural	JJ MURRAY
2011	Factory	None
	Agricultural	J DLAMINI
2012	Factory	R GENT
	Agricultural	KE MATHIAS
2013	Factory	A RAGHUNANDAN, CRC JENSEN, T MTEMBU and FEA AHMED
	Agricultural	JJ MURRAY, HNP STOLZ and JL BOUWER
2014	Factory	Prize shared by: M NDLAZI, RI SINGH and S NDLOVU; M MBUYAZI and S MHLONGO
	Agricultural	CPR CRONJE and P SAHADEO
2015	Factory	A MDAKANE and T NDHLALA
	Agricultural	None
2016	Factory	EM DLAMINI
	Agricultural	None
2017	Factory	FS MNCUBE, DJ LOVE, P SIKHAKANE, D OGLE and T MTEMBU
	Agricultural	AJ HARRIS
2018	Factory	C MARAIS, R LAUBSCHER, Q ENGELBRECHT and P FRANCOIS
	Agricultural	B SMALL
2019	Factory	T GOUNDEN, C CHILI, S NALA, M SULIMAN and Z RAMBAKUS
	Agricultural	N LECLER
2021	Factory	C KOTZE
2021	Agricultural (First)	RJ NICHOLSON and M KADWA
2021	Agricultural (Highly Commended)	M KADWA
2022	Factory	F MARAIS, C VAN DEN BERG and L BARNARD
2023	Agricultural (First)	R NICHOLSON
2023	Agricultural (Highly Commended)	R NICHOLSON, S DUBE, M LANDMAN and RT MASONDO
2024	Agricultural	KADWA M, and NICHOLSON R
2024	Factory	NAIDOO S, MNCUBE F, NDLOVU V and NINELA M

SASTA POSTER AWARDS 2000-2024

Year	Prize Award	Author(s)
2000	Factory	None
	Agricultural	SA McFARLANE and RA BAILEY
2001	Factory	None
	Agricultural	SA McFARLANE
2002	Factory	None
	Agricultural	C BEZUIDENHOUT and C GERS
2005	Factory	None
	Agricultural	MT SMITH, A SINGELS and J NEEN
2006	Factory	None
	Agricultural	M JONES and M VAN DEN BERG
2007	Factory	None – No Congress
	Agricultural	None – No Congress

2003	Factory	None
	Agricultural	None
2004	Factory	Y NAIDOO and R SIMPSON
	Agricultural	DJ NIXON
2009	Agricultural	PL CAMPBELL, GW LESLIE, SA McFARLANE, SD BERRY, R RHODES, R VAN ANTWERPEN, RS RUTHERFORD, T VAN ANTWERPEN DM MCELLIGOTT and DE CONLONG
Year	**Prize Award**	**Author(s)**
2010	Factory	None
	Agricultural	A JUMMAN and NL LECLER
2011	Factory	None
	Agricultural	CN BEZUIDENHOUT
2012	Factory	WK LAWLOR
	Agricultural	WA GILLESPIE, FJ MITCHELL, MJ WAY, TM WEBSTER and JH WITTHOFT
2013	Factory	H DU CLOU and SN WALFORD
	Agricultural	B BHENGU, T MASONDO, S HLELA, V DLAMINI and S MNGOMEZULU
2014	Factory	RC LOUBSER
	Agricultural	SA McFARLANE, LA MARTIN, D WILKINSON, AC KOCH, T VAN ANTWERPEN, N PILLAY and RS RUTHERFORD
2015	Factory	WK LAWLOR
	Agricultural	P SITHOLE and A PARASKEVOPOULOS
2008	Factory	B BARKER and J WESLEY-SMITH
	Agricultural	SA McFARLANE, T VAN ANTWERPEN, P GOVENDER and GF BUCHANAN
2009	Factory	SN WALFORD, S EGLI and B MARTINCIGH
2016	Factory	SN WALFORD
	Agricultural	Prize shared by: P TWEDDLE; PL CAMPBELL, A PARASKEVOPOULOS and S HURIPURSHAD
Year	**Prize award**	**Author(s)**
2017	Factory	B BARKER, S MADHO and S RAHIMAN
	Agricultural	Prize shared by: AB PATTON, ITR MAKHUBEDU and A WEIGEL, K McFARLANE and AD WALTON
2018	Factory	K FOXON
	Agricultural	P TWEDDLE
2019	Factory	K BOOYSEN, KM FOXON, and SN WALFORD
	Agricultural	PB TWEDDLE and AJ HARRIS
2021	Agricultural (Tie First)	PB TWEDDLE
2021	Agricultural (Tie First)	AC KOCH, CJ KISTAN, R GOVENDER, T VAN ANTWERPEN and SA McFARLANE
2021	Agricultural (Highly Commended)	A PARASKEVOPOULOS, RS RUTHERFORD and SA McFARLANE
2021	Factory	I GOVENDER
2022	Factory	T MOLOI
2023	Agriculture (First)	R JACOB, R LIGEGE, G MEYER and S SNYMAN
2023	Agriculture (Highly Commended)	M KADWA
2024	Agriculture (First)	CJ KISTAN, and SA McFARLANE
2024	Agriculture (Highly Commended)	MKHIZE L, and SNYMAN S
2024	Factory	GOPALDASS D AND VOGEL A

JUBILEE AWARDS 2000-2021

Year	**Prize Award**	**Author(s)**
2000	Factory	CRC JENSEN
	Agricultural	EJ SCHMIDT
2003	Factory	None
2011	Factory	Y NAIDOO
	Agricultural	V HARRACA
2015	Factory	PS JENSEN

	Agricultural	None		Agricultural	S RAMBURAN
2006	Factory	None	2018	Factory	W LAWLOR
	Agricultural	None		Agricultural	N MILES
2009	Factory	None	2021	Factory	K FOXON
	Agricultural	None		Agricultural	MW ADENDORFF
			2024	Factory	D BEZUIDENHOUDT
				Agricultural	S MCFARLANE

INNOVATION AWARDS 2000-2020

Year	Prize Award	Author(s)	Year	Prize Award	Author(s)
2000	Factory	L HELFRICH	2002	Agricultural	NOODSBERG CANEGROWERS'
	Agricultural	D DINKELMANN			ASSOCIATION (Proposed by G MAHER)
2001	Factory	B GOVENDER	2003	Factory	D DENNIS
	Agricultural	None		Agricultural	None
2002	Factory	S CHINASAMY	2004	Factory	None
2004	Agricultural	WH REDINGER	2007	Factory	None
2005	Factory	None		Agricultural	I HILLERMAN
	Agricultural	C GARNETT	2008	Factory	None
2006	Factory	None		Agricultural	A SINGELS
	Agricultural	E ALBERTSE			

ROBIN RENTON MEMORIAL AWARD (PGBI PRIZE/DRA GLOBAL) 2003-2020

Year	Author(s)		
			None
2003	LJ MELROSE	2012	PS JENSEN
2004	None	2013	S SHAH
2005	None	2014	DN BOOTE
2006	S RAMA	2015	None
2007	None – No congress held	2016	S HESS
2008	P SHARMA	2017	AJ HARRIS
2009	Z RAMBUKUS	2018	P NAIDOO
2010	A JUMMAN	2019	P Du TOIT
2011	T NDHLALA	2024	S RAHIMAN

SASTA STUDENT THESIS AWARD 2004-2007

Year	Prize Award	Author(s)	Year	Prize Award	Author(s)
2004	Agricultural	MH GRAHAM	2006		None
2005		None	2007		None

SASTA STUDENT AWARD 2008-2023

Year	Prize Award	Author(s)	Year	Prize Award	Author(s)
2008	Agricultural	AJ HARRIS	2015	Agricultural	BJ VAN VUUREN

2009	Agricultural	G DITTRICH-SCHRÖDER
2010	Factory	H DU CLOU
2011	Agricultural	P MUDAVANHU
2012	Factory	SN RAHIMAN
	Agricultural	TA GOBLE
2013	Agricultural	RL ROSSLER
2014	Agricultural	MS SIBOMANA
2016	Agricultural	AJ SERFONTEIN
2017	Agricultural	NW MBUMA
2018	Agricultural	NW MBUMA
2019	Factory	P NAIDOO
2021	Factory	TP MANUEL R MUTETE
2023	Agriculture	E MUGEHU, H SHIMELIS and LTM MPOFU
2024	Agriculture	SINGH S
2024	Agriculture (highly commended)	MAKHETA T
2024	Factory	J URAYAYI

AGRICULTURE SUCCESS STORY AWARD 2010-2013

Year	Author(s)	Year	Author(s)
2010	D SUTHERLAND	2012	None
2011	None	2013	None

FACTORY OPERATIONAL PAPER AWARD 2011-2013

Year	Author(s)	Year	Author(s)
2011	Q MASEKO	2013	B SKINNER
2012	S GARTNER		